Forschungszentrum Jülich

Institut für Festkörperforschung

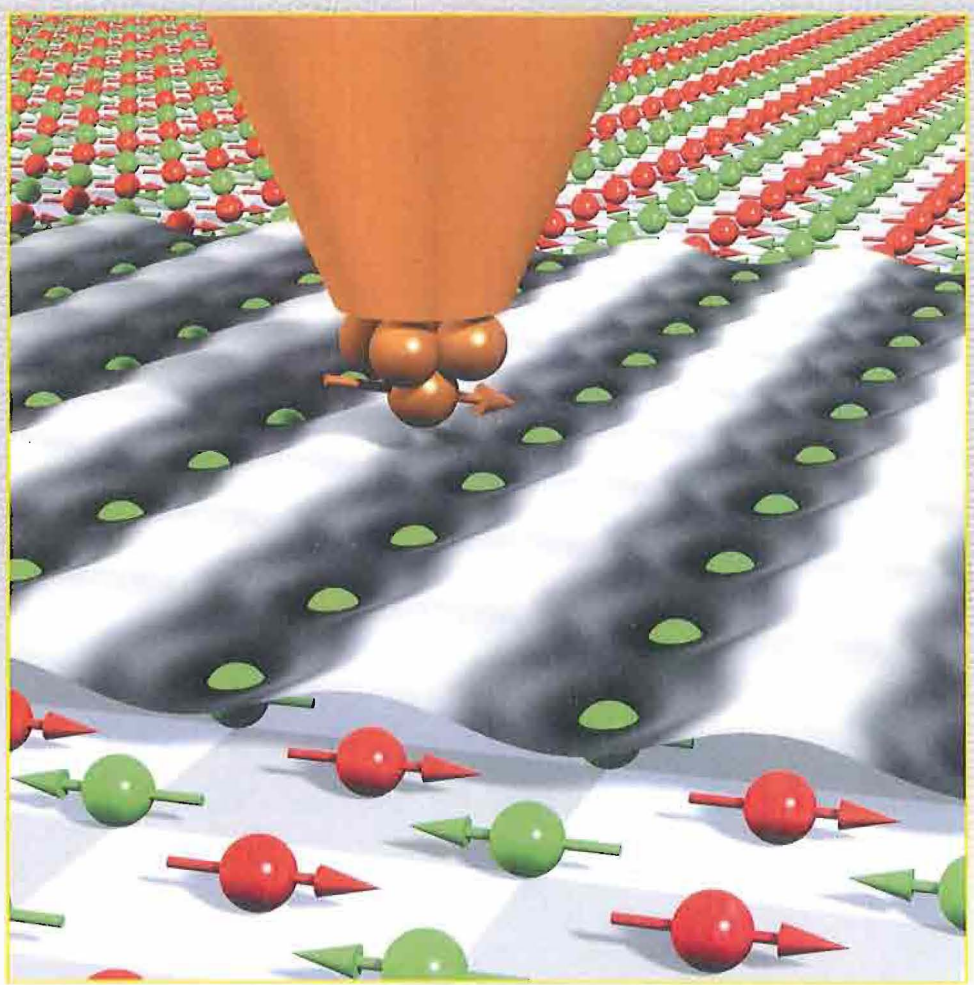

Scientific Report 2000/2001

Published by Forschungszentrum Jülich GmbH
D-52425 Jülich
Telephone: +49 2461 61-0 – Telex: 833556-0 kfa d
Responsible for content: the Managing Director of the IFF
tel: +49 2461 614465, fax: +49 2461 612410, e-mail: h.geisler@fz-juelich.de
Wholly set-up by BD-SG, Grafische Betriebe, Forschungszentrum Jülich GmbH
Time of going to press: 15.02. 2001

Institut für Festkörperforschung

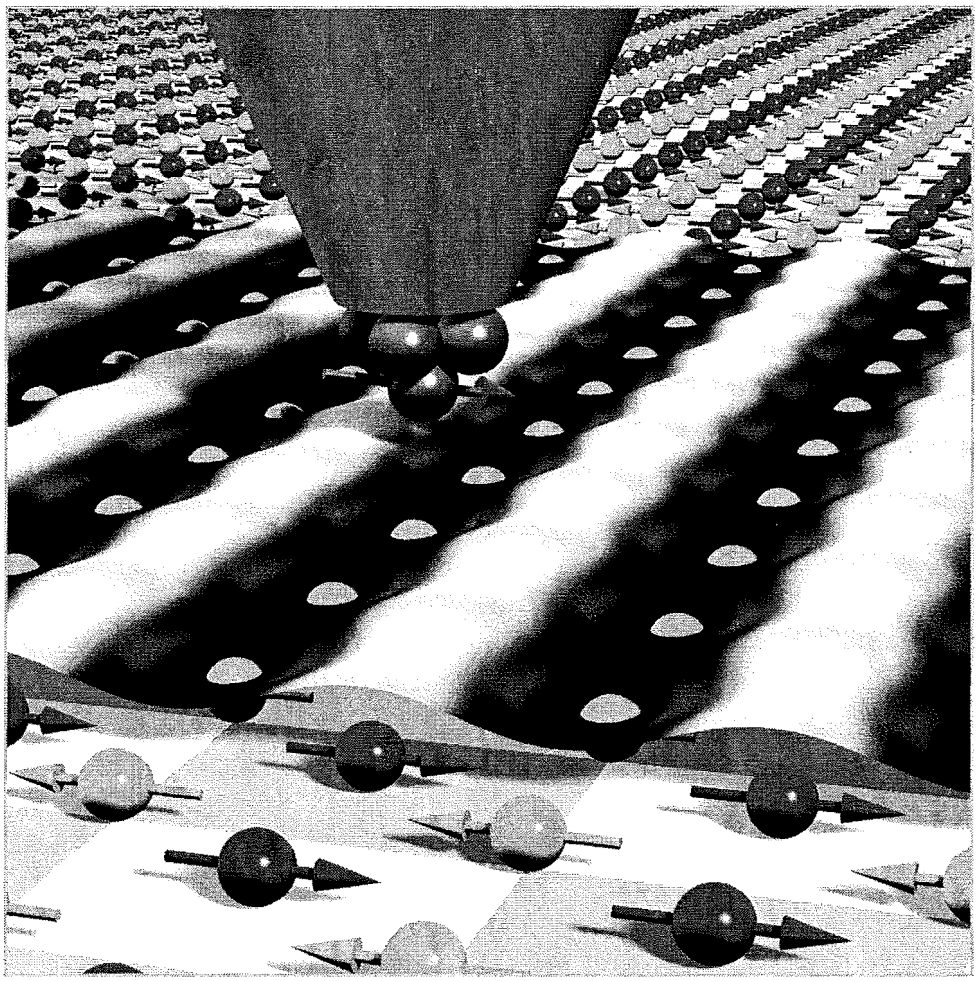

Scientific Report 2000/2001

Introduction

The "Institut für Festkörperforschung" (IFF) is devoted to research on condensed matter. Topics span from the physics and chemistry of liquids, via membranes, clusters, surfaces and thin films to homogeneous and inhomogeneous bulk solids. The IFF has a department structure consisting of 9 institutes and service groups. It's wide spectrum of experimental facilities and individual expertise enable the IFF to successfully tackle complex problems in close collaboration between preparative, experimental and theoretical groups. Specialized laboratories and facilities exist for preparation of polymers and ceramics or the growth of thin films and bulk single crystals. Besides standard methods for characterization, highly sophisticated techniques are available and constantly further developed such as ultra high resolution electron microscopy, neutron- and synchrotron x-ray scattering or fsec laser spectroscopy. Characteristic for an institute of the HGF (Hermann von Helmholtz Association of National Research Centers) is the fact that the IFF builds, operates and makes available to external users the neutron scattering instruments at the research reactor FRJ-2. Last but not least, the IFF has a long tradition in teaching and training of young researchers, not only through the approximately 30 IFF scientists teaching at universities, but in particular through the Spring Schools of the IFF and the annual Neutron Laboratory Course.

This annual report is intended to inform the international scientific community, including our scientific advisory board, about the scientific activities at the IFF during the past year. We have attempted to present a typical cross section through the research done at IFF, including scientific highlights as well as results of long term developments, for example the construction of new large scale instruments. I hope you will enjoy learning about our activities.

During the last few years, the IFF has seen a very significant restructuring, where out of originally 10 institutes, 5 institutes were closed and 4 institutes were formed focussing on new research fields. In 1997 the "Institute for Electroceramic Materials" and the "Institute for Scattering Methods" were created, followed by the "Institute Theory II" ("Complex Fluids and Soft Matter Research") in 1998. Finally, in January 2000, Prof. Jan Dhont joined the department to set up his activities in "Soft Matter Research". Now, with three out of nine institutes ("Neutron Scattering" (polymer research), "Theory II" and "Soft Matter Research") working in this field, it constitutes one of the main pillars of the IFF and provides attractive possibilities for cooperation within the research center itself.

The year 2000, as the first year of the new Millennium, was proclaimed "Jahr der Physik" ("Year of Physics") by the German federal government. Prof. Müller-Krumbhaar took a leading role in organizing the presentation of the accomplishments in condensed matter science to the broad public and many scientists of the IFF enjoyed the experience of explaining and discussing their research results during the exhibition "Stein der Weisen" in the "Bundeshaus" in Bonn. The communication within the scientific community reflects the productivity of the IFF with 310 publications, of which 256 articles were published in refereed journals, and a total of 346 external talks of which 245 were invited. The IFF continued to provide top candidates for faculty positions: Dr. S. Blügel received a call for a C3 professorship for Theoretical Physics at the University of Osnabrück, Dr. C. Carbone left the IFF to take up a position at the National Research Council in Trieste, Italy, and Prof. Dr. W. Eberhardt was offered a faculty position at the Technical University of Berlin and as scientific director of the BESSY GmbH. The international scientific recognition of the IFF is also expressed in prizes awarded to Prof. Dr. K. Urban (medal for Scientific Publishing of the German Physical Society) and Prof. R. Waser (Ferroelectrics Recognition Award of the IEEE) among other honors.

In view of the many and varied accomplishments of the year 2000, the IFF has had a good start into the new millennium. As long as the scientific freedom is preserved and room is left for true innovation, we can look optimistically into the future.

Th. Brückel
Managing Director 2001

Contents

Institute for Solid State Research (IFF)

1. Management and Structure

Prof. Dr. Th. Brückel
Institute 'Scattering Methods'
IFF-Managing Director for 2001

H. Geisler (Permanent Deputy of the Managing Director)

Institutes:

Institute 'Theory I'
Prof. Dr. G. Eilenberger

Institute 'Theory II'
Prof. Dr. G. Gompper

Institute 'Theory III'
Prof. Dr. H. Mueller-Krumbhaar

Institute 'Scattering Methods'
Prof. Dr. Th. Brückel

Institute 'Neutron Scattering'
Prof. Dr. D. Richter

Institute 'Electroceramic Materials'
Prof. Dr. R. Waser

Institute 'Soft Matter'
Prof. Dr. J. Dhont

Institute 'Microstructural Research'
Prof. Dr. K. Urban

Institute 'Electronic Properties'
Prof. Dr. W. Eberhardt

Special Group:
'Materials under high doses of radiation'
Prof. Dr. H. Ullmaier

Central Facilities:
'Networks and Numerical Methods'
H. Geisler

'Accelerator'
DI R. Hoelzle

'Construction'
H. Feilbach

'Mechanical Workshop'
K. Hirtz

'Administration'
H. Geisler

The Institute of Solid State Research (IFF) pursues research on condensed materials in the solid or liquid state. Based on its studies of bulk properties of condensed phases, the IFF is concerned with inhomogeneous systems and with the consequences of reduced dimensionality. This refers in particular to the physics of clusters, phase boundaries, thin films and membranes. With regard to both theory and experiment, the institute's research can be understood in terms of three strategically distinct categories:

- **Phenomena oriented research:** The search for, the discovery and explanation of general phenomena and behaviour in condensed matter systems, including the mathematical and physical concepts and structures underlying this behaviour.

- **Materials oriented research:** The investigation of specific materials or classes of materials with a view of gaining an understanding of their special properties and, where appropriate, exploring their potential for practical application. Production of novel materials, and preparation as well as characterisation of well-defined samples.

- **Method oriented research:** Development of new methods and the improvement of existing methods, both in the experimental and the theoretical/numerical sectors.

The general physical basis for these research areas is provided by statistical physics and quantum mechanics. Together they describe on a microscopic scale the behaviour and the reaction to external influences of electrons and atoms, the building blocks whose aggregation and cooperation is responsible for the formation of condensed phases. The issues to which these connections give rise in the context of current research form the basis of the work of *theoretical* and *experimental* groups within the institute.

Based on new techniques of preparation and characterization on a microscopic atomic scale, the *experimental* groups have increased their efforts to develop devices and taylor systems with new properties. This, in turn, has triggered the *theoretical* groups, employing modern techniques, to describe and come to an understanding of the extremely complex behaviour of these new systems.

In persuing a research strategy oriented towards the future, the IFF has extended its activities by a central topic "soft matter" in founding a new institute bearing this name and by dedicating the institute "Theory II". This emphasises the strategic decision in favour of this research area. It will also initiate extended and attractive cooperations within the research centre.

The following specific foci of work in the IFF are symptomatic of the nature and purpose of a Helmholtz-Research Centre:

- Contributing to the construction and operation of new experimental equipment and instruments for international sources of neutron and synchrotron radiation. In addition to the Jülich Research Reactor "DIDO", the neutron sources at Argonne, Berlin, Gaithersburg, Grenoble, München, Oak Ridge, Saclay and Appleton are used. The Jülich Research Centre contributes to the RD Program for the European Spallation Source *(ESS)*, a common project of 11 European countries. The IFF is involved in the ESS project via research into shock-wave effects in the liquid mercury target, the optimisation of the target and the moderators, as well as in the development of instrumentation. Experiments with synchrotron radiation are carried out at BESSY, DELTA and HASYLAB in Germany, and internationally at Argonne (APS), Berkeley (ALS), Brookhaven (NSLS), Grenoble (ESRF) and Trieste (ELETTRA).

- Using the Jülich Computer Centre, mainly for theoretical investigations and large-scale numerical simulations.

- Projects that require high levels of investment and/or the continuity of a highly qualified team of staff (in most cases in the context of national and international cooperative projects and services). Examples are the Centre for High-resolution Microscopy, the operation of accelerators, the Electro-ceramics laboratory, superconductor technology and the development of sophisticated numerical algorithms and programs.

Over the long term, the research results of the IFF have led to a broad and internationally recognized status. Special technical and scientific excellence was achieved in the following areas: application of synchrotron-radiation and neutron scattering, electron-microscopy, electron-spectroscopy, high-temperature

superconductivity, magneto-electronics, the physics of clusters, electron theory, dynamical features of phase-transitions, quasi-crystals and polymers.

A prerequisite for the focal areas of research in the IFF mentioned above and its position in the international community as a valued partner for cooperation is its strong position in basic research. The IFF carries out basic research in areas with potential for the future of condensed matter science, also as a hotbed for applied research projects.

Genuine innovation (as distinct from continuous development) occurs typically as a by-product of curiosity-driven research. This is exemplified particularly well by the discovery of the "giant-magnetoresistance" effect, which over the past years has become a very active area in solid state research. The effect has attractive applications for magnetic sensors e.g. as read heads for data storage and for control of moving parts. The license revenue from the patents on this effect represents the largest contribution to the total patent revenue of the Jülich Research Centre devolving from a single application! With this activity the IFF is also participating in the BMBF (Bundesministerium für Bildung und Forschung, i.e. Ministry of Education and Research) project "Magnetoelectronics" and also carries out accompanying basic investigations within the Strategy-Fund Project "Magnetoelectronics".

The IFF participates along with ISG (Institute for thin films and interfaces) in the Jülich's program "Basic Research in Information Technology" (PGI). With its strong basic research as foundation, the IFF has in recent years extended its facilities for technical development and component–design continuously. This has led to the acceptance of the IFF's research program within the framework of the HGF-Strategy-Fund Project "Microtechnology High-Performance Components – Microinductors" and also of the "SQUID-Microscopy" and the "Hilbert-Transformation-Spectroscopy" programs.

In 2000, the scientific work of the IFF generated 310 publications (256 in refereed journals and 54 others), 4 patents and 19 patent applications. 346 scientific talks were presented. Among these were 245 invited talks. 105 posters were presented at conferences. In addition IFF staff members gave 48 educational seminars at universities. 26 staff members are lecturers at universities.

The traditional IFF-Spring School was held in 2000 with the topic "Femtosecond and Nano-eV-Dynamics in Condensed Matter" and attracted 122 participants. In addition the IFF organises an annual two week lecture and practical laboratory course on "Neutron Scattering" in October. In the year 2000 we had 36 participants, 10 of which were from other european countries.

In 2000 13 diploma students and 12 doctoral students completed their thesis; 25 diploma students and 71 doctoral students worked at IFF.

2. Scientific and Technical Infrastructure

In the context of a general reduction in the number of personell at the research center Jülich, the IFF was forced to tighten its technical infrastructure. Through organisational and strategic measures, the IFF tried to maintain the optimal efficiency of the central services despite the decrease in the number of staff. As a consequence the central facilities *Electronics Laboratory* and *Numerical Methods and Data Processing* were merged into a group *Networks and Numerics*. These measures have now reached a critical limit.

Research "at the cutting-edge" requires the capability to build and maintain experimental facilities in high-tech areas. This holds as well for the basic research performed by the IFF at national and international sources as for its applied research. Equipment must meet high international standards, and especially so when the work performed is to be "relevant for industry". A basic requirement for the work of the Department is an infrastructure, within the IFF and the Research Centre itself, which supplies the necessary expertise, effectiveness and facilities.

The group *Networks and Numerics* maintains the workstation cluster and computer networks, and supports scientific staff in the design and performance of experiments. It supplies expert assistance in hard- and software, maintains the system-software of the IFF-Workstation-Cluster and trains mathematical-technical assistants.

The *Accelerator Group* is responsible for the operation of the Compact-Cyclotron and the Tandetron.

Construction and *Workshop* develop and build equipment for the IFF, from simple mechanical components to sophisticated modern technology. The facility works closely together with the scientists and engineers of the Institute to achieve the ambitious quality and tolerance goals set by the experimentalists.

Staff members in the central facilities:

K. v. Ameln, S. Berger, H.P. Esser, A. Bremen, H. Cremer, P. Eickenberg, M. Emmerich, H. Feilbach, U. Funk-Kath, R. Gehlhaar, E. Gundt, R. Heckmann, J. Heinen, D. Henkel, K. Hirtz, R. Hölzle, K.H. Johnen, S. Krahe, J. Lingenbach, T. Matulewski, W. Noack, T. Nguyen-Vu, P. Pickartz, M. Pohl, B. Radermacher, H. Sachsenhausen, L. Schätzler, H. Schnitzler, J. Schramm, T. Starc, P. Stefelmanns, W. Stellmacher, H. Terberger, E. Westphal, K. Wingerath.

J. Hengesbach (INC), L. Kasterke (IME), H. Schwalbach (ISG)

3. Other Scientific Activities: Collaborations with Universities, Institutions and Industry

The productivity of a Research Institute depends strongly on its capacity for scientific exchange and for scientific and technical cooperation. In this regard, the Jülich Research Center offers excellent possibilities. The Centre's top class infrastructure offers efficient assistance, also for visiting scientists. Modern neutron scattering instrumentation appropriate for cutting-edge studies are available to many IFF guest scientists in the DIDO reactor hall and in the neutron guide hall ELLA. The wide variety of collaborations in which the institutes for Neutron Scattering and Scattering Methods of the IFF are involved leads to optimal usage of these large scale instruments. On the other hand, the availability of complementary facilities at other institutions is essential for the IFF. With the construction of instruments the IFF contributed to the development and improved usage of external large scale facilities such as ILL and CEN (Grenoble), APS (Argonne, USA), DELTA (Dortmund), HASYLAB (Hamburg), BESSY (Berlin), NSLS (Brookhaven), and NIST (Washington).

Bilateral agreements have been concluded with the Paul-Drude Institute, Berlin, RWTH Aachen, IBM Rüshlikon, and the Universities Bonn, Göttingen and Kiel for the use of the Jülich centre for high-resolution microscopy for specialized studies in the area of quantitative and high-resolution microscopy, and the use of the Jülich microscope with correction of spherical abberation.

In the past years, the IFF has expanded its activities as a *sub-contractor* to large companies (e.g. Bosch, Siemens, Daimler-Benz, Thompson, Philips) and contract work has become the main focus of the scientific work of several groups, especially in the context of large national (German) and international projects. Of special importance is the IFF's participation in the BMBF-Project "Magnetoelectronics". Under the auspices of the Technology Transfer Bureau of the Jülich Research Centre, the IFF leases equipment to companies that have established themselves in the Jülich Technology Centre. In addition, the IFF has designed and built pilot equipment for industrial companies.

One of the most important duties of a Research Centre is to make its large scale instruments available to universities and other research organisations for research projects that need not necessarily have a direct connection with active research programs of the Centre. In this context it is of paramount importance for the IFF to keep the 16 neutron scattering instruments at the research reactor DIDO operating and to improve them further. In the year 2000, neutrons were available for users at 177 days altogether. During this time 87 experiments were performed by IFF scientists and 114 experiments by external groups (19

groups from each national and international universities, 4 groups from national and 11 from international research institutes and 5 groups from industry).

Many staff members of the IFF serve in scientific committees (e.g. advisory boards for institutes and scientific societies, program committees for international meetings, editors of proceedings, journals and databases, members or presidents of the boards of directors of scientific societies as well as referees, e.g. for the German Research Community, special research areas and prize committees).

Personal Honours, Awards and Distinctions

Dr. S. Blügel, Institute "Electronic Properties", was offered a C3-professor position at the University Osnabrück for Theoretical Physical (magnetism).

Prof. Dr. Th. Brückel was appointed chairman of the Scientific Council of the Institute Laue-Langevin at Grenoble.

Dr. C. Carbone, Institute "Electronic Properties", has accepted the offer of a position at the Italian National Research Council, Trieste.

Prof. Dr. W. Eberhardt received a call to the TU Berlin combined with the appointment as Scientific Director of BESSY GmbH.

Dr. Ch. Pithan, Institute "Electroceramic Materials", – together with Yukiko Ozaki, Kawasaki Stell Corporation – received the "48th Outstanding Paper Award of the Japanese Institute of Metals" for the publication "Scanning tunneling spectroscopy of high-resistance grain boundaries in sintered Mn-Zn-ferrite".

Prof. Dr. K. Urban and Dr. C. Jia, Institute "Microstructural Research", were awarded the Honour of Lifelong Guest Professor by the Wuhan University, Wuhan (China).

Prof. Dr. K. Urban has received the medal for Scientific Publishing from the German Physical Society. He was also appointed Honorary Member of the Materials Research Society of India.

Prof. Dr. R. Waser was elected member of the advisory board to the Ecole Polytechnique Federal de Lausanne, Switzerland. He also received the Ferroelectrics Recognition Award from the IEEE, branch UFFC (Ultrasonics, Ferroelectrics and Frequency Control Society).

Dr. H. Kohlstedt, Institute "Electroceramic Materials", completed successfully his "Habilitation" at the University Köln with a thesis entitled "On the Physics and Technology of Superconducting and Magnetic Tunnel Contacts".

Alexander von Humboldt Research Prize

Prof. T. Burkhardt, Temple University, Philadelphia, USA, Institute "Theory II".

Mrs. Prof. M. Olmstead, University of Washington, Seattle, USA, Institute "Electronic Properties".

Prof. N. Smith, Law. Berkeley Nat. Lab., Berkeley, USA, Institute "Electronic Properties".

Alexander von Humboldt Scholars

Dr. K. Maiti – IISC Bangalore, Bangalore, Indien
Dr. J. Wu – Beijing Lab. of Electron Microscopy, Beijing, China

Institute Reports with Selected Research Results 2000

Institute Theory I

General Overview

Research Areas

The main focus in the Institute is on gaining an understanding of electronic structure and atomic-scale processes and, wherever realistically possible, performing quantitative calculations. The term 'quantitative' is used here to draw a distinction to the other important 'qualitative' aspect of theory, which considers characteristic elements of physical reality in the abstract and represents these using the simplest possible theoretical or numerical representation. The individual themes that constitute this area of activity will be described in more detail below.

For a given collection of nuclei, the structure and properties of the resulting atomic assemblies are determined in the last analysis by the electrons. Thus the main focus of the Institute's work programme, referred to above, in fact spans the entire physics of condensed materials! The institute's choice of relevant problems in this area, which is addressed by a virtual army of theorists worldwide, is made according to the following aspects:

- current issues of a methodological or thematic nature,
- the expertise of staff members,
- the availability of computer programme-packages that have evolved over many years (and so can be compared to moderately expensive experimental equipment),
- special capabilities of the Jülich computer facility,
- status of competition and possibilities for collaboration, local, national and international.

In this sense, a central feature is the ongoing development and application of current density-functional/ab initio molecular dynamics programmes, especially in conjunction with the powerful computational facility in ZAM. Work in this area has been performed by Dr. Jones and Dr. Akola, with Prof. Ballone as a frequent guest. A new example of work in this research area can be found below.

The computer programmes run currently on the T3E. On-going development includes the testing of new, non-local approximations for the exchange-correlation energy functional. Such approximations are essentially empirical and not the result of ab initio theory. This leads to systematic deviations with respect to measured values and with values calculated for small systems by more reliable, but much more resource intensive quantum methods. Combining accuracy with ease of computation will remain a challenge into the future. The focus of applications has been to atomic clusters, especially those with light atoms (organic molecules, carbon-aggregates), which require 'hard' pseudopotentials and so represent difficult numerical problems. Simulation of time- and temperature depending processes (reactions) are of particular interest.

A further area of research concerns the interaction of electrons and electromagnetic fields in bulk materials (Prof. Sturm) and on sufaces (Dr. Liebsch). A perennial challenge to the condensed matter theorist is the problem of interactions and correlations among electrons. Whereas for s- and p-electron systems these effects are satisfactorily taken into account by density functionals, d- and f-electron systems show phenomena which are beyond the scope of LDA. Methods like dynamical mean field theory and have been generalized to multiband situations and applied by Dr. Silke Biermann and Pro. Lichtenstein. Work in this direction is reported below.

Dr. Harris builds on the experience of many years by applying density functional theory to materials problems, and together with Dr. Bringer is working on programmes to apply data mining methods for materials research at the institute.

An important research topic in the Institute is the atomic theory of friction and contact mechanics. A new result is presented below as an example of the general area of research. Over the past years, Dr. Persson had pioneered work in this area (much of which is summarized in his 1997 monograph on this topic). This remains an area whose

development is just breaking out of infancy, and has broad-based ramifications and many open questions and applications.

Another research area of the Institute, the theory of non-linear systems, had been transferred for the period 1997-99 to the 'Modelling Forum', where Dr Lustfeld, co-opted as a member of the Forum, was applying his know-how to environmental problems. There is now an ongoing cooperation between Dr. Lustfeld and two groups in the "Institute of Chemistry and Dynamics of the Geosphere" of FZJ concerning the behaviour of pollutants in the atmosphere and in soil. In a co-operation with colleagues from the Eötvös University, Budapest, mathematical problems of chaotic motion are treated.

The research area of Prof. Eisenriegler - 'Geometric Effects in Complex Fluids' - bears a close relationship to the theory of soft-matter. At the end of 2000, Prof. Eisenriegler joined the Institute Theory II and took this activity along with him.

External Funding and Collaborative Projects

- Between 1994 and 2000, Dr. Persson was granted annually support by the DFG to cover 3-months guest visits to IFF by Prof. Volokitin, University of Samara, Russia.
- As a participant on a 5-year BMBF(German Research Ministry)-supported German-Israeli Cooperative Project, Dr. Persson receives from 1998 to 2003 annual funding of 50,000 DM to cover guest visits and travel expenses.
- As a contributor in a collaboration between institutes from Jülich, Mainz and Heidelberg, Dr. Jones receives for the years 2000-2004 through a Materials Design Programme of the BMBF funding of in total 1 250 000 DM.

Gert Eilenberger

Personnel 2000/2001 and areas of activity

Staff members

Dr. A. Bringer	Problems of electron correlation, genetic algorithms for materials research	23.20.0
Prof. G. Eilenberger, Institute Director	Applications of supersymmetry in solid state problems, nonlinear dynamics	23.20.0 23.15.0
Dr. J. Harris	Practical applications of computational and informational methods to materials research	23.20.0
Dr. R.O. Jones	Structure and dynamics of clusters and amorphous and liquid systems; Project: "Chemistry-Laboratory Computer"	23.20.0
Dr. A. Liebsch	Linear and non-linear response, electronic correlation with quantum impurity methods	23.20.0
Dr. H. Lustfeld	Theory of nonlinear systems and its applications in atmospheric chemistry	23.15.0
Dr. B.N.J. Persson	Electronic response at surfaces, atomic friction, adsorbate modes, crack propagation	23.20.0
Prof. K. Sturm	Electronic response; dielectric properties of metals and semi-conductors (now retired)	23.20.0
Mrs Ch. Hake	Secretary	

Guests 2000

Prof. P. Ballone	(University of Messina, Italy) Development and applications of the DF/DM method	23.20.0
Dr. J. Bene	(Eötvös University, Budapest, Hungary) Theory of non-linear systems	23.15.0
Prof. K.H. Fischer	(FZ Jülich, retired) Vortices in d-wave and high T_c super-conductors	23.20.0
Dr. Z. Kaufmann	(Eötvös University, Budapest, Hungary) Theory of non-linear systems	23.15.0
Prof. A. Lichtenstein	(Catholic University Nijmegen, The Netherlands) Correlation problems in d-electron systems	23.20.0
Dr. C. Lopez	(Cuernavaca, Mexico) Optical phenomena at Ag surfaces	23.20.0
Dr. J. Maytorena	(Cuernavaca, Mexico) Optical phenomena at Ag surfaces	23.20.0
Prof. V.L. Popov	(Russian Academy of Sciences, Tomsk, Russia) Aspects of atomic friction	23.20.0
Prof. A. Volokitin	(Samara University, Samara, Russia) Adsorbates at surfaces	23.20.0
S. Zilberman	(Tel Aviv University, Tel Aviv, Israel) Theory of friction	23.20.0

Graduate students

Dr. S. Biermann	(Univ. Cologne) New schemes of approximation for the many particle problem in condensed matter [Doctor's degree awarded Nov. 2000]	23.20.0
R. Maaßen	(Univ. Cologne) Geometric effects in complex fluids	23.30.0

"Living polymers" – Why do they polymerize?

P. Ballone† and R. O. Jones
Institute Theory I

Last year we reported the results of density functional calculations on the reactions of lithium and sodium phenoxide molecules with the cyclic tetramer of bisphenol-A polycarbonate (BPA-PC). Both molecules catalyze ring-opening with small energy barriers ($\Delta E = 4.0, 2.5$ kcal/mol, respectively), and the reactants and products - a chain with a phenyl carbonate at one end and a phenoxide at the other - have almost the same total energies. The alkali atom at the end of the chain can repeat this process, producing long chains: a "living polymer". If the reaction, used in the industrial production of PC, is not exothermic, why does polymerization occur? We discuss here the role played by entropy using a classical simulation based on the mechanism suggested by the DF calculations.

F&E-Nr: 23.20.0

Density functional (DF) calculations are well-established as a means of computing the geometrical and electronic properties of molecules, and of simulating the behaviour of bulk systems. While such calculations avoid the use of parametrized force fields common in the study of polymers, for example, they are very demanding of computing resources. Our recent calculations of the energy surfaces for reactions involving $\sim$ 150 atoms are amongst the most extensive yet performed, and they provide unexpected insight into the mechanisms involved.

The structural unit of bisphenol-A polycarbonate (BPA-PC), one of the most important polymers in industrial production, contains 33 atoms. Many cyclic oligomers can be formed, and the tetramer – which is strain-free and shows the *cis-trans* isomerization found in polycarbonate chains – provides an ideal model for PC. The reaction of Li phenoxide with the carbonate group is representative of "nucleophilic attack", which often leads to the rupture of ring systems (ring-opening polymerization) [1]. The reactants and products of this reaction are shown in Fig. 1. As the LiOPh molecule approaches, the carbonyl group rotates, followed by the formation of an approximately tetrahedral CO_4 unit. Finally, a Li-O bond breaks, leading to a chain with an active -C-O-Li termination. A series of catalytic reactions can result, resulting in the breaking of all ring structures present and the formation of long chain segments. More details are provided in Ref. [2].

The energy barrier to the reaction and the change of energy between reactants and products are small. The absence of an exotherm is well-established experimentally and presents a puzzle, as entropy – the other possible driving force – might be expected to favor the presence of many small molecules rather than a small number of long chains. We have addressed this problem by performing numerous simulations using a simple model that mimics the ring-opening mechanism described above.

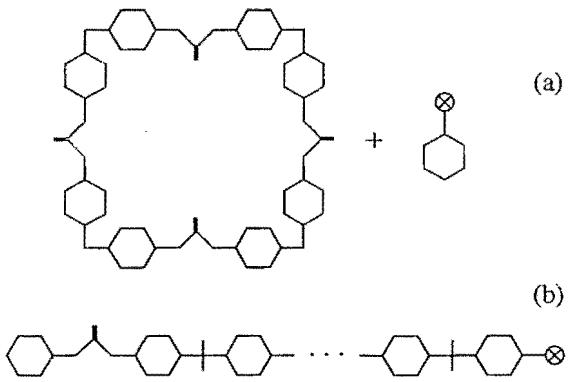

FIG. 1. Reaction of LiOPh with cyclic tetramer of BPA-PC. The product (b) is a Li-terminated chain.

In our model, diphenyl carbonate (DPC) units are represented by Lennard-Jones particles, with harmonic springs describing the covalent bonds in the polymer backbone. Each particle forms at most two harmonic bonds, so that the system comprises open chains or rings without branching. If we have $(N/4)$ cyclic tetramers, the potential energy is then:

$$V(\mathbf{r}_1, ..., \mathbf{r}_N) =$$
$$4\epsilon \sum_{i>j}^{N'} \left\{ \left(\frac{\sigma}{|\mathbf{r}_i - \mathbf{r}_j|} \right)^{12} - \left(\frac{\sigma}{|\mathbf{r}_i - \mathbf{r}_j|} \right)^{6} \right\} +$$
$$+ \frac{1}{2} k \sum_{\alpha=1}^{(N/4)} \left\{ (\mathbf{r}_{4\alpha-3} - \mathbf{r}_{4\alpha})^2 + (\mathbf{r}_{4\alpha-3} - \mathbf{r}_{4\alpha-2})^2 + \right.$$
$$\left. + (\mathbf{r}_{4\alpha-2} - \mathbf{r}_{4\alpha-1})^2 + (\mathbf{r}_{4\alpha-1} - \mathbf{r}_{4\alpha})^2 \right\} \quad (1)$$

where the prime on the first sum indicates that the Lennard-Jones interaction is turned off when i and j are connected by the harmonic potential.

The units of length and energy are σ and ϵ, respectively, and the density is measured in terms of the pack-

ing fraction η ($\eta = \pi\rho\sigma^2/4$ in 2D, $\eta = \pi\rho\sigma^3/6$ in 3D). The choice of k ($k = 3\epsilon$) leads to very floppy molecules and allows us to sample efficiently both the intra- and inter-molecular degrees of freedom. Angle bending and torsion contributions are neglected. We perform simulations for systems with fixed bonding patterns and for which one ("active") particle can interchange its bond with another particle. The active particle can form only one bond, so that it is always located at an end of a linear chain of at least two particles.

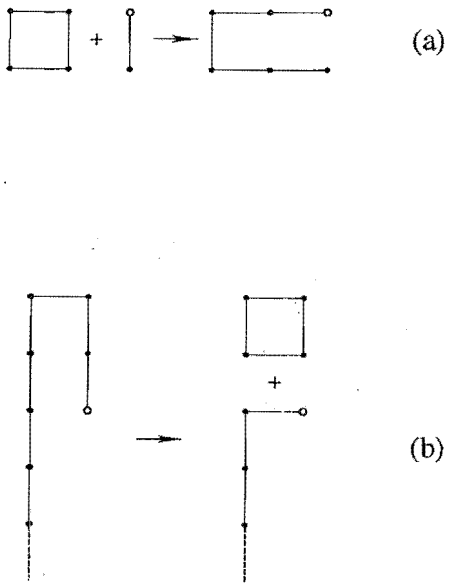

FIG. 2.

The simulation samples both different bonding configurations and the particle positions. At regular intervals we link the active particle and its nearest neighbor (excluding the particle connected to it by an intra-molecular bond), as well as two of their covalently bonded neighbors (Fig. 2). The interchange always conserves the total number of bonds, and is accepted or rejected using the Metropolis algorithm according to the change of the potential energy and temperature. In this way, we treat the system as a collection of N equivalent particles and $(N-1)$ bonds in thermal equilibrium. The successful bond interchange results in the incorporation of a ring into the active chain segment [2(a)] or – with equal intrinsic probability – into the separation of a ring from the active chain [2(b)]. The system potential energy is sampled by the (constant volume) Monte Carlo (MC) method.

The determination of the thermodynamic properties for chains of fixed length has been performed in 2D (3D) with systems of 10000 particles in a square (cubic) simulation box periodically repeated in space. The simulations of the equilibrium polymerization were performed for systems of 10002 particles, of which only one is active. The simulations were started from a system of 2500 tetramers and one dimer that carries the active particle. The simplicity of the model allows us to perform very long simulations with up to several million steps *per particle*. Dynamical properties, such as the diffusion coefficient or the viscosity coefficient, have been computed by microcanonical MD runs for systems of fixed bonding configuration, starting from atomic positions equilibrated by MC and initial random velocities selected from a Gaussian distribution. Full details will be provided elsewhere [3].

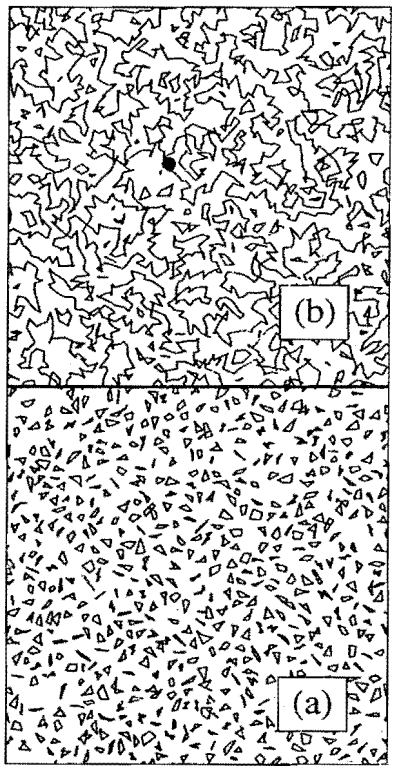

FIG. 3. Evolution of polymerization at $\eta = 0.4$, $T = 3$.

The model demonstrates a clear tendency towards polymerization that is enhanced by increasing the temperature T and particularly the packing fraction. Polymerization is highly reversible, i.e. it decreases upon decreasing the system density. A typical example is shown in Fig. 3 for $\eta = 0.4$, $T = 3.0$: the liquid-like starting assembly of tetramers (a) develops over time into a long linear chain, with residual rings of small and medium size (b). The system shows a pronounced polydisperse nature, i.e. a wide range of ring sizes. At equilibrium, we still observe large fluctuations in the length of the open chain, and a sizable mobility of the active head induced by the bond interchange mechanism.

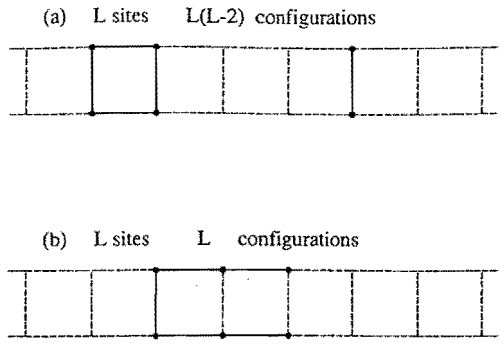

FIG. 4.

The reason for polymerization can be understood from a simple one-dimensional example. If the tetramers and the initiating dimer can move only on a 1D lattice comprising L sites [4(a)], the number of configurations available for the system is $L(L-2)$ (we assume that different particles cannot occupy the same lattice point). The elongated chain, on the other hand, has only L available configurations [4(b)], and (a) will be favored by entropy over (b), if the system can assume either configurations without intermixing. However, if the reacting system can transform reversibly from (a) to (b), it will have the sum of these configurations $(L(L-2)+L)$ and an equilibrium concentration of the elongated chain proportional to $L/[L(L-2)+L] = 1/(L-1)$. This concentration will be enhanced if the entropy advantage of the separated units is reduced, for instance by increasing the density.

Detailed results will appear in Ref. [3]. While the average length of the linear chains increases with increasing T, it is particularly interesting that there is a dramatic increase in the range $0.1 \leq \eta \leq 0.15$ in two dimensions (Figure 5). The transition appears to be first order, but further calculations are needed to confirm this. Possible reasons for the transition include: (a) The bond breaking mechanism results in a polydispersive system, increasing the number of possible configurations and the entropy. (b) The polymerized system appears to have an enhanced short/medium range mobility that compensates the loss of long range mobility accompanying the formation of large molecules. There is an obvious analogy to crystallization, in which particles sacrifice long range diffusion (ineffective at high density) to gain local entropy. Our observation that the transition is more sensitive to density than to temperature strengthens this analogy.

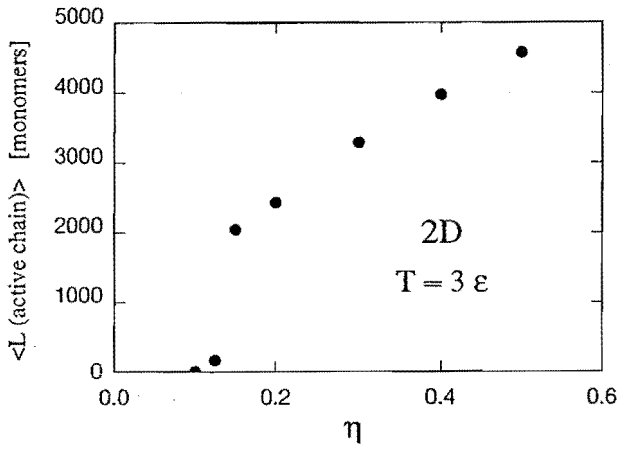

FIG. 5. Average chain length as a function of packing fraction.

† Permanent address: Università degli Studi di Messina, Dipartimento di Fisica, I-98166 Messina, Italy.

[1] D. J. Brunelle, In *Ring-Opening Polymerization: Mechanisms, Catalysis, Structure, Utility*; Edited by D. J. Brunelle, (Hanser, München, 1993), p. 1, p. 309.

[2] P. Ballone, B. Montanari, and R. O. Jones, J. Phys. Chem. **104**, 2793 (2000); P. Ballone and R. O. Jones, J. Phys. Chem., in press.

[3] P. Ballone and R. O. Jones, in preparation.

Density Functional Calculations of Elastic and Thermo-elastic properties.

John Harris
Institute Theory I, IFF.

The density functional scheme is now the standard method used to compute energies, equilibrium geometries and vibration frequencies in molecular and condensed-matter chemistry. Applications to mechanical properties of materials are less well established. Early work was limited to the lattice constants and bulk moduli of elemental materials or binary alloys. Computations of the full stiffness matrices of materials began to appear in the literature only in the 1990's. I give a brief review of the state of the art and demonstrate that the density functional scheme does give accurate results for the stiffness matrix. I also outline practical ways of computing thermo-elastic properties such as the thermal expansion coefficient. These remain to be tested.

F&E-Nr: 23.20.0

I. INTRODUCTION

Calculation of the stiffness matrices of materials proceed by applying the DF scheme to compute the energy differences when lattices are subject to strain fields. Establishing a viable computational scheme for the stiffness matrix of crystalline materials is particularly important because this is not an easy quantity to measure. Most of the experimental stiffness matrix data that exist were taken some time ago and,for example, the monograph by Simmons and Wang [1], which dates from 1971, is still a major source of data. The number of materials for which reliable data are publicly available is at a rough estimate 1500.

Early work showed that the DF method was able to track the energy of crystalline structures sufficiently well to allow computation of the bulk modulus. More recent work (see, for example, [2]) has shown that even the small energy changes associated with shear deformations can be determined with sufficient accuracy to allow computation of the full stiffness matrix. The computation of thermo-elastic properties like the thermal expansion coefficient is one stage more difficult, and accordingly the literature is relatively more sparse. The 'hard' part is the computation of the Grüneisen constant, which requires the volume derivatives of the phonon frequencies and a sum over phonon normal modes. Use of a Debye model for the phonons and an averaged Grüneisen parameter simplifies the computation greatly, but the cost in loss of accuracy is currently not determined.

II. COMPUTATIONAL METHOD.

The energy difference, $\delta\mathcal{E}$, between the energies of crystal lattices having the equilibrium values of the lattice parameters (zero strain) and a distorted lattice corresponding to strain $\vec{e}$, is written conventionally,

$$\delta\mathcal{E}\left(\vec{e}\right) = 1/2 \sum_i \sum_j C_{i,j} e_i e_j, \qquad (1)$$

where $C_{i,j}$ are the elements of the 6x6 stiffness matrix. The manner in which the strain fields are chosen and the required second derivatives determined is not entirely trivial. A novel, general and efficient statistically-based method has been developed recently by Le Page and Saxe. Once C is computed the standard moduli of elasticity can be determined via simple formulae which relate these to linear combinations of the $C_{i,j}$. Such calculations refer to 0K. The temperature dependence of the elastic properties is of course of considerable importance and can be treated theoretically at various levels. The framework for computing properties such as the thermal expansion coefficient were laid out in the original very elegant work of Grüneisen and involve a computation of derivative's of the material's phonon frequencies and a sum over normal modes. This scheme can be carried out in practice and is found to be highly accurate, but is quite CPU intensive (see, for example, [3] and references therein). A simpler level of theory, the so-called "Grüneisen-Debye" approximation, combines Grüneisen's theory with a Debye model for the phonons. The result is a set of simple formulae for the thermo-elastic constants that contain two essential material parameters, the "Debye Temperature" and an averaged "Grüneisen constant". Within this approach the only computed input required, in addition to the stiffness matrix, is the pressure-volume equation of state, from which the averaged Grüneisen parameter can be computed. This input allows calculation of all elastic constants, the transverse and longitudinal velocities of sound, and the coefficient of thermal expansion. Although data computed in the manner outlined above refer to perfect crystalline structures,the Voigt-Reuss-Hill method have evolved over the years for deriving from the crystalline data results for single-phase polycrystalline samples. This model has been implemented in computing the thermo-elastic properties of selected polycrystalline Laves phases [4] but more computations are required to establish the accuracy and limitations of the Grüneisen-Debye and the Voigt-Reuss-Hill approximations.

III. SAMPLE STIFFNESS MATRIX RESULTS

Tables 2.1 2.3 give a comparison of measured values with some computed stiffness matrix elements for three crystalline solids (the units are Gpa). The calculations were performed on a PC running Windows NT 4.0 and used the VASP module developed within Jürgen Hafner's group at the University of Vienna [5], as implemented in the MedeA software package, marketed by Materials Design. The Perdew-Wang 1991 gradient corrected exchange correlation functional (GGA) was used becaus this gave consistently better results than the local density approximation. All three sample calculations used the statistical method of Le Page and Saxe to determine the stiffness matrix from the energies of strained configurations, with a sampling of typically 2-3 energy points per degree of freedom. The results for cubic Ni3Al and tetragonal Rutile were obtained using ultra-soft pseudopotentials with standard values for plane wave cutoffs. They show a quite satisfactory agreement with experiment. This level of agreement is not untypical of the elemental and binary systems we have considered to date.

Tab.2.1 Elastic Constants of Ni_3Al

	Expt (6)	Calc.
C11	224	208
C12	148.6	148
C44	124.4	120

Tab.2.2 Elastic Constants of TiO_2 Rutile

	Expt (1)	Calc.
C11	273	261
C12	176	143
C13	149	145
C33	484	473
C44	125	109
C66	194	214

Combined with ab initio computations of lattice parameters, which showed typically errors of less than 1%, these, and other results for the stiffness matrix elements of alloys and compounds, illustrate that a solution of the Kohn-Sham equations using pseudo-potentials can deliver remarkable accuracy for the elastic behaviour of materials containing transition elements. Pseudo-potential calculations in the rare earth and actinide series are notoriously difficult but are possible using Blöchl's Projector Augmented Wave (PAW) method, which has recently been implemented within the VASP code.

Table 2.3 shows results for the stiffness matrix of Thorium Oxide as computed using the VASP PAW implementation. The excellent agreement with experiment illustrates that the addition of PAW's to the pseudopotential extends in principle the region of applicability of the plane-wave method to the rare-earths and actinides (though there is much work to be done to establish that a similar level of accuracy to that displayed in the table is to be expected in general).

Tab.2.3 Elastic Constants of ThO_2

	Exp (1)	Calc
C11	367	356
C12	106	108
C44	79.7	71

IV. CONCLUSIONS

The DFT Kohn-Sham method is sufficiently accurate to allow the determination of the stiffness matrices of materials of varying types with useful accuracy. Simple methods for computing thermal expansion coefficients and for deriving data for polycrystalline samples from calculations for perfect crystals have been implemented, but more work is needed to establish the bounds of accuracy of such methods.

Acknowledgement: This work is part of an ongoing collaboration with Peter Schmidt of the Technical University of Darmstadt, Jürgen Sticht and Paul Saxe of Materials Design and John Rodgers and Yvon Le Page of NRC, Canada

[1] "Single Crystal Elastic Constants and Calculated Elastic Properties", Gene Simmons and Herbert Wang, The M.I.T. Press, Cambridge, MA and London, England (1971)

[2] P. Ravindran, L. Fast, P. A. Korzhavyi, B. Johansson, J. Wills and O. Eriksson, Journal of Applied Physics 84, 4891-904 (1998)
J. Friedman, Technical Report No.102, Lab. for Computational Statistics, Stanford University (Nov 1988)

[3] A. I. Lichtenstein, R. O. Jones, S de Gironcoli and S. Baroni, Phys Rev. B 62 11487 (2000)

[4] B. Mayer, H. Anton, E. Bott, M. Methfessel, J.Sticht, J.Harris and P.C. Schmidt, (Intermetallics, to be published)

[5] G. Kresse and J. Furthmüller, Phys. Rev. B 54, 11169 (1996);
Computat. Mat. Sci. 6, 15 (1996)

[6] Metallurgical and Materials Transactions A. 30A, 2403-2408, (1999)

Hot-Electron Dynamics at Noble Metal Surfaces

C. López Bastidas, J.A. Maytorena* and A. Liebsch
Institute Theory I

The lifetime of hot electrons at noble metal surfaces is studied within a model focussing on the spatial variation of s-d screening. The lifetime is calculated using the *GW* approximation for the self-energy. The dynamics of electrons is treated within a two-component s-d electron model which permits explicit consideration of the mutual polarization of induced s and d electron densities. In the region of s electron spill-out near the surface the hot-electron lifetime is shown to be smaller than in the bulk due to a surface induced reduction of s-d screening.

F&E-Nr. 23.20.0

The availability of femto-second lasers has recently opened the possibility of studying the real-time decay of excited electrons. Since the quasi-particle lifetime governs the dynamics of charge transfer and electronic excitations in surface chemistry, the microscopic understanding of the processes contributing to the decay is of special interest.[1] The key quantity characterizing such processes is the nonlocal complex self-energy which yields the relaxation shift and broadening of an excited state due to its interaction with the surrounding system. In view of the difficulty of performing self-energy calculations, only few studies for realistic bulk metals have been performed so far. For metal surfaces, one-dimensional models focussing on the band structure in the direction normal to the surface were used which do not permit an adequate treatment of s-d screening effects in the case of noble metals.[2] Evidence for the importance of these effects was recently revealed in a variety experimental investigations of noble metal surfaces and nano particles.[3]

A fully three-dimensional treatment of surface screening for metals involving d electrons is computationally not yet feasible. To describe qualitatively the effect of s-d polarization on the decay of hot electrons at noble metal surfaces we make use of the fact that the sp bands exhibit nearly free electron character up to the interband onset ($\sim$ 4 eV for Ag). This suggests using a two-component s-d electron model in which the time-dependent nonlocal s electron response is treated within density functional theory for semi-infinite jellium and the occupied d bands are simulated by a local polarizable medium. Previously, this model had proven quite useful to explain the origin of the unusual dispersion relation of collective excitations on Ag surfaces.[4] An important feature incorporated in this model is the fact that the vacuum charge density spill-out stems primarily from the s electrons rather than the more tightly bound d electrons. Thus, as will be shown below, the absence of s-d screening in the surface region leads to stronger effective Coulomb interactions than in the interior of the metal. This implies shorter lifetimes of hot electrons at noble metal surfaces, in agreement with experimental observations. We also demonstrate that this lifetime depends in a remarkable way on frequency since decay into both particle–hole pairs and surface collective modes is feasible.

To evaluate the self-energy we use the so-called *GW* approximation where G is the quasi-particle propagator and W the fully screened Coulomb interaction. This interaction is given by the integral equation: $W = K + K\chi K$, where K is the bare Coulomb interaction and χ the full many-body density response function of the system. Within the present model, W can be reformulated as $W = K' + K'\chi_s' K'$, where K' includes screening via the polarizable d electron medium and $\chi_s' = \chi_s^0/(1 - K'\chi_s^0)$ accounts for the renormalization of the bare s electron susceptibility χ_s^0 due to both s and d electron screening. The above treatment corresponds to the RPA. Dynamical exchange–correlation contributions could be easily incorporated by using instead the time-dependent local density approximation. All of the quantities are nonlocal and frequency dependent. Employing a two-dimensional Fourier transformation, we have $W(z, z', k_\parallel, \omega)$, etc. As a result of the spatial characteristics of s and d electron densities in the surface region, the screened Coulomb interaction K' is not simply given by K/ϵ_d where $\epsilon_d(\omega)$ is the local dielectric function of the d electron medium. Instead, K' exhibits a more complicated dependence on both ϵ_d and the boundary z_d of this medium relative to the equilibrium distribution of s electrons in the surface region:[5]

$$K'(z, z', q_\parallel, \omega) = \frac{2\pi}{q\epsilon_d(z', \omega)}\Big[e^{-q|z-z'|} + \mathrm{sign}(z_d - z') \times \sigma_d\, e^{-q|z-z_d|}\, e^{-q|z'-z_d|}\Big]$$

where $q = |q_\parallel|$, $\sigma_d = (\epsilon_d - 1)/(\epsilon_d + 1)$ and $\epsilon_d(z, \omega) = [\epsilon_d(\omega), 1]$ for $[z \leq z_d, z > z_d]$. The above expression for K' follows from the modified Poisson equation satisfied by the total electrostatic potential and the boundary condition at z_d. The presence of the second term in K' ensures the inclusion of polarization charges generated by the d electron medium. Despite the non-symmetric form of K' the fully screened Coulomb interaction $W(z, z', q_\parallel, \omega)$ is symmetric in z, z' as required by reciprocity.

The inverse lifetime of an initial state ψ_0 at energy ω above the Fermi level E_F and with parallel momentum $k_\parallel$ is given by

$$\tau^{-1} = -2\int dz \int dz'\, \psi_0^*(z)\psi_0(z')\,\mathrm{Im}\,\Sigma(z,z',k_\parallel,\omega).$$

Replacing for simplicity in the expression for Σ the interacting propagator G by the bare G_0, one finds

$$\mathrm{Im}\,\Sigma(z,z',k_\parallel,\omega) = \int d^3q\, \psi_{q_z}^*(z)\psi_{q_z}(z')\,\mathrm{Im}\,W(z,z',q_\parallel,\omega')$$

where ψ_{q_z} are single-particle s electron wave functions of the final state. Energy and momentum conservation require $\omega' = \omega - q_z^2 - (k_\parallel + q_\parallel)^2$ with $0 \le \omega' \le \omega$. Thus, final states between E_F and ω contribute to the decay of the initial excited state at energy ω.

Fig. 1 shows the imaginary part of the self-energy for an Ag surface. The energy of the initially excited electron is 1 eV above E_F and its parallel momentum is assumed to vanish. The dynamical s electron response is evaluated for a semi-infinite electron gas with $r_s = 3\ a_0$. (The average bulk density is $n_s = 3/4\pi r_s^3$.) The local dielectric function $\epsilon_d(\omega)$ is taken from bulk optical data. To illustrate the decay of the initial state near the surface and in the interior, the results are plotted for two source points $z' = 0$ and $-9\ a_0$. Also, to demonstrate the effect of s-d screening in the surface region, Im Σ is shown for two boundaries of the d electron medium: $z_d = 0$ and $-1.5\ a_0$. The self-energy exhibits a main peak for $z \approx z'$ and dynamical Friedel oscillations in the vicinity. The inverse lifetime of a state is roughly determined by the peak area. As a result of s-d screening, the Ag self-energy is seen to be reduced relative to the corresponding bare s electron self-energy in the absence of d electrons. This screening reduction is strongest in the interior ($z' = -9\ a_0$) since an excited s electron perceives a nearly isotropic polarizable d electron density. However, an s electron forming part of the density spill-out near the surface ($z' = 0$) is less subject to s-d screening because of the limited spatial extent of the d electron density. An attractive feature of our model is that we can tune the range of s-d polarization by adjusting the boundary z_d of the d electron medium. Evidently, for $z_d = 0$ s-d screening is important even for source points z' at the surface so that the self-energy differs quite strongly from the s electron case, albeit not as much as in the bulk. Conversely, for $z_d < 0$ the region of reduced s-d screening increases and the self-energy near the surface begins to resemble the unscreened s electron self-energy. These results demonstrate the great sensitivity of the imaginary part of the self-energy to the details of the screening processes in the surface region.

Preliminary results at frequencies close to the onset of interband transitions near 4 eV show a very strong enhancement of the Ag self-energy due to decay into surface plasmons ($\omega_s \approx 3.7$ eV). Since the two-component s-d electron model used in the present work yields a fairly realistic $q_\parallel$ dispersion of this excitation, the enhancement should directly affect the lifetime of Ag image states just below the vacuum threshold (~ 4.5 eV) which have been the subject of various experimental investigations. For detailed calculations it would be desireable to combine the present scheme with one-dimensional potential models which provide the correct spatial character of wave functions normal to the surface. Such an extension is currently under progress.[6]

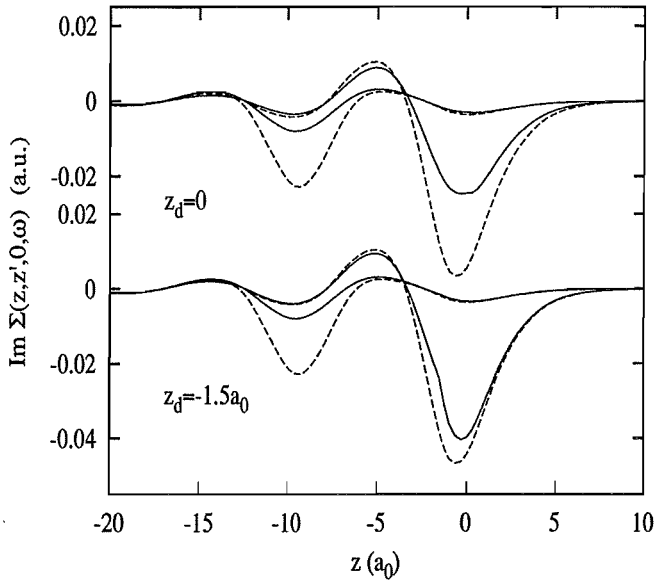

FIG. 1. Imaginary part of self-energy $\mathrm{Im}\,\Sigma(z,z',k_\parallel,\omega)$ for Ag surface ($\omega = 1$ eV, $k_\parallel = 0$). Solid (dashed) curves: with (without) s-d polarization. Left peak: $z' = -9\ a_0$; right peak: $z' = 0$. Upper panel: $z_d = 0$; lower panel: $z_d = -1.5\ a_0$. The metal occupies the half-space $z \le 0$; the polarizable d electron medium occupies $z \le z_d$.

In summary, we have developed a method of evaluating the influence of s-d polarization on the hot-electron dynamics at noble metal surfaces. The screened Coulomb interaction involves the nonlocal response of conduction electrons and the local dielectric properties of the occupied d bands. The absence of s-d screening in the region of s electron spill-out leads to an enhanced self-energy and therefore to a shortening of electronic lifetimes.

*Present address: Centro de Ciencias Físicas, UNAM, 62210 Cuernavaca, México

[1] See special issue of Chem. Phys. **251** (2000).
[2] I. Campillo, A. Rubio, J.M. Pitarke, A. Goldmann, and P. Echenique, Phys. Rev. Lett. **85**, 3241 (2000).
[3] C. Voisin et al, Phys. Rev. Lett. **85**, 2200 (2000); N.Nilius et al, ibid. **84**, 3994 (2000); L. Bürgi et al, ibid. **82**, 4516 (1999); J. Li et al, ibid. **81**, 4464 (1998).
[4] A. Liebsch, Phys. Rev. Lett. **71**, 145 (1993).
[5] C. López Bastidas, J.A. Maytorena and A. Liebsch, to be published.
[6] A. Liebsch, P. Echenique, et al.,to be published.

Elastoplastic contact between randomly rough surfaces

B.N.J. Persson
Institute Theory I

I have developed a theory of contact mechanics between randomly rough surfaces. The solids are assumed to deform elastically when the stress σ is below the yield stress σ_Y, and plastically when σ reaches σ_Y. I study the dependence of the (apparent) area of contact on the magnification. The theory has been applied to rubber friction and found to be in good agreement with experimental data.

F&E-Nr: 23.20.0

Even a highly polished surface has surface roughness on many different length scales. When two bodies with nominally flat surfaces are brought into contact, the area of real contact will usually only be a small fraction of the nominal contact area. We can visualize the contact regions as small areas where asperities from one solid are squeezed against asperities of the other solid; depending on the conditions the asperities may deform elastically or plastically.

How large is the area of *real* contact between a solid block and the substrate? This fundamental question has extremely important practical implications. For example, it determines the contact resistivity and the heat transfer between the solids. It is also of direct importance for sliding friction [1], e.g., the rubber friction between a tire and a road surface, and it has a major influence on the adhesive force between two solids blocks in direct contact.

I have developed a theory of contact mechanics [2], valid for randomly rough (e.g., self affine fractal) surfaces. In the context of rubber friction, for which the theory was originally developed, mainly elastic deformation occurs. However, the theory can also be applied when both elastic and plastic deformations occur in the contact areas. This case is, of course, relevant to almost all materials other than rubber.

The contact theory can be applied to surfaces with roughness on many different length scales. The classical contact theory of Greenwood [3] was developed for surfaces with roughness on a single length scale. Thus, in this theory the surface asperities are "approximated" by spherical caps of *identical* radius of curvature (but with a Gaussian height distribution). The Greenwood theory has been applied to real surfaces with roughness on many different length scales, by defining an average radius of curvature R. However, it turns out that R depends strongly on the resolution of the roughness-measuring instrument, or any other form of filtering, and hence is not unique. The contact theory I have developed is based on a completely different physical approach, and gives well defined results for surfaces with arbitrary surface roughness.

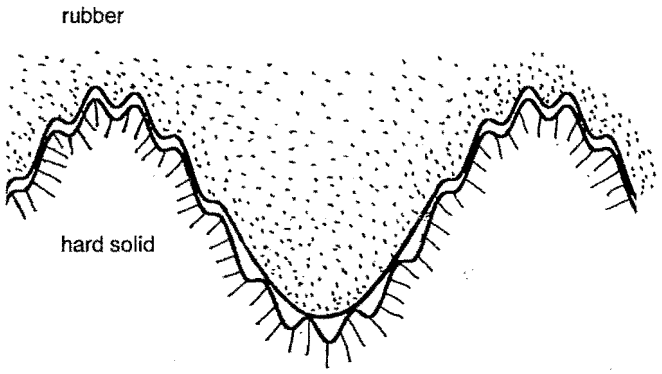

FIG. 1. An elastic solid (e.g., rubber) squeezed against a hard, rough, solid surface.

The basic idea behind the new contact theory is that it is very important not to *a priori* exclude any roughness length scale from the analysis. Consider a surface with surface roughness on two different length scales as indicated in Fig. 1. Assume that a rubber block is squeezed against the substrate and that the applied pressure is large enough to squeeze the rubber into the large "cavities" as indicated in the figure. It is clear that even if the rubber is able to make direct contact with the substrate in the large cavities, the pressure acting on the rubber at the bottom of a large cavity will be much smaller than the pressure at the top of a large asperity. Thus while, because of the high local pressure, the rubber may be squeezed into the "small" cavities at the top of a large asperity, the pressure at the bottom of a large cavity may be too small to squeeze the rubber into the small-sized cavities at the bottom of a large cavity. If $A(\lambda)$ is the (apparent) area of contact on the length scale λ [more accurately, I *define* $A(\lambda)$ to be the area of real contact if the surface would be smooth on all length scales shorter than λ, see Fig. 2], then I have studied the function $P(\zeta) = A(\lambda)/A(L)$ which is the relative fraction of the rubber surface area where contact occurs on the length scale $\lambda = L/\zeta$ (where $\zeta \geq 1$), with $P(1) = 1$. Here $A(L) = A_0$ denotes the macroscopic contact area [L is the diameter of the macroscopic contact area so that $A_0 \approx L^2$], and we define the nominal contact pressure $\sigma_0 = F_N/A_0$, where F_N is the load or perpendicular force.

I have shown that for an ideal elastic body (no plasticity) squeezed against a rigid self affine fractal surface without a short-distance cut off, $P(\zeta) \to 0$ as $\zeta \to \infty$.

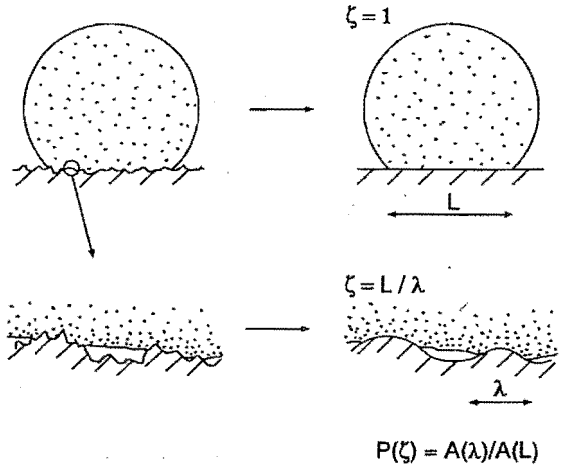

FIG. 2. An elastic ball squeezed against a hard, rough substrate.

If we assume that only elastic deformation occurs,

$$P(\zeta) = \frac{2}{\pi}\int_0^\infty dx\ \frac{\sin x}{x}\ \exp\left[-x^2 G(\zeta)\right], \qquad (1)$$

where

$$G(\zeta) = \frac{\pi}{4}\left[\frac{E}{(1-\nu^2)\sigma_0}\right]^2 \int_{q_L}^{\zeta q_L} dq\ q^3 C(q), \qquad (2)$$

where $q_L = 2\pi/L$, E is the elastic modulus and ν the Poisson ratio. The surface roughness power spectra

$$C(q) = \frac{1}{(2\pi)^2}\int d^2x\ \langle h(\mathbf{x})h(\mathbf{0})\rangle e^{-i\mathbf{q}\cdot\mathbf{x}},$$

where $z = h(\mathbf{x})$ is the height of the surface above a flat reference plane (chosen so that $\langle h\rangle = 0$), and $\langle ...\rangle$ stands for ensemble average.

We consider now the limit $\sigma_0 << E$, which is satisfied in most applications. In this case, for most ζ-values of interest, $G(\zeta) >> 1$, so that only $x << 1$ will contribute to the integral in (1), and we can approximate $\sin x \approx x$ and

$$P(\zeta) \approx \frac{2}{\pi}\int_0^\infty dx\ \exp\left[-x^2 G(\zeta)\right] = \left[\pi G(\zeta)\right]^{-1/2}. \qquad (3)$$

Thus, within this approximation, using (2) and (3) we get $P(\zeta) \propto \sigma_0$ so that the area of real contact is proportional to the load. This is the reason for why the friction coefficient in most cases is independent of the load. For automobile tires the condition $\sigma_0 << E$ is usually satisfied and as a result the tire-road friction coefficient is independent of the load. Consequently, on a dry road track one expects the same friction for wide and narrow tires, assuming that the rubber-road adheasional interaction is unimportant.

In the study above we have assumed that only elastic deformation occurs. However, the theory can be generalized to the case where also plastic deformation occurs. Let us introduce the functions $P_{\rm non}(\zeta)$ and $P_{\rm pl}(\zeta)$ which describe the fraction of the original (for $\zeta = 1$) macro contact area where, under the magnification ζ, non-contact, and contact with plastic yield has occurred, respectively. Thus we have

$$P_{\rm el}(\zeta) + P_{\rm non}(\zeta) + P_{\rm pl}(\zeta) = 1,$$

where $P_{\rm el}(\zeta) = P(\zeta)$ describe the fraction of the macro contact area where elastic contact occur on the length scale L/ζ. The functions $P_{\rm non}$ and $P_{\rm pl}$ are given by

$$P_{\rm non} = \frac{2}{\pi}\sum_{n=1}^{\infty}\frac{\sin\alpha_n}{n}\left(1 - \exp\left[-\alpha_n^2 G(\zeta)\right]\right), \qquad (4)$$

$$P_{\rm pl} = -\frac{2}{\pi}\sum_{n=1}^{\infty}(-1)^n\frac{\sin\alpha_n}{n}\left(1 - \exp\left[-\alpha_n^2 G(\zeta)\right]\right), \qquad (5)$$

where $\alpha_n = n\pi\sigma_0/\sigma_Y$, and where $G(\zeta)$ is given by (2). In the elastic limit, $\sigma_Y \to \infty$, $P_{\rm pl} = 0$, and $P_{\rm el} = 1 - P_{\rm non}$ reduces to equation (1).

The theory above is valid for surfaces with arbitrary random roughness, but has been applied to self-affine fractal surfaces. It has been found that many "natural" surfaces, e.g., surfaces of many materials generated by fracture, can be approximately described as self-affine surfaces over a rather wide roughness size region. A self-affine fractal surface has the property that if we make a scale change that is different for each direction, then the surface does not change its morphology. Recent studies have shown that even asphalt road tracks (of interest for rubber friction) are (approximately) self-affine fractal, with an upper cut-off length $\lambda_0 = 2\pi/q_0$ of order a few mm. For a self affine fractal surface $C(q) = 0$ for $q < q_0$, while for $q > q_0$:

$$C(q) = (q_0 h_0)^2 \frac{H}{2\pi}\left(\frac{q}{q_0}\right)^{-2(H+1)}, \qquad (6)$$

where $H = 3 - D_{\rm f}$ (where the fractal dimension $2 < D_{\rm f} < 3$), and where q_0 is the lower cut-off wavevector, and h_0 is determined by the rms roughness amplitude, $\langle h^2\rangle = h_0^2/2$.

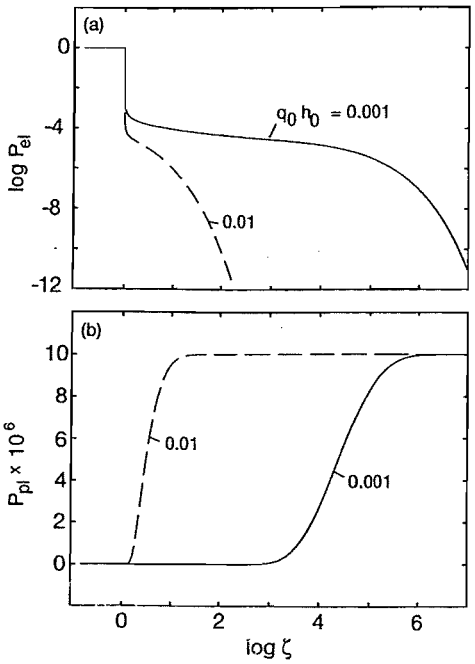

FIG. 3. The functions P_{el} and P_{pl} describes the fraction of the macroscopic contact area where elastic and plastic contact occur.

When $C(q)$ is given by (6), the functions P_{el} and P_{pl} depend only on H (or, equivalently, on the fractal dimension $D_f = 3 - H$), on σ_0/σ_Y, and on the *plasticity index* $\psi = (E/\sigma_Y)q_0h_0$. In Fig. 3 I show the dependence of P_{el} and P_{pl} on the magnification ζ. I have used parameters which correspond (roughly) to a cubic steel block ($L = 10$ cm), on a steel substrate. I assume $\sigma_0 = 10^4$ Pa, $\sigma_Y = 10^9$ Pa, and $E = 10^{11}$ Pa. The surface roughness of the substrate is assumed to be self affine fractal with $q_0h_0 = 0.001$ (solid lines) and 0.01 (dashed lines). The theory does not depend on q_0 directly (but only on the product q_0h_0), but if we choose the cut off wave vector $q_0 = 10^4$ m^{-1} (corresponding to the typical cut off length $\lambda_0 = 2\pi/q_0$ of order ≈ 1 mm), then $q_0h_0 = 0.001$ and 0.01 correspond to the rms roughness $h_0 = 0.1$ and 1 μm, respectively. In the calculations we have used the fractal exponent $H = 0.8$. Note that for the case $q_0h_0 = 0.01$ plastic deformation starts already at the cut off length $\lambda_0 \approx 1$ mm, and on the length scale $\lambda_0/10 \approx 0.1$ mm all junctions have yielded plastically. However, when $q_0h_0 = 0.001$ plastic yield start when ζ is of order a few 1000, corresponding to distances of order $\lambda_0/\zeta \approx 0.1\mu$m. On the length $\lambda \approx 20$ Å (corresponding to $\zeta \approx 3 \times 10^5$) all asperities have yielded plastically. However, on this short length scale steel may be much harder than the macroscopically observed yield stress; thus, for "real" steel mainly elastic deformation is likely to prevail when $q_0h_0 = 0.001$.

[1] B.N.J. Persson, *Sliding Friction: Physical Principles and Applications*, Sec. Ed. (Springer, Heidelberg, 2000).

[2] B.N.J. Persson, to be published.

[3] J.A. Greenwood, in *Fundamentals of Friction, Macroscopic and Microscopic Processes*, Ed. by I.L. Singer and H.M. Pollack (Kluver, Dordrecht, 1992).

Repelling systems and time dependent Poincaré maps

H. Lustfeld

Institute Theory I

It is shown that in repelling systems (i.e. in transient chaos) no direct relations exist between averages in a continuous time dynamical system (flow) and averages over the corresponding Poincaré map. However, this relation is restored if a *time dependent Poincaré map* is defined instead of the usual one. The properties of such maps with regard to escape rates, measures, shifts, and Lyapunov exponents are investigated in general and in particular for one dimensional systems.

F&E-Nr: 23.15.0

To find beyond the transient time regime the long time behavior of a continuous dynamical system it is sufficient in many cases[1] - e.g. in permanent chaos - to know its Poincaré map (PM) $x = f(x')$. After computation of the density $\rho_P(x)$ on the Poincaré surface (P), average values of relevant long time quantities can be determined: Measures, Lyapunov exponents, shifts etc. To get the corresponding quantities of the dynamical system the simple connections between time t and number of iterations n and between ρ_P and the density of the continuous system, ρ, are used:

$$t = n\langle\tau\rangle, \quad \rho = \langle\tau\rangle\rho_P \quad \langle\tau\rangle = \int_P \rho_P(x')\tau(x') \qquad (1)$$

where the return time $\tau(x')$ is the time between two successive hits on P. Obviously the return time τ is a rather irrelevant quantity, it just fixes the time scale.

It is demonstrated here that the situation is quite different for the neighborhood of a repeller. Still, results about the long time behavior of the system are easily obtained if the properties on P are known. It turns out, however, that now a time dependent Poincaré map (TPM) is needed since the above mentioned relevant quantities depend on τ *in an essential way*. The reason behind this is that the system remains transient in a sense. It becomes quasistationary and not stationary[2][3]: Trajectories are leaving the neighborhood of the repeller continously. Generically this phenomenon looks quite different whether one observes it on the scale n or the real time t.

To get information about the long time properties on P one can initialize a rather arbitrary bundle of trajectories and look at the long time behavior of that. An equivalent procedure consists in generating a current density on P with normal component $\rho_s(x,t)$. Again ρ_s may be chosen rather arbitrarily. (Let $\rho_s(x,t) \equiv 0$ for $t < 0$.) Because of mass conservation

$$\rho_P = \mathcal{L}\rho_P + \rho_s \qquad (2)$$

Here $\mathcal{L}$ defines the *time dependent* Frobenius Perron operator

$$[\mathcal{L}g](x,t) = \int_P dx' \int_0^t dt' \delta(x - f(x'))\delta(t - t' - \tau(x'))g(x',t') \qquad (3)$$

or in a form that emphasizes the time dependence :

$$[\mathcal{L}g](t) = \int_0^t dt' L(t-t')g(t') \qquad (4)$$

To get the relation between ρ_P and ρ for a repeller one has to keep in mind that averages are *not* computed with ρ_P alone but with the product $\Pi(T)\rho_P$ where Π projects out that part of the current density that will get lost in the time interval $[t, t+T]$. Now in the long time limit we need only the 'mass' in a tube around the trajectory beginning and ending on P. After dividing by the number of crossings of P this leads asymptotically to

$$\Pi(T)\rho(x') = \Pi(T)\rho_P(x')\langle\tau\rangle, \quad \langle\tau\rangle = \int_P d\mu\tau(x') \qquad (5)$$

μ being the natural measure that will be defined below. As in the non-repelling scenario there is a rather trivial connection between density of the flow and that of the *time dependent* Poincaré map.

In spite of this the return time *is* relevant and cannot be eliminated from eq.(2) except for $\kappa = 0$ (no repeller) or $\tau(x) = const$ (simple Poincaré map). Let us take a glance at the quasistationary regime. ρ_S is assumed to have vanished, still ρ_P remains time dependent because of the escape rate κ. We make the ansatz

$$\rho_P(x,t) = \rho_P(x)e^{-\kappa t} \qquad (6)$$

and we obtain from eq.(2) the selfconsistent equation for the conditionally invariant density

$$\rho_P(x) = \int dx' \delta(x - f(x'))e^{\kappa\tau(x')}\rho_P(x') \qquad (7)$$

To make this more explicit we look into the case when f can be reduced to a one-dimensional map $x_1 = f_1(x_1')$. This is possible if in proper coordinates the evolution of x_1 is nearly independent of the other components. This

may be due to strong dissipation. However, it is also possible in other cases, like in Baker maps. Let us chose the well known tent map with a possible opening as an example: $f_1(x) = x/a_0$ if $x < a_0$, $f_1(x) = (1-x)/a_1$ if $x > 1 - a_1$, where $a_0 + a_1 \leq 1$. For simplicity we assume $\tau(x)$ to be piecewise constant, namely $\tau(x) = \tau_0$ if $x < a_0$, $\tau(x) = \tau_1$ if $x > 1-a_1$. Escape occurs in case $a_0+a_1 < 1$ where the trajectory leaves the Poincare surface for $x \in (a_0, 1-a_1)$. Then the smooth, nonnegative solution of (7) is $\rho_P(x) = 1$ which accidentally is also the solution of the 1D eigenvalue equation. κ is implicitely given by $a_0 e^{\kappa\tau_0} + a_1 e^{\kappa\tau_1} = 1$.

To get ρ_P for all t the Laplace transform is taken (noted by $\tilde{}$) the adjoint Frobenius Perron operator is introduced

$$\tilde{L}^+(s)\tilde{g}(s) = \int_P dx' \delta(f(x) - x') e^{-s^*\tau(x)} \tilde{g}(x', s) \qquad (8)$$

and $\tilde{L}(s)$ as well as $\tilde{L}^+(s)$ are expanded into eigenfunctions (for each s)

$$\tilde{L}(s)\tilde{\varphi}_n(s) = \lambda_n(s)\tilde{\varphi}_n(s) \qquad (9)$$

$$\tilde{L}^+(s)\tilde{\psi}_n(s) = \lambda_n(s)\tilde{\psi}_n(s) \qquad (10)$$

$$\int_P dx' (\tilde{\psi}_n(x', s))^* \tilde{\varphi}_m(x', s) = \delta_{nm} \qquad (11)$$

Expanding $\tilde{\rho}_s$ into the eigenfunctions of $\tilde{L}(s)$ and applying the inverse Laplace transformation one can show that asymptotically

$$\rho_P(t \to \infty) \propto e^{-\kappa t} \tilde{\varphi}_0(-\kappa) \qquad (12)$$

with

$$\tilde{L}(-\kappa)\tilde{\varphi}_0 = \tilde{\varphi}_0 \qquad (13)$$

$$\kappa = -s_0,\ s_0 = \max\{s \text{ with } \lambda_n(s) = 1\} \qquad (14)$$

$\tilde{\varphi}_0(-\kappa)$ is the *conditional invariant measure of the TPM*.

If P has a periodic structure it can be reduced to a unit cell that is repeated again and again, (cf the 2 dimensional Lorentz gas). In this case the PM as well as the TPM can be separated into a reduced map from the unit cell into the unit cell plus a shift Δ. Then there is a 'shift source' $\mathcal{L}\rho\Delta$ and one gets for the shift density

$$S = \mathcal{L}S + \mathcal{L}\rho\Delta \qquad (15)$$

Applying again the Laplace transform and using the adjoint operator one finds asymptotically

$$\langle\Delta\rangle = \frac{\langle S(t)\rangle}{t} = \frac{1}{\langle\tau\rangle} \int_P d\mu\Delta \qquad (16)$$

with

$$\langle\tau\rangle = \int_P d\mu\, \tau = -\lambda_0'(-\kappa) \qquad (17)$$

and the *natural measure*

$$d\mu = dx \tilde{\psi}_0^*(x, -\kappa)\tilde{\varphi}_0(x, -\kappa) \qquad (18)$$

Similarly we get for the Lyapunov exponent

$$\lambda_{lyap} = \frac{1}{\langle\tau\rangle} \int_P d\mu \ln \mid f' \mid \qquad (19)$$

An example when averages over the natural measure play an important role is the following. One considers the dynamics to be the microscopic process of a diffusive system on a 1D lattice, such that this process decides in which direction the particle jumps on the lattice. Calculating average speed or diffusion coefficient needs an averaging over long trajectories. Take the tent map as

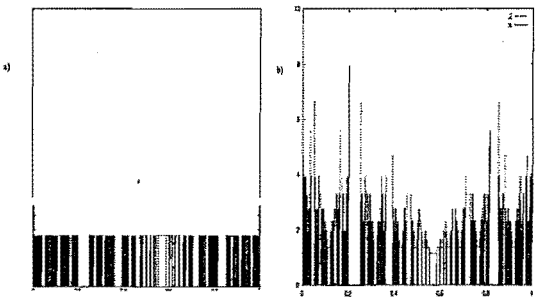

FIG. 1: *typical natural measure density $\mu(x)$ for the tent map of a repeller. a) Poincaré map, b) time dependent Poincaré map with same parameters.*

an example. The coordinate S may change by ± 1 depending on which subinterval of $[0, 1]$ contains x, namely $S(t + \tau(x)) = S(t) + \Delta(x)$ and $\Delta(x) = 1$ if $x \in [0, a_0]$, $\Delta(x) = -1$ if $x \in [a_1, 1]$. In this case the average speed is

$$\langle\Delta\rangle_{TPM} = \frac{a_0 \exp\kappa\tau_0 - a_1 \exp\kappa\tau_1}{a_0 \exp\kappa\tau_0 + a_1 \exp\kappa\tau_1}, \qquad (20)$$

while the natural measure of the 1D map yields $\langle\Delta\rangle_{PM} = \frac{a_0 - a_1}{a_0 + a_1}$. Note that it can even happen that $\langle\Delta\rangle_{TPM}$ and $\langle\Delta\rangle_{PM}$ have opposite sign.

Computing the Lyapunov exponent for the repelling tent map yields

$$\lambda_{TPM}^{(lyap)} = \frac{a_0 \exp\kappa\tau_0 \ln(1/a_0) + a_1 \exp\kappa\tau_1 \ln(1/a_1)}{a_0 \exp\kappa\tau_0 + a_1 \exp\kappa\tau_1}, \qquad (21)$$

in contrast to

$$\lambda_{PM}^{(lyap)} = -\frac{a_0 \ln(1/a_0) + a_1 \ln(1/a_1)}{a_0 + a_1} \qquad (22)$$

The inequality of the Lyapunov exponents demonstrates again that there is a *relevant* difference between the time dependent and the usual Poincaré map.

REFERENCES

[1] P. Gaspard, *Phys. Rev. E* **53**, 4379 (1996).

[2] H. Lustfeld, P. Szépfalusy, *Phys. Rev. E* **53**, 5882 (1996).

[3] Z. Kaufmann, A. Nemeth, H. Lustfeld, P. Szépfalusy, *Phys. Rev. Lett.* **78**, 4031 (1997).

Publications in refereed journals

Ballone P.; Montanari B.; Jones R.O.
Catalytic reactions of living polymers - density functional study of reactivity of phenol and phenoxides with the cyclic tetramer of polycarbonate
J. Phys. Chem. A104, 2793-2798, 2000
23.20.0

Ballone P.; Montanari B.; Jones R.O.
Density functional study of carbonic acid clusters
J. Chem. Phys. 112, 6571-6575, 2000
23.20.0

Bene J.1,; Bröcheler S.; Lustfeld H.
1Institute for Theoretical Physics, Eötvös University, Budapest, Ungarn
Simulating 2D Flows with Viscous Vortex Dynamics
J. Stat. Phys. 101, p. 567 (2000)
23.15.0

Bonn M.1,2; Hess Ch.1; Funk S.1; Miners J.1; Persson B.N.J.; Wolf M.1; Ertl G.1
1Fritz-Haber-Institut der MPG Berlin
2Leiden Institute of Chemistry, Leiden, Niederlande
Femtosecond surface vibrational spectroscopy of CO adsorbed on Ru(001) during desorption
Phys. Rev. Lett. 84, 4653 (2000)
23.20.0

Lichtenstein A.I.; Jones R.O.; de Gironcoli S.1; Baroni S.1
1Istituto Nazionale per la Fisica della Materia, Trieste, Italien
Anisotropic thermal expansion in silicates: A density functional study of β-euryptite and related materials
Physical Review B, 62, 17 (2000)
23.20.0

Liebsch A.; Liechtenstein A.1
1University of Nijmegen, Niederlande
Photoemission quasiparticle spectra of Sr2RuO4
Phys. Rev. Lett. 84, 1591 (2000)
23.20.0

Persson B.N.J.; Ballone P.1
1Istituto Nazionale per la Fisica della Materia, University of Messina, Italien
Boundary lubrication: layering transition for curved solid surfaces with long-range elasticity
Solid State Communications 115, 599 (2000)
23.20.0

Persson B.N.J.; Ballone P.1
1Istituto Nazionale per la Fisica della Materia, University of Messina, Italien
Squeezing lubrication films: layering transition for curved solid surfaces with long-range elasticity
J. Chem. Phys. 112, 9524 (2000)
23.20.0

Persson B.N.J.; Popov V.L.1
1Institute of Strength Physics and Materials Science, Tomsk, Russland
On the origin of the transition from slip to stick
Solid State Communications 114, 261 (2000)
23.20.0

Persson B.N.J.; Tosatti E.1
1SISSA, Trieste, Italien
Qualitative theory of Rubber Friction
J. Chem. Phys. 112, 2021 (2000)
23.20.0

Persson B.N.J.; Volokitin A.I.1
1Samara State Technical University, Russland
Comments on "Brownian Motion of Microscopic Solids under the Action of Fluctuating Electromagnetic Fields
Phys. Rev. Lett. 84, 3504 (2000)
23.20.0

Persson B.N.J.; Volokitin A.I.1
1Samara State Technical University, Russland
Dynamical Interactions in Sliding Friction
Surface Science 457, 345 (2000)
23.20.0

Persson B.N.J.
Electronic friction on a superconductivity surface
Solid Sate Communications 115, 145 (2000)
23.20.0

Persson B.N.J.
Friction dynamics for curved solid surfaces with long-range elasticivity
J. Chem. Phys. 113, 5477 (2000)
23.20.0

Persson B.N.J.
Layering transition: Dynamical instabilities during squeeze-out
Chem. Phys. Lett. 324, 231 (2000)
23.20.0

Persson B.N.J.
Sliding Friction: Theory and Applications
Second Edition (extended version), Springer 2000
23.20.0

Persson B.N.J.
Theory of time-dependent plastic deformation
Phys. Rev. B61, 5949 (2000)
23.20.0

Sturm A.; Gusarov A.1
1Faculte Polytechnique de Mons, Belgien
Dynamical correlations in the electron gas
Physical Review B, 62, 24 (2000)
23.20.0

Invited Talks

Harris J.
Calculation of Elastic Constants of Materials using Density Functional Theory
Washington, DC, American Chemical Society Meeting, 16.8.2000
23.20.0

Jones R.O.
Density functional calculations and force field parameters
Workshop on: Multiscale Modeling of Macromolecularsystems, Mainz 6.9.2000
23.20.0

Jones R.O.
Density functional calculations for polymers and clusters - present experience and future prospects
10. Workshop on Computational Materials Science, Villasimius (CA), Italien 8.-11.9.2000
23.20.0

Jones R.O.
Density functional study of molecules and polymers - structure, energetics, reactions
Department of Chemistry, University of Jyväskylä, Finland, 29.3.2000
23.20.0

Jones R.O.
Strukturen, Energien und Reaktionen in organischen Molekülen und Polymeren - eine Dichtfunktionalstudie des Polycarbonats
Institut für Theoretische Physik, Universität Paderborn
8.5.2000
23.20.0

Jones R.O.
Thermal expansion in silicates - or the remarkable stability of cook-tops towards thermal shock
Department of Physics, University of Jyväskylä, Finland
30.3.2000
23.20.0

Jones R.O.
Thermische Ausdehnung in Kochfeldern - ein Beispiel der vielen Anwendungen von Silikaten
Workshop BMBF Kompetenzentrum, MPI für Polymerforschung, Mainz 7.11.2000
23.20.0

Liebsch A.
Photoemission quasi-particle spectra of Sr2RuO4
European Physical Society Meeting
Montreux 17.3.2000
23.20.0

Liebsch A.
Quantum well behavior induced by dynamical screening in alkali metal films
Workshop Epioptics Erice 21.7.2000
23.20.0

Liebsch A.
Surface optics of Ag: influence of localized d electrons
Workshop Epioptics Erice 22.7.2000
23.20.0

Persson B.N.J.
10 Lectures on Friction presented at Dipartimento di Fisica G. Galilei,
Padova, Italien April und Mai 2000
23.20.0

Persson B.N.J.
12 Lectures presented "Troisieme cycle de la Physique"
Lausanne 13.4.2000; 27.5.2000; 4.11.2000
23.20.0

Persson B.N.J.
Dynamics of Small Confined Systems
MRS Fall meeting, Boston, USA 27.11.-1.12.2000
23.20.0

Persson B.N.J.
Four invited lectures presented at spring school on friction
Oulanka Biological Station, Finland 26.-30.3.2000
23.20.0

Persson B.N.J.
Participated as expert (presented a talk on friction) in an EU-meeting related to the founding of nano-scale materials physics by the European union
Brüssel 10.3.2000
23.20.0

Persson B.N.J.
Reibungsprobleme in dynamischen Systeme
Hannover 7.-8.12.2000
23.20.0

Persson B.N.J.
Summer School "Imaging and manipulation of matter at the nanometer scale
Mi-ra ores de la Sierra, Spanien 11.-16.9.2000
23.20.0

Persson B.N.J.
Third Swedish meeting on vacuum and materials science
CTH Gothenburg, Schweden 14.-16.8.2000
23.20.0

Persson B.N.J.
Workshop on Tribology
The Wiezmann Institute, Tel Aviv, Israel 3.4.2000
23.20.0

Persson B.N.J.
Workshop on nonequilibrium phenomena in confied systems and on solid friction
CECAM, Lyon 28.-31.8.2000
23.20.0

Other talks

Bene J.1; Bröcheler S.; Lustfeld H.
1Institute for Theoretical Physics, Eötvös University, Budapest, Ungarn
Simulating 2D-flows with viscous order dynamics
General Assembly der European Geophysical Society, Nizza
29.4.2000
23.15.0

Harris J.
Computational Methods in Materials Science
Institut Superieure des Materiaux du Mans, Le Mans, Frankreich 26.3.2000
23.20.0

Liebsch A.
Quantum well behavior induced by dynamical screening in alkali metal films
Physics Department, University of San Sebastian 4.7.2000
23.20.0

Liebsch A.
Role of d electrons in electronic surface excitations
Physics Department, University of San Sebastian 5.7.2000
23.20.0

Lustfeld H.; Kaufmann Z.1
1Department of Physics of Complex Systems, Eötvös University, Budapest, Ungarn
Comparison between flow and Poincare maps of simple repelelrs
MPI für Physik komplexer Systeme, Dresden 6.11.2000
23.15.0

Lustfeld H.; Poppe D.1; Bröcheler S.
1FZJ -ICG3
Charakterisierung periodischen Verhaltens der Reaktionsgleichungen von Spurengasen in der Troposphäre
Frühjahrstagung 2000 der AEFF der DPG, Bremen 24.3.2000
23.15.0

Posters

Lustfeld H.
Fast Slow behavior in the pollutant reaction equations of the troposphere
MPI für Physik komplexer Systeme, Dresden 18.5.-19.05.2000
23.15.0

Lecture courses

Bringer, A.
SS 2000: Numerische Methoden in der Physik
23.20.0

Eilenberger G.
WS 2000/2001: 5-stündige Vorlesung. Universität zu Köln: Analysis 1 für Physiker
23.20.0

Sturm K.
SS 2000: 2-stündige Vorlesung an der Universität Düsseldorf:
Elektronische Anregungen im Festkörper
23.20.0

Sturm K.
WS 1999/2000: Vorlesung im 31. IFF-Ferienkurs: Dynamik in kondensierter Materie
März 2000
23.20.0

Institute Theory II

General Overview

Introduction: Soft Matter Research

The main research topic of the Institute is the theory of "complex fluids" and "soft matter" systems. Soft matter physics is an interdisciplinary research area encompasing statistical physics, material science, chemistry, and biology. The systems are characterized by

- Supramolecular structure and self-assembly
- Typical length scales ranging from nano- to micro-meters
- Typical energy scales comparable to the thermal energy k_BT.

Classical examples of complex fluids are

- Polymer solutions, mixtures, and melts
- Mixtures of block copolymers and homopolymers
- Lyotropic liquid crystals
- Amphiphilic systems, i.e. mixtures of oil, water and amphiphiles
- Colloidal suspensions.

While these areas remain active fields of research, the focus has recently shifted to more complex systems which are obtained by combining two or more of the components listed above. A few examples are

- Colloidal particles in polymer solutions
- Mixtures of surfactants and amphiphilic block-copolymers
- Mixtures of several surfactants or lipids
- Colloids in liquid crystals

This brings the systems which are studied in physics closer to applications in material science or biology.

Since the structures in soft matter systems often contain a large numer of molecules, *mesoscale modelling* is typically required to bridge the length- and time-scale gap between the microscopic domain — of atoms and their interactions — and the emerging properties of supramolecular assemblies on meso- or macroscopic scales. Microscopic models are employed to study properties of complex systems on the molecular scale, and to provide a link of mesoscale models to molecular architecture.

A large variety of methods is used to study soft matter systems. In fact, a combination of analytical and numerical methods is often needed to successfully characterize these complex systems. In particular, simulation methods (Monte Carlo, molecular dynamics), computational hydrodynamics, field theory, perturbation theory, and exact solutions are employed in our institute.

A characteristic feature of soft-matter research is the fruitful interaction between theory and experiment. With a third of the IFF institutes [Neutron Scattering (Richter), Theory II and Soft Matter (Dhont)] now focusing on soft matter research, many of the essential aspects of these systems are investigated here.

Research projects and results:
(in alphabetic order)

1. *Polymer-mediated attraction between two small colloidal particles:*
   The second virial coefficient B_2 of a dilute solution of small colloidal particles shows an interesting *non-monotonic* dependence on the concentration n of free polymer chains in the embedding solvent. The quantitative form of this dependence, with a minimum at the overlap concentration $n \approx n^*$, is obtained by expressing B_2 in terms of the compressibility of the polymer solvent without particles. (E. Eisenriegler)

2. *Influence of chain self-avoidance on polymer depletion forces between colloidal particles:*
   Self-avoidance effects become more and more important the lower the dimension of the polymer-embedding space. For a dilute solution of long chains in *two* dimensions the density depletion profile around two touching disks is calculated exactly and the force between the disks is obtained. The force between two spheres in *three* dimensions can be estimated by interpolating between two and four dimensions. (E. Eisenriegler)

3. *Measuring bending rigidity in bicontinuous microemulsions:*
   We demonstrate a new approach to determine the bending rigidity of the amphiphile film in microemulsions and sponge phases from neutron scattering data. This method is precise enough to measure the logarithmic scale dependence of the bending rigidity and its universal prefactor for the first time. Furthermore, we show that in the mushroom regime the bending rigidity of a membrane decorated by amphiphilic block copolymers increases linearly with the polymer concentration on the membrane; the amplitude is found to be about a factor 1.5 larger than theoretical results for ideal chains. (G. Gompper, H. Endo, M. Mihailescu, J. Allgaier, M. Monkenbusch, D. Richter, B. Jakobs, T. Sottmann, R. Strey)

4. *Stability of inverse bicontinuous cubic phases in lipid-water mixtures:*
   We have investigated the stability of seven inverse bicontinuous cubic phases (G, D, P, $C(P)$, S, $I-WP$, $F-RD$) in lipid-water mixtures based on a curvature model of membranes. Lipid monolayers are described by parallel surfaces to triply periodic minimal surfaces. The phase behavior is determined by the distribution of the Gaussian curvature on the minimal surface and the porosity of each structure. Only G, D and P are found to be stable, and to coexist along a triple line. The calculated phase diagram agrees very well with experimental results for 2:1 lauric acid/DLPC. (G. Gompper, U.S. Schwarz)

5. *Diffusion in glasses:*
   The diffusion of interstitial particles in disordered systems without lattice translational invariance is investigated by a novel Monte Carlo approach. Experimental and simulated structures of silicate and alkali-silicate glasses are used to calculate the positions and energies of the minima and saddle points for the interstitials. The resulting transition rates are then utilized in Monte Carlo simulations, which can be extended to sufficiently long times to extract asymptotic diffusion coefficients. These show approximate Arrhenian behavior as functions of inverse temperature. (K. Kehr, K. Mussawisade)

6. *Phase separation of binary fluid mixtures in shear flow:*
   The phase separation of binary fluid mixtures in uniform shear flow has been studied numerically in the framework of continuum convection-diffusion equations based on a Ginzburg-Landau free-energy functional. The main results show the existence of domains with two typical length scales, whose relative abundance changes with logarithmic-time periodic oscillations. (A. Lamura, F. Corberi, G. Gonnella)

7. *Stability of a protein pore in a lipid membrane:*
   A membrane protein pore embedded in a fully hydrated bilayer lipid membrane is investigated by molecular dynamics simulations. It is found that the melittin pore decays from an initial tetrameric configuration into a stable trimer and one monomer. The expansion-induced formation of an interface between the pore-lining acyl chains of the lipids and the pore water is transformed into an energetically more favorable toroidal pore structure, where some lipid heads are translocated from the rim to the central part of the interface. (J.-H. Lin, A. Baumgärtner)

8. *Effects of size ratio and inter-chain overlap in colloid-polymer mixtures:*
   The depletion of long flexible polymers near the surface of a colloidal particle is an entropic effect and

depends apart from the distances of nearby particles in a crucial way on the ratio of the particle and chain sizes ond on the degree of overlap between the chains. We study both effects for the simple system of a single spherical particle embedded in a monodisperse solution of free nonadsorbing polymer chains. Both the density profile of the polymers and the solvation free energy of the particle are calculated. (R. Maassen, E. Eisenriegler, A. Bringer)

9. *Wetting behavior in amphiphilic systems:*
The wetting behavior of ternary amphiphilic systems, containing water, surfactant and vapor, has been investigated. We first study interfacial wetting in ternary mixtures with the most general nearest-neighbor pair interactions, and find Cahn-type wetting transitions near the critical end points. In a second step, we investigate the dependence of the contact angles on the amphiphilic strength of the surfactant molecules. [Supported by DFG priority program "Wetting and Structure Formation at Interfaces".] (T. Schilling, G. Gompper)

10. *Dynamics of swollen lamellar phases:*
Among the large variety of phases, which appear in amphiphilic systems, the lamellar phase plays a key role for the understanding of the physical properties of these systems, since its simple geometry allows for detailed theoretical and experimental investigations. We study the relaxation rates of lamellar phase in a ternary system of water, oil and amphiphile, which are governed by the hydrodynamics of the fluid layers. A direct comparison with light scattering and neutron-spin-echo experiments is possible. (T. Schilling, O. Theissen, G. Gompper)

11. *Hydrophobic interaction:*
We investigate idealized discrete models of the hydrophobic interaction. Our findings suggest that a solubility-enhancing increase of symmetry of the solvent particles decreases the solvent-mediated part of the potential of mean force between solute particles. This weakening of the hydrophobic attraction is in agreement with the notion that the effect is entropic in origin. (G.M. Schütz, I. Ispolatov, G.T. Barkema and B. Widom)

12. *Shocks in driven diffusive systems:*
Shocks in driven diffusive systems, i.e. abrupt changes in the local density, form collective excitations which are localized and stable over long periods of time. In a family of lattice models for driven diffusive systems we obtain detailed information about the microscopic structure of the shock as well as its large-scale properties by using special non-abelian symmetries for the exact analytical calculation of the time evolution of a shock measure. Numerical finite-size scaling analysis shows that the notion of a localized shock is meaningful also for very small systems, thus suggesting that coarse grained nonequilibrium theories involving shocks are applicable to small real systems. (G.M. Schütz, T. Antal, V. Belitsky, M. Dudziński, C. Pigorsch)

13. *Reaction-diffusion systems:*
The dynamics of a coupled two-component nonequilibrium reaction-diffusion system for dynamically activated hopping is examined by renormalization group analysis of a continuum field theory representing the corresponding master equation. For activators B subject to diffusion-limited reactions the activated particles A perform normal diffusion if the density of B particles attains a finite asymptotic value (active state), while strongly anomalous subdiffusive behavior occurs if the B density decays into an inactive state. For B pair annihilation the mean-square displacement of the A particles grows only logarithmically with time in $d \geq 2$ dimensions. For radioactive B decay, the A particles remain localized. (G.M. Schütz, S. Trimper, U.C. Täuber)

Some Remarks:

- Prof. Klaus Kehr, a member of the Institute Theory II from 1971 until 1999 and acting director during several periods (1976–1977, 1988–1990, and 1995–1999), unfortunately died last year shortly after his retirement. Many members of the IFF will remember Prof. Kehr as a helpful and friendly person, and as a very enthusiastic and excellent physicist.
- Prof. Erich Eisenriegler, who was a member of Institute Theory I from 1969 until 2000, has formally joined the Institute Theory II this year. Prof. Eisenriegler's main research interests have focused on soft matter systems already for quite a while. He brings his expertise on statistical field theory and the renormalization group, as well as on polymers near surfaces and colloids into the Soft Matter Theory group.
- Dr. G. Schütz spent the summer 2000 as visiting professor at the Cornell University in Ithaca, New York.
- Dr. Roland Winkler will join the Institute Theory II at the beginning of 2001.

Awards etc.:

- Dr. G. Schütz has been awarded the *Gustav-Hertz Preis 2000* by the Deutsche Physikalische Gesellschaft, in recognition of an excellent recently completed research project from the group of young scientists.
- Prof. T. Burkhardt (Temple University, Philadelphia, USA) has received an award from the *Alexander von Humboldt Stiftung*, which he used to spend half a year (Sept. 1999 to Febr. 2000) as a visiting scientist at the IFF.

Gerhard Gompper

Personnel 2000/2001 and areas of activity

Scientific Staff

Dr. A. Baumgärtner	Statistical mechanics of proteins and membranes;	23.30.0
Prof. E. Eisenriegler	Polymers near surfaces, colloid-polymer mixtures	23.30.0
Prof. G. Gompper Institute Director	Statistical mechanics of amphiphilic systems	23.30.0
Dr. G. Schütz	Driven diffusive systems, reptation models	23.30.0

Technical Staff

H. Paffen	Secretary	

Postdocs

Dr. A. Lamura	Hydrodynamics of simple and complex fluids	23.30.0

Diploma and Graduate Students

T. Auth	Polymers at membranes	23.30.0
K. Mussawisade	Diffusion in disordered materials	23.15.0
J.-H. Lin	Membrane proteins	23.30.0
M. Paeßens	Finite-size effects in entangled polymers	23.30.0
T. Schilling	Wetting in amphiphilic systems	23.30.0
R. Willmann	Polymer dynamics in disordered media	23.30.0

Guests

Prof. T. Burkhardt	(Temple University, Philadelphia, USA) Statistical mechanics of polymers; stochastic processes (Sep. 1999 - Feb. 2000)	23.30.0
C. Pigorsch	(Universität Halle) Shocks in many-body systems (Mar. 2000)	23.15.0
S. Miller	(Universität Stuttgart) Polymerized Membranes (May - June 2000)	23.30.0
E. Fouladvand	(Sharif University, Tehran, Iran) Driven many-body systems (Aug. - Sept. 2000)	23.15.0
Dr. T. Ihle	(University of Minnesota, Minneapolis, USA) Mesoscale simulations of hydrodynamics (Sep. - Oct. 2000)	23.30.0
Dr. J. Santos	(TU München) Reptation dynamics (Oct. 2000)	23.30.0
Dr. W. Goźdź	(Polish Academy of Sciences, Warsaw, Poland) Membrane shapes (Oct. - Dec. 2000)	23.30.0

Measuring Bending Rigidity of Membranes in Bicontinuous Microemulsions

G. Gompper[1], H. Endo[2], M. Mihailescu[2], J. Allgaier[2], M. Monkenbusch[2], D. Richter[2], B. Jakobs[3], T. Sottmann[3], and R. Strey[3]

[1] Institute Theory II [2] Institute for Neutronscattering
[3] Dept. of Physical Chemistry, Universität zu Köln

We demonstrate a new approach to determine the bending rigidity of the amphiphile film in microemulsions and sponge phases from neutron scattering data. This method is precise enough to measure the logarithmic scale dependence of the bending rigidity and its universal prefactor for the first time. Furthermore, we show that in the mushroom regime the bending rigidity of a membrane decorated by amphiphilic block copolymers increases linearly with the polymer concentration on the membrane; the amplitude is found to be about a factor 1.5 larger than theoretical results for ideal chains.

F&E-Nr: 23.30.0

Amphiphilic molecules in mixtures with water and/or oil spontaneously aggregate to form mono- or bilayers, if the sizes of the hydrophilic and hydrophobic parts are large enough. In this case, the description of the ensemble of amphiphile sheets by a random surface model, in which the shapes and fluctuations are controlled by the curvature elasticity, has been found to be very useful for understanding many phenomena in these systems. For a detailed comparison of theory and experiment, it is crucial to measure the parameters of this model, which are the preferred (or spontaneous) curvature c_0, the bending rigidity κ, and the saddle-splay modulus $\bar{\kappa}$. For many applications, it would of course be desirable not only to determine but also to control and tune the values of these elastic moduli.

We have developed a new approach, by which it is possible to determine the bending rigidity of membranes in bicontinuous microemulsions for the first time [1]. Here, the microemulsion is a macroscopically homogeneous, isotropic fluid phase; on a mesoscopic scale, it consists of two intertwined networks of oil- and water-channels, which are separated by an amphiphilic monolayer, compare Fig. 1. Our method is based on the analysis of neutron scattering data in ternary microemulsions, where by minute additions of amphiphilic diblock copolymers PEPx-PEOy (polyethylenepropylene/polyethyleneoxide with molecular weights x, y in kg/mol) the membrane properties can be tuned continuously [2]. Two length scales, the correlation length ξ and a characteristic wave vector $k = 2\pi/d$, where d is the average domain size, can be extracted from the scattering intensity in bulk contrast. The main result of our theoretical analysis is the relation

$$k\xi = \frac{64}{5\sqrt{3}} \frac{\kappa_R(\phi_s)}{k_B T} \qquad (1)$$

where κ_R is a scale-dependent, *renormalized* rigidity, which is given by

$$\kappa_R(\phi_s) = \kappa + \alpha \frac{k_B T}{4\pi} \ln(\phi_s) \qquad (2)$$

The theoretical analysis, which leads to Eq. (1), starts from results for the Gaussian-random-field model [3], localizes the inconsistencies of this model with recent Monte Carlo simulations of dynamically triangulated surfaces [4], and corrects the results in such a way as to give the proper thermodynamic singularities.

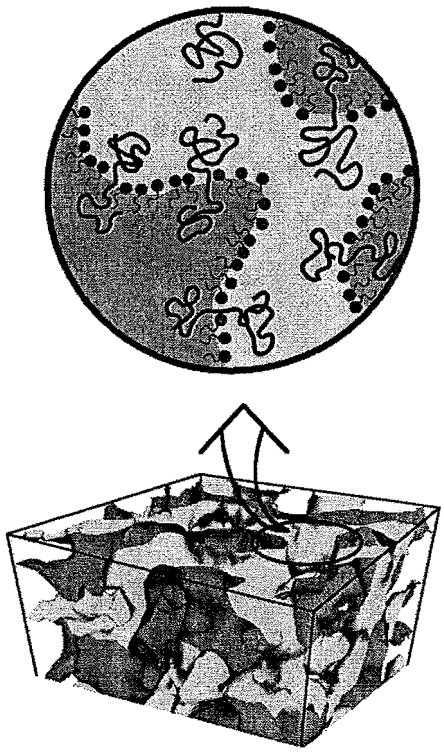

FIG. 1. Schematic presentation of the mesoscopic structure of a bicontinuous microemulsion, which contains small amounts of an amphiphilic block copolymer.

Results for the dimensionless product $k\xi$ were obtained from the analysis of the scattering data for different surfactant volume fractions ϕ_s and polymer volume fractions ϕ_δ in the mixture of both amphiphiles; the results are shown in Fig. 2. For fixed ϕ_s, the average domain size and thereby the characteristic wave vector k remain unchanged. The increase of $k\xi$ with ϕ_δ therefore indicates an increase of the correlation length with the polymer grafting density σ (which is proportional to the polymer volume fraction ϕ_δ). On the other hand, the surfactant volume fraction decreases along the three-phase-coexistence line, where the microemulsion coexists with both an almost pure oil and water phase, so that the weak dependence of $k\xi$ on ϕ_δ indicates a simulaneous decrease of k and increase of ξ.

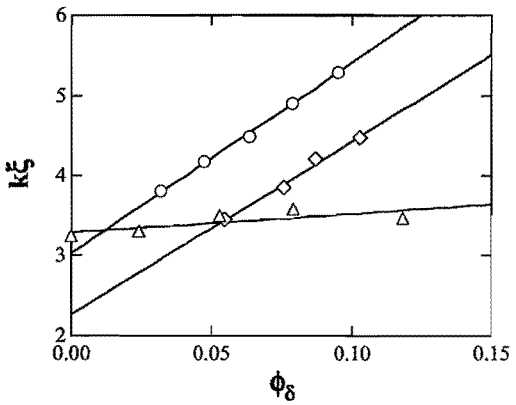

FIG. 2. Dimensionless ratio $k\xi$ of the two lengths scales characterizing the structure of a bicontinuous microemulsion. Data are shown for PEP5-PEO5 with membrane volume fraction $\phi_s = 0.12$ (○) and $\phi_s = 0.08$ (◇), and for PEP10-PEO10 along the three-phase coexistence line (△), in all cases as a function of the polymer volume fraction ϕ_δ in the mixture of both amphiphiles.

With the use of Eqs. (1) and (2), the effective bending rigidity of the polymer decorated membrane can be extracted. Fig. 3 shows that all data points collapse onto a single line, with a value of $\alpha = 2.96 \pm 0.09$ emerging form the fit. This settles a debate of about 15 years about the correct value of α. While our value is consistent with field-theoretical calculations [5] which give $\alpha = 3$, a *negative* value proposed recently by Helfrich can clearly be ruled out.

The data collapse in Fig. 3 shows that the weak dependence of $k\xi$ on the polymer volume fraction ϕ_δ along the three-phase coexistence line — compare Fig. 2 — arises from the competition of two effects. First, the effective bending rigidity increases due to the stiffening effect of the attached polymers; second, the rigidity decreases due to the increase of the domain size, which leads to a softening of the membrane as a result of thermal fluctuations, as described by Eq. (2). Fig. 2 indicates that these two effects nearly cancel along the coexistence line.

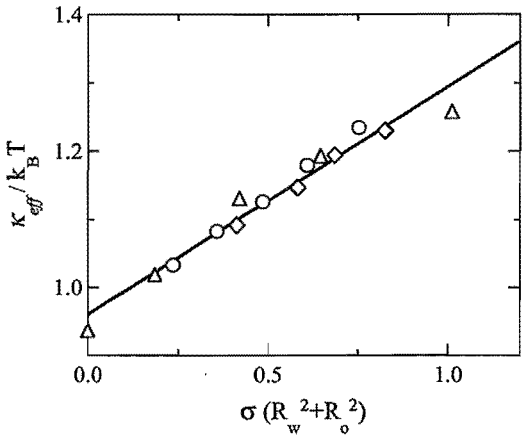

FIG. 3. The effective bending rigidity κ_{eff} of a membrane decorated by amphiphilic block colpolymer, as a function of the dimensionless grafting density $\sigma(R_o^2 + R_w^2)$, where $R_{o(w)}$ is the end-to-end distance of the hydrophobic (hydrophilic) block. Data are shown for surfactant volume fractions $\phi_s = 0.12$ (○) and $\phi_s = 0.08$ (◇) and along the three-phase coexistence line (△).

In the mushroom regime, where $\sigma(R_o^2 + R_w^2) < 2$, so that the polymer conformation on the membrane are not disturbed by the interaction with neighboring polymer chains, a linear dependence of the bending rigidity on the grafting density is expected theoretically. This is entirely consistent with the results of Fig. 3. Furthermore, a recent calculation of the bending rigidity for ideal chains (without self-avoidance) predicts a slope of $k_BT(1 + \pi/2)/12$ [6]. The slope of the straight line in Fig. 3 is found to be about a factor 1.5 larger than this theoretical result. We believe that this factor is due to the omission of self-avoidance effects in the calculations of the effective bending rigidity.

Our results show that the new approach to measure bending rigidities of membranes in bicontinuous microemulsions works very well. This approach can now be applied to many other systems, in which the bending rigidity can be varied by some external parameter.

[1] G. Gompper *et al.*, (preprint) (2001).
[2] B. Jakobs *et al.*, Langmuir **15**, 6707 (1999).
[3] P. Pieruschka and S. A. Safran, Europhys. Lett. **22**, 625 (1993).
[4] G. Gompper and D. M. Kroll, Phys. Rev. Lett. **81**, 2284 (1998).
[5] L. Peliti and S. Leibler, Phys. Rev. Lett. **54**, 1690 (1985).
[6] C. Hiergeist and R. Lipowsky, J. Phys. II France **6**, 1465 (1996).

Molecular Dynamics Simulations of Membrane Proteins

J.-H. Lin and A. Baumgaertner
Theorie II and Forum Modellierung

We have investigated the interaction of proteins with hydrated lipid bilayer membranes using molecular dynamics simulations. Two problems have been addressed : the protein-insertion problem and the stability of a protein pore embedded in a bilayer membrane. It is shown that in contrast to previous studies single proteins do not insert spontaneously, but are prohibited to do so by the interfacial barrier of the water-lipid interface. A tight protein pore expands due to electrostatic repulsion among the α-helices. The energetically unfavorable expansion-induced formation of an interface between the pore-lining acyl chains of the lipids and the pore water is transformed into an energetically more favorable toroidal pore structure where some lipid heads are translocated from the rim to the central part of the interface. It is hypothesized that pore growth, and hence cell lysis, is induced by a protein-mediated line tension of the pore.

F&E-Nr. 23.30.0

The Protein-Insertion Problem. The adhesion and partitioning of proteins into lipid bilayer membranes and their subsequent folding are fundamental processes in biological cells. It is known for a long time that short amphiphatic proteins spontaneously adsorb at and insert into membranes [1]. Despite many experimental facts indicating spontaneous adsorption and insertion under certain experimental conditions, our theoretical understanding of these processes are still poor. In particular, the specific interaction between the lipid-water interface and proteins is not well understood. Therefore, we have performed molecular dynamics simulations of an all atom system consisting of water, lipid molecules and proteins. As a specific system we have choosen the protein melittin, lipids of the type POPC (1-palmitoyl-2-oleoyl-*sn*-glycero-3-phosphocholine) and water of the TIP3P type [2]. The sequence of melittin is 26 amino acids long. The N-terminus part (Ile-Gly-Ala-Val-Leu) is more hydrophobic, whereas the C-terminus part (Lys-Arg-Lys-Arg-Gln-Gln) is positively charged and hence strongly hydrophilic.

Since the N-terminus part of melittin is very hydrophobic, one would expect that this protein would spontaneously insert into the membrane. This view had been suggested by free energy considerations [3,4] and supported by Monte Carlo simulations using a simplified membrane model and an effective medium approximation for water [5,6]. However, molecular dynamics simulations of the all atom model [2] do not support the latter findings, but rather indicate that melittin is weakly bound to the membrane surface. This solute state is stable for about 6 nanoseconds and there are no indications for an insertion process. This is demonstrated by the probability distribution of the location of the center-of-mass of melittin with respect to the normal of the membrane surface which is denote by z in Fig. 1. For comparison, Fig. 1 contains also the density profiles of water and the phosphate groups of the lipid heads which indicate the location of the water-lipid interface. It should be noted that the two interfaces, as indicated in Fig. 1 by the two PO_4 groups, belongs to a stack of membrane separated by an aqueous phase. The basic conclusions from the simulation studies are [2] :

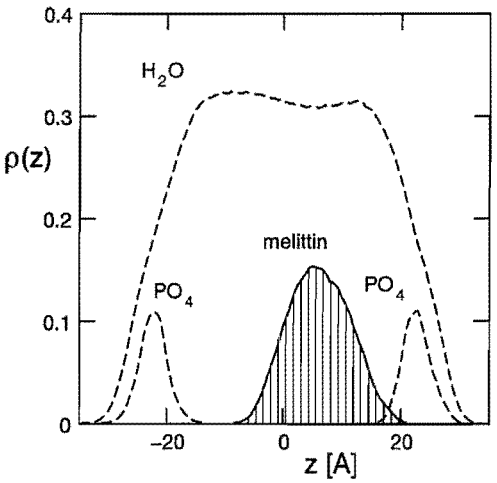

FIG. 1. Density profile of melittin, water, and lipid heads.

(1) a single hydrophobic protein cannot disrupt the water-membrane interface in order to intercalate and subsequently insert into the hydrophobic core of a bilayer membrane; (2) the hydrophilic terminus of a single protein cannot adsorb or even intercalate into the water-lipid interface of zwitter-ionic lipids (as in the present case of POPC); (3) a correct thermodynamic theory must include the energies of the water-lipid interface.

It is important to note that our findings are in agreement with observations and experiments on analogs of melittin, like alamethicin and others [1], at very high dilution. At higher concentrations, however, experiments indicate insertion of melittin in a probably aggregated form.

Stability of a Protein Pore. Although cell lysis by toxic peptides is a well known phenomena and has been investigated by many experiments, the molecular mechanism is not well understood. A particular popular toxin is the bee venom peptide melittin, which is known to cause hemolysis and to induce leakage of fluorescent dyes from lipid vesicles [7,8]. The currently accepted view is that insertion and aggregation take place at high salt concentration and at peptide/lipid molar ratio above 1/200. A central problem which has been addressed in many experiments is the type of aggregate and its lytic mechanism. A reasonable view at the present time is the formation of cylindrical pores build by transbilayer helices. However, in most cases the existence of pores has been concluded indirectly on the basis of the efflux of fluorescent dye molecules from large unilamellar vesicles.

We have studied the stability of a hypothetical melittin pore consisting of 4 monomers using molecular dynamics simulations [9]. Similar as in previous experiments we consider the pore to be embedded in a POPC bilayer membrane at pH value 7. During a simulation of 5.8 ns we found that the conformation of melittin is remarkably stable over the whole time scale. On the other hand, the initial closed-packed tetrameric configuration is unstable and decays continuously to a stable trimeric configuration and a separate monomer. The inital and final locations of the helices are indicated by dotted and full circles for initial and final states, respectively, in Fig. 2.

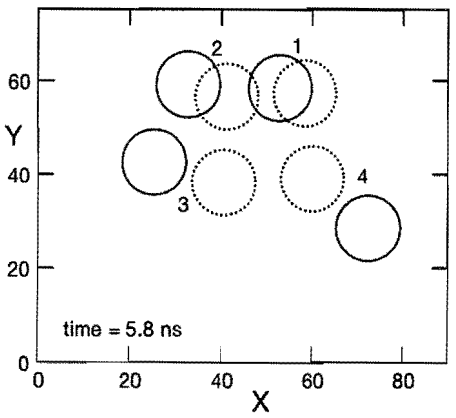

FIG. 2. Initial and final configuration of the tetrameric state.

Since the diameter of the aqueous pore increases with time, its cylindrical surface increases accordingly. Since also the distance between between the trimeric and the monomeric melittin increases with time, the initial shielding of water from direct contact with hydrophobic acyl chains, as in the initial tetrameric state, becomes less effective. Then, the hydrophobic parts of the lipids become exposed to water and the interesting question arises how this conflicting situation is resolved by the system. An analysis of these pore-forming lipids had revealed that some lipids had changed their orientation with respect to the membrane normal from a parallel to a perpendicular orientation. This reorientation is accompanied by a translocation of the lipid heads from the membrane surface to the surface of the pore. This is shown in Fig. 3, where those lipid heads exhibiting a transition from the membrane surface to the inner part of the pore are depicted by solid lines and are shown as a function of time; the dotted background corresponds to the other lipids.

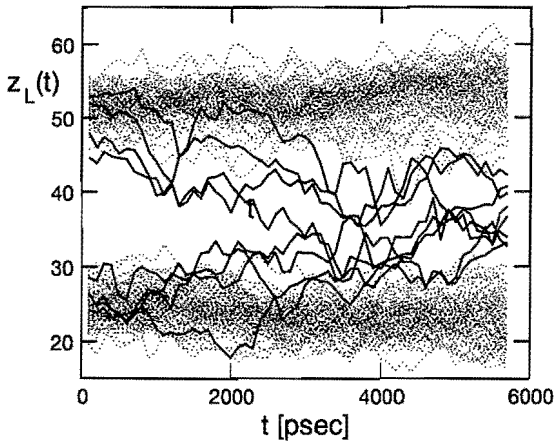

FIG. 3. Trajectories of lipid heads.

An important and interesting point is the intercalation of lipids between helices. It is conceivable that this spontaneous intercalation, once it has happened, leads to a destruction of the stable tetrameric aggregate. This event is induced by Coulomb repulsion between helices which leads to sufficiently large fluctuations of the interhelical distances.

[1] S. H. White,W. C. Wimley, Curr.Opin.Struct.Biol. **4**, 79 (1994).
[2] J.-H. Lin, A. Baumgaertner, Comput. Theor. Poly. Sci. **10**, 97 (2000).
[3] D. A. Engelman, T. A. Steitz, Cell **23**, 411 (1981).
[4] P.J. Park, W. Sung, Phys. Rev. Lett. **80**, 56897 (1998).
[5] M. Milik, J. Skolnick, Biophys. J. **69**, 1382 (1995).
[6] A. Baumgaertner, Biophys. J. **71**, 1248 (1996).
[7] A. S. Ladokhin, W. C. Wimley, S. H. White, Biophys. J. **69**, 1964 (1995).
[8] K. Matsuzaki, S. Yoneyama, K. Miyajima, Biophys. J. **73**, 831 (1997).
[9] J.-H. Lin, A. Baumgaertner, Biophys. J. **78**, 1714 (2000).

Lattice models of the hydrophobic interaction

G.M. Schütz[1,2], I. Ispolatov[2], G.T. Barkema[3]
and B. Widom[2]

(1) *Institut für Festkörperforschung (Theorie II), Forschungszentrum Jülich, D-52425 Jülich, Germany*
(2) *Department of Chemistry and Chemical Biology, Baker Laboratory, Cornell University, Ithaca, NY 14853-1301, USA*
(3) *Instituut voor Theoretische Fysica, Universiteit Utrecht, Princetonplein 5, 3584 CC Utrecht, The Netherlands*

We establish the equivalence of various lattice models of the hydrophobic interaction with the Ising model in a magnetic field with temperature-dependent strength. In order to capture the effect of symmetries of the solvent particles we introduce an extended model which is not of the Ising type. Our results for the solubility and the solvent-mediated part of the potential of mean force between solute particles suggest that an increase in symmetry enhances the solubility, but decreases the amplitude and range of the attractive force. This weakening of the hydrophobic effect observed in the model is in agreement with the notion that the effect is entropic in origin.

F&E-Nr: 23.30.0

The hydrophobic attraction is of importance in many areas of physical chemistry and biochemistry and has a long and multi-faceted history of study [1,2]. In the case of aqueous solutions the notion refers to an effective attraction between hydrophobic solute particles which is mediated by the solvent particles. The basic mechanism behind this phenomenon is believed to be a subtle interplay between an energy and entropy decrease associated with the solvation of a hydrophobic solute such as a hydrocarbon (or more complex) molecule. The energy decrease is a specific property of the solvent, but the entropy decrease can be understood more generally as resulting from the entropically unfavorable necessity to place the solvent molecules in some particular orientation in order to allow for the accomodation of a solute molecule between them (e.g. through hydrogen bonds). The low solubility of the hydrophobic particles indicates a positive balance between the two contributions to the free energy. However, the net increase in free energy when two such solute molecules are accomodated in the solvent is less when they are close together than when they are far apart. The consequence is an effective attraction between them which is superimposed on and may even dominate their direct interaction.

To investigate the consequences of such an interplay between favorable energy and unfavorable entropy we consider idealized lattice models where each solvent particle is allowed to be in one of q states which may be regarded as orientations with respect to some frame of reference. In the simplest realization of this approach [3] q is an integer and there is a nearest neighbor interaction between solvent particles with energy w if both particles are in one particular state and u (with $u > w$) otherwise. Solute particles may be accommodated only on the interstitial site between solvent particles, provided (because of the solvent-solute interaction) that both solvent particles be in that special energetically favorable orientation (Fig.1). The energy of interaction of an interstitial solute molecule with its neighbors is then taken to be v. As a function of temperature the solvent-mediated part of the potential of mean force between solute particles shows an inverse relationship between the magnitude of the attractive force and its range [3,4]. The solubility of the hydrophobe decreases with increasing temperature. In one dimension the decay of the potential of mean force with distance is monotonic, while in two and three dimensions there is an oscillatory modulation.

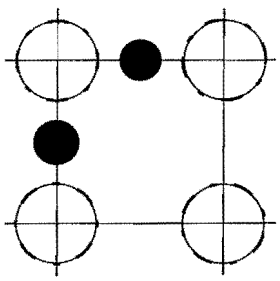

FIG. 1. Two-dimensional representation of the accommodation of solute particles (black disks) on the interstitial sites between solvent particles (circles) on a square lattice. Depending on the model the bold sections on the circumference of the circles have different interpretations in terms of orientations (see text).

This basic model can be extended to continuous state variables, thus being somewhat more realistic with regard to the interpretation of the molecular states as orientations. First we define the (still discrete) n^2-model with q discrete orientations (states). In the two-dimensional version a solvent particle (Fig. 1) is represented by a circle of $4q$ discrete points which consist of quadruples related to each other by a 90 degree rotation. Each quadruple defines one orientation and there is always one quadruple of points which is located on the lattice axis. The special states $1, \ldots, n$ correspond to quadruples of points on the dark sections of the circumference of the circles. A solute particle may be accommodated whenever special points of two neighboring molecules are located on the lattice axis. In the continuum limit $q, n \to \infty$ with

the ratio $\tilde{q} = q/n$ of special points fixed, a solute particle may be accommodated if dark segments of neighboring circles intersect with the lattice axis.

Moreover, symmetries of the solvent particles can be modelled in a simple fashion by allowing for the accommodation of solute particles between solvent molecules that are in any n rather than just one energetically favorable pair of special states. This n-model describes more structured solvent molecules which have chemically different surface regions. E.g. for $n = 2$ one would say that a solute particle could be accommodated if on both neighboring molecules either the long or the short dark segment intersect with the lattice axis, but not if for one molecule the long segments intersects and for the other molecule the short segment.

In the n^2-model all special states are indistinguishable, as are the non-special states. Hence any joint probability involving some state k depends only on whether k belongs to the group of special states or not. The equivalence to the Ising model is established by assigning Ising spins $s_i = +1$ to the n special states and $s_i = -1$ to the $q - n$ other states respectively [5]. Thus the partition function of the n^2-model (with the irrelevant global reference energy $u = 0$) turns into the partition of a ferromagnetic Ising model in a magnetic field with energy

$$\tilde{E} = -J \sum_{<i,j>} s_i s_j - h \sum_i s_i - const. \qquad (1)$$

The interaction parameters are given by the relations $J = -w/4$ and $h = -cw/4 - 1/2kT \ln(q/n - 1)$, with c the coordination number of the lattice and $w < 0$. In the continuum limit of the state variables the parameter $\tilde{q} = q/n$ becomes a continuous variable in the range $1 < \tilde{q} < \infty$. Hence the properties of the n^2-models are identical to those of the original 1^2-model [3,4] briefly reviewed above and equivalent to those of the Ising model in a temperature-dependent magnetic field.

Unfortunately, the n-model is *not* equivalent to an Ising model and nothing is known about the model in three dimensions. However, since the most important features of the 1^2-model were already seen in one dimension, we restrict our analysis of the n-model also to the one-dimensional case which can be solved exactly by diagonalizing its transfer matrix [5]. We calculate the solvent-mediated potential of mean force $W(r)$ between solute particles on the basis of the potential-distribution theorem [6]. One then finds [5]

$$W(r) = -kT \ln\left[1 + A e^{-(r-1)/\xi}\right]. \qquad (2)$$

The amplitude A is a monotonically increasing function of temperature T, approaching $A = q/n - 1$ in the regime relevant for modelling the hydrophobic effect. The inverse localization length $1/\xi$ may be written as a sum of two terms, $\xi^{-1} = \ln[b/q] + \ln[q/(q-n)]$ where $b = \exp(-w/(kT)) > 1$. Both A and ξ *decrease* as a function of the symmetry parameter n (Fig. 2).

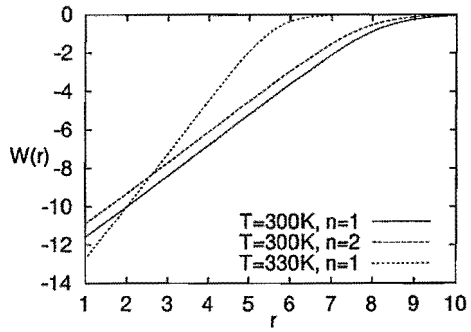

FIG. 2. Potential of mean force in units of kT_0 as a function of distance (in lattice units) at different temperatures and for different symmetry parameters with $T_0 = 300K$, $q = 110000$, $w/k = -3000K$ [3].

As solubility we define the dimensionless ratio $\Sigma = \rho_{\rm soln}/\rho_{\rm gas}$ where $\rho_{\rm soln}$ is the number density of the solute in the solution and $\rho_{\rm gas}$ is its number density in an ideal gaseous phase in osmotic equilibrium with the solution. For small solubility (such that the saturated solution is very dilute) this quantity is the Ostwald absorption coefficient. Within the lattice model one finds [5]

$$\Sigma = bn/q^2 e^{-v/(kT)} \qquad (3)$$

and therefore an increase with symmetry.

The most striking features of the original hydrophobic interaction model, the inverse relationship between amplitude and range of the potential of mean force and the decrease of solubility with increasing temperature in reasonable temperature ranges, are present also in the more symmetric n-model. However, the amplitude of the potential decreases with increasing degree of symmetry. This is in agreement with the notion that the origin of the hydrophobic effect is entropic. With increasing degree of degeneracy (and hence symmetry) the entropy decrease associated with the requirement to orient molecules in a particular direction is less and hence also the balance in the free energy difference is reduced.

[1] W. Kauzmann, Adv. Protein Chem. **14**, 1 (1959).
[2] A. Ben-Naim, *Hydrophobic Interactions*, (Plenum Press, New York, 1980).
[3] A.B. Kolomeisky and B. Widom, Faraday Discuss. **112**, 81 (1999).
[4] G.T. Barkema and B. Widom, J. Chem. Phys. (2000).
[5] G.M. Schütz, I. Ispolatov, G.T. Barkema and B. Widom, to be published in Physica A (Dec. 2000).
[6] B. Widom, J. Chem. Phys. **39**, 2808 (1963).

Numerical study of segregating binary mixtures in shear flow

A. Lamura
Institute Theory II

We study numerically the phase separation of a binary mixture in uniform shear flow in the framework of the continuum convection-diffusion equation based on a Ginzburg-Landau free energy for different temperatures both in 2 and 3 space dimensions. Our main results show the existence of domains with two typical sizes, whose relative abundance changes with time producing logarithmic-time periodic oscillations in the behavior of the average domains sizes and of other rheological observables.

F&E-Nr: 23.30.0

When a binary mixture is suddenly quenched from a disordered initial state to a coexistence region below the critical temperature, the two components segregate and form domains which grow with time. In the unsheared case a single length scale $R(t)$, which measures the average size of domains, characterizes the kinetics of phase separation. This length grows with the power law $R(t) \sim t^{\alpha} \sim t^{1/3}$ in a pure diffusive regime [1]. The physics of this coarsening process is that atoms evaporate from smaller droplets, that are dissolving, and diffuse through the other phase to larger droplets that are growing. The late stage growth is often called Ostwald ripening. The application of a shear flow greatly affects the phase separation process [2]. A large anisotropy is observed in typical patterns of domains which appear elongated in the direction of the flow. Previous numerical simulations confirm these observations. These studies, however, were carried out on rather small systems so that an accurate resolution of their spatial properties, which is usually inferred from the knowledge of the structure factor, is not available yet.

We investigated the segregation process by numerical simulation of large scale systems in order to compute at a fine level of resolution the structure factor. In the following we consider a binary mixture in shear flow described by a model with a coupling between a diffusive field φ, representing the concentration difference between the two components of the mixture, and a shearing velocity field. This approach neglects hydrodynamic effects. For weakly sheared polymer blends with large polymerization index and similar mechanical properties of the two species, however, the present model is expected to be satisfactory in a preasymptotic time domain when velocity fluctuations are small.

The fluid is described by the Langevin equation

$$\frac{\partial \varphi}{\partial t} + \vec{\nabla} \cdot (\varphi \vec{v}) = \nabla^2 \frac{\delta \mathcal{F}}{\delta \varphi} + \eta \qquad (1)$$

where $\vec{v}$ is the external velocity field describing plane shear flow with profile $\vec{v} = \gamma y \vec{e}_x$, γ and $\vec{e}_x$ being, respectively, the shear rate and the unit vector in the x direction. η is a gaussian white noise, representing the effects of thermal fluctuations. The term $\vec{\nabla} \cdot (\varphi \vec{v})$ describes the advection of the field φ by the velocity field and $\nabla^2(\delta \mathcal{F}/\delta \varphi)$ takes into account the diffusive transport of φ. The equilibrium free-energy can be chosen as

$$\mathcal{F}\{\varphi\} = \int d^d x \Big\{ -\frac{1}{2}\varphi^2 + \frac{1}{4}\varphi^4 + \frac{1}{2} \mid \nabla \varphi \mid^2 \Big\} \qquad (2)$$

in the ordered phase.

Eq. (1) has been simulated in spatial dimensions $d = 2$ and 3. The structure factor is $C(\vec{k}, t) = \langle \varphi(\vec{k}, t) \varphi(-\vec{k}, t) \rangle$ where $\varphi(\vec{k}, t)$ are the Fourier components of φ. Results are presented here for the two dimensional case at temperature $T = 0$ [3]. Similar results have been obtained for temperatures in the range $0 \leq T \leq 5$ and in $d = 3$ at $T = 0$ in Ref. [4].

A sequence of configurations at different values of the strain γt is shown in Fig. 1.

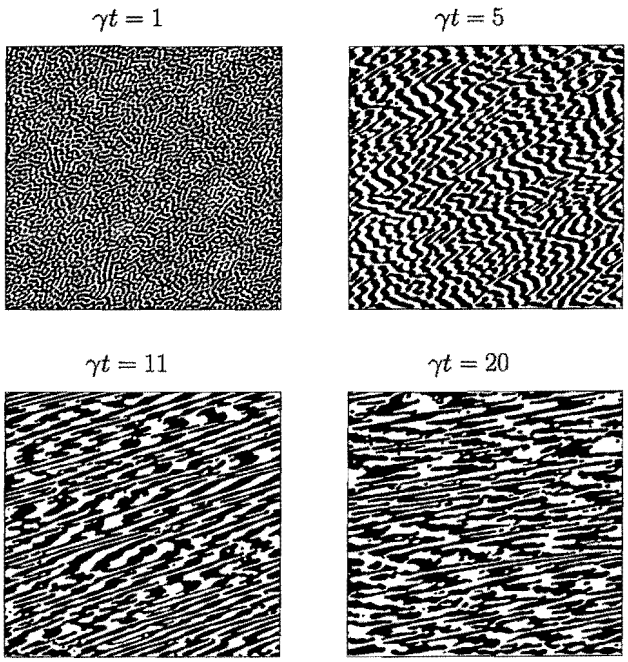

FIG. 1. Configurations of a portion of 512 × 512 sizes of the whole lattice are shown at different values of the strain γt at $T = 0$. The x axis is in the horizontal direction.

After an early time, when well defined interfaces are forming, the pattern of domains starts to be distorted for $\gamma t \gtrsim 1$. The growth is faster in the flow direction and domains assume the typical striplike shape aligned with the flow direction. As the elongation of the domains increases, nonuniformities appear in the system: Regions with domains of different thickness can be clearly observed at $\gamma t = 11$ and $\gamma t = 20$.

An analysis of length scales present in the system can be done by studying the behavior of the structure factor. At the beginning $C(\vec{k},t)$ exhibits an almost circular shape. Then shear-induced anisotropy deforms $C(\vec{k},t)$ into an elliptical pattern. The profile of $C(\vec{k},t)$ changes with time until it is separated in two distinct foils, each of them characterized by two peaks. Since the property $C(\vec{k},t) = C(-\vec{k},t)$ holds, the two foils are symmetric with respect to the origin of the k-space and it is sufficient to consider only the two peaks of one foil. The position of each peak identifies a couple of typical lengths, one in the flow and the other in the shear (vertical) direction. This corresponds to the observation of domains with two characteristic thicknesses (compare Fig. 1). The relative height of the peaks of $C(\vec{k},t)$ is demonstrated in Fig. 2 where the two maxima in each foil are observed to dominate alternatively at the times $\gamma t = 11$ and $\gamma t = 20$.

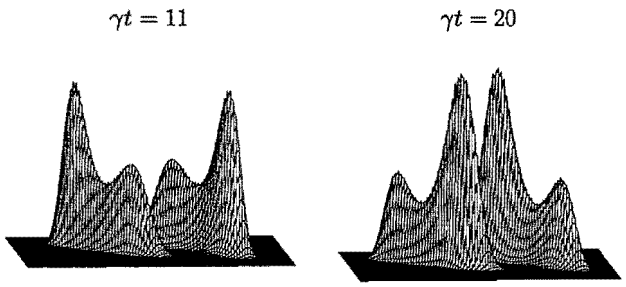

FIG. 2. The structure factor is shown at $\gamma t = 11$ and $\gamma t = 20$. The axes k_x and k_y are in the horizontal and vertical directions, respectively.

The competition between two kinds of domains is a cooperative phenomenon. In a situation like that at $\gamma t = 11$, the peak with the larger k_y dominates, describing a prevalence of stretched thin domains. When the strain becomes larger, a cascade of ruptures occurs in those regions of the network where the stress is higher and elastic energy is released. At this point the thick domains, which have not yet been broken, prevale and the other peak of $C(\vec{k},t)$ dominates, as at $\gamma t = 20$. Finite-size effects prevented us to follow the alternate predominance of the two peaks longer in time. Such a behavior was shown in Ref. [5], where the phase separation of binary mixtures in shear flow was addressed in the context of the large-N limit approximation.

This dynamics affects the behavior of the average size of domains, $R_x(t)$ and $R_y(t)$, in the flow and shear direction. These quantities have been calculated through $R_x(t) = (\int d\vec{k} k_x^2 C(\vec{k},t) / \int d\vec{k} C(\vec{k},t))^{-1/2}$, and analogously for $R_y(t)$; their behavior is shown in Fig. 3. Due to the alternative dominance of the peaks of $C(\vec{k},t)$, R_x and R_y increase with amplitudes modulated by a periodic oscillation in logarithmic time. Using a renormalization group approach we proved that $R_x \sim t^{4/3}$ and $R_y \sim t^{1/3}$, but simulations cannot give evidence of such a scaling regime due to finite-size effects [3]. The logarithmic periodicity of these oscillations in time is one of the most relevant results to be tested experimentally.

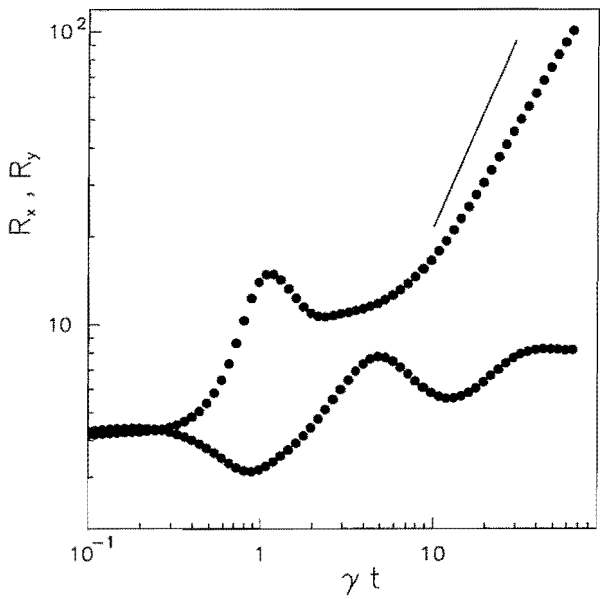

FIG. 3. Evolution of the average domain size in the shear (lower curve) and flow (upper curve) directions. The straight line has slope 4/3.

Stretching of domains requires work against surface tension and burst of domains dissipate energy resulting in an increase $\Delta\eta$ of the viscosity [2]. Starting from zero, $\Delta\eta$ grows oscillating up to a global maximum, then it relaxes to zero. The relative maxima of $\Delta\eta$ are found in correspondence of the minima of R_y when the domains are maximally stretched.

[1] A. J. Bray, Adv. Phys. **43**, 357 (1994).
[2] A. Onuki, J. Phys. Condens. Matter **9**, 6119 (1997).
[3] F. Corberi, G. Gonnella, and A. Lamura, Phys. Rev. Lett. **83**, 4057 (1999).
[4] F. Corberi, G. Gonnella, and A. Lamura, Phys. Rev. E **62**, 8064 (2000).
[5] F. Corberi, G. Gonnella, and A. Lamura, Phys. Rev. Lett. **81**, 3852 (1998).

Dynamics of the Swollen Lamellar Phase

T. Schilling, O. Theissen, and G. Gompper

Institute Theory II

We investigate the dynamical behavior of lamellar phases in ternary amphiphilic systems of water, oil and amphiphile. The interaction between neighboring amphihpilic monolayers is decribed by the steric interaction, which arises from the entropy loss due to the confinement of membrane fluctuations in a stack. The dynamics of the system is determined by the hydrodynamics of the fluid layers. Relaxation rates are calculated for arbitrary wave vectors q parallel and perpendicular to the average monolayer plane. We find a complex crossover behavior from a $q_\parallel^2$-law for small parallel wave vectors to a $q_\parallel^3$-law for large $q_\parallel$. The relevance of our results for the interpretation of dynamic scattering experiments is discussed.

F&E-Nr: 23.30.0

Among the large variety of phases, which appear in amphiphilic systems, the lamellar or L_α-phase plays a key role for the understanding of the physical properties of these systems [1]. Scattering experiments in the L_α-phase provide a large amount of information about the thermal fluctuations and dynamics of these systems, because the amphiphilic layers have a well-defined average orientation. The simple stack geometry also allows for detailed theoretical investigations, which can be carried out analytically. Finally, the theoretical results provide the necessary framework for the interpretation of the experimental data.

A frequently used experimental system is a ternary mixture of oil, water and amphiphile, which consists of alternating layers of oil and water, separated by monolayers of amphiphile. These systems are also known as swollen L_α-phases, because they can be obtained from a binary lamellar phase (of water and amphiphile) by swelling the bilayers with oil — or vice versa.

On length scales large compared to the size of a molecule, amphiphilic systems can be described successfully by continuum theories [1]. In this case, the monolayers are modelled as elastic sheets with a bending rigidity κ and a saddle-splay modulus $\bar{\kappa}$. For fixed topology, as is the case for the lamellar phase not too close to a phase transition to the sponge phase, the integrated Gaussian curvature is a topological invariant, so that $\bar{\kappa}$ gives only an irrelevant contribution to the free energy. Therefore the bending rigidity κ is the elastic constant of interest in this phase.

Dynamic light scattering has been used, in particular, to measure the bending rigidity of monolayers or bilayers [2]. In order to extract the value of the monolayer rigidity κ from these measurements, the measured relaxation rates have to be fitted to expressions obtained from the analysis of a theoretical model of the dynamics of the lamellar phase. Unfortunately, the extracted values of κ in the experiments of Ref. [2] differ by about a factor of three, depending on which mode has been measured. We will argue below that a possible explanation for this discrepancy is that the amplitude of the steric interaction, as predicted from Monte Carlo simulations [3] and field-theoretical calculations [4], is considerably *smaller* than Helfrich's estimate [5].

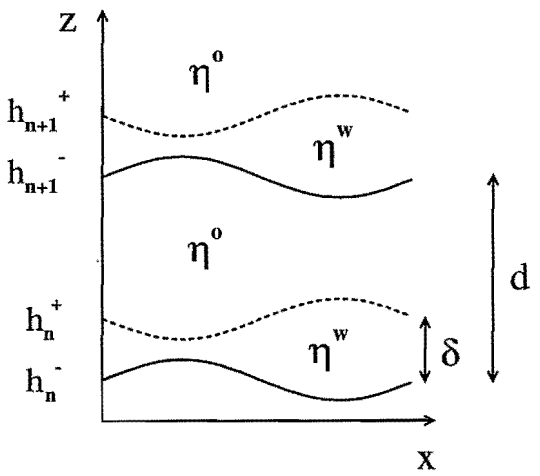

FIG. 1. Stack of membranes in a ternary mixture of water, oil and surfactant. Layer thicknesses and viscosities of the oil- and water-layers are indicated.

A schematic diagram of the swollen lamellar phase is shown is Fig. 1, which also introduces the notation of our model. We divide the stack into unit cells with lattice constant d in the z-direction. Each unit cell consists of a water layer of thickness δ and an oil layer of thickness $d-\delta$. We label the unit cells by an index n, which takes values from $-\infty$ to ∞. Within each unit cell, the oil and water layers are distinguished by an additional index, which is either o for oil or w for water. For example, the pressure of the water in the n-th unit cell is written as $p_n^w(x,y,z)$. In addition, each unit cell contains two different elastic sheets. One of them separates the $(n-1)$-th from the n-th unit cell, the other separates the n-th water layer from the n-th oil layer. The local positions of these two amphiphilic monolayers are denoted $h_n^-(x,y)$ and $h_n^+(x,y)$ respectively. Now it is straightforward to write down the elastic free energy [6]

$$\mathcal{H} = \sum_n \int dx\, dy \left\{ \frac{\kappa}{2} \left((\nabla^2 h_n^+)^2 + (\nabla^2 h_n^-)^2 \right) \right.$$
$$\left. + V_o(d-\delta)(h_n^- - h_{n-1}^+)^2 + V_w(\delta)(h_n^- - h_n^+)^2 \right\} \quad (1)$$

where $V_o(d-\delta)$ and $V_w(\delta)$ describe the direct (steric or electrostatic) interactions across the oil- and water-layers, respectively, and the hydrodynamic equations within each fluid layer

$$0 = \nabla u_n^o\,, \quad 0 = -\nabla p_n^o + \eta^o \nabla^2 u_n^o\,, \quad (2)$$
$$0 = \nabla u_n^w\,, \quad 0 = -\nabla p_n^w + \eta^w \nabla^2 u_n^w\,. \quad (3)$$

This set of equations can be solved by a Fourier ansatz for the directions parallel and a Bloch-like ansatz perpendicular to the average membrane plane; this introduces wavenumbers $q_\parallel$ and $q_\perp$, respectively. In the hydrodynamic limit, $q_\parallel d \ll 1$, there are two *barolinic modes* for $q_\perp d > 0$ with the relaxation rates

$$\omega_1(q_\parallel) = \frac{V_w(\delta)\delta^3}{12\eta^w}\, q_\parallel^2 \qquad \text{(baroclinic I)} \quad (4)$$
$$\omega_2(q_\parallel) = \frac{V_o(d-\delta)(d-\delta)^3}{12\eta^o}\, q_\parallel^2 \quad \text{(baroclinic II)}\,. \quad (5)$$

The baroclinic mode I is characterized by a constant thickness of the oil layers, while the water-layer thickness oscillates parallel to the membrane. Similarly, baroclinic mode II shows a constant thickness of the water layers, while the oil-layer thickness oscillates parallel to the membrane. Therefore, only the membrane interactions across and the viscosity of the water (oil) layers determine the relaxation rate ω_1 (ω_2).

For $q_\perp d = 0$, we obtain the relaxation rates

$$\omega_1(q_\parallel) = \frac{2\kappa}{\eta^w\delta + \eta^o(d-\delta)}\, q_\parallel^2 \qquad \text{(undulation)} \quad (6)$$
$$\omega_2(q_\parallel) = \frac{1}{12}\, \frac{\delta^3(d-\delta)^3\,[V_w(\delta) + V_o(d-\delta)]}{\eta^w(d-\delta)^3 + \eta^o\delta^3}\, q_\parallel^2$$
$$\text{(peristaltic)}\,, \quad (7)$$

again in the hydrodynamic limit. Here, the undulation mode has constant thicknesses of both oil and water layers, while the peristaltic mode is characterized by oscillations in the film thickness parallel to the membranes of both oil and water layers.

The behavior for general $q_\parallel$ and $q_\perp$ can still be calculated analytically, but the expressions become very lengthy [6]. These expressions therefore have to be evaluated analytically. A typical example for the baroclinic modes is given in Fig. 2. It shows a complicated crossover behavior from the $q_\parallel^2$ power law of Eqs. (4) and (5) for $q_\parallel d \ll 1$ to the $q_\parallel^3$ law of a free membrane for $q_\parallel d \gg 1$. Note that the whole function $\omega(q_\perp, q_\parallel)$ enters in a calculation of the scattering intensity in a neutron spin echo experiment, or in a light scattering experiment of very dilute lamellar phases.

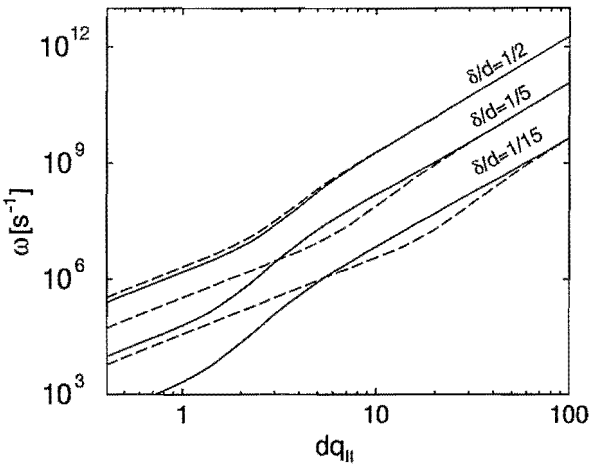

FIG. 2. Relaxation frequencies of the baroclinic mode as a function of the wave vector $q_\parallel$ for different ratios of the thicknesses of oil and water layers, as indicated. Baroclinic mode I and baroclinic mode II are shown by dashed and solid lines, respectively.

Finally, we want to comment on the discrepancy of the bending rigidities, which have been extracted in Ref. [2] from the analysis of the baroclinic and undulation modes. The system studied experimentally is dominated by the steric interaction across the oil layers, with $V_o(d-\delta) = \beta(k_BT)^2\kappa^{-1}(d-\delta)^{-2}$. The universal prefactor β was originally estimated by Helfrich [5] to be $\beta = 9\pi^2/128 = 0.683$, a value which seems to describe the experimental x-ray scattering data quite well. However, Monte Carlo simulations [3] and field-theoretical calculations [4] of the same model give the theoretically more reliable result of $\beta = 0.318$. If the latter result is used instead of Helfrich's estimate (which was employed in Ref. [2]), the discrepancy of the κ-values obtained from the undulation mode, Eq. (6), which is independent of β, and from the baroclinic mode II, Eq. (5), become consistent within error bars. Thus, this is the first indication that the theoretical value of $\beta = 0.318$ agrees with experimental observations.

[1] G. Gompper and M. Schick, in *Phase Transitions and Critical Phenomena*, edited by C. Domb and J. Lebowitz (Academic Press, London, 1994), Vol. 16, pp. 1–176.

[2] F. Nallet, D. Roux, and J. Prost, J. Phys. France **50**, 3147 (1989).

[3] G. Gompper and D. M. Kroll, Europhys. Lett. **9**, 59 (1989).

[4] M. Bachmann, H. Kleinert, and A. Pelster, Phys. Lett. A **261**, 127 (1999).

[5] W. Helfrich, Z. Naturforsch. **33a**, 305 (1978).

[6] T. Schilling, O. Theissen, and G. Gompper, Eur. Phys. J. E **4**, (to appear) (2001).

Publications in refereed journals

Antal T.1,2; Schütz G.M.
1 Universite de Geneve, Switzerland
2 FZ Jülich, Germany
Asymmetric exclusion process with short-range interaction: Some remarks on traffic flow and a nonequilibrium reentrance transition
Phys. Rev. E. 62, 83 - 89 (2000)
23.15.0

Corberi F.1; Gonnella G.2; Lamura A.
1 Univ. Salerno, Italy
2 Univ. Bari, Italy
Phase separation of binary mixtures in shear flow: A numerical study
Phys. Rev. E 62, 8064 - 8070 (2000)
23.30.0

Dudzinski M.1; Schütz G.M.
1 Univ. Köln
Relaxation spectrum of the asymmetric exclusion process with open boundaries
J. Phys. A 33, 8351-8364 (2000)
23.15.0

Eisenriegler E.
Polymers interacting with mesoscopic particles
J. Phys.: Condens. Matter 12, A227-A232 (2000)

Eisenriegler E.
Small mesoscopic particles in dilute and semidilute solutions of nonadsorbing polymers
Journ. Chem. Phys.: 113, 5091-5097 (2000)

Endo H.; Allgaier J.; Gompper G.; Jakobs B.1; Monkenbusch M.; Richter D.; Sottmann T.1; Strey R.1
1Univ. Koeln, Germany
Membrane Decoration by Amphiphilic Block Copolymers in Bicontinuous Microemulsions",
Phys. Rev. Lett. 85 102-105 (2000)
23.30.0

Gompper G.; Kroll D. M.1
1 Univ. Minnesota, Minneapolis, USA
Melting transition of a network model in two dimensions
Eur. Phys. J. E 1, 153-157 (2000)
23.30.0

Gompper G.; Kroll D. M.1
1 Univ. Minnesota, Minneapolis, USA
Statistical mechanics of membranes: freezing, undulations, and topology fluctuations
J. Phys.: Condens. Matter 12 A29-A37 (2000)
23.30.0

Kawasaki M.; Odagaki T.; Kehr K.W.
Absence of self-averaging in the complex admittance for transport through random media,
Phys. Rev. B 61, 5839-5842 (2000)
23.15.0

Kehr K.W.; Koza Z.1
1 Univ. Wroclaw, Poland
Hopping motion of lattice gases through nonsymmetric potentials under strong bias conditions
Phys. Rev. E 61, 2319-2326 (2000)
23.15.0

Kehr K.W.; Koza Z.1
1 Univ. Wroclaw, Poland
Hopping motion of lattice gases through nonsymmetric potentials under strong bias conditions
Phys. Rev. E 61, 72319-2326 (2000)
23.15.0

Lin J.-H.; Baumgärtner A.
Molecular Dynamics simulations of hydrophobic and amphiphatic proteins interacting with a lipid bilayer membrane.
Comput. Theor. Poly. Sci. 10, 97 (2000)
23.30.0
46.10.0

Lin J.-H.; Baumgärtner A.
Stability of a melittin pore in a lipid bilayer a molecular dynamics study.
Biophys. J. 78, 1714 (2000)
23.30.0
46.10.0

Pigorsch C.; Schütz G.M.
Shocks in the asymmetric simple exclusion process in a discrete-time update
J. Phys. A 33, 7919-7935 (2000)
23.15.0

Schwarz U.S.1; Gompper G.
1 Weizmann Inst. Rehovot, Israel
Stability of Inverse Bicontinuous Cubic Phases in Lipid-Water Mixtures
Phys. Rev. Lett. 85 1472-1475 (2000).
23.30.0

Schwarz, U.S.1; Gompper G.
1MPI-KG, Golm and Weizmann Inst. Israel
Stability of bicontinuous cubic phases in ternary amphiphilic systems with spontaneous curvature
J. Chem. Phys. 112, 3792-3802 (2000)
23.30.0

Schütz G.M.
Exact tracer diffusion coefficient in the asymmetric random average process.
J. Stat. Phys. 99, 1045-1049 (2000)
23.15.0

Schütz G.M.
Phasenübergänge in offenen Vielteilchensystemen fern vom Gleichgewicht
Phys. Blätt. 56, 69 - 73 (2000)
23.30.0

Trimper S.; Täuber U.C.; Schütz G.M.
Reaction-controlled diffusion
Phys. Rev. E 62, 6071-6078 (2000)
23.30.0

Other publications

Baumgaertner A.; Sambeth R.
Models of Cell Locomotion
In Stochastic Dynamics and Pattern Formation in Biological and Complex Systems, ed. by S.Kim, K.Lee, W.Sung,
AIP Conference Proceedings 501, Melville, New York, 2000.
23.30.0
46.10.0

Schütz G.M.
Dynamical theory of steady state selection in open driven diffusive systems, in: Traffic and Granular Flow '99, pp. 227 - 232, D. Helbing, H. J. Herrmann, M. Schreckenberg and D. E. Wolf (eds.), (Springer Verlag, Berlin, 2000)
23.30.0

Schütz G.M.
Exactly Solvable Models for Many-Body Systems Far From Equilibrium, in: Phase Transitions and Critical Phenomena 19, pp. 1 - 251, C. Domb and J. Lebowitz (eds.), (Academic Press, London, 2000), 23.15.0

Invited Talks

Baumgärtner A.
MD Simulations of Ionchannels
Second workshop on Protein-Lipid Interactions.
Brüssel, Belgien
17.11.-19.11. 2000
23.30.0

Baumgärtner A.
MD simulations of membrane proteins
Univ. Wageningen
20.12.2000,
23.30.0

Baumgärtner A.
Motility of biological cells.
Debye Winterschool.
Utrecht, Niederlande
22.3.-23.3. 2000
23.30.0

Baumgärtner A.
The protein-lipid interface
First meeting on protein-lipid interaction.
Brüssel, Belgien
23.4.-24.4. 2000
23.30.0

Baumgärtner A.
The protein-lipid interface
Univ. Utrecht, Niederlande
14.12.2000
23.30.0

Gompper G.
Applications of Random Surfaces to Fluid Mixtures
Reihe von zwei eingeladenen Vorträgen beim "10th Workshop on Statistical Mechanics and Non-perturbative Field Theory (SMFT 2000)"
Bari (Italy), 25. - 27. September 2000
23.30.0

Gompper G.
Recent Results on the Physics of Membranes
Eingeladener Vortrag beim "French-German Symposium on Present and Future Topics in Wetting"
Bad Honnef, 18. - 20. September 2000
23.30.0

Gompper G.
Soft Matter: Amphiphile, Membranen, Mikroemulsionen
Fachbereich Physik, Universität Essen
2. 2. 2000
23.30.0

Gompper G.
Statistical Physics of Membranes: Undulations, Defects, Topology Fluctuations
Institut für Biologische Informationsverarbeitung, FZJ
10. 3. 2000
23.30.0

Gompper G.
Weiche Materie: Amphiphile, Membranen, Schwamm-Phasen
Fakultät für Naturwissenschaften, Universität Magdeburg
7. 11. 2000
23.30.0

Schütz G.
Aging in Reaction-diffusion systems
Fachbereich Physik, Universität Halle
27. 4. 2000
23.15.0

Schütz G.
Nonequilibrium relaxation law for entangled polymers
83th Statistical Mechanics Conference, Ruttgers University, USA
7. 5. 2000
23.30.0

Schütz G.
Nonequilibrium relaxation law for entangled polymers
Department of Chemistry and Chemical Biology, Cornell University, USA
21. 5. 2000
23.30.0

Schütz G.
Phasenübergänge in offenen Vielteilchensystemen fern vom Gleichgewicht
64. Physikertagung, Dresden
22. 3. 2000
23.15.0

Other talks

Schütz G.
Nonequilibrium relaxation law for entangled polymers
Meco 25, Pont-a-Mousson, Frankreich
11. 3. 2000
23.30.0

Schütz G.
Stability and Branching of Shocks
DPG-Frühjahrstagung, Regensburg
30. 3. 2000
23.15.0

Posters

Döbereiner H.-G.; Gompper G.; Haluska C.; Petrov P. G.
Measurement of Spontaneous Curvature
Poster beim "3rd European Biophysics Congress", München, 9. - 13. September 2000
23.30.0

Gwan J.-F.; Baumgärtner A.; Seifert R.; Kaupp U.B.
Computer simulation study of the binding effect of various ions in cyclic
nuleotide-gated channels.
3rd European Biophysics Congress
9.-13.Sept. 2000, Muenchen
23.30.0
42.50.0

Sambeth R.; Baumgärtner A.
A 2-d model for cell locomotion based on actin polymerization.
Biophysics and biochemistry of motor proteins
27.9.-1.10.2000, Banff, Canada
23.30.0
46.10.0

Sambeth R.; Baumgärtner A.
A complete one dimensional model for force generation based on the
treadmilling of filaments.
Numerical simulations on polymer and cell dynamics.
13.6.-16.6.2000, Honnef
23.30.0
46.10.0

Sambeth R.; Baumgärtner A.
Signal induced motility in a complete two dimensional model for amoeboid
motion based on the polymerization of actin.
3rd European Biophysics Congress
9.-13.Sept. 2000, Muenchen, 23.30.0, 46.10.0

Schütz G.
Emergence of macroscopic non-equilibrium behaviour from microscopic dynamics in quantum spin chains
DPG-Frühjahrstagung, Regensburg
27. 3. 2000
23.15.0

Lecture courses

Baumgärtner A.
Einführung in die theoretische Biophysik I.
Universität Duisburg, V2
SS 2000

Baumgärtner A.
Einführung in die theoretische Biophysik II.
Universität Duisburg, V2
WS 2000/2001

Baumgärtner A.
Theoretische Physik fürs Lehramt II.
Universität Duisburg, V2, Ue2
WS 1999/2000

Eisenriegler E.
Statistische Physik von Polymeren
Universität Düsseldorf, 2-std.
SS 2000

Schütz G.
Gläser: Physikalische Konzepte und numerische Methoden
Universität Bonn, 2-std.
WS 2000/2001

Internal seminars

Baumgärtner A.
Simulationen von Membranproteinen
Soft Matter Tagung
Heimbach, 18.-20.10.2000
23.30.0

Baumgärtner A.
Simulationen von Membranproteinen
VSR-Kommission
Juelich, 7.11.2000
23.30.0

Gompper G.
Fluctuation Spectra of Non-Spherical Vesicles
Soft Matter Tagung
Heimbach, 18.-20.10.2000
23.30.0

Lamura A.
Equilibrium and Dynamical Properties of Microemulsions
Soft Matter Tagung
Heimbach, 18.-20.10.2000
23.30.0

Lamura A.
Phase separation of binary mixtures in shear flow
Seminarvortrag, IFF, FZ Jülich, 25.5.2000
23.30.0

Schütz G.
Non-equilibrium relaxation law for entangled polymers
Joint Soft Matter Seminar, IFF, FZ Jülich, 24.2.2000
23.30.0

Institute Theory III

General Overview

Research Areas

The institute *Theory III* investigates the mechanisms of the formation of structures and their consequences in condensed matter. The research starts from electronic properties which define the shortest length and time scales, but it also encompasses the macroscopic consequences. The analytical and numerical investigations are in many ways closely connected with experimental studies performed in other groups of the IFF, but also with activities in other institutes of the Research Center Jülich.

Central points of interest for the research in *Theory III* are in the field of electronic structure of solids (F&E-Nr. 23.20.0). Materials classes under consideration are metals and semiconductors, specifically with respect to their importance for information technology (F&E-Nr. 23.42.0). A second mainstream is formed by cooperative phenomena in condensed matter (F&E-Nr. 23.15.0). Questions here aim at the dynamics of structure and pattern formation and the statistical mechanics of order and disorder processes. Specific activities in the field of complex fluids (F&E-Nr. 23.30.0) are concerned with structure and dynamics of soft matter. The research of *Theory III* employs all analytical and numerical techniques applicable to many-body problems in condensed matter. In addition the development of new methodological concepts and numerical procedures is part of our research interest. The development of parallel program codes adapted to massively parallel computers has received special attention in recent years.

The explanation of the microstructure and dynamics of real solids requires the understanding of the electronic properties. One of the most important methods for the calculation of the electronic structure of real solids is the density functional theory in connection with appropriate numerical procedures. While in recent years bulk properties of metals and semiconductors have been at the center of our research a main concern now is directed towards the understanding of surface and interface properties, with particular emphasis on magnetism.

The technological success of the GMR-effect has also triggered new theoretical efforts in layered structures. A particular related problem is the tunneling of electrons through epitaxial multilayers of the type ferromagnetic-insulating-ferromagnetic. It was recently demonstrated by us that the tunneling process in this case can be understood in terms of the complex band structure of the bulk insulator, specifically the metal-induced gap-states in the energy-region of the gap. The decay of the wavefunction into the insulating region is described by an imaginary part of the Bloch vector. The spectral distribution of this part of the wave-vector has been calculated for various semiconductors like Si, GaAs, etc. One result is that in most cases and for large enough film thickness the tunneling is dominated by states of normal incidence on the interface. Based on these results we can discuss the spin-dependent tunneling in those junctions.

The growth of such layered structures is achieved through hetero- or homo-epitaxy, where the layers grow on some substrate of different or of the same material. For hetero-epitaxy with large lattice mismatch this growth-process does not give homogeneously growing layers but results in isolated islands growing in height, but not in width. To understand the atomistic reasons for different growth processes, pseudopotential-calculations based on local density-functional concepts were performed. In particular it was tried to understand the influence of a surfactants like As, Sb which can change the Stranski-Krastanov island growth into layer growth. These calculations give detailed explanations for the different observed growth modes and they are in full agreement with experiments for example for homo-epitaxial growth of As- or Sb-covered Si(111)-surfaces.

On larger scales the lattice-misfit between the substrate and a cluster adsorbed during the hetero-epitaxy-process leads to repulsive elastic forces between the adsorbed atoms of the cluster. This is a collective effect which becomes increasingly important with the size of the growing adsorbate cluster. We have studied the influence of the resulting elastic stress onto the growth-modes of the clusters. Large-scale computer-simulations employing a recently developed multigrid-scheme gave quantitative results for the different growth patterns. A scaling-theory was able to explain the large scale behavior. New laws for the growth-rates depending on a new elastically controlled length scale are obtained.

The investigation of glasses and supercooled liquids as disordered materials was further extended by molecular dynamics methods. The spatial heterogeneity is a major reason for the non-standard dynamics of the glass. In particular it is thought that this heterogeneity is the reason for non-exponential relaxation observed in experiments. To understand this effect, Lennard-Jones models and several other realistic microscopic models for

glasses were investigated. Large-scale simulations were performed concerning the diffusion and relaxation properties and their dependence on temperature and time. A non-Gaussian distribution of fluctuations is observed and traced back to collective hopping of groups of atoms. Based on our simulations we are lead to assume that this mechanism is common to all glass-forming systems. In consequence this heterogeneity will always increase in the intermediate time-domain, the beta-relaxation region, at all temperatures and in many types of materials.

Microstructural features evolve in crystalline solids by reaction-diffusion kinetics of defects. The results depend crucially upon the spatial dimension of the underlying diffusion process – as is well known for example in the process of Ostwald-ripening of inclusions – which here is commonly assumed to be three-dimensional. During irradiation of metals, however, clusters of interstitials will rather give rise to one-dimensional diffusion. It can even be argued, that additional transversal diffusion can lead to reaction-diffusion kinetics somewhere intermediate between one and three dimensions. An analytical theory for this effect is fully confirmed by Monte-Carlo simulations.

A non-scientific but nevertheless seemingly important activity during this past year 2000 was the organisation of the events for "2000: Jahr der Physik", a joint effort by the German Physical Society (DPG) and the sponsoring Bundesministerium für Bildung und Forschung (BMBF), an effort towards the "public understanding of science". Some 450 physicists have been involved in the presentation of exhibitions and lectures during five major events in Berlin and Bonn, the number increasing to about 2000 when one considers furthermore the around 200 satellite-events throughout the country. The reports about resonance in the public and in the press have been rather encouraging. As the coordinator for the German Physical Society I would like to thank the board of directors of the Research Center Jülich, J. Treusch, R. Wagner and H. Grübel, for their emphasis and continuous support during this year. I thank my colleagues at IFF for their help and patience in many occasions. My very special thanks go to the members of this institute Theory-3 for their understanding, support and encouragement, and for their generous tolerance in this special year 2000.

H. Müller-Krumbhaar

Personnel 1999/2000 and areas of activity

Scientific Staff

Dr. E. Brener	Kinetics of phase transformations	23.150
Prof. P.H. Dederichs	Electronic properties, interfaces and layered systems	23.200
Dr. K. Mika	Structure maps for binary systems	23.150
Prof. H. Müller-Krumbhaar, -Institute Director-	Non-linear dynamics of dissipative systems	23.150
Dr. R. Rzehak	Polymer dynamics and hydrodynamic flow	23.150
Dr. H. Schober	Statics and dynamics of glasses, defects and phonons	23.300
Prof. K. Schroeder	Electronic and atomic structure of defects in semiconductors	23.420
Dr. H. Trinkaus	Dissipative structure formation, reaction-diffusion problems	23.150,23.805, 23.420
Dr. R. Zeller	Electronic structure and magnetic properties of metals	23.200
L. Snyders	Secretary	

Visitors

Dr. I.A. Cabria (SP)	Relativistic KKR-Green's function methods	23.200
Dr. D. Caprion (F)	Dynamic of amorphous and liquid Se	23.300
Dr. H. Emmerich	Hydrodynamics of wetting	23.150
Dr. M. Freyss (F)	Spin-dependent transport	23.200
Dr. J. Matsui (JP)	Dynamics at the glass transition	23.300
Prof. V. Kozub	Phonons in amorphous materials	23.300
Dr. V. Luchnikov	Voronoi analysis of glasses	23.300
Prof. V. Marchenko (GUS)	Elastic effects during phase transformations	23.150
Dr. Ph. Mavropoulos (GR)	Complex bandstructure and transport	23.200
Prof. C. Misbah (F)	Solidification processes, non-linear dynamics	23.150
Dr. N. Papanikolaou (GR)	Ab-initio calculations of forces and lattice relaxations	23.200
Prof. N. Stefanou (GR)	Mesoscopic transport	23.200
Dr. D. Temkin (GUS)	Pattern formation at interfaces	23.150
Dr. J. Galanakis (GR)	Complex bandstructure and transport	23.200

PhD and Diploma Students (University = RWTH Aachen)

MSc. N. Atodiresei	Dispersion of localized electronic states of semiconductor surfaces	23.420
Dipl.-Phys. A. Antons	Ab-initio calculations on surface reconstruction	23.420
Dipl.-Phys. A. Baranov (GUS)	Magnetic adatoms of surfaces	23.200
Dipl.-Phys. V. Bellini (I)	Electron structure of magnetic layered systems	23.200
Dipl.-Phys. R. Berger	Polar surfaces of III-V-semiconductors	23.420
Dipl.-Phys. Y. Cao	Structural Stability of surfactant-covered semiconductor surfaces	23.420
Dipl.-Phys. F. Gutheim	Cluster growth on surfaces	23.150
Dipl.-Phys. M. Hartmann	Collective effects of cracks and dislocations	23.150
Dipl.-Phys. H. Höhler	Defects in semiconductors	23.420
Dipl.-Phys. D. Kienle	Transport coefficients in polymer solutions	23.150
Dipl.-Phys. M. Kluge	Binary metallic glasses	23.300
Dipl.-Phys. Wi. Kromen	Point defects and interfaces in Nitride-semiconductors	23.420
Dipl.-Phys. B. Nonas	Fully relativistic band structure methods	23.200
Dipl.-Phys. R. Spatschek	Collective effects of cracks in solids	23.150
Dipl.-Phys. O. Wunnicke	Tunneling Magneto Resistance (TMR)	23.200

Complex Band Structure and Tunneling through Insulators

Ph. Mavropoulos, N. Papanikolaou, M. Freyss, R. Zeller, and P. H. Dederichs
Institute IFF-Theory III

We investigate the importance of Metal-induced Gap States for the tunneling of metal electrons through insulator films. By introducing an imaginary part κ to the wavevector in order to describe the decay of the wavefunction in the insulator, we obtain the complex band structure in the gap region. The spectrum of the decay parameters κ is calculated for the semiconductors Si, Ge, GaAs, and ZnSe. In most cases, for large enough film thicknesses the tunneling is dominated by states of normal incidence on the interface; possible exceptions are considered. Based on our conclusions, we discuss the spin-dependent tunneling in Fe/Semiconductor/Fe (001) junctions.

F&E-Nr: 23.20.0

This report aims at understanding the tunneling through epitaxial Ferromagnet/Insulator/Ferromagnet junctions. In the literature the tunneling is often described by Jullière's model [1] or by a simple potential barrier, i.e., by approaches which lack microscopic justification. In a recent letter [2] we demonstrate that the tunneling process through insulators can be understood in terms of the complex band structure of the bulk insulator, in particular the Metal-induced Gap States (MIGS) in the energy region of the gap. As model systems for our discussion we use Fe/I/Fe sandwiches, where I refers to the semiconductors Si, Ge, GaAs and ZnSe. In the bulk of a crystal, the periodicity demands that the Bloch $\mathbf{k}$-vectors are purely real. But near a crystal surface or interface one can match a bulk wavefunction of complex $\mathbf{k}$ with the solution outside the half-crystal [3]. For the interface between a metal and an insulator the most important of such states are MIGS, being itinerant in the metal but exponentially decaying in the insulator (for energies in the gap). Such solutions for complex $\mathbf{k}$-vectors form the complex band structure of the insulator. Although they only occur at surfaces or interfaces, they are solutions of the bulk Schrödinger equation, since the interface-induced changes of the potential are confined in their greatest part to the first one or two monolayers. For the considered transport problem, under an infinitesimal applied voltage metallic electrons with energies at the Fermi level E_F impinge on the insulator interface. Due to the assumed perfect epitaxy the in-plane component $\mathbf{k}_{||}$ of the incident wave vector $\mathbf{k} = (\mathbf{k}_{||}, k_z)$ is conserved. Therefore in the insulator only evanescent states with a given (real) energy E_F and a real $\mathbf{k}_{||}$-component are allowed, so that only the perpendicular component $k_z = q + i\kappa$ can be complex, with the "decay parameter" κ describing the exponential decrease of the wavefunction in the insulator.

The central problem for tunneling is therefore the determination of these decay parameters κ, in particular the search for the smallest possible κ-value κ_{min} for a given Fermi energy in the gap. In fact in the limit of large barrier thickness only the state with the smallest decay parameter, $\kappa_{\min}$, survives and contributes to the tunneling current. The determination of $\kappa_{\min}$ can proceed in two steps. Firstly for given values of $\mathbf{k}_{||}$ and E_F one has to determine, out of the infinitely many solutions with different decay parameters, the one with the smallest $\kappa > 0$ value. In the second step one can then vary $\mathbf{k}_{||}$, and search for the absolute minimum $\kappa_{\min}$ compatible with E_F. Of course, states with κ close enough to $\kappa_{\min}$ will be also important.

The method used in this work for the calculation of the complex band structure is the simplest possible: we apply the local pseudopotential plane-wave technique with empirical form factors. Since these form factors have been fitted to spectroscopic data, this method gives a reasonably good description of the band structure in the gap region, this being the most important for the tunneling. Clearly local density functional calculations give a much better overall description of the band structure, but they have the well-known deficiency of underestimating the band gap by about 50%. Thus the above method is well suited for our purpose.

In the following we can only shortly sketch some of our results. Fig 1 shows the band structure of ZnSe for perpendicular incidence ($\mathbf{k}_{||} = \mathbf{0}$) on a ZnSe (001) interface, the real bands with k_z real in the middle panel and the complex parts for $q = 0$ in the left and for $q = 2\pi/a$ in the right panel. Here directly the dispersion of the decay parameter κ as a function of energy is plotted. For a given energy in the band gap the one with the smallest κ is that of symmetry Δ_1 (the identity representation) connecting the top of the Δ_1 valence band to the bottom of the Δ_1 conduction band. We expect this to be true quite generally when we are dealing with a direct gap characterized by a Δ_1 valence band maximum and a Δ_1 conduction band minimum. Then the loop connecting these particular extrema will be smaller than any other one, and so will be the corresponding value of the decay parameter.

The next larger κ-values arise from the degenerate Δ_3 and Δ_4 bands, and, additionally, infinitely many other inverse-parabolic states exist starting from higher bands,

having much larger κ-values. Departing from the $\bar{\Gamma}$-point, we know that the valence states are lowered energetically, the conduction states are raised and the gap increases. For this reason it is expected that the loops at $q = 0$ become larger for non-zero $\mathbf{k}_{||}$ values, and the corresponding values of κ increase.

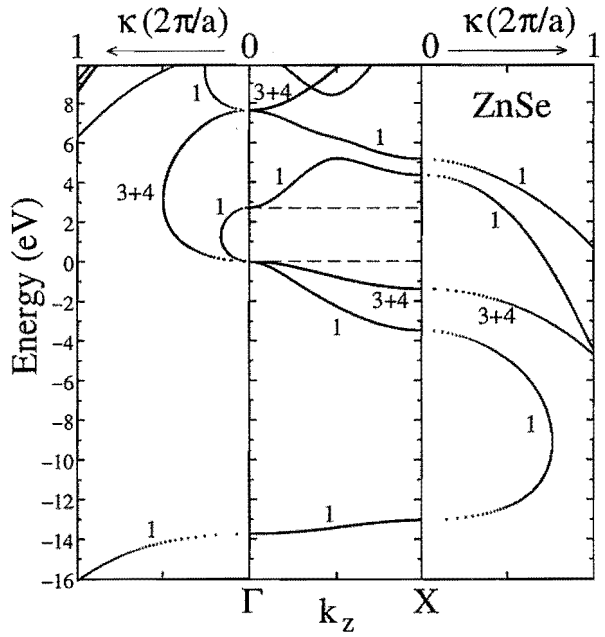

FIG. 1. The complex band structure of ZnSe, for $\mathbf{k}_{||} = \mathbf{0}$, at $q = 0$ (left panel) and $q = 2\pi/a$ (right panel). The real lines are forming loops and free-electron-like parabolas.

Thus, by proceeding the search for $\kappa_{\min}$, one can scan the whole two-dimensional surface Brillouin zone at a given energy. One would thus form a constant-energy surface in the $(\mathbf{k}_{||}, \kappa)$-space. This consists of many branches, corresponding to the (infinitely) many different complex bands for any given $\mathbf{k}_{||}$, but our attention should be focused on the lowest-lying one. This is shown in Fig. 2 for four materials, namely Si, Ge, GaAs, and ZnSe, for a typical value of E_F in the middle of the gap. We see that in all four cases the decay parameter is minimized at the $\bar{\Gamma}$-point. We also see that the difference of κ at the flatter part of the branch and at $\mathbf{k}_{||} = \mathbf{0}$ ($\kappa_{\min}$) increases monotonically with the band gap, this also following the order Si<Ge<GaAs<ZnSe. However other cases can also occur. For instance, for Si the $\kappa_{\min}$-state is determined by the complex band structure close to the X-point, if the Fermi energy approaches the conduction band minimum. The above results have important consequences for tunneling. In the metal only states of Δ_1-symmetry (in the nomenclature of the ZnSe T_d-symmetry group) can couple to the Δ_1-states in the semiconductor and thus for large insulator thicknesses only metallic states at the $\bar{\Gamma}$-point and with Δ_1-symmetry determine the tunneling currents. The different availability of these Δ_1-states in the majority and minority bands leads to magnetoresistance. Our analysis is fully consistent with the *ab initio* results of MacLaren *et al.* [4].

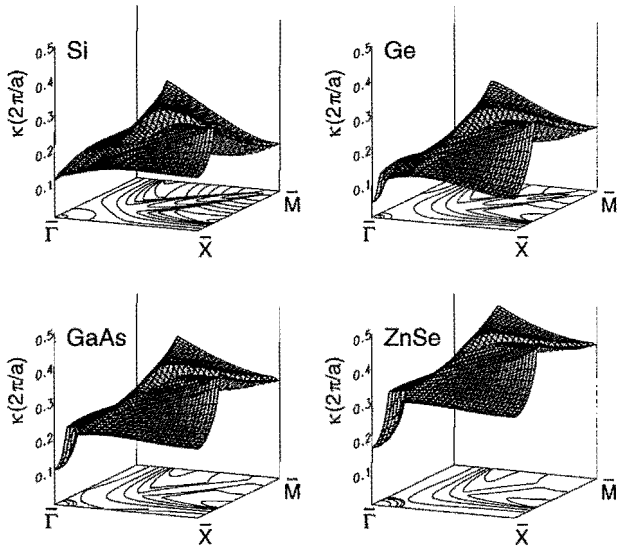

FIG. 2. The constant-energy surfaces $\kappa = \kappa(\mathbf{k}_{||})$ drawn in one-fourth of the surface Brillouin zone for Si, Ge, GaAs, and ZnSe. Only the lowest positive branches of the decay parameter κ are drawn. for an energy in the middle of the band gap. The decay parameter has its minimum at the $\bar{\Gamma}$-point in all four cases.

In short we have shown that conclusions about the tunneling in FM/I/FM epitaxial systems can be drawn by a simple inspection of the complex band structure of the insulator in the gap region. For the above cases this has been obtained using simple pseudopotential techniques, and as a matter of fact it can be understood, in a first approximation, just by looking at the real band structure and by noticing the symmetry of the real bands and their curvature at the minima and maxima. Thus it constitutes a very useful tool for the understanding and prediction of tunneling phenomena.

[1] M. Julliere, Phys. Lett. **54A**, 225 (1975)

[2] Ph. Mavropoulos, N. Papanikolaou, and P. H. Dederichs, Phys. Rev. Lett. **85**, 1088 (2000)

[3] V. Heine, Proc. Phys. Soc. **81**, 300 (1962); Surf. Sci. **2**, 1 (1964)

[4] J. M. MacLaren, X.-J. Zhang, W. H. Butler, and Xindong Wang, Phys. Rev. B **59**, 5470 (1999)

The Early Stage of Surfactant-mediated Homoepitaxy: Formation of Small Clusters on Si(111):As and Si(111):Sb

A. Antons, R. Berger, K.Schroeder, S.Blügel*
*Institute IFF-Theory III and *IFF-Electronic Properties*

Experimental observations of island growth during homoepitaxy on surfactant(As, Sb)-covered Si(111) are explained by *ab initio* calculations of the structure and binding energies of small clusters of Si-adatoms. We show that on Si(111):As the growth of double-layer steps with (1 × 1) structure is established already at an island size containing four Si-adatoms. On the contrary, on Si(111):Sb the growth proceeds by an alternating sequence of (1 × 1) and ($\sqrt{3} \times \sqrt{3}$) structures with monolayer steps. We find that individual Sb-trimers are nucleated on Si(111):Sb(1 × 1) terraces leading to a ($\sqrt{3} \times \sqrt{3}$) Sb-trimer structure on top of (1 × 1) terraces.

F&E-Nr: 23.42.0

The often observed Stranski-Krastanov growth mode in heteroepitaxial systems can be changed into layer growth by the use of surfactants. Using monolayers of group-V elements(As, Sb) on Si the surface reconstruction is modified due to the extra electron of the surfactant atoms. While Si(111):As shows a (1 × 1) surface structure in equilibrium, Si(111):Sb shows a ($\sqrt{3} \times \sqrt{3}$) structure. To study the effect of surfactants on island growth experiments of homoepitaxy on (As, Sb)-covered Si(111) have been performed [1]. On Si(111):As only islands with double-layer steps are found, whereas with Sb as surfactant, monolayer steps are observed and subsequent terraces show an alternating sequence of (1×1) and ($\sqrt{3} \times \sqrt{3}$) structures. From previous theoretical results [2] we know that the diffusion barrier for Si adatoms on top of the surfactant layer is comparable to the barrier for exchange with a surfactant atom. We have found that the equilibrium position of the Si adatom on a (1 × 1) terrace is the substitutional position. It can be reached by exchange of a single Si adatoms with an (As,Sb)-surfactant atom which is lifted to a NN adatom-site binding to the Si atom.

The following questions arise: (1) What is the sequence of clustering of substitutional Si atoms on the surfactant covered surface, (2) at what island size is the double layer step manifested on Si(111):As, and (3) when does the growth on Si(111):Sb start to deviate from that on Si(111):As (on the (1 × 1) terrace)?

We have investigated the structure and energies of small clusters ($n \leq 4$) of substitutional Si atoms decorated with an equal number of (As,Sb)-surfactants [3]. On Si(111):As(1×1) we find stable structures for compact clusters with increasing binding energies per substitutional Si atom. In Fig. 1 the energy gained in each step compared to the individual exchange on the (As, Sb)-covered (1×1) terrace is plotted together with the most stable structures of the clusters.

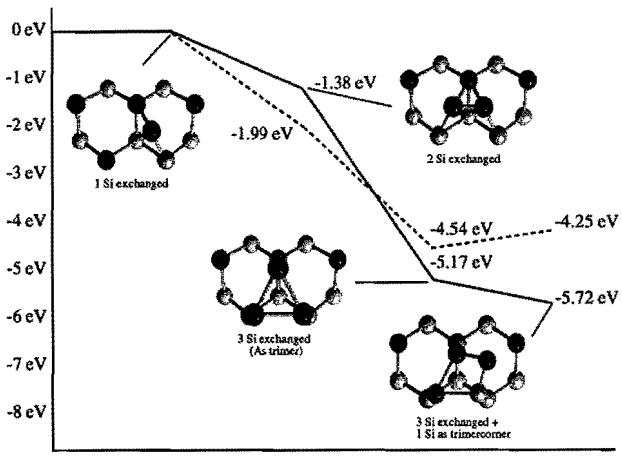

FIG. 1.
Development of small clusters on surfactant covered Si(111) during homoepitaxy. (a)**As**: The full line indicates the energy $E_{cl}^n - nE_B$ which is gained by an n-cluster compared to n isolated exchanged atoms. The relative energies between two configurations show the energy difference $E_{cl}^n - E_{cl}^{n-1} - E_B$ between a cluster with n Si atoms and an (n-1)-cluster plus an isolated exchanged Si atom. (b)**Sb**: The dashed line shows that an Si atom added to an Sb trimer leads to an increasing energy, leading to a ($\sqrt{3} \times \sqrt{3}$) trimer structure on top of the (1 × 1) terrace as is experimentally observed.

The structures are stabilized by the saturation of all bonds. Generally, Si dangling bonds are avoided, i. e. all Si atoms try to obtain a tetrahedral neighborhood, and the (As, Sb) atoms form three bonds and one doubly occupied dangling bond. In particular, the Si substitutional dimers show a large variety of possible metastable structures (see Fig. 2). The most stable dimer is shown in Fig. 1, it consists of two neighboring substitutional Si atoms, and the replaced As atoms each bind to one of the Si atoms and to the same neighboring As atom on the terrace. They also bond to each other, thus the configuration satisfies the bond saturation rule.

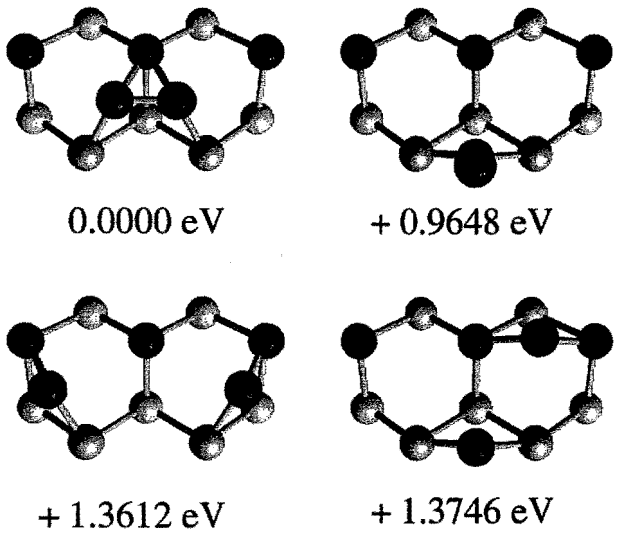

FIG. 2.
Metastable structures of a cluster containing two substitutional Si atoms on Si(111):As. The structures differ by the bonding of the As atoms replaced via an exchange step by the Si adatoms. Only when the two As atoms **bond to each other** and to the same As neighbor on the terrace the bond saturation rule is fulfilled. This constitutes the most stable dimer cluster. The energies are relative to this most stable dimer.

In the trimer the three exchanged Si atoms are located at neighboring sites in the As-layer, constituting a triangle which locally completes a double layer, and the three replaced As-atoms form a T4-centered trimer on top of the Si atoms. The fourth attached Si atom replaces one of the As atoms of the trimer and lifts it to a nearly ideal H3-position in the upper layer of the next double layer while the Si atom sits in the lower layer. This attachment is energetically favorable compared to the individual exchange on the As covered terrace. Thus, this cluster of four exchanged Si atoms (decorated with four As atoms) is the nucleus for the double layer islands observed in experiments. The critical nucleus for island growth on Si(111):As(1×1) shrinks to zero, since all clusters in the sequence have a higher binding energy per Si atom than the individual substitutional Si atom. The growth of the tetramer then proceeds by attachment of additional Si atoms lifting the other two As atoms also to the next layer. Our proposal is that then the neighboring As atoms from the terrace are replaced by Si atoms establishing on each side of the triangle a structure similar to an As decorated step edge of $(\bar{1}\bar{1}2)$ orientation. Further growth proceeds very similar to the motion of steps.

On Si(111):Sb(1×1) the clustering follows the same sequence as for As coverage up to $n = 3$. But the fourth Si atom is more favorably exchanged on the Sb-covered terrace rather than built into the existing Sb trimer. It serves as a nucleation center for a new Sb-trimer on top of a full Si double layer. Thus, for Sb-coverage individual T4-centered Sb trimers are formed on Si(111):Sb(1×1) which can grow to the coherent $(\sqrt{3}\times\sqrt{3})$ structure found in equilibrium for Si(111):Sb.

In summary, our findings are in full accord with the experimental observations. The different growth behavior of As- and Sb-covered Si(111) can be understood on the basis of these calculations. To establish a full kinetic picture, we are currently calculating the barriers for the qualitatively different attachment steps at clusters: from single substitutional Si atoms to dimers to trimers and to tetramers, and also at straight double steps of various orientations. We have also calculated the diffusion and exchange barriers for Si adatoms on the $(\sqrt{3}\times\sqrt{3})$ terrace of Si(111):Sb in order to understand the formation of the (1×1) structure [4]. The results show that the effective diffusion is much faster on the $(\sqrt{3}\times\sqrt{3})$ equilibrium terraces than on the (1×1) islands. This helps to understand the details of the island development on Si(111):Sb. In experiments, the (1×1) islands appear to be large and compact whereas the $(\sqrt{3}\times\sqrt{3})$ Sb-trimer structures on top of these island are very small clusters down to the scale of individual trimers.

[1] B. Voigtländer *et al.*, Phys. Rev. B**51**, 7583 (1995).
[2] K. Schroeder *et al.*, Phys. Rev. Lett. **80**, 2873 (1998).
[3] A. Antons *et al.*, Phys. Rev. B, to be published.
[4] K. Schroeder *et al.*, Phys. Rev. B, to be published.

Epitaxial Growth with Elastic Interaction: Layer and Cluster-Growth

F. Gutheim, H. Müller-Krumbhaar, and E. Brener
Institute IFF-Theory III

Heteroepitaxial growth of clusters in presence of elastic strain has been studied by means of a multi-grid Monte Carlo simulation. Deformation of the underlying substrate typically leads to a repulsive $1/r^3$ interaction-potential between the adsorbed atoms. We find an increased effective fractal dimension d_f on small scales, exhibiting a crossover to the conventional dimension of diffusion limited aggregation (DLA) on large scales. We show that the growth velocity of an advancing fractal step grown from a lattice gas of finite density reflects this crossover phenomenon and is linked to the fractal dimension of the aggregate by through the matching of length-scales.

F&E-Nr: 23.15.0

In heteroepitaxial growth the lattice mismatch between the adsorbed layers and a substrate of different material in general leads to elastic deformation of the substrate lattice. A single adsorbed cluster up to some limiting size will acquire the lattice structure of the substrate apart from a small local change in the lattice parameter. This "coherent" lattice deformation causes elastic stresses in both the adsorbate and the substrate, leading to effective long-range interactions between the adsorbate atoms mediated by substrate-deformations. This effective elastic interaction potential between any two adsorbed atoms is typically repulsive and depends on their distance r like $1/r^3$ [1].

Low deposition rates combined with sufficiently low surface diffusivity – and in particular edge diffusivity – lead to the formation of monatomic ramified clusters as long as the coverage remains small. This process has been studied in great detail under the name "diffusion limited aggregation" (DLA) [2]. Incorporating elastic effects the resulting overall fractal clusters look generally denser than clusters without long-range repulsive interaction and their structure can be characterized by an increase in the effective fractal dimension $d_{\text{eff}} > 1.7$ on short length-scales exhibiting a change [3] to conventional DLA-structure without interaction $d_f \approx 1.7$ at a crossover-length r_X. Thus the properties of the growing cluster change when the radius exceeds a critical radius r_X. This crossover-radius depends on the strength and the range of interaction, but remains finite even for the long-range elastic interaction without cutoff.

Feeling the repulsion of the tips of the cluster, a diffusing particle will enter a deep bay-like opening or fjord with increased probability. Having entered, the particle will diffuse the characteristic length r_X along the fjord before being captured by one of the walls, depending on the potential barrier, see [3] for details. As a result, the crossover length r_X can be understood as a kind of mean penetration depth.

While DLA-clusters grow by successive diffusion and aggregation of single ad-atoms, our multi-particle growth model based on [3] allows for the interaction and diffusion of many ad-atoms at a time and models an advancing fractal step on the substrate. On the basis of M. Uwaha's and Y. Saito's model [4] we study the steady state properties of a cluster growing inside a channel of width L with periodic boundary conditions perpendicular to the direction of growth. Far away from the growth front the lattice gas density n_g is kept constant.

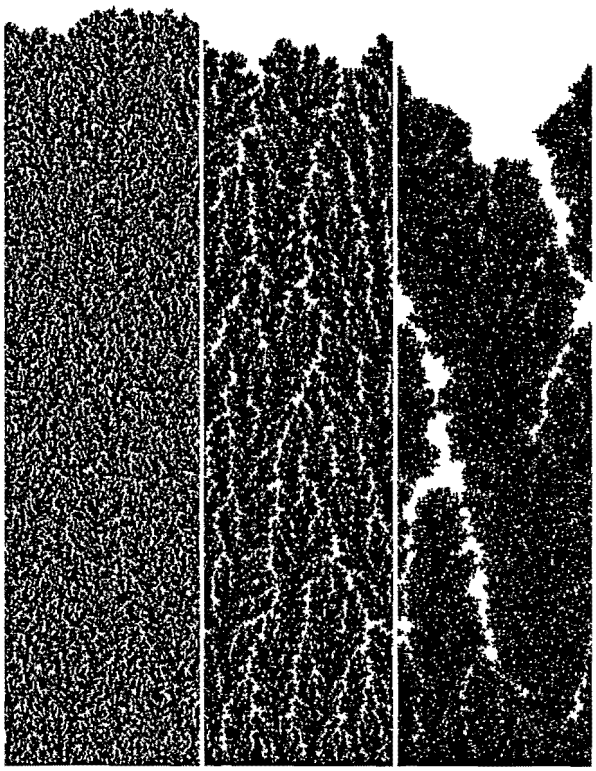

FIG. 1. Layers grown from lattice gas with density $n_g = 0.3$, increasing interaction strength from left to right, width $L = 1024$ lattice units

Our study is based on a two dimensional square lattice with gas atoms performing a biased random walk until they move next to a cluster atom and are added irreversibly to the cluster. Colliding gas atoms do not form new cluster seeds. Starting with a single cluster-line at the bottom and randomly distributed lattice gas,

the cluster begins to grow and a depletion layer evolves in front of the cluster. The cluster front advances with a constant velocity V which decreases with the strength of elastic repulsion. The cluster has a ramified branch like structure, which is similar to clusters grown by conventional DLA on small length-scales. Due to the stationarity of growth the overall cluster density will match the given gas concentration because material is conserved. Hence the structure of the cluster cannot remain fractal on large length-scales. Particles finally become uncorrelated and the correlation function approaches an equivalent to the average density value. This crossover defines a new length-scale, the characteristic length ξ_s of the cluster. Assuming a simple power-law decay of the correlation function $c(r) \sim r^{d_f-2}$ for the range where the fractal dimension rules the structure of the cluster and $c(r \to \infty) \sim n_g$ for greater distances, these two asymptotic laws define the crossover length $\xi_s \sim n_g^{1/(d_f-2)}$.

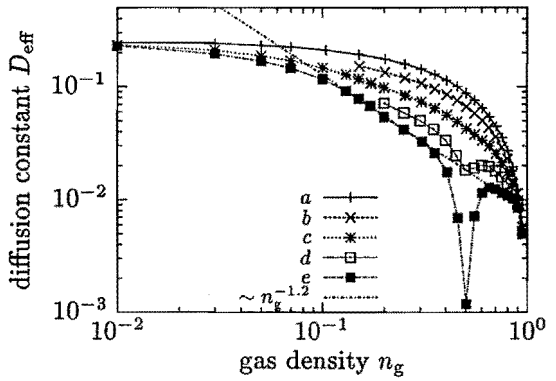

FIG. 2. Effective diffusion constant $D_{\rm eff}$ calculated from the autocorrelation of the particles $D_{\rm eff} = \langle(\vec{r}(t)-\vec{r}(0))^2\rangle/(4t)$ evaluated for large times t. Increasing interaction strength (a) to (e)

Including density and interaction dependent changes of the mobility of the particles into an effective diffusion constant $D_{\rm eff}(n_g)$ from the particles autocorrelation, see Fig. 2, the macroscopic diffusion length becomes the characteristic length ξ_g of the lattice gas and is related to the velocity of the cluster front $\xi_g \sim D_{\rm eff}/V$.

In absence of other length scales both lengths ξ_g and ξ_s should match, leading to the prediction

$$V/D_{\rm eff}(n_g) \sim n_g^{1/(2-d_f)} \qquad (1)$$

for the scaled velocity $V/D_{\rm eff}$. Depending on whether $\xi_s > r_x$ or $\xi_s < r_x$, ξ_s behaves like $\xi_s \sim n_g^{1/(d_f-2)}$ with d_f being either the fractal dimension of DLA or the increased effective dimension found in the presence of elastic effects.

Detailed investigation of the lattice gas leads to the insight that near $n_g = 0.5$ the gas becomes correlated as well and that the correlation length of the gas is in competition with the diffusion length. The rather drastic increase in correlation at this density value can be understood as some kind of resonance effect. However, for weak interaction strength (a) to (c) the scope of correlations in the gas is still of the order of unity and can be ignored. Yet for stronger interaction this length becomes relevant and is the cause for the irregular behavior of curve (d) in Fig. 3.

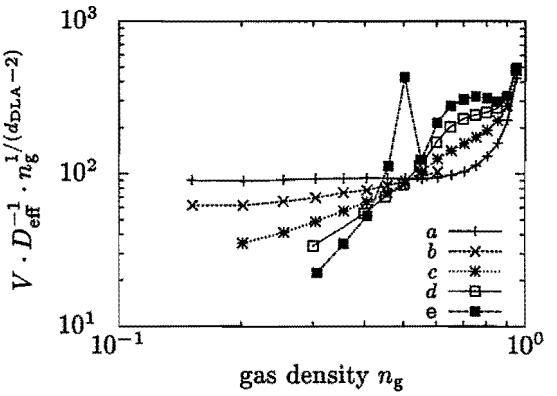

FIG. 3. Deviations from asymptotic scaling (1) for increasing interaction strength (a) to (d)

Starting with a fairly high density value of $n_g \approx 1/2$, the slope of the curves increases with the interaction strength in correspondence to the effective fractal dimension approaching the value $d_f = 2$ in the DLA simulation. In this regime the growth velocity can be characterized by an increased effective fractal dimension. Lowering the particle density the slope decreases as well, bounded by the slope of the non-interacting case (a). For relatively weak interaction (b) it is obvious that the slope converges to the value of (a), indicating that in the low density limit the velocity of growth is governed only by the fractal dimension of simple DLA $d_f \approx 1.7$.

The results indicate that the matching of characteristic length-scales survives as a valid mechanism of velocity selection in presence of elastic effects [5]. The crossover in fractal dimension found in our DLA simulation is shown to have a strong influence on the properties of fractal growth. In the low density limit, however, the velocity of growth is controlled by the fractal dimension of DLA only. While in the low density limit the velocity differs in factor only, with increasing density the scaling exponents change systematically due to the crossover in the effective fractal dimension.

[1] V.I. Marchenko and A.Y. Parshin, Sov. Phys. JETP **52**, 129 (1980)

[2] T.A. Witten and L.M. Sander, Phys. Rev. Lett. **47**, 1400 (1981)

[3] J. Steinbrecher *et al.*, Phys. Rev. E **59**, 5600 (1999)

[4] M. Uwaha and Y. Saito, Phys. Rev. A **40**, 4716 (1989)

[5] F. Gutheim *et al.*, in: Stochastic Processes in Physics, Chemistry, and Biology, J.A. Freund, T. Pöschel (Eds). Lecture Notes in Physics. Vol. 557 (2000)

Dynamic heterogeneity of relaxations in glasses and liquids

D. Caprion, M. Kluge, J. Matsui and H.R. Schober
Institute IFF-Theory III

Heterogeneity in super-cooled liquids and glasses is studied using the non-Gaussianity parameter. We simulate selenium and a binary Lennard-Jones system by molecular dynamics. In the non-Gaussianity three time domains can be distinguished: an increase on the ps-scale due to the vibrational (ballistic) motion of the atoms, followed by a growth, due to local relaxations (β-relaxation) at not too high temperatures and finally a slow drop at long times. The non-Gaussianity follows in the β-regime a $\sqrt{t}$ -law which can be explained by collective hopping.

F&E Nr.: 23.30.0

In recent years relaxations, both in glasses and in liquids, have been studied intensively by experiment and theoretically. One particular aim was to determine whether the relaxations involve only groups of atoms or are spread over the whole system. The first case, where relaxations are restricted to a few atoms only, is known as heterogeneous scenario; the other one as homogeneous. Spatial heterogeneity is often thought to be responsible for the non-exponential relaxations in super-cooled liquids.

To understand its effects, it is necessary to know the properties of the "dynamic heterogeneity" itself, e.g. the time and temperature dependence. Qualitatively it is known [1–3], that the system becomes homogeneous at all temperatures for sufficiently long times, corresponding to the α-regime. In the intermediate time domain, corresponding to the β-relaxation, heterogeneity becomes more pronounced when the system is cooled down.

This is closely related to collectivity of motion. Measurements of the isotope effect have shown that diffusion both in glasses and in super-cooled liquids is highly collective [4,5]. A similar very small isotope effect was also observed in simulations of a Lennard-Jones liquid [6]. In glasses, one observes collective jumps of chain-like structures [7–9]. Similar mobile structures are also observed in the under-cooled liquid [10,11].

Here we will focus especially on intermediate times, shorter than the typical diffusion time. We have shown [12] that there is, for different classes of materials, a common law governing heterogeneity at these intermediate time-scales which stretch, depending on temperature, over some ps or at least several ns.

To quantify the heterogeneity of the relaxations we follow previous work [13–17] and use the non-Gaussianity parameter (NGP) [18]:

$$\alpha_2(t) = \frac{3 < \Delta r^4(t) >}{5 < \Delta r^2(t) >^2} - 1, \qquad (1)$$

where $\langle ... \rangle$ denotes time averaging, $\Delta r^2(t)$ is the mean square displacement and $\Delta r^4(t)$ is the mean quartic displacement. Experimentally the NGP can be determined from the q-dependence of the Debye-Waller factor [13].

As shown previously, the non-Gaussianity increases markedly in this time domain. Here we want to go one step further. First we show that molecular dynamics simulations of two different systems, Se and binary Lennard-Jones (LJ), give strikingly the same law for the increase of the non-Gaussianity parameter (NGP), $\alpha_2(t)$. In this intermediate time domain the non-Gaussianity follows a power law $\alpha_2(t) \propto \sqrt{t}$, for both systems and both for temperatures above and below T_g.

To exemplify this behaviour we show in Fig. 1 for Se $\alpha_2(t)$ multiplied by t against time in a log-log plot. The most interesting feature of this plot is the appearance of an envelope curve for all temperatures stretching over a time domain from 10^{-1} ps to 10^3 ps, i.e. four orders of magnitude. It corresponds to a power law $t^{3/2}$ leading to $\alpha_2(t) \propto \sqrt{t}$.

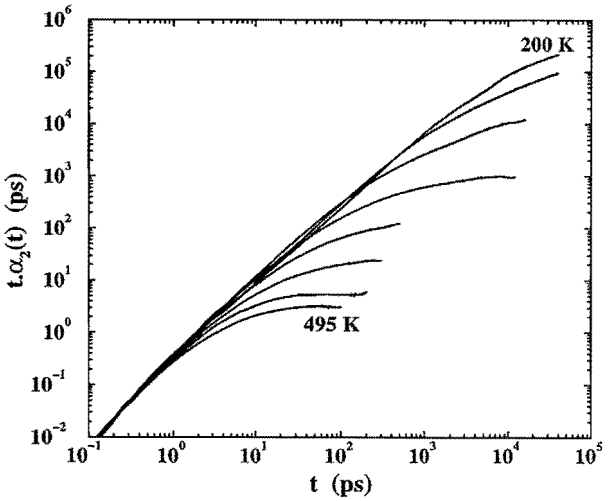

FIG. 1. Non-Gaussianity parameter multiplied by time against time in a log-log representation. The values are obtained from a molecular dynamics simulation of Se at the temperatures (from bottom to top): 495 K, 445 K, 400 K, 355 K, 330 K, 290 K, 255 K and 200 K.

We find the same behaviour for both components of the binary LJ-system, for a recent simulation of supercooled orthoterphenyl [19] and for our simulation of CuZr. From this we conclude that the NGPs of different types of

structural glasses and super-cooled liquids follow at intermediate times the same time dependence: $\alpha_2(t) \propto \sqrt{t}$. Therefore, we think that the mechanism responsible for the increase of the NGP, i.e. of the heterogeneity, is common to many kinds of glass-forming materials.

In our previous investigation of the non-Gaussianity [3], we have clearly shown that the increase of non-Gaussianity is due to relaxations. Moreover it has also been shown that in under-cooled liquids and in the glassy phase, clusters of so called mobile particles exist [8–11]. Theses move in a given time over greater distances than the average. Successive jumps are strongly correlated, showing that the major part of the atoms jumping collectively, but not all of them, will participate in a following jump [8]. We further know from experiments [1] and simulations [3] that on the long time scales of diffusion the NGP drops, which indicates that the heterogeneity decays.

Using these results, we build a simple model which explains the time dependence of the NGP. We make three assumptions, all based on previously known results. First, all atoms have a vibrational mean square displacement, increasing with temperature $\propto T$ and giving an initial $\alpha_2(t) \approx 0.2$. Secondly, there are groups of mobile atoms which jump collectively. And thirdly, after such a jump some atoms can leave while others enter a mobile group. Fig. 2 depicts such a collective jump schematically.

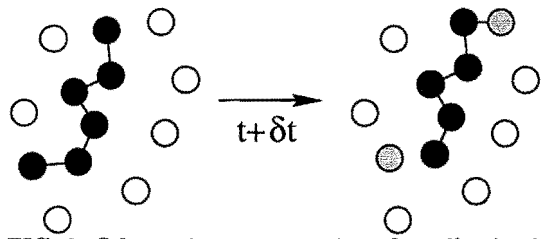

FIG. 2. Schematic representation of a collective jump (left configuration to right configuration). Mobile and immobile atoms are indicated by full and empty circles, respectively. The grey circles show the atoms which have changed their group. After the jump one previously mobile atom has left the group, i.e. it will not participate in the next jump. Another atom has joined the group instead.

This simple model reproduces the power law $\alpha_2(t) \propto \sqrt{t}$, found in the molecular dynamics simulation, which is striking due to the simplicity of the model and even more so to the fact that all details of the interaction in the materials are neglected. In other words, the model can be applied to many kinds of glass-forming material, once one believes in collective hopping of groups of particles. Therefore, we think that the behavior of the non-Gaussianity parameter will also be observed in oxide glasses such as silica and in polymeric glasses. In polymer glasses the long chains will probably limit the displacement of the atoms in the β-relaxation regime which might result in smaller maximal values of the NGP.

To conclude we have presented the results of two independent molecular dynamics simulations on completely different systems and of a simple model. All these results show the same power law for the non-Gaussianity in the intermediate time range, corresponding to the β-relaxations in under-cooled liquids and in glasses. This increase of the non-Gaussianity, i.e. of the heterogeneity of the relaxations, proportional to $\sqrt{t}$, can be understood as resulting from the collective hopping of groups of particles. Assuming that this mechanism is common to all kinds of glass-formers, we believe that heterogeneity will always increase in the intermediate time regime domain following the power law $\sqrt{t}$, at all temperatures and in many types of materials.

[1] A. Arbe and J. Colmenero, Phys. Rev. Lett. **81**, 590 (1998).
[2] W. Kob *et al.*, Phys. Rev. Lett. **79**, 2827 (1997).
[3] D. Caprion and H. R. Schober, Phys. Rev. B **62**, 3709 (2000).
[4] F. Faupel, P. W. Hüppe, and K. Rätzke, Phys. Rev. Lett. **65**, 1219 (1990).
[5] H. Ehmler *et al.*, Phys. Rev. Lett. **80**, 4919 (1998).
[6] M. Kluge and H. R. Schober, Phys. Rev. E **62**, 597 (2000).
[7] H. R. Schober, C. Oligschleger, and B. B. Laird, J. Non-Cryst. Sol. **156**, 965 (1993).
[8] C. Oligschleger and H. R. Schober, Phys. Rev. B **59**, 811 (1999).
[9] C. Oligschleger and H. R. Schober, Solid. State Commun. **93**, 1031 (1995).
[10] H. R. Schober, C. Gaukel, and C. Oligschleger, Defect and Diffusion Forum **143-147**, 723 (1997).
[11] C. Donati *et al.*, Phys. Rev. Lett. **80**, 2338 (1998).
[12] D. Caprion, J. Matsui, and H. R. Schober, Phys. Rev. Lett. **85**, 4293 (2000).
[13] R. Zorn, Phys. Rev. B **55**, 6249 (1997).
[14] H. Miyagawa, Y. Hiwatari, B. Bernu, and J. Hansen, J. Chem. Phys. **88**, 3879 (1988).
[15] W. Kob and H. Andersen, Phys. Rev. E **52**, 4134 (1995).
[16] B. Doliwa and A. Heuer, Phys. Rev. Lett. **80**, 4915 (1998).
[17] T. Odagaki and J. Matsui, in *Slow Dynamics in Complex Systems*, Vol. 469 of *AIP conference proceedings*, edited by M. Tokuyama and I. Oppenheim (AIP, Woodbury, NY, 1999), p. 484.
[18] A. Rahman, Phys. Rev. **136**, A405 (1964).
[19] S. Mossa, R. D. L. andG. Ruocco, and M. Sampoli, Phys. Rev. E **62**, 612 (2000).

1-D to 3-D diffusion reaction kinetics of defects in crystals

H. Trinkaus
Institut Theorie III

Microstructural features evolving in crystalline solids from diffusion-reaction kinetics of mobile components depend crucially on the dimension of the underlying diffusion process, which is commonly assumed to be 3-D. In metals, irradiation induced displacement cascades produce clusters of self-interstitials performing 1-D diffusion. Changes between equivalent 1-D diffusion lines and transversal diffusion result in diffusion reaction kinetics between 1-D and 3-D. An analytical approach suggests a single-variable function (master curve) interpolating between the 1-D and 3-D limiting cases. This is fully confirmed by kinetic Monte Carlo simulations.

F&E-Nr: 23.15.0

The characteristic length scale of spatial variations in a microstructure resulting from diffusion-reaction kinetics of mobile components is defined by the mean diffusion range of such components. For normal three-dimensional (3-D) diffusion, this length scale is larger, but in most cases not substantially larger, than the average distance between the relevant immobile reaction partners (precipitates, bubbles, voids). In many experimental studies of the microstructural evolution in metals under ion or neutron irradiation, characteristic length scales have been found to be more than one order of magnitude larger than expected in 3-D diffusion reactions kinetics. This surprising feature has been explained by the large range of 1-D diffusion of self-interstitial clusters produced in displacement cascades [1].

Recent efforts in modelling the microstructural evolution in metals subject to cascade damage indicate that the possibility of a continuous transition from 1-D to 3-D defect reaction kinetics must be taken into consideration [2]. Such a transition may be considered to be induced by an increasing disturbance of the 1-D diffusion due to spontaneous changes between crystallographically equivalent 1-D diffusion lines and/or transversal diffusion. In the resulting reaction kinetics, the mean 1-D diffusion length without sinks, l, represents a new crucial length scale in addition to the size of the sinks (radius R) and the 1-D mean free path, λ_1.

Here, the main results of analytical studies and kinetic Monte Carlo (KMC) simulations of such 1-D to 3-D diffusion reaction kinetics are reported. As long as $l >> R$, the kinetics keeps 1-D features. For this case, an analytical solution can be derived by applying a self-consistent embedding procedure. The two main steps in this procedure are: (1) analysis of the effect of an individual sink of type i, considered to be embedded into an absorbing continuum of given sink strength k^2,on the (steady state) diffusion field of defects diffusing along a certain 1-D line; (2) application of a self-consistency condition requiring the flux to an individual sink, multiplied by the respective sink density, to be equal to the absorption rate (sink strength) in the absorbing continuum. This procedure results in a solvable set of quadratic equations for the partial strengths of sinks of different types, k_i^2.

A straight-forward derivation of a closed form expression for general diffusion reaction kinetics, including the 3-D limiting case, $l << R$, does not seem to be possible. It is, however, possible to find the correct functional form for the dependence of the absorption rate/sink strength on the relevant system parameters by modifying the mean time between 1-D line changes properly [3]. Expressing the length scales R and λ_1 by the sink strengths k_1^2 and k_3^2 for the 1-D and 3-D limiting cases, respectively, and adjusting the numerical factors properly, a single-variable function for the sink strength interpolating between the limiting cases is obtained [2,3]. The corresponding "master curve" for the partial strength of sinks of type i, k_i^2, related to the corresponding 1-D limiting case, is plotted in Fig. 1.

KMC simulations of the 1-D to 3-D diffusion reaction kinetics have been performed for various values of sink size (radius R), sink density N and mean 1-D diffusion length l. In Fig. 1, simulation data are presented in the form as suggested by the analytical "master curve". Perfect agreement within the accuracy of the simulations is found.

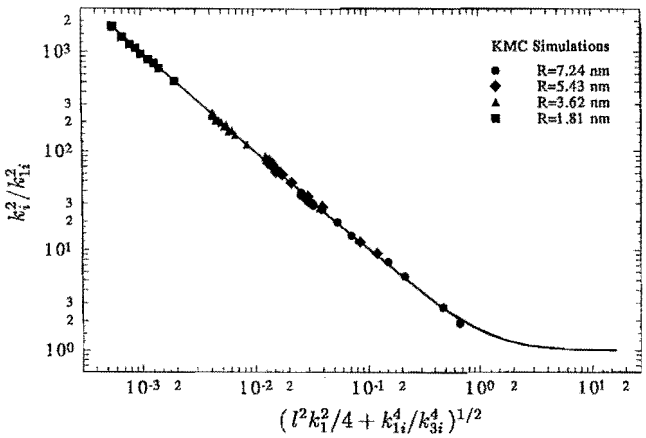

FIG. 1. "Master curve" interpolating between the sink strengths for the 1-D and 3-D limiting cases (solid line) and KMC simulation data for various sink radii (symbols).

[1] H. Trinkaus, B.N. Singh and A.J.E. Foreman, *J. Nucl. Mater.*, **199**, 1 (1992).
[2] H. Trinkaus, B.N. Singh and S.I. Golubov, *J. Nucl. Mater.*, **283**, 89 (2001).
[3] H. Trinkaus, H.L. Heinisch, A.V. Barashev, S.I. Golubov and B.N. Singh, to be published.

Publications in refereed journals

Berger R.; Blügel S.; Antons A.; Kromen Wi.; Schroeder K.
A Parallelized ab initio Molecular Dynamics Code for the Investigation of Atomistic Growth Processes
Proceedings of the NIC-Workshop "Molecular Dynamics on parallel Computers", Jülich, 08.-10. Februar 1999, p. 185-198 (World Scientific 2000)
23.42.0

Brener E. A.; Müller-Krumbhaar H.; Temkin D.E.1
1I.P. Bardin Institute of Ferrous Metals, Moscow
Structure Formation in Diffusional Growth and Dewetting
Solid State Ionics 131, 23 (2000)
23.15.0

Brener E.; Marchenko V. I.1; Müller-Krumbhaar H.; Spatschek R.
1P.L. Kapitza Institute for Physical Problems, Moskau
Coarsening kinetics with elastic effects,
Phys. Rev. Lett. 84, 4914 (2000)
23.15.0

Brener E.; Marchenko V.1; Müller-Krumbhaar H.; Spatschek R.
1P.L. Kapitza Institute for Physical Problems, Moskau
Coarsening Kinetics with Elastic Effects
Phys. Rev. Lett. 84, 4914 (2000)
23.15.0

Brener E.; Müller-Krumbhaar,H.; Temkin D.; Abel T.
Structure formation in diffusional growth and dewetting
Solid State Ionics 131, 23 (2000)
2315.0

Caprion D.; Kluge M.; Matsui J.1; Schober H.R.
1Kyushu University, Japan
Computer simulations of the dynamics in glasses and melts
Advances in Solid State Physics 40 (B. Kramer edt.), p. 469, Vieweg, Braunschweig, 2000
23.30.0

Caprion D.; Matsui J.1; Schober H.R.
1Kyushu University, Japan
Dynamic Heterogenity in Glasses and Liquids
Phys. Rev. 85, 4293 (2000)
23.30.0

Dederichs P.H.; Mavropoulos Ph.; Papanikolaou N.
Complex Bandstructure and Tunneling through Insulators
Tagungsband Statusseminar Magnetoelektronik 2000, p. 263, VDI Technologiezentrum
23.20.0

Diehl H.W.1; Eckhardt B.1; Grossmann S.2; Müller-Krumbhaar H.; Zimmermann W.3
1Universität GHS Essen
2Universität Marburg
3Universität Saarbrücken
Strukturbildung und Selbstorganisation
Kapitel 3.4 in "Physik - Denkschrift der Deutschen Physikalischen Gesellschaft zum Jahr der Physik", Herausgeber: Deutsche Physikalische Gesellschaft e.V., Bad Honnef; November 2000
23.15.0

Gutheim F.; Müller-Krumbhaar H.; Brener E.; Misbah C.1
1Lab. de Spectrometrie Phys., Univ. Joseph Fourier, Grenoble, Frankreich
Epitaxial Growth with Elastic Interaction: Layer and Cluster Growth
Stochastic Processes in Physics, Chemistry and Biology, J.A. Freud, T. Pöschel (Eds.), Lecture Notes in Physics, Vol. 557 (2000)
23.15.0

Gutheim F.; Müller-Krumbhaar H.; Brener E.; Misbah C.1
1Lab. de Spectrometrie Phys., Univ. Joseph Fourier, Grenoble, Frankreich
Epitaxial Growth with Elastic Interaction: Layer and Cluster Growth
Stochastioc Processes in Physics, Chemistry and Biology, p. 484,
J. A. Freund, T. Poeschel eds., Springer Verlag, Berlin 2000
23.15.0

Hauck J.; Mika K.
Architecture of crystal structures from square planes
Acta Crystallogr. B56, 750-765 (2000)
23.55.0

Hauck J.; Mika K.
Magnetic Ordering
J. Magn. Magn. Mat. 212, 389-400 (2000)
23.55.0

Hauck J.; Mika K.
Structure Maps of Surface Structures
Surface Review and Letters 7, 37-53 (2000)
23.55.0

Hauck J.; Mika K.
Structure and Interactions of Clusters
Int. J. Modern Phys. B 14, 1075-1092 (2000)
23.55.0

Hauck J.; Mika K.
Structure families of ZrO2 and CaTiO3 related ionic conductors
Solid State Ionics 127,1-21 (2000)
23.55.0

Hauck J.; Mika K.
The Jig-saw Puzzle of Crystal Structures: Alloys, Superconducting Oscides, Semiconductors, Ionic Conductors, Surface Adsorbates and Magnetic Structures
Jül-3732, Januar 2000, to appear in Progr. Solid State Chemistry
23.55.0

Kentzinger E.; Schober H.R.
Migration energies in L12 intermetallic compounds
J. Phys. Condens. Matter 12, 8145 (2000)
23.15.0

Kluge M.; Schober H.R.
Isotope effect of diffusion in a simple liquid
Phys. Rev. E. 62, 597 (2000)
23.30.0

Korhonen T.1; Settels A.; Papanikolaou N.; Zeller R.; Dederichs P.H.
1Helsinki University of Technology, Helsinki, Finland
Lattice Relaxations and Hyperfine Fields of Heavy Impurities in Fe
Physical Review B62, 452 (2000)
23.20.0

Levanov N.A.1; Stepanyuk V.S.1; Hergert W.1; Bazhanov D.I.2; Dederichs P.H.; Katsnelson A.3; Massobrio C.4
1FB Physik, Martin-Luther-Universität, Halle
2MPI für Mikrostrukturphysik, Halle
3Solid State Physics Department, Moscow State University, Moscow
4Institut de Physique e de Chimie des Materiaux de Strasbourg, Strasbourg, Frankreich
Energetics of Co adatoms on the Cu(001) surface
Phys. Rev. B61, 2330 (2000)
23.20.0

Luchnikov V. A.1; Medvedev N. N.1; Naberukhin Y. I.1; Schober H.R.
1Institute of Chemical Kinetics and Combustion, Novosibirsk, Russia
Voronoi-Delaunoy analysis of normal modes in a simple model glass
Phys. Rev. B 62, 3181 (2000)
23.30.0

Mavropoulos M.; Papanikolaou N.; Dederichs P.H.; Complex Bandstructure and Tunnelin throug Ferromagnet/Insulator/Ferromagnet Junctions
Phys. Rev. Lett. 85, 1088 (2000)
23.20.0

Müller-Krumbhaar H.; Emmerich H.; Brener E.; Hartmann M.
Dewetting hydrodynamics in 1+1 dimensions
Accepted Phys. Rev. E. (2000)
23.15.0

Müller-Krumbhaar H.; Saito Y.1
1KEIO University, Deoartment of Physics, Yokohama, Japan
Crystal Growth and Solidification (Review)
in Computer Simulation in Colloid an Interface Science, ed. M. Borowko, Dekker, N.Y., 2000
23.15.0

Müller-Krumbhaar H.
Nachwuchsmangel in Physik - ein Problem der Schule?
Praxis der Naturwissenschaften - Physik, Bd. 49, 1 (2000)
23.15.0

Nonas B.; Papanikolaou N.; Wildberger K.; Zeller R.; Dederichs P.H.
3d Impurities on the (001) surface of Fe
Clusters and Nanostructure Interfaces, ed. By P.Jena, S.N. Khanna and B.K. Rao (World Scientific, Singapore, 2000), p. 545-552
23.20.0

Papanikolaou N.; Nonas B.; Heinze S.1; Zeller R., Dederichs P.H.
1Universität Hamburg
Scanning tunneling spectra of impurities in the Fe(001) surface
Physical Review B62, 11118 (2000)
23.20.0

Ryazanov A.I.1; Trinkaus H.; Volkov A.E.1
1Russian Research Center, "Kurchatov Institute", Moscow
Incubation Dose for Ion Beam Induced Anisotropic Growth of Amorphous Alloys: Insight into Amorphous State Modifications
Phys. Rev. Lett. 84, 919 (2000)

Schober H.R.; Caprion D.
Structure and Relaxation in liquid and amorphous selenium
Phys. Rev. B 62, 3709 (2000)
23.30.0

Schroeder K.; Antons A.; Berger R.; Kromen Wi.; Blügel S.
Surface Diffusion and Models for the Kinetics of Epitaxial Growth
to be published in the Proceedings of the International Symposium on Structure and Dynamics of Heterogeneous Systems, Duisburg, 25.-26. Februar 1999, p. 71-94 (World Scientific 2000)
23.42.0

Settels A.; Schroeder K.; Korhonen T.1, Papanikolaou N.; Aretz M.; Zeller R.; Dederichs P.H.
1Helsinki University of Technology, Helsinki, Finland
In-donor complexes in Si and Ge: structure and electric field gradients
Solid State Commun. 113, 239 (2000)
23.20.0

Settels A.; Schroeder K.; Korhonen T.1; Papanikolaou N.; Aretz M.; Zeller R.; Dederichs P.H.
1Laboratory of Physics, Helsinki University of Technology, Espoo, Finland
In-Donor Complexes in Si and Ge: Structure and Electric Field Gradients
Solid State Comm. 113, 239 (2000)
23.42.0

Spettmann R.1; Entel P.1; Schroeder K.; Blügel S.
1Theoretische Tieftemperaturphysik, Gerhard-Mercator Universität Duisburg
Electronic Structure of Si(111):Sb((3 x (3) R30°: an ab initio Study
Proceedings of the International Symposium on Structure and Dynamics of Heterogeneous Systems, held at Duisburg, 25.-26.02.1999, p. 217-225 (World Scientific 2000)
23.42.0

Stepanyuk V.S.1; Hergert W.1; Bazhanov D.I.2; Kirschner J.2; Baranov D.I., Dederichs P.H.; Katsnelson A.3
1FB Physik, Martin-Luther-Universität, Halle
2MPI für Mikrostrukturphysik, Halle
3Solid State Physics Department, Moscow State University, Moscow
Atomic processes and the strain distribution in the early stages of thin films growth
Appl. Phys. A71, 1-4 (2000)
23.20.0

Stepanyuk V.S.1; Hergert W.1; Rennert P.1; Nonas B.; Zeller R.; Dederichs P.H.
1Martin-Luther-Universität Halle, Halle
Magnetic nanostructures on the fcc Fe/Cu(100) surfaces
Physical Review B61, 2356 (2000)
23.20.0

Trautmann C.1; Klaumünzer S.2; Trinkaus H.
1Gesellschaft für Schwerionenforschung, Darmstadt
2 HMI Berlin
Effect of Stress on Track Formation in Amorphous Iron Boron Alloy: Ion Tracks as Elastic Inclusions
Phys. Rev. Lett. 85, 3648 (2000)
23.15.0

Trinkaus H.; Holländer B.1; Rongen St.1; Mantl S.1; Herzog H.-J.2, Kuchenbecker J.2; Hackbarth T.2
1ISI, Forschungszentrum Jülich, Jülich
2Daimler Chrysler AG, Research and Technology, Ulm
Strain relaxation mechanism for hydrogen-implanted Si1-x Gex/Si(100) heterostructures
App. Phys. Lett. 76, 3552 (2000)
23.42.0

Invited Talks

Caprion D.
Dynamics of amorphous and liquid selenium
ESRF, Grenoble, 06.06.2000
23.30.0

Caprion D.
Relaxation dons les verres de selenium
Lab. de Matiere Condensee, Universite Paris 6, 20.03.2000
23.30.0

Dederichs P.H.; Papanikolaou N.; Zeller R.
Conceptional Improvements of the KKR Method
Psi-k conference: Ab-initio (from electronic structure) calculation of complex processes in materials
Schwäbisch Gmünd, 22-26.08.2000, 23.20.0

Dederichs P.H.
A Contribution to Understanding Tunneling Magnetoresistance
International Workshop on First-principles Simulation of Advanced Magnetic Materials
Suwa, Japan, 06.-07.03.2000
23.20.0

Dederichs P.H.
Ab-initio Rechnungen zum Tunnelmagnetowiderstand in Ferromagnet / Isolator Schichten
Kolloquium des MPI Metalphysik, Stuttgart, 11.07.2000
23.20.0

Dederichs P.H.
Ab-initio Rechnungen zum Tunnelmagnetowiderstand in Ferromagnet / Isolator Schichten
Seminar, 1. Physikalisches Institut, RWTH Aachen, 23.11.2000
23.20.0

Dederichs P.H.
Ein Beitrag zum Verständnis des Tunnelmagnetowiderstandes in Ferromagnet / Isolator / Ferromagnet Schichten
Forschergruppenseminar, Universität Regensburg, 25.02.2000
23.20.0

Kluge M.
Molecular Dynamics Simulations an Melts and Glasses of Cu33 Zr67
Ioffe-Institute, St. Petersburg, 15.06.2000
23.30.0

Müller-Krumbhaar H.
Ist Physik morgen noch interessant?
Studienkreis Schule + Wirtschaft in NRW, Leverkusen, 21.11.2000
23.15.0

Müller-Krumbhaar H.
Nachwuchsmangel in Physik - ein Bildungsproblem?
DPG-Frühjahrstagung, FV Didaktik, Hauptvortrag, 20.03.2000
23.15.0

Müller-Krumbhaar H.
Wie wächst ein Keim?
Physikalisches Kolloquium, Uni. Erlangen, 10.7.2000
23.15.0

Papanikolaou N.; Freyss M.; Bellini V.; Mavroupoulos Ph., Zeller R.; Dederichs P.H.
Ab-initio calculations for the electronic structure and transport properties of TMR junctions
Symposium on Spin-Electronics
Halle, 03.-06.07.2000
23.20.0

Papanikolaou N.; Mavropoulos Ph.; Dederichs P.H.
Complex band structure and tunneling through Metal/Insulator/Metal junctions
GMR-TMR miniworkshop, Prague, 12-13.04.2000,
23.20.0

Papanikolaou N.; Mavroupoulos Ph.; Freyss M.; Zeller R.; Dederichs P.H.
Spin dependent transport in metal-insulator junctions
Psi-k conference: Ab-initio (from electronic structure) calculation of complex processes in materials
Schwäbisch Gmünd, 22-26.08.2000
23.20.0

Schober H.R.; Caprion D.; Kluge M.
Simulationen zur Dynamik in Gläsern und Schmelzen
Regensburg 27.03.2000, DPG Frühjahrstagung
23.30.0

Schober H.R.
Collectivity of motion in glasses and supercooled liquids
MPI Dresden, 11.10.2000
Int. Workshop on Collective Phenomena in the Low Temperature Physics of Glasses
23.30.0

Schroeder K.; Antons A.; Berger R.; Blügel S.
Ab initio Rechnungen für Adatome auf Halbleiteroberflächen
Tagung der Theorie-Institute der RWTH Aachen, Altenberg, 18.02.2000
23.42.0

Schroeder K.; Antons A.; Berger R.; Blügel S.
Theory of surfactant-mediated growth
PSI-K 2000 Conference, Schwäbisch Gmünd, 22-26.08.2000
23.42.0

Schroeder K.; Antons A.; Berger R.; Blügel S.
Understanding surfactant-mediated growth, contributions from ab initio calculations
International Symposium on Structure and Dynamics of Heterogeneous Sytems, Duisburg, 28-29.08.2000
23.42.0

Schroeder K.
Mikroskopie des Kristallwachstums mit Surfactants: ab initio Rechnungen zur Kinetik von Adatomen auf Halbleiteroberflächen
Kolloquium des SFB 418, Fachbereich Physik der Martin-Luther-Universität Halle-Wittenberg, 03.05.2000
23.42.0

Zeller R.
Calculations for the electronic structure and lattice relaxations of defets
Berlin, 11.05.2000
23.20.0

Other talks

Antons A.; Berger R.; Blügel S.; Kromen Wi.; Schroeder K.
Ab initio Untersuchungen der Struktur von Inseln und Stufenkanten As-bedeckter Si(111)-Oberflächen
DPG-Frühjahrstagung Regensburg, 27.03.2000
23.42.0

Caprion D.; Schober H.R.
Does selenium have heterogeneous or homogeneous diffusion behaviour
DIMAT 2000, Paris 19.07.2000
23.30.0

Kluge M.; Schober H.R.
Molekulardynamik-Simulationen an Schmelzen und Gläsern aus Cu33 Zr67
28.03.2000, DPG Frühjahrstagung, Regensburg
23.30.0

Kromen Wi.; Blügel S.; Schroeder K.
Implementierung einer Projektor-augmentierten Pseudopotentialmethode
DPG-Frühjahrstagung Regensburg, 29.03.2000
23.42.0

Mika K.
A linear programming approach to the high temperature degeneracy of simple Ising systems
Ising Centenuial Conference, Universität Köln, 15.06.2000
23.15.0

Müller-Krumbhaar H.
2000: Jahr der Physik
mehrere Pressekonferenzen im Rahmen der Aktion von DPG und BMBF
23.15.0

Schroeder K.; Antons A.; Berger R.; Blügel S.
Adatome auf Si(111): Sb, Gleichgewichtslagen und Diffusion
DPG-Frühjahrstagung Regensburg, 27.03.2000
23.42.0

Spatschek R.; Brener E.; Marchenko V.I; Müller-Krumbhaar H.
1 P.L. Kapitza Insitute for Physical Problems, Moskau
Vergröberungsübergang unter Berücksichtigung elastischer Effekte
Frühjahrstagung der DPG, Regensburg, März 2000
23.15.0

Spatschek R.; Müller-Krumbhaar H.; Brener E.
Ostwald-Reifung unter elastischer Wechselwirkung
DFG-KickOff-Meeting zum SPP: "Phasenumwandlungen in mehrkomponentigen Schmelzen", Bonn, Okt. 2000
23.15.0

Posters

Antons A.; Berger R.; Blügel S.; Schroeder K.
Structure of Steps and small Islands on Si(11): As
CHIPPS'2000, Wandlitz bei Berlin, 15.-18.05.2000
23.42.0

Antons A.; Berger R.; Blügel S.; Schroeder K.
Structure of Steps and small Islands on Si(11): As
PSI-K 2000 Conference, Schwäbisch Gmünd, Germany, 22.-26.08.2000
23.42.0

Bellini V.; Papanikolaou N.; Zeller R.; Dederichs P.H.
Magnetic 4d monoatomic rows on Ag substrates
Psi-k Conference: Ab initio (from electronic structure) calculation of complex processes in materials
Schwäbisch Gmünd, 22.-26-08.2000
23.20.0

Cabria I.; Nonas B.; Zeller R.; Dederichs P.H.
Strong enhancement of orbital moments and anisotropy energies of adatoms on the Ag(001)surface
Psi-k Conference: Ab initio (from electronic structure) calculation of complex processes in materials
Schwäbisch Gmünd, 22.-26-08.2000
23.20.0

Dederichs P.H.; Mavropoulos Ph.; Papanikolaou N.
Complex band structure and tunneling through Metal/Insulator/Metal junctions
3rd Gordon Research Conference on Magnetic Nanostructures, February 2000, Ventura, California
23.20.0

Freyss M.; Papanikolaou N.; Mavropoulos Ph.; Zeller R.; Dederichs P.H.
Ab-initio calculations for the electronic structure and transport properties of TMR junctions
Psi-k Conference: Ab initio (from electronic structure) calculation of complex processes in materials
Schwäbisch Gmünd, 22.-26.08.2000
23.20.0

Gutheim F.; Brener E.; Müller-Krumbhaar H.
Cluster und Stufenwachstum unter elastischer Verspannung
Frühjahrstagung der DPG, Regensburg, März 2000
23.15.0

Kluge M.; Schober H.
Diffusion in Amorphous Solids and Liquids
DIMAT 2000, Paris, 18.07.2000
23.30.0

Mavropoulos Ph.; Papanikolaou N.; Dederichs P.H.
Complex band structure and tunneling through Metal/Insulator/Metal junctions
International Symposium on Nanoscale Magnetism and Transport
Sendai, Japan, 08.-10.03.2000
23.20.0

Papanikolaou N.; Mavropoulos Ph.; Dederichs P.H.
Complex band structure and tunneling through Metal/Insulator/Metal junctions
Symposium on Spin-Electronics, Halle, 3-6.07.2000
23.20.0

Papanikolaou N.; Nonas B.; Zeller R.; Dederichs P.H.
Scanning Tunneling Spectra of Impurities in the Fe (001)surface
3rd Gordon Research Conference on Magnetic Nanostructures, February 2000, Ventura, California
23.20.0

Schroeder K.; Antons A.; Berger R.; Kromen W.; Blügel S.
Kinetics of group-IV adatoms on As-covered Si(111): diffusion and exchange processes
CHIPPS'2000, Wandlitz bei Berlin, 15.-18.05.2000
23.42.0

Zeller R.
Energy Interpolation for the Tight-Binding Korringa-Kohn-Rostoker Structure Constants
Schwäbisch-Gmünd, 23.08.2000
23.20.0

Lecture courses

Blügel S.; Dederichs P.H.; Müller-Krumbhaar H.; Schroeder K.
Computeranwendungen in der Festkörperphysik, Physikalisches Seminar (6h), WS 2000/2001, RWTH Aachen
23.20.0
Schroeder K.
Capellmann H.1; Schroeder K.
1Institut für Theoretische Physik, RWTH Aachen
Theoretische Festskörperphysik I, Vorlesung (4h) und Übung (2h), SS 2000, RWTH Aachen
23.42.0

Blügel S.; Dederichs P.H.; Müller-Krumbhaar H.; .Schroeder K.
Computeranwendungen in der Festkörperphysik, Physikalisches Seminar (6h), WS 2000/2001, RWTH Aachen
23.42.0

Dederichs P.H.
Grundlagen der Elektronentheorie
31. IFF Ferienkurs "Femtosekunden und Nano-eV:Dynamik in kondensierter Materie", Jülich 13.-24.03.2000
23.20.0

Müller-Krumbhaar H.
Computeranwendungen in der Festkörperphysik
RWTH-Aachen, WS 00/01
23.15.0

Müller-Krumbhaar H.
Praktisches Rechnen für Naturwissemschaftler
RWTH-Aachen, WS 99/00.
23.15.0

Schroeder K.
Elementare Anregungen: Phononen und Magnonen
31. IFF-Ferienkurs "fs und neV: Dynamik in kondensierter Materie", Jülich, 13.-24.03.2000
23.42.0

Institute for Scattering Methods

General Overview

Modern solid state physics goes far beyond a phenomenological description and bases the understanding of solid state properties and phenomena on atomic theories. To obtain information about the atomic structure of solids, probes with sub-nanometer spatial resolution are needed. To study the excitation spectra, an appropriate energy resolution is necessary in addition. All these requirements can be met by scattering methods. In this sense, scattering methods provide the basis of our present understanding of the structure, excitations and phase transitions of condensed matter on a microscopic level.

At the Institute for Scattering Methods (ISM), synchrotron x-ray scattering and neutron scattering are employed for the investigation of condensed matter on an atomic microscopic level. The emphasis lies on exploiting fully the complementarity of the two probes. Besides the application of scattering methods to solid state problems, major activities are concentrated on the methodology. This includes the further development of experimental techniques by improving instrument components and data treatment algorithms, the development of new experimental methods and the corresponding instruments and the development, construction and operation of scattering instruments at large-scale facilities. At present, ISM operates five instruments at the research reactor DIDO of the Research Center Jülich and two instruments at the Hamburger Synchrotronstrahlungslabor HASYLAB. In addition, we participate in the operation of a sector at the Advanced Photon Source APS in Argonne, USA. These instruments are open for the use by external groups from universities, research centers and industry. The instrument responsibles from ISM provide scientific and technical support during the experiment and the data processing. ISM is open for all research areas in condensed matter science, where scattering methods can be applied. At present, the research activities are concentrated in the fields: "solid state magnetism", "structural disorder", "electrocatalytic processes" and "ultra thin liquid films". For the purpose of this research, ISM is also engaged in sample preparation (e.g. by molecular beam epitaxy and single crystal growth) and characterisation (e.g. AC and DC susceptibility and magnetisation measurements).

Instrumentation for neutron and synchrotron x-ray scattering

- *High Energy Side Station at the Advanced Photon Source in Argonne, USA (Th. Brückel, D. Hupfeld, P. Hiller in collaboration with Ames Laboratory and Argonne National Laboratory)*

During the last three years, an undulator beamline for scattering of high energy x-rays (30 - 130 keV) has been developed and built at the IFF. In fall 2000, the components were transported to Argonne National Laboratory, where the Forschungszentrum participates in the development and operation of a sector at the Advanced Photon Source APS in the framework of the MUCAT (Midwestern Universities Collaborative Access Team) collaboration. The components were installed and first radiation was received in the experimental enclosure during the last storage ring cycle in 2000. The first characterisation of the beam indicates that specifications concerning beam stability could be fulfilled. However, the full expected flux of about 10^{12} photons at 80 keV will only be available with the second generation of monochromator crystals (see detailed report).

- *Focusing Small Angle Scattering Instrument and Reflectometer KWS-3 (B. Alefeld, L. Dohmen)*

This new small angle camera and reflectometer is based on an entirely new principle employing mirrors as focusing elements. The mechanical design and construction of the instrument has been completed. The instrument has been erected in the neutron guide hall between the two small angle scattering instruments KWS-1 and KWS-2. We expect the instrument to be tested with neutrons in the beginning of 2001 after we obtain the permission for operation by the reactor safety commission.

- *Reflectometer HADAS (U. Rücker, E. Kentzinger, T. Sorkalla)*

The neutron reflectometer HADAS is the first instrument, which received the new instrument control electronics developed by the ZEL (central electronic department of FZ Jülich) for the new Munich reactor FRMII. The reflectometer has been equipped with polarisation analysis employing remanent supermirrors. With a position sensitive detector, it is now possible to collect the diffuse scattering under grazing incidence with full polarisation analysis. First experiments with polarised supermirrors show a so far unknown spin splitting of the diffuse scattering of these magnetic multilayers (see detailed report).

- *Neutron Spectrometer for Polarisation Analysis SV30 (H. Conrad, A. Ioffe, R. Mueller, S. Massalovitch, E. Küssel, B. Schmitz, Ch. Horriar-Esser)*

A new spectrometer for neutron polarisation analysis in the thermal neutron energy range up to 110 meV is under construction and will replace the old SV4 triple axis spectrometer at the DIDO reactor. Nuclear spin polarised ^{3}He in filter cells will be employed for polarisation analysis over a large solid angle. We study the possibility to use a neutron sensitive image plate as position sensitive detector. The design of the primary spectrometer has been essentially completed and the mechanical components have been delivered or are being built on side. Two large double focusing monochromators, one with PG 002 and one with Cu 002 crystals, are available. In the beginning of January 2001, SV4 has been dismantled and the new beam tube insert has been approved by the reactor safety commission. In parallel, we started a new approach for ^{3}He polarisation by spin exchange from potassium vapour. The appropriate 20 Watt laser has been purchased and the set-up is presently being installed (collaboration with ZEL, S. Appelt, F. Häsing).

- *ESS Target Station (H. Conrad and ESS Collaboration)*

The JESSICA experiment, a full size test stand of the target, moderator and reflector module of the European Spallation Neutron Source ESS, has been taken into operation at the COSY synchrotron. For the first time, thermal neutrons from a spallation source have been produced in Jülich. The measured thermal neutron spectrum coincides perfectly with the predictions of theory. A report about the JESSICA experiment is given in a special section of this annual report.

All these developments have only been possible with massive technical support by the central technical divisions at the Forschungszentrum Jülich. We especially want to acknowledge the support by ZAT, ZEL, ZFR, BD and the construction, mechanical workshop and electronics group at the IFF.

Scattering Methods

- *Theory of Grazing Incidence Diffraction (B. Toperverg, E. Kentzinger)*

The scattering theory for grazing incidence diffraction using a supermatrix formalism has been further developed and has been implemented in a software package for simulation and analysis of neutron as well as x-ray data. For the neutron case, full polarisation analysis has been implemented for arbitrary non-collinear magnetic structures of multilayers. The formalism has been extended to laterally structured multilayers within the Distorted Wave Born Approximation DWBA.

- *Resonant Exchange Scattering from Ferromagnets (D. Hupfeld, O. Seeck, J. Voigt, J. Bos, B. Schmitz)*

Magnetic x-ray scattering is several orders of magnitude weaker than charge scattering and therefore difficult to observe for ferromagnetic materials, where magnetic and charge scattering coincide. The traditional method is to measure the interference term between magnetic and charge scattering. We have developed a new method employing polarisation analysis, where in addition to the interference term, the pure magnetic resonant term (resonance exchange scattering) can be measured. The method has been applied to the ferromagnet EuS (see detailed report).

Solid State Magnetism

- *Critical Behaviour of the Spin Chirality (V. P. Plakhty, Th. Brückel, W. Schweika)*

In helically polarised antiferromagnets, the order parameter consists of not only the spin variables, but also the spin chirality, which describes whether the magnetic order is left or right handed. In a polarised neutron scattering experiment on the helimagnet holmium, we were able to determine the critical exponents for the average chirality β_c and the chiral susceptibility γ_c and found experimental evidence that the spin order transitions in chiral systems belong to new chiral universality classes. Note that in order to measure the chiral susceptibility, a four spin correlation function has to be determined, in contrast to the common believe that neutron scattering gives only access to spin pair correlations (see detailed report).

- *An Empirical Scheme of Spin Wave Exponents (U. Köbler, R. M. Mueller, K. Fischer)*

From spin wave calculations, F. Bloch predicted that in the limit of very small temperatures, the spontaneous magnetisation follows a $T^{3/2}$ term. We report here the experimental finding that in an intermediate temperature range up to 70 % of the critical temperature, the temperature dependence of the spontaneous magnetisation exhibits simple power laws with a T^2 behaviour holding in many cases (see detailed report).

- *Transition Metal Multilayers (W. Babik, E. Kentzinger, U. Rücker, J. Voigt, G. Goerigk, O. Seeck)*

Transition metal multilayers, relevant for applications in the field of magnetoelectronics, have been prepared by MBE techniques, the interface morphology has been determined by x-ray scattering under grazing incidence and the magnetic structure has been investigated with polarised neutron reflectometry. Trilayers of Co/Cu/Co have been

grown on sapphire as well as Si substrates. The interface morphology has been characterised with grazing incidence diffraction and will be linked to the magnetic properties. Similar studies have been performed in the Fe/Cr/Fe system. Fe/Mn/Fe and FeCo/Mn/FeCo trilayers have been investigated by means of polarised neutron reflectometry. It was found that in the FeCo samples, the Mn layer exhibits a spontaneous magnetisation, in contrast to bulk Mn and the Fe/Mn/Fe samples.

- *Rare Earth Multilayers (J. Voigt, D. Hupfeld)*

The magnetic structure and phase transitions in rare earth Er/Tb multilayers have been investigated by means of neutron diffraction and resonant magnetic x-ray scattering. A rich phase diagram could be established. As a result of proximity effects, the magnetic structures are quite different from the bulk. As an example, we have evidence from magnetic x-ray scattering at the Tb L_{II} and L_{III} edges that in the Tb layers a helical magnetic structure exists at low temperatures, where bulk Tb exhibits a basal plane ferromagnetism.

Research on Advanced Materials

- *Structure of Nanosized Metal Particle Networks (H.-G. Haubold, T. Vad, H. Jungbluth)*

Nanosized metal particles can be assembled into highly ordered arrays by interconnecting the metal particles with organic spaces. These new materials are expected to exhibit novel collective properties. The structure of such Pt/polymer hybrids has been investigated by anomalous small angle x-ray scattering and particle radii and distances could be determined (see detailed report).

- *Optimisation of the Composition and Synthesis of Storage Phosphors (M. Schlapp in collaboration with TU Darmstadt)*

The storage phosphor $BaFBr:Eu^{2+}$ finds application in x-ray image plate detectors. The dependence of the photo stimulated luminescence upon doping with alkaline earth metals has been studied and the spectral distribution of the stimulation could be optimised.

- *Phason Disorder in Quasicrystals (W. Schweika)*

The diffuse scattering of an icosahedral AlPdMn quasicrystal has been investigated. The scattering shows the characteristic behaviour expected for phason disorder. The temperature dependence of the diffuse intensity indicates the existence of a phason instability at lower temperatures.

- *Free Standing Polymer Films (O. Seeck, M. Mihaylova)*

Free standing polymer films have been investigated by grazing incidence scattering of synchrotron radiation. Films thicker than three times the radius of gyration behave like liquids, while in thinner films additional elastic terms seem to play an important role.

Examples for the work accomplished at the Institute for Scattering Methods during the year 2000 are given by the progress reports on the following pages.

Thomas Brückel

Personnel 2000/2001 and areas of activity

Scientific Staff

Dr. B. Alefeld *- until 30.06.2000 -*	Development of neutron scattering methods; instrument responsible for the lattice parameter instrument LAP; construction and development of the small angle scattering machine KWS III.	23.89.1
Prof. Dr. Th. Brückel	Institute director; neutron and synchrotron x-ray scattering; magnetism.	23.89.1
Dr. H. Conrad	European Spallation Source project ESS: target and moderators.	23.89.1
Dr. G. Goerigk -HASYLAB, Hamburg-	Material research with anomalous small angle x-ray scattering (ASAXS); instrument responsible for Jülich's user-dedicated small-angle scattering facility JUSIFA.	23.89.1
Dr. H.-G. Haubold	Anomalous small angle x-ray scattering ASAXS and x-ray absorption spectroscopy XAS from highly dispersive systems; in-situ studies of electro-chemical processes.	23.89.1
Dr. A. Ioffe *- since 01.07.2000 -*	Development of neutron scattering methods and instrumentation for Polarization Analysis. Instrument responsible for the triple axis spectrometer SV4; construction and development of the new polarized thermal neutron scattering instrument.	23.89.1
Dr. U. Köbler	Magnetisation and neutron diffraction studies of materials with fourth-order exchange interactions.	23.89.1
Dr. R. Mueller	Development of the ^{3}He filter for neutron polarisation analysis.	23.89.1
Dr. U. Rücker	Instrument responsible for the neutron reflectometer HADAS; preparation and characterisation of magnetic thin film systems.	23.89.1
Dr. W. Schweika	Diffuse neutron scattering for the investigation of short-range order in alloys, oxides, perovskites and quasi-crystals; instrument responsible for the diffuse neutron scattering instrument DNS.	23.89.1

Technical Staff

W. Bergs	Reflectometer HADAS.	23.89.1
A. Broch	Diffuse neutron scattering instrument DNS.	23.89.1
L. Dohmen	Project engineer for the small angle scattering instrument KWS III.	23.89.1
Dipl.-Ing. P. Hiller	Project engineer for μCAT-collaboration at the Advanced Photon Source APS; x-ray small angle scattering.	23.89.1
Ms. C. Horriar-Esser	Ultra low-temperature magnetometry and ^{3}He filter project.	23.89.1
H. Jungbluth	Software development for x-ray small angle scattering.	23.89.1
Ms. B. Köppchen	Secretary.	23.89.1
Dipl.-Ing. E. Küssel	Project engineer for the new polarised thermal neutron scattering instrument.	23.89.1
B. Olefs	Magnetometry, electronics and PC responsible.	23.89.1
B. Schmitz	Triple axis spectrometer SV 4 and cryotechniques.	23.89.1
T. Sorkalla *- since 06.09.2000 -*	Laboratory assistant.	23.89.1

Scientists

Dr. D. Hupfeld - APS, Argonne, USA-	Magnetic x-ray scattering; instrument responsible at the μ-CAT sector of the APS.	23.89.1
Dr. E. Kentzinger *- since 01.02.2000 -*	Neutron and synchrotron x-ray scattering from magnetic thin film materials.	23.89.1
Dr. O. Seeck -HASYLAB, Hamburg -	X-ray scattering from ultrathin liquid films in confined geometries; instrument responsible of the Wiggler beamline W1.	23.89.1
Dr. Th. Vad	Further development of the instrument control and data treatment programs for Jülich's user-dedicated small-angle scattering facility (JUSIFA); ASAXS measurements.	23.89.1

Dr. Th. Zeiske - *until 31.01.2000* -	Instrument responsible of the triple axis spectrometer SV 4; Design of the new polarised neutron spectrometer.	23.89.1

Thesis Students

Dipl.-Phys. W. Babik	(RWTH Aachen) Interface morphology of GMR and TMR layer structures.	23.89.1
M. Sc. K. Istomin	(RWTH Aachen) Interplay of charge, orbital and magnetic ordering in manganites.	23.89.1
cand. phys. R. Krug - *01.03.2000 until 31.07.2000* -	(RWTH Aachen) Investigation of the vacancy-oxygen-correlations in $Yba_2Cu_3O_{6+x}$ with diffuse neutron-scattering.	23.89.1
M. Sc. Milena Mihaylova - *since 06.12.2000* -	(HASYLAB, Hamburg) Liquids in confined geometry investigated by scattering methods.	23.89.1
cand. phys. S. Nerger - *until 31.05.2000* -	(RWTH Aachen) Structure and magnetic coupling in FeCo/Mn/FeCo layer systems.	23.89.1
Dipl.-Ing. M. Schlapp - *since 17.04.2000* -	(TU Darmstadt) Development of highly efficient materials and image plates for neutron detection.	23.89.1
cand. phys. J. Voigt - *until 14.04.2000* -	(RWTH Aachen) Elementspecific magnetization density distribution in rare-earth superlattices.	23.89.1
Dipl.-Phys. J. Voigt - *since 01.05.2000* -	(RWTH Aachen) Influence of proximity and reduced dimensionality on structure and phase transition in rare earth superlattices.	23.89.1

Guests

Dr. J. Bos - *since 01.03.2000* -	(RWTH Aachen) Preparation of powder and single crystal samples; magnetic structures and phase transitions by neutron- and x-ray scattering.	23.89.1
Dipl.-Phys. C. Byloos	(Università Ferrara, Italy) Shock waves in the ESS spallation target	23.89.1
Dr. S. Massalovitch - *since 15.09.2000* -	(Kurchatov Institute, Moscow, Russia) Development of a large-area image plate detector of thermal neutrons.	23.89.1
Prof. V. Plakhty - *until 15.03.2000* -	(Petersburg Nuclear Physics Institute, Russia) Neutron and synchrotron x-ray study of the spin chirality in holmium.	23.89.1
Dr. B. Toperverg - *01.02.2000 - 31.05.2000; since 01.09.2000* -	(Petersburg Nuclear Physics Institute, Russia) Theory for grazing incidence diffraction.	23.89.1
Dr. Y.-G. Wang - *until 31.05.2000* -	(Southeast University, Nanjing, China) Interface and magnetic characterization of magnetic multilayers using scattering methods.	23.89.1

Trainees

Ms. S. Bluhm
- *since 01.10.2000* -
A. Christ
- *since 29.08.2000* -
J. Thelen
- *until 30.09.2000* -

Undulator Beamline for High Energy X-Ray Scattering

Th. Brückel[1], D. Hupfeld[1], P. Hiller[1], J. Strempfer[1],
H. Feilbach[2], N. Bayer[2], M. Pohl[2], U. Probst[3],
A. Goldman[4], D. Robinson[4], E. Zoellner[4]
[1]*FZJ, Institute for Scattering Methods*
[2]*FZJ, IFF*
[3]*FZJ, ZAT*
[4]*Ames Laboratory, Ames, USA*

An undulator beamline for the photon energy range 30 to 130 keV has been constructed. The beamline has been installed at the Advanced Photon Source APS in Argonne, USA as part of the Midwestern Universities Collaborative Access Team (MUCAT) sector. First x-rays were delivered into the experimental enclosure in November 2000.

F&E-Nr: 23.89.1

Introduction

In 1998, the Forschungszentrum (FZJ) joined the Midwestern Universities Collaborative Access Team (MUCAT) at the Advanced Photon Source (APS) in Argonne, USA. The APS is one of worldwide three (ESRF (France), APS (USA) and SPRING8 (Japan)) third generation synchrotron radiation sources for the hard x-ray range. MUCAT (9 American universities, Ames Laboratory and FZJ) develops and operates a sector (bending magnet and undulator line) at the APS. The bending magnet line is funded and construction is in progress for a general purpose station for scattering and absorption spectroscopy. At the undulator line, the following instruments are operational in a x-ray energy range from 4 to 30 keV: diffractometer for magnetic scattering, liquid surface reflectometer, surface chamber and surface diffractometer. The contribution of FZJ was the design and construction of an undulator side station for the photon energy range from 30 to 130 keV. The side station can be operated in parallel with the stations of the main undulator line thus effectively doubling the usage of the undulator beam. Both lines together cover the complete energy range of hard x-rays up to the K-edges of transuranium elements thus allowing all kinds of anomalous and resonant scattering studies.

At high photon energies around 100 keV, x-rays penetrate several millimeters into bulk samples and in a way very similar to neutron diffraction, true bulk properties can be studied in a complex sample environment. MUCAT intends to apply high energy x-ray diffraction in various fields, such as non-resonant magnetic x-ray diffraction, the determination of local structures from diffraction measurements, in-situ studies of materials in complex sample environments or the study of phase transitions. The main interest of FZJ lies in magnetic x-ray diffraction, where the pure spin momentum can be measured separately from the orbital angular momentum without polarisation analysis. Besides problems in magnetism, structural disorder will be investigated by collecting diffuse scattering with an area detector.

Beamline Design

The layout of the undulator line is depicted in figure 1. The energy range from 4 to 30 keV can be covered by a double crystal monochromator displacing the beam by 26 mm in the vertical plane. High energy photons are transmitted through the cryogenically cooled thin web Si 111 crystal monochromator. These high energy photons are monochromised by Bragg diffraction from a water-cooled silicon monochromator, deflecting the beam in an angular range of 4.2 to 8.2° horizontally. The second crystal of the high energy double monochromator assembly is mounted on a translation stage covering a range of 4 m. Thus a double crystal monochromator in non-dispersive setting for energies between 30 and 130 keV can be realised with Si 111, 311 and 331 monochromator crystals. Annealed silicon crystals with a rocking curve width of 10" are used in order to increase the intensity by transmitting a larger wave length band. With a system of vacuum bellows, the beam is transported into the experimental enclosure HE, where it is offset horizontally by 600 mm with respect to the main undulator beam. To allow for a wide range of scattering experiments, a HUBER PSI diffractometer is installed, which is specially modified for high energy diffraction. The 2 θ goniometer is replaced by two crossed translational stages, thus allowing for the large distances between sample and analyser and analyser and detector, necessary for the required collimation. In addition this construction allows the installation of a heavy solid state detector. The Eulerian cradle can be removed and replaced by a system of double arc goniometer and x-y-z translational stages, so that heavy sample environment such as cryomagnets or furnaces can be mounted.

A serious design issue of the beamline is the handling of the high thermal power. Nearly 6 kW are emitted by the undulator at closed gap. A water-cooled tungsten mask reduces the beam cross section to 2 x 4 mm (vertical x horizontal) in front of the high energy monochromator crystal reducing the thermal load to 2 kW. A combination of C, Al and Cu filters removes the low energy part of the spectrum leaving a thermal load of a few hundred Watts for the first monochromator

crystal. With a filter assembly consisting of a 1 mm thick Al and a 1 mm thick Cu disk, a maximum temperature of 390°C is reached in the center of the Cu filter element. The remaining heat load of several hundred Watts still can produce a thermal bump on the first monochromator crystal leading to a serious decrease in reflectivity for the double crystal monochromator. This problem has been solved by working in Bragg geometry and soldering a Si crystal with triangular cross section into a water-cooled Cu holder. Details of this new approach will be published elsewhere.

Realisation

The beamline has been designed and built in Jülich and was transported to the US in September. The installation of the components was done during the October shutdown of the storage ring. In the November run of the synchrotron, the radiation survey was passed successfully and first light could be brought to the experimental station within a few days. At 30 keV with the Si 111 monochromator crystal, a flux of about 10^{12} photons/s was determined with a calibrated ionisation chamber. However, mechanical deformations of the monochromator crystals were detected, which give rise to a flux reduction and an inhomogeneity of the beam, especially for higher photon energies. This problem will certainly be overcome with a second generation of monochromator crystals and we expect to reach a flux of 10^{12} to 10^{13} photons at a photon energy of 80 keV for closed undulator gap. While the expected flux could not be reached, the thermal and mechanical stability of the beamline turned out to be impressive. No heat load effects could be detected. Despite the fact that the two monochromator chambers are mounted on separate support structures and separated in space by 4 to 8 m, the mechanical stability is such that no short term intensity fluctuations can be observed. Over the course of one day, intensity fluctuations are in the order of 10 %. These fluctuations can be suppressed by a piezo feedback system.

Summary and Outlook

In summary, the high energy side station of the MU-CAT sector at the APS has been successfully taken into operation. Improvements in the monochromator design to avoid mechanical strain will be implemented and first commissioning experiments performed in 2001. An image plate area detector for the collection of diffuse scattering has been ordered and will be installed in spring 2001. In parallel, an option for beam focussing with x-ray lenses or bend monochromator crystals will be developed. After about 1 year of commissioning, the beamline will become available for independent investigators during 25 % of the available beamtime.

Acknowledgement

The mechanical components were built with great precision in the workshops of IFF and FZJ. We received valuable support by technical staff from APS. Initial monochromator tests were done at HASYLAB by H. Schulte-Schrepping.

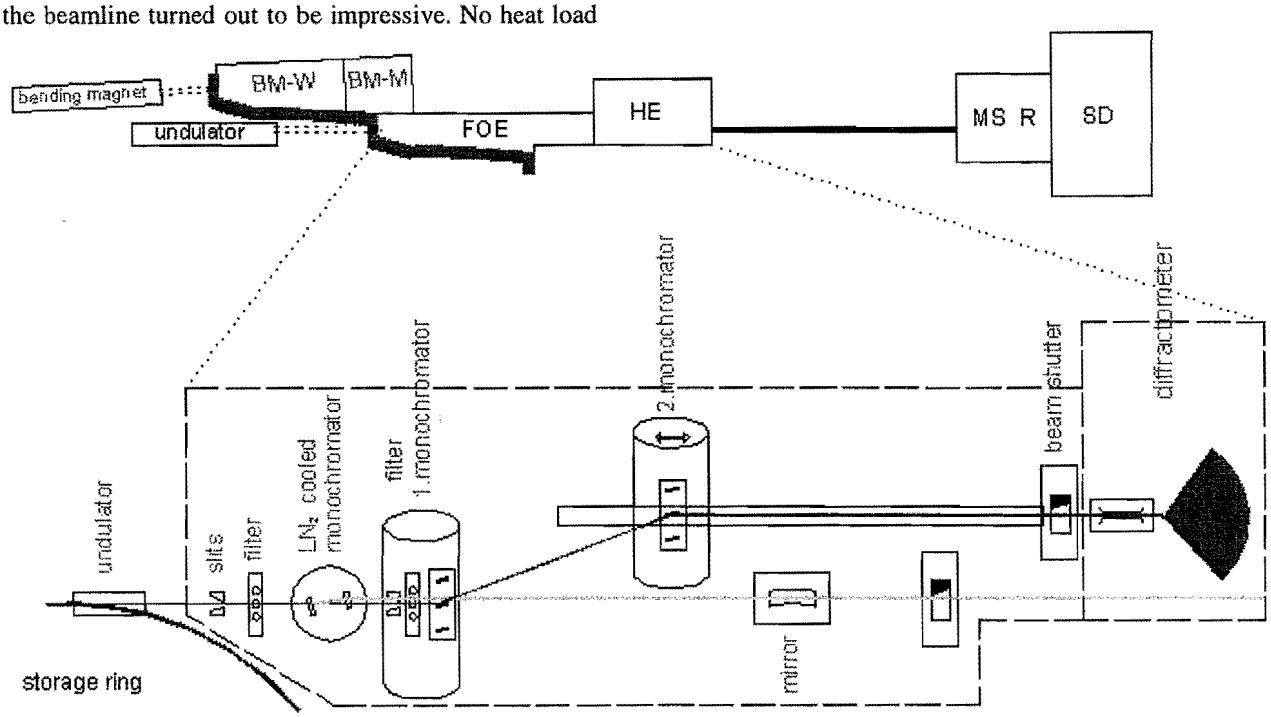

FIG. 1. Layout of the MuCAT-Sector at the APS (above) and schematic drawing of the undulator line (below).
BM-W: Bending Magnet, White Beam station
BM-M: Bending Magnet, Monochromatic Beam
FOE: Front optical enclosure for the Undulator line
HE: High Energy Station
MS: Magnetic Scattering
R: Liquid Surface Reflectometer
SD: Surface Diffraction

The Polarized Neutron Reflectometer HADAS

U. Rücker, E. Kentzinger, B. Alefeld, W. Bergs, Th. Brückel
Institute for Scattering Methods

On the basis of the previous cold triple-axis spectrometer HADAS in the neutron guide hall at the research reactor FRJ-2 (DIDO) in Jülich a polarized neutron reflectometer has been developed. This instrument is equipped with a 2D position sensitive detector and a polarization analyser covering the complete detector area, allowing to measure efficiently the diffuse scattering under grazing incidence from thin magnetic films with high resolution and polarization analysis.

F&E-Nr: 23.89.1

Neutron reflectivity is a powerful tool for analysing the depth profile of thin film systems, yielding information about the stacking sequence, interface morphologies, and, using polarized neutrons, a depth profile of the in-plane magnetization of the layered structure. But the specular reflectivity ($q_{||} = 0$) can resolve only information about structures perpendicular to the film surface, averaged over the lateral coordinate. The statistical information about the lateral morphology and magnetization can be found in the diffuse scattering under grazing incidence ($q_{||} \neq 0$). The intensity of the diffuse scattering is usually some orders of magnitude weaker than the intensity of the specular reflectivity at the same angle of incidence.

The HADAS instrument (Fig. 1) has been converted to a (non-polarized) reflectometer a few years ago. Between the double monochromator of pyrolytic graphite mosaic crystals and the sample position a collimation system with two adjustable vertical slits was introduced, which allows to adjust the horizontal divergence of the incident beam between 0.1 and 10 mrad. A vertically focussing monochromator allows illumination of small samples (down to 1 cm^2) with an intense beam with a high vertical divergence that does not affect the resolution of the instrument, which is only defined by the angular resolution in the scattering plane.

For polarized neutrons, a second beam path between the neutron guide and the unpolarized beam path is used, that touches a polarizing supermirror. By reflection on the supermirror, only the neutrons with the spin parallel to the magnetization of the mirror are reflected, the other species is absorbed. The polarizer is located in an electromagnet, with that it can be remagnetized, so that it can produce spin ↑ neutrons in the saturated and spin ↓ neutrons in the remanent state.

After reflection on the sample, a 2D position sensitive detector allows to separate the specular reflection from diffuse scattering and background. We planned to build a polarization analyser that covers the complete detector area (80 mm ∅) without disturbing the resolution and efficiency of the detector, i.e., it must not affect the horizontal coordinate of the impinging neutrons and all detector columns should be treated equally.

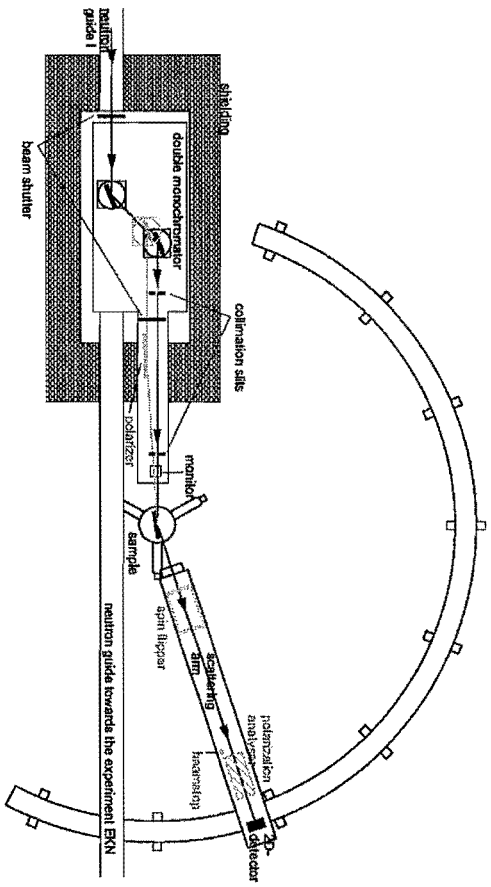

FIG. 1. Schematic view of the HADAS neutron reflectometer.

The final design consists of a vertical stack of 30 polarizing supermirrors which form a divergent collimator that is inclined by 0.75° against the direct view between sample and detector. For a sample size of 17 mm and below, all neutrons coming from the sample arrive at the polarization analyser within the range of angles, where a good polarization is achieved. The polarizing supermirrors are deposited on 0.21 mm thick float glass plates, so that the dead area of the polarization analyser is only about 10% of the detector area. The glass plates are self-supporting, so that no additional material, that could cause small-angle scattering or absorption, is in the beam. Fig. 2 shows a photo of the mounted polarization analyser together

with the hinge used to incline the device against the neutron beam coming from the sample.

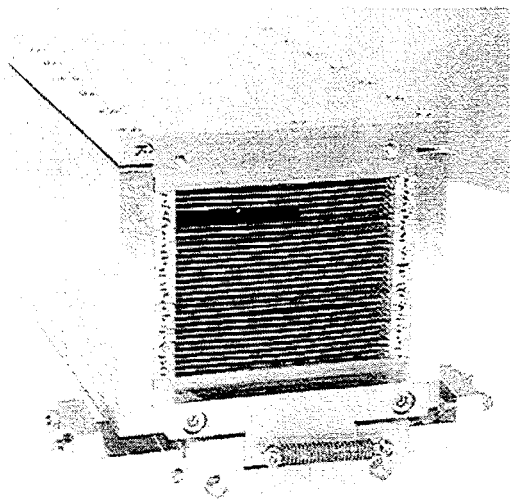

FIG. 2. Photo of the polarization analyser together with the hinge used to incline the device against the neutron beam. The device can be adjusted with a motorized micrometer screw lifting the back of the analyser.

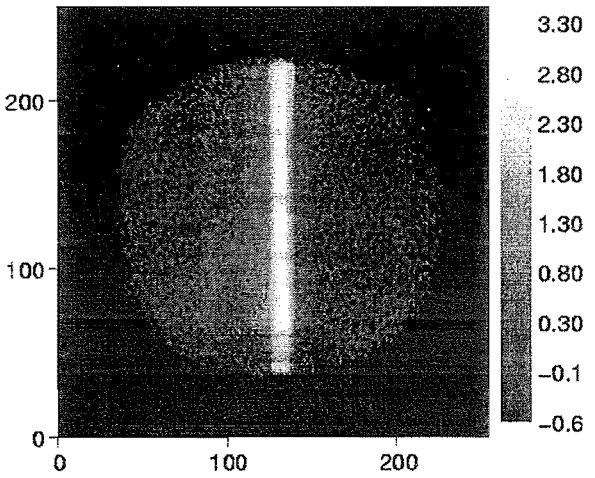

FIG. 3. 2D detector image of the reflection from a polarizing supermirror at α_i = 0.6° recorded with polarisation analysis (spin ↑). The colors represent a logarithmic intensity scale.

The first duty of the new device was to characterize the properties of the supermirrors used for polarization and polarization analysis in the instrument itself. Therefore the polarization analyser was mounted and the polarizer was set onto the sample position and illuminated with a well-collimated unpolarized beam. Fig. 3 shows the detector image of the reflection of the supermirror in the spin ↑ channel at the incident angle α_i = 0.6°. In the middle of the active detector area one can see the specular reflex. Its vertical structure shows a modulation due to the absorption of the individual analyser glass plates. As the distances between the self-supporting glass plates are not completely equal, a small variation between the transmission of the different channels can be seen. On the left of the specular reflex (i.e. at higher scattering angles) diffuse scattering can be seen, while on the right hand side the background signal is weak.

Fig. 4 shows a vertical integration of the detector pictures without polarization analysis (analyser horizontal) and with polarization analysis for spin ↑ and ↓, respectively.

The curve without polarization analysis shows strong diffuse scattering on both sides of the specular reflection. With polarization analysis it can be seen that the diffuse scattering is strongly spin polarized. Between the horizon (α_f = 0°) and the specular reflection, the diffuse scattering is spin ↓, while the diffuse scattering at higher angles is spin ↑. This distinct spin polarization shows, that the diffuse scattering has mainly magnetic origin, a thorough theoretical description of the observed effects is under way.

In conclusion, it can be stated, that the new instrument offers unique possibilities for the study of the magnetic contributions to the diffuse neutron scattering under grazing incidence from magnetic thin film structures. In parallel with the development of the adapted theoretical formalism it will be a powerful tool to find out important information about the behaviour of layered magnetic structures under the influence of varying magnetic fields.

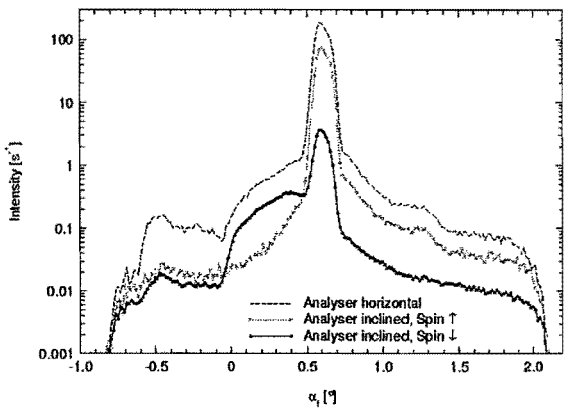

FIG. 4. Vertical integration along the detector columns of the 2D detector images of a neutron beam reflected from a polarizing supermirror. The dashed line shows the signal with the polarization analyser horizontal, i.e. with hardly any interaction between the incoming neutrons and the analyser mirrors. The gray line and the black line show the signal with the analyser inclined properly against the beam and the spin flipper off and on, respectively.

Resonant Exchange Scattering from Ferromagnetic Materials and Application to EuS

D. Hupfeld, O. H. Seeck, J. Bos, J. Voigt, B. Schmitz, K. Fischer and Th. Brückel
Institute for Scattering Methods

We report on a new method to investigate the magnetic properties of ferromagnetic materials with x-ray resonance exchange scattering. We were able to perform measurements on the sample system EuS with high accuracy.

F&E-Nr.: 23.55.0, 23.89.1

Introduction

The traditional tool for the investigation of ferromagnetic materials is neutron scattering, where the intensity of magnetic scattering is of the same order of magnitude as the scattering from the nucleus. Only very few ferromagnetic materials have been investigated with X-ray resonance exchange scattering because usually the charge scattering, which is observed at the same point in reciprocal space as the magnetic scattering, has an intensity several orders of magnitude larger than the magnetic scattering. The scattering intensity can be described by the following formula:

$$I = r_0^2 \left| f_c + i\frac{\lambda_c}{d} f_m \right|^2, \qquad (1)$$

where f_c represents the charge scattering and f_m the magnetic scattering. Therefore, to investigate ferromagnetic samples with x-ray resonance exchange scattering, a setup is used where a magnetic field is applied perpendicular to the scattering plane in horizontal scattering geometry. By switching the sign of the magnetic field, the interference term ($\propto f_c f_m$) between charge scattering and resonance exchange scattering changes sign. Therefore, the magnetic signal is observable as an intensity difference:

$$R_a \equiv \frac{I^{\uparrow} - I^{\downarrow}}{I^{\uparrow} + I^{\downarrow}}, \qquad (2)$$

where $I^{\uparrow}$ and $I^{\downarrow}$ represent the scattering intensity for magnetisation parallel or antiparallel to the scattering plane, respectively. For a detailed description of this method and a few examples see [1].

Experiment and results

We used the same experimental setup in an attempt to directly measure the magnetic intensity of a ferromagnetic sample. The new helium flow cryostat with superconducting coils of the Institute for Scattering Methods was used successfully for the first time. The design is equivalent to the standard "Orange cryostat" from AS Scientific with additional superconducting coils. The cryostat can be used in horizontal scattering geometry only. The coils produce a field up to 5 T perpendicular to the scattering plane. For a more detailed description of the magnet cryostat see [2].

EuS orders ferromagnetically below a Curie temperature of 17 K. It exhibits the largest collosal magnetoresistance effect of any substance known to date. On doping with a few percent Gd, the Curie temperature doubles and an insulator-metal transition takes place. Resonance exchange scattering is the ideal tool to investigate this drastic change in electronic structure as we have shown

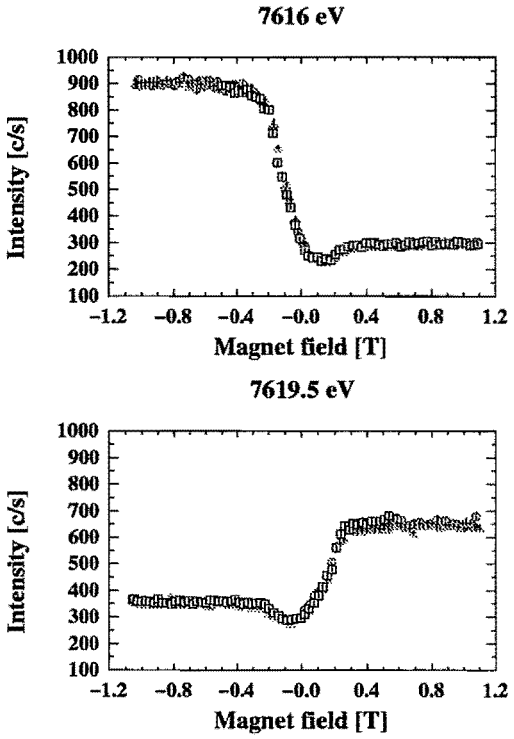

FIG. 1: Measurement of the field dependence of the scattering intensity at the (115) Bragg peak for 7616 eV and 7619.5 eV. At these two energies charge scattering, magnetic resonance exchange scattering and an interference term are contributing to the scattering intensity.

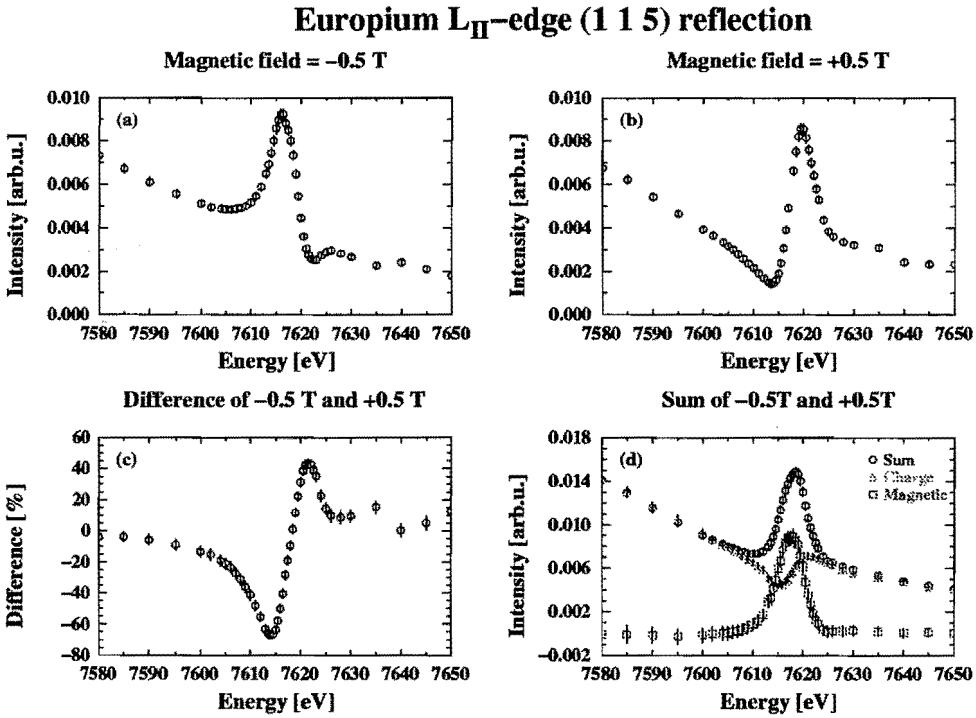

FIG. 2: Measurement of the energy dependence of the (115) Bragg peak of EuS close to the europium L_{II}-edge at 4.2 K. Each datum point in graph a) and b) represents the integral intensity of a rocking scan of the sample with a negative or positive magnetic field of 0.5 T applied perpendicular to the scattering plane, respectively. In graph c) the difference of the two measurements with positive and negative magnetic field is shown as described in equation 2. In graph d) the sum of the two measurements is depicted. To extract the pure magnetic signal, the charge scattering was measured well above the Curie-temperature at 40 K. The "magnetic" curve shows the typical resonance behaviour of the pure magnetic signal obtained as the difference between the magnetic and the charge scattering.

in our previous study of the antiferromagnetic order on the gadolinium rich side of $Gd_xEu_{1-x}S$ mixed crystals [3].

Despite the strong resonance enhancement at the europium L_{II}- and L_{III}-edges the scattering intensities at the Bragg positions are normally dominated by the charge scattering and only an interference term between charge and magnetic scattering can be measured. At the L_{II}-edge of europium the (115) Bragg peak has a 2Θ angle which is close to 90 degrees. The synchrotron radiation at the W1 experimental station is to more than 90 % linear polarised within the orbital plane. This leads to a strong suppression of the charge scattering for the (115) Bragg peak. To suppress the few percentage of radiation with the wrong polarisation we mounted a pyrolitic graphite crystal as a polarisation analyser. With this geometry magnetic scattering is comparable to charge scattering with an intensity of a few hundred counts per second. In figure 2 the energy dependence of the scattering intensity at the (115) Bragg peak is shown. It is possible to separate the magnetic contributions from the charge scattering (figure 2d). The change of sign of the interference term as a function of energy visible in figure 2c is described in detail in [1].

In figure 1 the dependence of the scattering intensity on the magnetic field is shown. The curve form is dominated by the change of sign of the interference term between charge scattering and resonance exchange scattering in the scattering amplitude.

Conclusions

In conclusion we were able to demonstrate that in special cases x-ray resonance exchange scattering can be used to obtain data from ferromagnetic samples with high accuracy. This is especially valuable for the investigation of disordered systems containing several magnetic elements because x-ray resonance scattering is element sensitive.

[1] S. Lovesey and S. Collins, *X-ray scattering and absorption by magnetic materials* (Oxford University Press, Oxford, 1996).

[2] O. H. Seeck *et al.*, Operation of a high-field magnet cryostat at the diffractometer ROEWI (W1.1), HASYLAB annual report, 2000.

[3] D. Hupfeld *et al.*, Europhys. Let. **49**, 92 (2000).

Chiral Criticality in Helimagnet Ho Studied by Polarised Neutron Scattering

V. P. Plakhty[1,2], Th. Brückel[2], W. Schweika[2], J. Kulda[3], S. Gavrilov[1], D.Visser[4,5,6]
[1]*Petersburg Nuclear Physics Institute*
[2]*FZJ, Institute for Scattering Methods*
[3]*ILL, Grenoble*
[4]*Department of Physics University of Warvick*
[5]*ISIS Facility, Rutherford Appleton Laboratory*
[6]*IRU, TU Delft*

The critical exponent for the average chirality, β_C = 0.79(3), and the chiral susceptibility, γ_C = 0.79(5), are determined for the spin-ordering transition in helimagnet Ho. The γ_C agrees with the Monte Carlo value for the *XY* chiral universality class, while the β_C is substantially higher than a predicted value. It is shown that $\beta_C > 2\beta = 0.67(1)$, which indicates that chirality is an additional component of the order parameter, but not simply a vector product of two spins.

F&E-Nr: 23.89.1

Introduction

The order parameter of helically polarised magnets (stacked-triangular lattice antiferromagnets (TLA) or helimagnets like rare-earth metals) includes, along with the ordinary spin variables $\mathbf{S}_R$, the spin chirality $\mathbf{C} = [\mathbf{S}_{R1} \times \mathbf{S}_{R2}]$, a relevant variable that describes the helix to be right-handed or left-handed. The chiral systems are being intensively studied, and the main interest arises from Kawamura conjecture that their spin-order transitions should belong to new, chiral universality classes (see [1] and Refs therein). These classes are characterised by modified conventional critical exponents α, β, γ and ν for the specific heat, order parameter (staggered magnetisation), susceptibility and correlation length, respectively. In addition, critical exponents for the average chirality, β_C, below T_N and the chiral susceptibility, γ_C, above T_N appear. This conjecture is strongly debated [2,3] as experimental values of the conventional critical exponents can be explained in a different way. The truly chiral exponents had never been measured before the recent experiments [4,5] performed for a TLA $CsMnBr_3$. Experimental values of the critical exponents β_C = 0.44(2) and γ_C = 0.84(7) are in a good agreement with the Monte Carlo results [6] β_C = 0.45(2) and γ_C = 0.77(5) for the chiral universality class of a *XY*-type TLA. Together with the fact that spin and chiral ordering occur at the same temperature and the scaling relation is fulfilled, this gives evidence for the validity of the chiral-universality scenario of the spin-ordering transition in the *XY* TLA.

The experimental values of the conventional critical exponents for the rare-earth helimagnets Ho, Dy, Tb are not very consistent [1]. For instance, most pronounced for the *XY* chiral universality class α, that should be very high (α = 0.34 ÷ 0.40 [6,7]) in the case of Ho varies from –0.02(1) [8] to 0.27(2) [9]. Two scales of fluctuations in the very vicinity of the phase transition further complicate the situation. The exponents γ and ν are very different: γ_1 = 1.24(15), ν_1 = 0.55(4) and γ_2 = 2 ÷ 5, ν_1 = 1.0(3) for the inverse correlation lengths of about 0.02 $Å^{-1}$ and 0.001 ÷ 0.002 $Å^{-1}$, respectively [10]. Existing values of conventional exponents would fit any universality class. Measurements of the chiral exponents could clear up the situation.

Theoretical Background

The β_C exponent for the average chirality can be obtained from the temperature dependence of the polarisation-dependent part of the magnetic satellite intensity [11] that is given by the second term in Eq.(1):

$$I(\mathbf{k}) \propto 2f^2(\mathbf{Q})\{\langle S_z\rangle^2[1+(\hat{\mathbf{Q}}\hat{\mathbf{C}})^2] + 2\langle \mathbf{C}\rangle(\hat{\mathbf{Q}}\hat{\mathbf{C}})(\hat{\mathbf{Q}}\mathbf{P}_0)(n_L - n_R)\}\delta(\mathbf{Q} - \mathbf{b}_i - \mathbf{k}) \quad (1)$$

where $\mathbf{k}$ is the satellite wave vector of a reflection with the reciprocal lattice vector $\mathbf{b}_i$, and n_L, n_R are the populations of the left- and right-handed domains.

$$\langle \mathbf{C}\rangle \propto \Delta(\mathbf{k}) = I^{\uparrow}(\mathbf{k}) - I^{\downarrow}(\mathbf{k}) \propto |\tau|^{\beta_C} \quad (2)$$

where $I^{\uparrow}(\mathbf{k})$ and $I^{\downarrow}(\mathbf{k})$ are the intensities measured with $\mathbf{P}_0$ parallel and antiparallel to $\hat{\mathbf{Q}}$, and $\tau = (T - T_N)/T_N$ is the reduced temperature. The conventional critical exponent β can be determined from the first term of Eq.(1) as

$$\langle S_z\rangle^2 \propto \Sigma(\mathbf{k}) = I^{\uparrow}(\mathbf{k}) + I^{\downarrow}(\mathbf{k}) \propto |\tau|^{2\beta} \quad (3)$$

With a known β_C, the γ_C may be found from the chiral crossover exponent, $\phi_C = \beta_C + \gamma_C$. The latter enters a power temperature dependence of the polarisation-dependent completely inelastic part of the cross-section, which appears due to the dynamical chirality (DC) - interaction between chiral fluctuations and a field-induced magnetisation above T_N [12]. This cross-section is given by the difference of intensities measured with opposite neutron beam polarisation, $\Delta(\varepsilon) = I^{\uparrow}(\varepsilon) - I^{\downarrow}(\varepsilon)$, which has been shown [4] to have at small ω the form:

$$\Delta(\omega) = A\frac{\varepsilon/\Gamma}{[1+(\varepsilon/\Gamma)^2]^2} \quad (4)$$

where $A \propto \tau^{-\phi_C}$.

Experiment and Results

A crystal of Ho with the mosaicity of about 0.1° was obtained by recrystallisation. A piece of about 1 cm^3 was cut off for the inelastic scattering above T_N. A cylinder of 3 mm in diameter and 3.5 mm long for the Bragg intensity measurements was cut off from the same crystal by electro-erosion. The cylinder axis was oriented along the [0 0 1] direction. To measure the average chirality one needs a non-equal domain population (1), which has been created like in Ref. [13] by the torsion deformation of about 2% (plastic) around the cylinder axis that is collinear to the **C**. For this purpose the cylinder had been welded by electronic beam to tails of 15 mm in diameter made of the polycrystalline holmium. To avoid any scattering from the tails they were painted with paint on the basis of gadolinium nitrate. The crystal in a torsion device shown in Fig. 1 was installed in the orange cryostat. The measurements of the Bragg intensities $I^{\uparrow}(\mathbf{k})$ and $I^{\downarrow}(\mathbf{k})$ were carried out on IN22 triple axis spectrometer (TAS) at a thermal neutron guide of the ILL reactor with a highest possible $\mathbf{k}_i = 4.1$ Å^{-1} to avoid extinction. The difference of $I^{\uparrow}(\mathbf{k})$ and $I^{\downarrow}(\mathbf{k})$ of a few percent is seen in the inset to Fig. 2. This difference was smaller than expected, but still high enough to provide sufficient statistics.

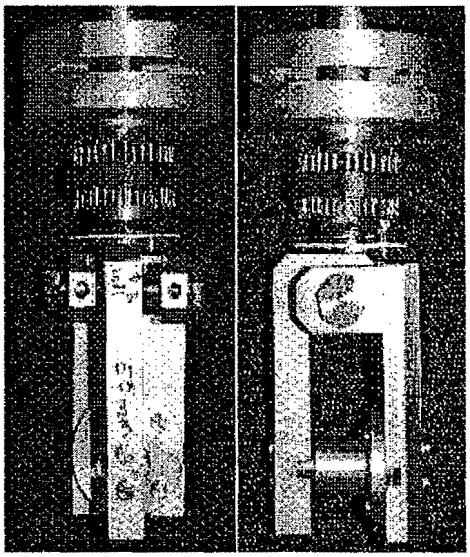

FIG. 1. Sample holder for the Ho-crystal under torsion deformation. A cylindrical Ho-crystal welded to the polycrystalline holmium tails is inside the thin-wall aluminum cylinder, which centers the crystal and avoids its bending.

The temperature dependence of the peak intensity of a satellite (0 0 μ) of the $\mathbf{b}_i = 0$ has been measured in the temperature range $120 \le T(\mathrm{K}) \le 132$. First of all a series of preliminary longitudinal (ω - 2θ) and transverse (ω) scans were made to determine the temperature dependence of the maximum position and to estimate the Néel point as $T_N = 130.5$ K. A smooth curve was drawn through the experimental intensities above T_N (background plus diffuse critical scattering). The critical scattering intensity at a definite $T_i > T_N$ corrected by the ratio C^+/C^- was subtracted together with background from the total intensity at $T = T_N - (T_i - T_N)$. We have used $C^+/C^- = 5$ from Table III of Ref. [14], which is close to the experimental and series value of 5.03(5) as well as to the ε-expansion value of 4.8. These corrections are known for the susceptibility, i.e., for the $\Sigma(T)$. As to the $\Delta(T)$, the corresponding correction for the chiral susceptibility is unknown. Fortunately critical chiral scattering is completely inelastic [12] and, as follows from Eq. (4), should vanish when being integrated over a narrow energy resolution interval. This was the case in Ref. [5]. In the present experiment, this interval is an order of magnitude wider, and some critical scattering is seen for Δ (T), although much weaker that for $\Sigma(T)$. It should be pointed out that the values of β_C and β have changed in the limits of a standard deviation when the correction is made using the mean-field ratio $C^+/C^- = 2$, i.e., the final result is not sensitive to this correction. The data were treated as follows: At a definite T_{Ni} the corrections for the critical scattering were made, and the corrected values were fit as $\log\Delta(\tau) = \log\Delta(\tau_0) + \beta_C \log|\tau|$ and $\log\Sigma(\tau) = \log\Sigma(\tau_0) + 2\beta \log|\tau|$. Then all the procedure was repeated at another T_{Ni}. The final values of $T_N = 130.55(1)$, $\beta_C = 0.79(3)$ and $2\beta = 0.67(1)$ have been chosen by the criteria of minimum of the residual least squares, $\chi^2_{min} = 2.1$ for the $\Delta(\tau)$ and $\chi^2_{min} = 1.1$ for the $\Sigma(\tau)$. The results of the final iteration are shown in Fig. 2. The transition temperature for chirality occurs to be at the T_N in the limits of a standard deviation, i.e., coincides with the spin ordering temperature with a relative precision of 10^{-4}.

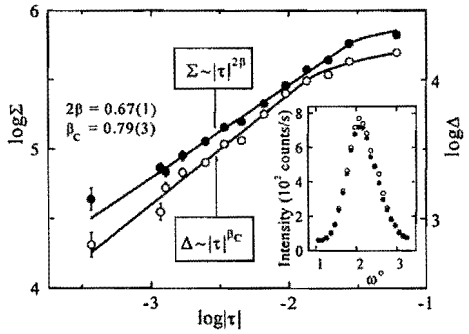

FIG. 2. Log-log plot of $\Delta = I^{\uparrow} - I^{\downarrow}$ and $\Sigma = I^{\uparrow} + I^{\downarrow}$ vs τ. The insert shows the rocking curves $I^{\uparrow}(\omega)$ and $I^{\downarrow}(\omega)$ described by the open and filled circles, respectively.

The DC part of the cross-section (4) has been measured using a cryomagnet with horizontal field up to 4 T. A crystal of holmium has been mounted in the cryomagnet with the hexagonal axis being horizontal. The field has been always applied along the hexagonal axis, i. e., along the chirality vector **C**. The DC cross-section is proportional to B in the low-field approximation [12]. The theoretical estimate for this limit is very crude, and the proportionality was checked up to 4 T at $\tau = 0.11$ in the $CsMnBr_3$ TLA [4]. To be on

the safe side, we have applied the smaller field of B = 2 T in the present experiment. In spite of the lower field, the effect, $\Delta(\varepsilon)$, is high enough due to the large moment value of Ho. A series of energy scans at the magnetic satellite (0 0 2-μ) position were made in the temperature range 132.20 ≤ T(K) ≤ 161.15. The experiment was performed on the IN12 spectrometer at the ILL with $\mathbf{k}_i$ = 1.5 Å^{-1} and with the energy resolution of 0.1 meV. The spectra $\Delta(\varepsilon) = I^{\uparrow}(\varepsilon) - I^{\downarrow}(\varepsilon)$ were measured at each temperature. As a result (Fig. 3) ϕ_C = 1.58(4) has been obtained, which occurs to be substantially higher than 1.22(5) for the XY chiral universality class as obtained by the Monte Carlo simulation for the TLAs [6] and the experimental value of 1.28(7) for a TLA CsMnBr3 [5].

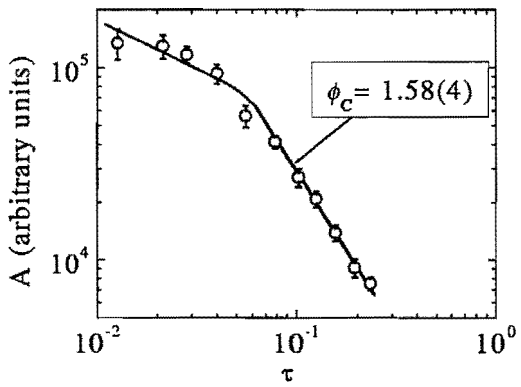

FIG. 3. Scale factor, A, of the DC inelastic spectrum $\Delta(\varepsilon) = I^{\uparrow}(\varepsilon) - I^{\downarrow}(\varepsilon)$ vs τ.

At $T = T_N$ + 1.65 K two energy widths were observed corresponding to the fluctuations on different scales mentioned above. The lifetimes are $t_1 = 2.1(2)\cdot10^{-10}$ s and $t_2 > 10^{-8}$ s for the short and the long scales, respectively. The latter is just an estimate, since no widening of the resolution function could be observed.

Conclusion

In conclusion we should point out that the discrepancy of ϕ_C is due to a rather high β_C = 0.79(3) in comparison with the Monte Carlo value of 0.45(2) for the XY chiral transition in a TLA [6] and the experimental one of 0.44(2). The chiral susceptibility exponent $\gamma_C = \phi_C - \beta_C$ = 0.79(5) is in good agreement with the γ_C = 0.77(5) for the XY chiral universality class [6]. The cause of this conflict is unclear. The RKKY interaction with the range of the order of the helix period could be the reason. Another point we would like to stress out is the established fact: $\beta_C > 2\beta$ = 0.67(1). (Naively one should expect $\beta_C = 2\beta$.) This means that chirality is not a simple vector product of two spins, but a new component of the order parameter.

We thank O. P. Smirnov for supervising the manufacturing of the sample torsion device.

[1] H. Kawamura, J. Phys.: Condens. Matter **10**, 4707 (1998).
[2] P. Azaria, B. Delamotte, and Th. Jolicoeur, Phys. Rev. Lett. **64**, 3175 (1990).
[3] S. A. Antonenko and A. I. Sokolov, Phys. Rev. B **49**, 1590 (1994).
[4] V. P. Plakhty, S. V. Maleyev, J. Kulda, J. Wosnitza, D. Visser and E. Moskvin, Europhys. Lett. **48**, 215 (1999).
[5] V. P. Plakhty, J. Kulda, D. Visser, E. V. Moskvin and J. Wosnitza, Phys. Rev. Lett. **85**, 3942 (2000).
[6] H. Kawamura, J. Phys. Soc. Japan **61**, 1299 (1996).
[7] R. Deutchmann, H. von Löhneysen, J. Wosnitza, R. K.Kremer and D. Visser, Europhys. Lett. **17**, 637 (1992).
[8] P. de Plessis, C. F. van Doorn and D. C. van Delden, J. Magn. Mag, Mat. **40**, 91 (1983).
[9] K. D. Jayasuriya, S. J. Campbell and A. M. Stuart, J. Phys. F: Met. Phys. **15**, 225 (1985).
[10] T. R. Thurston, G. Helgesen, J. P. Hill, D. Gibbs, B. D. Gaulin, P. J. Simpson, Phys.Rev. B **49**, 1573 (1994).
[11] S. V. Maleyev, V. G. Bar'yakhtar and R. A. Suris, Sov. Phys. Solid State **4**, 2533 (1963); M. Blume, Phys. Rev. **130**, 1670 (1963).
[12] S. V. Maleyev, Phys. Rev. Lett. **75**, 4682 (1995).
[13] V. I. Fedorov, A. G. Gukasov, V. Kozlov, S. V. Maleyev, V. P. Plakhty, I. A. Zobkalo, Phys. Lett. A **224**, 372 (1997).
[14] E. Brezin, J. C. Le Guillou and J. Zinn-Justin, in *Phase Transitions and Critical Phenomena*, edited by C. Domb and M. S. Green (Academic Press, London, 1976), p.127.

A New Empirical Scheme of Spin Wave Exponents in Magnetism

U.Köbler[1], A.Hoser[2,3] , R.M.Mueller[1], K.Fischer[4],
[1]*FZJ, Institute for Scattering Methods*
[2]*HMI-Berlin*
[3]*RWTH-Aachen*
[4]*FZJ, IFF*

In contrast to classical spin wave theories it was frequently observed experimentally that the thermal decrease of the spontaneous magnetization of ferromagnets can well be described by a single T^{ε} power term. We have performed systematic experimental studies of the T^{ε} laws and observed that the empirical spin wave exponent ε depends on the dimensionality of the magnetic interactions and on whether the spin quantum number is integral or half-integral. This implies a scheme of 6 different exponents ε. Surprisingly, for the same class of materials ε is independent of the spin order type.

F&E-Nr: 23.15.0

Introduction

In the year 1930 F.Bloch performed the first spin wave calculation [1]. According to this quantum mechanical theory the thermal decrease of the spontaneous magnetization of a ferromagnet should be given in first approximation by a $T^{3/2}$ term. Real ferromagnets such as Ni, Fe, CrO_2 and EuO exhibit T^2 laws over a temperature range of up to 0.7 of the critical temperature [2]. The reason for the different exponent and the much larger validity range of the empirical T^2 law is that Bloch assumed that the atomic spins are coupled only by Heisenberg exchange interactions. As we now know, the next higher class of interactions, the fourth-order exchange interactions, i.e., biquadratic, three-spin and four-spin interactions are nearly as strong as the conventional Heisenberg interactions and cannot be neglected. These interactions modify the spin dynamics fundamentally. Up to now no spin wave theory including fourth-order exchange interactions exists. It is therefore important to proceed empirically and to collect the many experimental facts necessary for the development of a more suitable theory. It appears that the magnetic interactions and the spin dynamics in magnetic solids are more complicated than was hitherto assumed and that a completely new concept is necessary for a satisfying understanding.

Spin wave theory versus empirical description

The Bloch theory was refined by F.J.Dyson who showed [3] that Bloch's $T^{3/2}$ law is the leading term of a power series and that the next higher terms are $T^{5/2}$ and $T^{7/2}$. The increasing number of coefficients (to be evaluated experimentally) as well as the unclear convergence of the Bloch-Dyson power series makes it a difficult task for any experimentalist to test the spin wave theory experimentally. In fact, up to now no convincing experimental proof exists for the Bloch-Dyson spin wave theory in spite of a large body of careful and accurate experiments reported in literature. The problem is not so much the experimental accuracy but the conceptual difficulties with power series expansions.

Already in 1929 Weiss and Forrer observed that the spontaneous magnetization of iron can well be described by a single T^2 power term [4]. The same observation was made in 1944 on the ferromagnet CrO_2 [5]. Meanwhile the T^2 law has been established for many materials [2].

In fig.1 we present as an example the T^2 dependence of the spontaneous magnetization of EuS. Shown are the zero field Nuclear Magnetic Resonance (NMR) frequencies at the ^{153}Eu nucleus vs. T^2. NMR is the most accurate method in magnetism.

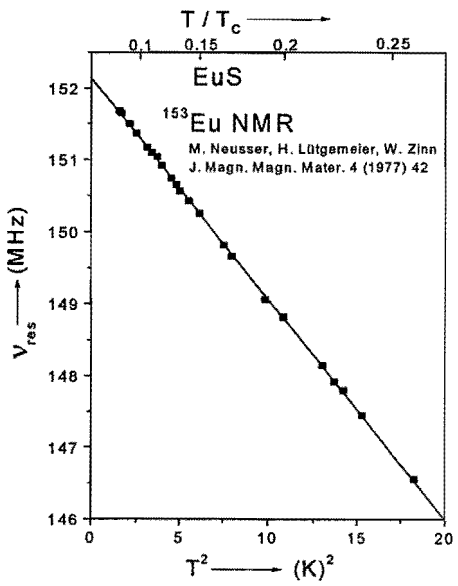

FIG. 1. ^{153}Eu NMR resonance frequency as a function of T^2. In the ordered state the hyperfine field induces a Zeeman splitting of the nuclear spin states. The resonance frequency samples the splitting and is proportional to the hyperfine field and therefore proportional to the spontaneous magnetization.

Integral and half-integral spin values

The Bloch-Dyson spin wave theory makes no difference between integral and half-integral spin quantum numbers. Experimentally a considerable difference is observed. Unfortunately most of the known magnetic materials have half-integral spins. Among the transition elements ionic compounds of Ni^{2+} (S=1) and Fe^{2+} (S=2) are good candidates for integral spin values. Also the antiferromagnet UO_2 is a good example for S=1. In fig.2 we show the normalized sublattice magnetization as a function of $T^{9/2}$. These data have been obtained from the neutron scattering intensities of the 0,0,1 Bragg reflection of a UO_2 single crystal. It can be seen that the thermal variation of the antiferromagnetic order parameter can be described until $T \sim 0.8T_N$ with $\varepsilon = 9/2$. The same exponent is observed also for NiO, $FeBr_2$, $KNiF_3$ and $NiCO_3$.

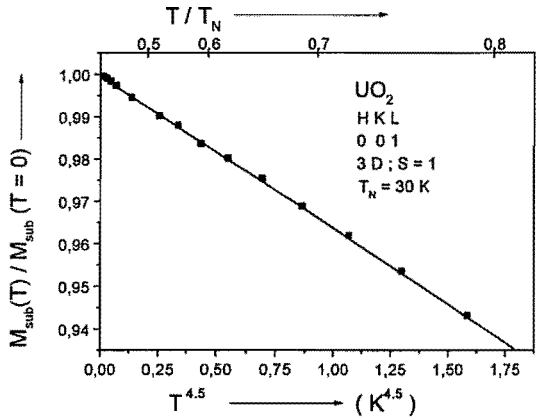

FIG. 2. Temperature dependence of antiferromagnetic order parameter of UO_2 as a function of $T^{4.5}$ obtained with neutron scattering on a single crystal.

Dimensionality of the magnetic interactions

This study restricts on materials with pure spin magnetism meaning that the magnetic atom has a spherical symmetric state. Depending on the symmetry of the crystalline lattice the exchange interactions can be anisotropic. For cubic materials the interactions can be assumed to be three-dimensional (3D) and isotropic. In non-cubic materials the interactions will still be 3D but anisotropic. It is a further empirical fact, that a distinction has to be made between 3D-isotropic interactions, 3D-anisotropic interactions and axial interactions. For those three cases particular spin wave exponents ε are observed for integral and half-integral spin quantum number. It is much surprising that the same exponent ε is observed for materials with planar (2D) interactions as for the 3D-anisotropic materials. For instance, the layered compound K_2NiF_4 (S=1) for which no spin wave dispersion is observed perpendicular to the layers exhibits like the orthorhombic Mn_2O_3 (S=2) a T^2 behaviour.
As an example for predominantly axial interactions we show in fig.3 neutron scattering results on antiferromagnetic MnF_2. The spherical symmetric spin state of the Mn^{2+} is well reflected by the perfect paramagnetic isotropy. In the orderd state the anisotropy of the interactions becomes apparent by the strong antiferromagnetic anisotropy with spin orientation parallel and antiparallel to the crystallographic c-axis.

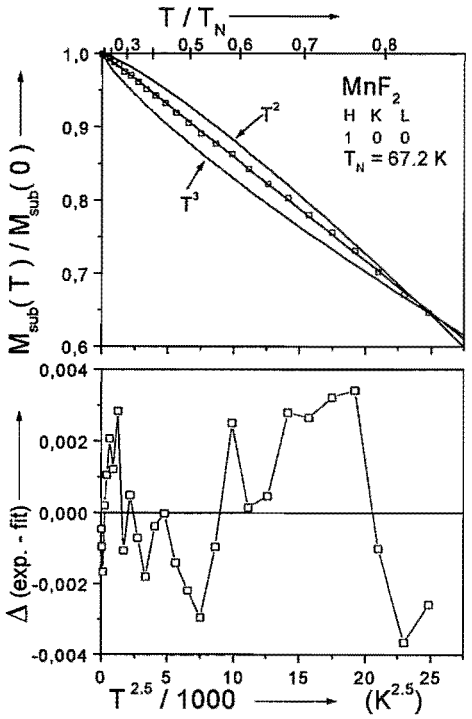

FIG. 3. Order parameter of antiferromagnetic MnF_2 obtained from 1,0,0 neutron scattering intensities vs. $T^{5/2}$. Lower diagram gives differences between experimental data and fit.

Five different exponents ε with values 9/2, 6/2, 5/2, 4/2 and 3/2 were observed. Table I attributes them to the dimensionality of the interactions and the spin quantum number. Only one prominent experimental example for each category is given.

Exchange interactions		integral spin		half-integral spin			
		$S=1$	$S=2$	$S=\frac{1}{2}$	$S=\frac{3}{2}$	$S=\frac{5}{2}$	$S=\frac{7}{2}$
3D isotropic		UO_2	$FeBr_2$	$KCuF_3$	$CrBr_3$	$CsFeF_4$	EuO
		$T^{\frac{9}{2}}$		T^2			
3D-anisotropic 2D		CrO_2	Mn_2O_3	K_2CuF_4	$CrCl_3$		Gd metal
		T^2		$T^{\frac{3}{2}}$			
1D (axial)			FeF_2			MnF_2	
		T^3		$T^{\frac{5}{2}}$			

[1] F.Bloch, Z.Physik **61** (1930) 206
[2] U.Köbler, A.Hoser, M.Kawakami, T.Chatterji, J.Rebizant, J.Magn.Magn.Mater. **205** (1999) 343
[3] F.J.Dyson,Phys.Rev. **102** (1956) 1230
[4] P.Weiss, R.Forrer, Ann.Physique **12** (1929) 20
[5] C.Guillaud, A.Michel, J.Bénard, M.Fallot, Comp.Rendus **219** (1944) 58

ASAXS investigation of 3-D Pt-metal particle networks

H.-G.Haubold[1], T.Vad[1], N. Waldöfner[2], H. Bönnemann[2]
[1]*Institute for Scattering Methods, FZJ*
[2]*MPI of Coal Research, Mühlheim/Ruhr*

We performed anomalous small angle x-ray-scattering (ASAXS) experiments with synchrotron radiation to study the 3-dimensional nanostructures of three metal/organic hybrids formed by crosslinking Al/organic stabilized Pt-particles with different bifunctional organic spacer-molecules. The advantage of ASAXS is the possibility of separating the particle scattering from that of the organic components thus providing unbiased information on particle size distribution and interparticle correlation. In order to obtain the structural information from the scattering data use was made of A. Vrij's equations for a multicomponent system of hard spheres. The results indicate that the Pt-particles are successfully interconnected by the organic spacers. However, the degree of ordering between the particles is less pronounced due to a quite large polydispersity of the Pt-particles.

F&E-Nr: 23.89.1

Introduction

The assembly of nanosized metal particles to highly ordered arrays has gained importance over the past few years. This topic is part of the fast evolving field of nanotechnology which is believed to be one of the key-technologies in the near future.

The resulting new materials are expected to exhibit novel collective properties which differ from those of the bulk materials. The major advantage is, that their properties can be *individually* designed by controlled variation of particle size and interparticle distances and may therefore contribute to improvements in a variety of fields, e.g., the development of faster micro-chips and memory-media, more effective absorbers for solar-energy, or special optical lattices.

Nanocrystal 2D-superlattices and metal colloid networks have been prepared by several groups. However, bottom-up preparations of nanoparticles to give three-dimensional structures still remain to be a challenge. Here, we report a way to characterize metal-organic networks formed by crosslinking Al-organic stabilized platinum nanoparticles with bifunctional spacer molecules.

Experimental

Three Pt-colloid-samples were prepared by a group of the *MPI of Coal Research (Mühlheim/Ruhr)*: The first sample is a Pt-colloid without any spacer-molecules, the second one is a hybrid material with the Pt-particles being interconnected by hydroquinone, and the third one a hybrid with 4,4-dihydroxy-biphenyl as spacer-molecule.

For the synthesis of these samples the method of *reductive stabilization of nanoparticles with aluminium-trialkyls* was used, a preparation method recently discovered by Bönnemann and coworkers [1]. This synthesis has proven to be a reliable method for the fabrication of small zero-valent transition-metal-particles over a wide range of different elements, e.g. Pt or Co. The key feature of this synthesis is the formation of a reactive metal-organic protecting shell around the particles. Reactive Al-alkyl groups present in the shell open up the possibility of chemical reactions at the surface of a colloidal particle. One example is the substitution of organic groups at the Al-atom in order to modify the dispersive properties of the colloids. If the substituents are bifunctional, e.g. diols like hydroquinone or 4,4-dihydroxy-biphenyl, a crosslinking of the particles can be brought about which leads to the formation of a 3D-colloidal network (see Fig. 1). Thus, the interparticle distance can easily be controlled by variation of the type (i.e. the length) of the spacer-molecule being used.

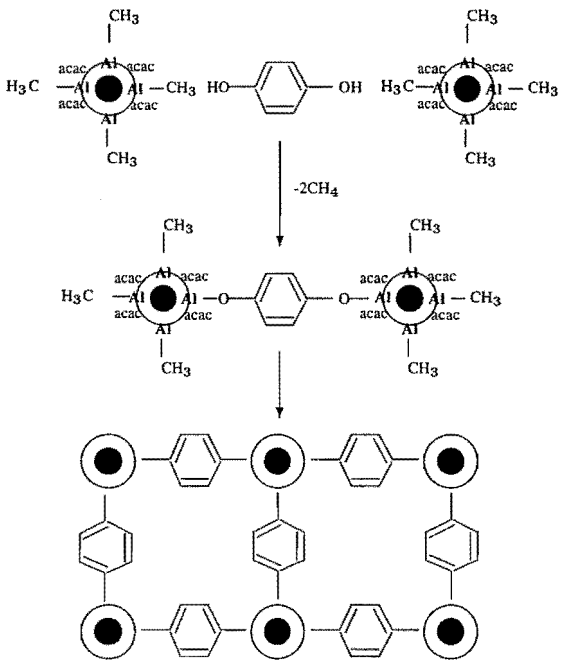

FIG. 1. General principle of reactive interparticle connection.

For the structural characterization of such colloids with typical metal-particle diameters and interparticle distances in the 1-10 nm regime Anomalous Small Angle X-ray Scattering with synchrotron radiation (ASAXS) allows to separate the particle scattering

from that of the surrounding organic components and is therefore a suitable method for the determination of the structural parameters.

We performed ASAXS experiments to study the nanostructure of the three different Pt colloids. Contrast-variation experiments at two different X-ray energies E_1=10.976 keV and E_2=11.551 keV near the L_3-absorption edge of Pt (E_{L3}=11.564 keV) were carried out in order to separate the particle scattering from the background. All measurements were performed at our ASAXS beamline JUSIFA [2] at DESY/HASYLAB.

Results and discussion

The separated particle scattering curves $d\Sigma/d\Omega_p = d\Sigma/d\Omega(E_1) - d\Sigma/d\Omega(E_2)$ along with their refined model functions are shown in Fig. 2, and the most interesting refined model parameters are given in Table 1. For the least-squares refinements of the scattering curves we applied a modified model function based on the work of A. Vrij [3] which describes the scattering of a mixture of hard spheres (i.e. the Pt-metal particles) with a continuous (log-normal) size distribution and an additional constant distance-parameter D_0 (for the spacer-molecules).

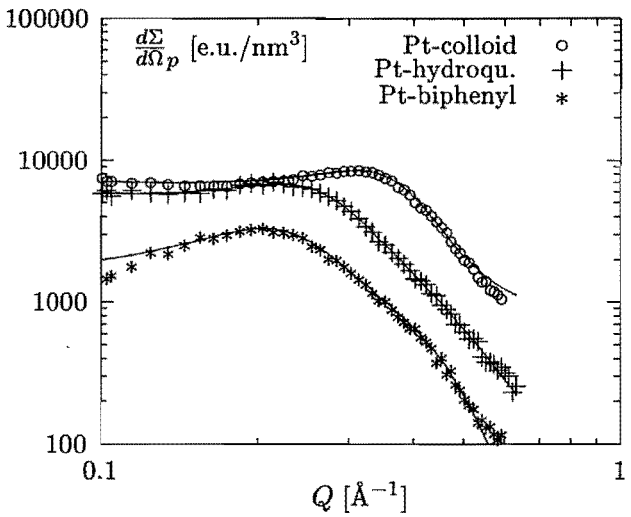

FIG. 2. Separated small-angle scattering- and refined model- curves for three different Pt-colloids.

The results for the (most frequently occuring) radius R_0 for the three investigated samples are in excellent agreement with those obtained from TEM-images [4]. The different D_0-values of the three samples are found consistent with the different types of spacer-molecules used for the interconnection of the metal-particles.

For the Pt-colloid the Pt-particles are not interconnected by spacer-molecules. For this sample, the refinement yields a D_0-value of approximately 4 Å. This value is twice the thickness D_{ps} of the Al-organic protective shell which surrounds each of the Pt-particles (D_0 =2D_{ps}). The result can be easily crosschecked by subtracting 2D_{ps} from the D_0-values of the other two samples.

TABLE 1. Refined model Parameters R_0,σ_0 and D_0 for three Pt-colloids

Sample	R_0 [Å]	σ_0	D_0 [Å]
Pt-colloid	5.5(3)	0.21(1)	3.7(8)
Pt-hydroquinone	5.3(3)	0.26(2)	9.8(8)
Pt-biphenyl	6.2(2)	0.17(3)	12.3(4)

The differences D_0-2D_{ps} = 6(1) Å for Pt/hydroquinone and D_0-2D_{ps} = 8.6(9) Å for Pt/4,4-dihydroxy-biphenyl are consistent with the theoretical spacer-lengths of d_{th} = 5.8 Å and d_{th} = 9.9 Å calculated by molecular modelling. This finding also indicates that the metal particles are completely interconnected by the spacers. However, the thickness of about 2 Å for the protective shell is quite small and corresponds approximately to the diameter of only one CH_3-group which implies that the major part of the Al-organic material must form some kind of 'alloy' on the particle surface, together with the Pt-atoms.

Conclusion

The results obtained so far show that the nanostructure in 3-D metal-particle networks can be investigated in ASAXS experiments.

The method of reactive interconnection of Al-organic stabilized metal particles by bifunctional spacers is found to work properly. However, the non-zero parameters σ_0 for the widths of the particle-size-distributions show the main problem which has to be solved in order to increase the degree of particle-ordering: The synthesis-method has to be improved to produce nearly monodisperse metal-particles with a uniform size and shape. This is the basic requirement for the creation of highly ordered nanolattices.

References

[1] H. Bönnemann et al.: Rev. Roum. Chim. 11-12, 1003-1010 (1999)

[2] H.-G. Haubold et al., Rev. Sci. Instr. 60, 1943-1946 (1989)

[3] A. Vrij: J. Chem. Phys. 71, 3267-3270 (1979)

[4] N. Waldöfner, H. Bönnemann, personal communication

Publications in refereed journals

Alefeld B.; Dohmen L.; Heidemann A.1
1ILL, Grenoble, France
GaAs as a backscattering crystal
Physica B 283 (2000) 299 - 301
23.89.1

Alefeld B.; Dohmen L.; Richter D.; Brückel Th.
Space technology from X-ray telescopes for focusing SANS and reflectometry
Physica B 276 - 278 (2000) 52 - 54
23.89.1

Alefeld B.; Dohmen L.; Richter D.; Brückel Th.
X-ray space technology for focusing small-angle neutron scattering and neutron reflectometry
Physica B 283 (2000) 330 - 332
23.89.1

Braun A.1; Bärtsch M.1; Schnyder B.1; Kötz R.1; Haas O.1; Haubold H.-G.; Goerigk G.
1PSI, Department of General Energy Research, Villigen, Switzerland
X-ray scattering and adsorption studies of thermally oxidized glassy carbon
Journal of Non-Crystalline Solids 260 (1999) 1 - 14
23.89.1

Futakawa M.1; Kikuchi K.1; Conrad H.; Stechemesser H.
1Japan Atomic Energy Research Institute, Tokai-mura, Japan
Pressure and stress waves in a spallation neutron source mercury target generated by high-power proton pulses
Nuclear Instruments and Methods in Physics Research A 439 (2000) 1 - 7
23.60.0

Hohlwein D.1,2; Zeiske Th.
1University, Institut für Kristallographie, Tübingen
2HMI, BENSC, 14109 Berlin
Paramagnetic short-range order in MnF2 beyond the critical region
Physica B 276 - 278 (2000) 584 - 585
23.89.1

Hupfeld D.; Schweika W.; Strempfer J.1; Mattenberger K.2; McIntyre G. J.3; Brückel Th.
1Ames Laboratory, Iowa State University, Ames, USA
2ETH, Laboratorium für Festkörperphysik, Zürich, Switzerland
3ILL, Grenoble, France
Element-specific magnetic order and competing interactions in Gd0.8Eu0.2S
Europhyics Letters 49 (1) (2000) 92 - 98
23.89.1

Irmer G.1; Monecke J.1; Verma P.2; Goerigk G.; Herms M.3
1University of Mining and Technology, Institute of Theoretical Physics, Freiberg
2Institute of Technology, Department of Electronics and Information Science, Kyoto, Japan
3Fraunhofer-Institut für Zerstörungsfreie Prüfverfahren, Dresden
Size analysis of nanocrystals in semiconductor doped silicate glasses with anomalous small-angle x ray and Raman scattering
Journal of Applied Physics 88 (2000) 1873 - 1879
23.89.1

Kaendler I. D.1; Seeck O. H.; Schlomka J.-P.1; Tolan M.1; Press W.1; Stettner J.1; Kappius L.2; Dieker C.2; Mantl S.2
1University, Inst. f. Exp. und Angw. Physik, Kiel
2FZJ, ISI, Jülich
Structural characterisation of oxidized allotaxially grown CoSi2 layers by x-ray scattering
Journal of Applied Physics 87 (2000) 133 - 139
23.89.1

Kentzinger E.; Rücker U.; Caliebe W.; Goerigk G.; Werges F.; Nerger S.; Voigt J.; Schmidt W.; Alefeld B.; Fermon C.1; Brückel Th.
1DRECAM/SPEC, CEA Saclay, 91191 Gif-sur-Yvette, France
Structural and magnetic characterization of Fe/(-Mn thin films
Physica B 276 - 278 (2000) 586 - 587
23.89.1

Kentzinger E.; Schober H. R.
Migration energies in L12 intermetallic compounds
J. Phys.: Condens. Matter 12 (2000) 8145 - 8158
23.89.1

Kümmerle E. A.1; Güthoff F.1; Schweika W.; Heger G.1
1University, Institute for Crystallography, Aachen
Single-Crystal Neutron Diffraction Investigations on the Phase Transitions in CeO1.800 and CeO1.765
Journal of Solid State Chemistry 153 (2000) 218 - 230
23.15.0

Meier G.1; Pawelzik U.1; Schweika W.; Kockelmann W.2
1MPI-Polymerforschung, Mainz
2ISIS, Rutherford Laboratory, UK
The static structure factor S(Q) of partially deuterated ethyl- and hexylmethacrylate polymers
Physica B 276 - 278 (2000) 369 - 370
23.89.1

Reif T.; Doerr M.1; Loewenhaupt M.1; Rotter M.1; Svoboda P.2; Welzel S.3
1Technische Universität, Institut für Angewandte Physik, Dresden
2Charles University, Department of Electron Systems, Prague,The Czech Republic
3HMI, Berlin
Magnetic structure of DyCu2 in the virgin and in the converted state
Physica B 276 - 278 (2000) 600 - 601
23.89.1

Rücker U.; Alefeld B.; Bergs W.; Kentzinger E.; Brückel Th.
The new polarized neutron reflectometer in Jülich
Physica B 276 - 278 (2000) 95 - 97
23.89.1

Rücker U.; Alefeld B.; Kentzinger E.; Brückel Th.
Monochromator design for the HADAS reflectometer in Jülich
Physica B 283 (2000) 422 - 425
23.89.1

Seeck O. H.; Kaendler I. D.1; Sinha S. K.1; Tolan M.2; Shin K.3; Rafailovich M. H.3; Sokolov J.3; Kolb R.4
1ANL, APS, Argonne, USA
2University, Inst. f. Exp. und Angw. Physik, Kiel
3SUNY, Dept. of Mat. Sci. and Engin., Stony Brook, USA
4Exxon Research, Annadale, USA
Analysis of x-ray reflectivity data from low-contrast polymer bilayers using a Fourier method
Applied Physics Letters 76 (2000) 2713 - 2715
23.30.0, 23.89.1

Strempfer J.1; Brückel Th.; Caliebe W.; Vernes A.2; Ebert H.2; Prandl W.3; Schneider J. R.1
1HASYLAB at DESY, Hamburg
2Universität, Institut für Physikalische Chemie, München
3Universität, Institut für Kristallographie, Tübingen
Form-factor measurements on chromium with high-energy synchrotron radiation
Eur. Phys. J. B 14 (2000) 63 - 72

23.89.1

Tolan M.1; Seeck O. H.; Wang J.2; Sinha S. K.2; Rafailovich M. H.3, Sokolov J.3
1University, Inst. f. Exp. und Angw. Physik, Kiel
2ANL, APS, Argonne, USA
3SUNY, Dept. of Mat. Sci. and Engin., Stony Brook, USA
X-ray scattering from polymer films
Physica B 283 (2000) 22 - 26
23.30.0, 23.89.1

Zeiske Th.; Hagdorn K.1; Hohlwein D.1; Ihringer J.1; Prandl W.1; Ritter H.1
1University, Institut für Kristallographie, Tübingen
Structure and magnetism of Ho0.2Ca0.8MnO3
Physica B 276 - 278 (2000) 624 - 625
23.89.1

Other publications

Brückel Th.; Eberhardt W.
Dynamik in kondensierter Materie
Vorlesungsmanuskripte des 31. IFF-Ferienkurses vom 13. - 24.03.2000 (2000), Schriften des Forschungszentrums Jülich, Reihe Materie und Material/Matter and Materials, Band 3, ISBN 3-89336-256-8, 1 - 32
23.89.1

Brückel Th.; Eberhardt W.
Vorwort zum 31. IFF-Ferienkurs 2000 "fs und neV: Dynamik in kondensierter Materie"
Schriften des Forschungszentrums Jülich, Reihe Materie und Material/Matter and Materials, Band 3, ISBN 3-89336-256-8
23.89.1

Brückel Th.
Elastic Scattering from Many-Body Systems
Schriften des Forschungszentrums Jülich, Reihe Materie und Material / Matter and Materials, Volume 5 (2000) 3-1 - 3-18
23.89.1

Brückel Th.
Magnetism
Schriften des Forschungszentrums Jülich, Reihe Materie und Material / Matter and Materials, Volume 5 (2000) 16-1 - 16-19
23.89.1

Conrad H.
Die Europäische Spallations-Neutronenquelle ESS - Spallationsmethoden
Vorlesungsmanuskripte des 31. IFF-Ferienkurses vom 13. - 24.03.2000 (2000), Schriften des Forschungszentrums Jülich, Reihe Materie und Material/Matter and Materials, Band 3, ISBN 3-89336-256-8, B4.1 - 20
23.89.1

Conrad H.
Neutron Sources
Schriften des Forschungszentrums Jülich, Reihe Materie und Material / Matter and Materials, Volume 5 (2000) 1-1 - 1-15
23.89.1

Schweika W.
Polarization analysis
Schriften des Forschungszentrums Jülich, Reihe Materie und Material / Matter and Materials, Volume 5 (2000) 4-1 - 4-19
23.89.1

Schweika W.
Quellen und Eigenschaften der Neutronen- und Synchrotronstrahlung
Vorlesungsmanuskripte des 31. IFF-Ferienkurses vom 13. - 24.03.2000 (2000), Schriften des Forschungszentrums Jülich, Reihe Materie und Material/Matter and Materials, Band 3, ISBN 3-89336-256-8, B1.1 - 20
23.89.1

Seeck O. H.; Sinha S. K.1; Kaendler I. D.1; Shu D.1; Shin K.2; Rafailovich M.2; Sokolov J.2; Tolan M.3
1ANL, APS, Argonne, USA
2SUNY, Dept. of Mat. Sci. and Engin., Stony Brook, USA
3University, Inst. f. Exp. and Angw. Physik, Kiel
Interfacial properties of soft matter thin films studied by x-ray scattering
in: Interfacial Properties on the Submicron Scale, ACS/Oxford Press (2000) ed. by J. Frommer, R. Overney
23.89.1

Seeck O. H.; Sinha S. K.1; Kaendler I. D.1; Wang J.1
1ANL, APS, Argonne, USA
Investigation of confined liquids with x-ray and neutron scattering
in: Exploration of subsurface phenomena by particle scattering, IAS Press (2000) ed. by N. Q. Lam, C. A. Melendres, S. K. Sinha
23.89.1

Seeck O. H.
Continuum description: Grazing Incidence Neutron Scattering
in: Neutron Scattering, Forschungszentrum Jülich GmbH (2000) 6-1 - 6-18, ed. by Th. Brückel, G. Heger, D. Richter
23.89.1

Tolan M.1; Seeck O. H.; Wang J.2; Sinha S. K.2; Rafailovich M. H.3; Sokolov J.3
1University, Inst. f. Exp. and Angw. Physik, Kiel
2ANL, APS, Argonne, USA
3SUNY, Dept. of Mat. Sci. and Engin., Stony Brook, USA
Surface structure of soft-matter thin films probes by diffuse x-ray scattering
in: Exploration of subsurface phenomena by particle scattering, IAS Press (2000) ed. by N. Q. Lam, C. A. Melendres, S. K. Sinha
23.89.1

Vasiliu-Doloc L.1; Rosenkranz S.2; Osborn R.2; Sinha S. K.3; Lynn J. W.1; Mesot J.2; Seeck O. H.; Preosti G.4; Fredo A.J.4; Mitchell J. F.2
1NIST Center for Neutron Research, Gaithersburg, USA
2ANL/MSD, Argonne, USA
3ANL, APS, Argonne, USA
4Northern Illinois University, Dept. of Phys., DeKalb, USA
Charge melting and polaron collapse in La1.2Sr1.8Mn2O7
Advanced Photon Source Research No. 3, April 2000
23.89.1

Invited Talks

Brückel Th.
Magnetism in a new light: Applications of resonant and non-resonant magnetic x-ray diffraction
USA, Iowa State University/Ames Laboratory, Seminar of the Solid State Physics Group, 05.10.2000
23.89.1

Brückel Th.
The High Energy Side Station at the MuCAT Beamline
USA, Advanced Light Source APS, Seminar, 12.10.2000
23.89.1

Conrad H.
Introduction to the ESS Mercury Target System Design
Tokai, Japan, 2nd International Workshop on Mercury Target and Cold Moderator Engineering, 13.11.2000
23.60.0

Conrad H.
Probleme in Target- und Moderatormaterialien
Simonskall, ESS-Tag, 17.04.2000
23.60.0

Conrad H.
Status Report on the Jülich ESS-related activities
Tsukuba, Japan, ICANS-XV, 09.11.2000
23.60.0

Goerigk G.
Anomalous Small Angle X-ray Scattering
Budapest, Technische Universität, Institutsseminar des Instituts für Physikalische Chemie, 09.11.2000
23.89.1

Goerigk G.
Materialuntersuchungen mit anomaler Röntgen-Kleinwinkelstreuung
Berlin, Kolloquium des Komitees Forschung mit Synchrotronstrahlung, 07. - 08.07.2000
23.89.1

Goerigk G.
Materialuntersuchungen mit anomaler Röntgen-Kleinwinkelstreuung
Rostock, Universität, Fachbereich Physik, Institutsseminar, 11.05.2000
23.89.1

Haubold H.-G.
Röntgenkleinwinkel-Streuung an Realkatalysatoren
Bochum, Ruhr-Universität, Graduiertenkolleg, 18.01.2000
23.89.1

Ioffe A.
Neutron Speed Echo Spectroscopy
Berlin, International Workshop on Neutron Spin Echo Spectroscopy, 16. - 17.10.2000
23.89.1

Köbler U.
Die dominierende Rolle der Austauschwechselwirkungen 4. Ordnung in reinen Spinmaterialien
Aachen, RWTH, Seminar über Kristall- und Strukturchemie, 03.11.2000
23.15.0

Mueller R.
The Yb fiber LASER for metastable 3He optical pumping at Jülich
Sanct Petersburg, Russia, PNCMI-2000 International Workshop, 22.06.2000
23.89.1

Seeck O. H.
Coherent X-ray Scattering on Layer Systems with Magnetic Roughness
Hamburg, DESY/HASYLAB, XFEL-Workshop, 20. - 21.07.2000
23.89.1

Seeck O. H.
Investigation of polymer bilayer interfaces with x-ray scattering
Amsterdam, The Netherlands, AMOLF, Seminar, 24.07.2000
23.89.1

Seeck O. H.
Untersuchung der Grenzflächeneigenschaften dünner "Soft-Matter"-Filme mittels Röntgenstreuung
Berlin, Hahn-Meitner-Institut, Seminar, 17.02.2000
23.30.0, 23.9.1

Other talks

Brückel Th.; Ioffe A.; Küssel E.; Massalovitch S.; Schlapp M.; Schmitz B.
Development of the high resolution image plate detector at the FZ Jülich
Grenoble, France, ILL, 2nd TECHNI Meeting, 12. - 13.10.2000
23.89.1

Brückel Th.; Rücker U.
Weiterentwicklung von Beugungsmethoden zur Untersuchung magnetischer Materialien mit Hilfe von Synchrotronstrahlung
Konferenzraum des IFF, Vollversammlung BMBF Verbund 04, 14. - 15.02.2000
23.89.1

Brückel Th.
Image Plate Detector for Thermal Neutrons
Abingdon, UK, The Cosener's House; TECHNI-Meeting, 30. - 31.03.2000
23.89.1

Brückel Th.
Polarised Neutron Scattering at the Jülich Research Center
Grenoble, France, ILL, ENPI-Meeting, 24. - 25.02.2000
23.89.1

Conrad H.
JESSICA, the ESS-like Target/Moderator/Reflector Mock-up and Cold Moderator Test Facility
Tsukuba, Japan, ICANS-XV, 08.11.2000
23.60.0

Conrad H.
Overview of the ESS Target and Moderator R&D
Tsukuba, Japan, ICANS-XV, 07.11.2000
23.60.0

Haubold H.-G.; Vad Th.; Jungbluth H.; Hiller P.
Nano Structure of Nafion: A SAXS Study
Noosa, Australia, ISPE 7, 06. - 11.08.2000
23.89.1

Hupfeld D.
The mu-CAT Undulator High Energy Side Station
APS, Argonne, USA, Technical Workgroup Meeting, 16.11.2000
23.89.1

Rücker U.; Bergs W.; Alefeld B.; Kentzinger E.; Brückel Th.
The new polarized neutron Reflectometer in Juelich
Sanct Petersburg, Russia, PNCMI-2000 International Workshop, 21.06.2000
23.89.1

Posters

Alefeld B.; Dohmen L.; Brückel Th.
GaAs as a backscattering crystal
Aachen, RWTH, 8. DGK Jahrestagung, 13. - 16.03.2000
23.89.1

Gebhardt R.; Lauer I.; Nawroth T.; Decker H.; Goerigk G.; von Krosigk G.
Structural Changes of Oxygen Transport Protein Hemocyamin Detected by pH-Dependent USAXS
Hamburg, HASYLAB, Usermeeting, 28.01.2000
23.89.1

Glück S.; Fischer P.; Schütz G.; Goerigk G.
Monitoring of the Circular Polarization State of Synchrotron Radiation at B1 (JUSIFA) Beamline
Hamburg, HASYLAB, Usermeeting, 28.01.2000

23.89.1

Goerigk G.; Williamson D. L.
Nanostructured Ge-Distribution in a-SiGe Alloys from Anomalous Small Angle X-ray Scatterinbg Studies
Hamburg, HASYLAB, Usermeeting, 28.01.2000
23.89.1

Hupfeld D.; Brückel Th.; Schweika W.; Strempfer J.1; Mattenberger K.2
1APS at ANL, Argonne, USA
2ETH, Zürich, Switzerland
Resonante Austauschstreuung an GdxEu1-xS-Mischkristallen
Aachen, RWTH, 8. DGK Jahrestagung, 13. - 16.03.2000
23.89.1

Hupfeld D.; Strempfer J.1; Voigt J.; Goldman A.2; Brückel Th.
1Northern Illinois University, de Kalb, USA
2Ames Laboratory, Iowa State University, Ames, USA
X-ray resonance exchange scattering from a Tb single crystal
Chicago, USA, 10th Advanced Photon Source (APS) User Meeting, 02. - 04.05.2000
23.89.1

Kentzinger E.; Rücker U.; Nerger S.; Caliebe W.; Goerigk G.; Werges F.; Brückel Th.
Charakterisierung von dünnen epitaktischen (-Mn-Schichten mit Elektronenbeugung sowie Reflektometrie und diffuser Streuung von Synchrotronstrahlung
Aachen, RWTH, 8. DGK Jahrestagung, 13. - 16.03.2000
23.89.1

Köbler U.
Fourth-order exchange interactions - the driving forces in magnetism
Berlin, HMI, Nutzertreffen, 05.05.2000
23.15.0

Nawroth T.; Gebhardt R.; Decker H.; Goerigk G.
XANES and EXAFS of Metalloproteins by Subtraction of True Reference Spectra Obtained with a Flow-Through Cell
Hamburg, HASYLAB, Usermeeting, 28.01.2000
23.89.1

Nerger S.; Kentzinger E.; Rücker U.; Voigt J.; Ott F.1; Seeck O. H.; Brückel Th.
1LLB, CEA/CNRS, France
Proximity effects in Fe1-xCox/Mn/Fe1-xCox trilayers
Sanct Petersburg, Russia, PNCMI-2000 International Workshop, 21.06.2000
23.89.1

Rücker U.; Bergs W.; Alefeld B.; Kentzinger E.; Brückel Th.
The new polarized neutron Reflectometer in Juelich
Sanct Petersburg, Russia, PNCMI-2000 International Workshop, 21.06.2000
23.89.1

Schweika W.; Ice G. E.1; Robertson J. L.1; Sparks C. J.1; Bai J.1
1ORNL, Oak Ridge, USA
Gitterverschiebungen und Fermiflächeneffekte in Cu3Au
Aachen, RWTH, 8. DGK Jahrestagung, 13. - 16.03.2000
23.89.1

Schweika W.
The Instrument DNS: Polarization Analysis for Diffuse Neutron Scattering
Sanct Petersburg, Russia, PNCMI-2000 International Workshop, 21.06.2000
23.89.1

Wang Y.-G.; Kentzinger E.; Rücker U.; Caliebe W.; Goerigk G.; Babik W.; Brückel Th.
Strukturelle Charakterisierung von Fe/Cr/Fe Schichtsystemen
Aachen, RWTH, 8. DGK Jahrestagung, 13. - 16.03.2000
23.89.1

Wang Y.-G.; Kentzinger E.; Rücker U.; Seeck O. H.; Brückel Th.; Schreiber R.; Bürgler D. E.; Grünberg P.
Characterization of the Buried Interfaces in Fe/Cr/Fe Trilayers using Synchrotron Radiation
Dresden, VDI-Tagung, 13. - 16.06.2000
23.89.1

Patents applied for

Dohmen L.; Alefeld B.
Geschwindigkeitsselektor zur Monochromatisierung eines Neutronenstrahls
PCT: PCT/DE 00/00238 (23.01.2000) (EP,US,JP)
PT 1.1656
23.89.1

Sonnenberg K.; Küssel E.
Verfahren und Vorrichtung zur Herstellung von Einkristallen sowie Kristallkeim
EP: 00105206.7 (13.03.2000) (BE,DE,FR,GB,IT,NL) US: 09/526,768 (16.03.2000)
PT 1.1681
23.89.1

Sonnenberg K.; Küssel E.
Vorrichtung zur Herstellung von Einkristallen
Deutsche Patentanmeldung 199 12 484.1-43 PCT/DE 00/02349 (16.03.2000) (EP,US,JP)
PT 1.1680
23.89.1

Lecture courses

Brückel, Th., Schweika, W.
Ferienschule (Praktikum) über Neutronenstreuung
TV 10 / TÜ 30, WS 00/01

Brückel, Th.
Festkörpermagnetismus und hochkorrelierte Elektronensysteme
RWTH Aachen, V2, SS 00
1.2 FKF

Internal reports

Nerger S.
Struktur und magnetische Kopplung in FexCo1-x/Mn/FexCo1-x-Schichtsystemen
Diplomarbeit in Physik, vorgelegt der RWTH, angefertigt am IFF
23.89.1

Voigt J.
Elementspezifische Magnetisierungsdichteverteilung in Seltenen-Erd-Übergittern
Diplomarbeit in Physik, vorgelegt der RWTH, angefertigt am IFF
23.89.1

Internal seminars

Brückel Th.; Eberhardt W.
Dynamik in kondensierter Materie
Auditorium der Zentralbibliothek, IFF-Ferienschule, 13.03.2000

23.89.1

Brückel Th.
Elastic Scattering from Many-Body Systems
IFF-Hörsaal, Neutron Laboratory Course, 26.09.2000
23.89.1

Brückel Th.
Magnetism
IFF-Hörsaal, Neutron Laboratory Course, 29.09.2000
23.89.1

Conrad H.
Die Europäische Spallations-Neutronenquelle ESS - Spallationsmethoden
Auditorium der Zentralbibliothek, IFF-Ferienschule, 13.03.2000
23.89.1

Conrad H.
Neutron Sources
IFF-Hörsaal, Neutron Laboratory Course, 26.09.2000
23.89.1

Kentzinger E.
Characterization of the buried interfaces in metallic multilayers using synchrotron radiation
IFF-Hörsaal, Informationstagung aus Anlaß der 15. Sitzung des Wissenschaftlichen Beirats, 13.04.2000
23.89.1

Schweika W.
Polarization analysis
IFF-Hörsaal, Neutron Laboratory Course, 27.09.2000
23.89.1

Schweika W.
Quellen und Eigenschaften der Neutronen- und Synchrotronstrahlung
Auditorium der Zentralbibliothek, IFF-Ferienschule, 13.03.2000
23.89.1

Seeck O. H.
Continuum description: Grazing Incidence Neutron Scattering
IFF-Hörsaal, Neutron Laboratory Course, 27.09.2000
23.89.1

Institute for Neutronscattering

General Overview

The year 2000 was a normal year of reactor operation. The FRJ-2 delivered neutrons for 177 days with good reliability. During that time all together 201 experiments were carried out, 114 of them with external participation. These experiments were performed out with the support of the Institute for Neutronscattering, the Institute for Scattering Techniques and external collaborating research groups. In 2000 the 4th Neutron Laboratory Course took place. This time, the participation was opened for European students and supported financially by the European Neutron Round Table. From the 36 accepted participants 12 came from outside Germany. Seven students performed the Laboratory Course as part of the advanced practical course in materials science in the frame of the physical chemistry curriculum at the University of Münster.

Neutron instrumentation (F&E-Nr. 23.89.1)
In 2000 at the NSE spectrometer in the ELLA laboratory a double spin echo set up was implemented. This device increased the accessible dynamic range to four orders of magnitude in time. Setting up a collimator system in front of the detector reduced the instrumental background significantly, allowing now the study of very weak incoherent scattering which is always a problem for spin echo spectroscopy. Here, the Jülich instrument provides now unique capabilities (see report A. Wischnewski).

The backscattering spectrometer (BSS 1) was equipped with a new set of analyzers featuring large perfect silicon crystals. In this way, the instrumental resolution was significantly improved. In particular the line shape of the resolution function was transformed from a Lorenzian to a Gaussian shape, enabling the instrument to detect minute amounts of quasielastic scattering close to the central peak (see report H. Grimm).

At the triple axis spectrometer (IN 12), by a number of instrumental improvements in particular using a big vacuum tank around the sample, the instrumental background in forward direction was significantly decreased. In this way e. g inelastic spectroscopy on glass forming liquids at very small Q-values became possible.

The design and construction of the backscattering spectrometer for the FRM-II in Munich proceeded according to the management plan. The design of the phase space transformation chopper and the analyzer system was completed; both items are now under construction. A new system for glueing perfect silicon crystals on the analyzer spheroids was developed and implemented. The doppler drive which uses aircushions was finally constructed. One remaining problem relates to the surface treatement of the guiding rails and grooves, which most likely is solved by atmospheric plasma spraying. An intermediate solution was chosen for the construction of the prototype.

Polymers, membranes and complex fluids (F&E-Nr.: 23.30.0)
Most of the research in the institute focuses on the study of soft condensed matter systems, emphasizing polymers and complex fluids. Such research requires a close collaboration between synthetic chemists and physicists. In the institute this is realized by a synthetic laboratory which provides the samples for the physics research.

Polymer synthesis
Aside of the standard preparation of homo- and block-copolymers two items deserve to be highlighted:

1. Model Polyolefins are generally derived from the anionic polymerization of dienes and subsequent catalytic hydrogenation. In general, thereby, not only two hydrogens or deuteriums are added at the double bond but further hydrogens are exchanged. For samples with mixed hydrogen deuterium content, this leads to important uncertainties in the scattering length density which often endangers a quantitative evaluation of experiments. Using p-Toluenesulphonylhydrazide-N, N, N-d_3 as a catalyst it became possible to saturate Polydienes without any significant H, D exchange. This technique was used in order to synthesize deuterated polyethylene chains with protonated labels at preordained positions.

2. A specialty of the chemistry lab is the synthesis of branched polymers. Standard characterization techniques for such polymers like GPC, light scattering, membrane-osmosis and NMR are not sensitive enough to detect small differences in the degree of branching. We investigated the possibilities of Temperature Gradient Interaction Chromatography (TGIC) as an alternative to GPC. It turned out, that it was possible to characterize branched polymers with an accuracy unknown in the past. Especially in the case of an partially deuterated H-polymer all different defect structures were unambiguously characterized. Furthermore, a strong isotope effect was found in TGIC - an effect, which was not yet reported for this class of chromatographic techniques. For partially

deuterated branched polymers this isotope effect can be used to increase the resolution power of TGIC even further.
As a new feature in the analytic laboratory a GPC triple detector is now in use, which allows an absolute determination of the molecular weights by online light scattering and universal calibration.

Polymer dynamics
Dynamic properties of polymers are investigated from large scale motions like reptation, reaching to local relaxation and the β-process in glass forming polymers.

- **Large scale motion**
  One of this years highlights was the direct observation of the mean squared proton displacement in polymer melts as a function of time by incoherent neutron scattering. These experiments became possible due to the excellent performance and stability of the Jülich NSE spectrometer and lead to the first direct observation of the cross over from the Rouse motion $\langle r^2(t)\rangle \approx t^{1/2}$ to local reptation $\langle r^2(t)\rangle \approx t^{1/4}$.
  Comparing the mesoscopic relaxation dynamics of a polymer with large intrachain barriers (Polyisobutylene) with one with basically no rotational barriers (Polydimethylsiloxane), it became possible to identify the molecular origin of so called intrachain viscosity effects in polymer solutions. From the detailed Q and t dependence of the relaxation spectra, it could be shown that the intrachain viscosity can be directly related to the dissipation from reorientational jumps across torsional barriers within a chain (collaboration with the group of Prof. Colmenero in San Sebastian).

- **Local dynamics**
  One of the most puzzling features of the glass transition is the strong increase of the fast pikosecond process with temperature which is found universally in neutron and light scattering studies. It could be shown that an interpretation in terms of a strong increase of low barrier relaxation centers above the glass transition explains not only the feature itself but also suggest a new view of the Vogel-Fulcher behavior of the viscosity and of the Kauzmann entropy crisis. In this view the Kauzmann and Vogel-Fulcher temperatures correspond to the point, where the fast pikosecond process extrapolates to zero. From a series of neutron measurements in polystyrene this point lies about 40K below the glass temperature in good agreement with Vogel-Fulcher data from the literature.

  Dielectric studies on the β-relaxation of different polymers and low molecular glass formers by dielectric spectroscopy could be interpreted in terms of the two level potential according to Gilroy and Philips, giving further support to this theoretical picture. NSE experiments on Polybutadienes with different degrees of deuteration tried to identify the dynamics related to different correlation functions in a glass forming melt. It turned out that below the merging temperature of the α- and β-process the dynamics of a sample, where the double bond is labeled is significantly and qualitatively different to that of a fully deuterated material. While the relaxation of the fully deuterated material follows the α-process, the labeled double bond appears to relax according the β law.

Structure formation in polymer solutions and complex fluids
In a collaboration with the group of Prof. Gompper (Theorie II), we exploited the ability to tune the surface elasticity of bicontinuous microemulsions by the addition of minute amounts of amphiphilic block copolymers. We showed that the bending elasticity can be directly read off from structural data. For the first time, we measured the spatial renormalization of the bending elasticity and determined the prefactor, which was under discussion for more than ten years (see report G. Gompper/Theorie II).

The dynamics of bicontinuous microemulsions was studied over a large range of composition and momentum transfer combining NSE and dynamic light scattering. In the range of the structural relaxation the data agree qualitatively with the prediction of the time dependent Landau-Ginzburg theory of Gompper. At more local scales the data assume asymptotically the behavior predicted by the Zilman and Granek theory.

Our studies on the micellarization properties of PEO-PEP amphiphilic diblockcopolymers were continued by measurements on symmetric species of the PEOx-PEPx type. A shape transition from spherical to rod like micelles was detected. The experimental results could be interpreted satisfactorily by a mean field model of Nagaraian and Ganesh (see report H. Kaya).

The short range order of polymers in the melt was investigated on a series of differently labeled Polyisoprene materials. The experimental structure factors were quantitatively compared with computer simulations (group of Prof. Colmenero/Univ. San Sebastian) achieving in general good agreement (see report R. Zorn). Now the

simulations are used in order to identify specific partial structure factors contributing to the observed experimental spectra.

Phase transitions
In a collaboration with the theory group of Prof. Löwen in Düsseldorf, careful studies on the phase diagram of star polymer colloid mixtures were undertaken. Thereby, the star arm number was varied from 2 to 32 and different star colloid size ratios were employed. A detailed comparison of experiment and theory lead to a consistent explanation of the experimental findings in terms of a soft star potential-colloid (see report J. Stellbrink).

The phase diagram of a three component polymer mixture consisting of a dPB/PS (deuterated Polybutadiene/Polystyrene) homopolymer blend of critical composition and different amounts of the corresponding dPB-PS diblock copolymer was explored. Beyond the Lifshitz line (at 6% diblock content) a micro emulsion phase was observed. First attempts were undertaken to determine the phase boundaries between disordered, bicontinuous, droplet, and ordered phases by applying theoretical approaches for the micro emulsion phases. Furthermore, as a function of temperature the Lifshitz line depends on the diblock concentration, an observation contradicting present mean field theories.

Branched polymers and rubbers
The work on rubbers concentrated on the role of fillers. Spherical silica particles aggregating in clusters and cylindrical fillers arising from microphase separations in a triblockcopolymer of the type Polybutadiene-Polystyrene-Polybutadiene were investigated. A careful analysis of the overstrain of the polymer matrix yielded a reinforcement factor for the silica fillers agreeing with a Padé-formulation of the strain amplification. To our surprise an analysis of the rod like filler does not reveal any strain amplification effect at all. A combination of SAXS and SANS results is consistent with an unaffected matrix network and limited strain orientation of the rods with subsequent breaking of the cylinders.

The work in the Brite Euram project on "The science and technology of long chain branching in Polyolefines and their process control", concentrated on the analysis of the relaxation behavior of partially labeled *H*-blockcopolymers. The theory development was performed in collaboration with Prof. Straube from Halle and Prof. McLeish from Leeds. An inclusion of the reduction of topological constraints due to dynamic dilution processes and the consideration of incompressibility leads now to a workable approach which gives a relatively good description of the SANS pattern as well as the rheological results.

Further work was carried out in an industrial collaboration with DSM, where the unperturbed chain dimensions of Nylon 6 were studied. These experiments were extremely difficult and needed the elimination of polyelectrolyte as well as intrachain hydrogen bonding effects.

Further research activities (F&E-Nr.: 23.15.0)

Tunneling systems
The study of rotational tunneling concentrated on the evaluation of defect structures and their influence on the tunneling spectra. Comparison of the tunneling spectra in glassy and crystalline toluene were performed in collaboration with the group of Prof. Colmenero in San Sebastian. A nice example of controlled defect structures and their effect on the rotational tunneling is reported in the contribution by M. Prager. Other than in glasses controlled defect structures allow to observe the subtle effects of environmental changes on the rotational tunneling properties of methyl groups.

Biological macromolecules
We studied the temperature – and humidity dependence of the self correlation of the hydrogen atoms in DNA as probe for the onset of configurational fluctuations. The measurements were extended to three different degrees of hydration and – in frequency – down to the GHz regime. The onset of relaxational motion at about 200K relates to a large extent to the presence of water and it is absent for dry DNA.

Dieter Richter

Personnel 2000/2001 and areas of activity

Scientific Staff

Dr. J. Allgaier	Polymer synthesis, microemulsions	23.30.0
Prof. Dr. U. Buchenau	Dynamics of glassforming materials	23.30.0
Dr. H. Grimm	Molecular crystals, oriented macromolecules Instrument Responsible: Backscattering spectrometer BSS1	23.30.0
Dr. M. Monkenbusch	Dynamics of polymers and complex liquids, development of new spin echo techniques Instrument Responsible: Spinecho Spectrometer NSE	23.30.0
Dr. M. Prager	Rotational tunneling Instrument Responsible: Thermal time of flight spectrometer SV 29	23.15.0
Dr. W. Pyckhout-Hintzen	Polymer networks, branched polymers, rheology Instrument Responsible: Small angle neutron scattering KWS 1	23.30.0
Prof. Dr. D. Richter *Institute Director*	Structure and dynamics of polymers, glass transition, complex liquids ESS Science Executive	23.30.0
Dr. D. Schwahn	Phase transitions in polymer systems, self assembly of crystalline copolymers Instrument Responsible: Small angle neutron scattering KWS 1 and double crystal diffractometer DKD	23.30.0
Dr. L. Willner	Polymer synthesis, polymer micelles	23.30.0
Dr. habil. R. Zorn	Rubbery electrolytes, glass transition, dynamics in confinement	23.15.0

Technical Staff

U. Bünten	Technician at KWS 1 and NSE	23.89.1
Ms. M. Hintzen	Technician in the polymer characterization laboratory	23.30.0
Dipl.-Ing. M. Heiderich	Engineer responsible for the KWS 1 and DKD instruments	23.89.1
M. Jungen	Technician at SV 29	23.89.1
Dipl.-Ing. T. Kozielewski	Engineer backscattering spectrometer FRM 2	23.89.1
Ms. U. Sausen-Malka	Electronics laboratory	23.89.1
J. Rademacher	Technician at SV 29 and KWS 3	23.89.1
Dipl.-Ing. R. Schätzler	Head of technical service group	23.89.1
K. Schönknecht (until 29.02.2000)	Technician at BSS 1 and NSE	23.89.1
T. Starc	Technician at BSS 1 spectrometer	23.89.1
R. Stollenwerk	Technician at KWS 2	23.89.1
Dipl.-Ing. G. Vehres	Electronics engineer, head of electronics laboratory Second Instrument Responsible: Thermal time of flight spectrometer SV 29	23.89.1
Ms. S. Oubenkhir	Secretary	

Scientists

Dr. L. Fetters	Self-assembly of crystalline: amorphous copolymers and rheological predictions of polymer systems.	23.30.0
Dr. H. Frielinghaus	Microemulsions Instrument Responsible: Small angle neutron scattering facility KWS 2	23.30.0
Dr. M. Heinrich	Polymer processing, influence of branched polymers	23.30.0
Dr. H. Hermes	Influence of solvent polymer interaction on the chain conformation of polyamide-6	23.30.0
Dr. S. Kahle	Dielectric spectroscopy, relaxations in complex polymer systems Second Instrument Responsible: Backscattering spectrometer BSS 1	23.30.0

Dr. O. Kirstein	Project scientist for backscattering instrument at FRM-II	23.89.1
Dr. M. Kreitschmann (until 29.02.2000)	Influence of polymer architecture on the aggregation properties of PI-PS blockcopolymers	23.30.0
Dr. W. Leube (until 31.10.2000)	Micellarisation and gelation of partially crystallizable polymers	23.30.0
Dr. M. Ohl	Second Instrument Responsible: D 23, IN 22 at the ILL	23.89.1
Dr. S. Perny	Synthesis of branched model polymers and analysis of the structural quality	23.30.0
Dr. A. Radulescu	Aggregation behavior of copolymers and wax crystallization	23.30.0
Dr. W. Schmidt	Instrument Responsible: IN 12 at the ILL	23.89.1
Dr. J. Stellbrink	Star polymers, colloid mixtures and living polymerization	23.30.0
Dr. A. Wischnewski	Topological constraints in polymer melts, ESS Scientific Advisory Committee (SAC) Assistant	23.89.1

Thesis Students (University of Münster)

Dipl.-Chem. B. Abbas	Critical concentration fluctuation; in blockcopolymer melts	23.30.0
Dipl.-Phys. A. Botti	Microscopic deformation of filled networks	23.30.0
Dipl.-Phys. D. Byelov	Cocrystallization of wax and copolymers	23.30.0
M.Sc. H. Endo	The role of amphiphilic polymers in the emulsification properties of microemulsions	23.30.0
M.Sc. M. Goad	Dynamic modulus and entanglement formation in polymer melts of polymer blends	23.30.0
Dipl.-Phys. S. Hoffmann	Dynamics of polymer blends	23.30.0
Dipl.-Ing. H. Kaya	Micellarisation of amphiphilic polymers	23.30.0
Dipl.-Ing. M. Mihailescu	Dynamic of microemulsions - influence of amphiphilic polymers	23.30.0
Dipl.-Phys. V. Pipich	Formation of structure in mixtures of two homopolymers and a diblockcopolymer	23.30.0

Guests

Dr. Ms. A. Arbe (Univ. of San Sebastian, Spain)	Primary and secondary relaxation in polymer glasses	23.30.0
Prof. Dr. J. Colmenero (Univ. of San Sebastian, Spain)	α–β relaxation in polymers	23.30.0
Dipl.-Phys. M. Heuberger (Weizmann Inst. of Science, Rheovot, Israel)	Investigation of PEP/PEP-PEO mixtures by small angle neutron scattering and neutron reflectivity	23.30.0
Dr. S. Koizumi (JAERI Tokai, Japan)	Heterogeneity in polymer glasses	23.30.0
Dr. Y. Melnichenko (Oak Ridge Nat. Lab., USA)	Critical behavior in polymer blends	23.30.0
Dr. Ms. H. Montes (ESPCI Paris, France)	Concentration fluctuations and dynamics in diblock copolymers, neutron scattering approach	23.30.0
Prof. E. Straube (Univ. Halle)	The influence of topological constraints at the microscopic level in polymer networks and blends	23.30.0
Dr. G. Wignall (Oak Ridge Nat. Lab., USA)	Ordering behavior of triblockcopolymers and polymers in solution	23.30.0

Trainees

R. Keller

B. Pütz

M. Riemenschneider

Rheology and the packing model: the case PVCH

M. Goad, W.Pyckhout-Hintzen, J. Allgaier, D. Richter, L. Fetters[1]
Institut for Neutronscattering
[1] *EXXON, Annandale, USA*

A rheological study on the behaviour of polymers with low plateau moduli was undertaken in view of the relationship between molecular structure and mechanical properties. The packing model relates both using the concept of the packing lenght p. New interesting relations have been found for typical high-to-medium plateau modulus polymers. The aim of this work is to synthesize first the highest possible packing length polymer at controlled conditions and to discuss its rheological parameters. The former observations could be confirmed at higher packiung lengths.

F&E-Nr: 23.30.0

The origin of the entanglement formation of polymers is not yet fully understood and several concepts have been forwarded [1]. It is now well established that the characteristic molecular weights, i.e. entanglement M_e and critical M_c in linear polymer melts can be related to the so-called packing length of the polymer. This length is given by the ratio of the volume and the chain stiffness $l_0^2 C_\infty$ where l_0 is the bond length and C_∞ the characteristic ratio. The packing model predicts for the plateau modulus $G_{No} \sim p^{-3}$. [2]. The investigated polymer polyvinylcyclohexane (PVCH) possesses the highest packing length which can be achieved retaining the quality of control of size and molecular weight distribution typical for the technique of anionic polymerization. PVCH serves as the extreme test to confirm the former (empirical)relations.

Synthesis of model PVCH polymers proceeded by catalytic hydrogenation of the anionically prepared polystyrene precursor. The hydrogenation is difficult to achieve due to the aromatic nature of the phenyl rings in the polystyrene [3]. Several catalyst systems were tested and it was possible to hydrogenate polystyrene up to molecular weights of $M_n = 3 \cdot 10^6$ using a specially activated palladium/carbon catalyst. For molecular weights higher than $M_n = 5 \cdot 10^5$ degradation of the polymer chains occurred. The degradation is due to chemical chain scission caused by traces of oxygen present in the hydrogenation reactor or by cleavage of C-C bonds caused by the catalyst. Difficulties involving chain degradation upon moulding by suitable stabilizers could be overcome succesfully. Dynamical-mechanical measurements were performed on a ARES (Rheometric Sci.) rheometer in parallel-plate geometry between $\omega = 10^{-3}$ and 100 rad/s at different temperatures. Master curves were obtained at a reference temperature $T_0 = 160°C$ by the WLF -time- temperature-equivalence shifting principle. Storage and loss moduli $G'(\omega)$ and $G"(\omega)$ from flow to transition regime at high frequencies were fitted in terms of the Winter model [4]. This model considers a relaxation time spectrum including two frequency distributions following power laws for the short-time (Rouse) and long time limit. It provides the only way to determine plateau moduli if contributions of the transition zone cannot be neglected and G' nor $G"$ can be extrapolated for $\omega \to \infty$. The fits are shown in Fig. 1. The exponents of the power laws revealed to be universal for all investigated polymers and independent of the packing length or chemical detail of the monomers. However, the Doi-Edwards prediction of $t^{\frac{1}{2}}$ in the plateau regime could not be found. Instead, $t^{\frac{1}{4}}$ of the non-reptational path length fluctuation mechanism showed up.

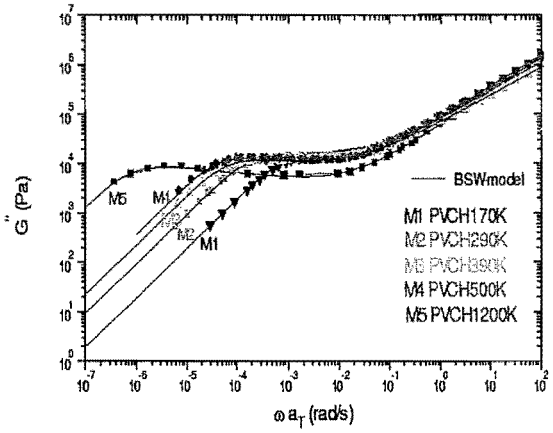

FIG. 1. Experimental $G"$ and fits for representative molecular weigths of PVCH. The hump is characteristic for the relaxation process of reptation-diffusion.

The zero-shear viscosities η_0 were obtained from the low frequency limit of the loss modulus as a function of molecular weights and shown in reduced way in Fig. 2.

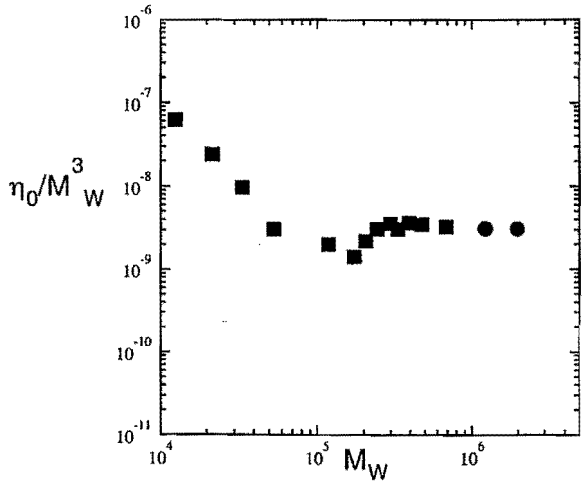

FIG. 2. Dependence of η_0 on molecular weight.

Three slopes are clearly identified from cross-over points. Below M_c a Rouse-scaling in M_w is seen, after which the well known $M_w^{3.4}$ scaling of reptation including path length fluctuations sets in. At $M_w = M_R$ pure reptation seems to take over which corresponds to the slope of M_w^3 (constant in the representation of η/M^3) as predicted by theory. Other anionic control polymers with low packing lengths from 2.2 to 4.5 (not shown here) behaved consistently in the same way at considerable higher M_R and all corroborate the predictions of the packing model for the dependence of the plateau modulus. As a common observation, the entanglement slope does not cross over to the pure reptational $\omega^{-\frac{1}{2}}$ as the viscosity does. The slope of 3.4 for the viscosity in the *sub-reptation* regime could be indicative for other "viscosity thinning" processes which would have vanished at long times. The analysis of all data further showed that the reptational molecular weight M_R is a sensitive function of M_c/M_e. As shown in Fig. 3 the independent determination of M_c from melt viscosity and M_e from plateau moduli clearly indicates that M_c/M_e is not 2 nor constant as assumed in literature but depends on the packing length of the system itself. Especially this ratio describes the entanglement proneness or how many entanglements are effectively required to build a constraining tube. As a main result, at a common p^* around 10 all characteristic molecular weights meet. This interesting feature awaits further synthesis work and would benefit from independent clarification from quasi-elastic scattering experiments.

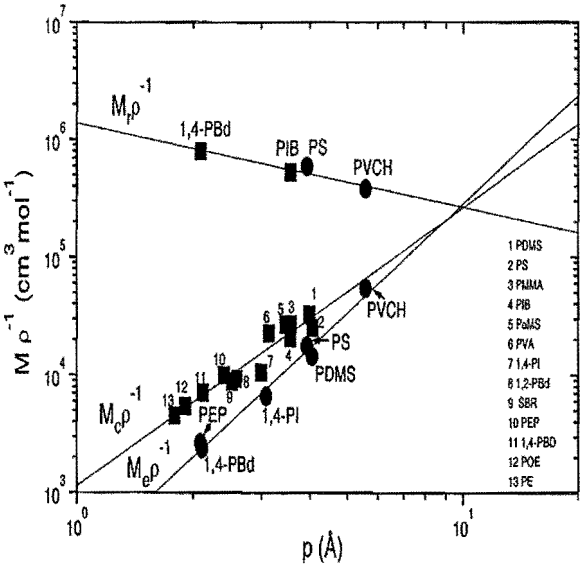

FIG. 3. Dependence of characteristic molecular weights upon packing length p.

[1] L.J. Fetters et al., Macromolecules, 1994, 27, 4639
[2] L.J. Fetters et al., Macromolecules, 1999, 32, 6847
[3] M. Gehlsen, J. Polym. Sci. B, Poly. Phys., 1995, 33, 1527
[4] H. Baumgaertel et al., Rheol. Acta, 1990, 29, 400

Upgrading of the backscattering spectrometer

H.Grimm, R.Schätzler and T.Starc

Institute for Neutronscattering

The backscattering spectrometer BSS at the research reactor FRJ2 allows for neutron scattering experiments in the range of GHz. Its performance has been strongly improved by the equipment with new analyzer plates – a step which is based on the availability of large silicon wafers. Thereby a much steeper resolution function is achieved. It is shown that this improvement is essential for the discernibility of small inelastic signals close to the usually dominant elastic line. In addition , the width of this line could be narrowed by 12% without loss of intensity. This improvement is based on the separate recording of the positive and negative acceleration periods of the doppler drive by means of a suitable gate.

F&E-Nr: 23.89.1

The continuous optimization of neutron spectrometers is mandatory because of the flux limitations of existing sources. The goal, thereby, is to improve usable flux, width and steepness of the resolution function as well as the signal/background ratio. Possible means are modified concepts and the availability of new materials. We report here on such a progress for the backscattering spectrometer BSS.

Such a spectrometer (Fig.1) selects thermal neutron energies with a relative accuracy of about 10^{-4} by restricting to Bragg angles of 90° [1]. In this limiting case, the influence of directional selection becomes comparable to that of the variance of the used lattice spacing (primary extinction). A variable energy transfer is achieved by moving the monochromator crystal (Doppler effect). Thus this technique provides access to the spectral range of μeV or GHz. Favored by the dominant incoherent cross section of thermal neutrons for hydrogen, major fields of interest are here diffusion or jump processes of hydrogen in condensed matter as well as rotational tunneling of e.g. methyl groups. The latter provides a highly sensitive probe for modeling of interatomic potentials.

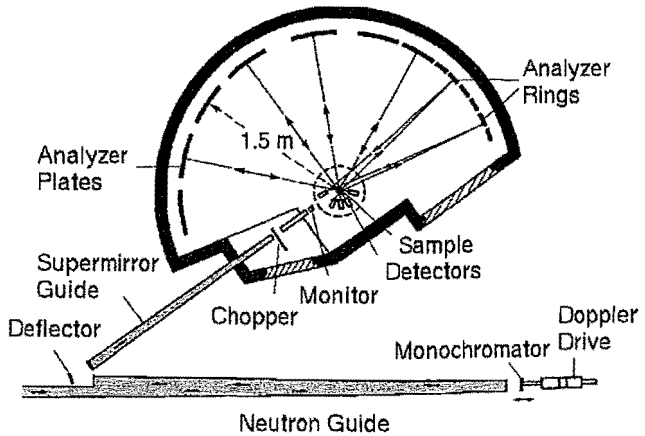

FIG.1 Schematic layout of the BSS1 at the external laboratory (ELLA) of the research reactor FRJ2 [1] .

The large analyzer plates (50cm x 90cm) represent spherical sections whose radius of curvature corresponds to their distance (1.5m) from the sample. Glued to their surface are elastically bent Silicon wafers of 0.5mm thickness in (111) orientation (Fig.2).

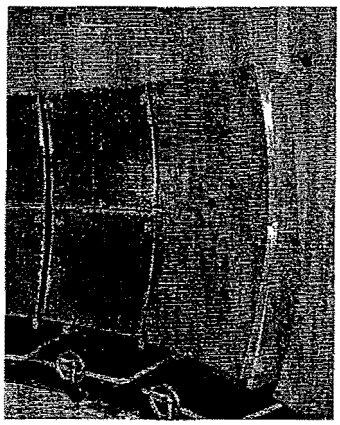

The uniformity of bending increases with the ratio of area to circumference of the wafers. The nowadays available larger Si wafers allowed for a change from the original effective diameter of about 3cm to about 11cm .

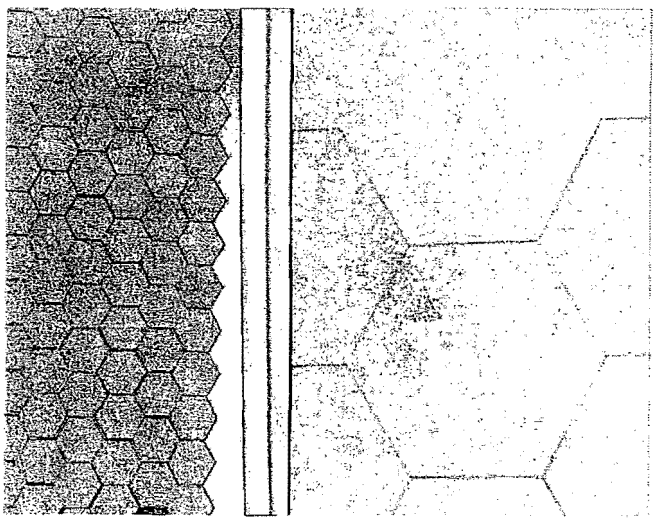

FIG.2 View at neighboring 'old' and 'new' analyzer plates centered at scattering angles Φ = 100° and 76°, respectively.

The first complete replacement of an analyzer plate was achieved in Feb'00. Care was taken to minimize the orientational variance of the indiviual (111) axes, i.e. using a single batch of wafers cut from the ingot and keeping track of their relative orientation by unique small grooves at two neighboring edges of the hexagons cut from wafers.

A study of rotational tunneling provided the first test of this new analyzer. The sample was the well known analgesic paracetamol which carries a methyl group attached to the amino group (Fig.3, insert). Symmetry entails a threefold potential for the rotation around the C-C axis. The difference of ground and first excited state is about 3μeV or 35mK. Due to the weak coupling between the rotational states and phonons, this excitation is observable with neutrons at temperatures up to 20K.

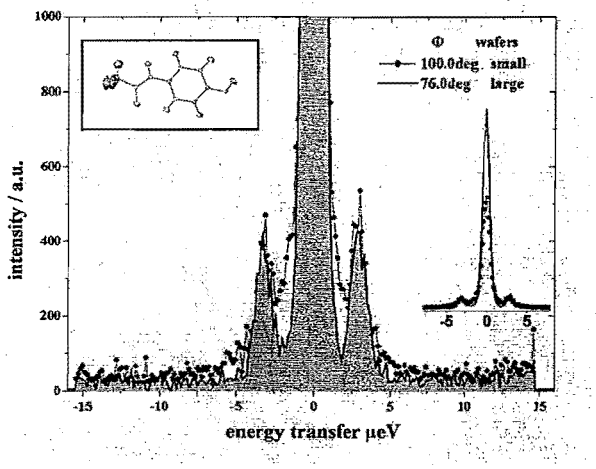

FIG.3 Tunneling spectrum for paracetamol measured at T=4.5 K with analyzer plates at scattering angles of 76° (large) and 100° (small wafers). Large wafers were used for the monochromator, as well.

The comparison of the spectra observed with the new (Φ=76°) and the old (Φ=100°) analyzer proves the progress achieved by using the large Si wafers, i.e. a relative gain of about 12% in energy resolution and – more important – a nearly Gaussian shape of the resolution function. The latter causes the much clearer distinction between the tunneling and elastic lines.

A new concept for the alignment of the spectrometer revealed the possibility to gain another 12% in the resolution without loss of intensity. The relevant alignment parameter is the travel time of the neutrons from the doppler drive to the detector. This time (counter-delay) associates doppler speed or energy transfer with a scattering event. A value of zero for both quantities occurs two times during the period of the doppler drive, i.e. with rising and falling speeds. A suitable gate for the counters allowed for recording of both events, separately, and thus for optimizing of the delay time (Fig.4).

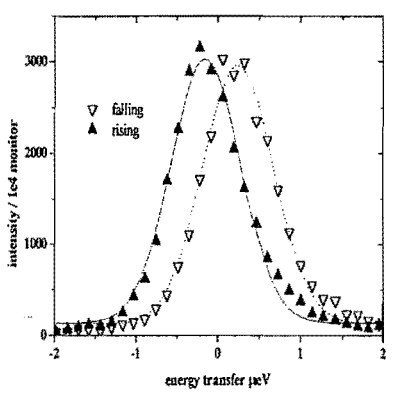

Fig.4 Elastic lines for 'falling' and 'rising' speeds of the doppler drive. The peak distance is 0.4μeV.

The origin of the energy transfer may be shifted by using a the mixed monochromator crystal $Si_{0.9}Ge_{0.1}$. Although this crystal has a wider lattice parameter variance than pure Si, the advantage of covering twice the inelastic range is essential for many experiments. The improvement of the spectrometer performance also in this mode of operation showed up clearly in a measurement of relaxational dynamics of DNA. In this case the relatively sudden appearance of a relaxational spectrum above a temperature of about 200K has been studied (Fig.4, insert). This behaviour seems to be rather common to large, hydrated biological molecules and signals the onset of conformational fluctuations [2].

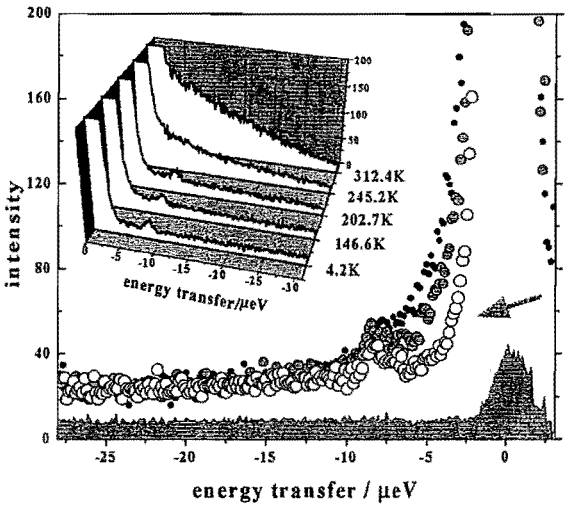

FIG.4 Spectrum of DNA at T~150K obtained at the replacement levels of 12.5%, 50% and 100% (small filled to large open symbols). The percentage refers to the contributing fraction of large analyzer crystals. The shaded area corresponds to the empty container. The insert provides an overview of the temperature dependence.

Measurements at different states of upgrading of the analyzer plates show the gradually increased discernibility of a small spectral feature at an energy transfer of about -8μeV (Fig.4). Its strength is about 0.5% of that of the elastic line, only. Obviously, the key to this improvement is the steeper resolution function (indicated by arrow in Fig.4).

[1] B.Alefeld ,T.Springer and T.Heidemann, Nucl.Sci. and Engineering, **110,** 84 (1992)
[2] A.P.Sokolov, H.Grimm, and R.Kahn, J.Chem.Phys., **110**, 7053 (1999)

Micellization of PEP-PEO Block Copolymers in Water: Molecular Weight Dependence

H. Kaya, L. Willner, J. Allgaier, J. Stellbrink, D. Richter
Institute for Neutron Scattering

A SANS study of the micellization of PEP-PEO block copolymer micelles as a function of molecular weight is presented and the results are compared with theoretical predictions. The experiments show that the low-molecular weight systems form rod-like micelles, while at high-molecular weights spherical micelles are formed

F&E-Nr: 23.30.0

The structures formed by amphiphilic block copolymer in aqueous solution have received considerable experimental and theoretical attention for many decades. Depending on the block copolymer characteristics one is able to produce a multitude of micellar structures which represent features of colloids, surfactant micelles, and star polymers.

PEP-PEO represent an ideal system in this context. Since the glass transition temperature is low, the micellar core is in a melt-like state, which gives the micelles the possibility to attain thermodynamic equilibrium. Combined with an exact preparation producing nearly monodisperse diblock copolymer chains, the system can be brought close to the ideal, yet simplified cases treated in theoretical studies of micellar structure. Previously we have published a profound study of the micellization behaviour of PEP-PEO as a function of the copolymer composition [1]. Here, the molecular weight dependence at constant composition will be presented. We have utilized small-angle neutron scattering (SANS) to obtain information on the structure of PEP-PEO micelles formed in water. SANS provides us with an unique tool for examining the structure of the micelles by virtue of the contrast variation technique.

Five block copolymers have been studied: PEP0.5--PEO0.5, PEP1-PEO1, PEP2-PEO2, PEP10-PEO10, and PEP22-PEO22; the digits denote the approximate molecular weights in units of 1000 Daltons. The common feature for these systems is that the blocks have equal volume. In addition we refer to the PEP5-PEO5 system measured by Poppe *et al* [2]. The three low-molecular weight systems were protonated and measured in D_2O, whereas for the three highest molecular weights, including PEP5-PEO5, the PEP blocks were partially deuterated. Here contrast variation was applied.

Representative results of the SANS experiments are displayed in Figures 1-3. An interesting morphological change is taking place upon decreasing the molecular weight, namely a transition from large and narrowly distributed spherical micelles at high molecular weights (evident from the high scattering intensity and the clear minima) to cylindrical micelles at low molecular weights (evident from the Q^{-1} power law seen at low and intermediate scattering vectors). A cross-over case is represented by the PEP2-PEO2 system, in which spheres and rods coexist in various ratios for concentrations above 0.1 v/v%, whereas upon dilution we observe only cylinders.

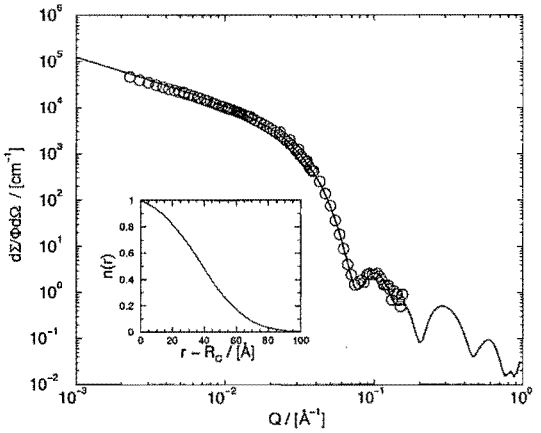

FIG. 1. SANS data of the PEP1-PEO1 in D_2O at 1 v/v% concentration. The solid line is a fit to the cylindrical core-shell model. The corona density profile is shown in the inset.

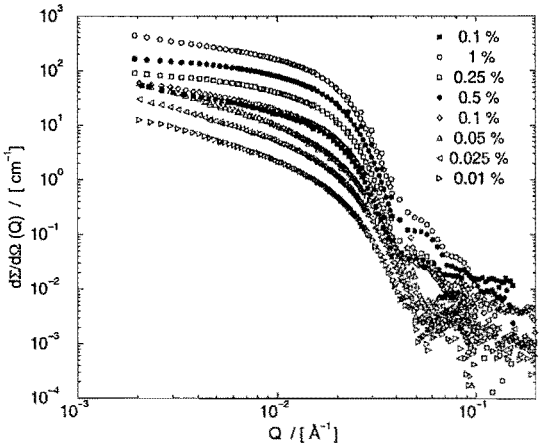

FIG. 2. Absolute SANS data for the PEP2-PEO2 system. Concentration dependent micellication is evident.

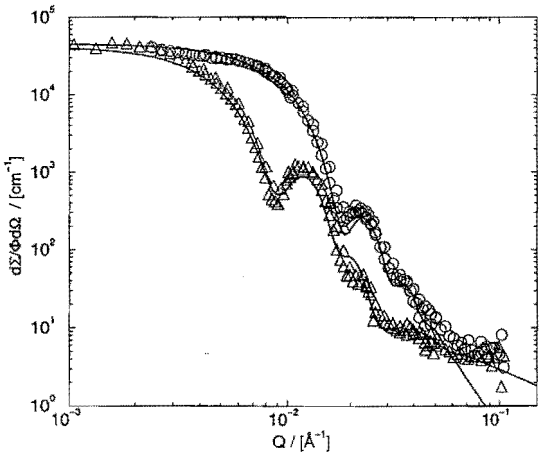

FIG. 3. Concentration-normalized SANS curves from the PEP10-PEO10 system in core (o) and shell (Δ) contrast. Solid lines represent fits to the core-shell model, performed simultaneous for both set of data.

For the quantitative analysis of the SANS curves we applied spherical and cylindrical core-shell form factors with the possibility of including density profiles within the micellar corona. The results for the fit parameters are shown in Table I. The most striking feature of the spherical micelles formed by the high molecular weight block copolymer are their high aggregation numbers. The hydrophobic part of the chains is densely packed in the micellar core. As for the cylinders, the micellar core is also solvent-free. However, the corona is more dense, containing about 60% solvent, and the PEO chains cover about 12% of the core surface, notably more than the 4% in the case of the spheres.

Comparing our results with predictions of the mean-field model of Nagarajan and Ganesh (NG) [3], we find excellent agreement between theory and experiment in the case of the spherical micelles. The calculated aggregation numbers are 1190, 2300, 3780, and 7200 for the PEP2-PEO2, PEP5-PEO5, PEP10-PEO10, and PEP22-PEO22 system, respectively. It should be noted that the assumptions made in this theory are fulfilled by our systems: the core is segregated from the corona and void of solvent; the corona is dilute and does not exhibit important internal density variations, and the micelle is large enough to ignore effects of curvature, chain coverage, and the errors imposed by the unphysical assumption of uniform chain stretching in the core.

TABLE I. *Micellar parameters extracted from core-shell models.*

Polymer composition	P (1)	λ_L (1/Å)	R_C (Å)	R_M (Å)
0.5-0.5	-	2.3	30	58
1-1	-	3.0	50	90
2-2	(1200)	3.5	73	150
5-5	2430	-	176	294
10-10	3860	-	253	468
22-22	7900	-	426	-

We applied the NG mean-field model on the low-molecular systems by modifying the equations to a cylindrical case, calculating the free energy change experienced by a singe chain upon transfer from the solution to an infinitely long cylindrical micelle. Upon minimization of the free energy we obtain the number of chains per length and the corona thickness. Several simplification should be mentioned: we have neglected end effects, and the entropy gain represented by the length polydispersity. The coverage of the core surface, however, is taken into account, but still the outcome theoretical calculations is systematically higher than the experimentally determined parameters. Better results are obtained when the the surface tension is reduced, something which could be caused by a non-neglible curvature [4]. In spite of these shortcomings, the model captures the main feature experimentally observed, namely the tendency to form cylinders increases as the molecular weight decreases.

The concentration dependent micellar structure and composition of the PEP2-PEO2 system can explained qualitatively [5], [6]. The transition from a saturated solution of block copolymers to a micellar solution requires the growing aggregates to pass a very high energy barrier given by the maximum of the grand potential [6]. Even if the equilibrium morphology is nonspherical, the lowest energy barrier for forming micelles can be that of a spherical micelle. Hence, spherical micelles will be formed as precursors. The dissolution of these metastable structures and reformation of the cylindrical micelles represent another barrier which vanishes at small concentrations, according to predictions by models based on self-consistent mean-field lattice models [7] and density-functional theory [8].

[1] Poppe, A., Willner, L., Allgaier, J., Stellbrink, J., and Richter, D., Europhys. Letters **51**, 628 (2000).
[2] Poppe, A., Willner, L., Allgaier, J., Stellbrink, J., and Richter, D., Macromolecules **24**, 7462 (1997).
[3] Nagarajan, R. and Ganesh, K., J.Chem. Phys. 5843 (1989).
[4] Puvvada, S. and Blankschtein, D., J.Chem. Phys. **92**, 3710 (1990).
[5] Shull, K. R., Macromolecules **26**, 2346 (1993).
[6] Semenov, A., Macromolecules **25**, 4967 (1992).
[7] Besseling, N. A. M. and Cohen Stuart, M. A., J.Chem. Phys. **110**, 5432 (1999) .
[8] Talanquer, V. and Oxtoby, D. W., J.Chem. Phys. **113** 7013 (2000).

Dynamics of microemulsions with polymeric cosurfactant

M.Mihailescu, H.Endo, J.Allgaier, M.Monkenbusch, D.Richter
Institute for Neutron Scattering

Using Neutron Spin Echo spectroscopy in combination with Dynamic Light Scattering we performed an extensive investigation of the bicontinuous (L3) phase in microemulsions. The dynamical behavior of different surfactant systems ($C_{10}E_4$, $C_{10}E_4$ mixed with polymeric cosurfactant - PEP_{10}/PEO_{10} and AOT) was studied under comparable conditions, at different length scales. The analysis reveals stretched exponential relaxation with q^3 scaling (q=momentum transfer) and an exponent of 0.75 in the asymptotic high q limit, and exponential relaxation with q^2 scaling at low q. On a local scale the relaxation rate increases almost linearly as function of the structure length - ξ. At intermediate length scales the relaxation rate in bulk contrast shows a minimum at $q = q0$ (the correlation peak position). Evidence for the modified elastic properties and additional interaction of the amphiphilic layers due to the polymer presence can only be found on a global scale.

F&E-Nr: 23.30.0

A common characteristic of amphiphilic surfactants is their preference to form extended two-dimensional membrane-like structure at the interface between two media (g.e water and oil). Within the well known Helfrich's model, the interface shape and fluctuations are controlled by the elastic bending energy and described by a few parameters: C_0 - the spontaneous curvature, κ - the bending rigidity modulus and $\overline{\kappa}$ - the saddle-splay modulus, respectively [1].

The combination of amphiphilic surfactants and polymeric cosurfactants in microemulsions has recently received much interest. The 'boosting 'effect on the emulsification power of a typical non-ionic amphiphile like $C_{10}E_4$ by addition of block-copolymers (PEO_x/PEP_y) and its influence on the structure of the bicontinuous phase has been demonstrated in studies of phase diagrams and SANS experiments [2].

It was suggested [3] that a homogeneous decoration of the amphiphilic layer with block-copolymer would increase the bending rigidity while decreasing the Gaussian rigidity.

The presented work offers the most complete view so far presented on the dynamical behavior of the bicontinuous phase in microemulsions around and beyond the scale of structural correlations. Parameters like temperature, surfactant concentration, polymer amount in surfactant and contrast are varied. The measurements were performed using a combination of NSE ($q = 0.009 - 0.2\mathring{A}^{-1}$) and respectively, DLS ($q = 8\times10^{-4} - 3\times10^{-3}\mathring{A}^{-1}$) techniques available in Jülich.

From a simple perspective, the relaxation of the impermeable amphiphilic layer is governed on a local scale (high q) by the bending rigidity, as the driving force, balanced by the friction of the layer with the surrounding solvent. This type of relaxation is accessed by observation of neutron scattering from a hydrogen rich interface layer (h-surfactant) separating deuterated liquids (d-water, d-oil, h-surfactant), due to the contrast (film contrast) between H and D. In bulk contrast (i.e. D_2O, h-oil) the fluctuation of the water and oil domains in between the surfactant sheets is probed. A common feature of the microemulsions dynamics in the high q regime is the stretched exponential behavior, $S(q,t) \simeq S(q)exp(-\Gamma_q t)^{\beta}$, (Fig. 1) and the q^3 power law of the relaxation rate (Γ_q) (Fig. 2).

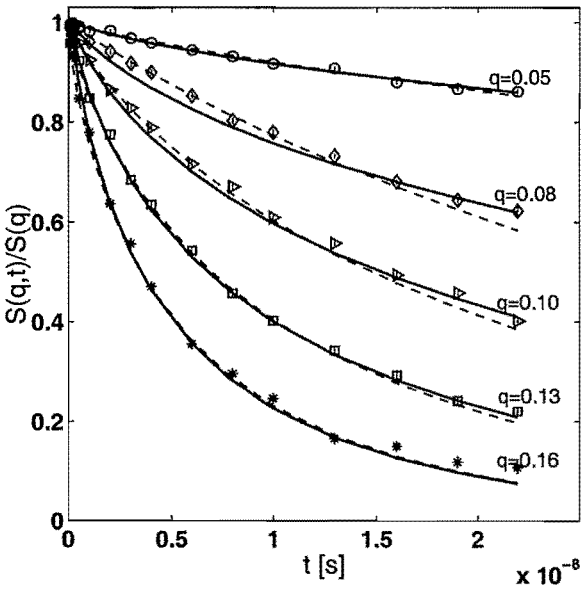

FIG. 1. Fitting curves using stretched exponential (dashed lines) and numerical calculation (solid lines).

Zilman and Granek [4] modeled the bicontinuous phase as a randomly oriented assembly of fluctuating plaquettes. They showed that a stretched exponential relaxation (with a β exponent of 2/3) results theoretically from a more general expression for the dynamic structure factor in the limits of high q and ($\kappa >> k_BT$). In order to avoid some approximations given in [4], numerical calculations were performed using their general expression of $S(q,t)$. The comparison with the experimental curves

is shown in Fig 1 together with a stretched exponential fit. The values of bending rigidity of the amphiphilic layer were found to be $\kappa \simeq 3 - 4k_BT$ at the highest q measured, for all the investigated systems. Given the unavoidable uncertainties, the eventual increase in rigidity due to addition of polymer to the pure amphiphilic layer could not be distinguished. By varying the temperature the viscosity of the bulk solvents was changed which led to an evident increase of the relaxation rate with temperature. Moreover, increasing the surfactant concentration (i.e. decreasing the structural length of the system) we found that the relaxation becomes slower (Fig. 2). At length scales around the correlation length of the systems ($q \simeq q_0$) we observe a minimum in the relaxation rate of bulk contrast at the peak of S(q) (Fig. 3). For film contrast a q-independent regime is found in agreement with [5].

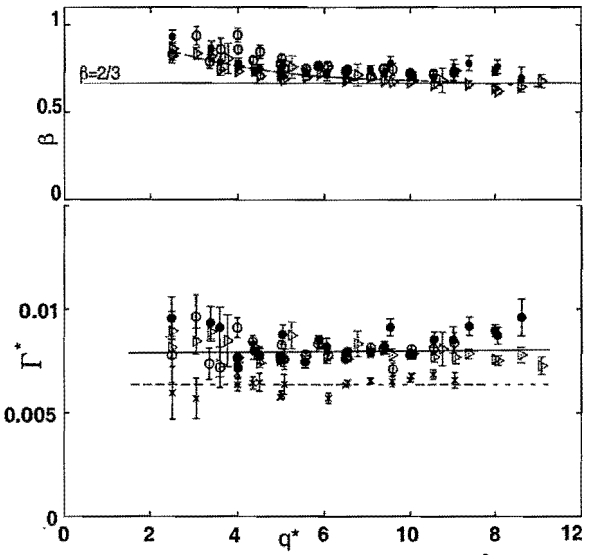

FIG. 2. Reduced relaxation rate $\Gamma^* = \Gamma_q \eta / q^3$ vs. reduced wavevector $q^* = q/q_0$ (lower half) and exponent β (upper half): $\circ - C_{10}E_4$; $\bullet - C_{10}E_4 + PEP_{10}$-$PEO_{10}$; $\triangleright - AOT$, at the same surfactant concentration ($\phi = 0.13$) and $\times - C_{10}E_4$ at ($\phi = 0.18$).

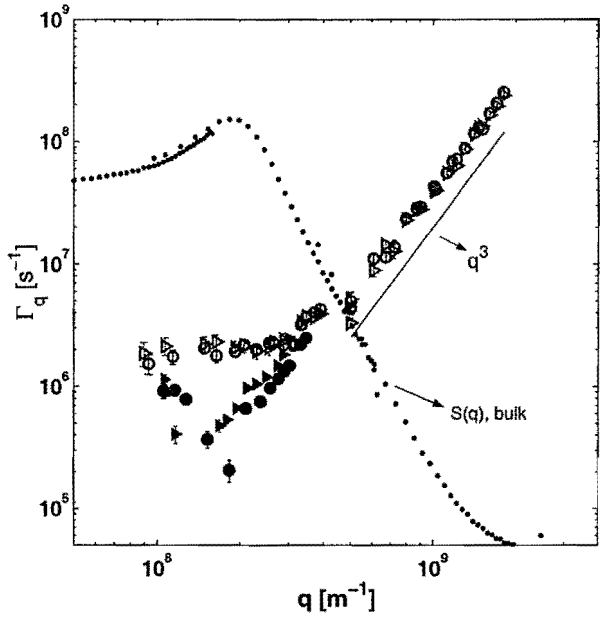

FIG. 3. Relaxation rate Γ_q vs q for $C_{10}E_4$+PEP_{10}/PEO_{10} microemulsions in film contrast (open symbols) and bulk contrast (full symbols) with varying polymer fraction ϕ_δ: $\bullet - (\phi_\delta = 0)$ and $\triangleright - (\phi_\delta = 0.05)$.

In conclusion we studied the dynamics of the bicontinuous phase in relation to the observed emulsification capacity enhancement observed in earlier phase diagram studies. In the high-q regime the scattering function proposed in the work [4] provides a direct relation to physical properties (bending rigidity, viscosity). Yet, we determine values for the bending modulus that are higher than those ($\simeq 1k_BT$) from structure and phase behavior measurements. We also find that the characteristic relaxation frequency is structure size dependent contrary to what is found in [6] on dilute sponge phases. Finally, the small polymer fraction in the surfactant layer makes a difference on a more global scale through the modified structure properties (rigidity, topology). In order to clarify some of the presented results an extension of the experiments to the lamellar phase is being planed.

The DLS results in the very low-q regime reveal the collective translational diffusion of the bulk water (oil) over large scales. Comparing systems of the same domain size but varying polymer amount in the amphiphilic layers we find an increasing diffusion rate D with the polymer amount. The values obtained for the diffusion coefficient with increasing polymer fraction in surfactant ϕ_δ are respectively: $D = 4.86\,m^2/s$ at $\phi_\delta = 0$, $D = 6.75\,m^2/s$ at $\phi_\delta = 0.05$ and $D = 7.16\,m^2/s$ at $\phi_\delta = 0.1$.

[1] Helfrich W., *Z.Naturforsch.* *C*,28 : 693 (1973)
[2] Jakobs B. et al., *Langmuir*, 15 (20): 6707, 1999
[3] Hiergeist C. and Lipowsky R., *J.Phys.II France*, 6 : 1465, 1996
[4] Zilman A.G. and Granek R., *Phys.Rev.Lett*, 77 (23): 4788, 1996
[5] Hennes M. and Gompper G., *Phys.Rev.E*, 54 (4) : 3811, 1996
[6] Freyssingeas E. et al., *J.Phys.II France*, 7 : 913, 1997

The effect of defect structures on the rotational tunnelling: 4-iodo-toluene

M. Prager, P. Schiebel[1], J. Combet[2]
Institute for Neutron Scattering
[1] *University of Tübingen, Tübingen, Germany*
[2] *Institut Laue-Langevin, Grenoble, France*

P-iodotoluene shows head-to-tail disorder. Methyl tunnelling rotation is used to study this disorder which manifests itself by the presence of two broad tunnelling transitions. Their relative intensities represent an order parameter. Average potential strengths and widths of gaussian potential distributions are derived. The potential shape is further refined by including methyl librations.

F&E-Nr: 23.15.0

Benzene derivatives containing methyl groups form a class of materials with an interesting variety of solid state phenomena. Already the simplest one, toluene, has a complex phase behaviour: it appears as glassy material and in two crystalline phases α and β. Tunnelling spectroscopy [1] allowed to obtain accurate rotational potential parameters.

A simple orientational disorder is found in monohalogenated p-iodo-toluene [2,3]. The material crystallizes in the space group $P2_12_12_1$ with Z=4 equivalent molecules in the unit cell. Staggering leads - ideally - to perfect chains of methyl groups on one side and of iodine on the other. However, due to very similar ionic radii of iodine and CH_3 the creation of stacking defects by head-to-tail disorder of the molecule requires only little energy. At room temperature (1-p)=0.2 of the molecules are statistically "misoriented". Disordered molecules are laterally displaced [3].

Four samples were investigated: fully protonated p-iodo-toluene and three mixed crystals containing 5%, 50% and 80% of p-iodo-toluene, respectively, diluted in "isostructural" 1,4-diiodo-benzene. Methyl rotational tunnelling was measured by high resolution neutron time-of-flight-spectroscopy at the IN5 instrument of the ILL, Grenoble. Spectra taken at sample temperatures of T=1.8K are shown in fig. 1. Pure p-iodo-toluene shows two pairs of tunnelling lines at $\hbar\omega = 54$ and $111\mu eV$. Despite the very low temperature all tunnel lines are significantly broadened. The inner line is weaker by a factor ~4. The dilute compounds show inelastic intensities centered at similar energy transfers but with significantly broadened lines. The relative intenities similarly change and approach $I_{inel1} \sim I_{inel2}$ for the 50:50 sample.

Lattice modes were measured in the energy regime 2-50meV using the new time-of-flight spectrometer SV29. Librational bands are observed around 7.3 to 8.3meV.

The existence of two tunnelling systems in pure p-iodo-toluene is the fingerprint of head-to-tail disorder. The line intensities represent occurrence probabilities and are in agreement with p=0.2 misoriented molecules obtained from diffraction [2]. Under the assumption of thermal equilibrium the relative line intensities yield an energy separation of the two orientations of $\delta E \sim 320K$. The width of the lines is the expression of additional disorder.

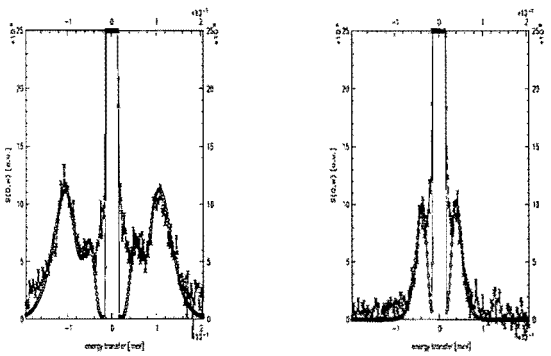

FIG. 1. Left: pure p-iodo-toluene, right: 5% p-iodo-toluene in 1,4-diiodo-benzene. T=1.8K, Instrument: IN5, λ=11Å. Solid lines: fits with Gaussian potential distributions.

The statistical occurrence of defects leads to different neighbourhoods each of which is connected with a specific rotational potential. Usually gaussian distributions of the potential strengths are assumed [4]

$$g(V) = \frac{1}{(2\pi)^{\frac{1}{2}}\delta V} exp(-\frac{1}{2}(\frac{V}{\delta V})^2).$$

Therefrom the distribution of tunnel intensities is obtained as

$$I(\hbar\omega_t) = -g(V)\frac{dV}{d(\hbar\omega_t(V))}$$

There is no analytical expression of the jacobian $\frac{dV}{d(\hbar\omega_t(V))}$. Thus we have fitted the exact solutions of the Schrödinger equation for a pure $cos(3\varphi)$ potential in the reliable range of potential strengths using the expression

$$\hbar\omega_t(V) = Bexp(-\alpha(\frac{V}{B})^\beta) \qquad for\ V < 5meV$$

$$\hbar\omega_t(V) = B(\gamma exp(-\delta\frac{V}{B}) + \gamma' exp(-\delta'\frac{V}{B}))\ for\ V > 5meV$$

with B=0.655meV the rotational constant of the methyl group, α=0.197596, β=1.73047, γ=1.33091meV, δ=0.119, γ'=0.13422meV, δ'=0.057 . The first term fits well the the free rotor regime [5]. The second one extents the range continuously to the largest potentials reliable for neutron scattering. The expression is sufficiently good for pure threefold potentials up to tunnel splittings of 0.1μeV. Compared to other work [4] the outlined expression has the advantage to include the regime of free rotors. The Gaussian potential distributions of Tab. I fit the tunnelling intensities very well (Fig. 1). With increasing disorder rotational potentials become stronger and the potential distribution widens up as expected, e.g. by a factor 3 at c=0.8.

concentr. 4-I-tol.	$\hbar\omega_t$ $[\mu eV]$	V_3 $[meV]$	δV_3 $[meV]$	occurrence probability
100%	54	17.6	1.60	0.25
	111	12.9	1.44	0.75
80%	25	23.0	5.0	0.36
	111	12.9	4.3	0.64
50%	25	23.0	4.5	0.5
	111	12.9	3.6	0.5
5%	41	19.5	2.0	1.0

TABLE I. Gaussian potential distributions derived from the tunnelling positions and linewidths[HWHM]. Intensities reflect the occurrence probabilities.

The rotational potential at defect sites is ~50% stronger than at ordered sites. This also means that the H-I pair interaction is stronger than the H-H interaction.

Methyl rotational potentials are generally determined up to second order of the Fourier expansion

$$V(\varphi) = \sum_{n=1}^{2} \frac{V_{3n}}{2}(1 - cos(3n\varphi))$$

Only by including the methyl librational energies allows to obtain the shape of the rotational potentials with this accuracy. As usual [1] larger tunnel splittings are combined with lower librational modes. We ignore disorder and evaluate only the mean tunnelling energies. The extracted potential parameters yield dominantly threefold potentials of the same strength as shown in Tab. I with weak (10%) sixfold terms. Thus the restriction to a purely threefold potential in describing disorder is justified.

	CH_3-chain			I-chain		
c	MMM	MMI	IMI	MMM	MMI	IMI
1.00	0.55	0.25	0.03	0.01	0.06	0.15
0.80	0.28	0.29	0.08	0.01	0.05	0.13
0.50	0.07	0.20	0.16	0.00	0.01	0.08
0.05	0.00	0.00	0.05	0.00	0.00	0.01

TABLE II. Probability distribution of neighborhoods around a central methyl group M in the methyl and the iodine chains assuming 20% head-to-tail misorientations. c is the concentration of p-iodo-toluene diluted in p-diiodo-benzene.

A most simple model can already describe the basic features: The relevant structural units are linear chains of methyl groups M. The inherent (1-p)~0.2 head-to-tail disorder 1) creates isolated M and makes 2) that the M chains are of finite length. Further the M concentration c is reduced by dissolving 4-I-toluene with di-iod-benzene. The M concentrations given by the combined effects of head-to-tail disorder and dissolution are $c_M = c * p$ and $c_I = c * (1 - p)$ within the M-chain and the I-chain, respectively. In each chain there is additional disorder due to statistical occurrence of flipped and guest molecules. Let us consider next neighbors only. The two neighbors of a methyl group are selected according to the binomial distribution p(n,N=2) using the respective c_i. Thus the occurrence probabilites of triples MMM, MMI and IMI are given by $c_i \cdot p(n, N = 2)$ (Tab. II). For cases with a single environment dominating (c=1.0 and c=0.05) the distribution of tunnelling intensity is rather sharp. For concentrations c_i around 50% chains are short and different environments get equally important. The corresponding disorder expressed by δV is large (Tab.). Keeping in mind that the situation is much more complex - methyl equilibrium orientations are also strongly influenced by disorder and further neighbors have to be taken into account - the number of different environments is much higher than in the simple model. The gaussian potential distribution is found to be a good description in the limit of very many weakly differing environments.

Disorder in glassy polymers is treated with similar distributions of rotational potentials. All cases known so far show strong average potentials with unresolvable tunnel splittings. This means that all conclusions live from an interpretation of the very edge of the potential distribution [4]. The weak rotational barrier of p-iodo-toluene allows to observe the complete potential distribution function. Thus te presented example confirms for the first time the concept of Gaussian potential distribution in disordered materials.

[1] M. Prager, A. Heidemann, Chem. Rev. **97**,2933(1997)

[2] Choong-Tai Ahn, S. Soled, G.B. Carpenter, Acta Cryst. **B28**,2152(1972)

[3] H. Serrano-Gonzales, K.D.M. Harris, S.J. Kitchin, A. Alvarez-Larena, E. Estop, X. Alcobe, E. Tauler, M. Labrador, D.C. Apperly, J. Sol. State Chem. **143**,285(1999)

[4] J. Colmenero, R. Mukhopadhyay, A. Alegria, B. Frick, Phys. Rev. Lett. **80**,2350(1998)

[5] S. Grondey, M. Prager, W. Press, A. Heidemann, J. Chem. Phys. **85**,2204(1986)

Phase Behavior and Flory-Huggins Interaction Parameter of Binary Polybutadiene Polymer Mixtures of with different Vinyl Content

D. Schwahn and L. Willner

Institute for Neutron Scattering

Binary blends of statistical polybutadiene copolymers of different vinyl content were explored by small angle neutron scattering. These samples represent the most simple class of statistical copolymer mixtures. Even though the components differ only slightly strong changes of phase behavior were observed with vinyl content; phase separation occurs between minus 230°C to more than plus 200 °C and the phase separation can even reverse from an enthalpic driven one at low temperatures (UCST) to an entropically driven one at high temperatures (LCST). While for most samples the experimentally determined entropic term of the Flory-Huggins parameter is in excellent agreement with Lattice Cluster Theory Calculations the theoretical enthalpic term does not at all describe our experimental data.

F&E-Nr: 23.30.0

The miscibility of two chemically different homopolymers is usually very poor and therefore of considerable interest in fundamental and applied research. Often, the compatibility between two polymers can be improved considerably if statistical copolymers are taken; an A-B statistical copolymer and a C homopolymer (A,B,C type of monomer) might be miscible even thought the A,B, and C homopolymers are not miscible with each other [1]. This phenomenon is interpreted by the interplay of *intermolecular* interactions between the A-C and B-C monomers and *intramolecular* interactions between the A-B monomers described by the enthalpic Flory-Huggins (FH) parameter in Eq.(1) according to

$$\Gamma_h = \varphi\Gamma_h(AC) + (1-\varphi)\Gamma_h(BC) - \varphi(1-\varphi)\Gamma_h(AB) \quad (1)$$

with φ representing the A monomer volume fraction of the copolymer. In case of a positive $\Gamma_h(AB)$ the total enthalpic Γ_h is reduced by the intramolecular interaction and therefore a better compatibility is achieved.

We report here about the phase behavior of binary mixtures of polybutadiene (PB) chains with different vinyl content. These mixtures represent the simplest possible class of statistical copolymer mixtures and are therefore a proper model system. We explored the following statistical copolymers: PB(1,4) with 7%, PB(1,2;1,4) with 54%, and PB(1,2) with 91% (1,2) vinyl content and of molar volume between 2k and 27 k in units of cm^3/mol.

The FH-interaction parameter Γ is a phenomenological parameter and represents a free energy of mixing with the, respectively, enthalpic and entropic contributions Γ_h and Γ_σ according to $\Gamma = \Gamma_h/T - \Gamma_\sigma$. This number is determined from the susceptibility S(0) obtained in neutron small angle scattering experiments (SANS) according to

$$S^{-1}(0) = 2[\Gamma_S - \Gamma]. \quad (2)$$

The susceptibility is derived from the structure factor S(Q) at wave number Q=0 and Γ_S represents the FH-parameter at the spinodal temperature. For 50% mixtures Γ_S is evaluated from the averaged molar volume according to 2/<V> [2].

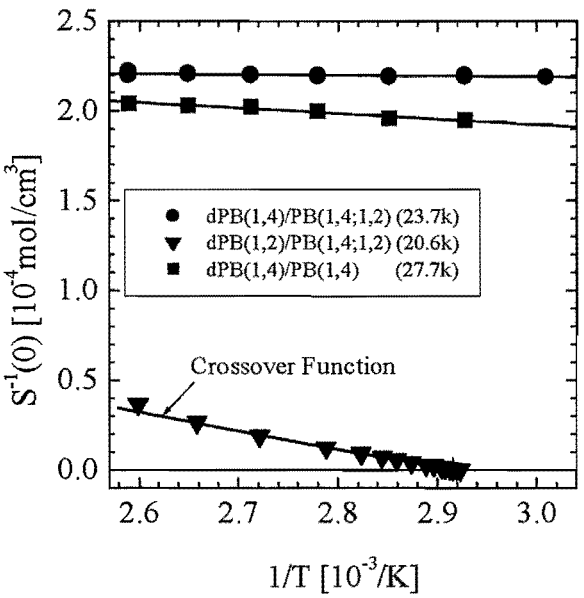

FIG.1 Inverse susceptibility versus inverse temperature of three PB mixtures of different microstructure

From our SANS experiments we got the following principle results:

(i) The mixtures of the 20k chains show very different compatibility. The (1,4)/(1,2) polymers were not miscible at all up to temperatures above 200°C; the (1,4)/(1,2;1,4) blend shows very good compatibility with an extrapolated critical temperature of about T_C=-235°C; the (1,2)/(1,2;1,4) blend already phase separate below 71°C. These observations were obtained from the temperature dependence of $S^{-1}(0)$ in the disordered phase as depicted in Fig.1; $S^{-1}(0)$ becomes zero at the critical temperature (Eq.(2)) and a mean field to 3D-Ising crossover behavior is observed for the (1,2)/(1,2;1,4) sample [2].

(ii) Strong chain-end effects of the FH-parameter were observed in consistence with Eq.(3)

$$\Gamma_h(V) = \Gamma_h + A_h / V; \quad \Gamma_\sigma(V) = \Gamma_\sigma + A_\sigma / V \qquad (3)$$

and which become visible by their molar volume dependence. The numbers of the entropic Γ_σ and enthalpic Γ_h as obtained from an extrapolation to an infinite molar volume have been plotted in Fig.2; for some combinations of vinyl content they even become negative.

(iii) From the FH-parameter in Fig.2 we can conclude that the phase behavior of these samples drastically change from showing the two-phase regime at low temperatures (UCST) to a complete different situation showing phase separation at high temperatures (LCST). A LCST system needs negative Γ_σ and Γ_h parameters; in case of $|\Gamma_\sigma| > \Gamma_S$ the negative Γ_σ acts as a driving force for the process of phase separation at high temperatures. The mixtures with the (1,2) PB chain as one component always show UCST behavior while blends with the (1,4) PB component reverse from an UCST to an LCST system for copolymers of vinyl content between 0.5 and 0.9. LCST behavior was first observed by Innai et al [4]. Their FH-parameters have been plotted as open triangles in Fig.2 after being corrected by us to infinite molar volume (see Eq.(3)).

So, our results clearly demonstrate a very strong influence of microstructure on the phase behavior in blends of PB statistical copolymers and, furthermore, show an appreciable inconsistence with the present theories as formulated in Eq.(1). So far this theory was mainly tested by cloud point measurements from which one could only determine Γ at the transition temperature and which, therefore, allows no separation into an enthalpic and entropic term. However, recent SANS experiments by us on the PB/PS blend with PB of different vinyl content have already shown that Eq.(1) does not correctly describe the phase behavior in statistical copolymer blends [5].

The present theoretical approaches of statistical copolymers give only a description of the enthalpic FH-parameter (Eq.(1)). This equation formulated for the conditions of our present PB samples gives $\Gamma_h=(1-\varphi)^2\Gamma_h(AB)$ and $\Gamma_h=\varphi^2\Gamma_h(AB)$ depending on whether the C monomer has been interchanged to the monomer A or B. In case of a 50% statistical copolymer (φ=0.5) both samples should have the same enthalpic FH-parameter. A comparison with the experiments in Fig.2 clearly shows that this is not the case; while a slightly negative number was found for the PB(1,4)/PB(1,2;1,4) a relativly large Γ_h was found for the PB(1,2)/PB(1,2;1,4) blend.

The situation of theoretical description seems to be more promising for the entropic contribution. Quite recently, the entropic term Γ_σ of statistical copolymer mixtures was calculated from Lattice Cluster Theory Calculation by Freed et al [6], which for the systems studied by us reads according to

$$\Gamma_\sigma = -(x-y)^2/(4z^2\Omega) \qquad (4)$$

with z representing the number of nearest neighbours (theoretical number z=6), Ω the monomer volume of PB (which is Ω=60.4 cm^3/mol), and x and y, respectively, being the vinyl content of the two components. Eq.(4) has been plotted as a solid line in Fig.2 assuming z=5.8 nearest neighbours; it correctly describes the experimental data with the PB(1,4) component measured by us (full triangles) and by Innai et al [4] (open triangles) after correction for chain-end effects. On the other hand, the blends with PB(1,2) shows deviations; some additional entropic contribution is seen to be relevant for the PB(1,2)/PB(1,2;1.4) sample.

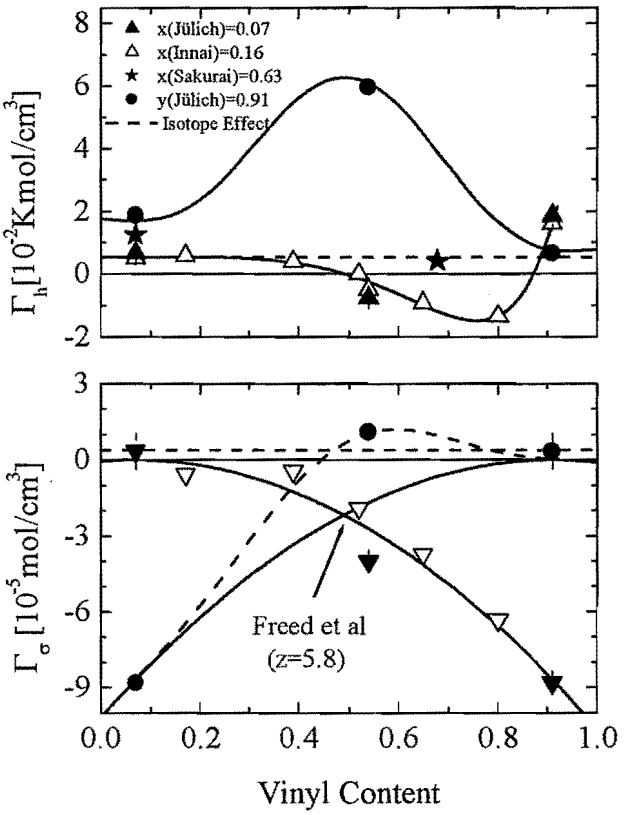

FIG.2 Enthalpic and entropic FH-parameters of a PB(1,4) and PB(1,2) mixed with a PB copolymer of different vinyl content. The FH-parameters represent the extrapolated numbers for infinite molar volume according to Eq.(3).

[1] D.R.Paul, J.W.Barlow *Polymer* **25**, 487 (1984); H.Wansoo and E.Karasz *Macromolecules* **25**, 1057 (1992).
[2] D.Schwahn, G.Meier, K.Mortensen, S.Janssen, *J. Phys.II (France)* **4**, 837 (1994)
[3] J.Dudowicz, K.Freed *Macromolecules* **26**, 213 (1993)
[4] H.Innai et al., *Macromolecules* **25**, 6087 (1992).
[5] H.Frielinghaus, D.Schwahn, L.Willmer, *Macromolecules* in press.
[6] J.Dudowicz, K.F.Freed, *Macromolecules* **33**, 3467 (2000)

Phase separation in star polymer-colloid mixtures

J. Stellbrink, J. Allgaier, and D. Richter
Institute Neutron Scattering, IFF, FZ Jülich, D-52425 Jülich, Germany

J. Dzubiella, A. Jusufi, C. N. Likos, C. von Ferber, and H. Löwen
Theoretical Physics II, Heinrich-Heine-Universität Düsseldorf, Universitätsstraße 1, D-40225 Düsseldorf, Germany

A. B. Schofield, P. A. Smith, W. C. K. Poon, and P. N. Pusey
Department of Physics and Astronomy, The University of Edinburgh, Mayfield Road, Edinburgh EH9 3JZ, United Kingdom

We examine the phase diagrams of star polymer-colloid mixtures for star arm numbers $f = 2, 6, 16, 32$ and different star-colloid size ratios q. In all samples with $q \approx 0.49$, addition of polymer to suspensions with volume fraction $\eta_c \sim 0.1 - 0.4$ brought about, successively, phase separation into colloidal gas and liquid (or demixing), triple coexistence of gas, liquid and crystal, and gas-crystal coexistence. In samples with $q \approx 0.18$, addition of polymer first led to fluid-crystal coexistence; a metastable gas-liquid binodal buried inside the equilibrium fluid-crystal coexistence region was encountered at higher polymer concentrations. Theoretically, we solve the thermodynamically self-consistent Rogers-Young integral equations for binary mixtures using three effective pair potentials obtained from direct molecular computer simulations. The numerical results show a spinodal instability. The demixing binodals are approximately calculated, and found to be consistent with experimental observations.

F&E-Nr: 23.30.0

Here we report a comprehensive study [1] combining experiment and theory on the phase behaviour of star polymer-colloid mixtures for star polymer with increasing arm numbers $f = 2, 6, 16, 32$, but constant radius of gyration R_g ≈50nm. Experimentally, we studied two sets of star polymer-colloid mixtures consisting of poly(methylmethacrylate) (PMMA) colloidal particles and poly(butadiene) (PB) star polymers with size ratios $q = 2R_g/\sigma_c \approx 0.49$ and $q \approx 0.18$, respectively (σ_c: diameter of the colloidal particle). PMMA particles in *cis*-decalin have been established as hard sphere models [2]. Their volume fraction $\eta_c = \frac{N_c}{V}\frac{\pi}{6}\sigma_c^3$ was calibrated using the onset of the hard sphere freezing transition, taken to be at $\eta_c = 0.494$ and observed as the nucleation of iridescent colloidal crystals. PB star polymers were prepared by anionic polymerization following an established procedure [3,4]. The molecular weights M_w of the PB arms were adjusted to give star polymers with values of $\langle R_g^2 \rangle^{1/2} = 0.0172 M_w^{0.609} f^{-0.403}$ [5] as close to 50 nm as possible. A linear PB polymer ($f = 2$) was prepared as a reference system.

The synthesis of such high molecular weight star polymers is a challenging task for each chemistry department, thus as a first step all used star polymers and colloids have been characterised carefully using small angle neutron scattering (SANS). This provides us the crucial size ratio q, which is necessary for a proper theoretical interpretation of the obtained experimental phase diagrams. Fig. 1 proofs the high quality of the used material: Here the star form factors for increasing f are shown as a function of scattering vector Q. All molecular parameters are summarized in tab. I.

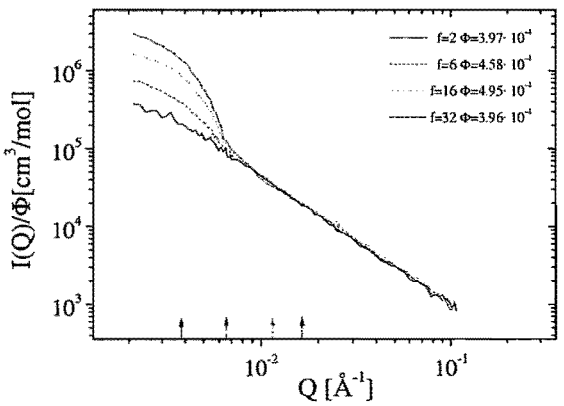

FIG. 1. $I(Q)$ in absolute units normalized to volume fraction Φ versus scattering vector Q for star polymers with increasing functionality f but constant radius of gyration R_g, $f = 2, 6, 16, 32$ (from bottom to top). Extrapolation to zero concentration gives the molecular form factors with parameters listed in tab. I. The arrows indicate the expected onset of the asymptotic power law regime which scales like $f^{1/2}$.

An analytic form for the star polymer-colloid pair potential can be found by integrating the osmotic pressure of one star along the spherical surface of a colloid, following an idea put forward by Pincus [6]. This can be achieved for arbitrary curvatures of the colloid but the analytical result below is accurate for size ratios $q \lesssim 0.7$ and reads [7]:

$$V_{sc}(r) = \Lambda k_B T f^{\frac{3}{2}} \frac{\sigma_c}{2r} \times$$
$$\begin{cases} \infty & r < \frac{\sigma_c}{2}; \\ \xi_2 - \ln(\frac{2z}{\sigma_s}) - (\frac{4z^2}{\sigma_s^2} - 1)(\xi_1 - \frac{1}{2}) & \frac{\sigma_c}{2} \le r < \frac{\sigma_s + \sigma_c}{2}; \\ \xi_2(1 - \mathrm{erf}(2\kappa z))/(1 - \mathrm{erf}(\kappa\sigma_s)) & \text{else,} \end{cases}$$

where $z = r - \sigma_c/2$ is the distance from the center of the star polymer to the surface of the colloid. The constants are $\xi_1 = 1/(1 + 2\kappa^2\sigma_s^2)$ and $\xi_2 = \frac{\sqrt{\pi}\xi_1}{\kappa\sigma_s}\exp(\kappa^2\sigma_s^2)(1 - \mathrm{erf}(\kappa\sigma_s))$. $\Lambda(f)$ and $\kappa(f)$ are fit parameters, obtained from computer simulations where the force between an isolated star and a hard flat wall is calculated. κ is in order of $1/\sigma_g$, whereas geometrical arguments yield a limit $\Lambda_\infty = 5/36$ for very large f. The so-called corona-diameter σ_s is related to the diameter of gyration through $\sigma_s \simeq 0.66\sigma_g$.

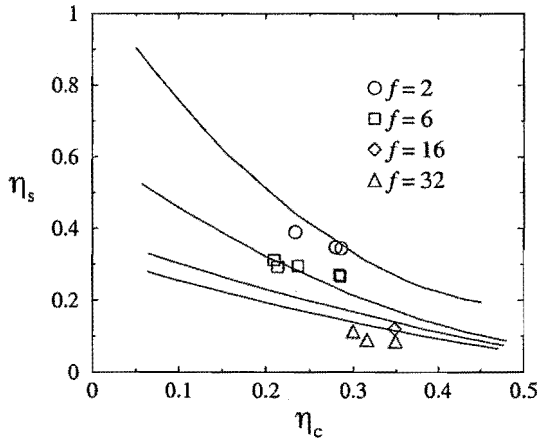

FIG. 2. Binodals for the mixing-demixing transition in star polymer-colloid mixtures for different arm numbers $f = 2, 6, 16, 32$ (from top to bottom) and size ratio $q \approx 0.49$. Symbols mark experimental results compared with theory (lines) for $q = 0.50$.

The results in Fig.2 show that theory and experiment are in good agreement. In particular, the same trends are found as functions of the system parameters f and q. By increasing f and keeping q fixed, the demixing transition moves to lower star packing fractions $\eta_s = \frac{N_s}{V}\frac{\pi}{6}\sigma_g^3$, as shown in Fig. 2. The largest differences occur at low arm numbers $f \lesssim 10$ which is theoretcially caused by the major changes in the star-colloid pair potential for low f. When q is decreased but f remains fixed, again a motion of the binodals to lower η_s is observed. This trend is *opposite* to the one predicted by the AO model [8]. The crucial parameter that determines the trends of the phase diagram is the non-additivity of the mixture. Systems interpolating between the fully additive hard sphere mixture and the fully nonadditive AO model can feature a depletion interaction which is more attractive than in the AO limit [9]. The agreement between theory and experiment is brought about *without* the use of any free parameters in the former that would allow for a rescaling of sizes or densities. All values are read off from experiment and the only free parameters of the theory appear on the level of the pair potentials and are used only in order to fit analytical expressions to the microscopically-determined star-star and star-colloid pair interactions.

To summarize, we have derived from first principles the effective interactions between the components of a star polymer-colloid mixture, proposing analytical expressions for these. We have used them to make theoretical predictions about the thermodynamic behavior of the fluid phase of the system finding very good agreement with the experimental results. Further work regarding, e.g., the crystallization properties of these mixtures is currently under way.

TABLE I. Molecular characteristics of PMMA colloids and PB star polymers.

Monomer	f	$M_w \cdot 10^{-6}$[g/Mol][a]	R_c[nm][b]	R_g[nm][a]
PMMA	-	-	104.0± 2.5	-
PMMA	-	-	289.0± 4.5	-
PB	2	0.86 ± 0.36	-	51.0 ± 3.5
PB	6	1.51 ± 0.06	-	52.1 ± 0.6
PB	16	3.45 ± 0.27	-	51.1 ± 0.5
PB	32	5.11 ± 0.39	-	51.4 ± 0.5

[a] small angle neutron scattering (SANS)
[b] static light scattering (SLS)

[1] J. Dzubiella *et al.*, submitted to Phys. Rev. Letters
[2] S. M. Ilett *et al.*, Phys. Rev. E **51**, 1344 (1995).
[3] J. Allgaier *et al.*, Macromolecules **29**, 1794 (1996).
[4] N. Hadjichristidis and L. J. Fetters, Macromolecules **13**, 191 (1980).
[5] G. S. Grest *et al.*, Adv. Chem. Phys. **XCIV**, 67 (1996)
[6] P. Pincus, Macromolecules **24**, 2912 (1991).
[7] A. Jusufi *et al.*, to be published
[8] M. Schmidt, private communication.
[9] R. Roth and R. Evans, to appear in Europhys. Lett.
[10] A. A. Louis *et al.*, Phys. Rev. Lett. **85**, 2522 (2000).
[11] P. G. Bolhuis *et al.*, preprint, cond-mat/0009093.

First direct observation of the Rouse-Reptation crossover in polyethylene by incoherent NSE

A. Wischnewski, M. Monkenbusch, D. Richter
Institute for Neutronscattering

The salient features of the motions of chains in high molecular weight polymer melts are well described by the famous Reptation model of DeGennes. The central ingredient of this model is a contorted virtual tube (of diameter d) around the contour of each polymer chain. The diffusion of chain segments feels only little influence of this confining tube for times too short for the mean squared displacements $\langle r^2(t)\rangle$ to reach its "walls". In that time regime the chain dynamics feels the environment only through a simple local friction - segmental diffusion follows the standard ROUSE behaviour. However, when $\langle r^2(t=\tau_e)\rangle$ becomes comparable to d the tube constraints become active and the segmental diffusion slows down. This slowing down at a crossover time τ_e would be directly observable if the mean squared displacements of some $(10\,\text{Å})^2$ could be measured over a time range of several nanoseconds. For the first time it has been possible to measure this effect on $\langle r^2(t)\rangle$ directly by analyzing the incoherent scattering from hydrogen in long-chain polyethylene segments in the proper range of momentum transfer and time using the Jülich neutron spinecho spectrometer.

F&E-Nr: 23.30.0

The Brownian motion of short chains in polymer melts is rather successfully described by the Rouse model which assumes Gaussian chains interacting solely by a simple local segmental friction. Intrachain interaction is restricted to entropic chain elasticity [1]. The Brownian motions and therefore the segmental diffusion is determined by the balance of viscous and entropic forces. The prediction of the Rouse model for the mean squared displacement of segments is $\langle r^2(t)\rangle \propto \sqrt{t}$.
For larger molecular weights topological constraints – entanglements – lead to characteristic deviations from the predictions of the Rouse model. In the limit of fully developed entanglements the viscosity is $\eta \propto M^{3.4}$ instead of $\eta \propto M$ in the Rouse regime, the diffusivity $D \propto M^{-2}$ instead of $D \propto M^{-1}$ and the melts exhibit a so-called elastic plateau modulus at intermediate frequencies, that resembles the behaviour of a transient rubbery network. These effects result from chain entanglements, the corresponding motional constraints cause a localization of the chain on intermediate time scales. The salient features of the constrained motions of chains in high molecular weight polymer melts are well described by the famous Reptation model of DeGennes. The central ingredient of this model is a contorted virtual tube (of diameter d) around the contour of each polymer chain if considered at time $t = 0$. The time evolution of the chain contour is Rouse model like as long as the segments do not reach the constraining tube "walls". Beyond that time the further relaxation can only proceed within the tube along its contour. Then the growth of the segmental mean squared displacement proceeds only according to $\langle r^2(t)\rangle \propto t^{1/4}$. The halt in further segmental diffusion beyond the tube walls also leads to a plateau in the time evolution of the single chain dynamic stucture factor $S(Q,t)$, where Q is the momentum transfer during scattering and t the Fourier time. The momentum transfer dependence of the plateau level resembles a form factor of the tube and allows for the extraction of the tube diameter.

$S(Q,t)$ determines the scattering intensity from polymer melts containing a few percent hydrogenated chains in a background melt of otherwise chemically equal deuterated chains. It may be investigated in the relevant Q-regime by neutron spinecho spectroscopy. Recently the accessible NSE time range could be extended up to 200 ns at the IN15 intrument at the ILL, Grenoble through the use of very long neutron wavelength. Thereby observations reaching now deeply into the plateau regime can be performed. The first of this extended time range experiments was performed on monodisperse polyethylene (PE, $M_w = 36000\,\text{g/mol}$, M_w weight averaged molecular weight) [2]. In this study the reptation model of De Gennes [3] was corroborated, while competing models could be ruled out. Meanwhile we extended this investigation by systematically varying the molecular weight from M_w=190 000 g/mol down to M_w= 8000 g/mol where De Gennes prediction starts to fail, indicating the end of the pure entanglement regime.

In the entanglement regime the fitting to DeGennes expression yields the tube diameter $d_{PE} \simeq 47$Å. The time τ_e, when the initial Rouse relaxation phase ends, is identified with the slowest Rouse mode of a chain with the end-to-end distance d, i.e. $\tau_e = d^4/(\pi^2 W l^4)$ where the Rouse rate Wl^4 is determined from the dynamics of low molecular weigth melts. Inferring $\tau_e \simeq 7$ ns from the $S(Q,t)$ measurements on IN15 is indirect and relies on the value of d_{PE} from the plateau levels. A direct trace of τ_e in the time dependence of $S(Q,t)$ is difficult since there is no theoretical prediction available that is valid in that regime.

For incoherent scattering the situation is different. In a hydrogenated sample the incoherent scattering from protons dominate the scattering intensity. The incoher-

ent scattering basically carries the information on the selfcorrelation of the individual protons. In the Q-range of interest only displacements larger than complete segments are relevant. Using high $M_w = 190000$ PE there are virtually only segements well inside the tube that determine the scattering. Assuming the Gaussian approximation for the diffusing segments the incoherent scattering function is:

$$S_{inc}(Q,t) = \exp\left[-\frac{1}{6}Q^2\langle r^2(t)\rangle\right] .$$

This directly yields the time dependence of the segmental diffusion $\langle r^2(t)\rangle = -6\log\left[S_{inc}(Q,t)\right]/Q^2$. There are expectations for this function for the szenario of reptating chains that are often quoted in textbook like the standard work of DOI & EDWARDS [4]. Figure 1 illustrates the time evolution of $\langle r^2(t)\rangle$ from the shortest to macroscopic times. Only the light window indicated in fig.1 is (currently) accessible to neutron scattering. It contains the crossover from free Rouse motion to constrained realxations in a tube (local reptation). For longer times $\tau_R < t < \tau_d$ (creep regime) the power law exponent returns to the 1/2 corresponding to a diffusion along a random walk. Finally at very long times normal center of mass diffusion behaviour is observed.

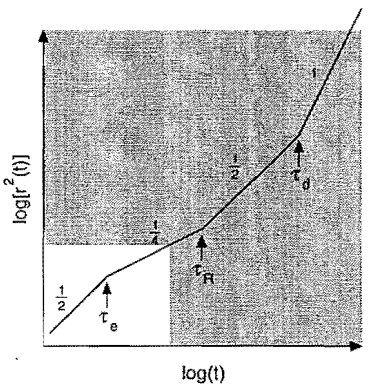

FIG. 1. Four different time regimes with different power-laws in the representation logarithm of the mean squared displacement versus logarithm of time (explanation see text).

Neutron spinecho spectroscopy covers the time range around the expected value of τ_e of a few nanoseconds. However the necessary observation of spin-incoherent scattering from protons in the sample that is a prerequisite to extract $\langle r^2(t)\rangle$ directly is difficult enough to have prevented the experiment until recently. The reasons for this are threefold: 1. incoherent scattering scatters neutrons uniformly into all directions ($\Delta\Omega = 4\pi$) unlike the coherent SANS which is concentrated on the small Q-values to be used in the experiment. 2. the spin-flip scattering that gives rise to the incoherence of the proton scattering interferes with the usual mechanism of spin preparation and analysis of the NSE and converts 2/3 of the intensity into background leaving a signal of 1/3 with a negative amplitude compared to coherent echo signals. 3. The necessary flippers and correction elements as well as sample containers contribute to background intensity that is comparable to the signal. Only extra measures to remove the background (collimator in front of analyzer-detector group), use of a large area detector to collect enough neutrons, long counting times (stability!) and very careful background subtraction allow for the reliable measurement of $S_{\rm inc}(Q,t)$. This is currently uniquely possible at the NSE spectrometer in Jülich. Figure 2 shows the result of 20 days of counting at two Q-values on a $M_w = 190000$ protonated PE sample.

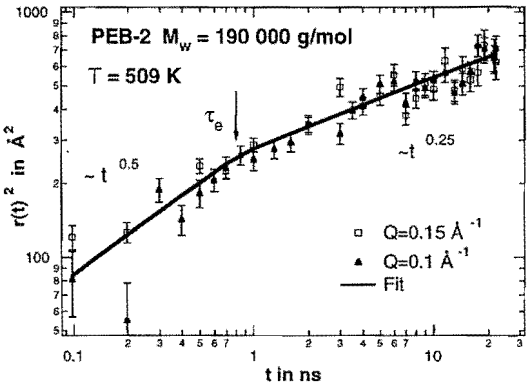

FIG. 2. Incoherent NSE data of fully protonated polyethylene with $M_w = 190\ 000$ g/mol for Q=0.1 Å^{-1} and Q=0.15 Å^{-1}. The lines represent a fit with the incoherent scattering function within the Rouse model (for $t < \tau_e$) and the Reptation model (for $t > \tau_e$) where τ_e is the only free parameter.

The crossover from the Rouse exponent 1/2 to the local reptation exponent 1/4 is clearly visible. The value of $\tau_e = 0.8$ ns however is rather compatible with a tube diameter $d \approx 30$Å than with the 47Å from the coherent experiments. But it is consistent with d-values inferred from mechanical measurements [5]. The explanation of this inconsistency needs further experiments on other polymers which are currently under way.

[1] W. Paul, G. D. Smith, D. Y. Yoon, B. Farago, S. Rathgeber, A. Zirkel, L. Willner and D. Richter, Phys. Rev. Lett. **80**, 2346 (1998)

[2] P. Schleger, B. Farago, C. Lartigue, A. Kollmar and D. Richter, Phys. Rev. Lett. **81**, 124 (1998)

[3] P. G. De Gennes, J. Physique **42**, 735 (1981)

[4] M. Doi and S. F. Edwards, *The Theory of Polymer Dynamics*, Oxford Science Publications, Clarendon Press, Oxford (1988)

[5] J. M. Carella, W. W. Graessley and L. J. Fetters, Macromolecules **17**, 2775 (1984)

Partial structure factors of polyisoprene – polarized neutron scattering experiments and computer simulation

R. Zorn, D. Richter, J. Eilhard, A. Zirkel, L. J. Fetters
Institute Neutron Scattering

F. Alvarez, J. Colmenero
Unversidad del País Vasco, San Sebastián, Spain

Polarized neutron scattering experiments have been carried out to obtain the coherent differential neutron scattering cross-section of partially deuterated polyisoprene. The results were corrected by a new algorithm for treating multiple-scattering contributions. The resulting differential neutron cross-section was compared to results from molecular dynamics simulation. The agreement is satisfactory and thus confirms the validity of such calculations for polymeric systems.

F&E-Nr: 23.30.0

Molecular dynamics (MD) simulation becomes more and more important in the calculation of the molecular structure of amorphous polymers. Therefore it is interesting to verify the results of such calculations by experiments on real materials. Neutron scattering plays an important rôle for this purpose because by selective deuteration different linear combinations of partial structure factors can be measured and compared to the same quantities from simulation.

Among the neutron diffraction methods those applying polarized neutrons are well-suited for this purpose: Firstly, they allow a separation of the coherent scattering part from the incoherent background. Secondly, because the coherent cross-section is measured in relation to the incoherent one a simple and most often reliable calculation of absolute cross-section values is possible.

The polarized neutron diffraction experiments [1] were performed on D7 at ILL, Grenoble. To suppress thermal excitations the samples were cooled to 1.5 K. The polyisoprene species used in this experiment were common polyisoprene (PI-h8: $(CH_2CH = C(CH_3)CH_2)_n$), methyl-group deuterated polyisoprene (PI-d3), chain deuterated polyisoprene (PI-d5), and fully deuterated polyisoprene (PI-d8).

In single scattering approximation the coherent differential cross-section from polarized neutron diffraction is

$$\left[\frac{\mathrm{d}\sigma_{\mathrm{coh}}}{\mathrm{d}\Omega}(Q)\right]_0 = \frac{2}{3}\frac{\sigma_{\mathrm{inc}}}{4\pi}\left(\frac{n_\uparrow(Q)}{n_\downarrow} - \frac{1}{2}\right). \qquad (1)$$

where $n_\uparrow(Q)$ is the number of neutrons scattered without spin flip and $n_\downarrow$ the respective number with spin flip. σ_{inc} is the incoherent neutron scattering cross-section.

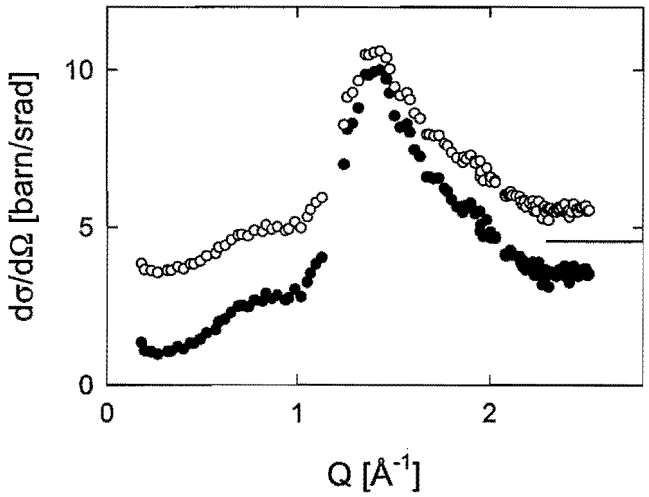

FIG. 1. Differential coherent neutron scattering cross-section (per monomer) of PI-d3 without (○) and with (●) multiple scattering correction. The line to the right indicates the high-Q limit expected from the tabulated coherent cross-sections of the nuclei present in PI-d3.

Figure 1 shows the data obtained in this way. In order to correct the data for the multiple scattering contribution a procedure was used similar to that described in [2] and [3] which will be subject of a separate publication [4]. The assumptions used in the derivation are: (i) subsequent scattering events have the same relative probability, (ii) multiple scattering is isotropic. This leads to a linear relation between the corrected and uncorrected differential cross-sections

$$\frac{\mathrm{d}\sigma_{\mathrm{coh}}}{\mathrm{d}\Omega}(Q) = A \cdot \left[\frac{\mathrm{d}\sigma_{\mathrm{coh}}}{\mathrm{d}\Omega}(Q)\right]_0 - B \qquad (2)$$

with the correction coefficients

$$A = \frac{3(\sigma_{\mathrm{inc}} + \overline{\sigma_{\mathrm{coh}}} + \sigma_{\mathrm{abs}})^2}{((4-T')\sigma_{\mathrm{inc}} + 3\sigma_{\mathrm{abs}} + 3T'\overline{\sigma_{\mathrm{coh}}})(\sigma_{\mathrm{abs}} + T'(\sigma_{\mathrm{inc}} + \overline{\sigma_{\mathrm{coh}}}))} \quad \text{and} \qquad (3)$$

$$B = (1-T')\frac{3T'\overline{\sigma_{\mathrm{coh}}}^3 + (2T'+1)\sigma_{\mathrm{inc}}\overline{\sigma_{\mathrm{coh}}}^2 + (2-T')\sigma_{\mathrm{inc}}^2\overline{\sigma_{\mathrm{coh}}} + \sigma_{\mathrm{inc}}^3 + (\sigma_{\mathrm{inc}}^2 + 3\overline{\sigma_{\mathrm{coh}}}^2)\sigma_{\mathrm{abs}}}{((4-T')\sigma_{\mathrm{inc}} + 3\sigma_{\mathrm{abs}} + 3T'\overline{\sigma_{\mathrm{coh}}})(\sigma_{\mathrm{abs}} + T'(\sigma_{\mathrm{inc}} + \overline{\sigma_{\mathrm{coh}}}))} \qquad (4)$$

where σ_{abs} is the neutron absorption cross-section and $\overline{\sigma_{coh}}$ is the coherent cross-section averaged over the wave vector range accessible by the instrument. The strength of the correction is controlled by T', the transmission probability of once scattered neutrons. Because there is no simple relation between this value and the experimentally measured transmission T of the incident neutrons a Monte Carlo simulation was done to derive T' from T.

The effect of the correction is demonstrated exemplary in figure 1. It can be seen that the corrected values allow an extrapolation to zero in the limit of low Q. In addition, the agreement with the expected high Q limit is improved. The results for the other species look similar with the exception of PI-d8 where the correction is only of the order of 5% because this sample's transmission is close to one.

Fully atomistic molecular dynamic simulations were carried out by using the Insight (Insight II 4.0.0 P) and the Discover-3 module from Molecular Simulations Inc. with the Polymer Consortium Force Field (PCFF). A cubic cell with periodic boundary conditions containing one polyisoprene chain of 100 monomer units was constructed at 363 K. Conjugate gradients minimization procedures were followed to minimize the structure, and subsequently dynamics were run for 1 ns in order to equilibrate the sample. The thus obtained cell was suddenly quenched to the glassy state at 100 K. Then a further equilibration of 10 ns was carried out. The system obtained in this way was used as a starting point for collecting data every 0.01 ps during a MD-run of 1 ns using the velocity Verlet algorithm in the NVT ensemble with a velocity scaling algorithm to keep the temperature constant.

The differential coherent neutron scattering cross-section of the simulated system was calculated from the atomic coordinates by

$$\frac{\mathrm{d}\sigma_{coh}}{\mathrm{d}\Omega}(Q) = \frac{1}{n_{mon}} \sum_{j,k=1}^{n} b_j b_k \exp\left(\mathrm{i}\mathbf{Q}\cdot\mathbf{r}_{jk}\right) , \qquad (5)$$

where the b_j stand for the nuclear scattering lengths for neutrons.

Figure 2 shows the comparison of experimentally determined coherent differential cross-sections and those from simulation. Only in the experimental case of PI-d8 a scaling factor 1.43 has been used because the uncertainty of proton content in the sample led to an obviously wrong normalization. Considering that in all other cases the comparison has no free parameter the agreement between experiment and simulation is highly satisfactory.

In addition it has to be taken into account that the simulation was carried out at 100 K while the experiment was done at a much lower temperature. This may be the source of some of the discrepancies. In order to show the significance of temperature in the simulation figure 2 also includes one run at 363 K for PI-d8 which shows a completely different intensity ratio between the first and second structure factor peak.

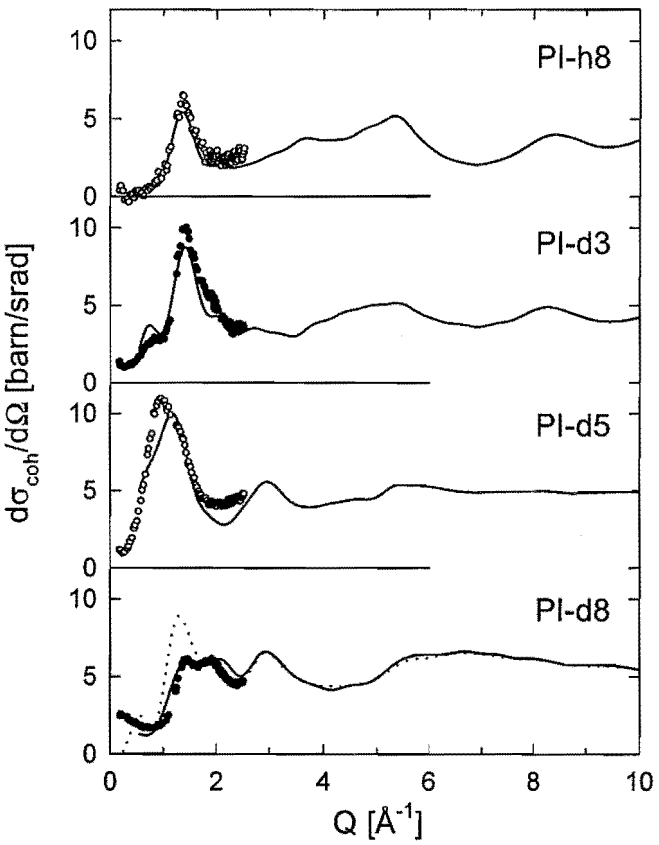

FIG. 2. Experimentally determined coherent differential cross-section (symbols, $T \approx 1.5$ K) and those from simulation (curves, $T = 100$ K) for the four PI species. The plots are offset in the vertical direction to enhance clearliness. The dotted curve shows the simulation result for PI-d8 at 363 K.

It can be seen that a significant part of the structure of the differential cross-sections lies outside the Q window observed here. Experiments with a higher Q range will be performed in the near future to scrutinize the results. On the side of the simulations calculations of partial structure factors (e.g. intra-chain, intra-group) are currently underway. Once the simulation procedure is confirmed by experiments these can ultimately lead to a detailed interpretation of the features in the structure factor.

[1] J. Eilhard, A. Zirkel, unpublished results (1995).
[2] P. Wells, R. Cywinski, Aust. J. Phys. **34**, 193 (1981).
[3] J. Mayers, R. Cywinski, Nucl. Instr. and Meth. A 241 519 (1985).
[4] R. Zorn, submitted to Nucl. Instr. and Meth. A.

Publications in refereed journals

Abbas B.; Schwahn D.; Willner L.
Concentrated diblock copolymer solutions in a pressure field
Physica B 276-278, 377-378, (2000)
23.30.0

Borbeley S.1.; Heiderich M.; Schwahn D.; Seidl E.2
1Research Institute for Solid State Physics and Optics, Hungary
2Atominstitut der Österreichischen Universitäten, Wien/Österreich
Resolution of the USANS diffractometer at the FRJ-2 reactor in Jülich
Physica B 276-278, 138-139 (2000)
23.30.0

Botti A.; Pyckhout-Hintzen W.; Richter D.; Straube E.1; Urban V.2; Kohlbrecher J.3
1Univ. Halle/Saale, FB Physik
2ESRF Grenoble, Frankreich
3PSI Villigen, Schweiz
Chain deformation in filled elastomers: a SANS approach
Physica B 276-278, 371-372 (2000)
23.30.0

Buzza D.M.1; Fzea A.H.2; Allgaier J.; Young R.N.3; Hawkins R.J.1; Hamley I.W.4; McLeish T.C.B.1; Lodge T.P.5
1Dep. of Phys. and Astronomy & Polymer IRC, Univ. Leeds/UK
2Dep. of Chem., Univ. Dundee/UK
3Univ. Sheffield/UK
4School of Chemistry, Univ. Leeds/UK
5Univ. Minnesota/USA
Linear melt rheology and small angle X-ray scattering of AB diblock vs A2B2 four arm star block copolymers
Macromolecules 2000, 8399-8414 (2000)
23.30.0

Endo H.; Allgaier J.; Gompper G.; Jakobs B.1; Monkenbusch M.; Richter D.; Sottmann T.1; Strey R.1
1Univ. Köln, Inst. für Physik. Chemie
Membrane decoration by amphiphilic block copolymers in bicontinuous microemulsions
Phys. Rev. Lett. 85, 102-105 (2000)
23.30.0

Hoffmann S.; Willner L.; Richter D.; Arbe A.1; Colmenero J.1; Farago B.2
1Departamento de Fisica de Materiales, Universidad del Pais Vasco, San Sebastian/Spain
2Institut Laue Langevin, Grenoble/France
On the Origin of Dynamic Heterogeneities in Miscible Polymer Blends - A Quasielastic Neutron Scattering Study
Phys. Rev. Lett. 80, 772 (2000)
23.30.0

Ibberson R.M.1; David W.I.F.1; Parsons S.2; Prager M.; Shankland K.1
1RAL, Chilton, Didcot, UK
2Univ. of Edinburgh, UK
The crystal structures of m-xylene and p-xylene, C8D10, at 4.5K
J. Mol. Struct. 524, 121 (2000)
23.15.0

Ibberson R.M.1; Morrison C.2; Prager M.
1RAL, Chilton, Didcot, UK
2Univ. of Edinburgh, UK
Neutron powder and ab-initio structure of orthoxylene: the influence of crystal packing on the phenyl ring
Chem. Commun. 2000, 539 (2000)
23.15.0

Inamura Y.1; Arai M.1; Otomo T.1; Kitamura N.2; Buchenau U.
1Inst. of Material Structure Science, KEK, Tsukuba/Japan
2Government Industrial Research, Inst. of Osaka, Ikeda/Japan
Density dependence of the boson peak of vitreous silica
Physica B 284-288, 1157-1158 (2000)
23.15.0

Kanaya T.1; Buchenau U.; Koizumi S.; Tsukushi I.1; Kaji K.1
1Inst. for Chem. Research, Kyoto University, Kyoto/Japan
Non-Gaussian behavior of crystalline and amorphous phases of polyethylene
Phys. Rev. B 61, 6451 (2000)
23.30.0

Kemner E.1; de Schepper I.M.1; Schmets A.J.M.1; Grimm H.; Overweg A.R.1,2; van Santen R.A.2
1Interfaculty Reactor Institute, Delft Univ. of Technology, The Netherlands
2Lab. of Inorganic Chem. and Catalysis, Eindhoven Univ. of Technology, The Netherlands
Molecular motion of ferrocene in a Faujaste-type zeolite: A quasielastic neutron scattering study
J. Phys. Chem. B 2000, 1560-1562 (2000)
23.15.0

Kemner E.1; de Schepper I.M.1; Schmets A.J.M.1; Grimm H.
1Interfaculty Reactor Institute, Delft Univ. of Technology, The Netherlands
Model independent determination of the elastic incoherent structure factor in neutron scattering experiments
Nuclear Instruments and Methods in Physics Research B 160, 544-549 (2000)
23.15.0

Kirstein O.; Kozielewski T.; Prager M.; Richter D.
The backscattering spectrometer for the FRM-II reactor in Munich
Physica B 291, 310-313 (2000)
23.89.1

Kirstein O.; Prager M.; Kozielewski T.; Richter D.
Phase space transformation used at the FRM II backscattering spectrometer: concepts and technical realization
Physica B 283, 361-364 (2000)
23.89.1

Koizumi S.1; Annaka M.1; Borbeley S.2; Schwahn D.
1Advanced Science Research Center, Japan Atomic Energy Research Institute, Tokai-mura/Japan
2Research Institute for Solid State Physics and Optics, Hungary
Fractal structures of a Poly(N-Isopropylacrylamide) gel studied by small-angle neutron scattering over a Q-range from 10-5 to 0.1Å-1
Physica B 276-278, 367-368 (2000)
23.30.0

Kurth D.G.1; Lehmann P.1; Volkmer D.2; Müller A.2; Schwahn D.
1MPI of Colloids and Interfaces, Potsdam
2University of Bielefeld, Dep. of Chemistrsy
Biologically inspired polyoxometalate-surfactant composite materials. Investigations on the structures of discrete, surfactant-encapsulated clusters, monolayers, and Langmuir-Blodgett films of (DODA)40(NH4)2[(H2O)n (Mo132O372(CH3CO2)30(H2O)72]
J. Chem. Soc., Dalton Trans., 3989-3998 (2000)
23.30.0

Lee S.A.1; Grimm H.; Pohle W.2; Scheiding W.2; van Dam L.3; Song Z.3; Levitt M.H.3; Korolev N.3.; Szabó A.1; Rupprecht A.3
1Dep. of Physics & Astronomy, Univ. Toledo, Ohio/USA
2Inst. für Molekularbiologie, Univ. Jena
3Division of Physical Chem., Univ. Stockholm/Schweden
NaDNA-bipyridyl-(ethylenediamine)platinum (II) complex: Structure in oriented wet-spun films and fibers
Phys. Rev. E 62, 7044, (2000)
23.15.0

Leube W.; Monkenbusch M.; Schneiders D.; Richter D.; Adamson D.1; Fetters L.1; Panagiotis D.2; Lovegrove R.2
1Exxon Mobil Research and Engineering Co., Strategic Corporate, Research Laboratories, Annandale, New Jersey, USA
2Infineum, Ltd. Milton Hill, Abingdon, England
Wax crystal modification for fuel oils by self-aggregating partially crystallizable hydrocarbon block copolymers
Energy&Fuels, Vol. 14 (2), 419-430 (2000)
23.30.0

McGrady G.S.1; Turner J.F.C.2; Ibberson R.M.3; Prager M.
1Kings College, London, UK
2Univ. of Tennessee, USA
3RAL, Chilton, Didcot, UK
Structure of the trimethylaluminum dimer as determined by powder neutron diffraction at low temperature
J. Mol. Struct. 19, 4398 (2000)
23.15.0

Monkenbusch M.; Schneiders D.; Richter D.; Willner L.; Leube W.; Fettes L.J.1; Huang J.S.1; Lin M.1
1Exxon Corporate Research, Annandale/USA
2Dept. of Mat. Sci., Princeton Univeristy/USA
Aggregation behavior of PE-PEP copolymers and the winterization of Diesel fuel
Physica B 276-278, 941 (2000), Conf. Proced. ICNS '99, Budapest/Hungary
23.30.0

Mortensen K.1; Schwahn D.; Frielinghaus H.; Almdal K.1
1Risø National Laboratory, Condensed Matter Physics and Chemistry Department, Roskilde, Denmark
Lifshitz critical line in the ternary mixture of homopolymer blend and diblock copolymer, studied by small-angle neutron scattering
J. Appl. Cryst. 33, 686-689 (2000)
23.30.0

Prager M.; Grimm H.; Parker S.F.1; McGrady S.2
1ISIS facility, RAL, Chilton Didcot, Oxon OX11 0QX, UK
2Kings College, London, UK
Rotational potentials of bridging and terminal methyl groups in trimethylaluminium-dimers
Physica B 276-278, 250-251 (2000)
23.30.0

Prager M.
The thermal time-of-flight spectrometer SV29 at FZ Jülich: focusing in space and time
Physica B283, 376 (2000)
23.89.1

Richter D.; Monkenbusch M.; Allgaier J.; Arbe A.1; Colmenero J.1; Farago B.2; Cheol Bae Y.3; Faust R.3
1Departamento de Fisica de Materiales, Universidad del Pais Vasco, San Sebastian/Spain
2Insitut Laue Langevin, Grenoble, France
3Department of Chemistry, University of Massachusetts-Lowell, Lowell/Massachusetts, USA
From Rouse dynamics to local relaxation: A neutron spin echo study on polyisobutylene melts
Journal of Chem. Phys. 111, 6107 (1999)
23.30.0

Richter D.
Neutron scattering in polymer physics
Physica B 276-278, 22-29 (2000)
23.30.0

Rush J.J.1; Udovic T.J.1; Berk N.F.1; Richter D.; Magerl A.2
1Center for Neutron Research, National Institute for Standards and Technology, Gaithersburg, USA
2Lehrstuhl für Kristallographie und Strukturphysik, Universität Erlangen-Nürnberg
Excited-state vibrational tunnel splitting of hydrogen trapped by nitrogen in niobium
Europhys. Lett. 48 (2), 187-193 (1999)
23.30.0

Schwahn D.; Mortensen K.1; Frielinghaus H.1; Almdal K.1; Kielhorn L.2
1Risø National Laboratory, Condensed Matter Physics and Chemistry Department, Roskilde, Denmark
2Bayer AG, Leverkusen
Thermal composition fluctuations near the isotropic Lifshitz critical point in a ternary mixture of a homopolymer blend and diblock copolymer
Journ. of Chem. Physics 112, 5454-5472 (2000)
23.30.0

Schwahn D.; Mortensen K.1; Frielinghaus H.; Almdal K.1
1Risø National Laboratory, Condensed Matter Physics and Chemistry Department, Roskilde, Denmark
3D-Ising and Lifshitz critical behavior in a mixture of a polymer blend and a corresponding diblock copolymer
Physica B 276-278, 353-354 (2000)
23.30.0

Schwahn D.
Ginzburg number and phase behavior of binary polymer blends in pressure fields
Macromol. Symp. 149, 43-52 (2000)
23.30.0

Skripov A.V.1; Combet J.2; Grimm H.; Hempelmann R.3; Kozhanov V.N.1
1Institute of Metal Physics, Urals Branch of the Academy of Sciences, Ekatarinenburg/Russia
2Institut Laue Langevin, Grenoble/Frankreich
3Inst. für Physik. Chemie, Univ. des Saarlandes
Quasielastic neutron scattering study of H motion in the hydrogen-stabilized C15-type phases HfTi2Hx and ZrTi2Hx
J. Phys. Cond. Matt. 12, 3313-3324 (2000)
23.15.0

Smith G.D.1; Paul W.2; Monkenbusch M.; Richter D.
1Dep. of Materials Science and Engineering / Dept. of Chemical Engineering and Fuels Engineering, Univ. Utah, USA
2Inst. für Physik, Univ. Mainz
A comparison of neutron scattering studies and computer simulations of polymer melts
Chem. Physics 261, 61-74 (2000)
23.30.0

Smith G.D.1; Paul W.2; Monkenbusch M.; Willner L.; Richter D.; Qiu X.H.; Ediger M.D.
1Dep. of Mat. Science and Engineering, University of Utah, Salt Lake City/USA
2Inst. für Physik, Universität Mainz
3Dep. of Chemistry, University of Wisconsin-Madison, Madison/USA
Molecular Dynamics of a 1,4-Polybutadiene Melt. Comparison of Experimental and Simulation
Macromolecules 32, 8857 (1999)
23.30.0

Sokolov A.P.1; Grimm H.; Kisliuk A.1; Dianoux A.J.2
1Dep. of Polymer Science, Univ. Akron/USA
2Institute Laue Langevin, Grenoble/Frankreich
Slow relaxation process in DNA at different levels of hydration
J. of Biological Physics 26, SN1-SN5, (2000)
23.15.0

Stellbrink J.; Allgaier J.; Monkenbusch M.; Richter D.; Lang A.1; Likos C.N.1; Watzlawek M.1; Löwen H.1; Ehlers G.2; Schleger P.2
1Univ. Düsseldorf, Theor Physik II
2Insitut Laue Langevin, Grenoble/Frankreich
Neither Gaussian chains nor hard spheres-star polymer seen as ultrasoft colloids
Progr. Colloid Polymer Sci. 115, 88-97 (2000)
23.30.0

Westermann S.1; Willner L.; Richter D.
1Goodyear Technical Center, Luxembourg
The evaluation of polyethylene chain dimensions as a function of concentration in nonadecane
Macromol. Chem. Phys. 201, 500-504 (2000)
23.30.0

Westermann S.; Pyckhout-Hintzen W.; Thiyagarajan P.1; Wozniak D.1; Richter D.; Straube E.2
1IPNS, Argonne, USA
2Universität Halle
A SANS study on thermal degradation kinetics in polyisoprene networks
Mat. Res. using cold neutrons at pulsed neutron sources, eds. P. Thiyagarajan, F. Trouw, B. Marzec, C.-K. Loong, World Scientific Publ., 210 - 213 (1999)
23.30.0

Willner L.; Poppe A.; Allgaier J.; Lindner P.1; Richter D.
1Institut Laue Langevin, Grenoble/France
Micellarization of Amphiphilic Diblockcopolymers in Water: Shape Transition and Meanfield to Scaling Cross Over
Europhysics Letters 51 (6), 628 (2000)
23.30.0

Wischnewski A.; Richter D.; Monkenbusch M.; Willner L.; Farago B.1; Ehlers G.1; Schleger P.1
Reptation in polyethylene-melts with different molecular weights
Physica B 276-278, 337 (2000)
23.30.0

Wischnewski A.; Richter D.
Comment on "What is the entanglement length in a polymer melt?" by M. Pütz, K. Kremer and G.S. Grest
Europhys. Lett. 52, 719-720 (2000)
23.30.0

Zorn R.; Monkenbusch M.; Richter D.; Matsuoka H.1; Yamamoto Y.1; Nakano M.1; Endo H.1; Yamaoka H.1; Seto H.2; Kawabata Y.2; Nagao M.3
1Dep. of Polymer Chemistry, Kyoto University/Japan
2FIAS, Hiroshima Univ./Japan
3Inst. of Solid State Physics, Univ. of Tokyo, Ibaraki/Japan
Neutron spin-echo study of the dynamic behavior of amphiphilic diblock copolymer micelles in aqueous solution
Langmuir 16, 9177-9185 (2000)
23.30.0

Zorn R.; Richter D.; Hartmann L.1; Kremer F.1; Frick B.2
1Univ. Leipzig, Inst. für Experimentalphysik
2Institut Laue Langevin, Grenoble/Frankreich
Inelastic neutron scattering experiments on the fast dynamics of a glass forming liquid in mesoscopic confinements
J. Phys. France IV, 10, Pr. 7-83 - Pr.7.86 (2000)
23.15.0

Other publications

Allgaier J.; Poppe A.; Willner L.; Stellbrink J.; Richter D.
PEP-PEO block copolymers as model system for the investigation of micellization in aqueous solution
ACS Symposium Series 765, Ed. J. Edward Glass (2000)
23.30.0

Buchenau U.
Relaxationsprozesse in Gläsern
Vorlesungsmanuskript des 31. IFF-Ferienkurs "Femtosekunden und Nano-eV", Vol. 3, C7.1 - 18 (2000)
23.15.0

Fetters L.J.1; Wheeler L.M.1; Xenidou M.; Richter D.
1Exxon Research and Engineering Co., Annandale/USA
Modification Potential for ShellvisTM Star Polymers
Exxon Research and Engineering Company; Proprietary Information, CR.17BU.99 (1999)
23.30.0

Monkenbusch M.
Introduction to soft matter systems
Neutron Scattering in Novel Materials, Proceedings of the 8th Summer School on Neutron Scattering, 102-116 (2000)
23.30.

Monkenbusch M.
Neutron spin-echo spectrometer, NSE
Lecture Notes of the Laboratory Course on "Neutron Scattering", Vol. 5, 11-1 - 11-18 (2000)
23.30.0

Monkenbusch M.
Neutronenspektroskopie
Vorlesungsmanuskript des 31. IFF-Ferienkurs "Femtosekunden und Nano-eV", Vol.3, B5.1 - 40 (2000)
23.30.0

Monkenbusch M.
Time-of-flight spectrometers
Lecture Notes of the Laboratory Course on "Neutron Scattering", Vol. 5, 10-1 - 10-23 (2000)
23.30.0

Prager M.
Translation an Rotation
Lecture Notes of the Laboratory Course on "Neutron Scattering", Vol. 5, 17-1 - 17-20 (2000)
23.30.0

Pyckhout-Hintzen W.; Botti A.; Heinrich M.; Richter D.; Straube E.1; Westermann S.2; Urban V.3
1Univ. Halle/Saale, FB Physik
2Goodyear Technical Center, Luxembourg
3ESRF Grenoble, France
SANS of polymer networks under deformation
Novel Materials, World Science Press (Singapore), 117-130 (2000)
23.30.0

Pyckhout-Hintzen W.; Westermann S.1; Botti A.; Richter D.; Straube E.2
1Goodyear Technical Center, Luxembourg
2Univ. Halle/Saale, FB Physik
Chain deformation in unfilled and filled polymer networks: a SAS approach
Notiziario Neutroni e Luce di Sincrotone 5, 34-40 (2000)
23.30.0

Richter D.; Monkenbusch M.; Farago B.1; Schleger P.1, Montes H.2
1Institut Laue Langevin, Grenoble/France
2ESPCI, Paris/France
Large scale motions in dense polymer systems
AIP Conference Proceedings 469, 587 - 598 (1999)

23.30.0

Richter D.
Dynamik von Polymeren
Vorlesungsmanuskript des 31. IFF-Ferienkurs
"Femtosekunden und Nano-eV", Vol. 3, C6.1 - 36 (2000)
23.30.0

Richter D.
Polymer dynamics
Lecture Notes of the Laboratory Course on "Neutron Scattering", Vol. 5, 15-1 - 15-29 (2000)
23.30.0

Richter D.
Polymer dynamics by neutron spin echo spectroscopy
in "Scattering in Polymeric and Colloidal Systems" Ed. by W. Brown and K. Mortensen, Gordon and Breach Science Publishers, London, Chap. 12, 535-575 (2000)
23.30.0

Richter D.
Properties of the neutron, elementary scattering processes
Lecture Notes of the Laboratory Course on "Neutron Scattering", Vol. 5, 2-1 - 2-21 (2000)
23.30.0

Rosov N.1; Rathgeber S.1; Monkenbusch M.
1NIST, Gaithersburg/USA
Neutron spin echo spectroscopy at the NIST Center
ACS Symposium Series 739 "Scattering from Polymers", Characterization by X-rays, Neutrons and Light, Ed. P. Cebe, B.S. Hsiao, D.J. Lohse
23.89.1 / 23.30.0

Schwahn D.; Mortensen K.1
1Risø National Laboratory, Condensed Matter Physics and Chemistry Department, Roskilde/Denmark
Thermal composition fluctuations in polymer blends studied with small angle neutron scattering
Chapter 8 in "Scattering in polymeric and colloidal systems", eds. W. Brown and K. Mortensen, Gordon and Breach Science Publishers (2000)
23.30.0

Schwahn D.
Small-angle scattering and reflectometry
Lecture Notes of the Laboratory Course on "Neutron Scattering", Vol. 5, 8-1 - 8-16 (2000)
23.30.0

Schwahn D.
Soft Matter Structure
Lecture Notes of the Laboratory Course on "Neutron Scattering", Vol. 5, 14-1 - 14-18 (2000)
23.30.0

Zorn R.
Correlations functions measured by scattering experiments
Lecture Notes of the Laboratory Course on "Neutron Scattering", Vol. 5, 5.1 - 5-24 (2000)
23.15.0

Zorn R.
Ionentransport in Elektrolyten
Vorlesungsmanuskript des 31. IFF-Ferienkurs
"Femtosekunden und Nano-eV", Vol. 3, D1.1 - 20 (2000)
23.15.0

Invited Talks

Buchenau U.
A new view of the glass transition
Workshop CPG 2000, Univ. Dresden, 02. - 13.10.00
23.15.0

Buchenau U.
Dynamics of glass formers
EPS CMD-18 Conference, Montreux/Switzerland, 14.03.00
23.30.0

Buchenau U.
Fast and slow relaxations at the glass transition
Workshop "Neutron scattering and computer simulation", Univ. San Sebastian/Spain, 15. - 17.06.00
23.30.0

Buchenau U.
I. Glasses; II. Glass transition; III. Inelastic scattering from glasses
Euroschool Dyn. Mat. 2000, Univ. Rostock, 04. - 05.09.00
23.15.0

Monkenbusch M.
Dynamics of homo- and blockcopolymer melts - Recent advances from neutron spin echo
CEA-CMRS Conference, Nagoya/Taiwan, 22.09.00
23.30.0

Monkenbusch M.
Next generation NSE instruments, What are the challenges?
Int. Workshop on NSE, HMI Berlin, 16.10.00
23.89.1

Ohl M.
Studies of dynamic and static properties of the orientational glasses
CEA, Grenoble/France, 09.12.99
23.15.0

Pyckhout W.
Local chain deformation in polymer networks by SANS
EPS CMD-18 Conference, Montreux/Switzerland, 13. - 17.03.2000
23.30.0

Pyckhout-Hintzen W.
SANS of polymer networks under deformation
Summerschool on Neutron Scattering, Zuoz/Switzerland, 08. - 12.08.00
23.30.0

Richter D.
Amphiphilic polymers as amphiphilicity boosters in microemulsion systems
219th ACS Conference, San Francisco/USA, 26. - 30.03.00
23.30.0

Richter D.
Die europäische Spallationsneutronenquelle - ein Leuchtturm für die Forschung
Jahresempfang des Forschungszentrum Jülich, Bonn, 20.09.00
23.30.0

Richter D.
Dynamics of homo- and blockcopolymer melts - recent advances from neutron spin echo
APS March Meeting, Minneapolis/USA, 20. - 24.03.00
23.30.0

Richter D.
Neutron scattering and the glass transition in polymers - Present status and future opportunities
VI Int. Workshop on "Non Crystalline Solids", Bilbao/Spain, 13.- 15.09.00
23.30.0

Richter D.
Neutron scattering and the glass transition in polymers - Present status and future opportunities
Workshop "Future perspectives for understanding the unsolved problem of the glass-transition by neutron scattering and computer simulation", San Sebastian/Spain, 15. - 17.06.00
23.30.0

Richter D.
Neutron scattering in polymer physics - recent highlights
Summer School "Recent developments in neutron scattering", Les Houches/France, 02. - 12.05.00
23.30.0

Richter D.
Neutron spin echo
Workshop on "Neutron Scattering in Soft Matter", Lungtan/Taiwan, 29. - 31.03.00
23.30.0

Richter D.
Polymer dynamics from local to the global scale
Workshop on "Neutron Scattering in Soft Matter", Lungtan/Taiwan, 29. - 31.03.00
23.30.0

Richter D.
The role of amphiphilic polymers in emulsification boosting in oil water microemulsion - a SANS and NSE Study
Kolloquium, MPI für Kolloid- und Grenzflächenforschung, Potsdam, 12.12.00
23.30.0

Richter D.
The role of amphiphilic polymers in emulsification boosting in oil-water microemulsions
Conference on "Scattering Studies of Mesoscopic Scale Structure and Dynamics in Soft Matter", Messina/Italy, 22. - 25.11.00
23.30.0

Schwahn D.
Investigations of polymer blends with small angle neutron scattering
The Dutch Polymer Institute (DPI), Eindhoven University of Technology/The Netherlands, 08.06.00
23.30.0

Stellbrink J.
Partial structure factors in star polymer/colloid mixtures
COST WG1-Meeting, Fribourg/Switzerland, 15.-16.12.2000
23.30.0

Wischnewski A.; Richter D.; Monkenbusch M.; Willner L.; Farago B.1; Ehlers G.1; Schleger P.1
1Institute Laue Langevin, Grenoble/France
Reptation in polymer melts - What's new?
EPS CMD-18 Conference, Montreux/Switzerland, 13. - 17.03.2000
23.30.0

Wischnewski A.; Willner L.; Monkenbusch M.; Richter D.; Farago B.1; Ehlers G.1; Schleger P.1
1Institut Laue Langevin, Grenoble/France
NSE: A method to observe constraints of motion in polymer melts
Int. Workshop on NSE, HMI, Berlin, 16.10.00
23.30.0

Zorn R.; Richter D.; Hartmann L.1; Kremer F.1; Frick B.2
1Fakultät für Physik und Geowissenschaften, Universität Leipzig
2Institut Laue Langevin, Grenoble/Frankreich
Inelastic Neutron Scattering Experiments on the Fast Dynamics of a Glass-Forming Liquid in Mesoscopic Confinements
Workshop "Dynamics in Confinement", Grenoble/France, 29.01.00
23.15.0

Zorn R.
Inelastische Neutronenstreuung als Werkzeug zur Beobachtung der mikroskopischen Dynamik in Polymersystemen
Kolloquium Physikalische Chemie, Univ. Hannover, 17.01.00
23.15.0

Zorn R.
Multiple scattering correction for polarized-neutron diffraction
Universität San Sebastian/Spanien, 28.07.00
23.15.0

Other talks

Allgaier J.; Poppe A.; Willner L.; Stellbrink J.; Richter D.
PEP-PEO block copolymers as model system for the investigation of micellization in aqueous solution
ACS Symposium Series 765, Ed. J. Edward Glass (2000)
23.30.0

Buchenau U.
Relaxationsprozesse in Gläsern
Vorlesungsmanuskript des 31. IFF-Ferienkurs "Femtosekunden und Nano-eV", Vol. 3, C7.1 - 18 (2000)
23.15.0

Fetters L.J.1; Wheeler L.M.1; Xenidou M.; Richter D.
1Exxon Research and Engineering Co., Annandale/USA
Modification Potential for ShellvisTM Star Polymers
Exxon Research and Engineering Company; Proprietary Information, CR.17BU.99 (1999)
23.30.0

Monkenbusch M.
Introduction to soft matter systems
Neutron Scattering in Novel Materials, Proceedings of the 8th Summer School on Neutron Scattering, 102-116 (2000)
23.30.

Monkenbusch M.
Neutron spin-echo spectrometer, NSE
Lecture Notes of the Laboratory Course on "Neutron Scattering", Vol. 5, 11-1 - 11-18 (2000)
23.30.0

Monkenbusch M.
Neutronenspektroskopie
Vorlesungsmanuskript des 31. IFF-Ferienkurs "Femtosekunden und Nano-eV", Vol.3, B5.1 - 40 (2000)
23.30.0

Monkenbusch M.
Time-of-flight spectrometers
Lecture Notes of the Laboratory Course on "Neutron Scattering", Vol. 5, 10-1 - 10-23 (2000)
23.30.0

Prager M.
Translation an Rotation
Lecture Notes of the Laboratory Course on "Neutron Scattering", Vol. 5, 17-1 - 17-20 (2000)
23.30.0

Pyckhout-Hintzen W.; Botti A.; Heinrich M.; Richter D.; Straube E.1; Westermann S.2; Urban V.3
1Univ. Halle/Saale, FB Physik
2Goodyear Technical Center, Luxembourg
3ESRF Grenoble, France
SANS of polymer networks under deformation
Novel Materials, World Science Press (Singapore), 117-130 (2000)
23.30.0

Pyckhout-Hintzen W.; Westermann S.1; Botti A.; Richter D.; Straube E.2
1Goodyear Technical Center, Luxembourg
2Univ. Halle/Saale, FB Physik
Chain deformation in unfilled and filled polymer networks: a SAS approach
Notiziario Neutroni e Luce di Sincrotone 5, 34-40 (2000)
23.30.0

Richter D.; Monkenbusch M.; Farago B.1; Schleger P.1, Montes H.2
1Instiut Laue Langevin, Grenoble/France
2ESPCI, Paris/France
Large scale motions in dense polymer systems
AIP Conference Proceedings 469, 587 - 598 (1999)
23.30.0

Richter D.
Dynamik von Polymeren
Vorlesungsmanuskript des 31. IFF-Ferienkurs "Femtosekunden und Nano-eV", Vol. 3, C6.1 - 36 (2000)
23.30.0

Richter D.
Polymer dynamics
Lecture Notes of the Laboratory Course on "Neutron Scattering", Vol. 5, 15-1 - 15-29 (2000)
23.30.0

Richter D.
Polymer dynamics by neutron spin echo spectroscopy in "Scattering in Polymeric and Colloidal Systems" Ed. by W. Brown and K. Mortensen, Gordon and Breach Science Publishers, London, Chap. 12, 535-575 (2000)
23.30.0

Richter D.
Properties of the neutron, elementary scattering processes
Lecture Notes of the Laboratory Course on "Neutron Scattering", Vol. 5, 2-1 - 2-21 (2000)
23.30.0

Rosov N.1; Rathgeber S.1; Monkenbusch M.
1NIST, Gaithersburg/USA
Neutron spin echo spectroscopy at the NIST Center
ACS Symposium Series 739 "Scattering from Polymers", Characterization by X-rays, Neutrons and Light, Ed. P. Cebe, B.S. Hsiao, D.J. Lohse
23.89.1 / 23.30.0

Schwahn D.; Mortensen K.1
1Risø National Laboratory, Condensed Matter Physics and Chemistry Department, Roskilde/Denmark
Thermal composition fluctuations in polymer blends studied with small angle neutron scattering
Chapter 8 in "Scattering in polymeric and colloidal systems", eds. W. Brown and K. Mortensen, Gordon and Breach Science Publishers (2000)
23.30.0

Schwahn D.
Small-angle scattering and reflectometry
Lecture Notes of the Laboratory Course on "Neutron Scattering", Vol. 5, 8-1 - 8-16 (2000)
23.30.0

Schwahn D.
Soft Matter Structure
Lecture Notes of the Laboratory Course on "Neutron Scattering", Vol. 5, 14-1 - 14-18 (2000)
23.30.0

Zorn R.
Correlations functions measured by scattering experiments
Lecture Notes of the Laboratory Course on "Neutron Scattering", Vol. 5, 5.1 - 5-24 (2000)
23.15.0

Zorn R.
Ionentransport in Elektrolyten
Vorlesungsmanuskript des 31. IFF-Ferienkurs "Femtosekunden und Nano-eV", Vol. 3, D1.1 - 20 (2000)
23.15.0

Posters

Edelmann K.1; Janich M.1; Hoinkis E.2; Pyckhout-Hintzen W.; Höring S.3
1Technische Hochschule Merseburg
2HMI, Berlin
3Universität Halle
Aggregationsverhalten von Ethylenoxid/Methylmethacrylat Diblock-Copolymeren in organischen Lösungsmitteln
GDCH, Merseburg, 20. - 21.03.2000
23.30.0

Heinrich M.; Pyckhout-Hintzen W.; Perny S.; Allgaier J.; Richter D.; Straube E.1
1Fachbereich Physik, Universität Halle
A SANS study of strained H-polymer melts in the quenched state
EPS, CMD-18, Montreux/Schweiz, 13. - 17.03.2000
23.30.0

Jakobs B.1; Sottmann T.1; Strey R.1; Endo H.; Allgaier J.; Richter D.; Gompper G.
Amphiphilic blockcopolymers: Efficiency boosters for microemulsions
14. Vortragstagung der Fachgruppe Waschmittelchemie der GDCH, Würzburg, April 2000
23.30.0

Kirstein O.; Kozielewski T.; Prager M.; Richter D.
Das Rückstreuspektrometer am FRM-II Reaktor
Wissenschaftliche Perspektiven 2001, Univ. München, 13.10.00
23.89.1

Knerr M.1; Krosigk G.2; Pyckhout-Hintzen W.; Göritz D.1
1Institut für Experimentelle und Angewandte Physik, Universität Regensburg
2DESY, Hamburg
Analyse der Dispergierung von Füllstoffen in Elastomeren mittels Ultrakleinwinkelstreuung
DPG Frühjahrstagung, Potsdam, 13. - 16.03.2000
23.30.0

Mihailescu M.
Dynamics of microemulsions with polymeric cosurfactant
EPS, CMD-18, Montreux/Schweiz, 13. - 17.03.2000
23.30.0

Prager M.
The thermal TOF spectrometer SV29 at the FRJ2-DIDO reactor, Jülich
FRM-2, Univ. München, 13.10.00
23.89.1

Pyckhout-Hintzen W.; Westermann S.; Botti A.; Richter D.; Straube E.1
1Fachbereich Physik, Universität Halle
Local chain deformation in polymer networks by SANS

EPS, CMD-18, Montreux/Schweiz, 13. - 17.03.2000
23.30.0

Willner L.; Allgaier J.
Synthese von amphiphilen Di-, Tri- und Sternblockcopolymeren via HO-funktionalisierter Polydiene
Vortragstagung: "Maßgeschneiderte Polymere", Merseburg, 20. - 21.03.00
23.30.0

Patents granted

Allgaier J.; Willner L.; Richter D.
Verfahren zur Herstellung von Hydrophob-Hydrophilen AB-Blockcoplymeren
EP 0904307 (28.06.2000) (DE,FR,GB,IT); PT 1.1375
23.30.0

Lecture courses

Buchenau U.; Schmid D.1
1Univ. Düsseldorf, Inst. für Festkörperspektroskopie
Experimentalphysik VI (Festkörperphysik)
SS 00, Univ. Düsseldorf
23.15.0

Grimm H.
Crystal spectrometer: triple-axis and back-scattering spectrometer
WS 00/01, Laboratory Course Neutron Scattering, FZ Jülich, 26.09. - 06.10.00
23.15.0

Grimm H.
Rotation and Translation
SS 00, Laboratory Course Neutron Scattering, FZ Jülich, 26.09. - 06.10.00
23.15.0

Monkenbusch M.
Introduction to soft matter systems
SS 00, Summerschool on Neutron Scattering, Zuoz/Switzerland, 08. - 12.08.00
23.30.0

Monkenbusch M.
Neutronenspektroskopie
WS 99/00, IFF Ferienschule: Femtosekunden und Nano-eV, FZ Jülich, 13.03. - 24.03.00
23.30.0

Monkenbusch M.
Time-of-flight spectrometers
WS 00/01, Laboratory Course Neutron Scattering, FZ Jülich, 26.09. - 06.10.00
23.89.1

Prager M.
Rotation and Translation
WS 00/01, Laboratory Course Neutron Scattering, FZ Jülich, 26.09. - 06.10.00
23.15.0

Richter D.
Dynamik von Polymeren
WS 99/00, IFF Ferienschule: Femtosekunden und Nano-eV, FZ Jülich, 13.03. - 24.03.00
23.30.0

Richter D.
Polymer dynamics
WS 00, Laboratory Course Neutron Scattering, FZ Jülich, 26.09. - 06.10.00
23.30.0

Richter D.
Properties of the neutron, elementary scattering process
WS 00, Laboratory Course Neutron Scattering, FZ Jülich, 26.09. - 06.10.00
23.30.0

Schwahn D.
Small angle scattering and reflectometry
WS 00/01, Laboratory Course Neutron Scattering, FZ Jülich, 26.09. - 06.10.00
23.30.0

Schwahn D.
Soft matter structure
WS 00/01, Laboratory Course Neutron Scattering, FZ Jülich, 26.09. - 06.10.00
23.30.0

Zorn R.
Correlation functions measured by scattering experiments
WS 00/01, Laboratory Course Neutron Scattering, FZ Jülich, 26.09. - 06.10.00
23.15.0

Zorn R.
Inelastic neutron scattering: dynamics of polymers
5th European School on Neutron Scattering Methods Applied to Soft Condensed Matter, Bombannes/France, 28.05. - 03.06.00
23.15.0

Zorn R.
Ionentransport in Elektrolyten
WS 99/00, IFF Ferienschule: Femtosekunden und Nano-eV, FZ Jülich, 13.03. - 24.03.00
23.15.0

Zorn R.
Neutron Spin Echo Spectrometer
WS 00/01, Laboratory Course Neutron Scattering, FZ Jülich, 26.09. - 06.10.00
23.15.0

Internal seminars

Allgaier J.
Polymersynthese
Jülich Soft Matter Days, Heimbach, 18. - 20.10.00
23.30.0

Endo H.
Polymer efficiency boosters in microemulsions: A SANS study to investigate the role of the polymer
Jülich Soft Matter Days, Heimbach, 18. - 20.10.00
23.30.0

Kahle S.
Glass transition and glassy state
Jülich Soft Matter Days, Heimbach, 18. - 20.10.00
23.30.0

Kirstein O.; Kozielewski T.; Prager M.; Richter D.
Rückstreuspektrometer für den FRM-II Reaktor
KFN-Tagung, FZ Jülich, 18. - 19.09.00
23.89.1

Mihailescu M.
Experiments describing the dynamics of microemulsions
Jülich Soft Matter Days, Heimbach, 18. - 20.10.00
23.30.0

Monkenbusch M.
Neutronenstreuung und Dynamik in "Soft Matter" Systemen
Jülich Soft Matter Days, Heimbach, 18. - 20.10.00
23.30.0

Pyckhout-Hintzen W.
Untersuchungen mit Neutronen and Netzwerken und verzweigten Polymerschmelzen
Jülich Soft Matter Days, Heimbach, 18. - 20.10.00
23.30.0

Schwahn D.
Phase behavior in ternary polymer mixtures
Jülich Soft Matter Days, Heimbach, 18. - 20.10.00
23.30.0

Stellbrink J.
Kolloidale Aspekte von Sternsystemen
Jülich Soft Matter Days, Heimbach, 18. - 20.10.00
23.30.0

Willner L.
Mizellarisierung von Polymeren
Jülich Soft Matter Days, Heimbach, 18. - 20.10.00
23.30.0

Wischnewski A.; Richter D.; Monkenbusch M.; Willner L.; Farago B.1; Ehlers G.1; Schleger P.1
1Institute Laue Langevin, Grenoble/France
Dynamik in Polymerschmelzen - Grenzen des Reptationsmodells
Beiratssitzung, IFF, FZ-Jülich, 13.04.2000
23.30.0

Zorn R.
Glass dynamics in confinement
Jülich Soft Matter Days, Heimbach, 18. - 20.10.00
23.15.0

Institute of Electroceramic Materials

General Overview

Research Areas

The research areas of the institute comprise (1) technologies for the integration of electroceramic materials into microelectronics and nanoelectronics, (2) dielectric and ferroelectric properties of oxide ceramics, and (3) the defect structure in the vicinity of internal and external interfaces in oxides. These areas are complementary to the research areas of the Institute for Electronic Materials 2 (IWE 2) at the Aachen Technical University (RWTH). Project groups often comprise staff members and students from both institutes.

The HGF project "PICCOLO"

In 2000, the major event has been the approval of the HGF project *'Piccolo* – Scaling Effects in Integrated Electroceramic Materials' and the start of the project in July. This project is embedded in the information technology program PGI (Physikalische Grundlagen der Informationstechnologie) of the Research Center Jülich. Beyond the Institut für Elektrokeramische Materialien (1), the (2) Institut für Mikrostrukturforschung IMF headed by K. Urban, (3) the Theorie III, headed by H. Müller-Krumbhaar, and (4) the Ion Technology (IT) group at the Institut für Schichten und Grenzflächen headed by S. Mantl are involved. Several national and international universities and research centers participate in "Piccolo", too. The main focus of the proposal "Piccolo" is a fundamental as well as applied research on scaling effects of electroceramic materials. Today, typically polycrystalline films exhibit grain sizes much smaller than the feature sizes of the microelectronic devices. However, along with the sustaining trend towards further miniaturization, the decreasing feature sizes in microelectronic technology will approach the typical crystallite sizes of the perovskite-type oxide structures. Specific scaling effects are anticipated along this route, due to the long-range nature of the ferroelectric interaction of the oxides involved. The project aims at an (1) elucidation of the physical origin of these scaling effects, (2) an exploitation and extension of the limits to which the ferroelectric properties and high permittivities of the oxides involved can be used, and (3) the development of technological design rules for the integration of the perovskite-type oxides on a decreasing scale. It will combine production-type processes and research-type methods. The spectrum of designated results of the project comprises (semiquantitative) models for the superparaelectric limit of ferroelectric (FE) oxides, the dead layer at interfaces, the phase stability and segregation processes of perovskite films during annealing, the nucleation and growth of films by MOCVD, recipes for the deposition of single grain capacitors and ultrathin FE films as well as for reactive ion etching and a ferroelectric field-effect transistor (FE-FET) as a demonstrator. In summary the project "Piccolo" is an initiative to pursue research on the basic properties of electroceramic materials under scaling and the relevance of these effects for the integration of perovskite-type oxides into microelectronics.

Integration Technologies

Our main deposition method for oxide thin films is the MOCVD technique (MOCVD = Metal Organic Chemical Vapor Deposition). In cooperation with AIXTRON AG, a multiwafer planetary reactor has been installed for the development and optimization of $(Ba,Sr)TiO_3$ films (BST). Systematic parameter studies have been performed, and BST films are produced on platinized Si wafer which set new international standards in thickness and compositional uniformity on 6" wafers. Equipment for the electrical characterization of MOCVD processed BST films has been built and tested as part of an ESPRIT project (HECTOR 300). Our horizontal MOCVD research reactor has been tested by the deposition of new model systems, such as the $(Ba,Pb)TiO_3$ solid solution which allows the materials tuning in a broad range of tetragonal ferroelectric distortions. Thin films made by CSD (Chemical Solution Deposition) at the IWE 2 in Aachen were prepared to provide high-precision compositional standards for the XRF analysis of the MOCVD films for both, the multiwafer planetary reactor and the horizontal reactor. As a supplement, we use high pressure oxygen sputtering for the deposition of ultrathin PZT film within the Piccolo project. For the patterning of the ceramic films and electrode / ceramic film stacks, the Reactive Ion Beam Etching (RIBE) technique is employed. In contrast to the situation in the standard Si and compound semiconductor technologies, dry etching processes of oxide ceramics have hardly been investigated yet and therefore represent a research area in which basic studies and industrially funded applied research can be linked in a beneficial manner. The integration processes are complemented by metallization methods based on electron beam and sputter techniques. Within this area, our studies aim at a better understanding of the processes and material parameters which govern the adhesion, the mechanical stress, and the microstructure.

Dielectric and ferroelectric properties

The second research area focuses on the *dielectric and ferroelectric properties* of oxide thin films and bulk ceramics, which are being investigated in Jülich as well as in Aachen. The material systems are based on compositions used for practical devices and model systems, e.g. $SrTiO_3$, $BaTiO_3$, $SrBi_2Ta_2O_9$, $Pb(Zr,Ti)O_3$ and $(Ba_{1-x}Pb_x)TiO_3$. One of the research topics is the microscopic understanding of ferroelectric hysteresis including new approaches for the separation of *reversible* and *irreversible* contributions to polarisation based on the analysis of frequency-dependent small and large signals. These studies are linked to the *aging* (imprint) phenomenon, i.e. the polarisation-dependent shift of the hysteresis curve with time and to the ferroelectric *fatigue* process, i. e. the reduction of the remanent polarisation by cycling. Both aging and fatigue processes play an important role in the operation of the novel non-volatile memories (Ferroelectric Random Access Memories, FeRAM). Impedance spectroscopy in the lower GHz regime is employed to determine the relaxation of the ferroelectric *domain wall* motion and to separate this contribution from the contribution of the crystal lattice. By varying the microstructure of the ceramics and by comparison between bulk ceramics and thin films, the model of Arlt will be extended with respect to the impact on 2D constraints imposed by mechanical stress due to the presence of substrates. The investigations of the ferroelectric properties are now additionally focussed on the scaling properties and nano-size effects. For *dielectric* ceramics, impedance spectroscopy is used to elucidate the interrelation of *extrinsic* losses and lattice defects. This activity includes the development and characterization of new microwave ceramics and is embedded into a cooperation with Norbert Klein's group at the ISG (Institut für Schichten und Grenzflächen) within the framework of a BMBF-Leitprojekt. In the case of ferroelectric materials, existing theories are further developed and extended towards a more quantitative description of the dielectric, piezoelectric, and elastic properties. Numerical *finite-element-methods* are used to describe the mutually coupled mechanical, thermal, and electrical properties of ceramic components such as multilayer capacitors and actuators.

Lattice disorder in the vicinity of internal interfaces

Our third research area comprises the *lattice disorder in the vicinity of internal interfaces* (grain boundaries) and external interfaces (surfaces and electrode interfaces) and their impact on electronic and ionic (oxygen ions and protons) charge transport. In the case of acceptor and donor doped titanate ceramics, the studies are focused on the formation of space charge depletion layers at grain boundaries as well as the related potential barriers and the transport of charge carriers along and across the grain boundary barrier. A hot-pressing technology has been developed to decorate the grain boundary area with additional dopants and to study the influence of these artifical grain boundary states. In some material systems, such as titanate-zirconate solid solutions, it is necessary to determine the equilibrium constants of the defect reactions and the diffusion constants of the system in order to create the basis for the research on interfaces. In this respect, the comparison of bulk ceramics and thin films of the same composition is of vital interest. In thin film systems, the significant influence of the electrode metals, the unexpectedly high stability under conditions of dc-voltage-induced resistance degradation, as well as the tolerance of the lattice concerning the incorporation of non-stoichiometries represent current research topics. In semiconducting, donor-doped $SrTiO_3$, the emphasis is placed on the interrelationship between point defects and extended defects involved in oxidation and reduction processes using single crystals and ceramics.

Rainer Waser

Institute of Electroceramic Materials

Head: Prof. Dr.-Ing. Rainer Waser
Secretariat: Maria Garcia
Tel. (02461) 61 5811; Fax: (02461) 61 2550
e-mail: r.waser@fz-juelich.de/m.garcia@fz-juelich.de

Personnel 2000/2001 and areas of activity

SCIENTISTS:

Dr. R.R. Arons	Structure of magnetoresistive and ferroelectric oxides; charge transport in proton conductors	23.42.0
Dr. P. Ehrhart	MOCVD methods for electroceramic thin films; X-ray diffraction and optical spectroscopy	23.42.0
Dr. S.Hoffmann-Eifert	High-permittivity electroceramic thin films: MOCVD, dielectric properties, charge transport, defect chemistry	23.42.0
Dr. H. Kohlstedt	Reactive ion beam etching of ceramic and metallic materials, magnetic and ferroelectric tunnel junctions	23.42.0
Dr. W. Krasser	Optical excitation-processes in electroceramic materials;light-annealing processes	23.42.0
Dr. P. Meuffels	Processing of electroceramic materials; defect chemistry of electroceramic materials	23.42.0
Dr. Ch. Pithan	Processing of hot pressed nanocrystalline and grain boundary decorated bulk electroceramics	23.42.0
Prof. T. Schober	High temperature proton conduction, thermogravimetry, impedance spectroscopy, transmission electron microscopy	23.90.0
Dr. H. Schroeder	Technology and properties of (metal) electrodes for electroceramic thin films; mechanical properties and electromigration in thin films and interconnects	23.42.0
Dr. K. Szot	Study of surface layer of perovskite materials of ABO_3 structure	23.42.0
Prof. R. Waser	Electronic ceramics and integration of ceramic thin films	23.42.0

TECHNICAL ENGINEERS:

H. Bierfeld	Ceramic technology and sputtering techniques	23.42.0
U. Dedek	Electrical characterization of electronic ceramics; design of measuring setups	23.42.0
DI J. Friedrich	Thermogravimetric analysis; Transmission electron microscopy	23.42.0
DI H. Haselier	Metallization and thin film technology as well as clean-room technology	23.42.0
B. Hermanns	MOCVD, RIBE, sputtering of magnetic materials	23.42.0
DI H. John	Clean-room technology, microlithography and optical laboratory; LRP	23.42.0

Ph.D. STUDENTS

O. Baldus (TH Aachen)	Laser annealing of CSD, MOCVD electroceramic thin films	23.42.0
F. Fitsilis (TH Aachen)	Thin film capacitors for future DRAM applications using the MOCVD technology	23.42.0
R. Ganster (TH Aachen)	Heterostructures of Titanate thin films, MOCVD growth and numerical simulations	23.42.0
Ch. Ohly (TH Aachen)	Defect structures in doped titanate thin films: electrical and morphological properties	23.42.0
St. Regnery (TH Aachen)	MOCVD planetary reactor processes	23.42.0
J. Rickes (TH Aachen)	Reconfigurable multimedia processors based on ferroelectric RAM (FeRAM)	23.42.0

S. Ritter (TH Aachen)	MOCVD growth of ultrathin ferroelectric thin films and electrical characterization	23.42.0
J. Rodriguez (Uni Köln)	Ferroelectric capacitors with oxide electrodes and tunneling	23.42.0
S. Schmitz, (TH Aachen)	Influence of the contact metal on leakage current and dielectric permittivity of electroceramic thin film capacitors	23.42.0
R. Schmitz (Uni Köln)	Magnetic tunnel junctions, fabrication and experiments	23.42.0
St. Schneider (TH Aachen)	Reactive ion etching (RIE) and reactive ion beam etching (RIBE) of ceramic thin films.	23.42.0
P. Schäfer (TH Aachen)	Evaluation of novel MOCVD systems for the deposition of ferroelectric thin films	23.42.0
S. Stein (Uni Köln)	Spinjection devices	23.42.0

GRADUANTS:

S. Strapatsakis (TH Aachen)	Modification and optimization of an automatic probe station for the electrical characterization of electroceramic thin films	23.42.0

GUEST SCIENTISTS:

Dr. N. Pertsev A.F. Ioffe Institute St. Petersburg (Russia)	Theoretical calculations on the effects of strain and stress on the dielectric response of ferroelectric thin films grown on the sole substrates	23.42.0

Microstructural and electrical properties of electroceramic thin films deposited by MOCVD

F.Fitsilis[1], S.Regnery [1,2] , P. Ehrhart[1]

[1] *Institute of Electroceramic Materials*
[2] *AIXTRON AG, Aachen*

$(Ba_xSr_{1-x})TiO_3$, (BST), is one of the prime candidates as a high-k-dielectric in integrated high-density capacitors for future multi-GBit DRAM memory cells[1] as well as for dielectric tuneable devices and remarkable progress has been achieved in the metal-organic chemical vapor deposition (MOCVD) of thin BST films[2] on a laboratory scale. We report on the performance of a planetary multi-wafer reactor which offers, due to batch mode processing, a high throughput and a low cost of ownership as a production tool. Film growth is discussed within a wide parameter field and the finally achieved electrical properties, e.g., permittivity, loss tangent, leakage current, are discussed in relation to the microstructural properties.

F&E-Nr: 23.42.0

The electrical properties of BST thin films, which are necessary for the envisaged applications, depend critically on the stoichiometry, the microstructure, as well as on the films thickness. We deposited BST thin films on $Pt/TiO_2/SiO_2/Si$ wafers, and through process variations we systematically changed the film properties within this broad parameter field. For the present discussion we select films of a composition around $(Ba_{0.7}Sr_{0.3})TiO_3$ and slightly different Ti content i.e.: different Group-II/Ti ratios. We first discuss the thickness dependence of the film properties and concentrate then on films with a thickness of 30nm, which is close to envisaged application for DRAMS. We selected films which are slightly Ti rich to discuss the influence of the growth temperature (565°C to 655°C) on the microstructure and the electrical properties.

An AIXTRON 2600G3 Planetary Reactor® was used, which can handle five 6-inch wafers simultaneously. A liquid precursor delivery system, ATMI-300B, mixes the liquid precursors of three different sources: 0.35 molar solutions of $Ba(thd)_2$ and $Sr(thd)_2$ and a 0.4 molar solution of $Ti(O\text{-}iPr)_2(thd)_2$. The liquid mixture is delivered by a micro-pump to the vaporizer on top of the reactor. The gas inlet is in the center of the reactor providing a pure horizontal gas flow, which yields a radial flow system.

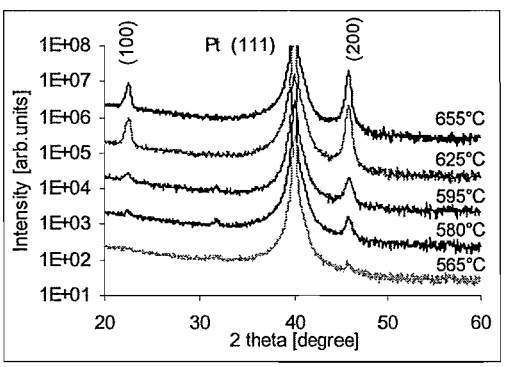

Fig.1: XRD-diagrams for films which were deposited at different temperatures and are slightly Ti-rich

The efficiency of the precursor use, defined as the ratio of the quantity deposited on all 5 wafers and the amount of the individual precursor elements contained in the consumed liquid, is an important parameter for the costs of ownership. The observed values of 45% for Ti and 35-40% for Ba and Sr are extraordinarily high as compared to the values reported for conventional showerhead reactors. Finally, due to the gas-foil rotation principle we obtained a good homogeneity of stoichiometry and film thickness over 6"

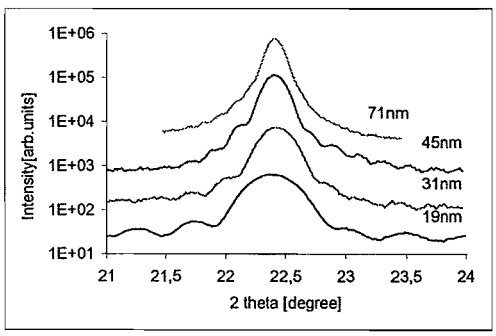

Fig.2: Thickness oscillations close to the (100) reflection of samples grown at 655°C

wafers[3]. These results are supported by recent ellipsometric data which yield as an example a thickness of 32,4 ± 0,4 nm and a variation in stoichiometry of 53,8 ± 0,3 at% Ti. Similarly small differences were observed between the five simultaneously processed wafers.

Fig.1 shows the XRD patterns of slightly Ti-rich films deposited at different temperatures on Pt-substrates with a strong (111)-texture. We observe a very strong (100)-texture for depositions above 595°C and a transition to more polycrystalline and finally poorly crystalline growth at lower temperatures. The (100)-oriented films observed at high deposition temperatures show a width of the rocking curves of only 2-3 degrees; as this width is similar to that of the underlying Pt[3], we observe locally a nearly epitaxial growth. These results indicate perfectly mono-crystalline structure documented by the details of the line profiles as shown in Fig.2: thickness fringes are clearly visible in high

resolution (100)-oriented grains and sharp interfaces. This conclusion is supported by HRTEM, Fig. 3, which directly demonstrates this (100)-orientation of the BST on (111)-Pt and the clean and sharp interfaces. For depositions at T ≥ 625°C, the dominant (100)-growth is stable over a rather wide range of stoichiometries (Gr-II/Ti = 0.92 to 1.03), and only if the films are far off stoichiometric composition there is a polycrystalline growth.

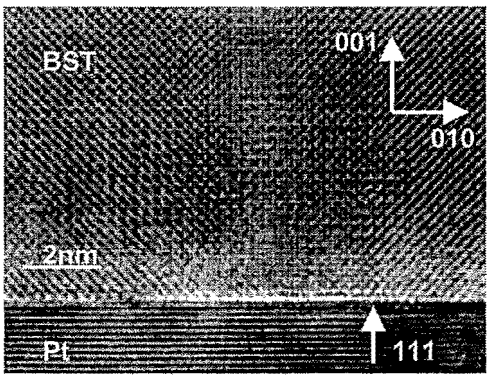

Fig.3: HRTEM micrograph showing the Pt-BST interface for a sample deposited at 655°C (C.L. Jia IFF/IMF)

The absolute value of the lattice parameter, as measured normal to the film plane, is, however, smaller than the expected bulk value. This difference results from a tensile stress of the film, which is thermally induced during cooling down of the film due to the different thermal expansion coefficients of BST and of the Si-substrate. The resulting tetragonal distortion of the film can be quantified by the c/a-ratio = (d+Δd)/d with values between 0.994 and 0.989. This c/a-ratio is opposite to the ferroelectric phase, which is characterized by a larger c-axis. The substrate induced lattice distortion yields therefore a plausible argument for

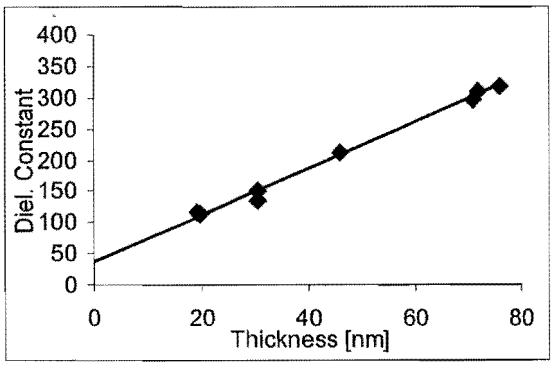

Fig.4: Thickness dependence of the dielectric constant for films grown at 655°C

the suppression of the ferroelectric phase transition in these thin films.

For the electrical characterisation Pt top electrodes were deposited by magnetron sputtering. An additional post-annealing was performed ex-situ. The standard characterisation included the dielectric permittivity, ε_r, measured at a frequency of 1 kHz and the dissipation loss, tanδ. More detailed investigations include the leakage current, the frequency dependence of the relative permittivity and the relaxation characteristics as well as the response to DRAM pulses.

Fig. 4 shows the permittivity for the crystallographic perfect samples shown in Fig. 2. We observe the expected increase with thickness, which has been discussed in terms of dead/or interface layer[1,3]. No obvious change of ε_r, close to the ideal stoichiometric ratio of Gr-II/Ti = 1 is observed in spite of a change in the lattice parameter which indicates a different incorporation of the surplus elements and the change in crystallinity and/or texture. There is, however, a dependence on the deposition temperature, i.e., a decrease of ε_r with decreasing temperature. In particular, we obtain a typical value of $\varepsilon_r \approx 208$ for Ti-rich films (GrII/Ti ≈ 0.97) grown at 625°C, which corresponds to a specific capacitance of C/A = 59.1 fF/μm². For a film at 565°C this value is reduced to $\varepsilon_r \approx 110$ or 30.2 fF/μm². The dissipation factor, tanδ, has values between 0,002-0,004 and shows no systematic variation within the investigated range of deposition parameters.

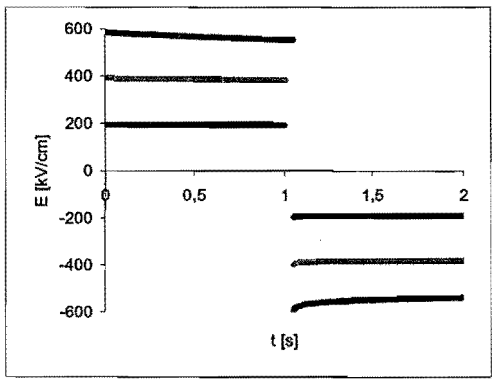

Fig.5: DRAM pulse test for a 30 nm thick sample

Fig. 5 shows the DRAM characteristics for a sample grown at 625 °C. After application of a 400 kV/cm (1.3 V) field we obtain 4% voltage drop in the first second after pulse load and these losses are independent of the direction of the applied field. Similar DRAM pulse measurements[8] on all samples showed less than 5% loss of charge in the first second after pulse load up to a field of 300 kV/cm; hence, these losses show no strong dependence on stoichiometry or details of the microstructure.

In summary, even films deposited at low temperature show electrical properties which are within the limits for DRAM specifications.

1. A.I. Kingon, S.K. Streiffer, C. Basceri, S.R. Summerfelt, *MRS Bulletin* **21**, 7, 46 (1996)
2. B.W. Wessels, *Annu. Rev. Mater. Sci.* **25**, 525 (1995) and references therein.
3. F. Fitsilis, S. Regnery, P. Ehrhart, R. Waser, F. Schienle, M. Schumacher, M. Dauelsberg, P. Strzyzewski, and H. Juergensen, accepted for publication in *J. European Cer. Soc.*

Electrical Conductivity and Segregation Effects of Doped $SrTiO_3$ Thin Films

Christian Ohly, Susanne Hoffmann-Eifert, Krzysztof Szot and Rainer Waser

Institute of Electroceramic Materials

The potential of perovskite type thin films for applications in electronic devices or oxygen sensors strongly relies on a detailed understanding of electrical properties. While the electrical conductivity of bulk $SrTiO_3$ is known in detail, the conductivity behavior of thin films (mainly as a function of oxygen partial pressure and temperature) is still unknown. The subject of this work, besides building a special measuring setup, is to examine the conduction characteristics of thin films. First results have shown an unexpected behavior accompanied by segregation effects, which lead to a certain restructuring of the film's morphology.

F&E-Nr: 23.42.0

$(Ba_{1-x}Sr_x)TiO_3$ is one of the most interesting material systems for memory devices in microelectronics as well as for oxygen sensoring applications due to its exceptional electrical properties [1][2]. Current research activities address the question, in how far these properties are changed with the ongoing miniaturization of the structures to nm-scale dimensions.

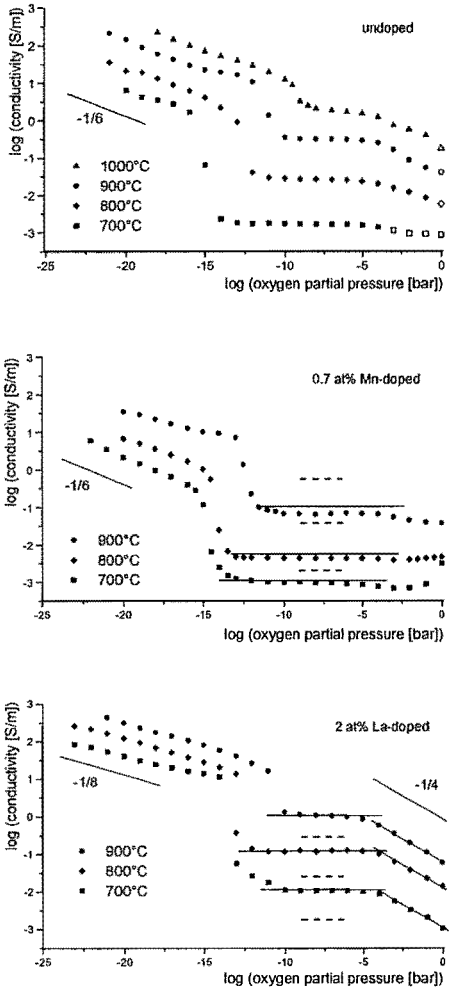

FIG. 1: Electrical conductivity vs. pO_2 of doped and undoped $SrTiO_3$ thin films. The thickness is about 500nm.

One of the far-reaching means to vary the electrical conductivity, of $SrTiO_3$ for example, is by changing the defect structure. This can be achieved by doping or by a controlled nonstoichiometry of the oxygen sublattice. The content of oxygen vacancies depends directly of the ambient oxygen partial pressure. Usually, the conduction behavior is described through defect chemical reactions and equilibrium considerations [3]-[5].

To determine the conductivity as a function of pO_2 and temperature, the common method of performing a 4-point dc-measurement under controlled atmospheric conditions was improved to fulfil specific demands by the highly resistive thin film samples. The measurement parameters range from 700°C to 1000°C in temperature and between 10^{-20} bar and 1 bar in oxygen partial pressure through the use of a solid state YSZ oxygen pump [6].

Thin film samples were grown on sapphire substrates by means of chemical solution deposition (CSD) to a final thickness of about 500nm. Doping was achieved by adding manganese (acceptor type) or lanthanum (donor doping) to the precursor solution [7]. XRD analysis of the films revealed a perovskite structure without second phases, an additional analysis by SEM showed a columnar morphology of the films (see FIG. 2).

The conduction behavior of bulk single crystal $SrTiO_3$ versus the oxygen ambient was widely investigated in the past [3]-[5]. If $\log(\sigma)$ is plotted vs. $\log(pO_2)$, a characteristic slope of (–¼) under reducing conditions is found. After passing an intrinsic minimum in mid-range pO_2, σ increases towards higher partial pressures and oxidizing conditions with a characteristic slope of now (+¼).

In contrast to this, the characteristics of $SrTiO_3$ thin films are quite different. FIG. 1a) shows the behavior of an undoped $SrTiO_3$ thin film of 500nm thickness. Under reducing ambients, a somewhat smaller slope can be seen. This is followed by a sharp drop to a plateau region of constant conductivity values. However, this region is broader at the lower temperatures than at higher, where the drop shifts towards higher pO_2. For all temperature levels this plateau region ends at about 10^{-5} bar, after where the conductivity decreases again. Open symbols mark values, where the conductivity is affected by leakage currents. In FIG 1 b) and c) the respectively influence of acceptor (0.7 at% Mn) and donor doping (2 at% La) is shown. As expected for bulk material, the acceptor doping results in decreased values, whereas donor doping gives a higher overall conductivity. While the donor doped sample

exhibits a clear (–¼)-slope at oxidizing atmospheres, the behavior of the manganese doped sample shows a changing behavior with increasing temperature.
The occurrence of a drop and a plateau region, which are common to all thin film samples, are fundamentally different to bulk material and are therefore attributed to a special thin film characteristic.

Regarding the dimensions of the films, additional examinations of the film's morphology were suggested by recent investigations of the chemical and structural stability of $SrTiO_3$ single crystal surfaces [8]-[10].
FIG. 2 shows the morphology of a $SrTiO_3$ film after deposition.

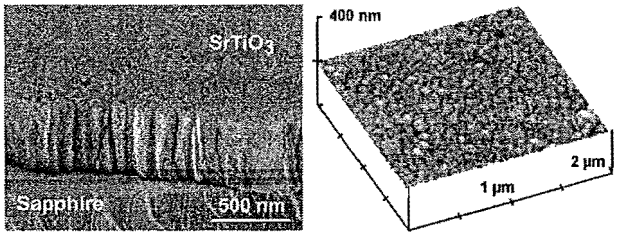

FIG. 2: $SrTiO_3$ thin film as deposited: SEM micrograph of the cross section (left) and topographical analysis of the surface by AFM (right).

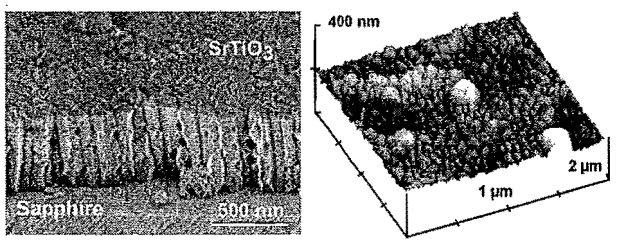

FIG. 3: $SrTiO_3$ thin film after measurements: SEM micrograph of the cross section (left) and AFM analysis of the surface (right).

After a set of measurement cycles at different temperatures from 700°C to 1000°C, the film's morphology looks considerably different (Fig. 3). The SEM picture reveals a noticeable increasing porosity along grain boundaries and, via AFM, a visibly higher roughness (approximately 10 times) caused by mass transport can be seen.
Because this can indicate the formation of second phases with a different conduction behavior and/or shifted values, it is necessary to find out when these segregation effects become critical to the measurements. The aim is to assign the morphological changes with particular measurement parameters like the electrical field or a certain oxygen partial pressure. This was studied through an annealing series, where samples of the undoped $SrTiO_3$ thin film were annealed at 900°C for several hours under selected oxygen partial pressures between 10^{-20} and 1 bar. But up to now, the parameters for the activation of the segregation effects are not sufficiently clarified.
Nevertheless, the observed morphological changes demonstrate a strong correlation between the conduction mechanisms and the defect structure depending on the ambient oxygen partial pressure and by this a rather complex interaction between the morphology, the defect structure and the conduction mechanisms.

Regarding the dimensions of the films, the point defect chemistry does not seem to be the appropriate model for explanation.
To get a deeper understanding of the different effects in play, a clear separation of intrinsic conduction mechanisms and extrinsically induced segregation effects must be accomplished first. Therefore, the morphological phenomena have to be elucidated with respect to its chemical nature and the influence on the conductivity behavior. In parallel, the different regimes of the conductivity curves will be investigated in more detail. In this context, an identification of the charge carrier types and the real defect structure (point defects, extended defects or a combination of both) will be addressed.

1. Kotecki, D. et al., *IBM Journal of Research & Development*, 1999, **43**, 367-82.
2. York, R. A., Nagra, A. S., Speck, J. S., Auciello, O. H. & Streiffer, S. K., to be published in *Integr. Ferroelectrics*, (ISIF 2000).
3. Waser, R. & Smyth, D. M., Gordon Breach, 1996, **47**.
4. Moos, R. & Härdtl, K. H., *J. Am. Ceram. Soc.*, 1997, **80**, 2549-62.
5. N. H. Chan, R. K. Sharma, D. M. Smyth, Nonstoichiometry in $SrTiO_3$. *J. Electrochem. Soc.*, 1981, **128**, 1762-9.
6. Ohly, C., Hoffmann, S., Szot, K. & Waser, R, to be published in *Integr. Ferroelectrics*, (ISIF 2000).
7. Hofman, W., Hoffmann, S. & Waser, R., *Thin Solid Films*, 1997, **305**, 66ff.
8. Szot, K., Speier, W., Herion, J. & Freiburg, C., *Appl. Phys. A*, 1997, **64**, 55-9.
9. Szot, K. & Speier, W., *Phys. Rev. B*, 1999, **60**, 5909-26.
10. Szot, K., Speier, W., Breuer, U., Meyer, R., Szade, J. & Waser, R., *Surf. Sci.* 2000, **460**, 112-28.

Dry Etching Characteristics of Noble Metal Electrode

St.Schneider and H. Kohlstedt

Institute of Electroceramic Materials

A reactive etch process to pattern noble metal electrodes is considered necessary for future generations of Dynamic Random Access Memories (DRAMs) integration and desirable for ferroelectric memory (FRAMs) applications. Conventional, sputter driven etch processes either yield in redeposition problems (fences) or in a severe sloping (CD loss) and are not acceptable for high density integration architectures. To systematically investigate possible reactive etch process regions, characterized by volatile etch products, we used a reactive ion beam etching (RIBE) tool with a filament free ICP source, that gives us exact control over the beam energy and the current density, and allows to use reactive gases. An energy dispersive quadrupole mass spectrometer is fitted to the chamber for in situ monitoring.

F&E-Nr: 23.42.0

The objective of this work, is to develop a process to pattern noble metal electrodes (e.g. Platinum and Iridium) in a effective and efficient way. A potential process has to met the well known stringent requirements like steep slope of the side wall, minimal change in the feature size, no fences, and no residues on the wafer. Yield considerations from manufacturing impose totally different requirements like high mean time between clean (MTBC) to be able to cut down production costs.

Conventional low temperature processes only work in the sputter driven etch regime. Due to the lack of a chemical etch rate one either ends up with quite steep side walls, to the cost of redeposition on the mask material (fences), or with fence free structures with very poor control over the feature size and an unacceptable slope [2-5]. Furthermore sputter etching offers only a very limited selectivity as well to the mask and as the substrate. Beside those disadvantages a sputter process results in a coating of the inside of the etch chamber leading to particle problems as well as plasma instabilities, which require often wet cleans of the tool.

To understand the high temperature etch process of Platinum we systematically investigated different etch regimes and plasma chemistries. In order to separate the plasma physic from the surface chemistry, we choose a Reactive Ion Beam Etching (RIBE) tool, instead of a conventional plasma reactor.

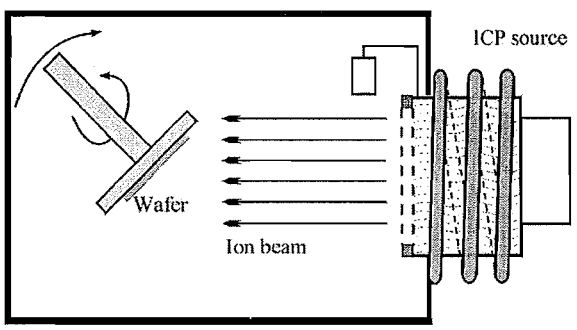

Fig. 1 Schematic drawing of the Reactive Ion Beam Etching (RIBE) chamber

The main advantage of ion beam etching tools is the precise control over the beam energy as well as the beam current density in contrast to plasma reactors, where those plasma parameters are a result of the energy input from the generators and have to be measured for each process.

Our Ionfab 300^{plus} from Oxford Plasma Technology is able to handle 6" as well as 4" wafers. The beam source is designed filament free with an inductively coupled plasma (ICP) source powered with a 13,56 MHz generator. This enables us to feed reactive gases like flourine, chlorine, or bromine containing chemistries directly into the source region.

The beam extraction takes place through a set of two grids (acceleration and screen grid) which accelerate and focus the beam. A filamentless beam neutralizer (FBN) mounted on top of the discharge chamber takes care of the charge neutrality of the beam to etch insulating specimen as well. The process region extending to a beam energy up to 1000 eV and beam currents up to 300 mA is comparable to industrial plasma reactors.

The wafer is clamped to a temperature controlled electrode with Helium- backside cooling to ensure thermal coupling. In the low temperature regime (-15°C up to 80°C) a dedicated chiller control the electrode temperature while in the high temperature regime (50° up to 300°C) a resistant heating system takes over. The wafer can be rotated during the process as well as tilted towards the beam. For the system configuration is shown in Fig. 1.

A further advantage of ion beam etching tools is the large dimension of the process chamber, which ease the use of probes without interfering with the beam and potentially tampering the process.

To study the process mechanisms an energy dispersive quadrupole mass spectrometer (Hiden EPQ) is attached to the chamber. The mass regime of the probe extents from 0 amu up to 500 amu with a resolution below 1 amu. The energy range goes from 0 to ± 1000 eV with a resolution below 1 eV.

The energy dependence of the platinum etch rate was investigated to get a baseline for the sputter etch regime, as well as to confirm compatibility of the ion source process regime with conventional plasma reactors. As can be seen in Fig. 2, the etch shows the expected behavior and starts at a threshold energy (about 30 V), increases linear with increasing energy and drops off slightly to a parabolic dependence at higher energies and beam currents larger as 100 mA. For the ion density dependence a very similar behavior is found. The etch rate increases linear with increasing beam current in the range from 75 mA to 250 mA.

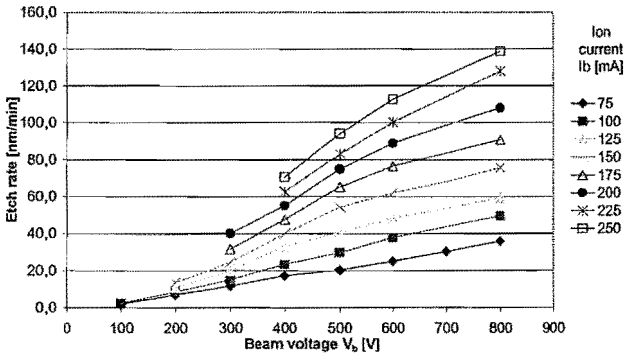

Fig. 2 Ion energy dependence for a Chlorine low temperature process

A possible solution to increase the volatility of the etch products is to increase the etch temperature in conjunction with the use of reactive gases. The vapor pressure of, e.g. Platinumtetrachloride is at room temperature about the typical lower limit of a process pressure of 1 mTorr and reaches for elevated temperature, e.g. 600 K about 700 mTorr.
Experimental data confirm the platinum etch rate with pure chlorine processes to start to increase significantly above 200-250 °C wafer temperature. The dependence of the etch rate with temperature follows a exponential function, which is a clear sign the etch mechanism being of chemical nature.

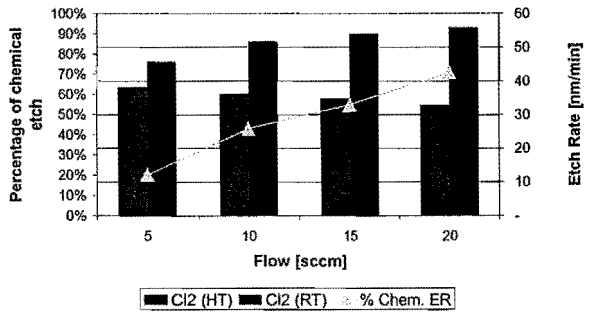

Fig. 3 Etch rate dependence on total flow for a Chlorine process at low and high temperatures, respectively

The total flow is one important parameter to tailor the etch behavior. As can be seen in Fig. 3, the dependence of the etch rate is opposite for low and for high temperatures with increasing flow. In the low (room temperature) region the platinum etch rate decreases with increasing flow, while in the high temperature region (300°C), the etch rate increases with increasing flow. From the mass spectrum sown in Fig. 4, we can learn, that for higher gas flows the dissociation yields more Cl^+ ions. At low temperature, the platinum etch process is a pure sputter process, thus with an increasing Cl^+ the concentration of Cl_2^+ concentration decreases and the average mass decreases, too. A decreasing mass results in turn in a drop of the sputter rate. In the high temperature region, on the other hand it is favorable to have a complete dissociation of the chlorine in the plasma, to offer Cl^+ ions to the platinum surface, which react to volatile $PtCl_4$.
As is true for the pure sputter etch regime at low temperatures, also the high temperature etch regime requires a threshold energy to be passed - as platinum is not etched spontaneously- before significant etch takes place. If the beam energy on the other hand is increased too much, the remaining sputter component prevails over the chemical component. The total etch rate still increases, but the fraction of the chemical etch rate decreases, rendering this regime not useful for a successful process.

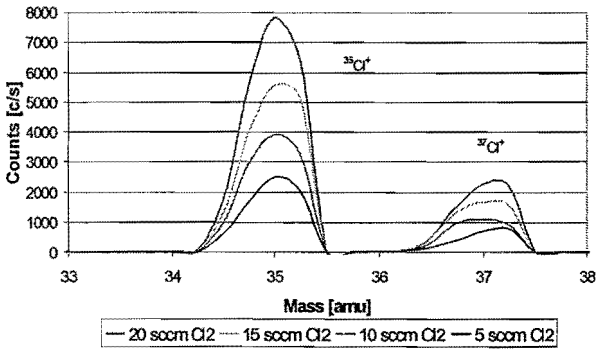

Fig. 4 Mass spectrum of a chlorine process for different gas flows

Photoresist masks are unstable at temperatures higher as 100 °C. The most common hardmask used for high temperature application would be a silicon oxide based material. To preserve the mask integrity during the etch is important to control the feature size. A pure chlorine process would be to aggressive. The addition of oxygen to the plasma chemistry helps to decrease the SiO_2 etch rate.
In summary, a high temperature etch of platinum is feasible. The dissociation of chlorine in the plasma controls the chemical character of the etch. Additives, like oxygen, allow to control the reactivity and the selectivity, especially to keep the mask integrity.

S. Yokoyama, et al., *Jpn. J. Apl. Phys.* Vol 34 (1995) pp.767-770
K.R. Milkove, C.X. Wang, *J. Vac. Sci. Technol.*, **A 15**, 596 (1997)
K.R. Milkove, J.A. Coffin, C.Dzionkowski, *J. Vac. Sci. Technol.*, **A 16**, 1483 (1998)
H. Kim, et a., *J. Vac. Sci. Technol.*, **A 17**, 2151 (1999)
K. Kwon, et al., *J. of the Electrochem. Society*, **147** (5) 1807-9 (2000)

A new probe station for electrical characterization of thin film insulators

S. Schmitz and H. Schroeder

Institute of Electroceramic Materials

Mixed oxide thin film insulators are promising candidates to replace SiO_2/SiN_x in future ultra-low-scale integrated Gbit-DRAM chips, e.g. as dielectric in capacitors of memory cells and as gate oxide in MOSFETs. Although some materials, e.g. $(Ba_xSr_{1-x})TiO_3$ (BST), have properties suitable for these applications, the underlying mechanisms of these properties are often less well understood. We report on a new "probe station", an apparatus specialized for the electrical characterization of metallized thin oxide films with the ability of a wide variation of external parameters and of measurements with high resolution necessary for mechanistic studies. First results on leakage currents are compared to published data and the need for additional experimental and theoretical work is demonstrated by the attempt to fit these data to commonly applied models.

F&E-Nr: 23.42.0

Thin film insulators such as mixed oxides with perowskite-type crystal structure gain more and more interest in the fast-growing information technology industry because of their unique electrical properties: Very high permitivity, ferroelectricity, piezoelectricity. They are or will be used e.g. in micro-electro-mechanical (MEM) devices or as components in ultra-large-scale integrated (ULSI) silicon-based chips such as Gbit dynamical random access memories (DRAMs), ferroelectric memories (FeRAMs) presently used in smart-cards or future field-effect transistors with ferroelectric gate oxide (FeFET).

Although some oxides, e.g. $(Ba,Sr)TiO_3$ or $Pb(Zr,Ti)O_3$, are already suitable for the above mentioned applications the underlying mechanisms for their superior properties are not fully understood which calls for mechanistic studies on these material systems. We therefore have designed and built a new apparatus to investigate the electrical properties of metallized thin oxide films with controlled and wide variation of many external parameters. On the other, hand it can also be used for service measurements of commercial wafers up to 8" diameter.

The new probe station is shown in Fig. 1. It consists of an oven plate as sample holder and several arms with needles for electrical contact (see Fig. 2) completely set up in a vacuum chamber, which is placed on a vibration isolated table.

The main features of this apparatus are:

Fully automated system including positioning of sample (x,y-direction) and contact arms (z-direction), temperature control, measurement sequence and data collection.

A silver plate oven with heating and cooling giving a wide temperature range (-100 to 500°C) also under oxidizing atmosphere.

Low friction bearing of contact arm and electromagnetic load control of the contact needles in order not to damage the thin films (metal-oxide interface or the oxide film itself).

Parallel measurements with up to ten contact arms.

Triaxial cable to the contact needle to minimize electromagnetic noise in order to measure very small signals (e.g. 3 10^{-14} A in current).

Environmental control (vacuum, gases).

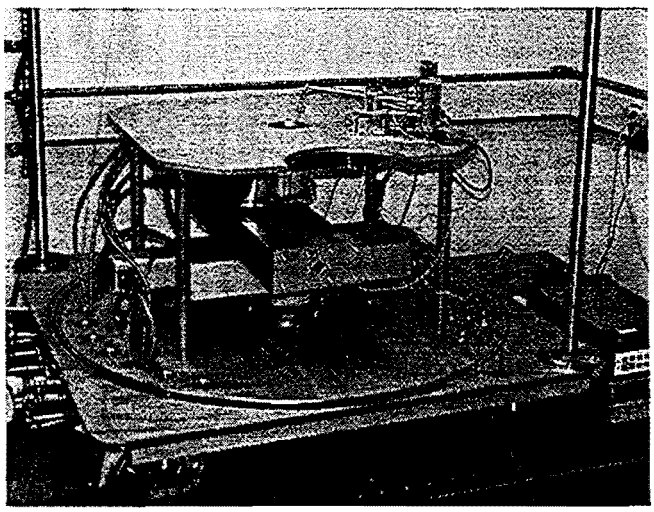

Fig. 1: New probe station (dome of vacuum vessel has been removed).

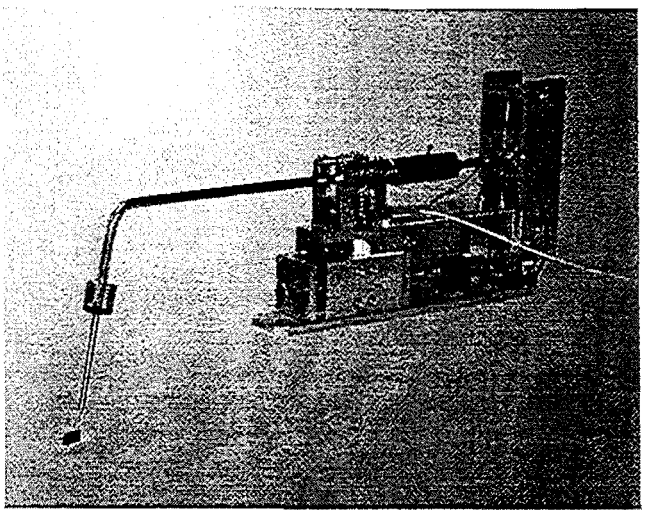

Fig. 2: Contact arm with load control and low friction bearing

As first experiments the leakage currents of 150nm thick $SrTiO_3$ (STO) films with Pt electrodes were measured. The samples were grown by chemical solution deposition (CSD) and crystallized at 750°C for 30' in oxygen leading to columnar grains with mean diameter of about the film thickness. The grains have a strong <111>-fiber texture.

The results of leakage current densities are plotted in Figs. 3 and 4, vs. temperature and applied field, respectively, together with published data [1-4] of differently grown STO and $(Ba,Sr)TiO_3$ (BST) samples which are representative for the Pt/(STO/BST)/Pt capacitor system.

From the Arrhenius plot in Fig. 3 two distinct temperature regimes can be extracted from our data (■): At temperatures T>400K a large slope, i.e. a large effective activation energy (Φ_{eff}=1.34eV), for T<400K a very low Φ_{eff} The other data have been collected mainly in the high temperature regime at very different fields with different thicknesses of the samples. For the thicker CSD-samples Φ_{eff} is 1.16eV and 1.34eV, while the thinner samples show much smaller values, 0.59eV and 0.75eV, respectively.

The interface between Pt (workfunction Ψ_{Pt}=5.3 to 5.6eV) and n-conducting STO/BST (workfunction $\Psi_{STO/BST}$ <5.3eV) will form a Schottky-contact with a barrier height of about 1.3 ± 0.2eV (the affinity of STO/BST is about 4eV) [5]. Therefore most authors (as the referenced ones did) model their data with the well-known Schottky effect (field-assisted thermionic emission), i.e. electrode limited currents, and the measured currents are the maximum currents the electrode can inject into the oxide by this mechanism. Assuming a constant (i.e. the applied) field in the specimens one can calculate the zero field Schottky-barrier height Φ_0.

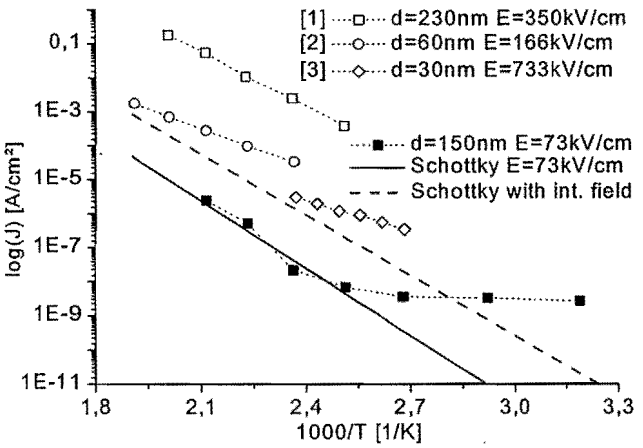

Fig. 3: Temperature dependence of leakage currents. Results of fitting: (■ HT: Φ_{eff}=1.34eV, Φ_0=1.39eV); (■ LT: Φ_{eff}=0.05eV, Φ_0=0.01eV); (: Φ_{eff}=1.06eV, Φ_0=1.16eV); (○: Φ_{eff}=0.75eV, Φ_0=0.82eV); (◊: Φ_{eff}=0.59eV, Φ_0=0.74eV);(Redrawn from [1-3])

Except at very high fields the increase to Φ_0 is beyond the uncertainties of Φ_{eff}, if the correct dynamic dielectric constant $\varepsilon_r \approx 5$ is used. To get into the range of $\Phi_0 \geq 1.1$eV (as suggested by the theoretical values) for the 30 and 60nm thick samples, internal fields at the injecting electrode of 4MV/cm and 9MV/cm, respectively, have to be present. They would lead to much higher absolute currents than the measured ones. An example for the effect of an internal field at the electrode (1MV/cm) is given in Fig. 3 for the Schottky-effect with same parameters as the fit of our HT-data. Such internal fields may be created by space charges at very high defect concentrations, e.g oxygen vacancies.

The other possible injection mechanism, tunneling through the Schottky-barrier (e.g. Fowler-Northeim) results in much lower currents using the same parameters.

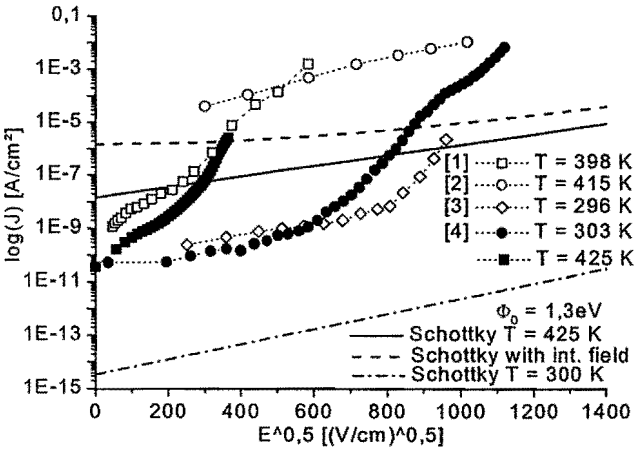

Fig. 4: Field dependence of leakage currents. (Results redrawn from [1-4])

The interpretation of the field dependence of the measured currents with simple models is even worse. In Fig. 4 measured data sets by the same authors and an additional data set of MOCVD–BST samples (30nm thick) grown in our institute are shown in the common "Schottky-plot". The large differences between the MOCVD-samples and the others are partly due to the different temperatures. Compared to the simulated "Schottky"-plots with Φ_0=1.3eV (at 300K and 425K, at 425K with int. field 1MV/cm) neither the field dependence nor the absolute values can be fitted. In contrast most of the data are larger than the Schottky-limit. The use of the evaluated barrier heights Φ_0 would also not result in a quantitative description. Fitting of the slopes would lead to unphysical values of ε_r much smaller than 1!

As before the limiting currents can be enlarged only by very high internal fields (as shown in Fig. 4), but the field dependence would much smaller than that of the data, so that electrode limited currents do not apply. Once more currents by tunneling are even lower.

A possible improvement for the field dependence may be the introduction of low-ε_r interface layers ("dead" layers or reaction layers), which would increase the applied field at the interface by some factor, or of high concentrations of mobile ionic defects which accumulate at the electrodes in dependence on internal and external fields.

In conclusion: The carrier injection into thin oxide films is still an open question (as the conduction through the insulator) which calls for mechanistic experimental and theoretical research.

[1] G.W. Dietz et al. *J. Applied Physics* **82**, 2359 (1997)
[2] S. Zafar et al., *Applied Physics Letters* **73**, 3533 (1998)
[3] J.D. Baniecki et al., *J. European Cer. Soc.* **19**, 1457 (1999)
[4] F. Fitsilis, S. Regnery, P. Ehrhart, privat communication
[5] e.g.: J.F. Scott et al., *Ferroelectrics* **225**, 83 (1999)

High temperature proton conductors for the injection of hydrogen into gases and vacua

T. Schober[1], P. Meuffels[1], J. Friedrich[1], H. Ringel[2], T. Schwickert[2]
[1]*Institute of Electroceramic Materials*
[2]*Central Department of Technology*

Abstract – High temperature proton conductors are very useful for the p_{O2} –control of inert gases such as Ar and for the controlled injection of hydrogen into a vacuum.

F&E-Nr: 23.55.0

Perovskite-type cerates and zirconates of the form ABO_3 (A=Ba, Sr; B=Ce, Zr) may dissolve significant amounts of water when doped with trivalent elements such as Y or Yb. Because the protons are mobile these systems become good proton conductors at elevated temperatures (high temperature proton conductors, HTPCs). When tubes are fabricated from these proton conductors and when electrodes are applied to these inside and outside a variety of electrochemical experiments become possible two of which are listed below.

P_{O2}-control of inert gases

Let us assume that Ar flows though a tube of the proton conductor $BaZr_{0.9}Y_{0.1}O_{2.95}$ held at 700 °C and that the outside atmosphere contains hydrogen, either in the form of water or in the form of dilute hydrogen. Behind the tube the effective p_{O2} is measured with a λ-type sensor. Without applying a voltage to the electrodes of the tube a background p_{O2} of roughly 5×10^{-5} mbar is measured which corresponds to the gas purity and outgassing effects. If, however, a negative potential of a few hundred mV is applied to the inner electrode the positive protonic charge carriers are attracted to it and eventually recombine at this cathode to molecular H_2. The latter reacts with the residual oxygen and forms water vapor. This effect leads to a decrease of the p_{O2}. Fig. 1 shows the dependence of this p_{O2} with applied negative potential. Even below the dissociation potential of water (~1.1 V) a gradual decrease of the oxygen level is noted until the 10^{-6} mbar level is reached. Further increase of U leads to a precipitous drop of the p_{O2} down to about 10^{-21} mbar. It is seen that adding small amounts of hydrogen to an inert gas using a HTPC allows to adjust the p_{O2} within wide limits. A further refinement of the technique consists in irreversibly trapping or gettering the generated water vapor *behind* the HTPC tube either with a cold trap or a zeolite trap. This lowers the attainable p_{O2}'s even further.

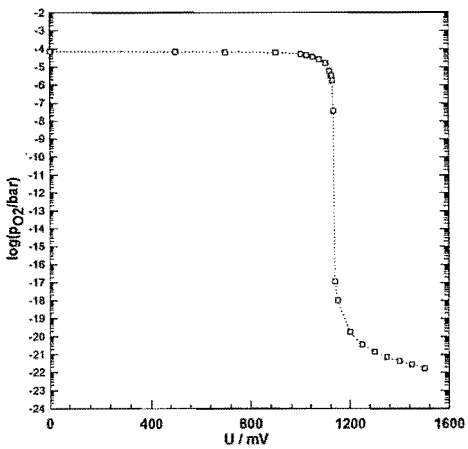

Fig. 1. Gas titration curve using a $BaZr_{0.9}Y_{0.1}O_{2.95}$ tube. Outside: moist air. The residual oxygen is increasingly consumed by the hydrogen introduced. Below the 10^{-7} mbar level we effectively deal with a moist hydrogen- argon mixture.

Injection of hydrogen into a vacuum

The classical techniques of introducing hydrogen into a vacuum are a) the use of mechanical leak valves, b) Pd-Ag permeation tubes, and c) thermal decomposition of unstable hydrides such as UH_3. Here, we present a novel electrochemical technique using a HTPC. As Fig. 2 shows a HTPC tube is interfaced to a support tube using glass solder which in turn leads to the vacuum system. The whole arrangement has a leak rate < 10^{-8} mbar l/s. As before, electrodes are applied to the inside and outside of the HTPC tube which is held at around 700 °C. The HTPC tube outside is flushed with a hydrogen containing gas.

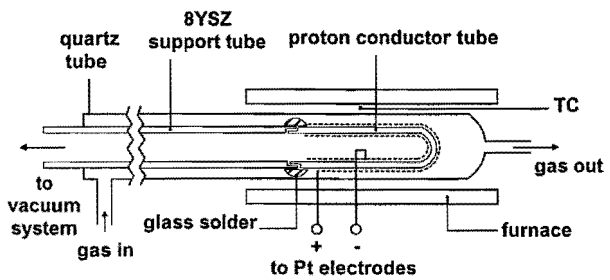

Fig. 2. Hydrogen vacuum leak valve using a HTPC. Applying negative potentials to the tube inside drives protons to the vacuum side. Recombination leads to H_2 molecules.

Fig. 3 shows the linear increase of the partial pressure of

hydrogen as measured with a mass spectrometer with current J. As predicted by Faraday's law the number of moles of hydrogen injected into the vacuum per second is given by:

$$n_{H2} = J/2F$$

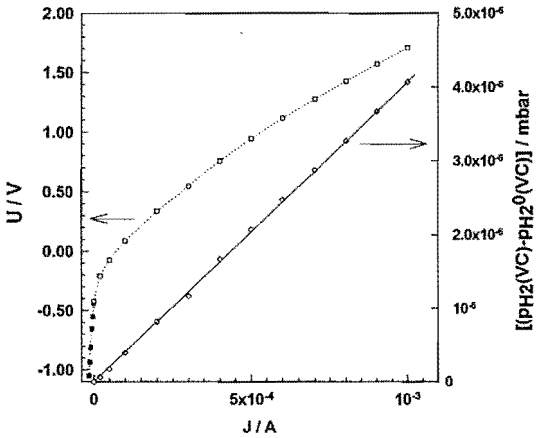

Fig. 3. Injection of hydrogen into a vacuum - details in text. Here, a tube of $CaZr_{0.9}In_{0.1}O_{3-x}$ is used.

Also depicted in Fig. 3 is the voltage U imposed by the galvanostat. As shown in Ref. (2) there is a balance of 3 voltages at the electrochemical cell as described by:

$$J_{H^+} < R_{H^+} > = U - \frac{RT}{2F} \ln \frac{p_{H_2}(L)}{p_{H_2}(0)}$$

The left hand term is the ohmic voltage drop in the electrolyte, the first term right hand side is the applied voltage, and the second the Nernst voltage at the cell due to the difference in hydrogen chemical potential on either side of the cell.

Fig. 4 proves that only hydrogen is generated at the cathode. It shows the mass spectrum of the vacuum system *with* a small proton current flowing. Before the application of a voltage –not shown due to space limitations - the background H_2^+-peak had the size of the CO^+ peak. With the applied potential the H_2^+-peak has increased roughly tenfold while all the other peaks have remained unchanged. Further increase of the pumping current brings the partial pressure of hydrogen easily into the 10^{-5} to 10^{-4} mbar range.

The following HTPC compositions were successfully tested for injecting hydogen into vacuum systems in the present work:

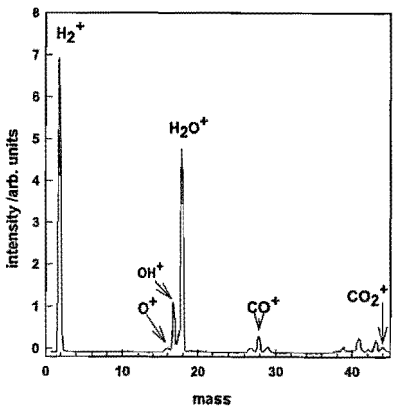

Fig. 4. Mass spectrum with applied voltage at the HTPC showing a drastically increased H_2^+ level compared to the state without voltage.

1. $BaZr_{0.9}Y_{0.1}O_{2.95}$
2. $CaZr_{0.9}In_{0.1}O_{3-x}$
3. $BaCa_{0.393}Nb_{0.606}O_{2.91}$

For high drain applications we favor composition 1.

Composition 2 is more suited for potentiometric work but will also hold for low to medium drain applications.

References

1. T. Schober, Solid State Ionics, (in press)
2. T. Schober, P. Meuffels, J. Amer. Ceramic Soc.(in press)
3. T. Schober, P. Meuffels, J.Vac.Sc. &Techn. (in press)
4. H. G. Bohn, T. Schober, J. Am. Ceram. Soc. 83 (2000) 768
5. T. Schober, H. G. Bohn, Solid State Ionics 127 (2000) 351
6. H.G. Bohn, T. Schober, T. Mono, W. Schilling, Solid State Ionics 117 (1999) 219
7. T. Schober, H. G. Bohn, T. Mono, W. Schilling, Solid State Ionics 118 (1999) 173
8. T. Schober, J. Friedrich, Solid State Ionics 125 (1999) 319
9. T. Schober, K. Szot, M. Barton, B. Kessler, U. Breuer, H.J. Penkalla, W. Speier, J. Solid State Chemistry 149 (2000) 262

Publications in refereed journals

Allen C.W.; Schroeder H.; Hiller J.M.
In situ study of dislocation behaviour in columnar Al thin films on Si-substrate during thermal cycling
Materials Research Society (MRS) Symposium Proceedings 594, 123 (2000)
23.42.0

Andoh H.; Harnach O.; Darula M.; Beuven St.; Kohlstedt H.
Superconductivity and its applications: Dynamics of order parameter and microwave emission for a YBa2Cu3O7-delta bicrystal junction
Physica C 339/4, 237 (2000)
23.42.0

Franken K.; Maier H.; Prume K.; Waser R.
Finite-Element Analysis of Ceramic Multilayer Capacitors: Failure Probability Caused by Wave Soldering and Bending Loads
J. Am. Cer. Soc., 83 (6), 1433-40 (2000)
23.42.0

Grossmann M.1; Bolten D.1; Lohse O.1; Böttger U.1; Waser R.
1 Institut für Werkstoffe der Elektrotechnik, RWTH Aachen
Correlation between switching and fatigue in PbZr0.3Ti0.7O3 thin films
Applied Physics Letters, Vol. 77, No. 12, 1894-1896
23.42.0

Grossmann M.1; Lohse O.1; Bolten D.1; Boettger U.1; Waser R.
1 Institut für Werkstoffe der Elektrotechnik, RWTH Aachen
Lifetime estimation due to imprint failure in ferroelectric SrBi2 Ta2O9 thin films
Applied Physics Letters, Vol. 76, No.3, 363-365.(2000)
23.42.0

Harnack O.; Darula M.; Beuven St.; Kohlstedt H.
Noise and conversion properties of Y-Ba-Cu-O Josephson mixers at operating temperatures above 20 K
Appl. Phys. Lett. 76, 1764 (2000)
23.42.0

Hwang S.C.; Waser R.
Study of Electrical and Mechanical Contribution to Switching in Ferroelectric/Ferroelastic Polycrystals
Acta mater. 48, 3271-3282 (2000)
23.42.0

Liedtke R.1; Grossmann M.1; Waser R.
1 Institut für Werkstoffe der Elektrotechnik, RWTH Aachen
Capacitance and admittance spectroscopy analysis of hydrogen-degraded Pt/(Ba,Sr)TiO/Pt thin-film capacitors,
Appl. Physics Letters, Vol. 77, No. 13, 2045-2047
23.42.0

Liedtke R.1; Hoffmann S.; Waser R.
1 Institut für Werkstoffe der Elektrotechnik, RWTH Aachen
Recrystallization of Oxygen Ion Implanted Ba0,7Sr0,3TiO3 Thin Films
Journal of the American Ceramic Society, 83, (2), 436-438 (2000)
23.42.0

Liedtke R.; Hoffmann S.; Waser R.
Recrystallization of Oxygen Ion Implanted Ba0.7Sr0.3TiO3 Thin Films
J. Am. Ceram. Soc. 83, 436-438 (2000)
23.42.0

Nielen H.; Goebel H.; Eppler I.; Schroeder H.; Schilling W.
Stress and plasticity in passivated interconnect lines
Proc. Of 5th Int. Workshop on "Stress-induced Phenomena in Metallization", Stuttgart (Germany), AIP Conf. Proc. 491, 277 (1999)
23.42.0

Nordlund K.; Partyka P.; Averback R.S.; Robinson L.K.; Ehrhart P.
Atomistic simulation of diffuse x-ray scattering from defects in solids
J. Appl. Phys. 88 (2000) 2278-2288
23.42.0

Pertsev N.A.; Koukhar V.G.; Waser R.; Hoffmann S.
Curie Weiss-type law for strain and stress effects on the dielectric response of ferroelectric thin films
Appl. Phys. Lett. 77, 2596-2598 (2000)
23.42.0

Petzelt J.; Ostapchuk T.; Kamba S.; Rychetsky I.; Savinov M.; Volkov A.; Gorshunov B.; Pronin A.; Hoffmann S.; Waser R.; Lindner J.
High-Frequency Dielectric Response of SrTiO3 Crystals, Ceramics and thin Films
Ferroelectrics 239, 117 (2000)
23.42.0

Petzelt J.; Ostapchuk T.; Kamba S.; Rychetsky I.; Savinov M.; Volkov A.; Gorshunov B.; Pronin A.; Hoffmann S.; Waser R.;. Lindner J.
High-Frequency Dielectric Response of SrTiO3 Crystals, Ceramics and thin Films
Ferroelectrics 239, 117 (2000)
23.42.0

Prume K.1; Waser R.; Franken K.; Maier H.
1 Institut für Werkstoffe der Elektrotechnik, RWTH Aachen
Finite-Element Analysis of Ceramic Multilayer Capacitors: Modeling and Electrical Impedance Spectroscopy for a Non-Destructive Failure Test
J. Am. Ceram. Soc., 83 (5), 1153-59 (2000)
23.42.0

Rottländer P.; Kohlstedt H.; Grünberg P.; Girgis P.
Ultraviolet light oxidation for magnetic tunnel junctions
J. Appl. Phys. 87, 6067 (2000)
23.42.0

Rottländer P.; Kohlstedt H.; de Gronckel H.M.A.; Girgis E.; Schelten J.; Grünberg P.
Magnetic tunnel junctions prepared by ultravioet light assisted oxidation
J. Magn. Magn. Mat. 210, 251 (2000)
23.42.0

Schober T.; Bohn, H.G.
Water vapor solubility and electrochemical characterization of the high temperature proton conductor BaZr0.9Y0.1O2.95
Solid State Ionics 127 (2000) 351-360
23.55.0

Schober T.; Szot K.; Barton M.; Kessler B.; Breuer U.1; Penkalla H.J.1; Speier W.1
1 Institut für Chemie und Dynamik der Geosphäre, FZJ
Cation loss of BaCa0.393Nb0.606O2.91 in aqueous media: amorphization at room temperature,
J. Solid State Chemistry 149, 262-275 (2000)
23.55.0

Schober T.; Szot K.; Barton M.;.Kessler B.; Breuer U.; .Penkalla H.J.; Speier W.
Cation Loss of BaCa0.393Nb0.606O2..91 in Aqueous Media: Amorphization at Room Temperature
Journal of Solid State Chemistry 149, 262 (2000)
23.42.0

Schäfer P.; Waser R.
MOCVD of perovskite thin films using an aerosol-assisted liquid delivery system
Adv. Mater. Opt. Electron. 10 (2000) 169-175
23.42.0

Setter N.1; Waser R.
1 EPFL, Lausanne, Switzerland
Electroceramic Materials
Acta mater. 48, 151-178 (2000)
23.42.0

Singh B.N.; Eldrup M.; Horsewell A.; Ehrhart P.; Dworschak F.
On recoil energy dependent void swelling in pure copper: part I. Experimental results
Phil. Mag. A 80 (2000) 2629-2650
23.42.0

Slowak R.1; Hoffmann S.; Liedtke R.1; Waser R.
1 Institut für Werkstoffe der Elektrotechnik, RWTH Aachen
Functional graded high-K (Ba1-xSrx)TiO3 thin films for capacitor structures with low temperature coefficient
Integrated Ferroelectrics 24, 169-179 (1999)
23.42.0

Szot K.; Speier W.; Breuer U.; Meyer R.1; Szade J.; Waser R.
1 Institut für Werkstoffe der Elektrotechnik, RWTH Aachen
Formation of micro-crystals on the (100) surface of SrTiO3 at elevated temperatures
Surface Science 460, 112 (2000)
23.42.0

Szot K.; Speier W.; Pawelczyk M.; Kwapulinski J.; Huliger J.; Hesse H.; Breuer U.; Quadakkers W.;
Chemical inhomogeneity in the near-surface region of KTaO3
J.Phys. : Condens. Matter 12, 4687 (2000)

Tyagi A.K.; Szot K.; Czyrska-Filemonowicz A.; Naumenko D.; Quadakkers W.J.
Significance of Crystallographic Grain Orientation for Oxide Scale Formation on FeCrAl ODS Alloys studied by AFM TEM and SIMS/SNMS
Materials at High Temperatures 17,159 (2000)
23.42.0

Ujma Z.; Szymczak L.; Handerek L.; Szot K.; Penkalla H.J.
Dielectric and pyroelectric properties of Nb-doped Pb(Zr0.92Ti0.08)O3 ceramics
Journal of the European Ceramic Society 20, 1003 (2000)
23.42.0

Waser R.; Hagenbeck R.
Grain Boundaries in Dielectric and Mixed-Conducting Ceramics
Overview No. 137, Acta mater. 48, 797-825 (2000)
23.42.0

de Gronckel H.A.M.; Kohlstedt H.; Daniels C.
Prerequisites for high-quality magnetic tunnel junctions: XPS and NMR study of Co/Al bilayers
Appl. Phys. A 70 (4), 435 (2000)
23.42.0

Invited Talks

Böttger U.1; Waser R.
1 Institut für Werkstoffe der Elektrotechnik, RWTH Aachen
Dielectric losses in ferroelectric thin films by reversible domain wall motion
12th IEEE Int. Symp. on the Applications of Ferroelectrics, Honolulu, Hawaii, 31.07.-02.08.2000
23.42.0

Ehrhart P.; Fitsilis F.; Regnery S.; Waser R.; Schienle F.1; Schumacher M.1; Dauelsberg M.1; Strzyzewski P.1; Jürgensen H.1
1 Aixtron AG, Aachen, Germany
Growth of (Ba,Sr) TiO3 thin films in a multiwafer MOCVD reactor
MRS Fall Meeting, Boston, 27.11.-01.12.00
23.42.0

Ehrhart P.; Waser R.; Schneller T.; Hoffmann-Eifert S.
Chemical deposition methods for ferroelectric thin films
Asian Meeting on Ferroelectrics, Hongkong, 13.12.00
23.42.0

Ehrhart P.
Chemical deposition methods II: MOCVD
12th Int. Symp. Integrated Ferroelectrics, Aachen, 12.03.-15.03.00
23.42.0

Fitsilis F.; Regnery S.; Ehrhart P.; Waser R.; Schienle F.1; Schumacher M.1; Lindner J.1; Miedl S.1; Jürgensen H.1
1 Aixtron AG, Aachen, Germany
BST thin films growth in a multiwafer MOCVD reactor
Int. Conf. on Electroceramics VII, Portoroz, Slovenia, 03.-06.09.2000
23.42.0

Grossmann M.1; Bolten D.1; Böttger U.1; Lohse O.1; Waser R.; Tiedke S.1; Schmitz T.1; Kall U.1; Hartner W.; Kastner M.; Schindler G.
1 Institut für Werkstoffe der Elektrotechnik, RWTH Aachen
The influence of the experimental procedures on the reliability issues of ferroelectric thin films in view of memory applications
12th Int. Symp. Integrated Ferroelectrics, Aachen, 12.03.-15.03.00
23.42.0

Hoffmann-Eifert S.
Processing-microstructure-property relationship of CSD and MOCVD derived oxide thin films
12th IEEE Int. Symp. on the Applications of Ferroelectrics, Honolulu, Hawaii, 31.07.-02.08.2000
23.42.0

Kohlstedt H.H.
Al2O3 Tunnelbarrieren in supraleitenden und magnetischen Tunnelkontakten
Ruhr-Universität Bochum, 19.05.00
23.42.0

Kohlstedt H.H.
Bauelemente zur nicht-flüchtigen Informationsspeicherung: Grundlagen und Entwicklungstendenzen
Graduierten Kolleg Workshop, Institut für Angewandte Physik der Universität Karlsruhe, 21.02.-22.02.2000
23.42.0

Kohlstedt H.H.
Dry-etching of oxides materials and refractory metal electrodes
Penn State University, USA, 21.11.2000
23.42.0

Kohlstedt H.H.
Magnetic tunnel junctions for non-volatile memory application
Wilhelm-Else Hereaus Stiftung, Metal-Nonmetal Structures for Magnetoelectronics, Bad Honnef, 05.01.-07.01.2000
23.42.0

Kohlstedt H.H.
Physics and technology of superconducting and magnetic tunnel junctions with aluminium oxide barriers
Universität Saarbrücken, 15.12.2000
23.42.0

Kohlstedt H.H.
Ätztechniken bei der Herstellung elektronischer Bauelemente
Arbeitskreis "Dünnschichten in der Mikroelektronik, Caesar, Bonn, 17.11.2000
23.42.0

Liedtke R.1; Waser R.
1 Institut für Werkstoffe der Elektrotechnik, RWTH Aachen
Capacitance and admittance spectroscopy analysis of hydrogen-degraded Ba0.7Sr0.3TiO3 thin films
12th IEEE Int. Symp. on the Applications of Ferroelectrics, Honolulu, Hawaii, 31.07.-02.08.2000
23.42.0

Lohse O.1; Grossmann M.1; Bolten D.1; Böttger U.1; Waser R.
1 Institut für Werkstoffe der Elektrotechnik, RWTH Aachen
Relaxation mechanisms in ferroelectric thin film capacitors for FERAM application
12th Int. Symp. Integrated Ferroelectrics, Aachen, 12.03.-15.03.00
23.42.0

Meyer R.1; Waser R.; Helmbold J.; Borchardt G.
Thermodynamics versus kinetics of perovskites: defect chemistry in the transition state
12th IEEE Int. Symp. on the Applications of Ferroelectrics, Honolulu, Hawaii, 31.07.-02.08.2000
23.42.0

Meyer R.1; Waser R.
1 Institut für Werkstoffe der Elektrotechnik, RWTH Aachen
Advances in point defect chemistry: space-charge controlled surface reactions
Int. Conf. on Electroceramics VII, Portoroz, Slovenia, 03.-06.09.2000
23.42.0

Nasini A.1; Dernovsek O.1; Fritz M.1; Waser R.; Wersing W.1
1 Siemens AG München
Innovative microwave filter design with a new high dielectric LTCC-material
MIOP Conference, 2001, Stuttgart
23.42.0

Ohly C.; Hoffmann S.; Szot K., Waser R.
Electrical conductivity and segregation effects of doped SrTiO3 thin films at high temperatures
Int. Conf. on Electroceramics VII, Portoroz, Slovenia, 03.-06.09.2000
23.42.0

Ohly Ch.
Chemical Solution Deposition und elektrische Leitfähigkeit von SrTiO3-Dünnschichten
Universität Karlsruhe, 24.10.2000
23.42.0

Pertsev N.A.; Koukhar V.G.; Waser R.; Hoffmann S.
Effects of domain formation on the dielectric properties of ferroelectric thin films
12th Int. Symp. Integrated Ferroelectrics, Aachen, 12.03.-15.03.00
23.42.0

Petzelt J.; Gregora I.; Ostapchuk T.; Kamba S.; Pokorny J.; Bovtun V.; Porokhonskyy V.; Savinov M.; Kadlec F.; Vanek P.; Rychetsky I.; Yuzyuk Y.; Almeida A.; Chavez R.; Hoffmann S.; Waser R.; Rafaja D.; Dobiasova L.; Perina V.
Polar clusters in pure bulk SrTiO3 ceramics
Int. Conf. on Electroceramics VII, Portoroz, Slovenia, 03.-06.09.2000
23.42.0

Petzelt J.; Ostapchuk T.; Kamba S.; Gregora I.; Rychetsky I.; Pokorny J.; Bovtun V.; Porokhonsky V.; Savinov M.; Hoffmann S.; Waser R.; Lindner J.
Far infrared, microwave and Raman spectroscopy of the ferroelectric soft mode in SrTiO3 thin films and ceramics
12th Int. Symp. Integrated Ferroelectrics, Aachen, 12.03.-15.03.00
23.42.0

Reichmann K.; Hoffmann S.; Schneller T.; Hasenkox U.; Waser R.
Morphology and electrical properties of SrTiO3-films on conductive oxide films
Int. Conf. on Electroceramics VII, Portoroz, Slovenia, 03.-06.09.2000
23.42.0

Rickes J.; Waser R.; Kall U.1; Bartic A.2; Wouters D.2
1 Institut für Werkstoffe der Elektrotechnik, RWTH Aachen
2 IMEC Leuven, Belgium
Comparison between standard and chain-type FERAM architectures employing a sophisticated ferroelectric capacitor model
12th Int. Symp. Integrated Ferroelectrics, Aachen, 12.03.-15.03.00
23.42.0

Schneider St.; Kohlstedt H.H.; Waser R.
Etching characteristics of noble metal electrode
MRS Fall Meeting, Boston, 27.11.-01.12.00
23.42.0

Schneller T.1; Ehrhart P.
1 Institut für Werkstoffe der Elektrotechnik, RWTH Aachen
Chemical deposition methods CSD and MOCVD
12th Int. Symp. Integrated Ferroelectrics, Aachen, 12.03.-15.03.00
23.42.0

Schober T.
Tubular high-temperature proton conductors: transport numbers and hydrogen injection
7th Euroconference on Ionics, Calcatoggio, Corsica, 02.10.2000
23.55.0

Schober T.
Water vapor solubility and impedance of the high temperature proton conductor SrZr0.9Y0.1O3-x
10th Int. Conf. on Solid State Protonic Conductors, Montpellier, France, 25.09.2000
23.55.0

Schulte T.; Waser R.; Römer E.W.J.; Bouwmeester H.J.M.; Nigge U.; Wiemhöfer H.-D.
Development of oxygen-permeable ceramic-membranes for NOx-sensors
Int. Conf. on Electroceramics VII, Portoroz, Slovenia, 03.-06.09.2000
23.42.0

Shur V.Ya.; Blankova E.B.; Subbotin A.L.; Borisova E.A.; Barannikov A.V.; Bolten D.1; Gerhardt R.1; Waser R.
1 Institut für Werkstoffe der Elektrotechnik, RWTH Aachen
Kinetics of pyrochlore-perovskite transformation during rapid thermal annealing of sol-gel PZT films
Int. Conf. on Electroceramics VII, Portoroz, Slovenia, 03.-06.09.2000
23.42.0

Szot K.; Hoffmann S.; Speier W.; Breuer U.; Siegert M.; Waser R.
Segregation phenomena in thin films of BaTiO3
12th Int. Symp. Integrated Ferroelectrics, Aachen, 12.03.-15.03.00
23.42.0

Szot K.
Oberflächenschicht in Perowskit-Materialien
Institut für Angewandte Photophysik, Universität Dresden, 18.01.00
23.42.0

Szot K.
Restructuring of the surface region in ABO3 materials
University of Mining and Metallurgy, Krakow, 10.04.00
23.42.0

Szot K.
Solid state reaction in surface layer of perovskite
Silesian University of Katowice, 15.12.00
23.42.0

Waser R.; Lohse O.1; Grossmann M.1; Bolten D.1; Böttger U.1
1 Institut für Werkstoffe der Elektrotechnik, RWTH Aachen
Transient behavior of the polarization in ferroelectric thin film capacitors
MRS Fall Meeting, Boston, 27.11.-01.12.00
23.42.0

Waser R.; Schneller T.1; Hoffmann S.
1 Institut für Werkstoffe der Elektrotechnik, RWTH Aachen
Advances in CSD technology for electroceramic thin films
Int. Conf. on Electroceramics VII, Portoroz, Slovenia, 03.-06.09.2000
23.42.0

Waser R.
Chemical solution deposition of complex electronic oxide thin films
Material Science Division, Argonne National Labs., Chicago, 01.12.00
23.42.0

Waser R.
Dielectric losses in ferroelectric thin films by reversible domain wall motion
12th IEEE Int. Symp. on the Applications of Ferroelectrics, Honolulu, Hawaii, 31.07.-02.08.2000
23.42.0

Waser R.
Oxidkeramische Materialien in der Mikroelelektronik und Nanotechnologie
10. Vortragstagung der Gesellschaft Deutscher Chemiker-Fachgruppe Festkörperchemie und Materialforschung: Anorganische Funktionsmaterialien, Münster, 26.09.-29.09.2000
23.42.0

Weber U.; Greuel G.; Böttger U.; Weber S.; Hennings D.; Waser R.
Dielectric properties of Ba(Zr,Ti)O3-based ferroelectrics for capacitor applications
Int. Conf. on Electroceramics VII, Portoroz, Slovenia, 03.-06.09.2000
23.42.0

Posters

Bachhofer H.1; Reisinger H.1; Dehm D.; von Philipsborn H.1; Waser R.
1 Siemens AG, München, Germany
Relaxation effects and steady-state conduction in non-stoichiometric SBT films
12th Int. Symp. Integrated Ferroelectrics, Aachen, 12.03.-15.03.00
23.42.0

Baldus O.; Krasser W.; Hoffmann S.; Waser R.; Kreutz E.
Laserannealing studies of strontium-titanate thin films using short laser pulses
12th Int. Symp. Integrated Ferroelectrics, Aachen, 12.03.-15.03.00
23.42.0

Bolten D.1; Böttger U.1; Grossmann M.1; Lohse O.1; Waser R.
1 Institut für Werkstoffe der Elektrotechnik, RWTH Aachen, Germany
Irreversible processes in donor and acceptor doped Pb(zr,Ti)O3 thin films
12th Int. Symp. Integrated Ferroelectrics, Aachen, 12.03.-15.03.00
23.42.0

Bolten D.1; Böttger U.1; Grossmann M.1; Lohse O.1; Waser R.
1 Institut für Werkstoffe der Elektrotechnik, RWTH Aachen, Germany
Reversible and irreversible polarization processes in ferroelectric thin films
12th IEEE Int. Symp. on the Applications of Ferroelectrics, Honolulu, Hawaii, 31.07.-02.08.2000
23.42.0

Böttger U.1; Bolten D.1; Lohse O.1; Grossmann M.1; Waser R.
1 Institut für Werkstoffe der Elektrotechnik, RWTH Aachen, Germany
Dielectric losses in ferroelectric thin films by reversible domain wall motion
12th Int. Symp. Integrated Ferroelectrics, Aachen, 12.03.-15.03.00
23.42.0

Ehrhart P.; Fitsilis F.; Regnery S.; Waser R.; Schienle F.1; Schumacher M.1; Lindner J.1; Dauelsberg M.1; Strzyzewski P.1; Jürgensen H.1
1 Aixtron AG, Aachen, Germany
Deposition of BST thin films in a multi-wafer MOCVD reactor
12th Int. Symp. Integrated Ferroelectrics, Aachen, 12.03.-15.03.00
23.42.0

Falter S.T.; Du K.M.; Loosen P.; Poprawe R.; Baldus O.; Waser R.
UV beam sources for double pulse generation
Conference on Lasers and Electrooptics 2000, Nizza, France, 04.-08.09.2000
23.42.0

Grossmann M.1; Bolten D.1; Böttger U.1; Lohse O.1; Waser R.; Hartner W.; Kastner M.; Schindler G.
1 Institut für Werkstoffe der Elektrotechnik, RWTH Aachen, Germany
Imprint properties of SBT thin films
12th Int. Symp. Integrated Ferroelectrics, Aachen, 12.03.-15.03.00
23.42.0

Grossmann M.1; Lohse O.1; Bolten D.1; Böttger U.1; Waser R.
1 Institut für Werkstoffe der Elektrotechnik, RWTH Aachen, Germany
Imprint in ferroelectric thin films: trapped charges model
12th IEEE Int. Symp. on the Applications of Ferroelectrics, Honolulu, Hawaii, 31.07.-02.08.2000
23.42.0

Haegel F.-H.; Janssen M.; Dams P.; Dornseiffer J.; Otterstedt R.; Triefenbach D.; Pithan C.
Synthesis of oxidic nanoparticles from microemulsions
10th Int. Conf. On Colloid and Interface Science, Bristol, Great Britain, 23.07.-28.07.2000
23.42.0

Hartner W.1; Bosk P.1; Schindler G.2; Dehm C.1; Mazuré C.2; Schroeder H.; Waser R.
1 Siemens AG, München, Germany,
2 Infineon Technologies, München, Germany
Degradation mechanisms of SrBi2Ta2O9 ferroelectric thin film capacitors during forming gas annealing
12th Int. Symp. Integrated Ferroelectrics, Aachen, 12.03.-15.03.00
23.42.0

Hofer C.1; Weber U.1; Waser R.
1 Institut für Werkstoffe der Elektrotechnik, RWTH Aachen, Germany
Electrical characterization of grain boundary decorated strontiumtitanate ceramics
Int. Conf. on Electroceramics VII, Portoroz, Slovenia, 03.-06.09.2000
23.42.0

Hoffmann M.1; Küppers H.1; Schneller T.1; Böttger U.1; Schnakenberg U.1; Mokwa W.1; Waser R.
1 Institut für Werkstoffe der Elektrotechnik, RWTH Aachen, Germany
A new concept and first development results of a PZT thin film actuator
12th IEEE Int. Symp. on the Applications of Ferroelectrics, Honolulu, Hawaii, 31.07.-02.08.2000
23.42.0

Küppers H.1; Hoffmann M.1; Leuerer T.1; Schneller T.1; Böttger U.1; Schnakenberg U.1; Waser R.; Mokwa W.
1 Institut für Werkstoffe der Elektrotechnik, RWTH Aachen, Germany
Piezoelectric bending actuator for microelectro-mechanical applications
12th Int. Symp. Integrated Ferroelectrics, Aachen, 12.03.-15.03.00
23.42.0

Liedtke R.1; Hoffmann S.; Waser R.
1 Institut für Werkstoffe der Elektrotechnik, RWTH Aachen, Germany
Hydrogen induced degradation of (Ba,Sr)TiO3 thin films
12th Int. Symp. Integrated Ferroelectrics, Aachen, 12.03.-15.03.00
23.42.0

Liedtke R.1; Hoffmann S.; Waser R.
1 Institut für Werkstoffe der Elektrotechnik, RWTH Aachen, Germany
Recrystallization of oxygen ion implanted Ba0.7Sr0.3TiO3 thin films
12th IEEE Int. Symp. on the Applications of Ferroelectrics, Honolulu, Hawaii, 31.07.-02.08.2000
23.42.0

Ma, W.; Schäfer P.; Ehrhart P.; Waser R.
Metalorganic chemical vapor deposition of BaTiO3 and SrTiO3 thin films using a single solution source with a non-contact vaporizer
12th Int. Symp. Integrated Ferroelectrics, Aachen, 12.03.-15.03.00
23.42.0

Meyer R.1; Liedtke R.1; Waser R.
1 Institut für Werkstoffe der Elektrotechnik, RWTH Aachen, Germany
Modeling of the time dependent current in BST thin films in the short time range
12th IEEE Int. Symp. on the Applications of Ferroelectrics, Honolulu, Hawaii, 31.07.-02.08.2000
23.42.0

Mitze C.1; Hasenkox U.1; Waser R.
1 Institut für Werkstoffe der Elektrotechnik, RWTH Aachen, Germany
On the magnetic structure of grain boundaries in doped manganates
12th Int. Symp. Integrated Ferroelectrics, Aachen, 12.03.-15.03.00
23.42.0

Mört M.1; Schindler G.2; Hartner W.1; Kasko I.1; Kastner M.1; Dehm C.1; Waser R.
1 Siemens AG München, Germany
2 Infineon Technologies, München, Germany
Low-temperature-process and thin-SBT-films for ferroelectric memory devices
12th Int. Symp. Integrated Ferroelectrics, Aachen, 12.03.-15.03.00
23.42.0

Ohly C.; Hoffmann S.; Szot K.; Waser R.
High temperature conductivity behaviour of doped SrTiO3 thin films
12th Int. Symp. Integrated Ferroelectrics, Aachen, 12.03.-15.03.00
23.42.0

Ohly Ch.; Hoffmann S.; Szot K.; Waser R.
Doped alkaline earth titanates: from the defect chemistry of bulk ceramics to the conduction behavior of thin films
12th IEEE Int. Symp. on the Applications of Ferroelectrics, Honolulu, Hawaii, 31.07.-02.08.2000
23.42.0

Prume K.1; Hoffmann S.; Waser R.
1 Institut für Werkstoffe der Elektrotechnik, RWTH Aachen, Germany
Finite-element simulations of interdigital electrode structures on high permittivity thin films
12th Int. Symp. Integrated Ferroelectrics, Aachen, 12.03.-15.03.00
23.42.0

Prume K.1; Waser R.
1 Institut für Werkstoffe der Elektrotechnik, RWTH Aachen, Gemany
Finite element simulation of multiplayer structures and devices
12th IEEE Int. Symp. on the Applications of Ferroelectrics, Honolulu, Hawaii, 31.07.-02.08.2000
23.42.0

Rickes J.T.; Waser R.
The effect of imprint on read and write operations in ferroelectric random access memories for lifetime prediction
12th IEEE Int. Symp. on the Applications of Ferroelectrics, Honolulu, Hawaii, 31.07.-02.08.2000
23.42.0

Roelofs A.1; Grossmann M.1; Hoffmann M.1; Schneller T.1; Böttger U.1; Waser R.; Schlaphof F.2; Eng L.M.2
1 Institut für Werkstoffe der Elektrotechnik, RWTH Aachen, Germany
2 TU Dresden, Germany
Nanoscale characterization of chemical solution deposition derived Ba{0.5}Pb{0.5}TiO3 thin films with scanning force microscopy
12th Int. Symp. Integrated Ferroelectrics, Aachen, 12.03.-15.03.00
23.42.0

Roelofs A.1; Schlaphof F.2; Schneller T.1; Grossmann M.1; Böttger U.1; Waser R.; Eng L.M.2
1 Institut für Werkstoffe der Elektrotechnik, RWTH Aachen, Germany
2 TU Dresden, Germany
Nanoscale characterization of chemical solution deposited PbTiO3 thin films with scanning force microscopy
12th IEEE Int. Symp. on the Applications of Ferroelectrics, Honolulu, Hawaii, 31.07.-02.08.2000, 23.42.0

Schroeder H.
On leakage current models applied to thin films
12th Int. Symp. Integrated Ferroelectrics, Aachen, 12.03.-15.03.00
23.42.0

Schäfer P.; Ma W.; Waser R.
Preparation of (Pb,Ba)TiO3 thin films by MOCVD using an aerosol-assisted liquid delivery system
12th Int. Symp. Integrated Ferroelectrics, Aachen, 12.03.-15.03.00
23.42.0

Schäfer P.; Ritter S.; Ganster R.; Hoffmann S.; Waser R.
Preparation of (Pb,Ba)TiO3 thin films by MOCVD using an aerosol-assisted liquid delivery system
12th Int. Symp. Integrated Ferroelectrics, Aachen, 12.03.-15.03.00
23.42.0

Schäfer P.; Ritter S.; Hoffmann S.; Waser R.
(Pb1-xBax)TiO3 thin films prepared by MOCVD: film formation and electrical properties
Int. Conf. on Electroceramics VII, Portoroz, Slovenia, 03.-06.09.2000
23.42.0

Shur V.Y.; Nikolaeve E.V.; Shishkin E.I.; Baturin I.S.; Bolten D.; Waser R.
Fatigue in PZT thin films
MRS Fall Meeting, Boston, 27.11.-01.12.00
23.42.0

Slowak R.1; Schneller T.1; Waser R.
1 Institut für Werkstoffe der Elektrotechnik, RWTH Aachen, Germany
High-permittivity temperature independent devices up to 2000C by modified graded thin films
12th Int. Symp. Integrated Ferroelectrics, Aachen, 12.03.-15.03.00
23.42.0

Waser R.; Hölbling Th.1
1 Institut für Werkstoffe der Elektrotechnik , RWTH Aachen, Germany
1D modelling of charge transport in SrTiO3 ceramics
Int. Conf. on Electroceramics VII, Portoroz, Slovenia, 03.-06.09.2000
23.42.0

Patents applied for

Hoffmann S.; Waser R.; Slowak R.1; Liedtke R.1
1RWTH Aachen
Dünnschichtkondensator
PCT: PCT/EP 00/09319 (26.08.2000) (EP,US,JP,KR)
PT 1.1726
17.22.0

Kohlstedt H.; Rodriguez J.
Verfahren zur Erzeugung eines Tunnelkontaktes sowie eine Vorrichtung umfassende Mittel zur Erzeugung eines Tunnelkontaktes
DE: 100 59 357.7 (29.11.2000)
PT 1.1859
23.42.0

Kohlstedt H.; Rottländer P.
Verfahren zur Herstellung eines magnetischen Tunnelkontaktes sowie magnetischer Tunnelkontakt
PCT: PCT/EP 00/07012 (21.07.2000) (EP, US,JP;KR)
PT 1.1721
23.42.0

Kohlstedt H.; Stein S.
Dreitorbauelement
DE: 100 31 401.5-33 (03.07.2000)
PT 1.1810
23.42.0

Kohlstedt H.
Anordnung zum Messen eines Magnetfeldes und Verfahren zum Herstellen einer Anordnung zum Messen eines Magnetfeldes
DE: 100 09 944.0 (02.03.2000)
PT 1.1782
23.42.0

Kohlstedt H.
Speicherkondensator
PCT: PCT/DE 00/02184 (04.07.2000) (EP,US,JP)
PT 1.1713
23.42.0

Schober T.; Meuffels P.; Friedrich J.
Verfahren zur Wasserstoffdosierung
DE: 100 53 986.6 (31.10.2000)
PT 1.1850
23.42.0

Szot K.; Speier W.
Teleskopartiger Mikromanipulator mit Piezomaterialien
PCT: PCT/DE 00/01070 (05.04.2000) (EP,US,JP,KR,CN)
PT 1.1679
23.42.0

Waser R.; Baldus O.; Krasser W.
Lasersystem mit steuerbarer Pulsdauer
PCT: PCT/DE 00/04314 (04.12.2000) (EP,US,JP,KR)
PT 1.1754
23.42.0

Waser R.; Baldus O.; Krasser W.
Verfahren zur Herstellung einer kristallisierten keramischen Schicht durch Laser-Annealing
PCT: PCT/DE 00/04313 (04.12.2000) (EP,US,JP,KR)
PT 1.1755
23.42.0

Lecture courses

Schroeder H.
Ausgewählte Kapitel der Metallkunde
Fakultät für Bergbau, Hüttenwesen und Geowissenschaften der RWTH Aachen, WS 99/2000 und WS 2000/01
23.42.0

Waser R.
Vorlesung Werkstoffe der Elektrotechnik
Sensoren und Sensormeßtechnik I+II
RWTH Aachen
23.42.0

Waser, R.; Ehrhart P., Hoffmann S.; Kohlstedt H.H.; Schroeder H.
Neue Materialien und Bauelemente für die Informationstechnik I (WS 99/2000)
Vertiefungsfach II
RWTH Aachen, WS 1999/2000
23.42.0

Institute for Soft Condensed Matter Physics

General Overview

The Institute "Weiche Materie" was founded in Jan. 2000. The main focus of the institute is on properties of colloidal systems. The aim is to understand:

- Macroscopic, Non-equilibrium Phenomena on a Microscopic Basis, and
- Dynamics and Microstructural order in Suspensions in Equilibrium.

To make progress in this area it is a necessity to be able to

- synthesize colloids and develop the synthesis of new model systems.

The research in the institute is done within "projects", which will be described below.

At this moment the further development of the institute is severely hindered by lack of laboratory facilities. Most of the planned laboratories can not yet be built for reasons that go beyond the jurisdiction of the FZJ. Some of the planned research can not be started, while other research themes can only be performed in part in improvised laboratories.

The following projects have been defined within the Institute "Weiche Materie":

Cooperative phenomena in condensed matter (F&E-Nr.: 23.15.0)

Non-equilibrium Phenomena

Project leader:	Prof. J.K.G. Dhont
Personnel:	D. Triefenbach (Technician)
	Dr. S. Rathgeber (Habilitand, started april 2000)
	Dr. P. Lettinga (Post Doc, started july 2000)
	T. Lenstra (Post Doc, will start in march 2001)

The subjects under investigation in this project are :

1. **Shear-banding and Rheology of "hairy Colloids" and Suspensions of rod-like Particles (S. Rathgeber)**

   Shear-banding is a hydrodynamic instability in systems under flow that occurs whenever the stress decreases with increasing shear-rate. The stationary state is now a state where regions of different microstructure and sometimes different shear-rates "coexist". The shear-banding instability occurs in the neighbourhood of spinodals, so that actual demixing kinetics is determined by the interplay between the thermodynamic and hydrodynamic shear-banding forces. The kinetics of demixing under shear flow and the structure of banded states will be studied by means of heterodyne, spatially resolved dynamic light scattering, spatially resolved birefringence measurements and rheology. Two systems will be investigates : "hairy colloids" (colloidal spheres coated with long polymer chains) and rigid rod-like particles. A system of hairy colloids where shear-banding has been observed will be investigated in cooperation with Dr. J. Vermant (University of Leuven). Another, well defined hairy colloid has been developed in the Institute for Neutron Scattering (see the next theme). When this system exhibits shear-banding, it will play an important role in our investigations. Simulations on hairy colloids in shear flow will be performed in the Insitute Theory II. There is an ongoing collaboration with prof. W. Briels (University of Twente) on the theory of the shear-banding transition in systems of rigid rods.

2. **Shear induced Polymer Brush Deformation (S. Rathgeber)**
   Colloidal particles with a small core in comparison to the length of the polymers that are attached to their

surface have been developed in the Institute for Neutron Scattering by Dr J. Allgaier and Dr. L. Willner. These systems will be used to study the polymer brush deformation under shear flow by means of birefringence measurements and small angle neutron scattering on very dilute samples, in cooperation with Dr. L. Willner and Dr. W Pyckhout-Hintzen (Institute for Neutron Scattering) and Dr. P. Lindner (ILL, Grenoble). For this purpose we developed a quartz shear cell in cooperation with Dr. W. Pyckhout-Hintzen and Dr. P. Lindner. In a later stage we will also perform rheology experiments and scattering experiments at larger concentrations, in order to probe the effect of the brush deformation on the microstructure. These investigations are part of a European project (HUSC, Hard to Ultra Soft Colloids).

3. **Critical Phenomena under Shear Flow (P. Lettinga)**
In mixtures of stearyl silica spheres and small PDMS polymers (Polydimethylsiloxane) in cyclohexane, depletion attractions can give rise to gas-liquid phase separation. Non-linear microstructural response to oscillatory shear flow near the gas-liquid critical point in these systems is studied by means of time resolved small angle light scattering. This set up is operational. The aim is to detect higher order harmonics in the time dependent response of the structurefactor, which are responsible for non-linear viscoelastic response.

4. **Dynamics and Structure of "Polymer-colloids" (S. Rathgeber)**
Suspensions of polymeric particles of a colloidal size are studied by means of small angle neutron scattering and neutron spin echo experiments. This concerns the shape, internal structure and dynamics of the colloidal particles. The systems that are studied are two different kind of dendrimers, cellulose derivatives and bottlebrush macromolecules, in cooperation with T. Pakula (Max Planck Institute for Polymer Research in Mainz). Scattering experiments and rheology measurements at higher concentration are planned.

5. **Nucleation and Crystal Growth under Shear Flow Conditions**
Small angle, time resolved static light scattering will be used to examine nucleation and crystal growth under the influence of shear flow. The shear induced shift of the liquid-solid bimodal will be a point of interest also. Since the crystals will probably be anisometric, scattering experiments are planned where the incident light beam is either directed along the gradient direction or the vorticity direction.

Dynamics in Equilibrium Systems

Project leader: Dr. G. Meier (started Aug. 2000)

The subjects under investigation in this project are :

1. **Dynamics of Polymer Mixtures and Colloids under high Pressure**
Pressure is an external variable that can be used to continuously vary the compatibility of polymers. The polymers can either be free polymers or polymers bound to the surface of colloidal particles. Besides by pressure, monomer-monomer pair-interaction potentials can also be changed systematically by changing the H/D composition of the polymers. This offers the possibility to gain insight in the microscopic origin of the rich phase behaviour and dynamics of these systems. The phase behaviour and (critical) dynamics of polymer mixtures and mixtures of polymers and polymer-coated colloidal particles will be the topic of this project.

2. **Phonon Dispersion in heterogeneous Systems**
Colloidal systems represent heterogeneous systems, in which the dynamics of acoustic modes will be studied. There will almost certainly be a dependence of the properties of acoustic excitations on the structural properties of the colloidal suspensions. The degree of heterogeneity can be changed continuously by changing the size and/or concentration of the colloidal particles.

3. **Rotational Diffusion of Rods near Phasetransition Lines**
Rotational diffusion of rod like colloids and polymers in the neighbourhood of a gas-liquid and isotropic-nematic phase boundary will be studied. Near a gas-liquid phase transition line, the attractive interactions between the rods will probably lead to a severe change of the rotational diffusion coefficient, since attractions favor parallel alignment of neigbouring rods over perpendicular alignment. On approach of the isotropic-

nematic spinodals, the rotational diffusion coefficient tends to zero in a way that is not known, that is, the critical exponent for the rotational diffusion coefficient is as yet unknown.

4. **Rotational Diffusion away from Phasetransition Lines (P. Lettinga)**
   Rotational diffusion coefficients of colloidal spheres and rods in bulk solution and within porous media are investigated by means of Time resolved Phosphorescence Anisotropy (TPA) and Fluorescence Recovery After Photobleaching (FRAP). These experiments are performed at the University of Utrecht in collaboration G. Koenderink and prof. A.P. Philipse. Also of interest is rotational diffusion of rigid rods under stationary shear flow, where FRAP and heterodyne dynamic light scattering experiments are planned.

We plan to built a combination of set ups which allows one to investigate dynamics in the time range 10^{-13}-10^{2} s. Dynamic light scattering covers a dynamic range of 10^{-7}-10^{2} s. A Sandercock tandem interferometer will be used to cover the time range 10^{-9}-10^{-11}s. The gap between these time ranges can be covered employing a confocal interferometer. The very fast dynamics will be studied by means of Raman scattering.

The project "Dynamics in Equilibrium Systems" can not start due to missing laboratory facilities.

Equilibrium Phase Behaviour and Structure

Project leader: To be appointed
Personnel: Dr. Z. Dogic (Humboldt scholarship, will start in April 2001)

To start with, Dr. Z. Dogic will synthesize a "diblock colloid" (see the project "Synthesis"), and, when successful, study the phase behaviour of this new colloidal model system.

Correlation between Interactions and ordered Structures

Project leader: Dr. J. Hauck

Dr. J. Hauck has been at the IFF for a longer time. His work in the Inititute Weiche Materie is a continuation of part of the work that has been done by J. Hauck during the past, applied to ordered structures in various colloidal systems.

Theory

Project leader: Dr. G. Nägele (started Jan. 2001)
Personnel: Dr. M. Kollmann (will start in April 2001)
Dr. H. Wang (will start in March 2001)

The aim of this project is two-fold: (i) developing theory on subjects that are, or may become, of experimental interest to the Institute, and (ii) to assist experimentalists with devising new experiments and with data interpretation.

Currently, the following subjects are being investigated :

1. **Electrokinetic Effects in Colloids**
   In particular, electrolyte friction is studied on the basis of mode coupling theory for a binary system : the large colloidal particles and the counter ions. A remarkable result is that hydrodynamic interactions play an essential role. A treatment of non-linear electrolyte friction response is within the validity of the present approach.

2. **Diffusion in Two-dimensional Space**
   Inspired by experiments that are performed by Dr. K. Zahn and Prof. G. Maret (University of Konstanz), diffusion coefficients have been calculated in case of a spatial dimension equal to 2. The surprising divergence

of the ensemble averaged hydrodynamic interaction function (commonly denoted as H(q)) is confirmed by theory. In addition, unexpected scaling behaviour has been predicted theoretically.

3. **Linear Viscoelastic Behaviour of spherical Colloids**
   A Green-Kubo formula for the linear shear viscosity of colloids, where hydrodynamic interactions are important, has been derived and evaluated numerically on the basis of a mode coupling approach.

Polymer, membranes and complex fluids (F&E-Nr.: 23.30.0)

Structure and Dynamics of Colloids at Interfaces

Project leader: Dr. P. Lang (started Oct. 2000)

The subjects under investigation in this project are :

1. **Structure and Dynamics of Interfaces between Coexisting Phases**
   The colloidal systems that will be investigated are rigid rods, like silica coated boehmite rods and semi-flexible fd-virus (in isotropic-nematic coexistence), and spheres (in gas-liquid or liquid-crystal coexistence).

2. **Structure and Dynamics close to a Wall**
   Like in the previous theme, rods and spheres will be investigated. We also plan to investigate depletion forces near a wall in mixtures of long polymers and small colloidal spheres. This will be done in cooperation with Dr. E. Eisenriegler (Institute Theory II).

At this moment, Dr. P. Lang is constructing an instrument with options for static and dynamic light scattering of evanescent waves (EWLS), total internal reflection microscopy (TIRM), capillary wave spectroscopy (CWS), ellipsometry and Brewster angle microscopy (BAM). The TIRM option is being built in cooperation with Dr. C. Bechinger (University of Konstanz).

In addition, P. Lang is working on the synthesis of "soft colloidal rods" (see the project "Synthesis").

Within the project "Structure and Dynamics of Colloids at Interfaces", the yet non-existing laboratories are essential for it's further development.

Further research activities (F&E-Nr.: 23.30.0)

Synthesis

Project leaders: Dr. J. Buitenhuis (will start in March 2001)
Dr. W. Sager (will start in April 2001)
Personnel: D. Jablonski (practical training started Oct. 2000)

The first aim will be to built up know how concerning the synthesis of commonly used colloidal model systems (like coated silica spheres, latex spheres, coated boehmite rods and gibbsite platelets, fd-virus and DNA fragments). D. Jablonski and D. Triefenbach have already synthesized stearyl silica-coated boehmite rods under the guidance of J. van Wijnhoven (Colloid Synthesis Facility in Utrecht). The development of new colloidal systems will the long term aim of this project. The synthesis of colloidal systems using microemulsion systems as templates is an area in which Dr. W. Sager is a specialist. Two synthesis projects have been started at the end of 2000 : the synthesis of "soft colloidal rods" (by Dr. P. Lang) and of "diblock colloids" (by Dr. Z. Dogic.) The soft colloidal rods are synthesized in a cylindrical microemulsion, where polymers are cross-linked. This could lead to flexible colloidal rods, of which the length is about 200 nm with an aspect ratio of about 20. The main problem here will probably be to fractionate the system in order to reduce the polydispersity in length. The diblock colloids will be synthesized by coupling of a stiff and flexible biological molecule.

The polymer synthesis know how that is available in the Institute for Neutron Scattering (Dr. L. Willner and Dr. J. Allgaier) will be of great advantage in developing certain classes of new colloidal systems.

The project "Synthesis" can not be satisfactorily realized due to the lack of laboratory facilities.

Jan Dhont

Personnel 1999/2000 and areas of activity

Scientific Staff

Prof. Dr. J.K.G. Dhont	Non-equilibrium structure and dynamics	23.150
Dr. J. Hauck	Structures and Interactions of Colloids, Polymers, Lipids and Bacteriae	23.150
Dr. G. Meier	Dynamics of mixtures, critical scattering, high pressure techniques	23.150

Technical Staff

Ms. K. Sellinghoff	Technician in the polymer characterization laboratory	23.150
Dipl.-Ing. D. Triefenbach	Chemical Engineer in polymer laboratories	23.150
Ms M.-L. Schüsseler	Secretary	

Scientists

Dr. Z. Dogic (ab 01.11.00)	Synthesis and phase behaviour of di-block colloids	23.150
Dr. P. Lang (ab 01.10.00)	Structure and dynamics of interfaces in colloidal systems	23.300
Dr. P. Lettinga (ab 01.07.00)	Study of the non-linear and linear viscoelastic, response of colloidal dispersions	23.150
Dr. S. Rathgeber	Structure and dynamics of polymer – colloids, polymer & colloid mixtures and biological colloids	23.150

Trainees

D. Jablonski (01.10.00)

Institute for Microstructure Research

General Overview

The Institut für Mikrostrukturforschung (Institute for Microstructure Research) is working in a number of fields. These were selected with an emphasis on modern-materials aspects, the importance of an atomistic and microstructural understanding for materials performance and the possibility to contribute to the development of technology. In some of these fields the competence spans the whole range from materials preparation via basic physics investigations to technical devices. In others access to interesting materials and device problems is provided by qualified collaborations. Besides this general-physics and technology part of the institute there is a second part of special competence. This is structure research by means of modern transmission electron microscopy and scanning tunnelling microscopy. This work is carried out within the Jülich Centre for High-Resolution Electron Microscopy. It is operated by the institute and serves a wider community of users.

Research Fields

(1) *Ceramic Superconductors*: Here the emphasis is on thin-film and heterostructure production, Josephson effects, and their application in magnetometer systems and spectroscopic techniques.

(2) *Semiconductors*: Here the emphasis is on structural investigations, mainly by transmission electron microscopy, of thin films and heterostructures. In collaboration with various research groups we are studying growth-related problems, like the relaxation mechanisms in SiGe films or the influence of doping on the microstructure in as-grown and annealed low-temperature grown GaAs films. Device relevant topics are addressed by studies on the interdiffusion in III-V heterostructures and by investigations of the microstructure of thin film solar cells of microcrystalline silicon. Another topic is the study of electronic states in compound semiconductors by scanning tunnelling microscopy employing a technique pioneered in our group. It permits, via the detection of the far-reaching Debye screening cloud at the surface, an investigation of charged doping or impurity atoms in the bulk of the samples.

(3) *Metallic Alloys*: These are at present quasicrystalline alloys and related normalcrystalline approximants. We are growing large single-quasicrystals for our own research but also for users world-wide, in particular for the participants in the DFG priority program on quasicrystals. Our own work on quasicrystals and approximants concentrates on phase-diagrams, plasticity and surface physics.

(4) *Electroceramics*: In the field of electroceramic materials we take advantage of our long-standing experience with respect to perovscitic materials both in preparation and in transmission electron microscopy. In collaboration with the Institut für Electrokeramische Materialien (Prof. Waser) we dedicate a large research capacity to the investigation of the structural aspects of the production and properties of electroceramic thin films.

(5) *High-Resolution Electron Microscopy*: The theoretical and technical aspects of atomic-resolution transmission electron microscopy have in recent years become one of the central fields of interest of our group. Computer program packages for the exit wave-function reconstruction developed in the institute are in use world-wide. In collaboration with EMBL Heidelberg and TU Darmstadt we developed the word's first aberration-corrected transmission electron microscope with record resolution, 1.3 Å at 200 kV. These developments are continued (see below).

Equipment

The institute has at its disposal sputtering deposition machines, some of them with three-target facilities, which were developed and built in the institute for the high-quality deposition of ceramic superconductor thin films and heterostructures. For device production local clean room, structuring and packaging facilities are available. The institute operates the Jülich Centre for High-Resolution Electron Microscopy with two 400 kV JEOL machines of the type 4000 EX/FX, a JEOL 2000 EX, a PHILIPS CM20 FEG, the spherical-aberration corrected PHILIPS CM200 FEG and a JEOL 840A scanning microscope. The priority in scanning tunnelling microscopy is on high-temperature investigations a field only rarely served by other competing groups. We have at our disposal two microscopes with in-situ cleaving facilities and ex-situ heating up to 750 °C. These instruments were designed and built inside the institute. An in-situ heating STM (Omicron) is used since early 2000. For the work on alloy plasticity a Zwick mechanical testing system has been installed in 1998. The collaboration with the Max-Planck-Institut für Mikrostrukturphysik at Halle in this field is continued. The institute operates together with the Institut für Streumethoden (Prof. Brückel) the IFF laboratory for crystal-growth.

Special results and developments

The institute was very successful in recent years in application of high-temperature superconductivity to communication systems. In particular the multipole dielectric filters designed in the institute received considerable attention world-wide. In

1998, as partner of BOSCH, we won the competition for a project "High-Temperature Superconductivity for the Communication Technology of the Future" which became one of the five priority programs of the German Federal Minister of Science and Technology. During the year 1999, in the course of a reorganisation of our institute, the whole high-frequency research group was transferred to the Institut für Schicht- und Ionentechnik (ISI). The free capacity, both with respect to personnel and funds, offered to us an excellent opportunity for development of new research competence.

Due to our unique position in this field we chose to direct our resources towards the development of Hilbert-transform spectroscopy on the basis of the ac-Josephson effect. This technique provides an excellent and novel tool for spectroscopy in the frequency range of 10^{10} to 10^{13} Hertz. It is broad band and orders of magnitude faster than Fourier spectroscopy. Here we have an excellent collaboration with the Institute for Radioelectronics (IRE) in Moscow. We succeeded in acquiring a BMBF-project for the development of a fast gas-spectrometer and a project with DESY, Hamburg. The latter is a consequence of our successful test of Hilbert-transform spectroscopy for the determination of the shape of electron bunches in the beam of the TESLA test facility in Hamburg. The goals are: Improving the sensitivity of the technique by development of even better Josephson junctions and constructing facilities for fast molecule spectroscopy in our own group.

Our dc-SQUIDs on the basis of ramp-type junction geometry continue their success both in performance and in their acceptance on the market. As a supplier of TRISTAN Company (USA, formerly Conductus) we deliver a larger number of SQUIDs and magnetometers per month. The market demands represent challenges to science and technology, and our work in this field will be continued as long as we can derive good science from these. The strategy for further developments in superconductivity will be to use our expertise in front technology in this field to develop applications which can also be used for our own research. Hilbert-transform spectroscopy has already been mentioned. SQUID-microscopy is another field. This project has been intensively followed since 1999 in a collaboration (joint patents) with ZEL (Prof. Halling) with the aim to built a SQUID-microscope prototype. Current delays are due to loss in personell and difficulties with suppliers. First tests are expected during 2001. An industry company has been found which is interested in marketing the new instrument.

The successful project of the spherical-aberration corrected transmission electron microscope described above has triggered new activities in electron optics world wide. The novel technology is considered a quantum jump of great commercial impact. New generations of instruments are under construction or in the planning phase in Europe, Japan and the US. Together with other institutions, in particular the Max-Planck-Institut für Metallforschung, we have contributed to the installation of a priority program of the DFG. In the framework of this program 3.8 Mio DM were granted in 1998 to our institute for the development, in collaboration with CEOS Company, Heidelberg, and ZEISS-LEO, Oberkochen, of the world's first Subangström-Instrument. Besides ultra-high resolution the 200 kV machine will contain a monochromator and an in-column energy filter of the Krahl-type. This will maintain the institute's position as a pioneer in advanced instrument development. The institute is partner of PHILIPS Electron Optics with respect to theory and application of exit-wave function reconstruction in high-resolution electron microscopy. Also in this field our institute is respected as an international leader. Recent developments, in particular in computer-controlled alignment, will be subject of further industry collaboration.

The quasicrystal group has currently three DFG funded projects and has submitted proposals for another four in the last phase of the DFG priority program. Great efforts went into new PhD programs with the Russian Academy of Sciences and other GUS state universities and universities in China. In the framework of this special program designed by the institute and the partners abroad the PhD students are working two to three years in Jülich on a grant supervised by the Jülich Doktorandenausschuß, but they will pass their examina in their home university.

Outstanding results of the year 2000:

- In Hilbert-transform spectroscopy, a high dynamic power range of around 5 orders and broad spectral range of 2 orders have been realised by high-Tc grain-boundary Josephson junctions. A prototype of terahertz Hilbert-transform spectrum analyser integrated into a Stirling cooler has been developed and its application for the optimisation of single line operation of far-infrared optically-pumped gas laser has been demonstrated (in collaboration with IRE RAS, Moscow).
- The aberration corrected 200 keV transmission electron microscope has, after the curing of a large number of operation difficulties, at last reached stable high-quality operating conditions. The enormous, partially very frustrating efforts dedicated to the prototype in recent years are bearing ample fruit in the form of excellent high-resolution results.
- Studies of the structure of n-i-p microcrystalline solar cells revealed that the nucleation of the intrinsic absorber layer on the highly crystalline n-type contact layer determines the microstructure. The local epitaxy results in crystalline columns extending throughout the whole intrinsic layer, even if highly amorphous growth conditions are chosen.
- We have achieved a world record in high Tc SQUID sensitivity of 6 $fTHz^{-½}$ at 77 K. This was demonstrated together with our industrial partners, Tristan Inc. and STL, at exhibitions at HvH Symposium at PTB Berlin and at ASC2000 in the US.

Prof. Dr. Knut Urban

Institute for Microstructure Research

Personnel 2000/2001 and areas of activity

Scientific Staff

Dr. Y. Divin	Hilbert-spectroscopy	(23.42.0)
Dr. Ph. Ebert	Scanning tunneling microscopy of semiconductors and quasicrystals	(23.55.0, 23.42.0)
Dr. M. Faley	High-T_c-Superconductor SQUIDs, Multilayer structures, SQUID-Microscopy	(23.42.0)
Dr. M. Feuerbacher	Plasticity of quasicrystals	(23.55.0)
Dr. B. Grushko	Crystal growth, phase diagrams of alloys	(23.55.0)
Dr. C.L. Jia	Characterization of superconductors, diamond and electroceramic films by high-resolution electron microsopy	(23.42.0)
Dr. M. Lentzen	Reconstruction techniques in high-resolution electron microscopy, Cs-corrected transmission electron microscopy for imaging of interfaces in semiconductors and of superconducting materials	(23.42.0, 23.55.0)
Dr. M. Luysberg	Transmission electron microscopy of semiconductor heterostructures, low-temperature GaAs and microcrystalline silicon	(23.42.0)
Dr. U. Poppe	Superconductivity, tunneling spectroscopy, High-T_c superconductor thin films and multilayers, SQUID-Microscopy	(23.42.0)
Dr. A. Thust	Reconstruction techniques in high-resolution electron microscopy, Cs-corrected transmission electron microscopy for imaging of interfaces in semiconductors, electron microscopy of superconducting materials	(23.42.0, 23.55.0)
Prof. Dr. K. Urban	Head of Institute	(23.42.0, 23.55.0)

Technical Staff

M. Beyss	Crystal growth, Materials preparation and characterization	(23.55.0)
DI W. Evers	Physical experimental technique, low temperature technique, thin film production	(23.55.0, 23.42.0)
A. Fattah	Crystal growth, Materials preparation and characterization	(23.55.0)
K. Fischer	Crystal growth, Materials preparation and characterization	(23.55.0)
R. Fischer	Metallography, Materials preparation and characterization	(23.55.0)
DI K.-H. Graf	Electronics, Electronic data processing, scanning tunneling microscopy	(23.55.0, 23.42.0)
D. Meertens	Metallography, semiconductor preparation, scanning- and transmission electron microscopy	(23.55.0, 23.42.0)
W. Pieper	Technical supervisor, Centre for High Resolution Electron Microscopy	(23.55.0, 32.42.0)
I. Rische-Radloff	Secretary	
K. Schwill	Trainee	
R. Speen	SQUID-Microscopy, Sputtering systems	
C. Thomas	Crystal growth, Materials preparation and characterization	(23.55.0)
G. Waßenhoven	Photolaboratory, photography technique	(23.55.0, 23.42.0)
E. Würtz	Metallography, semiconductor preparation, scanning and transmission electron microscopy	(23.55.0, 23.42.0)

Junior scientists

Dr. Y. Qin	Cs-corrected transmission electron microscopy of electroceramic thin films	(23.42.0)
Dr. L. Houben	Structure characterization of microcrystalline silicon thin films and solar cells. Investigation of potential distributions at grain boundaries in semiconductors and semiconductor devices by holographic imaging.	(23.42.0)
Dr. K. Tillmann	Quantitative analysis of semiconductor heterostructures by high-resolution transmission electron microscopy and finite element simulations	(23.42.0)

Doctor students

V. Chirotov	Broadband Hilbert-Transform Spectroscopy with high-T_c Josephson junctions	(23.42.0)
M. Heggen	Plasticity of quasicrystals and complex intermetallic phases	(23.55.0)
B. Jahnen	Interdiffusion in antimonide-based heterostructures	(23.42.0)
H.Z. Jin	Investigation of electroceramic thin films by high resolution electron microscopy	(23.42.0)
P. Schall	Plasticity of quasicrystals and related intermetallic phases	(23.55.0)
F. Kluge	Scanning tunneling microscopy of quasicrystals	(23.55.0)
S. Mi	Formation of intermetallic and quasicrystalline phases in ternary alloys of aluminium with transition metals	(23.55.0)
U. Semmler	Diffusion and dynamic effects on compound semiconductor surfaces	(23.42.0)
J. Wang	The nature of plasticity in quasicrystalline alloys and related approximants	(23.42.0)
M. Winter	Microwave frequency standards	(23.42.0)
M. Yurechko	Formation of intermetallic phases in ternary alloys of aluminium with transition metals	(23.55.0)

Diploma students

D. Kirch	He-Implantation into SiGe/Si Heterostructures	(23.42.0)
Th. Lange	Microstructural investigations of icosahedral Zn-Mg-RE quasicrystals	(23.42.0)
C. Scholten	Influence of the microstructure of microcrystalline silicon solar cells on their optoelectronic properties	(23.42.0)

Guests

P. Shadrin	AFM and LSM of high T_c Josephson junctions	
Dr. M. Vijayalakshmi	Irradiation-induced phase transformations in quasicrystals	(23.55.0)
Dr. J. Wu	Electronmicroscopy and production of oxide films	(23.42.0)
Prof. Dr. R. Wang	Quasicrystalline alloys	(23.55.0)
Prof. Dr. J. Gui	Ferroelectrics	(23.42.0)
Prof. Ohnuki	Irradiated metallic heterostructures	(23.55.0)

Structural Properties of Microcrystalline Si Solar Cells

C. Scholten, L. Houben, M. Luysberg

Institut für Mikrostrukturforschung

The structural properties of high efficiency microcrystalline nip solar cells grown by plasma enhanced chemical vapor deposition are investigated by transmission electron microscopy, X-ray diffraction, and Raman spectroscopy. Surprisingly, solar cells with the highest efficiency of about 8% [1] do *not* have the highest degree of crystallinity. Best performance is achieved at a crystalline volume fraction of about 70%, where small crystalline columns are surrounded by amorphous material. In general, the microstructure of all solar cells investigated is greatly affected by the nucleation onto the highly crystalline n-layers. Even under nearly amorphous deposition conditions of the i-layer individual crystalline columns extend throughout the whole solar cell.
F&E-Nr: 2342 8000

Recently, the interest in microcrystalline solar cells increased, because their production by plasma enhanced chemical vapor deposition is cheap, easily implemented onto large area and compatible with the amorphous silicon technology. For the solar cells investigated here first, n-type microcrystalline contact layers are deposited onto textured ZnO substrates choosing highly crystalline growth conditions, in order to achieve high conductivity. Secondly, intrinsic absorber layers are grown with different SiH_4 concentrations in H_2 (SC) ranging from 2% to 7%. Thirdly the p-type μc-Si:H layer is grown at a SC of 2% followed by the deposition of the ZnO front contact. In all cases investigated columnar structures of the microcrystalline silicon layers are observed. The dark field electron micrograph (Fig. 1) is obtained from a solar cell, where the i-layer was grown at a SC of 6.5%. Bright areas are caused by crystallites, which have the same crystallographic orientation with respect to the electron beam. The TCO (transparent conductive oxide, ZnO) appears dark. The columns consisting of highly twinned crystallites always extend perpendicular to the textured TCO substrate's surface resulting in a fan-like arrangement at the cusps. Further investigation of the nucleation of the n-layer on the ZnO substrate by high resolution electron microscopy shows a high density of randomly orientated crystallites forming a porous layer, which is in agreement with our previous observations for the growth of highly crystalline Si films e.g. on glass substrates [2,3]. Thus, the nucleation of μc-Si on ZnO is similar to that on glass substrates.

Choosing more amorphous-like growth conditions for the i-layer, i.e. a SC of 7%, results in individual crystalline columns extending throughout the whole layer. This is seen

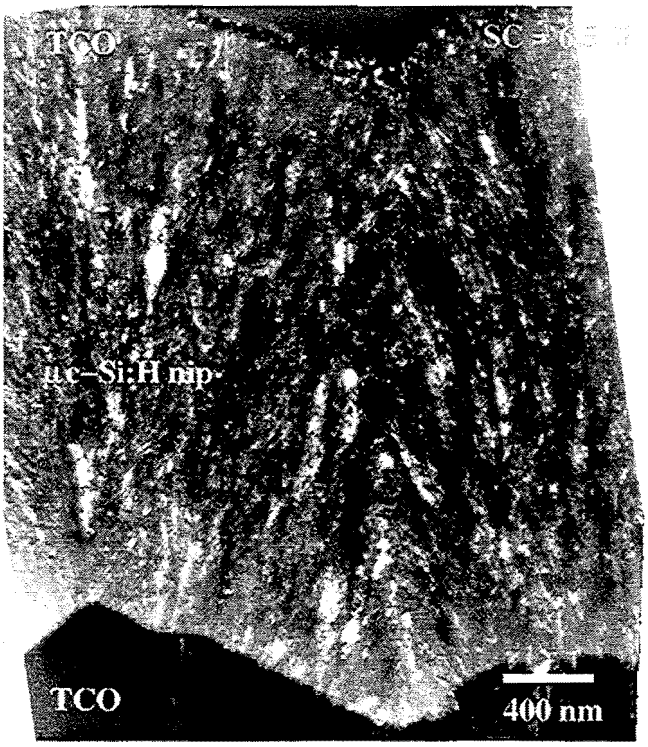

Figure 1: Dark field electron micrograph showing a microcrystalline solar cell grown at a SC of 6.5% in cross section. The ZnO (TCO) appears dark (bottom). Bright areas corrspond to crystallites of the same crystallographic orientation.

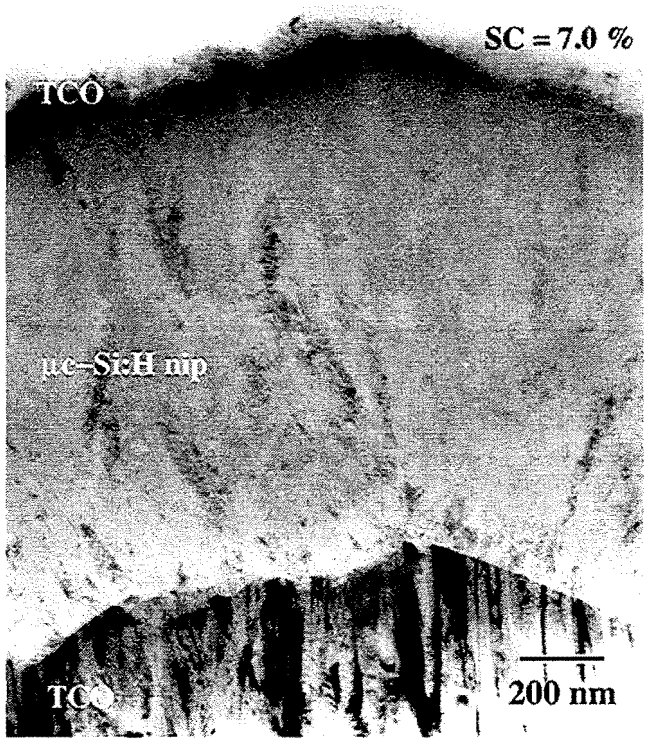

Figure 2: Bright field electron micrograph showing a solar cell grown at a SC of 7%. Dark areas correspond to crystallites fulfilling the Bragg condition. The contrast variation within the TCO (bottom) reflects its polycrystallinity.

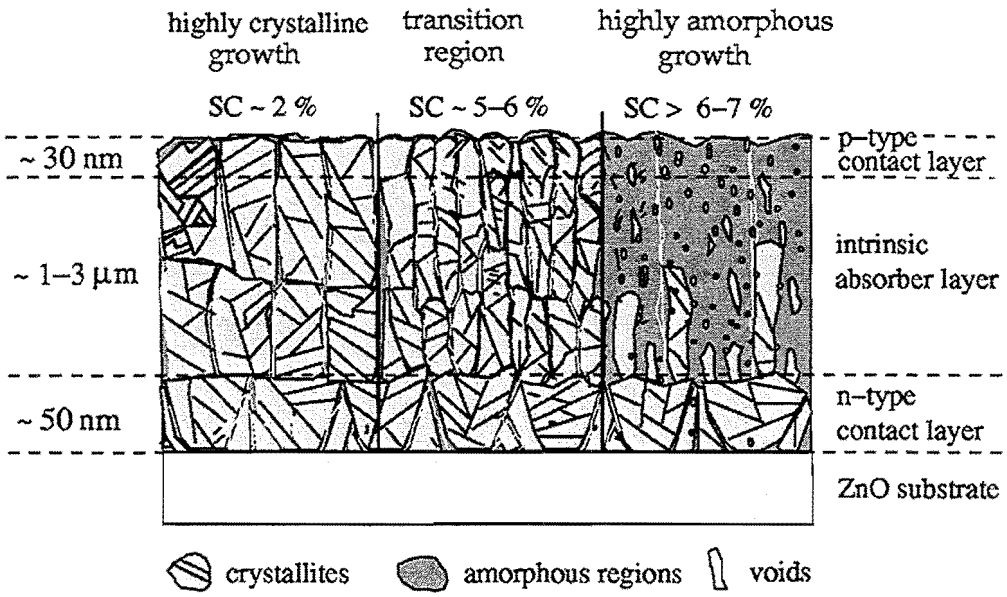

Figure 3: The characteristic microstructure for three solar cells grown under highly crystalline (left hand side) to nearly amorphous (right hand side) conditions are shown schematically. For details see text.

on the bright field image of such a solar cell (Fig.2), where dark areas correspond to crystalline regions fulfilling the Bragg condition. Dark field images of this sample reveal that additionally to the isolated crystalline columns, small crystallites are formed within the amorphous matrix. The polycrystallinity of the ZnO substrate is reflected by the change in contrast (bottom of Fig.2). The observation of extended crystalline columns is in contradiction to the growth on glass substrates, where small crystallites embedded in an amorphous matrix are formed through spontaneous nucleation [2].

The results of our structural characterizations are summarized in Figure 3, where solar cells with crystalline volume fractions of 90% (left and side), 70% (middle) and about 10 % (right hand side) are shown schematically. The n-doped contact layer of a thickness of about 50 nm is always highly crystalline. The crystalline grains show the typical highly twinned behavior. The nucleation of the intrinsic µc-Si:H on top of the n-layer follows a local epitaxy. As a result, the interface to the n-layer of highly crystalline i-layers cannot be detected by TEM, revealing a perfect epitaxy of individual crystallites with respect to the nuclei of the n-layer. In nearly amorphous material the local epitaxy leads to the growth of individual crystalline columns starting from the n-type layer. Thus, the structural properties of the intrinsic µc-Si:H are determined by the presence of the crystalline nuclei within the n-layer. Finally, the p-conductive layer cannot be distinguished from the i-layer, in all cases investigated. Therefore, the structure of the p-layer, is also dominated by local epitaxy, i.e. despite the highly crystalline growth conditions, the structure is determined by that of the intrinsic microcrystalline Si layer. In all solar cells a high density of cavities was observed, which are predominantly located between the crystalline columns. In particular, the fan-like arrangement of the columns results in large cavities extending from the cusps throughout the whole solar cell.

The maximum conversion efficiency is obtained for solar cells grown close to the transition to amorphous growth [1]. In this case the microstructure is dominated by small crystalline columns embedded into amorphous material, as schematically shown in the middle of Figure 3. The structure of the incoherent grain boundaries between the columns can be assumed to be amorphous-like, which implies that the paramagnetic defects caused by dangling bonds are reduced due to hydrogen passivation. For our solar cells, the maximum of the conversion efficiency is correlated to a maximum of the fill factor, which indicates a minimum of the recombination losses [1]. It may possibly be concluded, that the reduction of the recombination loss can be attributed to the structure of the grain boundaries. However, further analysis of the electrical properties of grain boundaries in microcrystalline silicon are required to support this view.

Acknowledgments

The growth and electrical characterization of the solar cells as well as the fruitful discussion with O.Vetterl, F. Finger, and R. Carius (IPV) are greatfully acknowledged.

References

[1] O.Vetterl, R. Carius, L. Houben, C. Scholten, M. Luysberg, A. Lambertz, F. Finger, H. Wagner, Materials Research Society Symposium, Vol. 609, in press

[2] L. Houben, M. Luysberg, P. Hapke, R. Carius, F. Finger, H. Wagner, Phil. Mag. A, 77, 1447 (1998)

[3] M. Luysberg, P. Hapke, F. Finger, R. Carius, Phil. Mag. A, **75**, 31 (1997)

Low Noise HTS dc-SQUID Flip-Chip Magnetometers and Gradiometers

M.I.Faley[1], U.Poppe[1], K.Urban[1], D. N. Paulson[2], T. N. Starr[2], and R. L. Fagaly[2]

[1] *Institut für Festkörperforschung, FZ-Jülich GmbH, D-52425 Jülich, Germany*
[2] *Tristan Technologies inc., San Diego, CA 92121 USA*

We have fabricated HTS dc-SQUID flip-chip sensors with large area multilayer flux transformers. Different layouts of the flux transformers provide a large variety of magnetometers and planar gradiometers. For the magnetometers a resolution ~ 6 fT/√Hz and the planar gradiometers a resolution of about ~ 30 fT/cm·√Hz were routinely obtained at 77 K. The noise was nearly white down to frequencies of few Hz. The sensors were vacuum-tight encapsulated together with a heater and a feed-back coil. This makes the handling of the sensors more reproducible and convenient. Production of the magnetometers and gradiometers in small series was proven. [1]
F&E-Nr: 23420

The flip-chip sensor consisted from a dc-SQUID and a multilayer flux transformer made on a separate substrates. Single- or 30° bicrystal 1 cm x 1 cm $SrTiO_3$ substrates were used for the preparation of the dc-SQUIDs. For the preparation of the flux transformers we have used single crystal 10 mm x 10 mm $SrTiO_3$ substrates and ∅ 30 mm $LaAlO_3$ or $SrTiO_3$ wafers.

Due to the damage-free interfaces and a gently sloping edges produces by a Br-ethanol etching we have achieved the critical current of the transformer inner coil of about 100 mA at 77 K. For the 8 mm HTM-8 magnetometer (see Fig. 1) the pick-up loop has an inductance ~ 20 nH. Limited by the critical current of the flux transformer, the dynamic range of the magnetometer is about 60 μT (peak-to-peak). This allows performing sensitive measurements with the HTM-8 magnetometer even after a movement in earth's field.

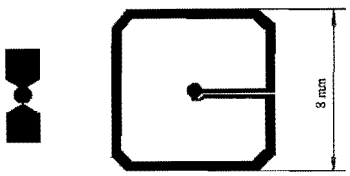

Fig.1. The dc-SQUID and 8 mm multilayer flux transformer (HTM-8) used for the flip-chip magnetometers.

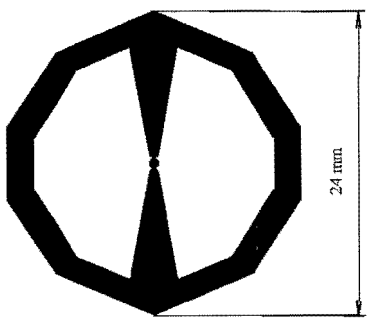

Fig.2. The gradiometric flux transformer for HTG-10R gradiometer. The 1 mm multi-turn coil is placed in the middle of the flux transformers.

A layout of the gradiometric flux transformer used for HTG-10R gradiometer is presented in Fig. 2. The gradiometric flux transformers have a length of about 24 mm and a baseline of about 10 mm.

We have observed that the flip-chip arrangement significantly reduces the effective SQUID inductance and provides a high effective area for the sensors. The effective inductance of the present SQUIDs inductively coupled to the flux transformers is of about 100 pH. In Fig. 3 the flux sensitivity of our flip-chip magnetometers HTM-8 and HTM-16 is compared with the one of the direct-coupled magnetometers [2] and [3] having known SQUID inductance.

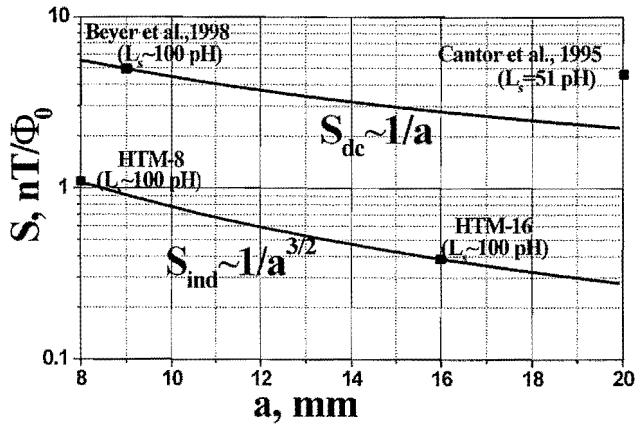

*Fig.3. Flux sensitivity "**S**" vs pick-up loop size "**a**" for direct coupled (S_{dc}) and inductively (flip-chip) coupled (S_{ind}) magnetometers.*

The effective area A_{eff} of a direct-coupled magnetometers A_{eff} is proportional to $A_{pickup}/L_{pu} \sim \mathbf{a}$, where **a** – size; $A_{pickup} \sim \mathbf{a}^2$ – area; and $L_{pickup} \sim \mathbf{a}$ – inductance of the pickup coil. For inductive coupled magnetometers with an optimized multiturn input coil of the flux transformer the effective area is $A_{eff} \sim A_{pickup}/\sqrt{L_{pickup}} \sim \mathbf{a}^{3/2}$. The flux sensitivity $S(nT/\Phi_0) \sim 1/A_{eff}$. The large area flip-chip magnetometers have a significant advantage in flux sensitivity compared to direct-coupled magnetometers.

TABLE 1
FLUX SENSITIVITIES AND NOISE ACHIEVED FOR THE FLIP-CHIP SENSORS

Sensor type	Flux sensitivity	Noise at 1 kHz
HTM-8	1 nT/Φ_0	20 fT/√Hz
HTM-16	0.4 nT/Φ_0	6 fT/√Hz
HTG-10	2.2 nT/cmΦ_0	40 fT/cm√Hz
HTG-10R	1.7 nT/cmΦ_0	30 fT/cm√Hz

The typical sensitivities and noise achieved for the flip-chip sensors are listed in the Table 2. The noise spectra of the HTM-8, HTM-16 magnetometers, and HTG-10 gradiometer are presented in Fig.4-6, correspondingly. Recently, the noise data of our magnetometers were independently confirmed during a common measurement with STL-electronics in the new shielded room of PTB (Berlin).

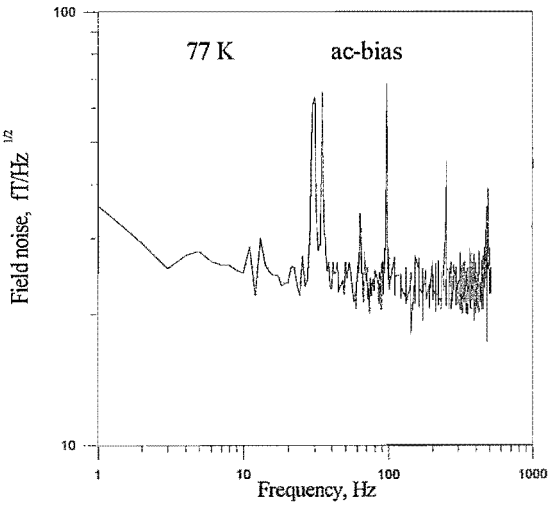

Fig.4. Noise spectrum of HTM-8, measured inside a 3-layer μ-metal shield and a superconducting shield.

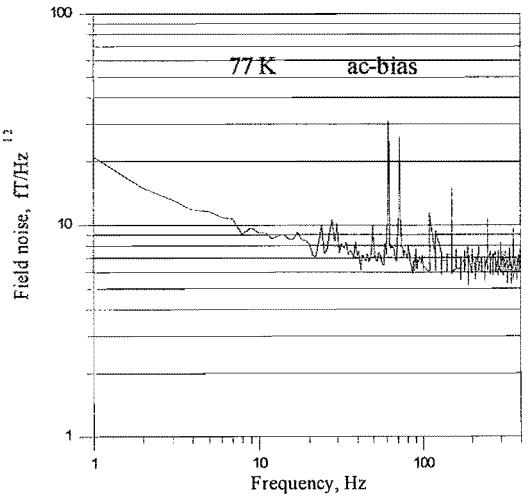

Fig.5. Noise spectrum of HTM-16, measured inside a 3-layer μ-metal shield and a superconducting shield.

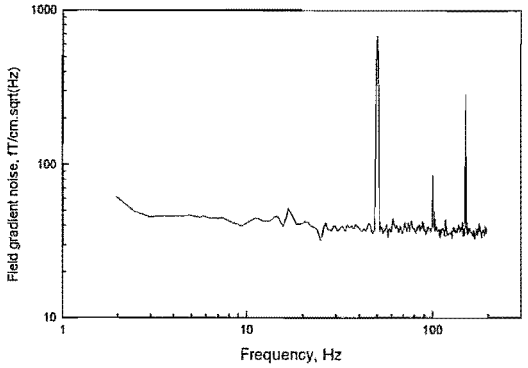

Fig.6. Noise measurement with a flip-chip gradiometer in a weak magnetic shielding. The shielding factor is about 100 at 50 Hz.

To ensure a long and reliable service life for the sensors, they need to be encapsulated. We enclose the sensors in fiber-glass epoxy capsulations. The capsulations are vacuum-tight sealed. This prevents the HTS films from degradation by ambient atmosphere and humidity. Inside the capsulation a modulation coil and nonmagnetic Pt resistor are integrated. The latter one is fixed to the SQUID and serves both as a thermometer or as a heater. The heater allows easy removal of trapped magnetic flux to improve the noise properties of the magnetometer.

The flux noise of the HTM-16 is about 15 $\mu\Phi_0/\sqrt{Hz}$. For the 100 pH SQUIDs a flux noise ~ 5 $\mu\Phi_0/\sqrt{Hz}$ was achieved (see, *e.g.*, [4]). This means that for our sensors there is a significant potential for further improvements in the field and the field gradient resolution even with the present layouts. A resolution of the HTM-16 magnetometers of about 2 fT/√Hz seems to be possible in future. Similar field noise originates from Al-coated Mylar foil used for a thermal insulation in fiber-glass cryostats intended for operation with liquid helium (4.2 K). An optimum construction of the liquid nitrogen cryostats can be made with a modified thermal insulation without such foil. Thus, one can expect to achieve later a field resolution below 1 fT/√Hz for the HTS systems operating at 77 K. For this purpose a magnetometers with a larger pickup coils (~30 mm) need to be developed.

[1] M.I.Faley, U.Poppe, K.Urban, D.N.Paulson, T.N.Starr, and R.L.Fagaly, Submitted to Applied Superconductivity Conference, ASC 2000, Sept. 17-22, 2000, Virginia, USA. Report 5EK05.

[2] J.Beyer, D.Drung, F.Ludwig, T.Minotani, and K.Enpuku, *Appl. Phys. Lett.*, **72**, No. 2, pp. 203-205 (1998).

[3] R.Cantor, L.P.Lee, M.Teepe, V.Vinetskiy, and J.Longo, *IEEE Transactions on Appl.Supercond.* **5**, No. 2, pp. 2927-2930 (1995).

[4] K.Enpuku, T.Minotani, F.Shiraishi, A.Kandori, and S.Kawakami, *IEEE Transactions on Appl.Supercond.*, **9**, No. 2, pp. 3109-3112 (1999).

$YBa_2Cu_3O_7$ [100]-tilt grain boundary bicrystal Josephson junctions with high I_cR_n products

U. Poppe, Y.Y. Divin, M. I. Faley, C. L. Jia and P. M. Shadrin

Institut für Mikrostrukturforschung

The surface morphology, microstructure and transport properties of epitaxial $YBa_2Cu_3O_7$ thin films deposited on vicinal substrates of $SrTiO_3$ by high pressure oxygen sputtering were studied. Furthermore the electrical and structural properties of $YBa_2Cu_3O_7$ Josephson junctions on vicinal offcut $SrTiO_3$ bicrystals with different grain boundary types were investigated in detail. This included junctions with a 2x 12° tilt or twist of the $YBa_2Cu_3O_7$ c-axis across the grain boundary. In comparison to conventional [001]-tilt grain boundaries bicrystal Josephson junctions showed high I_c R_n –products of up to 1.2 meV at 77 K and up to 8 meV at 4.2 K. IV-curve instabilities, probably of magnetic origin due to flux flow in the electrodes, often could be observed for junctions biased with high current densities.

F&E-Nr: 23420

The use of tilted substrates for the growth of high-T_c thin films can lead to improved properties for different applications. The c-axis of the film usually follows the c-axis orientation of the substrate for vicinal substrates. For larger tilt angles, due to the layered structure of high-T_c materials, the transport properties [1], [2] become more anisotropic and the surface roughness increases due to step bunching and the appearance of grains elongated along the ab-planes of $YBa_2Cu_3O_7$. While [001]-tilt grain boundary junctions with c-axis oriented $YBa_2Cu_3O_7$ thin films are frequently used for fundamental and applied research (e. g. [3], [4], [5]), -apart from step edge junctions- only a few reports on Josephson junctions with different types of grain boundaries have been investigated. Beside early work of Dimos et al [3], who studied the properties of very differently oriented bicrystal junctions, Tafuri et al [6] reported on biepitaxial tilt and twist boundaries with a 45° c-axis tilt of $YBa_2Cu_3O_7$.

We investigated [7] the growth of of 12° c-axis tilted $YBa_2Cu_3O_7$ films deposited on vicinal $SrTiO_3$ bicrystal substrates by high pressure oxygen sputtering and Josephson junctions properties. Furthermore a comparison of [100]-tilt boundary junctions with conventional [001]-tilt grain boundary junctions is presented. Films were patterned for the IV-measurements of the bicrystal Josephson junctions by deep UV photolithography and nonaqueous etching with a 0.1% bromine solution in ethanol. Several bridges with a width between 1 and 16 µm and a length of 6 or 10 µm were patterned across the bicrystal grain boundary for the junction measurements. A schematic diagram showing the crystallographic relations of the bicrystal junctions is given in Fig. 1. The surface morphology of the film and the grain boundary were investigated with a atomic force microscope (AFM) in the acoustic mode. In the AFM image in Fig. 2 one can recognize elongated grains and a [100]-tilt grain boundary (arrow) of the "valley" type, where the c-axes of both crystal parts were 12° tilted towards the grain boundary (see also Fig. 1c). The meandering width was of the order of the grain width which was about 100 nm. Different types of boundaries namely [100]-tilt grain boundaries and [100]-twist grain boundaries were investigated for junctions of different width.

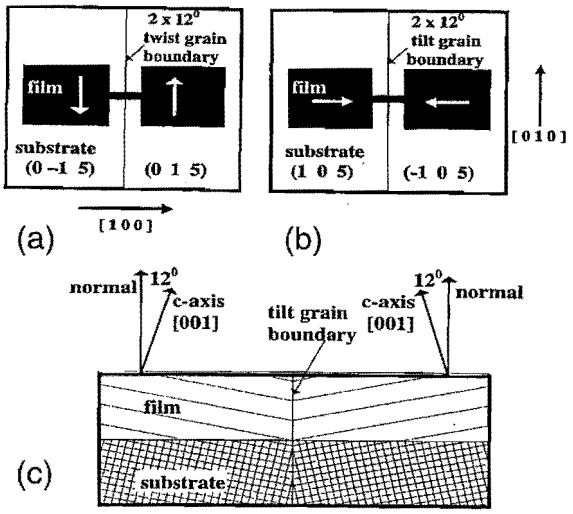

Fig. 1. Schematic diagram showing the crystallographic relations of the bicrystal junctions.

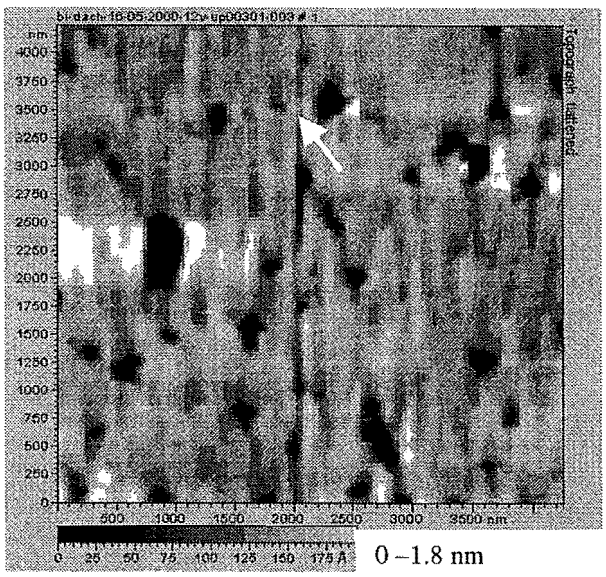

Fig. 2. AFM image (4 µm x 4 µm) of the surface of a $YBa_2Cu_3O_7$ film on a 2x12° bicrystal substrate with a [100]-tilt grain boundary marked by an arrow.

In table I some junction properties for several junctions on several chips (A, B, C, D, E) -which were produced in three different sputtering systems- are listed. All films were approximately 100 nm thick. Most of the junctions showed RSJ-like IV-characteristics and the junction resistance R_n did not significantly change with temperature.

TABLE I
BICRYSTAL JUNCTION PROPERTIES

Sample Number	Ic Rn [mV] 4.2 K	77 K	Rn [Ohm]	Junction width [μm]	Type 2x12° [100]-
A1	6.75	0.46	1.3	5	tilt
A2	7	0.63	1.8	3	tilt
A3	7	0.3	1.3	5	tilt
B1	8.3	1.1	1.8	2.5	tilt
B2	7	1.0	1.5	2.5	tilt
B3	8	1.2	1.9	2.5	tilt
B4	7.5	1.1	1.5	2.5	tilt
C1		0.3	1.0	8.5	tilt
C2		0.23	1.5	6	tilt
C3		0.6	2.7	3.5	tilt
C4		0.72	0.6	16	tilt
E1	3	0.2	12	4	twist
E2	3.4		26	4	twist

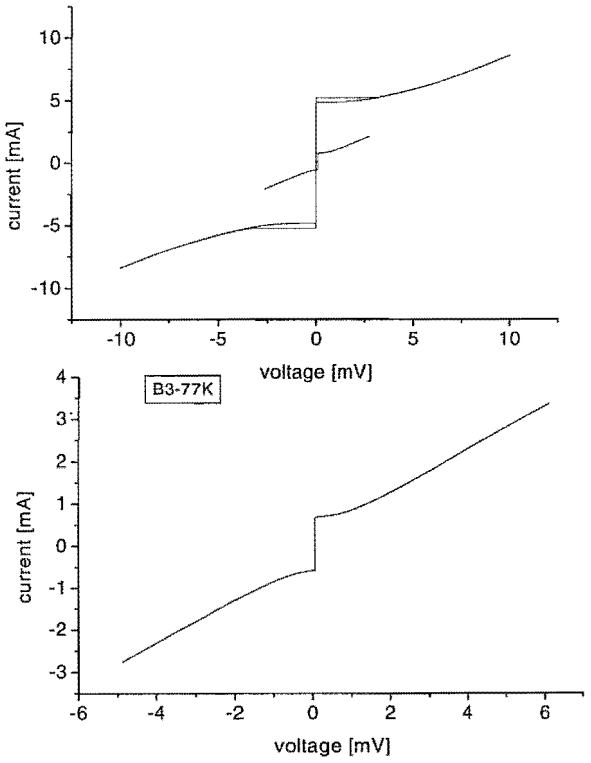

Fig. 3. IV-characteristics of the junction B2 (upper graph) at 4.2K with a slightly hysteretic curve in the range up to 10 mV and at 77K in the range up to 2.5 mV (small curve in the center). Lower graph: IV-curve of junction B3 at 77K.

All junctions were slightly hysteretic at a temperature of 4.2K and non-hysteretic at 77K (Fig. 3). The critical current densities of the tilt junctions varied between 1-2 x 10^6 A/cm^2 at 4.2K and between 0.3-2 x 10^5 A/cm^2 at 77K. Only at higher temperatures (77K) and at voltages above about 7 mV the differential resistance started to increase, indicating flux flow behavior of the c-axis tilted film or a heating effect on the junction. IV-curve instabilities with hysteretic behavior -probably of magnetic origin due to motion of vortices in the electrodes- could often be observed for junctions biased with high current densities. The scattering of the values for I_c and R_n is not too large for junctions of comparable width on one chip as can be seen for the junctions B1-B4 in table I. This might be explained by the fact that the [100]-tilt grain boundary is quite straight showing not much faceting in comparison to conventional [001]-tilt boundaries as can be seen from Fig.2. If one compares the I_c R_n values at 77 K from table I with the data of bicrystal junctions with [001]-tilt boundaries (e. g. [4], [5]) one finds similar results but for junctions at much lower temperatures.

As discussed by Mannhart et al [16] or Tafuri et al [6] due to symmetry reasons the order parameter at the grain boundary should be not so much suppressed in the case of [100]-tilt or [100]-twist boundaries in comparison to conventional [001]-tilt boundaries. Furthermore the local strain near the grain boundary e.g. due to faceting should be lower for the first kind of junctions.

In conclusion Josephson junctions produced on vicinal bicrystals of the 2x12° [100]-tilt type showed very high I_cR_n –products of up to 1.2 meV at 77 K and up to 8 meV at 4.2 K. The reasons might be attributed to the grain boundary microstructure and the different symmetry relations of the order parameter across the boundary in comparison to conventional [001]-tilt boundaries

Acknowledgments:

The authors gratefully acknowledge helpful discussions with J. S. Wu and V. Shirotov as well as technical assistance of W. Evers. This work was supported in part by German Ministry of Sciences under Grant No. 13N7335/8.

References

[1] Y.Y. Divin, U. Poppe, J.-W. Seo, B. Kabius and K. Urban, *Physica C*, **235-240**, 675 (1994)

[2] P. S. Czerwinka, R. Campion, K. Horbelt, P. King, S. Misat, S. Morley, H. U. Habermeier, B. Leibold, *Physica C*, **324**, 96 (1999).

[3] D. Dimos, P. Chaudhari, J. Mannhart, *Phys. Rev. B*, **41**, 4038 (1990)

[4] H. Hilgenkamp, J. Mannhart, *Appl. Phys. Lett.*, **73**, 265 (1998)

[5] K. Enpuku, T. Minotani, F. Shiraishi, A. Kandori, and S. Kawakami, *IEEE Transactions on Appl. Supercond.*, **9**, 3109, (1999)

[6] U. Poppe, Y.Y. Divin, M. I. Faley, J. S. Wu, C. L. Jia, P. M. Shadrin, K. Urban, to be published *in IEEE Trans.on Applied Supercond.* (March 2001)

[7] F. Tafuri, F. Miletto Granozio, F. Carillo, F. Lombardi, U. Scotti Di Uccio, K. Verbist, O. Lebedev, G. van Tendeloo, *Physica C*, **326**, 63 (1999)

[8] J. Mannhart, and H. Hilgenkamp, *Supercond. Sci. Technol*, **10**, 880 (1997)

Investigation of the Al-Cu-Rh phase diagram in the vicinity of the decagonal phase

B. Grushko and M. Yurechko

Institut für Mikrostructurforschung

Phase equilibrium was studied in Al-rich Al-Rh and Al-Cu-Rh alloys. We present a partial Al-Rh phase diagram. In addition to previously reported Al-Rh phases, two complicated orthorhombic compounds were found close to the Al_3Rh composition. Partial 900 and 800°C isothermal sections of the Al-Cu-Rh phase diagram were studied in the vicinity of the decagonal phase. At these temperatures the stable decagonal phase was found to be the only ternary compound. It is in equilibrium with the ternary extensions of three binary Al-Rh phases and at 900°C also with the liquid.

F&E-Nr:

To date a little work has been carried out on the Al-Cu-Rh alloy system where the existence of a stable decagonal phase was reported. Even the binary Al-Rh phase diagram was not known although several Al-Rh compounds were revealed. We report the first investigation of the Al-Rh phase diagram and the phase equilibrium involving the Al-Cu-Rh decagonal phase.

Binary Al-Rh compounds. The Al-Rh phase diagram was found to contain a number of phases isostructural to those in Al-Co [1]. They are AlRh (β-phase) of the CsCl-type structure corresponding to AlCo, hexagonal Al_5Rh_2 (H-phase) corresponding to Al_5Co_2 and monoclinic Al_9Rh_2 corresponding to Al_9Co_2. In addition, high-temperature cubic (C) and monoclinic (V) phases were found close to Al_5Rh_2 and two new orthorhombic phases of close compositions were found at about Al_3Rh.

The O_2-phase of a slightly lower Al concentration exhibited a powder XRD pattern similar to that of orthorhombic Al_3Pd [2], TEM examination also revealed electron diffractograms very similar to those observed in Al-Pd. The patterns can be indexed assuming an orthorhombic unit cell with a=2.34, b=1.65 and c=1.24 nm, which is close to the corresponding Al-Pd phase. The O_1-phase was found at 76 at.% Al. Its electron diffraction pattern can be indexed assuming an orthorhombic unit cell with a=2.38, b=1.64 and c=3.28 nm and systematic extinctions of l=2n+1 for *0kl*, h=2n+1 for *hk0*, $h+l$=2n+1 for *h0l*. The lattice parameters of the O_1-phase and the O_2-phase are related as $a_1 \approx a_2$, $b_1 \approx b_2$ and $c_1 \approx \tau^2 c_2$, where τ is the golden mean. Both orthorhombic phases are related to decagonal phases.

The available data concerning the phase compositions and transition temperatures are summarized in Fig.1. The lattice parameters of the Al-Rh phases are presented in Table 1. All the phases apart from AlRh and the high-temperature C-phase did not show pronounced compositional ranges. The lower temperature limits of the V-phase and C-phase regions have not yet been determined. We have also been unable to clarify the melting temperature of the O_1-phase as yet.

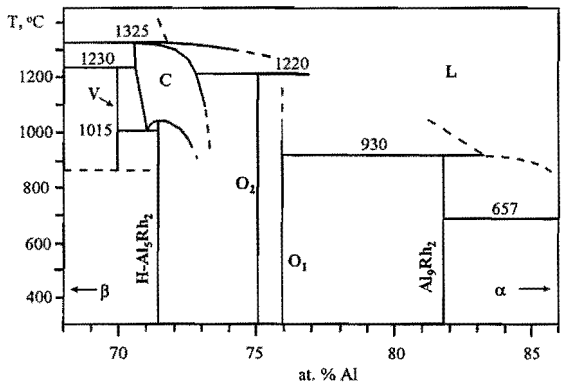

Fig.1. The partial Al-Rh phase diagram. For the phase designation see Table 1, the liquid is designated L, α is fcc Al.

Partial isothermal 900° C and 800°C sections of Al-Cu-Rh. The partial 900°C section of Al-Cu-Rh is shown in Fig.2. Three Al-Rh phases exhibited high Cu solubility. The β-phase extends to more than 35 at.% Cu and its Al concentration achieves 55 at.% at high Cu. The C-phase can contain up to about 13 at.% Cu and the O_2-phase up to about 11 at.% Cu. The Al concentrations of the C-phase and O_2-phase decrease sharply with the increase of the Cu concentration.

The C-phase exhibited a superstructure ordering at its low-Al composition limits. It has there the doubled lattice parameter a=1.5380(2) nm. The existence subregions of C and C_1 were not studied in detail, in Fig.1 the range of the cubic phase is conditionally divided between C and C_1 by

a broken line. The Al_9Rh_2 and H-Al_5Rh_2 phases were found to contain less than 0.5 at.% Cu. The Rh solubility in Al_2Cu formed in the solidified liquid was less than 1 at.%. At 900°C the Al-Cu-Rh decagonal phase is stable in a range of 1-2 at.%, whose center is at about $Al_{64.5}Cu_{16.8}Rh_{18.7}$. It coexists with the liquid and the ternary extensions of the β-phase, the C-phase (including C_1) and the O_2-phase. The decagonal range in Al-Cu-Rh coincides with the higher-Cu part of the decagonal range in Al-Cu-Co [3]. The diffraction patterns of the Al-Cu-Rh and Cu-rich Al-Cu-Co decagonal phases are similar. In a wide range of Cu concentrations the C-phase (including C_1) is in equilibrium with β, and the O_2-phase is in equilibrium with the liquid. The regions marked by (?-s) were not studied in detail.

The investigated part of the 800°C isothermal section is quite similar to that at 900°C. The ranges of the β-phase and O_2-phase extend to still higher Cu than at 900°C. Zero solubility of Cu in H-Al_5Rh_2 was found at this temperature. The decagonal phase is in equilibrium with the ternary extensions of the β-phase, the C-phase (including C_1) and the O_2-phase but not with the liquid. Instead, the O_2-phase was found in equilibrium with β at this temperature. The decagonal region lies around about $Al_{64.0}Cu_{18.0}Rh_{18.0}$. It is slightly shifted from the decagonal region at 900°C towards AlCu. This shift is smaller than that observed in Al-Cu-Co.

A part of the experimental work was performed by J. Gwóźdź, from the Institute of Physics and Chemistry of Metals, University of Silesia, Katowice, Poland, during his visit in FZJ.

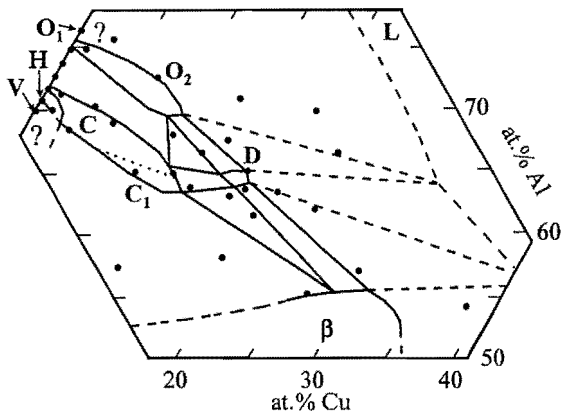

Fig.2. Phase equilibrium at 900°C in Al-Cu-Rh. For the phase designation see Table 1, the liquid is designated L. The compositions of the studied alloys are marked by spots.

References

[1] B. Grushko, R. Wittenberg, K. Bickmann, C. Freiburg, J. Alloys Comp. 233 (1996) 279.
[1] B. Grushko, M. Yurechko, N. Tamura, J. Alloys Comp. 290 (1999) 164.
[3] B. Grushko, Phil. Mag. Lett. 66 (1992) 151.

Table 1. The Al-Rh phases

	Formula	Space group	Lattice parameters *a*, nm	*b*, nm	*c*, nm	*β*,°
	Al_9Rh_2	$P2_1/a$	1.0149	0.6290	0.8557	142.4
O_1	"Al_3Rh"	*	2.38	1.64	3.28	-
O_2	"Al_3Rh"	*	2.34	1.65	1.24	-.
H	Al_5Rh_2	$P6_3/mmc$	0.7905	-	0.7861	-
C	Al_5Rh_2	$Pm\bar{3}$	0.7680	-	-	-
V	Al_7Rh_3	**	1.0309	0.3808	0.6595	102.4
β	AlRh	$Pm\bar{3}m$	0.2980	-	-	-

* Orthorhombic
** Monoclinic

Conservative antiphase boundary in $SrTiO_3$ films on $LaAlO_3$ substrates with $SrRuO_3$ buffer layers

J.S. Wu, C.L. Jia, and K. Urban
Institut für Festkörperforschung, Forschungszentrum Jülich GmbH,
D-52425 Jülich, Germany

J.H. Hao, and X.X. Xi
Department of Physics, The Pennsylvania State University, University Park,
Pennsylvania 16802, USA

We have studied the microstructure of $SrTiO_3$ films on $LaAlO_3$ substrates with $SrRuO_3$ buffer layer using high-resolution transmission electron microscopy. The {111} stacking fault in the $SrRuO_3$ buffer layer propagates into the $SrTiO_3$ film, giving rise to a new type of antiphase boundary in the {110} plane with a crystallographic shear vector of $a/2<001>$. The boundary is a conservative one which does not lead to any charge defects. A model based on dislocation interactions is proposed to explain the generation mechanism of the antiphase boundary.
F&E – Nr: 23.42

In $SrTiO_3$ thin films, a columnar structure has been reported as the dominant structural characteristic [1,2,3,4]. The columnar subgrain boundaries were found to be associated with misfit dislocations at the film/substrate interface in epitaxial $SrTiO_3$ films on $LaAlO_3$ substrates [4]. Recently, employing $SrRuO_3$ as the buffer layer, high-quality $SrTiO_3$ films with near single-crystal level dielectric loss were successfully prepared on $LaAlO_3$ substrates [5]. In this letter, we report a detailed structural analysis of these films by high-resolution transmission electron microscopy (HRTEM). A new type of conservative antiphase boundary was observed. A high density of planar defects in the $SrRuO_3/LaAlO_3$ interface was found in agreement with earlier observations in single-layer $SrRuO_3$ films on $LaAlO_3$ substrates [6]. Instead of perfect misfit dislocations, stacking faults bounding partial dislocations were found to play an important role in misfit accommodation. However, in the $SrTiO_3/SrRuO_3$ interface we hardly find any misfit dislocations since the misfit between $SrTiO_3$ and $SrRuO_3$ is small. The antiphase boundaries identified in $SrTiO_3$ layer are the results of planar defects in the $SrRuO_3$ layer which run across the interface into the $SrTiO_3$ device layers.

The bilayer $SrTiO_3/SrRuO_3$ films were grown by pulsed laser deposition on single crystal $LaAlO_3$ substrates. Details of the growth procedure are given in the literature [5,7].

Figure 1 shows a cross-sectional HRTEM image the $SrTiO_3/SrRuO_3$ interface taken along the [110] zone axis. A $(1\,\bar{1}\,1)$ stacking fault in the $SrRuO_3$ layer (lower part of the image) propagates upward until it reaches the $SrTiO_3/SrRuO_3$ interface. As a consequence, an antiphase boundary is introduced in the $SrTiO_3$ crystal. The stacking fault in the $SrRuO_3$ layer can be determined as an extrinsic one with an extra plane inserted between two $(1\,\bar{1}\,1)$ lattice planes. We use a Burgers circuit exhibiting three closure failures to identify the Burgers vector of the dislocation at the junction of the stacking fault and the antiphase boundary. The projected Burgers vector of the dislocation can be calculated as:

$\boldsymbol{b}_{proj} = a/3[\bar{1}\,1\,\bar{4}] + a/2[1\,\bar{1}\,1] + a/2[\bar{1}\,12] = a/6[\bar{2}\,21]$.

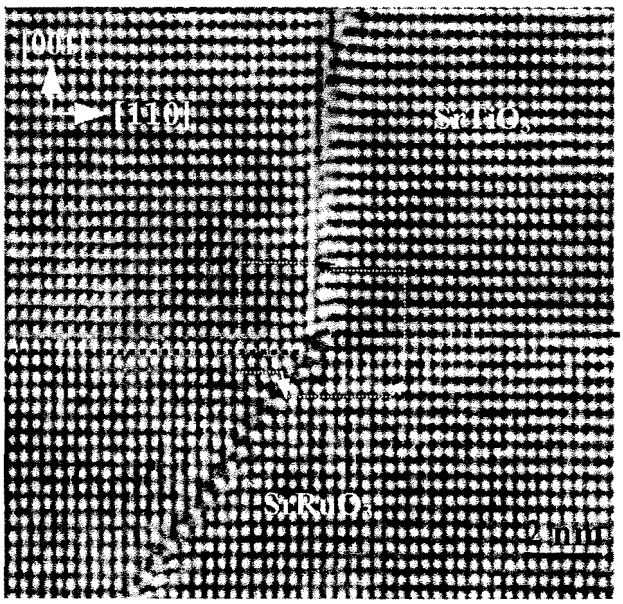

Fig.1 A Cross-sectional HRTEM image of the $SrTiO_3/SrRuO_3$ interface. A staking fault in the $SrRuO_3$ layer propagates upward to the $SrTiO_3$/ $SrRuO_3$ interface and introduces an anti-phase boundary in the $SrTiO_3$ layer.

In general, antiphase boundaries are characterized by a crystallographic shear vector $\boldsymbol{R}$ describing the relative displacement of the two parts of the crystal on either side of the interface. In fig.2, the antiphase boundary in the $SrTiO_3$ layer is in the $(\bar{1}\,10)$ plane. According to figure 1, the crystallographic shear of the antiphase boundary has two possible vectors. The first type is $\boldsymbol{R}=a/2[001]$, as shown in fig. 2(a), while

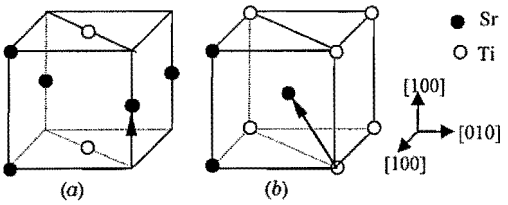

Fig.2 Two atomic structural models of the antiphase boundaries in the $(\bar{1}10)$ plane, with a crystallographic shear vector $\boldsymbol{R}=a/2[001]$ (a) and $\boldsymbol{R}=a/2[\bar{1}\,\bar{1}\,1]$ (b).

the second type has $\boldsymbol{R}=a/2[\bar{1}\,\bar{1}\,1]$ in fig. 2(*b*). The shear vector can only be identified if the same type of defect is studied along another direction, *e.g.* [100].

Figure 3 shows a cross-sectional image of the $SrTiO_3/SrRuO_3$ interface taken along the [100] direction. In order to distinguish the Sr and Ti positions in the $SrTiO_3$ crystal, we construct a structural model of the $SrTiO_3/SrRuO_3$ interface with the atomic layer sequence of $\cdots(SrO)(RuO_2)(SrO)(TiO_2)\cdots$. The simulated image which best matched the experimental one was inserted in the left-hand part of fig.3, where the atomic planes are also indicated. In the $SrRuO_3$ layer part of the image, the relatively bright dots correspond to the Sr atomic positions. In the $SrTiO_3$ layer part under the same imaging conditions, however, there is no pronounced difference in image contrast between the Sr and Ti atomic positions. Connecting those dots representing Sr atoms to form the perovskite cubic unit cells as shown by white rectangles, it is found that they are related to each other by a shear of $a/2[001]$ crossing the antiphase boundary. Thus, the crystallographic shear vector $\boldsymbol{R}$ is determined as $a/2[001]$ which is consistent with the atomic structural model in fig.2(*a*).

We note that the anti-phase boundary is in the $(\bar{1}10)$ plane and the displacement vector $\boldsymbol{R}$ is $a/2[001]$.

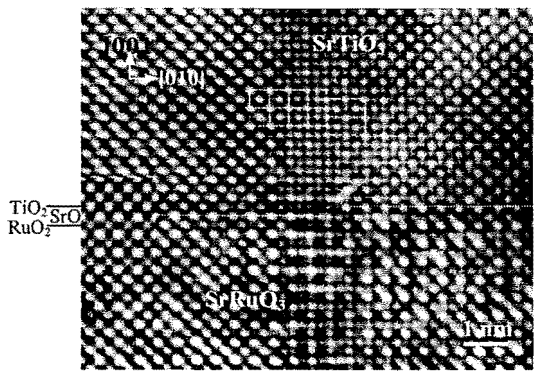

Fig.3 Cross-sectional image taken along the [100] direction. In the middle, an antiphase boundary grows into $SrTiO_3$ crystal from $SrRuO_3$ layer. A simulated image of $SrTiO_3/SrRuO_3$ interface for a defocus value of −68 nm and a sample thickness of 5.2 nm is patched in.

Since $\boldsymbol{R}\cdot\boldsymbol{n}=0$ where $\boldsymbol{n}$ is the normal vector of the boundary plane, the antiphase boundary is a conservative one. It implies that this type of antiphase boundary does not change the local composition nor does it generate any charged defects.

In $SrRuO_3$ crystal with perovskite structure, the {111} stacking fault can be extended by a gliding movement of Shockley partial with $\boldsymbol{b}=a/3\langle 112\rangle$ [8]. As shown in fig.1, the dislocation with projected Burgers vector in the $(\bar{1}10)$ plane being $a/6[\bar{2}21]$ is found at the junction of the $(1\,\bar{1}\,1)$ stacking fault and the $(\bar{1}10)$ antiphase boundary. Considering the possible reactions between dislocations, we can derive the dislocation reaction as:

$$a/3[\bar{1}12] \rightarrow a/6[\bar{2}21] + a/2[001]$$

Since the vector $a/6[\bar{2}21]$ is in the (110) plane, its projection on the plane yields the same result. The Burgers vector $\boldsymbol{b}=a/2[001]$ is obviously the crystallographic shear vector $\boldsymbol{R}$ of the antiphase boundary. In such a way, a {111} stacking fault in $SrRuO_3$ layer transforms smoothly into a {110} antiphase boundary in the $SrTiO_3$ layer.

In conclusion, the columnar subgrain boundary in the $SrTiO_3$ on the $SrRuO_3$ buffer is determined as a new type of antiphase boundary in the $(\bar{1}10)$ plane with a crystallographic shear vector $\boldsymbol{R}$ of $a/2[001]$. Composition fluctuations at the grain boundaries and charged defects harmful to the physical properties are avoided since this type of antiphase boundary is a conservative one. The partial dislocation with $\boldsymbol{b}=a/2\langle 001\rangle$ producing the antiphase boundary in the $SrTiO_3$ layer is dissociated from a Shockley partial with $\boldsymbol{b}=a/3\langle 112\rangle$ bounding a {111} stacking fault in the $SrRuO_3$ buffer layer. This type of antiphase boundary is generated by the stacking fault in the buffer layer which can be considered as the result of 'defect epitaxy'.

J.S. Wu is grateful for support from the Alexander von Humboldt-Stiftung.

References

[1] S. Yamamichi, T. Sakuma, K. Takemura, and Y. Miyasaka, Jpn. J. Appl. Phys., Part 1 **30**, 2193 (1991).
[2] H. Yamaguchi, S. Matsubara, and Y. Miyasaka, Jpn. J. Appl. Phys., Part 1 **30**, 2197 (1991).
[3] M.E. Tidjani and R. Gronsky, Appl. Phys. Lett. **58**, 765 (1991).
[4] L. Ryen, E. Olsson, L.D. Madsen, X. Wang, C.N.L. Edvardsson, S.N. Jacobsen, U. Helmersson, S. Rudner, and L.-D. Wernlund, J. Appl. Phys. **83**, 4884 (1998).
[5] H.C. Li, W.D. Si, A.D. West, and X.X. Xi, Appl. Phys. Lett. **73**, 190 (1998).
[6] P. Lu, F. Chu, Q.X. Jia, and T.E. Mitchell, J. Mater. Res. **13**, 2302 (1998).
[7] V.I. Merkulov, J.R. Fox, H.C. Li, W.D. Si, A.A. Sirenko, and X.X. Xi, Appl. Phys. Lett. **72**, 3291 (1998).
[8] O. Eibl, P. Pongratz, and P. Skalicky, Phil. Mag. **B 57**, 521 (1988).

Publications in refereed journals

Apostolopoulos G.1; Herfort J.1; Däweritz l.1; Ploog K.H.1; Luysberg M.
1 Paul Drude Institut, Berlin
Reentrant Mound Formation in GaAs(001) Homoepitaxy Observed by ex situ Atomic Force Microscopy
Phys. Rev. Lett. 84, 3358 (2000)
23.42.0

Baier F.1; Müller M.A.1; Grushko B.; Schäfer H.E.1
1 ITAP, Univ. Stuttgart 70569 Stuttgart, D
Atomic defects in quasicrystals: an approach with positron annihilation spectroscopy and time differential dilatometry.
Mat. Sci. Eng. A294-296, 650-653 (2000)
23.55.0

Bartsch M.1; Geyer B.1; Häussler D.1; Feuerbacher M.; Urban K.; Messerschmidt U.1
1 Max-Planck-Institut für Mikrostrukturphysik, Weinberg 2, Halle/Saale, D-06120, Germany
Plastic properties of icosahedral Al-Pd-Mn single quasicrystals
Mat. Sci. Eng. A294-296, 761 (2000)
23.55.0

Blüher R.1; Frank W.1,2; Grushko B.
1 ITAP, Univ. Stuttgart 70550 Stuttgart, D
2 MPI f. Metallforshung 70506 Stuttgart, D
Diffusion of 103Pd and 195Au in icosahedral Al 70.2Pd21.3Mn8.5 under proton irradiation.
Mat. Sci. Eng. A294-296, 689-692 (2000)
23.55.0

Damson B.1; Weller M.1; Feuerbacher M.; Grushko B. ; Urban K.
1 MPI f. Metallforschung 70174 Stuttgart, D
Mechanical spectroscopy of quasicrystals.
J. of Alloys and Compounds 310, 184-189 (2000)
23.55.0

Damson B.1; Weller M.1; Feuerbacher M.; Grushko B.; Urban K.
1 MPI f. Metallforschung 70174 Stuttgart
Mechanical spectroscopy of d-AlNiCo and i-AlPdMn.
Mat. Sci. Eng. A294-296, 806-809 (2000)
23.55.0

Divin Y.Y.; Poppe U.; Volkov O.Y.1; Pavlovskii V.V.1
1 Institute of Radioengineering & Electronics of RAS, Moscow 103907, Russian Federation
Frequency-selective incoherent detection of terahertz radiation by high-Tc Josephson junctions
Appl. Phys. Lett., Vol. 76, No. 20, 2826-2828 (2000)
23.42.0

Döblinger M.1; Wittmann R.1; Gerthsen D.1; Grushko B.
1 Lab. Elektronenmikroskopie, Univ. Karlsruhe 76128 Karlsruhe, D
Structural relationship and mutual transformation of approximants of the decagonal Al-Co-Ni phase.
Mat. Sci. Eng. A294-296, 131-134 (2000)
23.55.0

Ebert Ph.; Chao K.J.1; Niu Q.1; Shih C.K.1; Plummer E.W.2; Urban K.
1 Department of Physics, University of Texas, Austin
2 Department of Physics, University of Tennessee, Knoxville
Scanning tunneling microscopy of defects in quasiperiodically ordered surfaces
Mat. Sci. Eng. A, 294-296, 826-829 (2000)
23.55.0

Ebert Ph.; Urban K.; Aballe L.1; Chen C.H.1; Horn K.1; Schwarz G.1; Neugebauer J.1; Scheffler M.1
1 Fritz-Haber-Institut Berlin
Symmetric versus non-symmetric structure of the phosphorous vacancy in InP(110)
Phys. Rev. Lett. 84, 5816-5819 (2000)
23.55.0

Ebert Ph.
Atomic structure of Point Defects in Compound Semiconductor Surfaces.
Current Opinion in Solid State and Materials Science, in press
23.55.0

Feuerbacher M.; Klein H.1; Bartsch M.2; Messerschmidt U.2; Urban K.
1 European Synchrotron Radiation Facility, Pluo E202, BP 220, 38043 Grenoble Cedex, France
2 Max-Planck-Institut für Mikrostrukturphysik, Weinberg 2, D-06120 Halle, Saale, Germany
A comparative study of the plastic behaviour of icosahedral and x'-Al-Pd-Mn.
Mat. Sci. Eng. A 294-296, 736 (2000).

Gavilano J.L.1; Mushkolaj S.1; Ott H.R.1; Apih T.1; Dolinsek J.1; Dubois J.M.1; Urban K.
1 Ecole des Mines de Nancy, LSG2M, Nancy F
NMR Studies of an icosahedral Al72.4 Pd20.5 Mn 7.1 quasicrystal
Physica B 284-288, 1167-1168 (2000)
23.42.0

Gebauer J.1; Börner F.1; Krause-Rehberg R.1; Staab T.E.M.2; Bauer-Kugelmann W.1; Kögel G.1; Triftshäuser W.1; Specht P.3; Lutz R.C.3; Weber E.R.3; Luysberg M.
1 ISG, FZ Jülich
2 Laboratory of Physics, Helsinki University of Technology, Finnland
3 Department of Materials Science, University of California, Berkeley, Ca 94720, USA
Defect identification in GaAs grown at low temperatures by positron annihilation
J. Appl. Phys. 87, 8368 (2000)
23.42.0

Gebauer J.1; Krause-Rehberg R.1; Domke C.; Ebert Ph.; Urban K.; Staab T.E.M.2
1 FB Physik, Universität Halle
2 Lab. of Physics, Helsinki University of Technology
Direct identification of As vacancies in GaAs using positron annihilation calibrated by scanning tunneling microscopy
Phys. Rev. B, in press
23.55.0

Geyer B.1; Bartsch M.1; Feuerbacher M.; Urban K.; Messerschmidt U.1
1 Max-Planck-Institut für Mikrostrukturphysik, Weinberg 2, Halle/Saale, D-06120, Germany
Plastic deformation of icosahedral Al-Pd-Mn single quasicrystals.
I. Experimental Results
Phil. Mag. A 80, 1151-1163 (2000)
23.55.0

Grushko B.; Gwózdz J.; Yurechko M.
Investigation of the Al-Cu-Rh phase diagram in the vicinity of the decagonal phase
J. Alloys Comp., 305, 219-224 (2000)
23.55.0

Grushko B.
Composition and precipitation behavior of icosahedral Al-Pd-Mn quasicrystals.
Mat. Sci. Eng. A294-296, 45-48 (2000)
23.55.0

Gwozdz J.1; Grushko B.; Surowiec M.1
1 University of Silesia, Inst. Phys. Chem. Metals. 40-007 Katowice, Poland
Mosaic structure of single quasicrystals.
Mat. Sci. Eng. A294-296, 49-52 (2000)
23.55.0

Heggen M.; Feuerbacher M.; Schall P.; Klein H.1; Fisher I.R.2; Canfield P.C.2 Urban K.
1 European Synchrotron Radiation Facility, Pluo E202, BP 220, 38043 Grenoble Cedex, France
2 Ames Laboratory and Department of Physics and Astonomy, Iowa State University, Ames, Iowa 50011, USA
Plastic deformation of icosahedral Zn-Mg-Dy single quasicrystals
Phil. Mag. Lett., Vol. 80, No. 3, 129-136 (2000)
23.55.0

Heggen M.; Feuerbacher M.; Schall P.; Klein H.1; Fisher I.R.2; Canfield P.C.2; Urban K.
1 European Synchrotron Radiation Facility, Pluo E202, BP 220, 38043 Grenoble Cedex, France
2 Ames Laboratory and Department of Physics and Astonomy, Iowa State University, Ames, Iowa 50011, USA
Plasticity of icosahedral Zn-Mg-Dy single quasicrystals
Mat. Sci. Eng. A 294-296, 781 (2000)
23.55.0

Jia C.L.; Siegert M.1; Urban K.
1 ISI, FZ Jülich
Structure and defects of the interface between BaTiO3 thin films and MgO substrates
23.42.0

Jiang X.1; Fryda M.1; Jia C.L.
1 Fraunhofer-Institut für Schicht- und Oberflächentechnik, Bienroder Weg 54, 38108 Braunschweig
High-quality CVD diamond films on silicon: recent progresses
Diamond Relat. Mater. 9, 1640 (2000)
23.42.0

Jiang X.1; Jia C.L.
1 Fraunhofer-Institut für Schicht- und Oberflächentechnik, Bienroder Weg 54, 38108 Braunschweig
Direct epitaxy of diamond on Si(100) and surface-roughening-induced crystal misorientation
Phys. Rev. Lett. 84, 3658 (2000)
23.42.0

Khoukaz C.1; Galler R.1; Mehrer H.1; Canfield P.C.2; Fisher I.R.2; Feuerbacher M.
1 Institut für Metallforschung1, Universität Münster, D-48149 Münster, Germany;
2 Ames Laboratory and Department of Physics and Astonomy, Iowa State University, Ames, Iowa 50011, USA
Diffusion of 57Co in Decagonal AlNiCo-Quasicrystals
Mat. Sci. Eng. A, 294-296, 697 (2000)
23.55.0

Klein H.1; Feuerbacher M.; Urban K.
1 European Synchrotron Radiation Facility, Pluo E202, BP 220, 38043 Grenoble Cedex, France
Dislocations in Al-Pd-Mn approximants: an HREM study.
Mat. Sci. Eng. A294-296, 769 (2000)
23.55.0

Klein H.; Feuerbacher M.; Schall P.; Urban K.
Bending experiments on the ('-(Al-Pd-Mn) quasicrystal approximant
Phil. Mag. Lett., Vol. 80, No. 1, 11-18 (2000)
23.55.0

Kluge F.; Ebert Ph.; Grushko B.; Urban K.
Influence of grown-in voids on the structure of cleaved icosahedral Al-Pd-Mn quasicrystal surfaces
Mat. Sci. Eng. A 294-296, 874-877 (2000)
23.55.0

Lei C.H.; Jia C.L.; Lisoni J.G.1; Siegert M.1; Schubert J.1; Buchal Ch.1; Urban K.
1 ISI, FZ Jülich
Structural studies of epitaxial BaTiO3 film deposited on MgO-buffered r-plane cut sapphire
J. Crystal Growth 219, 397 (2000)
23.42.0

Lei C.H.; Jia C.L.; Siegert M.1; Urban K.
1 ISI, FZ Jülich
Investigation of {111} stacking faults and nanotwins in epitaxial BaTiO3 thin films by high-resolution transmission electron microscopy
Phil. Mag. Lett., Vol. 80, No. 6, 371-380 (2000)
23.42.0

Lentzen M.; Urban K.
Reconstruction of the projected crystal potential in transmission electron microscopy by means of a maximum-likelihood refinement algorithm
Acta Cryst. A 56, 235-247 (2000)
23.42.0

Messerschmidt U.1; Bartsch M.1; Geyer B.1; Feuerbacher M.; Urban K.
1 Max-Planck-Institut für Mikrostrukturphysik, Weinberg 2, Halle/Saale, D-06120, Germany
Plastic deformation of icosahedral Al-Pd-Mn single quasicrystals.
II. Interpretation of the experimental results
Philosophical Magazine A 80, 1165-1181 (2000)
23.55.0

Messerschmidt U.1; Bartsch M.1; Geyer G.1; Häussler D.1; Feuerbacher M.; Urban K.
1 Max-Planck-Institut für Mikrostrukturphysik, Weinberg 2, Halle/Saale, D-06120, Germany
Microprocesses of the plastic deformation of icosahedral Al-Pd-Mn single quasicrystals.
Mat. Sci. Eng. A.294-296, 761 (2000)
23.55.0

Quadbeck P.; Ebert Ph.; Urban K.; Gebauer J.1; Krause-Rehberg K.1
1 FB Physik, Universität Halle
Effect of dopant atoms on the roughness of III-V semiconductor cleavage surfaces
Appl. Phys. Lett., Vol. 76, No. 3, 300-302 (2000)
23.55.0

Schall P.; Feuerbacher M.; Bartsch M.1; Messerschmidt U.1; Urban K.
1 Max-Planck-Institut für Mikrostrukturphysik, Weinberg 2, D-06120 Halle, Saale, Germany
Dislocation arrangement and density in deformed Al-Pd-Mn single quasicrystals
Mat. Sci. Eng. A 294-296, 697 (2000)
23.55.0

Schroers J.1; Holland-Moritz D.1; Herlach D.M.1; Urban K.
1 DLR Köln
Growth kinetics of quasicrystalline and polytetrahedral phases of Al-Pd-Mn, Al-Co, and Al-Fe from the undercooled melt
Phys. Rev. B, Vol. 61, No. 21, 14500-14506 (2000)
23.42.0

Semmler U.; Ebert Ph.; Urban K.
Effect of charge carriers on the barrier height for vacancy formation on InP(110) surfaces
Appl. Phys. Lett., Vol. 77, No. 1, 61-63 (2000)
23.55.0

Semmler U.; Simon M.; Ebert Ph.; Urban K.
Stoichiometry changes by selective vacancy formation on (110) surfaces of III-V semiconductors: Influence of electronic effects
J. Chem. Phys., in press
23.55.0

Thust A.; Lentzen M.; Urban K.
The Use of Stochastic Algorithms for Phase Retrieval in HRTEM
Scanning Microscopy Supplement, 11, 435-452 (2000)
23.42.0

Tillmann K.1; Jäger W.1; Rahmati B.; Trinkaus H.; Vescan L.; Urban K.
1 Centrum für Materialanalytik, Universität Kiel, D24143 Kiel
Finite element analysis of the strain induced vertical ordering of islands and determination of compositional modifications in LPCVD-grown GexSi1-x-Si bilayers on Si(001)
Phil. Mag. A, Vol. 80, 255-277 (2000)
23.42.0

Tillmann K.; Lentzen M.; Rosenfeld R.
Impact of column bending in high-resolution transmission electron microscopy on the strain evaluation of GaAs/InAs/GaAs heterostructures
Ultramicroscopy 83, 111-128 (2000)
23.42.0

Yang W.1; Wang R.1; Feuerbacher M.; Schall P.; Urban K.
1 Department of Physics, Wuhan University, Wuhan 430072, China
Determination of the Burgers vector of dislocations in icosahedral quasicrystals by a high-resolution lattice-fringe technique
Phil. Mag. Lett., Vol. 80, No. 5, 281-288 (2000)
23.55.0

Yurechko M.; Grushko B.
A study of the Al-Pd-Co alloy system.
Mater. Sci. Eng. A294-296, 139.142 (2000)
23.55.0

Other publications

Belin E.1; Thiel P.A.2; Tsai A.-P.3; Urban K.
1 Laboratoire de Chime Physique-Mat. et Rayonnement, Paris
2 Iowa State University, Ames
3 National Research Institute for Metals, Tsukuba
Quasicrystals
Materials Research Society Symposium Proceedings, to be published (2000)
23.55.0

Gaehler F.1; Kramer P.2; Trebin H.-R.1; Urban K.
1 Universität Stuttgart
2 Universität Tübingen
Mat. Sci. Eng. A, 294-296, 1 (2000)
23.55.0

Urban K.; Paul G.1
1 Frankfurter Allgemeine Zeitung (FAZ), Frankfurt/Main
Physik im Wandel
Rotbuch Verlag (2000).
23.55.0

Invited Talks

Divin Y. Y.; Poppe U.; Shirotov V.V.; Volkov O.Y.1; Pavlovskii V.V.1; Urban K.
1 Institute of Radioengineering & Electronics of RAS, Moscow 103907, Russian Federation
Applications of Hilbert-Transform-Spectroscopy and terahertz spectral analysis by ac Josephson effect in high-Tc bicrystal junctions
Proceedings of the 7. Statusseminar "Supraleitung und Tieftemperaturtechnik" 14./15. Dezember 2000, Garmisch Partenkirchen, Germany
23.42.0

Divin Y.Y.; Poppe U.; Jia C.L.; Seo J.W.1; Glyantsev V.2
1 Institute de Physique Universite de Neuchatel,CH-2000, Switzerland
2 Conductus Inc., Sunnyvale, CA 94086, USA
Epitaxial (101) YBa2Cu3O7-x thin films on (103)NdGaO3 bicrystal substrates
Applied Superconductivity 1999. Ed.: X. Obradors, F. Sandiumenge and J. Fontcuberta, Inst. of Physics Conf. Ser. No.167, IOP Publishing Ltd., Bristol, p.p. 29-32 (2000)
23.42.0

Divin Y.Y.; Poppe U.; Urban K.; Volkov O.Y.1; Pavlovskii V.V.1
1 Institute of Radioengineering & Electronics of RAS, Moscow 103907, Russian Federation
Terahertz Spectral Analysis by Frequency-Selective Incoherent Detection in High-Tc Josephson Junctions
8th International Conf. on Terahertz Electronics, 28-29 September 2000, Darmstadt, Germany
23.42.0

Divin Y.Y.; Volkov O.1; Pavlovskii V.1; Poppe U.; Urban K.
1 Institute of Radioengineering & Electronics of RAS, Moscow 103907, Russian Federation
Terahertz Spectral Analysis by ac Josephson Effect in High-Tc Bicrystal Junctions
Applied Superconductivity Conference, ASC 2000, Virginia, USA, September 17 - 22, 2000
23.42.0

Ebert Ph.; Chao K.-J.; Niu Q.; Shih C.K.1
1 University of Tennessee, Knoxville
Dislocations, phason defects, and domain wall in a one-dimensional superstructure of a metallic thin film.
DFG Schwerpunktkolloquium 'Quasicrystals, Structure and Physical Properties', Jülich, Germany, 5.-7. April 2000.
23.42.0

Ebert Ph.; Kluge F.; Semmler U.; Zhang Tianjiao; Simon M.; Zhang Zhenyu; Urban K.
Clusterung von geladenen Zn-Dotieratomen in GaAs
Frühjahrtagung der Deutschen Physikalischen Gesellschaft, Regensburg, Germany, 27.-31.3.2000.
23.42.0

Ebert Ph.; Shih C.K.1
1 University of Tennessee, Knoxville
Critical thicknesses and quasiperiodic superstructures of ultrathin Ag overlayers on (110) surfaces of III-V semiconductors.
Materials Research Society Fall Meeting, Boston, Massachusetts, November 27-December 1, 2000.
23.42.0

Ebert Ph.
Cleavage Surfaces of Quasicrystals.
219th National Meeting of the American Chemical Society, San Francisco, California, March 26-30, 2000.
23.55.0

Ebert Ph.
Defekte auf III-V-Halbleiteroberflächen.
Symposium Rekonstruktion und Wachstum von III-V-Halbleiteroberflächen der Fachverbände Halbleiter- und Oberflächenphysik. DPG Frühjahrstagung des Arbeitskreises Festkörperphysik, Hamburg, Germany, 26.-30.3.2001.
23.42.0

Ebert Ph.
Factors affecting the structure and composition of cleavage surfaces of quasicrystals.
Materials Research Society Fall Meeting, Boston, Massachusetts, November 27-December 1, 2000.
23.55.0

Ebert Ph.
Spaltoberflächen von Quasikristallen.

Symposium 'Quasicrystalline Surfaces' des Schwerpunkts Quasikristalle der Deutschen Forschungsgemeinschaft, Bommerholz bei Dortmund, Germany, 9.-11. November 2000.
23.55.0

Faley M.; Jia C.L.; Wu J.S.; Poppe U.; Urban K.
Dependence of the microstructure of ReBa2Cu3O7-x films on the conditions of high-oxygen pressure dc-sputtering (INVITED PAPER)
M2S-HTSC-VI: 6th International Conference, Materials and Mechanisms of Superconductivity and High Temperature Superconductors, Houston, Texas, February 20-25 (2000)
23.42.0

Faley M.I.; Poppe U.; Urban K.; Paulson D.N.1; Starr T.1; Fagaly R.L.1
1 Tristan Technologies Inc. San Diego, CA 92121, USA
HTS dc-SQUID with gradiometric multilayer flux transformer
Applied Superconductivity 1999. Ed.: X. Obradors, F. Sandiumenge and J. Fontcuberta, Inst. of Physics Conf. Ser. No.167, IOP Publishing Ltd., Bristol, p.p.509-512 (2000)
23.42.0

Faley M.I.; Poppe U.; Urban K.; Paulson D.N.1; Starr T.1; Fagaly R.L.1
1 Tristan Technologies Inc. San Diego, CA 92121, USA
HTS dc-SQUID with gradiometric multilayer flux transformer
Proceedings of the 4rd European Conference on Applied Superconductivity (EUCAS 99), Barcelona, Spanien; Published in: Inst. Phys. Conf. Ser., No. 167, 509-512 (2000)
23.42.0

Faley M.I.; Poppe U.; Urban K.; Paulson D.N.1; Starr T.N.1; Fagaly R.L.1
1 Tristan Technologies Inc. San Diego, CA 92121, USA
HTS dc-SQUID flip-chip magnetometers and gradiometers
12th International Conference on Biomagnetism, Biomag 2000, Helsinki, 13.-17. August (2000)
23.42.0

Jahnen B.; Luysberg M.; Urban K.; Ungermanns Ch.1; Schmidt R.1
Bestimmung von Konzentrationsprofilen in GaSb/AlSb Heterostrukturen
1 ISG, FZ Jülich
Proceedings of the General Conference of the Condensed Matter Division European Physical Society, Regensburg, Europhysics Conference Abstracts (2000)
23.42.0

Khoukaz C.1; Galler R.1; Feuerbacher M.; Mehrer H.1
1 Institut für Metallforschung, Universität Münster, D-48149 Münster
Self-Diffusion of Ni and Co in decagonal Al-Ni-Co quasicrystals.
Proc. DIMAT 2000
23.55.0

Kim J.; Maciel A.; O'Sullivan E.D.; Ryan J.F.; Schwarz A.; Kaluza A.; Hardtdegen H.H.; Schapers T.; Lüth H.; Meertens D.; Dieker C.
Fermi-edge singularities in the photoluminescence spectrum of modulation-doped GaAs v-groove quantum wires
9th International Conference on Modulated Semiconductor Structures. MSS9
May 2000
Physica E, Vol.7, No.3-4, 517 (2000)
23.42.0

Kluge F.; Grushko B.; Ebert Ph.; Urban K.
Investigations of the structure and composition of decagonal Al-Ni-Co cleavage surfaces.
DFG Schwerpunktkolloquium 'Quasicrystals, Structure and Physical Properties', Jülich, Germany, 5.-7. April 2000.
23.42.0

Lentzen M.
Prospects of Cs-correction for structure imaging in HRTEM
4th Meeting of the Societe Francaise des Microscopies, 6-8 September 2000, Toulouse/F
23.42.0

Luysberg M.; Specht P.1; Weber E.R.1
1 Department of Materials Science, University of California, Berkeley, Ca 94720, USA
Influence of Be doping on the structural properties of low-temperature grown GaAs
SIMC XI 2000, Canberra, Australien (accepted for publication) (2000)
23.42.0

Maciel A.C.; Kim J.; Davies H.D.M.; O'Sullivan E.D.; Ryan J.F.; Schwarz A.; Kaluza A.; Hardtdegen H.H.; Schapers T.; Meertens D.; Dieker C.; Lüth H.
Fermi-edge singularities in the photoluminescence and magneto-optical spectra of modulation-doped v-groove quantum wires
Proceedings of 13th International Conference on the Electronic Properties of Two-Dimensional Systems
Physica E, Vol.6, No.1-4, 530 (2000)
23.42.0

Petukhov B.V.1; Messerschmidt U.1; Bartsch M.1; Dietzsch Ch.1; Geyer G.1; Häussler D.1; Ledig L.1; Feuerbacher M.; Schall P.; Urban K.
1 Max-Planck-Institut für Mikrostrukturphysik, Weinberg 2, Halle/Saale, D-06120, Germany
Dislocation mobility versus dislocation substructure controlled deformation of icosahedral Al-Pd-Mn single quasicrystals.
Proc. ICSMA 2000
23.55.0

Poppe U.; Divin Y.Y.; Faley M.I.; Wu J.S.; Jia C.L.; Shadrin P.; Urban K.
Properties of YBa2Cu3O7 Thin Films Deposited on Substrates and Bicrystals with Vicinal Offcut and Realization of High IcRn Junctions
Applied Superconductivity Conference, ASC 2000, Virginia Beach (2000)
23.42.0

Rotenberg E.; Barman S.R.; Paggel J.J.; Theis W.; Horn K.; Ebert Ph.; Urban K.; Gille P.
Photoemission study of valence band dispersion in quasicrystals. Aperiodic 2000, Nijmegen, The Netherlands, July 4-8, 2000.
23.55.0

Schwarz A.; Kaluza A.; Schapers T.; Hardtdegen H.H.; Lüth H.; Meertens D.; Dieker C.; Maciel A.C.; Kim J.; O'Sullivan E.D.; Ryan J.F.
Electron transport in modulation-doped GaAs v-groove quantum wires
Ninth International Conference on Modulated Semiconductor Structures. MSS9
May 2000
Physica E, Vol.7, No.3-4, 760 (2000)
23.42.0

Semmler U.; Ebert Ph.; Urban K.
Einfluß der Ladungsträger auf die Bildungsbarriere von Leerstellen in InP(110) Oberflächen
Frühjahrtagung der Deutschen Physikalischen Gesellschaft, Regensburg, Germany, 27.-31.3.2000.
23.42.0

Shadrin P.M.; Divin Y.Y.
Spread of critical currents in thin-film YBa2Cu3O7-x bicrystal junctions
Applied Superconductivity Conference, ASC 2000, Virginia, USA, September 17 - 22, 2000.
23.42.0

Shirotov V.; Divin Y.Y.; Urban K.
Dynamic Range of Frequency-Selective Response of High-Tc Josephson Detector to Millimeter-Wave Radiation
Applied Superconductivity Conference, ASC 2000, Virginia, USA, September 17 - 22, 2000.
23.42.0

Specht P.1; Cich M.J.1; Zhao R.1; Jäger N.D.1; Weber E.R.1; Gebauer J.2; Börner F.2; Krause-Rehberg R.2; Luysberg M.
1 Department of Materials Science, University of California, Berkeley, Ca 94720, USA
2 Fachbereich Physik, Universität Halle/Saale
Defect engineering in MBE grown GaAs-based materials
SIMC XI 2000, Canberra, Australien (accepted for publication) (2000)
23.42.0

Thust A.; Jia C.L.
Advances in atomic structure determination using the focal-series reconstruction method
12th European Congress on Electron Microscopy, Brno, Czech Republic, July 9 - 14, 2000.
Proceedings 12th EUREM, Vol III, p. 107.
23.42.0

Thust A.
Advanced Techniques for HRTEM of Defects
Euro Summer School on Electron Crystallography, Aachen, Germany, July 31 - August 4, 2000.
23.42.0

Thust A.
Obtaining 0.1 nm interpretable resolution in electron microscopy by combining a series of images
Fall Meeting of the Dutch and Belgian Societies for Electron Microscopy,
Papendal, The Netherlands, December 7-8, 2000.
23.42.0

Thust A.
Techniques for direct atomic structure determination in HRTEM
International symposium on the occasion of the inauguration of the Tecnai F30 electron microscope at the Angstrom Laboratory, Uppsala, Sweden, April 14, 2000.
23.42.0

Thust A.
The technique of focal-series reconstruction
7th Annual Summer School on Computer-Interactive HRTEM at the Lawrence Berkeley Labs,
Berkeley, California, June 24 - 30, 2000.
23.42.0

Urban K.
Spherical aberration corrected transmission electron microscopy
Congress of the Int. Mat. Res. Soc. Beijing 1999
23.42.0

Vetterl O.1; Carius R.1; Houben L.; Scholten C.; Luysberg M.; Lambertz A.1; Finger F.1; Wagner H.1
1 IPV, FZ Jülich
Effects of structural properties of (c-Si:H absorber layers on solar cell performance
MRS Spring Meeting, San Francisco (accepted for publication) (2000)
23.42.0

Volkov O.Y.1; Pavlovskii V.V.1; Divin Y.Y; Poppe U.
1 Institut für Festkörperforschung, Forschungszentrum Jülich GmbH, 52425 Jülich, Germany
2 Institute of Radioengineering & Electronics of RAS, Moscow 103907, Russian Federation
Far-infrared Hilbert-transform spectrometer based on Stirling cooler
Applied Superconductivity 1999. Ed.: X. Obradors, F. Sandiumenge and J. Fontcuberta, Inst. of Physics Conf. Ser. No.167, IOP Publishing Ltd., Bristol, p.p. 623-626 (2000)
23.42.0

Other talks

Ebert Ph.
Quasikristalle und ihre Oberflächen.
Kolloquium des Instituts für Festkörperforschung, Forschungszentrum Jülich, Germany, February 4, 2000.
23.55.0

Ebert Ph.
Surfaces of Quasicrystals.
Seminar at the Institut d'Electronique et de Microélectronique du Nord, Villeneuve d'Ascq, France, May 25, 2000. (Prof. Dr. D. Stiévenard)
23.55.0

Grushko B.
Composition and precipitation behavior of icosahedral quasicrystals in Al-Pd-Mn.
Frühjahrstagung des Arbeitskreises Festkörperphysik bei der DPG. Regensburg, Germany. März 2000.
23.55.0

Grushko B.
Decagonal and related phases in Al-Cu-Rh
Lab. f. Kristallogr., ETH Zürich, Schweiz
23.55.0

Grushko B.
Metallurgy of the aluminum-transition metals alloy systems forming quasicrystals
CRMC2/CNRS, Marseille, France June 2000
23.55.0

Posters

Lemster K.1; Estermann M.A.1; Haibach T.1; Steurer W.1; Grushko B.
1 ETH Zuerich, 8092 Zurich, Switzerland
Dekagonale Approximanten hoher Ordnung im System Al-Co-X (X=Ni, Ta).
8. Jahrestagung der Deutschen Gesellschaft für Kristallographie. Aachen, Germany. März 2000.
23.55.0

Yurechko M.; Gwózdz J.1; Grushko B.
1 University of Silesia, Inst. Phys. Chem. Metals. 40-007 Katowice, Poland
Phase equilibrium in Al-Cu-Rh in the vicinity of the decagonal phase.
SPQK-Kolloquium 2000 Jülich, Germany, April 2000.
23.55.0

Yurechko M.; Grushko B.
Orthorhombic "Al3TM" phases in Al-Pd and Al-Rh
Frühjahrstagung des Arbeitskreises Festkörperphysik bei der DPG. Regensburg, Germany. März 2000
23.55.0

Patents granted

Divin Y.Y.: Seo J.W.; Poppe U.
Schichtenfolge mit wenigstens einer epitaktischen nicht c-Achsen orientierten Schicht aus einer mit Hochtemperatursupraleitern kristallographisch vergleichbaren Struktur
EP: 0868753 (12.04.2000) (DE, FR, GB)
PT 1.333
23.42.0

Klein A.; Scholen A.
"Dual-mode"-Mikrowellen-Bandpaßfilter aus Hochgüterresonatoren
EP: 0896744 (31.05.2000) (De, ES, IT, FR, GB, SE)
PT 1.1369
23.42.0

Soltner J.; Zhang Y.1; Zander W.1; Banzet M.1; Schubert J.1
1ISI
Anordnung zur Ankopplung eines rf-SQUID-Magnetometers an einem supraleitenden Tankschwingkreis auf einem Substrat
DE: 196 11 900 (1007.2000)
PT 1.1356
29.85.0

Patents applied for

Poppe U.; Faley M.; Zimmermann E.1; Halling H.1
1ZEL
Magnetflußsensor mit schleifenförmigen Magnetfeldleiter sowie dessen Herstellung
PCT: PCT/DE 00/00962 (30.03.2000) (EP, US, JP)
PT 1.1674
23.42.0, 52.90.0

Zimmermann E.1; Glass W.1; Halling H1.; Soltner H.; Faley M.
1ZEL
SQUID-Mikroskop
DE: 100 53 034.6 (26.10.2000)
PT 1.1838
FE 23.420.0

Lecture courses

Ebert Ph.
Oberflächen von Quasikristallen
Physikalisches Kolloquium, RWTH Aachen, Germany, April 10, 2000.
23.55.0

Internal seminars

Poppe U.; Divin Y.Y.
Hilbert-Transform-Spetroskopie
INFO-PHYS-TECH, Nr.29/ Juni 2000, VDI-Technologiezentrum , Düsseldorf, Germany
23.42.0

The IFF Institute Electronic Properties

General Description of the Research Program

The research program of the IFF institute 'Electronic Properties' is devoted towards the investigation of the electronic structure of atoms, clusters, nanostructures, and solids. The ultimate goal is the development of an understanding and thus a base for the control of the properties of (new) materials. The electronic structure constitutes the microscopic base for all materials properties. The electronic interactions determine whether a solid is metallic, insulating, or semiconducting, whether it is transparent or exhibits a distinctive color, whether it is a magnet or a superconductor. Even the elastic properties and the thermal conductivity and heat capacity are determined by the electronic structure.
The electronic structure of simple solids consisting of a regular lattice formed by one or two atomic constituents, like pure metals or semiconductors such as GaAs, is quite well understood. Thin film systems introduce a modification of the intrinsic materials properties due to the interaction at the surface and the interfaces. In structures where at least one of the dimensions is in the nanometer range, the interface or surface properties in conjunction with quantum size effects result in significant modifications of the materials properties. This has led to the concept of 'atomic engineering of materials', whereby the materials properties are controlled by a variation of the atomic constituents at the microscopic atomic level. These concepts establish the central and interconnecting aspect of our research program, where we use both experimental as well as theoretical tools for our explorations. In our research we are not only interested in the ground state properties but also in the dynamic short time response to an external stimulation, as for example a short, intense light pulse.
A large part of our research program is devoted towards the development of a microscopic understanding of classes of materials with a direct connection to a technological application. Such materials where the microscopic control and the variation of the atomic constituents have a dominating influence for the technological application include semiconductor heterostructures as well as thin film magnetic systems for sensors and storage media.
Oriented towards these technological applications the research efforts of the institute are organized in the following areas:

- **Magnetism of thin Films and Nanostructures; from Basic Research to Magnetoelectronics**

- **Clusters as new Materials**

Additionally in our institute there is a considerable effort to develop new

- **Methods and Instrumentation**

Hereby the application of synchrotron radiation plays a central role. This includes the design and construction of beamlines and instruments for research with synchrotron radiation. In the following these programs are described in more detail. At the end of each section current research highlights are listed which either are included as short reports or have appeared in print recently.

A.1. Magnetism of thin films and nanostructures

Thin film systems and nanostructures such as magnetic quantum wires or dots exhibit distinctively different magnetic properties than their bulk counterparts. Obviously there is a close connection between the control of the magnetic properties of these novel nanostructured systems and the understanding derived from basic research on an microscopic atomic level. This has recently led to significant advances in technological applications of thin film systems as magnetic sensors and storage media. Additionally, this development is in line with the demand put forward by the increase in miniaturization in information technology.

Our long range goal is to develop a microscopic understanding of the magnetic phenomena. Magnetism is an electronically derived collective phenomenon influenced by the structure, composition and dimensionality of the system. As experimental techniques we are using spin and angle resolved photoemission, circular dichroism, and other synchrotron radiation related techniques in combination with (relativistic) band structure calculations. With spin- and angle resolved photoemission we determine the bandstructure $E(\sigma,k)$ of the occupied electronic states. These data can be directly compared with bandstructure calculations based on the density functional theory. Element specific magnetic information about multilayer and multicomponent systems is obtained making use of the circular dichroism at core level absorption edges. In addition these studies yield element specific information about the collective ordering phenomena as a function of temperature

As outlined above, electronic structure theory is an integral part of our research program and central to the development of a microscopic understanding of magnetic materials. The existence of a magnetically ordered phase is determined by a delicate balance between the exchange interaction and the kinetic energy of the electrons. The symmetry of the magnetic order (ferromagnetic or anti ferromagnetic) is also determined by the electronic structure and the geometry of the system. Spin-orbit interactions, which in general contribute only a small amount to the total energy of the system, determine macroscopic parameters such as the magnetic anisotropy, the coercivity, and the magneto optical properties. The existence of a preferred orientation also leads to the breaking of symmetries and a lifting of the degeneracies of electronic states. At the present level most calculations do not yet incorporate these effects and efforts are undertaken to include some of these, for example non-collinear spin structures, into the calculations in order to get a more realistic treatment.

Scientific highlights of 2000

- Real Space Imaging of Two-dimensional Antiferromagnetism on the Atomic Scale
  S. Heinze, M. Bode, A. Kubetzka, O. Pietzsch, X. Nie, S. Blügel, R. Wiesendanger,
  Science **288**, 1805 (2000)
- One Dimensional Spin-Polarized Quantum Wire States in Au on Ni(110)
  C. Pampuch, O. Rader, T. Kachel, W. Gudat, C. Carbone, R. Kläsges, G. Bihlmayer, S. Blügel, W. Eberhardt, Phys. Rev. Lett. **85**, 2561 (2000)
- Electronic bandstructure of Gd: a consistent description
- Development of a non-erasable magnetic security strip and testing of prototypes

A.2. Magnetoelectronics; a new field of information technology

Magnetoelectronics is one of the key areas of information technology with a large potential for future expansion. In general the term magneto electronics has been coined to describe electronic devices where, in analogy to the microelectronics, the spin dependent charge transport is used for data storage and processing as well as for sensor applications. In the year 1999 we were successful in obtainig approval and funding for this project within the framework of the HGF-Strategiefonds.

The roots of magnetoelectronics can be found in the discovery of antiferromagnetic coupling in thin magnetic films separated by a non-magnetic metallic spacer and the "giant magneto resistive" properties of these multilayers by P. Grünberg (FZ Jülich) and A. Fert (Paris) in the late 1980's.

Even though it was not part of a technology roadmap or forecast, this unexpected quantum mechanical effect in the area of nanostructured devices has made its way from basic research to commercial devices in the amazingly short time span of less than 8 years. New types of magnetic field sensors were developed which are incorporated into the latest generation of readout heads for magnetic discs. This has resulted in an unexpected strong increase in storage density, since these new heads have a much higher sensitivity. New rotary sensors are being developed which are of interest in robotics and for multiple applications in automobiles. Further applications of the GMR sensors may be in non-destructive testing of structural materials, such as reinforced concrete, or of high speed train wheels, with high spatial resolution. Additionally prototypes for novel non-volatile magnetic random access memory devices (MRAM) are being developed, based upon the resistance change in magnetic tunnel junctions (TMR) upon reversal of the magnetization of one of the layers. GMR sensors with applications as readout heads in hard discs or video recorders and as sensors in car-electronics guarantee a high volume and large revenues. The MRAM development on the basis of the TMR effect offers the possibility to build all solid state memory devices, which are non-volatile and directly compatible with integrated CMOS technology. The worldwide market for (semiconductor) memory devices amounted to 38 Billion $ in 1998 and is projected to increase to more than 100 Billion $ in the year 2002.

Short description of the research objectives in the HGF-Program Magnetoelectronics

The main goal of the HGF-program is to carry out a series of focused basic research projects in order to improve and expand the knowledge and materials basis for GMR sensors and TMR MRAM devices which are currently being developed jointly with industry within the framework of the "BMBF Leitprojekt Magnetoelektronik". The HGF-program is organized as a joint effort bridging institute boundaries whereby scientists from the IFF, the IGV and the ISI participate in this research. These novel magnetoelectronics devices are functional nanostructures consisting of ultrathin metal or metaloxide films, which have a thickness of only a few nanometers. Accordingly, quantization phenomena modify the electronic states and thus influence the magnetic properties. The alternating exchange coupling in magnetic thin films separated by a non-magnetic metallic spacer, which was at the origin of the development of GMR sensors, is indeed caused by the energetics of quantized conduction band states of the metallic spacer layer. Therefore it is obvious that the morphology of the layers and interfaces and their electronic properties determine the device characteristics. With respect to layout development questions arise concerning the transition into the superparamagnetic behavior with increasing miniaturization. Furthermore cross talk and the general influence of the lateral shape of the memory cells need to be investigated.

Until recently, the development of actual GMR sensors was largely empirical by trying out a large number of material combinations and process conditions. The development of TMR elements on the other hand is even less advanced. For both kinds of devices even the basic limitations for the optimum achievable performance, which are subject to the proper choice of materials and the modification of the interfaces, have not yet been established.

In the case of GMR sensors, for example, the relationship between the resistivity of the layers and the interface roughness has not yet been quantified. The development of artificial antiferromagnetic structures, such as FeMn multilayers is just at the beginning. Furthermore the influence of an antiferromagnetic insulating substrate, such as NiO, on the characteristics of the sensor is largely unexplored. Currently NiO has been used to pin the magnetization of one of the sensor layers and was found to also increase the GMR effect.

Concerning TMR junctions for the MRAM development, for the influence of the height of the tunneling barrier and even in general the variation of the spin dependent tunneling current upon magnetization reversal are not explained on a quantitative scale. Another largely unexplored, but nevertheless very important area, concerns the magnetization dynamics of thin film systems for MRAM cells. Furthermore, so far all TMR developments have used Al_2O_3 as the oxide barrier,

mostly due to historical reasons. Different oxides might lead to an improvement of the TMR characteristics.

Scientific highlights of the year 2000 (IFF only)

- Interface magneto-crystalline anisotropy probed by dynamical diffraction of soft X-rays
- Oszillatory interlayer exchenge coupling across an epitaxial FeSi spacer and ist unconventional temperature dependence
- Influence of the anisotropy on the FMR frequency of polycrystalline pinned and unpinned thin permalloy films

B. Clusters as new materials

Clusters are aggregates with a well defined, selectable number n of atoms. In our studies this number n varies between 3 and about 100, whereby we can select each size individually. In these experiments we can study the transition from the single atom to the solid. Of special interest is that this transition is not smooth and continuous, but rather leaves ample room for 'surprises'. The 'materials properties' of individual clusters are quite unique and may in general not be extrapolated from the properties of the corresponding infinite solid. The most famous example is C_{60}, the soccer ball shaped cluster, which can be condensed into a solid consisting only of carbon atoms. Thin films of C_{60} become superconducting at temperatures above 30 K when 'doped' with alkali atoms, and exhibit in general distinctly different properties than graphite or diamond, the other forms of solid carbon. A special highlight in this context a few years ago was our determination of the electron phonon coupling parameters from high resolution photoemission spectra of C_{60}^-. Thus we could show that the mechanism of the superconductivity of the alkali doped fullerenes, which are second in terms of their transition temperatures only to the high Tc materials, may be explained by BCS-theory. This is only one example how cluster research can lead to the discovery and development of new materials.

Our cluster research program exhibits quite some anologies to the corresponding research programs in solid state physics (magnetism, electronic properties) and surface physics (chemisorption, catalysis). This is in accordance with the main goals formulated above for our research program to develop an understanding for the properties of new materials on the microscopic atomic level.

B.1. Electron spectroscopy of mass-selected clusters in a molecular beam

Clusters of a monoatomic size are quite difficult to produce and separate in large quantities. Accordingly the investigation of the electronic properties of these individual mass selected clusters requires methods far beyond the capabilities of conventional electron spectroscopies.

Laser excited photoemission from anionic mass selected clusters has turned out to be a method which can be appplied to this task on a large variety of clusters in a mass selected molecular beam experiment. The clusters are produced by condensation of a plasma generated by a focussed laser beam or an electric discharge in a high pressure He atmosphere. Following adiabatic expansion and the formation of a molecular beam the cluster anions are accelerated by a pulsed electric field. According to their mass difference the anions thus arrive at different times in the ionization region of the magnetic bottle electron spectrometer. Adjusting the timing sequence of the laser used to excite the photoelectrons (detachment) electron spectroscopy on clusters of an unique mass can be performed. The electron energy distribution spectra reveal the electronic structure of the individual clusters. Under favorable conditions vibrational substructures may be resolved which reveal characteristic vibrational modes of the cluster and thus give additional information about the geometry of the atomic positions in the cluster. For the interpretation of these spectra and the identification of unique cluster structures a comparison with high level calculations and a collaboration with theory plays an important role.

In the year 2000 the major emphasis was shifted towards using femtosecond pump-probe techniques to study the mechanisms of energy transfer and relaxations processes. Here energy relaxation processes may be followed in real time for systems where the total energy remains localized spatially to a few atoms and correspondingly only a few degrees of freedom. Thus these processes evolve quite different than in solid state systems, where the total energy is spread rapidly over an extended volume of the sample involving more and more atoms. The energy can only be removed from the cluster by the emission of an electron or photon or by evaporation of an atom. This may occur finally after the system was evolving over a timescale up to the msec range. On the other hand very fast fs electronic relaxation processes may be observed also including the dissociation. Thus one is able to follow the development of the electronic structure as the fragments separate. This enables us to gain data about short lived transition states, which govern the pathways in chemical reactions. Accordingly these states are essential in developing a deeper understanding of chemical reactions. For the development of this field of fs-chemistry, A. Zewail was awarded the 1999 Nobel Prize in chemistry.

Scientific highligths of the year 2000

- Ultrafast hot-electron dynamics observed in Pt_3^- using time resolved photoelectron spectroscopy N. Pontius, P.S. Bechthold, M. Neeb, W. Eberhardt, Phys. Rev. Lett. **84**, 1132 (2000)
- Pump-probe photoelectron spectroscopy on mass-selected metal cluster anions
- Time-resolved Photofragmentation of Metal Carbonylclusters

B.2. Deposition of mass selected clusters on surfaces

For technological applications the individual properties of the clusters have to be conserved. This can be achieved by depositing mass selected clusters onto a suitable substrate. For this purpose we have developed a high intensity source capable of delivering a sufficient amount of mass selected clusters onto a substrate within a few minutes to prevent contamination. Cluster ions are produced in a specially designed high intensity laser vaporization source. The cluster-ions present in the molecular beam following the adiabatic expansion are accelerated and deposited onto a substrate after mass selection by a sector magnet. The substrate can be prepared and characterized in a conventional XPS/UPS system before and after the deposition. Samples are exchanged between these systems using a small, portable UHV sample transfer chamber. This way the substrates can also be transferred to additional facilities, foremost STM and STS characterization in-house as well as spectroscopy with synchrotron radiation.
Typical areas of applications for deposited mass selected clusters are in catalysis or nanoelectronics. In catalysis it is well known that small particles may exhibit special properties, increasing the reactivity or more important the selectivity of the process. It is expected that these properties can be enhanced or tuned by mass selecting the catalyst particles. In electronic applications (nanoelectronics) the concept of a 'single electron transistor' can be realized using deposited clusters. This is due to the fact that the clusters have discrete quantized electronic states, whereby the 'Fermi level' of a small cluster may change by an energy on the order of 1 eV, when a single electron is added to it or removed from it.

Our major research interests are:

- Characterization of the properties of the deposited clusters --- including the atomic geometry and electronic structure in comparison with the 'free' cluster in a molecular beam, diffusion and agglomeration phenomena, and generally the interaction with the support material
- Catalytic properties of mass selected deposited clusters
- Electronic properties of nanocontacts on semiconducting substrates
- Magnetism of nanostructures

Scientific highlights of the year 2000

- A 'metallic' endohedral fullerene: La@C_{60}
  R. Klingeler, G. Kann, I. Wirth, S. Eisebitt, P.S. Bechthold, M. Neeb, W. Eberhardt
  (submitted to Nature)
- Scanning tunneling spectroscopy of size selected endohedral fullerenes

C. Methods and instrumentation

Both aspects, the design and realization of new instruments as well as the development of novel methods for spectroscopy, are part of our research efforts. The powerful infrastructure provided by a large research center is especially helpful when designing new and complex instruments. Our interests in this area are centered around the application of synchrotron radiation. On the hardware side this includes the design and construction of synchrotron radiation beamlines or specific spectrometers and detectors.
Additionally new methods for spectroscopy and scattering are also being explored, concerning the aspects of resonance excitation conditions as well as exploiting the coherence of synchrotron radiation. In the laboratory two-color pump-probe photoemission spectroscopy with fs time-resolution using lasers is a major experimental development. At the future FEL-sources the synchrotron beam properties will match the performance of laboratory laser sources with respect to coherence, pulse power, and timestructure (pulse-lengths) in the fs range. This will extend the capabilities we currently have at visible and UV photon energies into the VUV and (soft) X-ray range and open up the possibilities for a whole set of new and exciting experiments.

C.1. Synchrotron radiation beamlines; spectroscopy and scattering

We have installed an undulator beamline for the photon energy range from 10 eV to 300 eV the DELTA storage ring. This beamline was planned for bandstructure investigations and high resolution core level spectroscopy of magnetic thin film systems for magnetoelectronics, solid state systems and cluster materials. We have built a plane grating type monochromator, since this type of instrument is, for the selected photon energy range, best suited to match the performance of the existing undulator source at DELTA. Unfortunately DELTA so far was unable to offer stable and reproducible operational conditions.
Additionally in the year 2000 we have installed an undulator based beamline with a spherical grating monochromator at the BESSY II storage ring for the photon energy range from 50 eV to 1.5 keV. The source consists of a pair of undulators offering adjustable polarization of the light, which is extremely useful for element specific investigations of magnetic systems including the determination of magnetic moments by using the sum rules developed for CMXD. We will also employ resonant inelastic X-ray scattering at this new BESSY beamline, a method which we have developed over the past years extensively. This beamline produced a first calibration spectrum in December and is currently being commissioned.
In the past year we have built up a new experimental station to conduct scattering experiments with coherent soft X-ray photons. This work was featured as the cover story in Synchrotron Radiation News. Even before the reconstruction of the interference pattern observed has been succesfully demonstrated last year, we had the vision that this might become a very interesting field of research in the future for the study of dynamical processes (m-sec) in magnetic systems, semiconductors and polymers with an exceptional sensitivity tunable on the length scale ranging from a few to 100 nanometers. As a special progress it should be mentioned that we recently were able to demonstrate that linear dichroism yields sufficient contrast to identify the axial orientation of domains on the surfaces of antiferromagnetic materials.

Scientific highlights of the year 2000

- Development of RIXS as a method to determine the bandstructure of solids (review article by S. Eisebitt and W. Eberhardt), J. Electr. Spectrosc. **110-111**, 335 (2000)
- Speckle in coherent Resonant Soft X-Ray Scattering obtaining antiferromagnetic contrast
- Further advances in investigations of hydrophobic fluoro-alcyl-silanes

C.2. Fs two color pump probe photoelectron spectroscopy

Time resolved pump probe photoemission spectroscopy is a new and very exciting field of physics. These experiments directly reveal the electron scattering and relaxation processes following the creation of an optical excited state in real-time. The shortest observed timescales of a few fs are due to electron electron scattering, whereas electron phonon scattering involves slightly larger timescales in the sub-ps regime. These processes also serve to populate electronic conduction band states not necessarily accessible by direct optical excitation. Recording the photoelectrons in an angle resolved mode allows the observation of the scattered excited electrons at specific points of the bandstructure. Since the excited electrons are observed directly, this technique does not require the presence or existence of recombination centers, which are exploited in ultrafast luminescence studies.

In the past we have largely studied charge transfer and excited electronic states involving C_{60} either as a film on a metal substrate or as an acceptor in a photoconductor system. Since we were able to improve the time resolution of our laser system recently, we also can study electronic relaxation processes at metal surfaces directly now. In the future, we will follow up on our earlier work on the timescales of the magneto optical recording process and continue with investigations of the magnetization dynamics of thin film systems with fs-spin-resolved photoemission.

Scientific highlights of the year 2000

- Dynamics of image potential states on the Ni(111) surface

C.3. Theory and experiments concerning STM image interpretation

The theory activities of the institute are largely concentrated in two areas. One of them is the theory of magnetism in thin films including electron transport phenomena in magnetoelectronics as introduced above and the second topic concerns the theoretical modeling of STM images. This latter activity starts with the calculation of the electronic structure of the surface under investigation and the calculation of the tunneling current into a tip represented by an atomic s-, p- or d-wavefunction which is supposed to resemble the tip atom mostly responsible for the tunneling process. In the future a more accurate inclusion of the electronic structure of the tip is planned. However, even on the basis of this simple Tersoff-Hamannn model (s-wavefunction) effects like the corrugation reversal of metallic substrates and the contributions to the STM image from atoms buried below the surface of metals could be observed, helping in the interpretation and correct assignment of some experimental puzzles. Previously these effects had only been reported for semiconductor surfaces, where electron screening is much less effective.

In the future we also plan to conduct experiments along these lines of the image development of the STM using our newly purchased variable temperature STM. Together with the theoretical activities we want to furnish compelling experimental evidence that even for metallic systems the STM images are substantially determined by the details of the electronic structure of the surface.

Scientific highlights of the year 2000

- Real Space Imaging of Two-dimensional Antiferromagnetism on the Atomic Scale S. Heinze, M. Bode, A. Kubetzka, O. Pietzsch, X. Nie, S. Blügel, R. Wiesendanger, Science **288**, 1805 (2000)
- Resolving complex atomic scale spin structures by SP-STM

I hope that I could give a satisfactory overview of our research program and the common thread linking all these activities. Foremost in importance however are the people engaged in these activities and therefore I would like to conclude with a few general remarks about the changes among the members of the institute

Dr. C. Carbone has left the institute after more than a decade of highly interesting and successful research on the determination of the electronic and magnetic properties of thin magnetic films, nanostructures and multilayers. He has been appointed as Professor and group leader at the Institute for the Structure of Materials in Trieste. We wish him all the best for the future.

Dr. S. Blügel has an offer to be appointed as professor in theoretical physics at the University of Osnabrück.

I myself have an offer for the position as Scientific Director of Bessy in conjunction with a professorship at the TU Berlin.

Prof. M. Olmstead from the University of Seattle has received an A.von Humboldt award and has spent several months with us working on the growth and dynamics of semiconductor nanostructures.
Dr. N.V.Smith from the Advanced Lights Source in Berkeley, has also won this distinguished award from the A. von Humboldt society and is spending half a year with us collaborating in the area of magnetic nanostructures and fs spectroscopy of image potential states.
Dr. K. Maiti and Dr. S.S. Yan have each won a stipend from the A. von Humboldt foundation. Dr. Maiti works with us on the determination of the electronic structure of metal-oxide interfaces and Dr. Yan investigates magnetic thin film systems for magnetoelectronics.
Apart from these the following guests have spent extended periods time collaborating with us during the past year: Dr. G. Bihlmayer, Dr. S. Clarke, Dr. R. Gareev, Prof. B.Kuanr, Dr. S. Madsen, L. Sacharow, and Dr. X. Nie
A. Karl, P. Kurz, D. Olligs, and F. Voges have graduated and received a PhD during the last year and M. Breidbach, C. Friedrich, F. Förster, M. Lörgen D. Schondelmaier, and D. Wortmann have finished their Diploma thesis in the institute during the year 2000.

I woud like to close this report by thanking all members of the instirtute for their efforts, contributions and discussions during the past year which have again resulted in a creative atmosphere and many scientific accomplishments

Wolfgang Eberhardt

Institute "Electronic Properties"

December 2000

Director: Prof. Dr. W. Eberhardt
Tel.: 4428, Fax: 2620

Secretary: J. Gollnick
Tel.: 5814, Fax: 2620

Groups	Research Areas
Dr. K. Maiti A. Dallmeyer (PhD-student) M. Malagoli (PhD-student)	Thin film magnetism Spin-polarized photoemission and CMXD with synchrotron radiation
Dr. L. Baumgarten Dr. H. Dürr C. Zilkens (PhD-student) F. Kronast (Diploma-student)	F-sec laser photoemission and high resolution photoemission from solids
S. Link (PhD-student) H. Rhie (PhD-student) J. Sievers (Diploma-student)	Photoelectron microscopy
Dr. S. Cramm M. Freiwald (PhD-student) D. Schondelmaier (PhD-student)	Beamlines at DELTA and BESSY II Characterization of functionalized surfaces
Dr. S. Eisebitt R. Scherer (PhD-student) G. Kann (PhD-student) I. Wirth (PhD-student) M. Lörgen (PhD-student) A. Zimina (Diploma-student)	Soft x-ray emission spectroscopy STM microscopy and spectroscopy
Dr. S. Blügel Dr. G. Bihlmayer Dr. G. Madsen P. Kurz (PhD-student) F. Förster (Diploma-student) D. Wortmann (PhD-student)	Electronic structure theory of solids and multilayers STM-theory
Dr. P.S. Bechthold Dr. M. Neeb R. Klingeler (PhD-student) G. Lüttgens (PhD-student) N. Pontius (PhD-student)	Electronic structure, geometry and materials properties of clusters F-sec dynamics of clusters
Dr. J. Morenzin S. Barnes P. Holik	Development of a magnetic security system
J. Lauer H. Pfeifer Dr. P. Swiatek S. Schubert	Electronic-Laboratory
K. Bickmann B. Küpper	Vacuum-Laboratory

Research Group "Magnetic Multilayers"

Prof. Dr. P. Grünberg Dr. D. Bürgler Dr. R. Gareev Prof. B. Kuanr J. Wingbermühle (PhD-student) M. Buchmeier (PhD-student) M. Breidbach (PhD-student) F.-J. Köhne R. Schreiber	Magnetic multilayers for sensors and memory applications

Electronic band structure of Gd: a consistent description

K. Maiti[1], M.C. Malagoli[1], E. Magnano[2], A. Dallmeyer[1], and C. Carbone[1]
[1]*Institute for Electronic Properties*
[2]*Laboratorio Nazionale TASC, INFM, Strada Statale 14 - Km.163.5, Basovizza, I-34012 Trieste, Italy*

The dispersion of the Gd (5d6s)-valence bands has been investigated by means of spin- and angle- resolved photoemission. The spin analysis of various spectral features shows that their weak dispersion and unusual broadening is due to the photoelectron lifetime rather than to correlation induced band narrowing as previously proposed. These results resolve a longstanding discrepancy between theoretical and experimental descriptions of the rare earth band structure.
F&E-Nr.: 23200

The unique electronic and magnetic properties of lanthanides result from the coexistence of *both* highly localized $4f$ and delocalized ($5d6s$)-levels in the valence region. While the excited- and ground-state configurations in the photoemission of the $4f$ electrons are indeed well understood, no satisfactory picture of the ($5d6s$)-states exists so far. The band structure calculations based on the local spin density approximations (LSDA) predict a large bandwidth for the ($5d6s$)-states in rare earths similar to that of the preceding elements (alkali and alkaline earth metals) in the Periodic Table. These latter cases exhibit strongly dispersive photoemission features that are reasonably well interpreted within the paradigms based on effective single particle approximations. However, various observations seem to indicate a failure of such descriptions to the ($5d6s$)-photoemission and suggest the importance of correlation effects.

In order to address the issue, we investigate the electronic band structure of Gd by means of spin- and angle-resolved photoemission spectroscopy, which is the most extensively studied lanthanide element for its importance as a prototypical Heisenberg ferromagnet ($T_C = 293$ K). The experiments were carried out on the TGM5 wiggler-undulator beamline at BESSY I, Berlin. The overall experimental resolution was 160 meV with angular resolution better than $\pm 0.5°$. Gd(0001) films of 30 monolayer (ML) thickness were epitaxially grown on a clean W(110) surface at room temperature and subsequently annealed at 600 K. The crystalline structure of the films was confirmed by very sharp LEED patterns.

Various state-of-the-art LSDA calculations result to a large energy dispersion along $\Gamma - A$ (Δ_1 and Δ_2 bands) as shown in Fig.1(a) for the ferromagnetic ground state. The spin-integrated normal emission spectra of the valence band at room temperature (RT) and 120 K are shown in Fig.1(c) and (d), respectively. The bulk feature around 1.8 eV at RT splits to a pair of features at 2.3 eV and 1.4 eV at 120 K indicating an exchange splitting of about 0.9 eV in close agreement with the theoretical results. The increase in photon energy ($h\nu$) from 34 eV ($\equiv \Gamma$) to 50 eV ($\equiv A$) exhibit a small energy shift of the bulk feature. In previous photoemission studies [1], the bandwidth of the Δ_2 bands was estimated to be about 0.5 eV from the spectra virtually identical to the ones presented here. This appears to be less than half of the energy dispersion expected for the magnetic ground state (see Fig.1(a)). Notably, such band narrowing in Gd appears to be much larger than that in the strongly correlated $3d$ transition metals, an unusual fact that has not been understood so far. Interestingly, the linewidth of the Δ_2 spectral feature increases substantially for photon energies beyond 40 eV. We show in the following that the knowledge of the spin characters of the various features leads to very different conclusions.

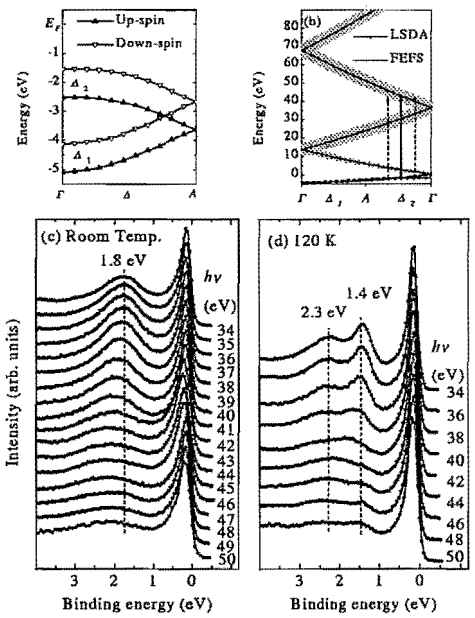

FIG. 1. (a) Band dispersion in the ferromagnetic ground state of Gd along ΓA. (b) A schematic diagram illustrating the k-broadening effect for a typical electronic transition. Spin-integrated normal emission valence band spectra of 30 ML Gd(0001) film at (c) room temperature and (d) at 120 K as a function of photon energy.

Spin-resolved spectra at some selected $h\nu$ are shown in Fig.2(a). The surface feature is predominantly of up-spin character. The Δ_2 emission at $h\nu = 34$ eV is resolved into a broad up- and a narrow down- spin component at about 2.3 eV and 1.4 eV, respectively. The spin-resolved

components exhibit distinct changes with $h\nu$ as is most evident in the expanded down-spin spectra in the figure. The lineshape of the down-spin feature can clearly be described as a combination of a strongly dispersive feature and a nearly nondispersive component at about 1.4 eV. This spectral modification could not be identified in the spin-integrated measurements (as in Fig.1(d)) due to the unresolved and overlapping emissions from both the spin channels. Most significantly, the peak around 2.5 eV in the spectra at $h\nu = 49$ eV turns out to have predominantly down-spin character. In the spin-integrated study, this structure was assumed to be due to up-spin states [1] and led thus to an incorrect estimate of the band dispersion. While the highly dispersive feature represents well the dispersion of the LSDA bands, the nondispersive feature does not have any correspondence in the theoretical results. The degeneracy with the bulk bands and its insensitivity to the surface contaminations rule out the possibility of surface character of this feature.

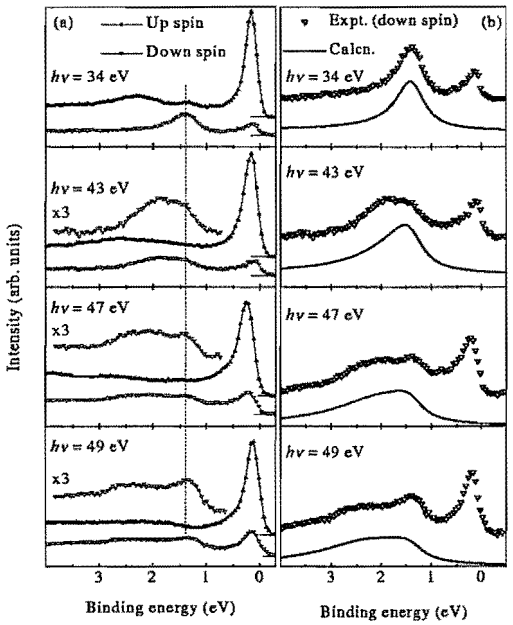

FIG. 2. (a) Spin-resolved spectra of 30 ML Gd film at 120 K. (b) The down-spin spectra and corresponding simulated spectral functions from the LSDA results.

It is to note here that the decay of the photoelectron wave functions due to various inelastic scattering processes while traveling through the solid introduces a momentum broadening as indicated in the inset of Fig.1(b) [2]. In order to investigate the influence of the momentum broadening, we simulate the down-spin spectral functions using the calculated ground state band and the free-electron final states (FEFS) as shown in the figure. The spectral function, $S(k_\perp, E)$ can be expressed as, $S(k_\perp, E) \propto \int\int d\epsilon_h dk'_\perp S'(k'_\perp, \epsilon_h) \frac{\Gamma_h}{(\epsilon_h - E)^2 + \Gamma_h^2} \times \frac{\Gamma_k}{(k'_\perp - k_\perp)^2 + \Gamma_k^2}$ where Γ_k $(= \frac{1}{2\lambda}$; λ = electron escape depth) represents the momentum broadening and Γ_h $(= \Gamma_0 + \alpha \times (BE)^2$; $\Gamma_0 = 0.15$ eV and $\alpha = 0.075$ eV^{-1}; BE = binding energy) represents the hole lifetime effect. $k_\perp$ is the perpendicular component of the reciprocal lattice vector; the parallel component, $k_\parallel$ is zero for normal emission geometry. $S'(k_\perp, \epsilon_h)$ is obtained from the Δ_1 and Δ_2 bands shown in Fig.1(b). The only parameter, Γ_k is varied to simulate the experimental spectra at all $h\nu$. It is necessary to shift the calculated dispersions by about 0.2 eV towards E_F to compare with the experimental spectra. The calculated results for $\Gamma_k = 0.17 \pm 0.03$ Å^{-1} are shown in Fig.2(b) by solid lines. While there is a little discrepancy in the relative intensity of the features possibly due to the neglect of matrix element effects, the spectral weight transfer and the presence of a nondispersive feature is clearly manifested in the simulated spectra consistently with the experimental ones.

Thus, considering the limitations and the simplicity of the model, the agreement with the experimental spectra is remarkable. Γ_k corresponds to $\lambda \sim 3$ Å; a reasonable estimate at these photon energies. Therefore, the observation of the narrow Δ_2 band can be attributed to the photo-electron lifetime effect rather than the strong electron correlation as previously proposed. The large DOS due to the relatively flat dispersion close to the Γ-point gives rise to substantial intensity at all photon energies and is the origin of the nondispersive feature. The RT spectra as a function of $k_\perp$, and the band dispersion at RT and 120 K as a function of $k_\parallel$ could also be simulated consistently with the experimental observations with the same parameters. Such consistency with the spectra probed at different experimental conditions provides strong confidence to the estimated parameters. The small shift of the calculated spectra with respect to the experimental ones might be related to the weak electron correlations, similar to that in alkali and alkaline earths.

In summary, this study resolves the long standing conflict between theory and experiment on the electronic band structure of rare earth metal systems. Spin-resolved measurements establish a clear correspondence between the experimental band dispersion as it is probed by angle resolved photoemission and band structure calculations. The results point out the importance of photoelectron lifetime in determining the experimental band dispersions and significantly reassess the role of correlation effects on the ($5d6s$)-states in rare earths.

[1] B. Kim *et al.*, Phys. Rev. Lett. **68**, 1931 (1992).

[2] E. Jensen and E.W. Plummer, Phys. Rev. Lett. **55**, 1912 (1985).

Interface magneto-crystalline anisotropy probed by dynamical diffraction of soft x-rays

H.A. Dürr
Institute 'Electronic Properties'

M. Münzenberg, W. Felsch
I. Physikalisches Institut, Universität Göttingen, 37073 Göttingen, Germany

S.S. Dhesi
ESRF, BP 220, 38043 Grenoble Cedex, France

The magnetic domain configurations of Fe $3d$ spins in Fe/CeH_2 multilayers was measured by soft x-ray resonant magnetic scattering. The interface region could be probed by setting up x-ray standing waves due to the multilayer periodicity. Resolving first- and second-order magnetic scattering contributions we show that the latter probes directly the magneto-crystalline anisotropy which is dominated by the Fe interface layers causing a spin reorientation transition when the temperature is lowered.

F&E-Nr. 23200

The interfaces between magnetic and non-magnetic layers are of high importance for many magnetic properties such as the magneto-crystalline anisotropy (MCA). Electronic hybridization at the interfaces can lead to a spin orientation perpendicular to the layers preferred for magneto-optical recording applications. However, a direct experimental observation is difficult even with element specific magnetometry such as magnetic circular x-ray dichroism (MCXD). MCXD has been successfully used to measure element specifically the anisotropy of the orbital magnetic moment which probes the easy direction of magnetization [1]. Recently van der Laan proposed a direct measurement of the MCA by probing the anisotropy of the spin-orbit expectation value with x-ray magnetic linear dichroism (XMLD) [2]. All of these methods, however, suffer from the drawback that interface properties such as MCA are only indirectly accessible through a variation of the magnetic and non-magnetic layer thicknesses. The lattice mismatch at the interface can then easily lead to undesired structural changes.

We used a more direct approach to interface magnetism based on dynamical scattering effects. This technique is well known from structural studies in single crystals where standing x-ray wave fields are set up near certain Bragg conditions. As the transferred wavevector is scanned through the Bragg peak two types of standing wave fields can be produced. They have their intensity maxima either at the position of the atoms or in-between them. Therefore, the amount of absorbed photons and, thus, the diffracted intensity depends on the type of standing wave field. In analogy to this technique we set up wave fields in Fe/CeH_2 multilayers. Interface sensitivity is achieved by tuning the scattering conditions so that the x-ray intensity maxima in the multilayer coincide with the position of the interfaces. We then used magnetic scattering effects [3] to extract information about interfacial magnetic properties.

Fe has strong absorption edges in the soft x-ray region where the wavelength (λ=17.5Å) matches that of the multilayer periodicity. The resonant electrical dipole scattering amplitude consists of three contributions [4]: (i) scattering due to the charge distribution of the selected electronic shell, (ii) magnetic scattering which is linear in the magnetic moment and (iii) magnetic scattering which is quadratic in the magnetic moment. In absorption (ii) causes MCXD whereas (iii) is responsible for XMLD and is a direct measure of the MCA [2].

The magnetization of Fe/CeH_2 is oriented perpendicular to the layer planes in a multidomain configuration at low temperatures. This is caused by a strong interface MCA that promotes a spin orientation perpendicular to the layers. Such a magnetization configuration is considerably stabilized via magnetostatic interactions when the multilayer magnetization splits up into adjacent spin-up and down domains of regular size (stripe domains). Stripe domains allow us to separate the scattering processes (i)-(iii) [3]. For the experimental geometry shown in the inset of Fig. 1 process (i) contributes only to the specular peak while (ii) and (iii) produce first and second-order magnetic superstructure peaks, respectively.

Fig. 1 displays Fe L_3 edge XRMS spectra of a [Fe(16Å)/CeH_2(10Å)]x60 sample measured at an x-ray incidence angle of 15°. The measurements were performed at the ESRF beamline ID12B. The spectra clearly show two magnetic satellite features located symmetrically around the specular peak. They appear below the spin reorientation transition of 235 K and become more pronounced as the temperature is lowered further. The two magnetic scattering signals show distinctly different temperature behaviors (see inset of Fig. 1). While the

second-order scattering yield saturates below 100 K the first-order intensity increases down to the lowest measured temperature.

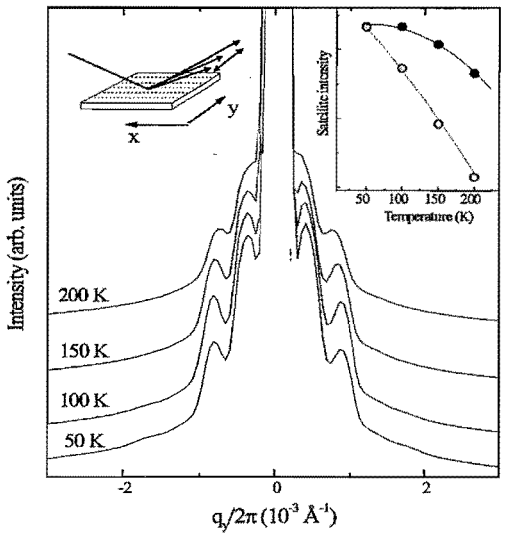

FIG. 1. Fe L_3 edge XRMS scans for various sample temperatures. The left-hand inset shows schematically the experimental geometry. The temperature dependence of the background corrected intensity of the first-order (solid circles) and second-order (solid diamonds) magnetic peaks is shown on the right.

In Fig. 2 the specular intensity (A) together with the first- (B) and second-order scattering peak height (C) is plotted as the x-ray incidence angle is varied through the first multilayer Bragg condition. At resonance the x-ray structure factor is large enough so that a diffracted wave with sufficient intensity is formed in order to create standing wave fields inside the multilayer. Since at the Fe L_3 resonance the $3d$ valence shell is probed the reflected specular intensity monitors the case when the wave field maxima pass through the Fe layers. With decreasing incidence angle the wave field maxima are continuously shifted towards the CeH_2 layer center and the specular intensity decreases. The sharp intensity decrease at the high-angle side is caused by the reflected x-rays moving partly off the detector. The first-order magnetic satellite intensity follows closely that of the specular intensity. In contrast the second-order magnetic scattering peaks at significantly different incidence angles corresponding to the position when the wave field maxima move towards the CeH_2 layer centers. This demonstrates that first- and second-order contributions probe different magnetic properties localized at different parts of the Fe layer.

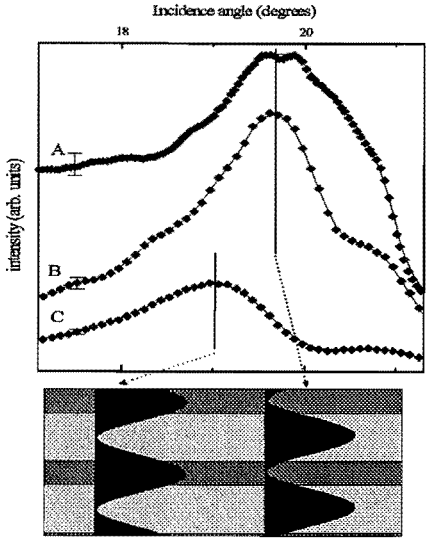

FIG. 2. Fe L_3 edge XRMS intensity taken at 200 K of A) the specular, B) the first-order magnetic and C) the second-order magnetic peak versus x-ray incidence angle. The lower part of the figure shows schematically how the x-ray standing wave field intensity (black sinusoidal areas) varies across the Bragg condition. The Fe and CeH_2 layers are indicated as light and dark shaded areas, respectively.

While the first-order magnetic peaks are caused by scattering from the Fe magnetic moments the second-order peaks arise because of the existence of a spin-orbit quadrupole moment which is directly proportional to the MCA [2]. The measurements shown in Fig. 2 demonstrate that the MCA of the Fe $3d$ electrons is an interface property. The temperature variation of the Fe $3d$ interface MCA as momitored by the second-order magnetic scattering intensity (see inset of Fig. 1) is most likely a consequence of Ce $5d$ / Fe $3d$ hybridization effects. The Fe MCA temperature variation reflects the temperature dependent Fe $3d$ quasiparticle band occupation [6]. This increases the MCA perpendicular to the layers as the temperature is lowered and leads to the observed spin reorientation transition.

[1] H.A. Dürr, et al., Science **277**, 213 (1997).
[2] G. van der Laan, Phys. Rev. Lett. **82**, 640 (1999).
[3] H.A. Dürr et al., Science **284**, 2166 (1999).
[4] J. Luo, G.T. Trammell, J.P. Hannon, Phys. Rev. Lett. **71**, 287 (1993).
[5] O. Schulte et al., Phys. Rev. B **52**, 6480 (1995).
[6] T. Herrmann, M. Pothoff, W. Nolting, Phys. Rev. B **58**, 831 (1998).

Oscillatory Interlayer Exchange Coupling across an Epitaxial FeSi Spacer and its Unconventional Temperature Dependence

R. R. Gareev, D. E. Bürgler, M. Buchmeier, D. Olligs, R. Schreiber, and P. Grünberg
Institute "Electronic Properties"

We study the interlayer exchange coupling in epitaxial Fe/$Fe_{0.56}Si_{0.44}$/Fe trilayers. Iron-silicide spacers with high structural and compositional homogeneity for thicknesses up to 34 Å are grown by co-evaporation from two electron beam sources. The coupling oscillates as a function of spacer thickness with two antiferromagnetic maxima at 12 and 26 Å. The bilinear coupling as a function of temperature shows a maximum near 80 K which we relate to the temperature-dependent resistance of the spacer. We qualitatively discuss our results in terms of existing theories of interlayer coupling.

F&E-Nr.: 23.42.0

Since the discovery of the antiferromagnetic (AF) exchange coupling between ferromagnetic layers separated by a nonmagnetic metal spacer this phenomenon has been observed for a wide range of metallic spacer materials. A further increased interest in this field has been stimulated by the finding of strong AF coupling across iron-silicide spacers [1] prepared by interdiffusion at the Si/Fe interfaces. Due to the metallic character of the iron-silicide an oscillatory behavior of the coupling is expected. However, no evidence of oscillations was observed so far. Moreover, recent reports of an exponential decrease of the coupling strength with spacer thickness in epitaxial Fe/FeSi/Fe trilayers [2] and a strong enhancement of the coupling strength through Si-rich FeSi demonstrate that the mechanism of exchange coupling through iron-silicides is still far from being understood.

The essential demand for a proper investigation of oscillatory interlayer coupling through binary compounds is a high degree of structural and compositional homogeneity of the spacer layer. We employ co-deposition of Fe and Si to obtain more homogeneous Fe_xSi_{1-x} spacers with a nominal composition $x \approx 0.5$ close to the one of the stoichiometric B2 phase with CsCl structure or the B20 (ϵ–FeSi) phase. Epitaxial Fe/FeSi-wedge/Fe sandwiches are grown in an ultra-high vacuum multichamber molecular beam epitaxy system by e-gun evaporation onto GaAs(100)/Fe(1 nm)/Ag(150 nm) substrate-buffer systems. The composition and the structure of the Fe/FeSi/Fe trilayers are verified *in-situ* by Auger electron spectroscopy (AES) and low-energy electron diffraction (LEED), respectively.

The magnetic properties are checked by longitudinal magneto-optic Kerr effect (MOKE) measurements with the external field applied in the sample plane. The MOKE setup based on an optical cryostat allows temperature dependent measurements in the range from 20 K to 300 K. Easy-axis MOKE hysteresis loops for the spacer thickness $d_{FeSi} = 26$ Å taken at 20 K and 300 K are shown in the insets of Fig. 1. Low-field non-linearities in the left inset are caused by second-order MOKE effects and have no influence on the discussion below. For very large in-plane, four-fold anisotropy K or negligible K the saturation field can be used as a measure of the total coupling J. For our epitaxial samples, $Kt \approx 0.2$ mJ/m^2 (t is thickness of the magnetic layers) is of the same order of magnitude as J, and we cannot derive an analytical relation between the saturation field and the coupling strength. However, we can define for all our MOKE loops a switching field H_S (see e.g. arrows in the left inset) where the magnetizations of the Fe films jump either to saturation or to a symmetric alignment with both magnetizations slightly deviating from the field axis. Numerical simulations including anisotropy K, bilinear (J_1) and biquadratic (J_2) coupling, and the external field confirm this behavior and yield for $Kt \gtrsim J_1 + J_2$ the relation

$$H_S = -c_1(J_1 + J_2)/(M_S t), \qquad (1)$$

where M_S denotes the saturation magnetization of the magnetic layers. The constant c_1 varies between 1 and 1.2 depending on the ratio $Kt/(J_1 + J_2)$. Hence H_S provides an estimation of the total coupling $J = J_1 + J_2$.

The dependence of H_S on the spacer thickness is measured for different temperatures ranging from 20 K to 300 K (Fig. 1). We observe an oscillatory behavior of the coupling *versus* spacer thickness for all temperatures. We note that this result represents the first observation of oscillatory interlayer coupling across an FeSi spacer

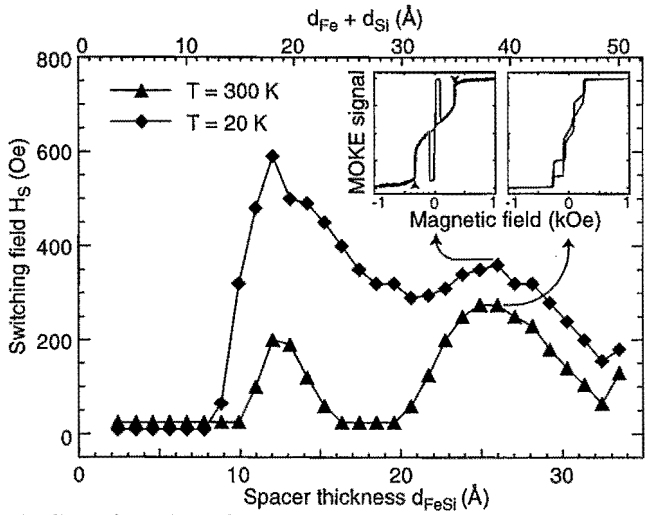

FIG. 1. Switching field H_S *versus* spacer thickness d_{FeSi} of a wedge-type Fe(5 nm)/$Fe_{0.56}Si_{0.44}(d_{FeSi})$/Fe(5 nm) trilayer measured at 300 K and 20 K, respectively. Insets show the hysteresis loops for both temperatures at $d_{FeSi} = 26$ Å.

layer. The position of the first peak matches the results of de Vries *et al.* [2], but the second peak contradicts their exponential decay of the coupling. We relate this discrepancy to (i) the more homogeneous spacer of our samples and (ii) the larger epitaxial spacer thickness range accessible in our experiments.

The temperature dependence of the switching fields at the first and second coupling maximum $H_S^{(1)}$ and $H_S^{(2)}$ is shown in Fig. 2(a). A qualitative inspection of the hysteresis loops indicates that $H_S^{(2)}$ is dominated by bilinear (AF) coupling in the whole temperature range. In contrast, the impacts of bilinear and biquadratic coupling on $H_S^{(1)}$ are of the same order and lead to a temperature-dependent remanent magnetization M_R [Fig. 2(a)]. Intuitively, M_R decreases with increasing J_1. We confirm this behavior again by numerical simulations and obtain

$$\frac{M_R}{M_S} = \frac{1}{2} - \frac{c_2}{4}\frac{J_1}{J_2} \quad ; \quad 0 < c_2 \leq 1. \qquad (2)$$

The constant c_2 depends on the value of the anisotropy term Kt: $c_2 = 0$ for $Kt \gg J$ and $c_2 \approx 1$ for $Kt \ll J$. The linear dependence of Eq. (2) is valid at least for $J_1/J_2 < 1$. In our epitaxial samples Kt is of the same order of magnitude J, and for the first coupling maximum J_2 dominates. Therefore we can combine Eqs. (1) and (2) to obtain expressions for $J_1^{(1)}$ and $J_2^{(1)}$. The resulting decomposition of the coupling in the first maximum in bilinear and biquadratic contributions is shown in Fig. 2(b). $J_1^{(1)}$ has a clear maximum around 80 K. With the chosen normalization this qualitative behavior is not affected by the parameters c_1 and c_2. Note that the shape and in particular the position of the maximum of $J_1^{(1)}(T)$ are the same as for the $H_S^{(2)}(T)$ dependence. Hence, the temperature dependence of the bilinear coupling in both peaks has a smooth maximum around 80 K.

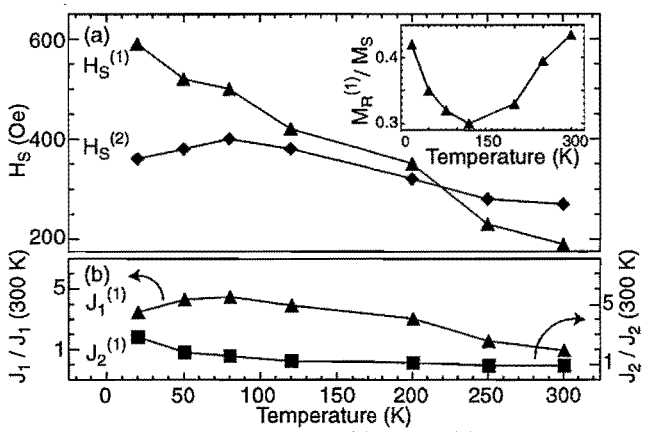

FIG. 2. (a) Switching fields $H_S^{(1)}$ and $H_S^{(2)}$ at the first and second coupling maxima, respectively, as a function of temperature. The inset shows the temperature dependence of the remanent magnetization in the first coupling maximum. (b) Bilinear and biquadratic contributions to the first coupling maximum $J_1^{(1)}$ and $J_2^{(1)}$ derived from Eqs. (1) and (2) with $c_1 = 1$ and $c_2 = 0.5$. The curves are normalized to their value at 300 K and vertically offset.

The temperature dependence of the bilinear coupling strength for metallic and insulating spacers can be described by the quantum interference model [3]. Oscillations and an increase of the coupling strength upon cooling are found for metallic spacers. In contrast, for insulating spacers the coupling strength is expected to exponentially decay with spacer thickness and to decrease with decreasing temperature. Hence, the smooth maximum in Figs. 2(a) and (b) might be related to a metal-insulator transition of the FeSi spacer material.

In order to check this possibility we measure the in-plane resistivity $R(T)$ of our samples using a four-point geometry. We find two distinct ranges with different temperature coefficients $\alpha = R(T)/T$. The change of α by two orders of magnitude describes the transition from a good metal to poor metal with a rather wide transition range (80–280 K).

The temperature dependence of J_1 seems to be connected with the resistance behavior of the FeSi spacer that grows either in the epitaxially stabilized B2 phase or in the bulk stable B20 phase. Hence, we can think of three possible scenarios: (i) The FeSi spacer is fully relaxed in the B20 bulk phase. This phase shows a transition to a Kondo insulator below 100 K. Our resistivity data cannot exclude the presence of an insulating spacer because the two Fe layers contribute to the in-plane conductivity, too. According to Bruno's theory [3] the presence of an insulating spacer would nicely explain the change of slope of J_1 (Fig. 2). However, the observation of oscillatory interlayer coupling from RT down to 20 K excludes this scenario. In fact, the observed oscillations require that the spacer material is non-insulating in the whole temperature range. (ii) We assume that the spacer is crystallized in the non-relaxed B2 phase and that our $R(T)$ data roughly reflect the temperature-dependent resistivity of the B2 phase. The drop of the temperature coefficient α by two orders of magnitude indicates a significant reduction of the number of carriers near the Fermi level. This could lead to a decrease of the bilinear (AF) coupling [3]. However, for our growth conditions a mixture of B2 and B20 phases is the most likely situation due to the almost equal heat of formation. In this scenario (iii) both effects described above can in principle contribute to the unconventional temperature dependence of J_1, and the metallic B2 phase gives rise to the oscillatory behavior in the whole temperature range.

In conclusion, we have demonstrated for the first time oscillatory interlayer coupling across FeSi spacer layers. The bilinear coupling exhibits an unconventional temperature dependence with a maximum which we connect with strong changes of the number of carriers in the spacer.

[1] E. E. Fullerton *et al.*, J. Magn. Magn. Mater. **117**, L301 (1992).

[2] J. J. de Vries *et al.*, Phys. Rev. Lett. **78**, 3023 (1997).

[3] P. Bruno, Phys. Rev. B **52**, 411 (1995).

Anti-counterfeit magnetic signatures

P.Holik, S.Barnes, P.Swiatek, D.Schondelmaier, J.Morenzin and W.Eberhardt

Institute 'Electronic Properties', Project 'MagSigno

We are working on new magnetic features for product security. The research and development is based on a patent pending technology of thin layers having a unique magnetic characteristic[1].
Informations are stored within the production process, and can be read out and tested for authenticity with conventional means. Reproducing is difficult, which makes the magnetic tag suitable for a wide range of security applications. Our goal is a quick transfer of the scientific results into products which are in line with the market.

Product piracy is a major problem in nearly every product section worldwide, which causes yearly about 500 billion dollars[2] losses in sales in the developed countries. Moreover, image impairment and legal consequences are threatening the existence of high quality product manufacturers. If grey markets have established once, in most cases a separation of genuine and faked goods isn't possible any more. Product security not only relates to valuable goods like electronic or mechanical components, clothes, media or tickets, but also comprises means of payment such as credit cards, bank notes, cheques or credit notes and official documents like passes, driving licenses, etc..
We are developing a inexpensive, reliable and simple solution to protect these items from counterfeiting. An easy to handle security label, which can be provided on objects and which can be constructed suitable to the customers needs. The devices for reading and checking for genuineness can be i.e. hand-held pens or integrated units.

Basic properties

The signature is made by texturing a special magnetic thin film system. The information is encoded within the production process and cannot be altered afterwards. The magnetic signature holds an information which can be read by ordinary magnetic reading heads, i.e. the wide spread reading technology can be used for this purpose.
The information encoded can not be manipulated by any means. The magnetic signature has an unique behaviour while applying an external magnetic field. Reproducing a system with a similar behaviour needs a high effort.
Only a few simple hardware modifications on standard magnetic readers are required for testing the signature whether it is genuine or a counterfeit. This allows low cost and small devices for both reading and verifying to be manufactured. Verifying can be performed without any online connection to an external host.

Technical progress

First goal of the project was to demonstrate the technology in its fundamental principles. In the first step a simple magnetic stripe which basically has the advantage of not being alterable after the information has been encoded was produced. This system based on a credit card could be read by conventional magnetic readers and was demonstrated on several trade fairs (CeBIT, Hannover-Messe, SECURITY). The high level of protection against forgery and the unique magnetic properties of the technology was proven with several samples, where the characteristics could be shown with a optical magnetic viewer.

Market potential

To perform a precise development typical markets for a respective security product have been estimated. In this field of application the separation from known low cost systems based on conventional magnetic tapes is given by the high protection against forgery and a much better temperature stability. Other more costly systems like i.e. chemical markings can be beaten by costs, especially regarding the verification technology. Separation against holograms or other one-bit systems can be made by unification, that means by varying the stored information and thus preventing black-markets for the anti-counterfeit tags to establish.

Outlook

The next step is focussing onto concrete products with a high market potential and developing prototypes of anti-counterfeit tags and the corresponding reading and verification devices. For each system the principle advantages and disadvantages compared to competing products and the acceptable price have to be estimated to evaluate the chances for a profitable production. That also involves planning the design of a batch production machine. All these application-oriented works are accompanied by fundamental research activities to improve the systems magnetic and mechanical properties.

---

[1] Offenlegungsschrift *DE 198 52 368*, deutsches Patent- und Markenamt
[2] W. Steinke, *Wirtschaftsschutz und Sicherheit*, **8-9** (2000) 20, Hüthig Verlag

Influence of anisotropy on FMR frequency of polycrystalline pinned and unpinned thin Permalloy films

Jörg Wingbermühle, Bijoy K. Kuanr, Daniel E. Bürgler, and Peter Grünberg
Institute "Electronic properties"

Employing a nonresonant broadband technique, we have measured the complex scattering matrix S-parameters, (S_{11} and S_{12}) of polycrystalline permalloy (Py) from 1 MHz to 20 GHz to estimate resonance as well as off-resonance high frequency losses. Our technique employs a Vector Network Analysator (VNA) Hewlett–Packard model HP8720B sending a phase-locked signal into a coaxial transmission line (50 Ω), which is terminated by the thin film sample. It is well known that NiO/Py interfaces give rise to an unidirectional anisotropy called exchange anisotropy (H_{ex}). We have used the VNA technique to measure the exchange anisotropy and the field-induced uniaxial anisotropy (H_U) in pinned (NiO/Py) and unpinned Py films.

F&E-Nr.: 23.42.0

The interaction of ferromagnetic (FM) and antiferromagnetic (AFM) layers at their interface leads to a unidirectional type of anisotropy (H_{ex}). This so-called exchanged-bias (EB) was discovered more than four decades ago [1]. The effect produces a shift of hysteresis loop in addition to an enhanced coercivity. It has recently been given considerable attention because of its application in high density magnetic recording and storage devices. It is generally accepted that the net moment appearing at the surface of an uncompensated antiferromagnet which is ferromagnetically or antiferomagnetically coupled to the moments of the ferromagnet is responsible for the exchange anisotropy [1]. Ferromagnetic resonance (FMR) spectra of EB coupled systems (for example: NiO/Py) are a rich source of information on this unique anisotropy. In addition to the FMR frequency, the frequency linewidth $\Delta\omega$ of frequency-swept FMR spectra is a direct measure of the relaxation rate η of the uniform precession. Note that $\Delta\omega$ should not be confused with the field-swept FMR spectra linewidth ΔH as observed from convential FMR at a fixed frequency.

We have used a non-resonant type transmission line-technique in the frequency domain [2,3] to measure magnetic thin-films. In the Corbino-geometry the sample is covered with silver paste except for a ring with inner and outer diameters $2a$ and $2b$. The inner and outer silver areas made direct contact to the inner and outer conductor of the modified SMA receptacle RF-excitation cell (spring-loaded receptacle with coax end, Suhner-type) with a cutoff frequency $f_c = 2c/(\pi[D+d]\sqrt{\epsilon_r})$ of 28 GHz and a characteristic impedance $Z = 60/\sqrt{\epsilon_r} \cdot \ln(D/d)$ of 50 Ω, where D and d are inner an outer diameters of the excitation cell. ϵ_r is the dielectric constant of the dielectric material (i.e. for Teflon $\epsilon_r = 1.65$) and c is the velocity of light. The RF signal supports a TEM mode propagation for the whole frequency range studied. In this geometry h_{rf} is applied radially between the silver areas in the plane of the sample surface. We also used the stripline geometry to measure the complex S-parameters from transmission line approach as a function of frequency (fig. 1). These parameters are derived after a two-port OSL (Open, Short and Load) calibration of the VNA taking into account the measurement error and substrate effects.

The samples are prepared by ion-beam sputtering with a field applied in the sample plane during deposition in order to induce a well defined EB-axis and at the same time an uniaxial anisotropy in the Py films. We measured the resonance frequencies (f_{res}) of thin polycrystalline Py films in frequency domain. The figure 1 displays a FMR-spectrum along with a χ^2-fit to the experimental absorption curve. This shows that the FMR absorption

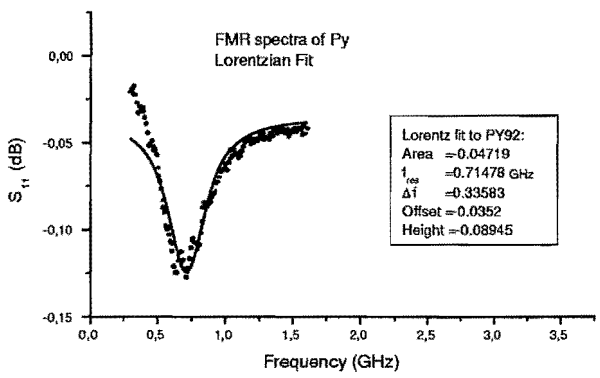

FIG. 1. VNA-FMR spectrum of a single Py film.

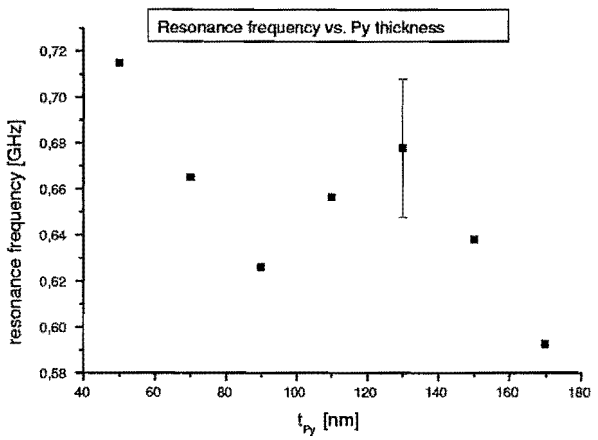

FIG. 2. FMR-frequency versus Py-thickness.

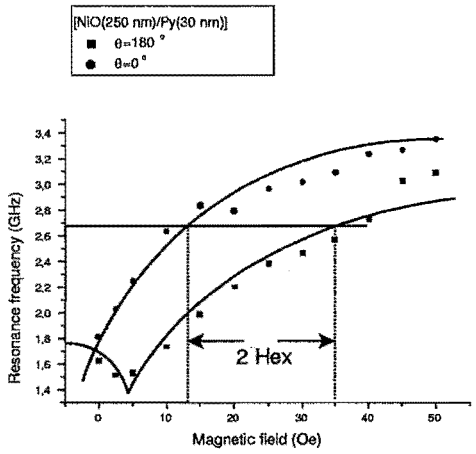

FIG. 3. Resonance frequency of a NiO/Py-layer as a function of the field applied in the EB-direction (dots) and opposite to it (squares). The solid lines are guide to eyes.

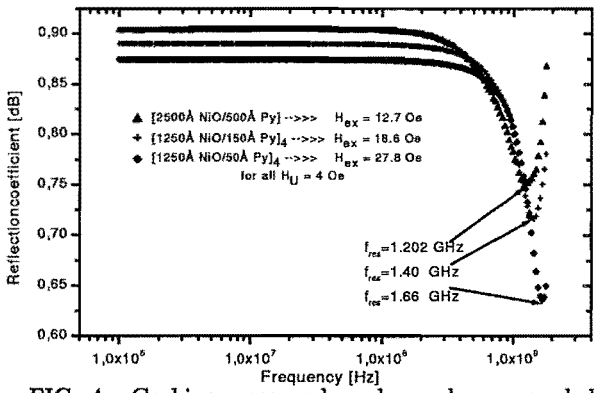

FIG. 4. Corbino-measured exchange-layer coupled with NiO.

lineshape is Lorentzian. Resonance frequency and 3-dB frequency linewidth are obtained from this Lorentzian fit. Figure 2 shows the resonance frequencies as a function of the Py layer thickness. The resonance frequency is independent of the Py thickness, which means that the field induced uniaxial anisotropy (H_U) is the same for all thicknesses of the Py films studied here.

Figure 3 shows the variation of the resonance frequency as a function of the magnetic field applied in the direction of EB (θ=0°) and opposite to it (θ=180°). At a fixed field there is always one resonance mode. When $\vec{H}$ is applied in the exchange-direction f_{res} is higher for all field values compared to the situation when $\vec{H}$ is applied opposite to the exchange-direction. The difference reflects the value of the exchange anisotropy: At a fixed frequency the difference between the two directions of the magnetic field gives $2H_{ex}$ [4,5] as indicated in fig.3. Here the H_{ex} value comes out to 12 Oe for a NiO(250nm)/Py(30nm)-film. It is to be noted here that these two mode positions are identical for an unpinned Py film, where the exchange anisotropy is zero. Thus, the mode positions yield a direct measure of the exchange anisotropy.

We have calculated the unidirectional exchange anisotropy for pinned structures from f_{res} and compared them to their MOKE results. Prior to FMR measurements, the Py films are characterized by MOKE with the field applied both parallel and antiparallel to the unidirectional axis. The loop shift in the parallel configuration gives the unidirectional exchange-anisotropy field H_{ex}, and the uniaxial anisotropy field H_U is obtained from initial slope of the in-plane hard-axis MOKE hysteresis loop.

In order to understand whether the phenomenon of exchange anisotropy is a bulk or a interface effect, we have produced multilayers consisting of alternate Py and NiO layers keeping total thickness of NiO and Py almost constant or varying the number of interfaces. Figure 4 shows FMR-spectra for three different multilayer configurations with NiO and Py thicknesses indicated. The spectra clearly show an increase of f_{res} when the number of interfaces between Py and NiO increases. The shift of the resonance frequency indicates a sharp increase of the exchange anisotropy field (H_{ex}) by more than 100%. The MOKE measurements in the easy axis yield the same values for H_{ex}. For all of these samples we have used an uniaxial anisotropy of H_U = 4 Oe, which we have measured from the hard axis MOKE hysteresis loops. Figure 2 confirms that H_U is independent of the Py thickness.

In conclusion, we have used Network Analyzer spectroscopy in frequency-domain to probe exchange anisotropy as well as field induced uniaxial anisotropy in pinned and unpinned Py films. The increase of exchange anisotropy for pinned films leads to the conclusion that exchange anisotropy is strongly influenced by the number of interfaces for a fixed total Py thickness.

[1] W.H. Meiklejohn, Phys. Rev. **102**, 1413 (1956)
[2] J.C. Booth, D.H. Wu, and S.M. Anlage, Rev. Sci. Instrum. **65**, 2082 (1994)
[3] A. Schwartz and S.M. Anlage, Phys. Rev. B **61**, R870 (2000)
[4] A. Layadi *et al.*, IEEE Trans. Magn. **23**, 2993 (1987)
[5] J.C. Scott, J. Appl. Phys. **57**, 3681 (1985)
[6] R.D. McMichael *et al.*, Phys. Rev. B **58**, 8605 (1998)

Scanning Tunneling Spectroscopy of Size-Selected Endohedral Fullerenes

R. Klingeler, G. Kann, I. Wirth, S. Eisebitt, P.S. Bechthold, M. Neeb, and W. Eberhardt
Institute "Electronic Properties"

Abstract. The density of electronic states in the vicinity of the Fermi level has been investigated on individual La@C_{60}, Ce@C_{60}, and C_{60} clusters deposited on highly oriented pyrolytic graphite (HOPG) using scanning tunneling spectroscopy (STS). The question weather a metallic or semiconducting behavior is observed depends on the type of encapsulated atom. Ce@C_{60} exhibits a non-metallic behavior with a band gap of about 0.3 eV, whereas La@C_{60} is found metallic at room temperature (RT). However, for La@C_{60} low temperature STS reveals the reversible opening of a 40 meV gap below 28 K, which is most likely due to the freezing of the "rattling" mode. The spectra are interpreted in terms of free C_{60}, including charge transfer and Jahn-Teller-distortion.

F&E-Nr: 23200

Endohedral fullerenes are of high interest due to their diversity and imaginable numerous applications [1]. Inspired by the robust carbon cage and its large hollow interior, endohedral fullerenes represent a new class of technologically relevant composites as they join both metallic and fullerene-like properties. One of the most intriguing aspects of endohedral fullerenes is the expected metallic or even superconducting character. Charge transfer from the metal (M) into the unoccupied carbon-cage orbitals, predicts M@C_{60} and other endohedral fullerenes to exhibit metallic properties. So far, no endohedral fullerene with $n \leq 60$ has been purified by chemical extraction (exception: Eu@C_{60}). In fact, all endohedral fullerenes produced so far reveal a zero density of states at the Fermi level in contrast to the intuitive metal-to-carbon charge transfer picture. As proposed by Weaver *et al.*, crystals of pure La@C_{60} are expected to be metallic due to a charge transfer best described as 3+ [2]. This has not been experimentally proven so far because La@C_{60} has not been isolated in pure form. However, a wide range of endohedral fullerenes from 30 to about 150 carbon atoms, including endohedrally doped M@C_{60}, are available by deposition from a mass-selected metal-fullerene cluster beam [3]. Combining this deposition

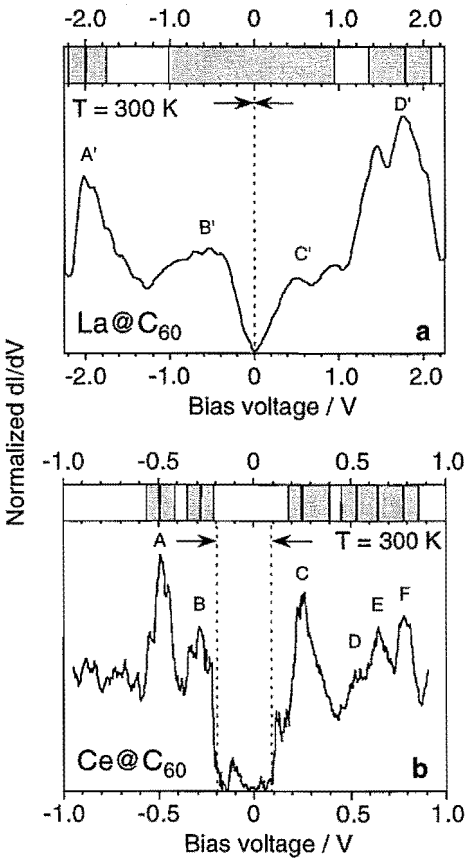

FIG. 1: Scanning tunneling spectra of La@C_{60} (a) and Ce@C_{60} (b) on HOPG at 300 K [5]. The normalized differential tunneling conductivity (dI/dV)·(V/I) reveals a metallic-like density of states at the Fermi level (zero voltage) for La@C_{60}. The distinct gap of ~0.3 eV at the Fermi level of Ce@C_{60} identifies it as a "semiconducting" molecule. The reproducible STS features are marked by the bars and shaded areas in the diagram at the top of the STS spectra.

Fig. 1 R.Klingeler et al.

technique with STS [4], we have probed the local density of electronic states near the Fermi level of La@C_{60} and Ce@C_{60} on HOPG (highly oriented pyrolytic graphite).

The clusters were synthesized by pulsed laser vaporization of a graphite-metal rod (100:1) and condensation in a He-atmosphere. After supersonic expansion, the cluster cations were mass-selected by a magnetic sector field (m/Δm≈250) and deposited onto a sample area of ~1x1 mm^2. In order to avoid damage upon surface impact, the clusters have softly been landed at an ion kinetic energy of < 200 meV/atom [3,4]. Following deposition, the cluster-covered sample was transferred into a variable temperature scanning tunneling microscope under ultra high vacuum conditions. The STS spectra have been taken with a chemically etched tungsten tip on top of individual clusters.

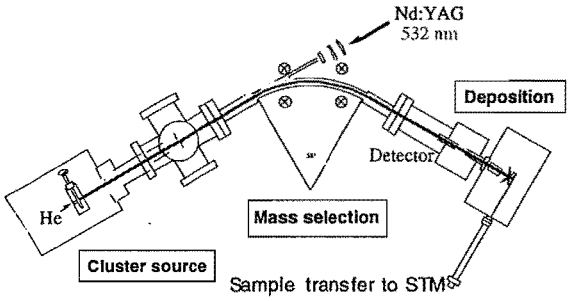

Scanning tunneling microscopy of the surface topology demonstrates the size-selected and non-destructive deposition of pure and doped C_{60}^+ onto HOPG [5]. According to investigations on free molecules, C_{60} on HOPG exhibits semiconducting behavior with a 1.7 eV band gap as measured by STS. The valence region of doped C_{60} is governed by C_{60}-derived orbitals, and a metal-to-cage charge transfer shifts the Fermi level into the t_{1u} (LUMO of pristine C_{60})-derived cage orbital. Fig. 1 shows the normalized dI/dV curves of La@C_{60} and Ce@C_{60}. The t_{1u} and t_{1u} derived orbitals, degenerated in pristine C_{60} due to I_h symmetry, split under the Jahn-Teller effect. It is induced by the charge transfer and an off-center metal ion position. The removal of degeneracy is clearly visible in the spectrum of Ce@C_{60}. Moreover, a 0.3 eV band gap indicates semiconducting behavior, and a 4+ formal Ce state is likely. In contrast, La@C_{60} exhibits non-zero density of states at the Fermi level.

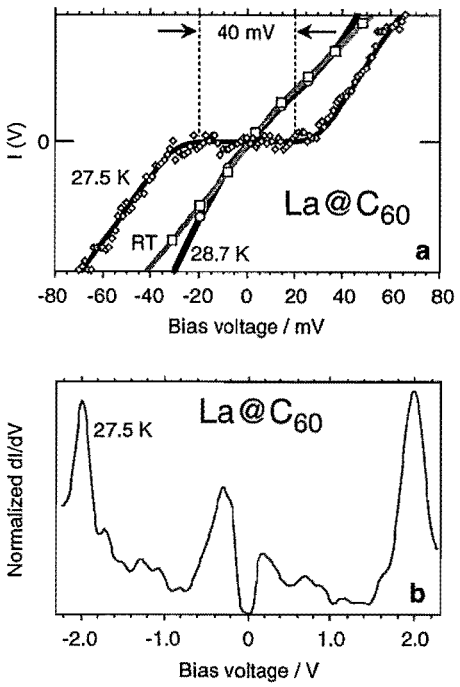

Fig. 2 R.Klingeler et al.

FIG. 2: Temperature-dependent scanning tunneling spectra of La@C_{60} [5]. Panel (a) shows the I(V) characteristic curve at room temperature (RT), 28.7 K and 27.5 K, respectively. Panel (b) shows the normalized differential tunneling conductivity (dI/dV)·(V/I) at 27.5 K as measured between -2.2 and 2.2 V. Note the occurrence of an energy gap below the transition temperature of 28 K. An error of ±1 K has been specified for the sample temperature.

In fact, it is the first endohedral fullerene proven to have metallic character. Moreover, a reversible metal-to-semiconductor transition occurs at 28 K (Fig. 2). It is attributed to the freezing of the rattling mode, the motion of the encapsulated metal ion.

[1] Bethune, D.S., et *al.*, Nature **366**, 123 (1993)

[2] Weaver, J.H., et *al.*, Chem. Phys. Lett. **190**, 460 (1992).

[3] Klingeler, R., Bechthold, P.S., Neeb, M., Eberhardt, W., J. Chem. Phys. **113**, 1420 (2000).

[4] Neeb, M., Klingeler, R., Bechthold, P.S., Kann, G., Wirth, I., Eisebitt, S., Eberhardt, W., Appl. Phys. A., in press.

[5] Klingeler, R., Kann, G., Wirth, I., Eisebitt, S, Bechthold, P.S., Neeb, M., Eberhardt, W., Nature submitted

R. Klingeler, G. Kann, I. Wirth, S. Eisebitt, P.S. Bechthold, M. Neeb, and W. Eberhardt

Speckle in Coherent Resonant Soft X-ray Scattering: Obtaining Antiferromagnetic Contrast

S. Eisebitt, M. Lörgen, R. Scherer, W. Eberhardt
IFF, Forschungszentrum Jülich, Germany

A. Rahmin, S. Tixier, T. Tiedje
Dept. of Physics, University of British Columbia, Canada

J. Lüning, J. Stöhr
SSRL, Stanford University, USA

Coherent resonant scattering has been performed in the soft x-ray range. We demonstrate, that contrast due to a domain pattern of *anti*ferromagnetic domains can be obtained.

Soft x-rays, with wavelengths ranging from approximately 1 nm to 25 nm are well suited for structural investigations of nanostructured materials. They are not sensitive to atomic distances (no Bragg peaks) but to the entities of interest on the nanometer length scale. In particular, domains in magnetic thin films are such entities, ranging in size from macroscopic down to the nanometer range, depending on the system under investigation. *Anti*ferromagnetic surfaces are particularly difficult to access due to their magnetically compensated nature. However, exploiting the x-ray magnetic linear dichroism (XMLD) effect in the *absorption* cross-section for soft x-rays, antiferromagnetic domains have been recently imaged in a real space technique [1]. We have exploited the corresponding term in the resonant *scattering* cross-section [2] in order to develop a reciprocal space technique which is sensitive to antiferromagnetic domains. In order to be sensitive to the individual domain configuration (also for non-periodic arrangements) we perform *coherent* resonant scattering, using synchrotron radiation. Antiferromagnetic thin films, especially when coupled to ferromagnetic films, are of technological importance in the magnetic recording and storage industry (magnetic RAM, GMR disk read heads).

While longitudinal coherence can be produced by a monochromator at a synchrotron radiation beamline, transverse coherence is not a parameter that can be controlled at a typical beamline. Consequently, the experiments were performed using a custom designed ultra high vacuum chamber containing a spatial coherence filter, consisting of two subsequent pinholes of diameters ranging from 1μm to 50μm. Experiments were performed at beamline 8 of the Advanced Light Source, Berkeley, and at the UE56/1 Undulator at BESSYII, Berlin. The coherence is characterized by modelling the diffraction patterns from known objects.

As an example we present in Fig. 1 the diffraction pattern obtained in the soft x-ray version of Young's double slit experiment. In our case, we have used radiation of 3 nm wavelength, coherently scattered from two pinholes with 1μm diameters, separated laterally by 10 μm.

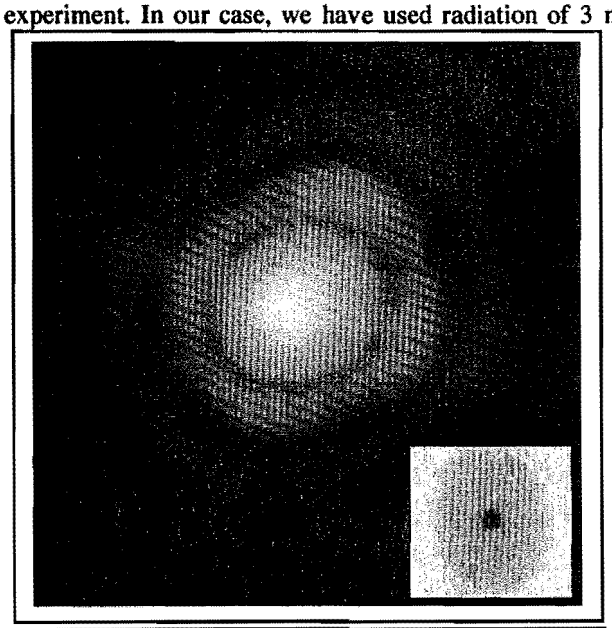

Fig.1 Diffraction pattern from two 1 μm pinholes, laterally separated by 10 μm. The wavelength of the radiation is 3 nm, the raw undulator output in the 1st harmonic without monochromatization was analyzed. In the center, transmission of the soft x-rays through the 4 μm Fe substrate can be observed. The 2D Fourier transform of the coherent scattering image shown in the inset indicates the real space positions of the two pinholes.

Coherent, resonant scattering of soft x-rays was observed from $LaFeO_3$ films, grown in an oxide molecular beam epitaxy system by means of a block-by-block growth method on a $SrTiO_3$ (100) substrate. $LaFeO_3$ is an antiferromagnet. The antiferromagnetic axis of the $LaFeO_3$ includes an angle of 45° with the sample surface and can assume two orientations with their respective projections on the sample surface perpendicular to each other. The

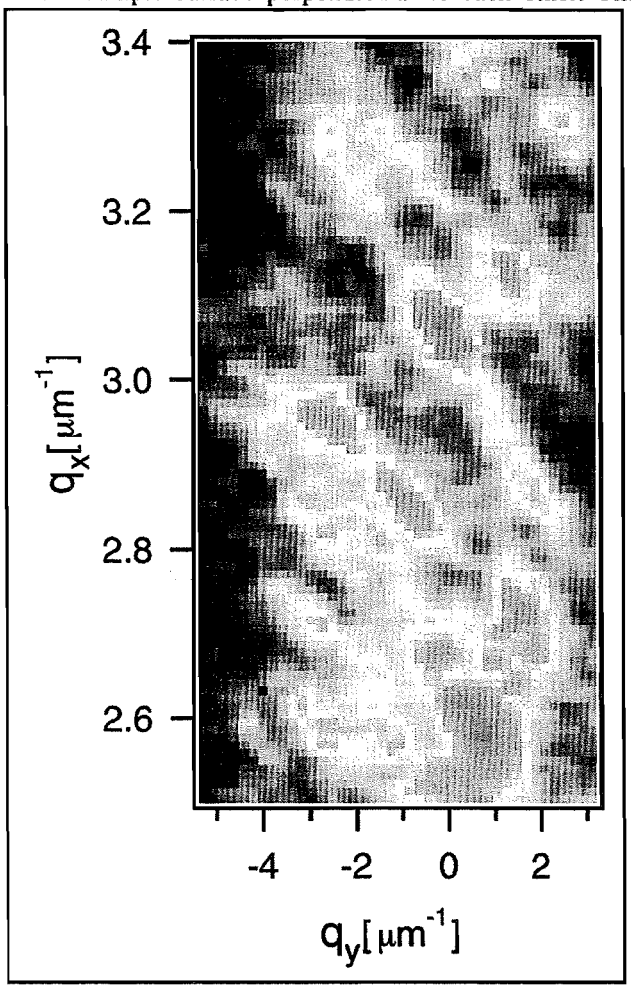

Fig. 2.
Speckle structure in the coherent scattering from a $LaFeO_3$. The intensity map is linear in false color. q_y=0 defines the scattering plane. The glancing angle of incidence on the sample is 7°, the incident photon energy is 708.5 eV

samples were imaged by XMLD-spectromicroscopy [1] and were mounted with one of the antiferromagnetic axis directions in the scattering plane. We will call these domains $\parallel$-domains as opposed to the $\perp$-domains, which are characterized by a projection of their antiferromagnetic axis on the sample surface that is perpendicular to the scattering plane. In our experimental setup, the direction of the electric field vector of the incident x-rays **e** is kept perpendicular to the scattering plane. As the XMLD term in the resonant scattering contains the scalar product **e**·**M**, where **M** is the local magnetic moment [2], the $\parallel$-domains cannot contribute to the XMLD scattering and only the $\perp$-domains in our sample will contribute to the magnetic scattering. As a result, the domain pattern acts as an amplitude pattern for the scattering, and we observe indeed speckle structure in the coherent scattering, as expected for an irregular arrangement of scatterers. In Fig. 2, a part of the scattering as measured in parallel by a position sensitive detector is reproduced in a false color map.

The incident radiation is tuned to 708.5 eV (1.75 nm), corresponding to a specific resonance within the Fe L_3 absorption edge, which exibits the XMLD effect. To proof the existence of antiferromagnetic contributions to the scattering, we change the incident photon energy to 710.1 eV. This small change in energy brings us to another distinct resonance within the Fe L_3 edge, where the XMLD scattering amplitude changes its sign. We observe a reproducible change in the speckle pattern [3], when we change the incident energy between the two resonances. This observation indicates, that the observed speckle pattern cannot be solely due to topology scattering due to the sample surface roughness, but that it contains contrast due to the distribution of the antiferromagnetic domains.

Recently, it has been demonstrated that soft x-ray speckle patterns can be used to probe the dynamics of a system even in thermal equilibrium [4] and that the real space information can be obtained from speckle patterns using an algorithm and oversampling in order to solve the phase problem [5]. On the basis of our results, we expect that similar information will be experimentally accessible in the future for surfaces with antiferromagnetic domains.

[1] J. Stöhr et. al. Phys. Rev. Lett. **83**, 1862 (1999)

[2] J. P. Hannon, G. T. Trammell, M. Blume, D. Gibbs, Phys. Rev. Lett 61, 1245 (1988)

[3] S. Eisebitt, M. Lörgen, R. Scherer, W. Eberhardt, A. Rahmin, S. Tixier, T. Tiedje, J. Lüning, J. Stöhr, to be published.

[4] A. C. Price et. al., Phys. Rev. Lett. **82**, 755 (1999).

[5] J. Miao, P. Charalambous, J. Kirz, D. Sayre, Nature **400**, 342 (1999).

Further advances in investigations of hydrophobic Fluoroalkyl Silanes

D. Schondelmaier, S. Cramm, R. Klingeler, C. Zilkens, and W. Eberhardt

Institute 'Electronic Properties'

In the last annual report we gave details about investigations of new hydrophobic materials suited for the application as self-cleaning surfaces by use of the Lotus effect. Due to its characteristics like self orientation and formation of monolayers on several substrates, these Fluoroalkyl Silanes (FAS) proved to be an interesting representative for an industrial application. This year, one emphasis of our researches was the orientation of FAS again. We compared computer simulated and experimental measured XANES spectra. Additional XANES measurements of molecules with various chain length are given. Another property of such FAS was found. It concerns a partial desorption of the molecules by UV irradiation. This phenomenon also called 'cracking' opens a multiplicity of new applications.

F&E-Nr.: 23.20.0

Since the exact geometries and the electronic structure of the molecule, witch are needed for the interpretation of the XANES experiments, were not found in the literature. Therefore we have calculated the chemical bonds using the density functional. Starting with a singlet electronic configuration $C_6F_9H_4Si(OH)_3$ molecule, the geometries were fully optimized within the local density approximation.

The calculated FAS molecule pattern is given in Fig.1 .The helical symmetries of C-F bonds is a new interesting detail of this calculation. **Fig.1 :**

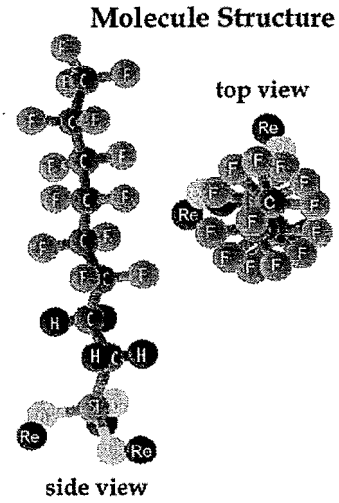

In order to determine the orientation of the FAS molecules relative to the surface, polarization dependent XANES (X-ray Absorption Near Edge Structure) measurements were done at the fluorine K-edge by use of the linear polarized synchrotron radiation of DELTA (Dortmund).

In addition to the study of last year, we have examined on clean silicon wafers three FAS molecules of different chain lengths: $C_8F_{13}H_4Si(Re)$, $C_6F_9H_4Si(Re)$ and $C_{10}F_{17}H_4Si(Re)$. The molecules differ only in their C-F chain length. The strength of the polarization dependence is compatible with the different molecule sizes and supports even on the longer chains the picture of a monolayer with the molecules oriented perpendicular to the surface.

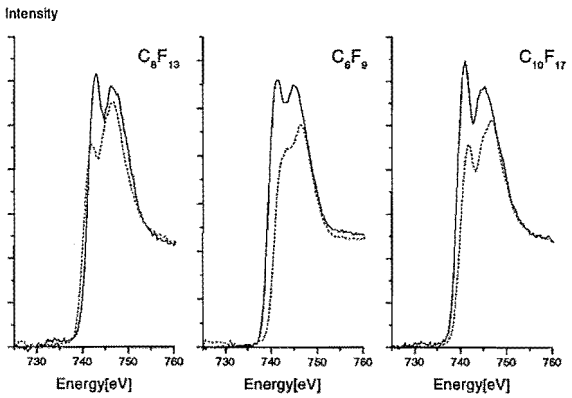

Fig. 2 : Absorption at the F K-edge with the E-vector of the x-rays parallel (solid line) and perpendicular (dotted) to the surface.

The absorption signal for the different polarization angles was simulated based on the p-like states found in the calculations. The results are given in Fig. 3. The angular dependence of the spectrum is the same in both, simulation and measurement, indicating that our geometric model is correct. **Fig.3 :**

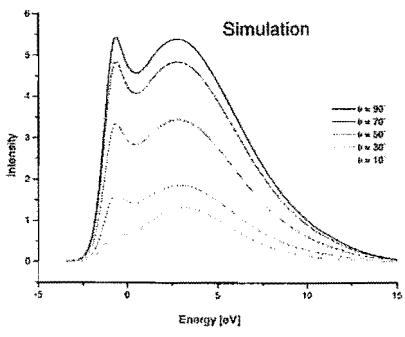

Pump-probe photoelectron spectroscopy on mass-selected metal cluster anions

N. Pontius, G. Lüttgens, P.S. Bechthold, M. Neeb and W. Eberhardt
Institute "Electronic Properties"

The combination of femtosecond light pulses with pump-probe technique has enabled to study ultrashort electron dynamics in metallic systems in real time. Of emerging interest is the dynamics of excited electrons in a non-equilibrium state, which is created when an electron is photoexcited by an ultrashort light pulse. To explore such energy thermalization processes in clusters we have set up a photoelectron experiment for time-resolved pump-probe photoelectron spectroscopy on mass selected transition metal cluster anions. The experimental setup consisting of a laser vaporization cluster source, a time-of-flight mass spectrometer and a magnetic-bottle time-of-flight electron spectrometer is shown in Fig. 1.

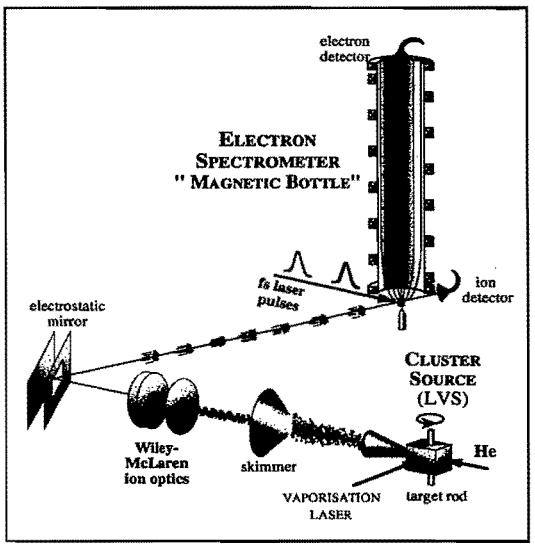

Fig. 1. Experimental setup for fs-spectroscopy on mass-selected metal cluster anions.

Pump-probe photoelectron spectra of Pd_3^-, Pd_4^- and Pd_7^- are shown in Fig. 2 which are recorded with two femtosecond pulses at a photon energy of ~1.5 eV. The relaxation dynamics of an excited electronic state is monitored by an exciting pump pulse and a second probe pulse which photodetaches an electron from the photoexcited cluster after a certain delay time. The time delay can reliably be controlled from 10 fs to 1 ns. The energy scales in Fig. 2 refer to

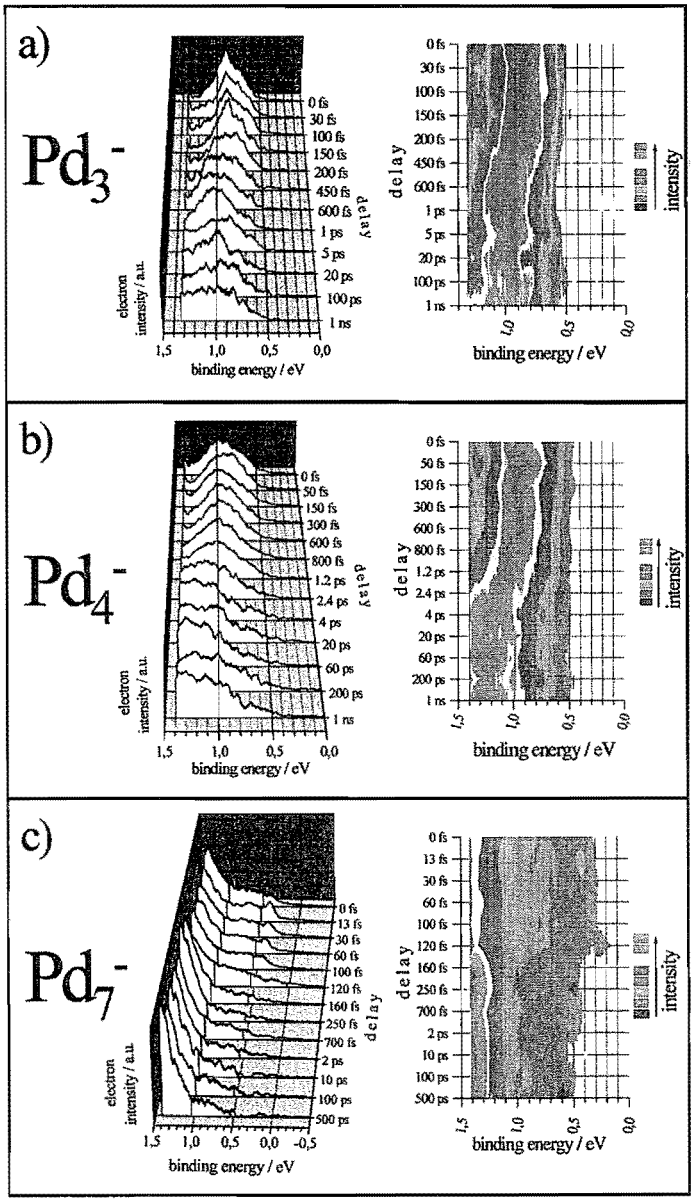

Fig. 2: Time-resolved photoelectron spectra of Pd-cluster anions using two subsequent fs-laser pulses of 1.5 eV.

the electron binding energies of the photoexcited Pd_n-cluster anions: $E_{bin}(Pd_n^*) = h\nu - E_{kin}$. Zero defines the vacuum level while the Fermi level (chemical potential) is located at a binding energy of 1.5 eV (Pd_3^-), 1.45 eV (Pd_4^-) and 1.9 eV (Pd_7^-), respectively. The minimum binding energy of the photoexcited cluster is given by

$$E_{bin,\min}(Pd_n^{-*}) = h\upsilon - E_{kin,\max}^{2h\upsilon} = EA - h\upsilon.$$

With increasing time delay a redistribution of the two-photon photoelectron intensity from lower to higher binding energies is clearly obvious for all three Pd-clusters. At zero delay the two-photon photoemission spectra of Pd_3^- and Pd_4^- show a broad asymmetric single feature between 0.5 and 1.2 eV. After 400 fs the intensity within the high binding energy region increases considerably. At a delay of > 2 ps the intensity above 1.2 eV reaches a maximum value while the intensity on the low binding energy flank is continuously reduced. At a delay of > 10 ps the intensity distribution is more or less constant indicating that a quasi steady state has been reached. In the right panel of Fig.2 contour plots are displayed which emphasise the trend of a continuous intensity shift from lower to higher binding energies within 1 ps. The dynamics of the photoexcited Pd-clusters can be interpreted by the relaxation of a non-thermal electron distribution that is created at the moment of photoabsorption. The excited electronic state scatters into degenerate electronic states which tends to maxime the internal entropy.

In order to extract the relaxation time for the optically excited states in Pd_3^-, Pd_4^- and Pd_7^- we have applied a least square fit based on a first-order exponential population dynamics N(t). The probed photoelectron intensity P(τ) as a function of the delay time τ is proportional to the integral of the population dynamics times the temporal intensity distribution of the probe pulse I(t):

$$P(\tau) \propto \int_{-\infty}^{+\infty} I(t-\tau)\cdot N(t)dt$$ [1]. Taking into account the temporal width of the pump and probe pulses (80 fs) an effective lifetime of 90 ± 30 fs has been derived for Pd_3^-, 200 ± 20 fs for Pd_4^- and 80 ± 20 fs for Pd_7^-. The electron relaxation times are about one order of magnitude smaller than those of optically excited electrons in bulk metals [2].

We note that the total photoelectron intensity in Fig. 2 decreases by a factor of 2-5 from 100 fs to 1 ns. This decrease can be explained by a cooling of the electron system. After about 100 fs the thermalized electronic system can be rationalized by a Fermi-distribution of 1.5 eV internal energy (Fig. 3). With increasing time the energy is withdrawn from the electronic system at the expense of an increasing temperature of the vibrational system leading to vibrational excitation and isomeric structures. Thus the total number of excited electrons above the Fermi energy (chemical potential) decreases the more the energy drains off into the vibrational system. A simulation of the cooling of the electron system is shown in Fig. 3 assuming a density of states with a mean level spacing of 40 meV and 25 electronic states/eV.

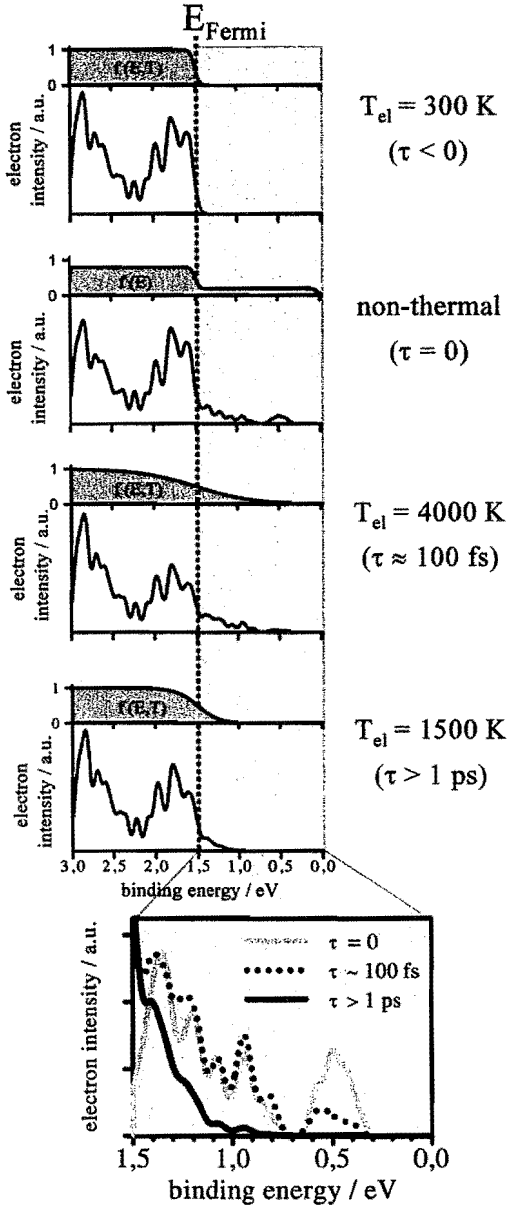

Fig.3. Simulation of hot-electron distributions of a discrete level system at an excitation energy of 1.5 eV.

[1] N. Pontius et *al.*, Phys. Rev. Lett. **84**, 1132 (2000).
[2] E. Knoesel, et *al.*, Surf. Sci. **368**, 76 (1996).

We thank A. Bringer, IFF/Theory, for stimulating discussions.

Time-resolved Photofragmentation of Metal-Carbonylclusters

G.Lüttgens, N.Pontius, P.S.Bechthold, M.Neeb, and W.Eberhardt
Institute "Electronic Properties"

The dissociation of the cluster-adsorbate-systems $Pt_2(CO)_5^-$ and Au_2CO^- have been recorded by measuring femtosecond-time-resolved 2-photon-photoelectron-spectra. Both clusters loose one CO-molecule after absorption of a 1.5eV-pump-photon. While the dissociation of Au_2CO^- seems to occur via a dissociative state within some hundred fs after excitation, $Pt_2(CO)_5^-$ evaporates CO in a statistical manner after thermalization of the absorbed energy. An ultrafast electronic relaxation process of the photo-excited state can in addition be seen in the spectra at low binding energies.

F&E-Nr. 23200

Cluster-adsorbate-systems can serve as model systems for adsorption sites in catalysts. Therefore studies of molecules adsorbed to clusters are expected to improve our knowledge about the nature of the bonding at such sites, particularly with respect to bond activation. The use of time-resolved two-photon-techniques allows to study the energy relaxation and the breaking of bonds in such systems.

The dissociation of the saturated $Pt_2(CO)_5^-$ and Au_2CO^- could be recorded in real time in a 2-photon-photoemission-experiment using a femtosecond laser. The cluster-adsorbate-systems were produced in a laser vaporization source with an additional CO-adsorbate-gas-valve. The cluster-adsorbates were mass-selected in a time-of-flight mass spectrometer and then excited by a 70 fs-pulse of 1.5eV-photons produced in an amplified Ti:Sapphire-femtosecond-lasersystem ('pump'-pulse, pulse energy ca. 1.0 mJ). 3eV-photoelctron-spectra were taken with a frequency-doubled and delayed 'probe'-pulse (time delay up to 3ns).

Pump-probe-spectra of $Pt_2(CO)_5^-$ are shown in Fig. 1. At short delay times one can see a vibrationally resolved double peak structure at a binding energy of 0.5 eV corresponding to the state excited by the pump-photon. This structure vanishes very quickly within 200 fs due to the fast thermalization of the excitation energy into the vibronic degrees of freedom of the clusters. At long delay times, the 2-photon-spectra develop into the spectrum of $Pt_2(CO)_4^-$ which leads to the conclusion that the clusters evaporate one CO-molecule statistically after excitation.

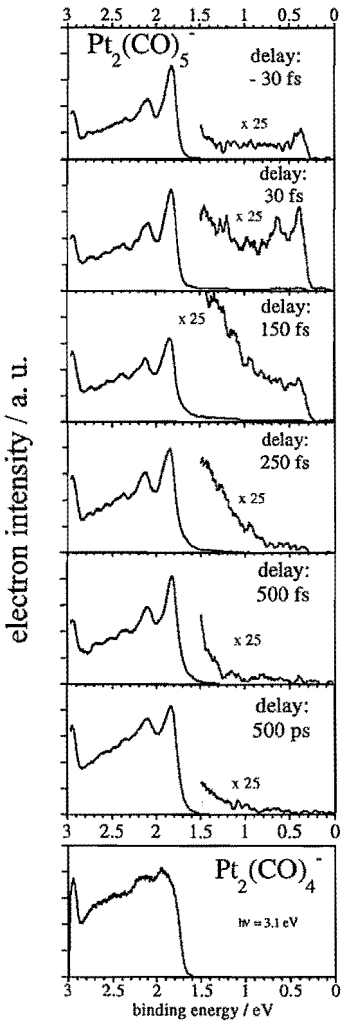

Fig. 1: Femtosecond-time-resolved photoelectron spectra of $Pt_2(CO)_5^-$

In contrast to this scenario, the dissociation of Au_2CO^- after excitation with a 1.5eV-photon does not occur statistically, but directly via a dissociative state. The 2-photon-photoelectron-spectra are shown in Fig. 2. A peak at a binding energy of 2.0 eV rises up in the spectra with a time constant of some hundred fs. This peak belongs to the dissociated product Au_2^-, as can be seen by comparison with the pure Au_2^-- spectrum at the bottom of Fig. 2.

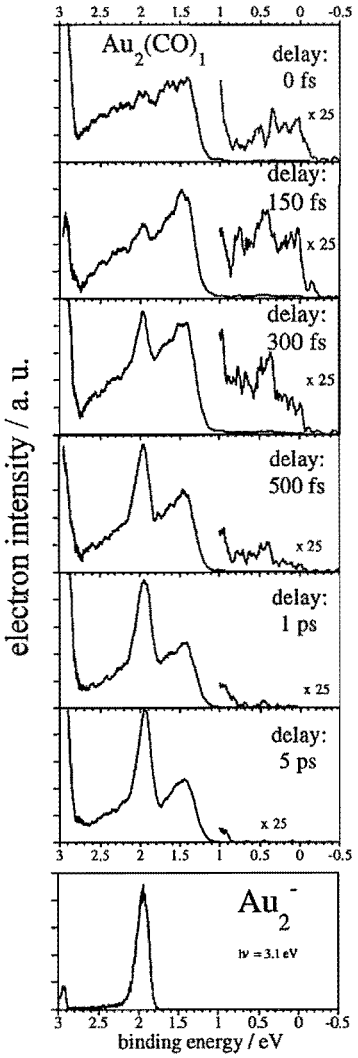

Fig. 2: fs-time-resolved photofragmentation of $Au_2(CO)^-$

The fast dissociation can be explained by the direct population of a dissociative state by the 1.5 eV-photon as shown schematically in Fig. 3.
An empiric potential energy curve of the dissociative state is found by fitting the parameters of an Born-Mayer potential to the experimental data (dissociation time and estimated kinetic energy) in a semiquantitative way. The 1/e-lenght of the potential is obtained to be about 0.5 Å.

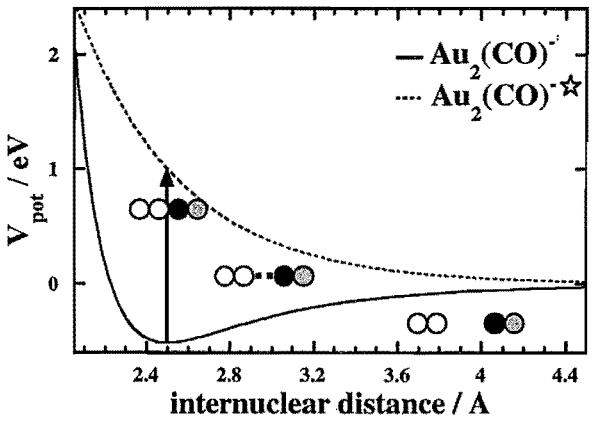

Fig. 3: Potential energy scheme of the dissociation of $Au_2(CO)^-$

For the near future further measurements on other metal-carbonylclusters and on metal-nitrogen-clusters are in preparation. A mass spectrum of the first copper-

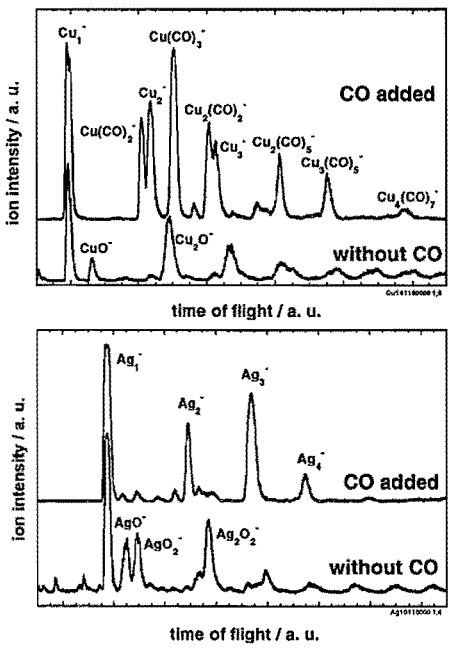

Fig. 4: Mass spectra of pure and CO-adsorbed Cu- and Ag-clusters

carbonyl-clusters produced is shown in fig. 4. Note that adding CO suppresses the oxidation of the clusters. This effect can also be seen with silver clusters, which do not adsorb CO-molecules (Fig. 4).

Dynamics of image-potential states on the Ni(111) surface

S. Link, J. Sievers, H.S. Rhie, H.A. Dürr and W. Eberhardt
Institute "Electronic Properties"

Using time-resolved two photon photoemission spectroscopy we have investigated the population dynamics of image-potential states on the clean and hydrogen-covered Ni(111) surface. On the clean surface a lifetime of 7±3 fs for the n=1 state is obtained. The adsorption of hydrogen increases the lifetime by a factor of two to 14±4 fs.

F&E-Nr. 23200

When electrons approach a metal surface they can be trapped by their own image charge inside the metal. This attractive interaction leads to a series of bound states if the metal surface is characterized by a high electron reflectivity usually provided by a gap in the electronic band structure. The binding energies of these so-called image-potential states (IPSs) depend on quantum numbers $n = 1, 2, ...$ and are given by $E(n) = E_{Vac} - 0.85eV/(n+a)^2$ converging towards the vacuum level, E_{Vac}. The quantum defect a is related to the phase shift upon electron reflection at the crystal. IPSs are mainly localized in front of the surface and very closely represent a two-dimensional electron gas.

Theory predicts IPS lifetimes to increase with n^3 [1]. This was indeed observed for the $n > 1$ states on the (100) surfaces of Cu and Ag with time-resolved two-photon photoemission spectroscopy (TR2PPE) [2]. However, the lifetimes depend strongly on the wavefunction overlap with bulk states. This effect is especially pronounced on noble metal (111) surfaces where the $n > 1$ IPSs are almost degenerate with bulk bands [3] [4]. As a consequence their lifetimes are dramatically reduced. The n=1 IPS on the other hand is still located inside the band gap and its lifetime was found to be mainly determined by decay into electron-hole pairs [5]. For this energy relaxation process the surface electronic structure has to be taken into account. While for noble metal surfaces the IPS decay mechanisms are now very well understood there is still little direct information available for transition metal surfaces. On these surfaces the partially unoccupied d-levels should provide a very efficient decay mechanism.

In a TR2PPE experiment the n=1 state on Ni(111) is populated from an occupied state through the frequency-tripled output (4.7 eV) of a Ti:sapphire laser system operating with a repetition rate of 250 kHz. A second frequency-doubled laser pulse (3.13 eV) was used to excite the electrons from the IPS above the vacuum level, E_{Vac}. The kinetic energy of the ejected electrons was measured at normal emission with a hemispherical analyzer. Both pump (hν =4.7 eV) and probe (hν =3.13 eV) pulses were 80 fs long as was measured directly at the sample. Measurements were performed in a UHV chamber with a base pressure in the lower 10^{-10} mbar range. The Ni(111) crystal was cleaned by cycles of 500 eV Ar^+ sputtering and subsequent annealing up to 900 K. All experiments were performed at room temperature. Hydrogen was adsorbed on the surface by filling the chamber with H_2 gas.

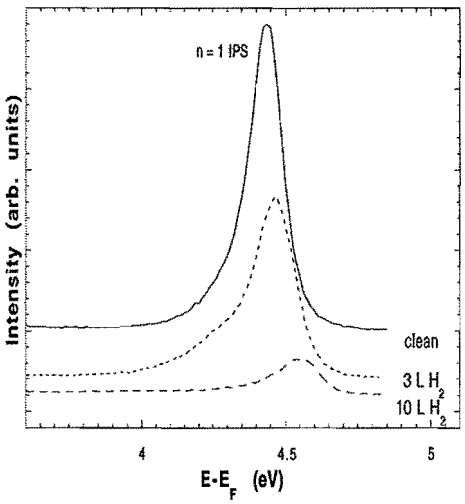

FIG. 1. Normal emission photoelectron energy distribution curves obtained from the clean Ni(111) surface and for different hydrogen exposures. One 4.7 eV is absorbed to populate the n=1 IPS while a 3.13 eV photon is used to probe its occupancy.

Fig. 1 displays 2PPE spectra of the n=1 IPS for the clean Ni(111) surface (solid line) and for different hydrogen exposures up to saturation (dashed lines). The spectra were taken at zero time delay between pump and probe pulses and are caused by two-photon photoemission processes. On the clean surface we obtain a binding energy relative to the vacuum level of 0.77±0.03 eV which is close to the value of 0.80±0.03 eV observed by Giesen et al. [6]. The binding energy increases to 0.83±0.03 eV at saturation coverage. Since the IPSs are pinned to the vacuum level a work function change caused by the adsorbat will be reflected in a shift of the energy position of

the n=1 IPS relative to E_F. In addition there is a strong intensity attenuation of the emission from the IPS. This is caused by the quenching of the occupied Λ_1 surface state which provides a very efficient excitation channel on the clean surface due to the large wavefunction overlap with the IPS [6]. The shoulder at the low energy side of the IPS is caused by two-photon photoemission from bulk states.

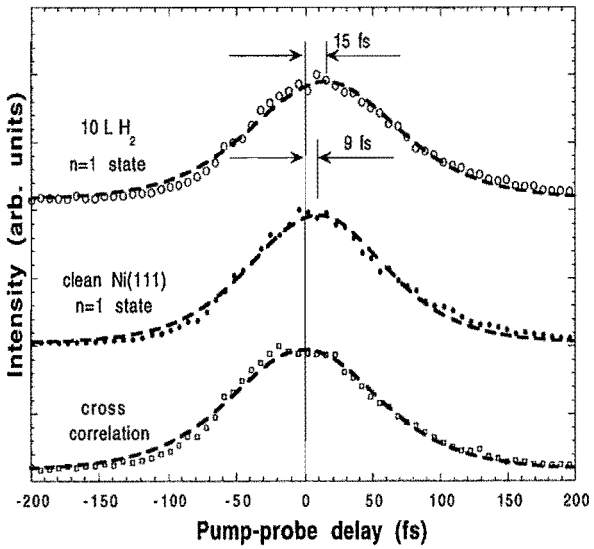

FIG. 2. Transient response of the IPS as a function of delay between pump and probe pulses for the clean (filled circles) and hydrogen-saturated (open circles) Ni(111) surface.

The lifetime of the image-potential state was measured by setting the electron analyzer to the n=1 IPS peak and scanning the pump-probe pulse delay. Typical results are displayed in Fig. 2 for the clean (solid circles) and hydrogen-saturated (open circles) Ni(111) surface. The instrumental cross-correlation trace was measured at kinetic energies just below the n=1 IPS peak and is shown in Fig. 2 (open squares). Assuming $sech^2$-shaped laser pulses, a fit to the instrumental cross-correlation trace gives a width of 125 fs (solid line). The most obvious effect observed in the n=1 IPS transient response of is the shift of the center position towards larger pump-probe delays upon hydrogen exposure. For lifetimes shorter than the pump-pulse duration the description of the experimental results by a theoretical model employing the solution of the Liouville-von-Neumann equation is capable of describing the IPS population dynamics [2] [7]. It is known that lifetimes below about 20 fs are given by the shift of the transient response towards larger time-delays [8]. From fits to the data (dashed lines) we obtain lifetimes of 7±3 fs and 14±4 fs for the n=1 state on the clean surface and hydrogen saturated surface, respectively.

The lifetime of the n=1 IPS on Ni(111) is much shorter than on other surfaces [2] [3] [4]. The decay of image-potential states is governed mainly by two effects. A strong wavefunction overlap of the IPS with energetically degenerate bulk states can cause the IPS population to decay into the bulk of the crystal. This effect strongly reduces the IPS lifetime especially for higher n when the IPS series is located near the top of the bulk band gap [3] [4]. Hydrogen adorption on Ni(111) increases the sample work function and moves the IPS series energetically closer to the upper band gap edge. However, the n=1 IPS is still far enough localized inside the gap and we do not observe any decrease of its lifetime. On the contrary, the lifetime nearly doubles for the hydrogen-saturated surface. This demonstrates that τ is dominated by the decay of the IPS electrons into unoccupied states closer to E_F. Energy and momentum conservation requires the creation of electron-hole pairs. The decay rate is, therefore, determined by both the unoccupied and occupied density of states near E_F. Surface states were found to play a significant role in this process since the wavefunction overlap with the IPS is much stronger than that of bulk states. The quenching of the occupied Λ_1 surface state should, therefore, account to a large extent for the observed lifetime increase.

It is worthwhile to note that the IPS lifetime on Ni(111) and H/Ni(111) is considerably shorter than that on Pd(111) ($\tau = 25 \pm 4$ fs) [9]. This indicates that the IPS decay is significantly influenced by the d-level occupancy which is ultimately also responsible for the ferromagnetic properties of Ni.

[1] P.M. Echenique and J.B. Pendry, J. Phys. C 11 (1978) 2065.

[2] I.L. Shumay, U. Höfer, Ch. Reuß, U. Thomann, W. Wallauer and Th. Fauster, Phys. Rev. B 58 (1998) 13974.

[3] R.W. Schoenlein, J.G. Fujimoto, G.L. Eesley and T.W. Capehart, Phys. Rev. B 43 (1991) 4688.

[4] M. Wolf, E. Knoesel and T. Hertel, Phys. Rev. B 54 (1996) R5295.

[5] S. Schuppler, N. Fischer, Th. Fauster and W. Steinmann, Phys. Rev. B 46 (1992) 13539.

[6] K. Giesen, F. Hage, F.J. Himpsel, H.J. Riess and W. Steinmann, Phys. Rev. B 33 (1986) 5241.

[7] J. C. Diels and W. Rudolph, Ultrashort Laser Pulse Phenomena, Academic Press, San Diego, 1996.

[8] T. Hertel, E. Knoesel, M. Wolf and G. Ertl, Phys. Rev. Lett. 76 (1996) 535.

[9] A. Schäfer, I.L. Shumay, M. Wiets, M. Weinelt, Th. Fauster, E.V. Chulkov, V.M. Silkin and P.M. Echenique, Phys. Rev. B 61 (2000) 13159.

Resolving Complex Atomic-Scale Spin-Structures by SP-STM

D. Wortmann, S. Heinze†, Ph. Kurz, G. Bihlmayer, and S. Blügel
Institute "Electronic Properties"

We propose the application of the constant-current (topography) mode of a spinpolarized scanning tunneling microscope (SP-STM) to investigate the complex (e.g. non-collinear) atomic-scale magnetic structure of otherwise chemically equivalent atoms. The power of this method has recently been demonstrated to give the first experimental evidence of a two-dimensional antiferromagnet.

F&E-Nr. 23420

The field of magnetism has experienced an incredible expansion in both basic and applied research over the past 15 years. To understand the complex materials involved in detail, we need to understand the behavior of surfaces and interfaces as function of their electrical and magnetic properties. The most important issues relate to the magnetic structure at these surfaces and the change of the magnetic properties when the atoms are confined to one or two dimensions (2D). In many cases, the geometrical arrangement of the atoms does not allow to satisfy the competing exchange interactions between neighboring atoms, which leads to frustrated spin structures. Well-known examples are ferromagnetic films in contact with antiferromagnetic ones as it is common for exchange-bias systems used in the magnetic recording industry and in magnetoelectronics or for antiferromagnets on a triangular lattice. Magnetic frustration is known to give rise to a wide variety of complex magnetic structures, e.g. antiferromagnetism, spin-density waves (SDW), and general non-collinear spin-structures, which determine the magnetic structure at the surfaces of thin films.

These spin-structures in nano-scale devices are still poorly understood because of the inability of traditional techniques to spatially determine the magnetic structure of the antiferromagnetic thin film. The size of the magnetic structure is below the spatial resolution of neutron diffraction topography (about 70 μm), X-ray diffraction topography (1-2 μm) and the fundamental resolution limit (about 0.2 μm) set by diffraction for optical and non-linear optical techniques. Currently two groups, S. Heinze *et al.* [1] and A. Scholl *et al.* [2] have developed independent techniques to image the magnetic structure of surfaces and interfaces in great detail. Scholl *et al.* used polarization-dependent X-ray magnetic dichroism spectro-microscopy and we [1] suggested the use of the spin-polarized scanning tunneling microscopy (SP-STM) in the constant current (topography) mode. The potential of the latter approach has recently been demonstrated proving experimentally for the first time the existence of collinear two-dimensional antiferromagnetism in monolayer (ML) Mn films on W(110) [1].

In Ref. [3], we go one step further: By generalizing the Tersoff-Hamann model to the case of SP-STM and considering the effect of the vacuum barrier on the lateral resolution of the STM, we propose the topography mode of SP-STM to investigate more complex atomic-scale magnetic structures. As an example we calculate SP-STM images of a monolayer Cr on Ag(111), which has a 120° Néel magnetic ground state as we deduce from total-energy calculations.

We derived the spin-dependent tunneling current, I, for the case of SP-STM:

$$I(\mathbf{R}_T, V, \theta) = I_0(\mathbf{R}_T, V) + I_P(\mathbf{R}_T, V, \theta) \tag{1}$$

$$= \frac{4\pi^3 C^2 \hbar^3 e}{\kappa^2 m^2} \left[n_T \tilde{n}_S(\mathbf{R}_T, V) + \mathbf{m}_T \tilde{\mathbf{m}}_S(\mathbf{R}_T, V) \right], \tag{2}$$

where V is the bias-voltage, $\mathbf{m}_T = (n_T^{\uparrow} - n_T^{\downarrow})\mathbf{e}_M^T$ is the magnetization of the tip and $\theta(\mathbf{R}_T)$ denotes the angle between the direction of the magnetization of the tip and the sample at the position of the tip, $\mathbf{R}_T$. Furthermore, we have introduced the integrated local density of states (ILDOS) of the sample $\tilde{n}_S(\mathbf{R}_T, V)$ and the the integrated local vector magnetization density of states of the sample $\tilde{\mathbf{m}}_S(\mathbf{R}_T, V)$ given by an energy integral of the local magnetization density of states, $\mathbf{m}_S(\mathbf{R}_T, \epsilon)$:

$$\mathbf{m}_S(\mathbf{R}_T, \epsilon) = \sum_{\mu} \delta(\epsilon_\mu - \epsilon) \Psi_\mu^{S\dagger}(\mathbf{R}_T)\, \boldsymbol{\sigma}\, \Psi_\mu^S(\mathbf{R}_T) \tag{3}$$

$$\tilde{\mathbf{m}}_S(\mathbf{R}_T, V) = \int d\epsilon\, g_V(\epsilon)\, \mathbf{m}_S(\mathbf{R}_T, \epsilon), \tag{4}$$

with $g_V(\epsilon) = f(\epsilon - \epsilon_F) - f(\epsilon + eV - \epsilon_F)$, where $f(\epsilon)$ is the Fermi function. Notice that $\tilde{\mathbf{m}}_S$ depends on $\mathbf{R}_T$ and thus includes the non-collinear spin-structure of the surface. Analogously, the ILDOS of the sample $\tilde{n}_S(\mathbf{R}_T, V)$ is defined by Eq. (3) and Eq. (4) by replacing Pauli's spin matrix $\boldsymbol{\sigma}$ by the unit matrix. Eq. (1) states that the tunneling current can be separated into a non-spinpolarized part, I_0, depending on the local DOS of the sample at the position of the tip and a spinpolarized contribution, I_P, given by the projection of the vector of the local magnetization DOS to the magnetization direction of the tip.

The STM image, given by the vertical adjustment $\Delta z(\mathbf{r}_\parallel, V, \theta)$ of the tip to constant tunneling current I, is determined by the change ΔI of the tunneling current. For a surface with 2D translational symmetry, ΔI can be written in terms of a 2D Fourier expansion:

$$\Delta I(\mathbf{r}_\parallel, z, V, \theta) = \sum_{n \neq 0} \Delta I_{\mathbf{G}_\parallel^n}(z, V, \theta)\, e^{i\mathbf{G}_\parallel^n \mathbf{r}_\parallel} \tag{5}$$

where $\mathbf{G}_\parallel^n$ denotes the reciprocal lattice vectors parallel to the surface, and $\Delta I_{\mathbf{G}_\parallel^n}(z,V,\theta)$ is the tip-sample distance (z) dependent expansion coefficient. This expansion can be applied to the non-spinpolarized part of the current, I_0, as well as to the spinpolarized part, I_P, of Eq. (1). The expansion coefficients decay exponentially with increasing length of $\mathbf{G}_\parallel^n$ and hence the STM image is dominated to a good approximation by the smallest non-vanishing reciprocal lattice vector $\mathbf{G}_\parallel^{(1)}$:

$$\Delta I(z,V) \approx \Delta I_{\mathbf{G}_\parallel^{(1)}}(V)\, e^{-2z\sqrt{\frac{2m}{\hbar^2}|\epsilon_F+eV|+(\frac{1}{2}G_\parallel^{(1)})^2}}. \quad (6)$$

Any magnetic superstructure lowers the translational symmetry. Therefore, smaller reciprocal lattice vectors become relevant for the spinpolarized part of the tunneling current, I_P, with coefficients which are consequently exponentially larger than those of the non-spinpolarized part, I_0. An SP-STM image thus reflects the magnetic superstructure rather than the chemical unit cell.

Now we apply this approach to resolve the spin-structure of one ML Cr on Ag(111). The nearest neighbor exchange interaction of Cr is antiferromagnetic and the Ag(111) substrate provides a triangular lattice, thus, we expect a frustrated spin-structure. We determined the ground-state spin structure of 1ML Cr on Ag(111) by performing self-consistent *ab initio* calculations based on the density-functional theory in the local spin-density approximation (LSDA). We apply the full-potential linearized augmented plane-wave (FLAPW) method in film geometry as implemented in the program FLEUR [4] recently extended by Ph. Kurz *et al.* [5] to treat non-collinear magnetic structures such as spiral SDWs. We found that the coplanar non-collinear periodic 120° Néel state (a 2D non-collinear structure with three atoms per surface unit-cell, which consists of spins forming 120° angles between nearest neighbors, see Fig. 2) is lower in energy than the the row-wise antiferromagnetic state (RW-AFM) (a unit-cell of two atoms, with spins which are ferromagnetically aligned along a row of nearest-neighbor atoms and antiferromagnetically aligned from row to row, see Fig. 1), and thus the magnetic ground-state.

Fig. 1 shows the calculated STM images for the RW-AFM structure. Fig. 1(a) shows an image calculated for a non-magnetic STM tip resulting in a hexagonal pattern corresponding to the chemical unit cell. Fig. 1(b) displays the SP-STM image calculated for a magnetic tip with a magnetization axis parallel to the one of the sample. We find a stripe pattern reflecting the broken symmetry between the atoms of different rows. Atoms with a magnetic moment parallel to the magnetization of the tip are imaged as protrusions while atoms with antiparallel magnetic moments appear as depressions. This setup provides maximal magnetic contrast as the angle between the direction of the magnetization of the tip and the magnetization of the sample is zero. A different angle would simply lead to a reduction of the magnetic contrast, restoring Fig. 1(a) for $\theta \to 90°$.

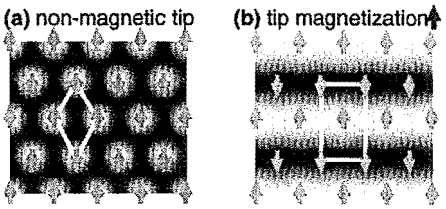

FIG. 1. Calculated STM images (grey scale plot) for the RW-AFM structure at a bias voltage of −0.5 V for a tip-sample distance of 3.7 Å and a fully spinpolarized tip. The structure of the unit-cell (yellow), the directions of the magnetic moments (red), and its projection on the direction of the moment of the tip (green) are superimposed.

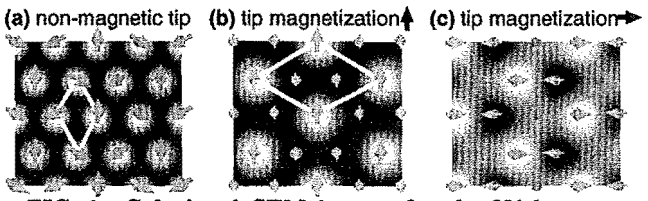

FIG. 2. Calculated STM images for the Néel structure. The image for conventional STM (non-magnetic tip) and for two different directions of the tip magnetization, i.e. for two different values of θ, are displayed.

Now we turn to the Néel structure displayed in Fig. 2. Fig. 2(a) shows again the STM image as expected for a conventional, non-spinpolarized tip. The two other plots [Fig. 2(b) and Fig. 2(c)] correspond to SP-STM images calculated for magnetic tips with two different directions of the magnetization. For Fig. 2(b) the magnetization of the tip has been chosen parallel to the magnetic moment of one of the three magnetically inequivalent atoms while the projection of the magnetic moment of the two other atoms onto the tip magnetization is the same. Consequently, the image displays a $(\sqrt{3}\times\sqrt{3})$ superstructure. If the projected magnetization, $\tilde{\mathbf{m}}_S\mathbf{e}_M^T$, is different for all atoms in a surface unit-cell as in Fig. 2(c), additional features appear in the image and the contrast is reduced. We conclude that not only the magnitude of the magnetic contrast but also the detailed pattern of the SP-STM image depends on the direction of the magnetization of the tip for the 120° Néel structure. It is obvious that the RW-AFM and the Néel state can be easily distinguished depending on whether a stripe pattern or a $(\sqrt{3}\times\sqrt{3})$ superstructure will be found.

† Present address: Microstructure Research Center, University of Hamburg, Jungiusstrasse 11, D-20355 Hamburg.

[1] S. Heinze, M. Bode, A. Kubetzka, O. Pietzsch, X. Nie, S. Blügel, and R. Wiesendanger, Science **288**, 1805 (2000).
[2] A. Scholl *et al.*, Science **287**, 1014 (2000).
[3] D. Wortmann, S. Heinze, Ph. Kurz, G. Bihlmayer, and S. Blügel, submitted to Phys. Rev. Lett.
[4] http://www.flapw.de
[5] Ph. Kurz, G. Bihlmayer, K. Hirai, and S. Blügel, accepted at Phys. Rev. Lett.

Publications in refereed journals

Bihlmayer G.; Asada T.1; Blügel S.
1Shizuoka University, Hamamatsu, Japan
Electronic and magnetic structure of the (001)-surfaces of V, Cr, and V/Cr
Phys. Rev. B 62, R11937 (2000)
23.20.0

Bihlmayer G.; Kurz Ph.; Blügel S.
Overlayers, interlayers, and surface alloys of Mn on the Cu(111) surface
Phys. Rev. B 62, 4726 (2000)
23.20.0

Clarke S.; Bihlmayer G.; Blügel S.
Chemical effects in rare gas adsorption
Phys. Rev. B (accepted)
23.20.0

Dallmeyer A.; Carbone C.; Eberhardt W.; Pampuch C.1; Rader O.1; Gudat W.1; Gambardella P.2; Kern K.2
1BESSY, Berlin
2Institut de Physique Experimentale, EPF-Lausanne, CH-1015 Lausanne
Electronic states and magnetism of monatomic Co and Cu wires
Phys. Rev. B 61, R5133 (2000)
23.20.0

Dhesi S.S.1; Dürr H.A.; Dudzik E.1; van der Laan G.1; Brookes N.B.2
1Daresbury Laboratory, Warrington, UK
2ESRF Grenoble, France
Magnetism and electron redistribution at Ni/Co interface
Phys. Rev. B 61, 6866 (2000)
23.20.0

Dudzik E.1; Dhesi S.S.1; Dürr H.A.; Collins S.P.1; Roper M.D.1; van der Laan G.1; Chesnel K.2
1Daresbury Laboratory, Warrington, UK
2CEA/Grenoble, France
Influence of perpendicular magnetic anisotropy on closure domains studied with x-ray resonant magnetic scattering
Phys. Rev. B 62, 5779 (2000)
23.20.0

Dürr H.A.; Dudzik E.1; Dhesi S.S.1; Goedkoop J.B.2; van der Laan G.1; Belakhovsky M.3; Mocuta C.3; Marty A.3; Samson Y.3
1Daresbury Laboratory, Warrington, UK
2University of Amsterdam, NL
3CEA/Grenoble, F
Magnetization profile of ultrathin FePd films
J. Synchrotron Rad. 7, 178 (2000)
23.20.0

Eisebitt S.; Eberhardt W.
Band structure information and resonant inelastic soft X-ray scattering in broad band solids
J. of Electron Spectroscopy and Related Phenomena 110-111, 335 (2000)
23.20.0

Eisebitt, S.; Wirth I.; Kann G.; Eberhardt W.
Statistical analysis of the electronic structure of single-wall carbon nanotubes
Phys. Rev. B 61, 5719 (2000) und Phys. Rev. B 62 , 4756 (2000)
23.20.0

Grünberg P.
Layered magnetic structures in research and application
Acta mater. 48, 239 (2000)
23.42.0

Hase T.P.A.1; Pape I.1; Read D.E.1; Tanner B.K.1; Dürr H.A.; Dudzik E.2; van der Laan G.2; Marrows C.H.3; Hickey B.J.3
1Department of Physics, University of Durham, UK
2Daresbury Laboratory, Warrington, UK
3Department of Physics and Astronomy, University of Leeds, UK
Soft x-ray magnetic scattering evidence for biquadratic coupling in Co/Cu multilayers
Phys. Rev. B 61, 15331 (2000)
23.20.0

Hase T.P.A.1; Pape I.1; Tanner B.K.1; Dürr H.A.; Dudzik E.2; van der Laan G.2; Marrows C.H.3; Hickey B.J.3
1Department of Physics, University of Durham, UK
2Daresbury Laboratory, Warrington, UK
3Department of Physics and Astronomy, University of Leeds
Soft x-ray resonant magnetic diffuse scattering from strongly coupled Cu/Co multilayers
Phys. Rev. B 61, R3792 (2000)
23.20.0

Heinze S.; Bode M.1; Kubetzka A.1; Pietzsch O.1; Nie X.; Blügel S; Wiesendanger R.1
1Zentrum für Mikrostrukturforschung, Universität Hamburg
Real-space imaging of two-dimensional antiferromagnetism on the atomic scale
Science 288, 1805 (2000)
23.20.0

Klingeler R.; Bechthold P.S.; Neeb M.; Eberhardt W.
Mass spectra of metal-doped carbon and fullerene clusters
J. of Chem. Physics 113, 1420 (2000)
23.20.0

Klingeler R.; Kann G.; Wirth I.; Eisebitt S.; Bechthold P.S.; Neeb M.; Eberhardt W.
La@C60, a metallic endohedral fullerene
Nature (submitted)
23.20.0

Kurz Ph.; Bihlmayer G.; Blügel S.; Hirai K.1; Asada T.2
1Department of Physics, Nara Medical University, Nara, Japan
21Shizuoka University, Hamamatsu, Japan
Comment on "Ultrathin Mn films on Cu(111) substrates: Frustrated antiferromagnetic order
Phys. Rev. B (accepted)
23.20.0

Kurz Ph.; Bihlmayer G.; Hirai K.1; Blügel S.
1Department of Physics, Nara Medical University, Nara, Japan
Three-dimensional spin-structure on a two-dimensional lattice: Mn/Cu(111)
Phys. Rev. Lett. (accepted)
23.20.0

Link S., Scholl A., Jacquemin R.; Eberhardt W.
Electron dynamics at a Ag/C60 metal semiconductor interface
Solid State Comm. 113, 689 (2000)
23.20.0

Link S.; Dürr H.A.; Bihlmayer G.; Blügel S.; Eberhardt W.; Chulkov E.V.1; Silkin V.M.1; Echenique P.M.1
1Donostia International Physics Center (DIPC), San Sebastian, E
Electron dynamics of image potential states on the clean and oxygen covered Pt(111) surface
Phys. Rev. B (submitted)
23.20.0

Link S.; Dürr H.A.; Eberhardt W.
Lifetimes of image potential states on the Pt(111) surface probed by time-resolved two-photon photoemission spectroscopy
Appl. Phys. A 71, 525 (2000)
23.20.0

Link S.; Sievers J.; Dürr H.A.; Eberhardt W.
Lifetimes of image-potential states on the clean and hydrogen covered Ni(111) surface
J. Electron Spectrosc. & Rel. Phenom. (in press)
23.20.0

Lüttgens G.; Pontius N.; Friedrich C.; Klingeler R.; Bechthold P.S.; Neeb M.; Eberhardt W.
Chemisorption of benzene on metal dimer anions: A study by photoelectron detachment spectroscopy
J. Chem. Phys. (submitted)
23.20.0

Maus M.; Ganteför G.; Eberhardt W.
The electronic structure and the band gap of nano-sized Si particles: competition between quantum confinement and surface reconstruction
Appl. Phys. A 70, 535 (2000)
23.20.0

Mirone A.1; Sacchi M.1; Dudzik E.2; Dürr H.A.; van der Laan G.2; Vaures A.3; Petroff F.3
1LURE, Université Paris-Sud, Orsay, F
2Daresbury Laboratory, Warrington, UK
3Unite Mixte CNRS/Thompson-LRC, Orsay, F
Study of the magnetic order in a Co/Cr multilayer by magnetic Bragg diffraction at the Co 2p resonance
J. Magn.&Magn. Mat. 218, 137 (2000)
23.20.0

Morenzin J.; Kietzmann, H.; Bechthold P.S.; Ganteför G., Eberhardt W.
Localization and "Bandwidth" of the 3d-orbitals in "magnetic" Ni and Co clusters (invited paper)
Pure and Applied Chemistry (2000) (submitted)
23.20.0

Neeb M.; Klingeler R.; Bechthold P.S.; Kann, G.; Wirth I., Eisebitt S.; Eberhardt W.
Deposition of endohedral fullerenes from a laser evaporation cluster source
Appl. Phys. A (accepted)
23.20.0

Pampuch C.1; Rader O.1; Kachel T.1; Gudat W.1; Carbone C.; Kläsges R.; Bihlmayer G.; Blügel S.; Eberhardt W.
1BESSY Berlin
One-dimensional spin-polarized quantum-wire states in Au on Ni(110)
Phys. Rev. Lett. 85, 2561 (2000)
23.20.0

Pontius N.; Bechthold P.S.; Neeb M.; Eberhardt W.
Femtosecond multi-photon photoemission of small transition metal cluster anions
J. of Electron Spectrosc. and Rel. Phenomena 106, 107 (2000)
23.20.0

Pontius N.; Bechthold P.S.; Neeb M.; Eberhardt W.
Time-resolved photo-electron spectroscopy on mass-selected metal clusters using a regenerative femtosecond amplifier up to 100 Hz
Appl. Phys. B 71, 351 (2000)
23.20.0

Pontius N.; Bechthold P.S.; Neeb M.; Eberhardt W.
Time-resolved photoelectron spectra of optically excited states in Pd3-
J. of Electron Spectrosc. and Relat. Phenom (in press)
23.20.0

Pontius N.; Bechthold P.S.; Neeb M.; Eberhardt W.
Ultrafast hot-electron dynamics observed in Pt3- using time-resolved
photoelectron spectroscopy
Phys. Rev. Lett. 84, 1132 (2000))
23.20.0

Rottländer P.; Kohlstedt H.; de Gronckel H.A.M.; Girgis E.; Schelten J.; Grünberg P.
Magnetic tunnel junctions prepared by ultraviolet light assisted oxidation
J. of Magnetism and Magnetic Materials 210, 251 (2000)
23.42.0

Wortmann D.; Heinze S.; Bihlmayer G.; Blügel S.
Interpreting STM images of the MnCu/Cu(100) surface alloy
Phys. Rev. B 62, 2862 (2000)
23.20.0

Wortmann D.; Heinze S.; Kurz Ph.; Bihlmayer G.; Blügel S.
Resolving complex atomic-scale spin-structures by SP-STM
Phys. Rev. Lett (submitted)
23.20.0

Yan S.-S.; Schreiber R.; Grünberg P., Schäfer R.
Magnetization reversal in (001) Fe thin films studied by combining domain images and MOKE hysteresis loops
J. Magn. Magn. Mat. 210, 305 (2000)
23.42.0

Other publications

Asada T.1; Blügel S.; Bihlmayer G.; Handschuh S.; Abt R.
1Shizuoka University, Hamamatsu, Japan
First-principles investigation of the stability of 3d monolayer/Fe(001) against bilayer formation
(44th Magnetism and Magnetic Materials Conference)
J. Appl. Phys. 87, 5935 (2000)
23.20.0

Bihlmayer G.; Abt R.; Blügel S.; Asada T.1
1Shizuoka University, Hamamatsu, Japan
Influence of magnetism for the alloy formation of ultrathin films
(International Symposium on Structure and Dynamics of Heterogeneous Systems)
Editors: P. Entel and S.E. Wolf, page 179 (World Scientific, 2000)
23.20.0

Dhesi S.S.1; Dudzik E.1; Dürr H.A.; Brookes N.B.2; van der Laan G.1
1Daresbury Laboratory, Warrington, UK
2ESRF Grenoble, F
Correlation between L3 absorption satellite and spin moment in ultrathin Ni films
Surf. Sci. 454-456, 930 (2000)
23.20.0

Dhesi S.S.1; Dudzik E.1; Dürr H.A.; van der Laan G.1; Brookes N.B.2
1 Daresbury Laboratory, Warrington, UK
2ESRF Grenoble, F
Electron correlation and charge transfer at the Ni/Co interface
J. Appl. Phys. 87, 5466 (2000)
23.20.0

Dudzik E.1; Dhesi S.S.1; Collins S.P.1; Dürr H.A.; van der Laan G.1; Chesnel K.2; Belakhovsky M.2; Marty A.2; Samson Y.2; Goedkoop J.B.3
1 Daresbury Laboratory, Warrington, UK
2CEA/Grenoble, F
3University of Amsterdam, NL
X-ray resonant magnetic scattering from FePd thin films
J. Appl. Phys. 87, 5469 (2000)
23.20.0

Eberhardt W.; Klingeler R.; Bechthold P.S.; Neeb M.
Metal doped fullerenes: Endohedral and networked dopants
Proceedings of the International Winterschool on Electronic Properties and Novel Materials, Kirchberg, Austria (submitted)
23.20.0

Eisebitt S.; Eberhardt W.
Soft X-ray spectroscopy as a probe of the electronic structure of nanostructured solids
In: Frontiers of Nano-Optoelectronic Systems, Ed. L. Pavesi, E. Buzaneva, Nato Science Series II, 6, p. 347 (Kluwer Aacademic, London, in print)
23.20.0

Eisebitt S.; Karl A.; Zimina A.; Scherer R.; Freiwald M.; Eberhardt W.; Hauke F.1; Hirsch A.1; Achiba Y.2
Electronic structure of doped fullerenes and single wall carbon nanotubes
In: Electronic Properties of Novel Materials: MolecularNanostructures, Ed. H. Kuzmany, J. Fink, M. Mehring. S. Roth (AIP Conference Proceedings, Melville, in print)
23.20.0

Grünberg P.; Rottländer P.; Girgis E.; Bürgler D.E.; Eberhardt W.; Kohlstedt H.; Gareev R.; Herrnsdorf J.1.; Schneider M.1
1HL-Planar, Dortmund
Preparation of materials for TMR type sensors
Tagungsband des Statusseminars über Magnetoelektronik, ed. by St. Mengel, VDI Düsseldorf, Juni 2000
23.42.0

Kurz Ph.; Bihlmayer G.; Blügel S.
Non-collinear magnetism of Cr and Mn monolayers on Cu(111)
(44th Magnetism and Magnetic Materials Conference)
J. Appl. Phys. 87, 6101 (2000)
23.20.0

Marty A.A.1; Samson Y.1; Gilles B.1; Belakhovsky M.1; Dudzik E.2; Dürr H.A.; Dhesi S.S.2; van der Laan G.2; Goedkoop J.B.3
1CEA Grenoble, F
2Daresbury Laboratory, Warrington, UK
3University of Amsterdam, NL
Weak-stripe magnetic domain evolution with an in-plane field in epitaxial FePd thin films: Model versus experimental results
J. Appl. Phys. 87, 5472 (2000)
23.20.0

Van der Laan G.1; Dudzik E.1; Collins S.P.1; Dhesi S.S.1; Dürr H.A.; Belakhovsky M.2; Chesnel K.2; Marty A.2; Samson Y.2; Gilles B.2
1Daresbury Laboratory, UK
2CEA/Grenoble, F
Soft X-ray magnetic scattering from striped magnetic domain structures
Physica B 283, 171 (2000)
23.20.0

Invited Talks

Bechthold P.S.
Electronic structure of small metal clusters (invited lecture)
10th Int. IUPAC Conf. on High Temperature Materials Chemistry, Jülich
13.04.2000
23.20.0

Bihlmayer G.; Kurz Ph.; Förster F.; Blügel S.
The FLAPW method applied to complex magnetic systems
Psi-k-2000: Network conference on electronic structure theory, Schwäbisch-Gmünd
22. - 26.08.2000
23.20.0

Blügel S.; Nie X.; Bihlmayer G.
Magnetic anisotropy in low dimensional systems
Psi-k-2000: Network conference on electronic structure theory, Schwäbisch-Gmünd
22. - 26.08.2000
23.20.0

Blügel S.
Der Schatz im Quantensee
Stein der Weisen, Veranstaltung im Rahmen des Jahres der Physik, Bundeshaus Bonn
21.09.2000
23.20.0

Blügel S.
Elektronen, Atome und Magnetismus im Nanokosmos
Fachbereich Physik der Universität Regensburg
05.05.2000
23.20.0

Blügel S.
Kristallwachstum von Halbleitern mit Surfactants aus mikroskopischer Sichtweise
Seminar and der LMU München, Institut für Kristallografie und Mineralogie
12.05.2000
23.20.0

Blügel S.
Magnetism in the nano-world
Talk at the electron group (National Institut for Standards (NIST)
24.07.2000
23.20.0

Blügel S.
Nanomagnetism meets magnetoelectronics
Symposium am Institut für Angewandte Physik, Universität
22.06.2000
23.20.0

Blügel S.
Nanomagnetismus im Zeitalter der Magnetoelektronik
Kolloquiumsvortrag am Fachbereich Physik, Christian-Albrecht-Universität zu Kiel
14.11.2000
23.20.0

Blügel S.
Von der Quantentheorie der Elektronen zu neuen Nanomaterialien
Fachbereich Physik, TU Clausthal, Osnabrück
24.01.2000
23.20.0

Blügel S.
Von der Quantentheorie der Elektronen zu neuen Nanomaterialien
Kolloquium am Fachbereich Physik, Universität Kaiserslautern
12.12.2000, 23.20.0

Blügel S.
Von der Quantentheorie der Elektronen zu neuen Nanomaterialien
Zentrales Kolloquium des Hahn-Meitner-Instituts Berlin
01.03.2000
23.20.0

Bürgler D.E.
Magnetische Zwischenschichtkopplung in Fe/Cr/Fe Schichtungen: Morphologie und Fermiologie
SFB-Kolloquium TU Dresden
27.04.2000

Bürgler D.E.
Magnetische Zwischenschichtkopplung und Magnetowiderstand in Fe/Cr-Schichtungen: Morphologie und Fermiologie
SFB-Kolloquium, Universität Göttingen
13.11.2000
23.42.0

Bürgler D.E.
Magnetische Zwischenschichtkopplung und Magnetowiderstand in magnetischen Schichtungen: Morphologie und Fermiologie
Kolloquium Universität Halle-Wittenberg
16.12.2000
23.42.0

Bürgler D.E.
Magnetoelektronik
Universität Regensburg
22.05.2000
23.42.0

Bürgler D.E.
Magnetoelektronik: Vom Kompass zum Datenspeicher von morgen
Kolloquium, Universität Basel
09.06.2000
23.42.0

Dürr H.A.
Angular resolved photoelectron spectroscopy
International Symposium on Spectroscopy of Materials
Schloss Ringberg
07.03.2000
23.20.0

Dürr H.A.
Anisotropic magnetic ground-state moments probed by soft X-ray spectroscopy
WE-Heraeus Seminar "Ground-state and Finite-temperature Bandferromagnetism", Berlin
04.10.2000
23.20.0

Dürr H.A.
Electron correlation and magnetism in low-dimensional solids
Seminar , Physikalisches Institut, Universität zu Köln
10.07.2000
23.20.0

Dürr H.A.
Femtosecond Laser Spectroscopy
Euro Summer School 2000, Rostock
29.08.2000
23.20.0

Dürr H.A.
Femtosecond spectromicroscopy of magnetic nanostructures
XFEL - Workshop on Hard Condensed Matter
20.07.2000
23.20.0

Dürr H.A.
Image potential state lifetime on transition metal fcc (111) surfaces
Image Potential State Workshop, San Sebastian, Spain
25.06.2000
23.20.0

Dürr H.A.
Magnetic domain correlations in transition metal films and multilayers
INFP Kolloquium, Forschungszentrum Karlsruhe
12.01.2000
23.20.0

Dürr H.A.
Magnetocrystalline anisotropy at interfaces probed by soft x-ray spectroscopy
Seminar im Physikalischen Institut, Universität Göttingen
19.06.2000
23.20.0

Dürr H.A.
Magnetocrystalline anisotropy of low dimensional systems probed by soft x-ray spectroscopy
Seminar
Hahn-Meitner-Institut Berlin
05.04.2000
23.20.0

Dürr H.
Stars and stripes in magnetism
Ward Plummer Symposium: Frontiers in Surface Science, Knoxville, TN, USA
14.10.2000
23.20.0

Eberhardt W.
Cluster als neue Materialien; elektronische Struktur und atomare Geometrie
11. Edgar-Lüscher-Seminar, Serneus, Schweiz
Februar 2000
23.20.0

Eberhardt W.
Clusters as new materials
Oak Ridge National Laboratory, USA
16.03.2000
23.20.0

Eberhardt W.
Clusters as new materials
Physik-Kolloquium, Universität Greifswald
11.05.2000
23.20.0

Eberhardt W.
Clusters as new materials
Universität Basel
23.06.2000
23.20.0

Eberhardt W.
Combination of lasers and synchrotron radiation sources
ESF/PESC Workshop on "Future Advanced Light Sources", Zürich, Schweiz
24.10.2000
23.20.0

Eberhardt W.
Forschung mit Synchrotronstrahlung
Kolloquium, TU Berlin
06.06.2000
23.20.0

Eberhardt W.
Fs-spectroscopy of clusters
Workshop on Atomic, Molecular and Cluster Physics with Free Electron Lasers, Hasylab, Hamburg
04.09.2000
23.20.0

Eberhardt W.
Future direction for research with lasers and synchrtron radiation
LS WAVE 2000, Berlin
26.08.2000
23.20.0

Eberhardt W.
Metal doped fullerenes: Endohedral and networked dopants
International Winterschool on Electronic Properties and Novel Materials, Kirchberg, Austria
23.20.0

Eberhardt W.
Opportunities for science using the time structure and coherence of a VUV-FEL
Erstes Blankeneser Gespräch über Forschung mit Synchrotronstrahlung, Workshop zum BESSY FEL, Blankensee
01.07.2000
23.20.0

Eberhardt W.
Overview of soft X-ray techniques
Workshop on "Soft X-ray Science in the Next Millennium: The Future of Photon-/In/Photon-Out Experiments, Pikeville, Tennesse, USA
18.03.2000
23.20.0

Eberhardt W.
Soft X-ray emission spectroscopy
Workshop Research with Synchrotron Radiation, Berlin
07.07.2000
23.20.0

Eberhardt W.
Ward Plummer Symposium: Frontiers in Surface Science, Knoxville, TN, USA
14.10.2000
23.20.0

Förster F.
Untersuchung vonnichtkollinearem Magnetismus in ultradünnen Filmen
Seminarvortrag am 1. Physikalischen Institut der RWTH Aachen
07.11.2000
23.20.0

Grünberg P.
Exchange anisotropy, interlayer exchange coupling and GMR in research and application
3rd European Conference on Magnetic Sensors and Actuators (EMSA), Dresden
Juli 2000
23.42.0

Grünberg P.
Kompass zum Datenspeicher: Magnetoelektronik
Veranstaltung "Stein der Weisen", Bonn
September 2000
23.42.0

Grünberg P.
Layered magnetic structures - history, highlights, applications
International, Conference on Magnetism 2000, Recife, Brazil
August 2000
23.42.0

Grünberg P.
Layered magnetic structures: Facts, figures, future
Euro Summer School 2000, Rostock
03.09.2000
23.42.0

Grünberg P.
Layered magnetic structures: History, highlights, applications
International Symposium on Nanoscale Magnetism and Transport, Sendai, Japan
März 2000
23.42.0

Grünberg P.
Layered magnetic structures: History, highlights, applications
Symposium on Magnetic Materials for Magnetoelectronic Devices, Ames Iowa, USA
Mai 2000
23.42.0

Grünberg P.
Magnetische Schichtstrukturen in Forschung und Anwendung
Physikalisches Kolloquium der RWTH Aachen
Januar 2000
23.42.0

Grünberg P.
Magnetische Schichtstrukturen in Forschung und Anwendung
Physikalisches Kolloquium der Universität Regensburg
Juli 2000
23.42.0

Grünberg P.
Magnetoelektronik: Vom Kompass zum Datenspeicher
Helmholtz Syposium 2000, Zukunft braucht Wissenschaftsthemen aus der Physik,
November 2000
23.42.0

Grünberg P.
Preparation of materials for TMR type sensors
Statusseminar Magnetoelektronik, Dresden
Juni 2000
23.42.0

Heinze S.
Interpretation of STM experiments on transition-metal structures by ab initio calculations
Research Institute for Materials, University Nijmegen, NL
19.01.2000
23.20.0

Kann G.
Rastertunnelmikroskopische Untersuchungen an Buckypaper und endohedralen Lanthanid-C60-Fullerenen
Seminar, Institut für Materialphysik, Universität Wien
11.12.2000
23.20.0

Kurz Ph.; Bihlmayer G.; Blügel S.; Hirai K.1
1Department of Physics, Nara Medical University, Nara, Japan
Magnetism of two-dimensional itinerant antiferromagnets on a triangular lattice
ESCM-2000: Electronic Structure and Magnetism in Complex Materials, Washington, D.C., USA
26. - 28.07.2000
23.20.0

Kurz Ph.; Bihlmayer G.; Blügel S.; Hirai K.1
1Department of Physics, Nara Medical University, Nara, Japan
Magnetism of two-dimensional itinerant antiferromagnets on a triangular lattice
SDHS'00: International Symposium on Structure and Dynamics of Heterogeneous Systems, Duisburg
28.- 29.08.2000
23.20.0

Neeb M.
Metalldotierte Fullerencluster aus der Laserverdampfung
Symposium Cluster und Fullerene, Hauptvortrag, DPG-Tagung, Bonn
April 2000
23.20.0

Wortmann D.; Heinze S.; Bihlmayer G.; Blügel S.
STM-Theorie von Übergangsmetalloberflächen und -grenzflächen
Seminarvortrag im Rahmen Forschergruppe 353, Christian-Albrecht-Universität zu Kiel
13.11.2000
23.20.0

Other talks

Blügel S.; Kurz Ph.; Bihlmayer G.
Nichtkollinearer Magnetismus von Monolagen auf Ag(111) und Cu(111)
DPG-Frühjahrstagung Regensburg
März 2000
23.20.0

Blügel S.
Magnetism of two-dimensional itinerant antiferromagnets on a triangular lattice
1st Washington Conference on Electronic Structure of Complex Materials
27.07.2000
23.20.0

Breidbach M.; Bürgler D.E.; Olligs D.; Grünberg P.
Strukturuntersuchungen dünner Goldpuffer auf GaAs (001)
DPG-Frühjahrstagung Regensburg
März 2000
23.42.0

Breidbach M.
Strukturuntersuchungen dünner Goldpuffer auf GaAs
DPG-Frühjahrstagung Regensburg
März 2000
23.42.0

Buchmeier M.
Inverser GMR-Effekt in Fe/Cr/Au/Co-Schichtsystemen
DPG-Frühjahrstagung Regensburg
März 2000
23.42.0

Bürgler D.E.; Meisinger F.1; Schmidt C.M.1; Schaller D.M.1; Güntherodt H.-J.1; Grünberg P.
1Universität Basel
In-plane momentum conservation and Fermi surface effects in magnetic interlayer coupling
EPS-CMD18, Montreux (CH)
16.03.2000
23.42.0

Clarke S.; Nie X.; Weinert M.1; Bihlmayer G.; Blügel S.
1Physics Department, Brookhaven National Laboratory, Upton, New York, USA
Ab initio investigations of the effect of an applied electric field on the Fe(001) surface
DPG-Frühjahrstagung Regensburg
März 2000
23.20.0

Clarke S.
An ab initio investigation of the effect of an applied field on the Fe(001) surface
DPG-Frühjahrstagung Regensburg
März 2000
23.20.0

Dallmeyer A.; Gambardella P.1; Maiti K.; Malagoli M.; Carbone C.; Eberhardt W.; Kern K.1
1Institut de Physique Experimentale, EPF-Lausanne, Switzerland
Magnetismus von eindimensionalen Co-Drähten
DPG-Frühjahrstagung Regensburg
März 2000
23.20.0

Dallmeyer A.; Malagoli M.; Maiti K.; Wingbermühle J.; Carbone C.; Eberhardt W.; Nagy D.L.1; Deak L.1; Bottyan L.1; Rüffer R.2; Leupold O.2
1KFKI Research Institute for Particle and Nuclear Physics, Budapest, Hungary
2European Synchrotron Radiation Facility , Grenoble, France
Nicht-kollinearer Magnetismus in fcc-Fe/Co(100)-Filmen
DPG-Frühjahrstagung Regensburg
März 2000
23.20.0

Dürr H.A.; Münzenberg M.1; Felsch W.1; Dhesi S.S.1
1Universität Göttingen
Interface magnetic anisotropy in Fe/CeH2 multilayers
International Workshop on X-ray Spectroscopies of Magnetic Solids
09.12.2000
23.20.0

Dürr H.A.
Magnetic stripe domains probed by soft x-ray resonant magnetic scattering
ESRF Monday Seminar, ESRF Grenoble, France
21.02.2000
23.20.0

Dürr H.A.
Magnetization dynamics of magneto-electronics devices probed by femtosecond photoelectron microscopy
Kolloquium zum Schwerpunktprogramm "Dynamik von Elektronentransferprozessen an Grenzflächen", Walberberg
14.02.2000
23.20.0

Eberhardt W.
Spektroskopie an Clustern im Molekularstrahl
Erstes Blankeneser Gespräch über Forschung mit Synchrotronstrahlung bei BESSY
01.07.2000
23.20.0

Eisebitt S.
Soft X-ray Speckle from antiferromagnetic domains
International Workshop on Soft X-ray Science in the Next Millennium:
The Future of Photon-in/Photon-out Experiments
Pikeville, USA
16.03.2000
23.20.0

Heinze S.; Abt. R.; Blügel S.; Gilarowski G.1.; Niehus H.1
1Institut für Physik, Humboldt-Universität zu Berlin
Vergrabene Übergangsmetallstrukturen auflösbar durch STM
DPG-Frühjahrstagung Regensburg
März 2000
23.20.0

Heinze S.; Bode M.1; Kubetzka A.1; Pietzsch O.1; Wortmann D.; Kurz Ph.; Nie X.; Blügel S.; Wiesendanger R.1
1Institut für Angewandte Physik, Universität Hamburg
Real space imaging of two-dimensional antiferromagnetism on the atomic scale
ICSFS-10: International Conference on Solid Films and Surfaces, Princeton University, N.J., USA
09. - 13.07.2000
23.20.0

Heinze S.; Wortmann D., Bihlmayer G.; Blügel S.
Ab-initio calculations of tunneling through MgO barriers on Fe(001)
228. WE-Heraeus-Seminar "Metal-Nonmetal Structures for Magnetoelectronics"
Bad Honnef
5. - 7. Januar 2000
23.20.0

Heinze S.; Wortmann D.; Blügel S.; Bode M.1; Wiesendanger R.1
1Zentrum für Mikrostrukturforschung, Universität Hamburg
Ab initio Rechnungen zum spinpolarisierten STM
DPG-Frühjahrstagung Regensburg
März 2000
23.20.0

Klingeler R.
Mass spectra of metal-doped fullerene clusters and electronic structure of Ce@44
DPG-Frühjahrstagung Bonn
April 2000
23.20.0

Kuanr B.; Wingbermühle J.; Bürgler D.E.; Grünberg P.
Influence of anisotropy on FMR frequency of polycrystalline pinned and unpinned thin Permalloy and epitaxial Fe films
16th ICMFS, 16th International Colloquium of Magnetic Films and Surfaces
Natal, Brazil
15.08.2000
23.42.0

Kuanr B.
Magnetic interlayer exchange coupling investigated by means of Brillouin-Light Scattering
Workshop 2000 des DEGA - Fachausschuss Physikalisches Akustik der DPG
Bad Honnef
05.10.2000
23.42.0

Link S.; Dürr H.A.; Eberhardt W.
Lifetimes of image-potential states on the clean and oxygen covered Pt(111) surface
DPG-Frühjahrstagung, Regensburg
März 2000
23.20.0

Lüttgens G.; Pontius N.; Friedrich Ch.; Klingeler R.; Bechthold P.S.; Neeb M.; Eberhardt W.
Chemisorption von Benzol an kleinen Metallclusteranionen: Eine photoelektronen-spektroskopische Studie
DPG-Frühjahrstagung Bonn
April 2000
23.20.0

Malagoli M.; Maiti K.; Magnano E.1; Dallmeyer A.; Carbone C.
1Laboratorio Nazionale TASC, Padriciano, Trieste, Italy
Lifetime and correlation effects in photoemission from the Gd valence band
DPG-Frühjahrstagung Regensburg
März 2000
23.20.0

Neeb M.
Time-resolved photodetachment spectroscopy on transition metal cluster anions
International Conference on Small Particles and Inorganic Clusters ISSPIC, Atlante, USA
12.10.2000-09-26
23.20.0

Neeb M.
Time-resolved photodetachment spectroscopy on transition metal cluster anions
International Workshop on Photoionization IWP 2000, Carry le Rouet, France
08.10.2000
23.20.0

Nie X.; Blügel S.
Investigation of chemical trends of the magnetocrystalline anisotropy for monolayers
DPG-Frühjahrstagung Regensburg
März 2000
23.20.0

Olligs D.; Bürgler D.E.; Grünberg P.
GMR in epitaktischen Fe/Cr/Fe-Schichten
DPG-Frühjahrstagung Regensburg
März 2000
23.42.0

Olligs D.; Bürgler D.E.; Grünberg P.
GMR in epitaktischen Fe/Cr/Fe-Schichten: Einfluss der Grenzflächenrauhigkeit
DPG-Frühjahrstagung Regensburg
März 2000
23.42.0

Pontius N.; Bechthold P.S.; Neeb M.; Eberhardt W.
Dynamik heißer Elektronen in kleinen Übergangsmetall-Clustern
DPG-Frühjahrstagung Bonn
April 2000
23.20.0

Schondelmaier D.
Orientation and self-assembly of hydrophobic fluoro-alcyl-silanes
DPG-Frühjahrstagung Regensburg
März 2000
23.20.0

Wingbermühle J.; Grünberg P.; Bürgler D.E.
Exchange Bias Eigenschaften von NiO/Permalloy Schichten, hergestellt mit Hilfe von Ionenstrahlsputtern
DPG-Frühjahrstagung Regensburg
März 2000
23.42.0

Wortmann D.; Heinze S.; Bihlmayer G.; Blügel S.
Ab initio calculations of tunneling through MgO barriers on Fe(001)
Workshop on TMR and GMR, Dresden
Dezember 2000
23.20.0

Wortmann D.; Heinze S.; Bihlmayer G.; Blügel S.
Ab-initio Berechnungen von STM-Aufnahmen einer Oberflächenlegierung: c(2x2)MnCu/Cu(100)
DPG-Frühjahrstagung Regensburg
März 2000
23.20.0

Wortmann D.; Heinze S.; Bihlmayer G.; Blügel S.
Ab-initio Berechnungen zum Tunneln durch eine MgO-Barriere auf Fe(001)
DPG-Frühjahrstagung Regensburg

März 2000
23.20.0

Wortmann D.; Heinze S.; Kurz Ph.; Bihlmayer G.; Blügel S.
Resolving complex atomic-scale spin-structures by SP-STM
Workshop on TMR and GMR, Dresden
Dezember 2000
23.20.0

Posters

Bihlmayer G.; Nie X.; Blügel S.
Magnetismus von dekorierten Stufenkanten
DPG-Frühjahrstagung Regensburg
März 2000
23.20.0

Bringer A.; Eberhardt W.
Eisebitt S.; Karl A.; Zimina A.; Scherer R.; Freiwald M.; Cramm S.; Schondelmaier D.;
Bringer A.; Eberhardt W.
The electronic structure of doped fullerenes investigated by soft X-ray emission
14th International Winterschool on Electronic Properties of Novel Materials - Molecular Nanostructures, Kirchberg, Tirol
08.03.2000
23.20.0

Buchmeier M.; Schreiber R.; Bürgler D.E.; Grünberg P.
Inverse GMR effect in Fe/Cr/Au/Co systems
VDI Statusseminar "Magnetoelektronik", Dresden
14. - 16.06.2000
23.42.0

Bürgler D.E.; Meisinger F.1; Schmidt C.M.1; Schaller D.M.1; Güntherodt H.-J.1; Grünberg P.
1Universität Basel
In-plane momentum conservation and Fermi surface effects in magnetic interlayer coupling
EPS-CMD18, Montreux (CH)
16.03.2000
23.42.0

Bürgler D.E.; Meisinger; F.1; Schmidt C.M.1; Schaller D.M.1; Güntherodt J.-J.1; Grünberg P.
1Universität Basel
In-plane momentum conservation and Fermi surface effects in magnetic interlayer coupling
Gordon Research Conference on Magnetic Nanostructures, Ventura, CA (USA)
14.02.2000
23.42.0

Clarke S.; Nie X.; Blügel S.; Bihlmayer G.; Weiner M.1
1Department of Physics, Brookhaven National Laboratory, Upton, NY, USA
An investigation of the effect of applied static electric fields on magnetic surfaces
Psi-k2000 Konferenz, Schwäbisch-Gmünd
August 2000
23.20.0

Dürr H.A.
Magnetic domain correlations in transition metal films and multilayers
228. WE-Heraeus-Seminar "Metal-Nonmetal Structures for Magnetoelectronics"
Physikzentrum Bad Honnef
07.01.2000
23.20.0

Eberhardt W.
Magnetoelectronics: Basic research, characterization and optimization of multilayer-
Systems for GMR-sensors and nonvolatile memeory diveces (MRAM)
BMBF-Statusseminar "Magnetoelektronik"
IFW Dresden
16.06.2000
23.20.0

Eisebitt S.; Karl A.; Zimina A.; Scherer R.; Freiwald M.; Cramm S.; Schondelmaier D.; Bringer A.; Eberhardt W.
The electronic structure of doped fullerenes investigated by soft X-ray emission
14th International Winterschool on Electronic Properties of Novel Materials: Molecular Nanostructures, Kirchberg, Österreich
März 2000
23.20.0

Friedrich Ch.; Lüttgens G.; Pontius N.; Neeb M.; Bechthold P.S.; Eberhardt W.
Erhöhung der Massenauflösung zur Photoelektronenspektroskopie von Cluster-Adsorbat-Systemen im Molekularstrahl
DPG-Frühjahrstagung Bonn
April 2000
23.20.0

Heinze S.; Bode M.1; Kubetzka A.1; Wortmann D.; Kurz Ph.; Pietzsch O.1; Nie X.; Blügel S.; Wiesendanger R.1
1Institut für Angewandte Physik, Universität Hamburg
Real space imaging of surface antiferromagnetism on the atomic scale
2nd Internationl Conference on Scanning Probe Spectroscopy , Hamburg
19.07.2000
23.20.0

Heinze S.; Wortmann D.; Bihlmayer G.; Blügel S.
Ab-initio calculations of tunneling through MgO barriers on Fe(001)
228. WE-Heraeus Seminar "Metal-Nonmetal Structures for Magnetoelectronics"
Physikzentrum Bad Honnef
05.01.2000
23.20.0

Kann G.; Wirth I.; Eisebitt S.; Klingeler R.; Neeb M.; Eberhardt W.
Scanning tunnelling spectroscopy of La@C60: A metallic endohedral fullerene
8th International Conference on Electronic Spectroscopy and Structures
Berkeley, USA
08. - 12.08.2000-07-06
23.20.0

Klingeler R.
La@C60: A metallic endohedral fullerene
10th International Symposium on Small Particles and Inorganic Clusters, Atlanta, USA
13.10.2000
23.20.0

Klingeler R.
Mass spectra of metal-doped fullerene clusters MxCn>120 (M = Ce, Gd; x = 1,2
DPG-Frühjahrstagung Bonn
06.04.2000
23.20.0

Klingeler R.
Metal doped fullerenes: Endohedral and networked dopants
14th International Winterschool on Electronic Properties of Novel Materials: Molecular Nanostructures, Kirchberg, Österreich
März 2000
23.20.0

Kuanr B.K.; Wingbermühle J.; Grünberg P.
Influence of anisotropy on FMR frequency of thin Permalloy and epitaxial Fe
Symposium on Spin-Electronics, Halle
05.07.2000
23.42.0

Link S.; Sievers J.; Dürr H.A.; Eberhardt W.
Lifetimes of image-potential states on the transition metal surfaces of Pt(111) and Ni(111)
8th International Conference on Electronic Spectroscopy and Structures
Berkeley, USA
08. - 12.08.2000
23.20.0

Morenzin J.; Kietzmann H.; Ganteför G.; Bechthold P.S.; Eberhardt W.
Magnetic properties of transition-metal clusters
10th Int. IUPAC Conf. on High Temperature Materials Chemistry, Jülich
11.04.2000
23.20.0

Morenzin J.; Kietzmann H.; Ganteför G.; Bechthold P.S.; Eberhardt W.
Spectroscopic evidence for the magnetic behavior of rhodium and ruthenium clusters
International Symposium on Small Particles and Inorganic Clusters (ISSPIC 10),. Atlanta, USA
11.10.2000
23.20.0

Pontius N.; Bechthold P.S.; Neeb M.; Eberhardt W.
Time-resolved photoelectron spectroscopy of small metal cluster anions
8th International Conference on Electronic Spectroscopy and Structures
Berkeley, USA
08. - 12.08.2000
23.20.0

Rottländer P.; Kohlstedt H.; Girgis E.; Schelten J.; Grünberg P.
Transportmessungen an UV-oxidierten Tunnelmagnetowiderstandselementen
DPG-Frühjahrstagung Regensburg
März 2000
23.20.0
23.42.0

Wang Y.G.; Kentzinger E.; Rücker U.; Seeck O.H.; Brückel Th.; Schreiber R.; Bürgler D.E.; Grünberg P.
Characterization of the buried interfaces in Fe/Cr/Fe trilayers using synchrotron radiation
VDI Statusseminar "Magnetoelektronik", Dresden
14. - 16.06.2000
23.42.0

Wortmann D.; Heinz S.; Bihlmayer G.; Blügel S.
Ab-initio calculations of tunneling through MgO barriers on Fe(001)
SSE-2000: Symposium on Spin-Electronics, Halle, Germany
03.-06.07.2000
23.20.0

Patents applied for

Morenzin J.; Eberhardt W.
Markierungseinrichtung sowie Verfahren zum Auslesen einer solchen Markierungseinrichtung
DE: 100 08 097.9 (22.02.2000); PT 1.1777
23.20.0

Morenzin J.; Eberhardt W.
Positionsmeßeinrichtung
DE: 100 52 086.3 (20.10.2000); PT 1.1853
23.20.0

Nie X.
Magnetisches Schichtsystem sowie ein solches Schichtsystem aufweisendes Bauelement
DE: 10046782.2 (21.09.2000)
23.20.0

Schondelmaier D.; Eberhardt W.
Verfahren zur Behandlung von Oberflächen sowie mit diesem Verfahren hergestellte Gegenstände und Verwendung von Verbindungen als photochemisch spaltbare Reagenzien
DE: 100 30 797.3 (29.06.2000), PT 1.1798
23.20.0

Lecture courses

Bechthold P.S.
Cluster und Clustermaterie
Universität zu Köln
SS2000
23.20.0

Bechthold P.S.
Ultrakurze Laserimpulse: Erzeugung, Handhabung, Nachweis
31. IFF-Ferienschule 2000 Femtosekunden und Nano-eV: Dynamik in kondensierter Materie
13. - 23.03.2001
23.20.0

Blügel S.
Dynamik in kondensierter Materie
31. IFF-Ferienschule 2000 Femtosekunden und Nano-eV: Dynamik in kondensierter Materie
13. - 23.03.2001
23.20.0

Bürgler D.E.; Grünberg P.
Magnetoelektronik in Forschung und Anwendung
31. IFF-Ferienschule 2000 Femtosekunden und Nano-eV: Dynamik in kondensierter Materie
13. - 23.03.2001
23.42.0

Bürgler D.E.
Beitrag zur Ringvorlesung "Kondensierte Materie III"
Universität Basel
SS2000
23.42.0

Bürgler D.E.
Magnetoelektronik in Forschung und Anwendung
31. IFF-Ferienschule 2000 Femtosekunden und Nano-eV: Dynamik in kondensierter Materie
13. - 23.03.2001
23.42.0

Dürr H.A.
Fsec-Magnetism
31. IFF-Ferienschule 2000 Femtosekunden und Nano-eV: Dynamik in kondensierter Materie
13. - 23.03.2001
23.20.0

Eberhardt W.
Oberseminar "Magnetoelektronik"
Universität zu Köln
WS2000/01
23.20.0

Eisebitt S.
Resonante inelastische Röntgenstreuung: Messungen mit atomarer Stoppuhr
31. IFF-Ferienschule 2000 Femtosekunden und Nano-eV: Dynamik in kondensierter Materie
13. - 23.03.2001
23.20.0

Neeb M.
Molekulardynamik chemischer Reaktionen auf der Femtosekundenskala: "Die schnellste Kamera der Welt"
31. IFF-Ferienschule 2000 Femtosekunden und Nano-eV: Dynamik in kondensierter Materie
13. - 23.03.2001
23.20.0

Internal reports

Blügel S.
Nanomagnetismuslabor: Supercomputer
ZAM-aktuell Nr. 86, Juni 2000
23.20.0

Internal seminars

Blügel S.
Magnetismus im Nanokosmos
Vortragsveranstaltung der VSR-Kommission des FZJ
19.06.2000
23.20.0

Special Group „Materials under heavy irradiation loads“

General Overview

Research Fusion Materials

An essential part of the activities of the group is still concerned with radiation damage effects in candidate structural fusion materials. This work is a contribution of the IFF to the Nuclear Fusion Project in Jülich which is financed to 25 and 45%, respectively, by EURATOM. The research topics are part of the European Fusion Programme. In addition to these activities, the group is increasingly involved in materials investigations for the targets of the planned European high-power spallation neutron source ESS (see below).

Scientific goal of the work are investigations of irradiation-induced changes of properties of technical- and model-material. Because an intensive source of fusion neutron is still missing, their action is simulated by light ion bombardment at a cyclotron. The emphasis of the efforts is an improvement of the basic understanding of processes underlying radiation damage effects. A close interaction with theoreticians is therefore mandatory and the close long-standing and fruitful collaboration with H. Trinkaus (Institut Theorie II) was continued.

In the field of **metallic structural fusion materials** the work concentrated on the combined influence of atomic displacements, hydrogen and helium on the mechanical properties and the hydrogen permeation of martensitic steels, particularly their low activation versions. These investigation will be extended to steel-ceramics composites in order to test the effectiveness of ceramic layers as diffusion-barriers for hydrogen isotopes.
The influence of (n, α)-produced helium in beryllium (a favourite **plasma-facing candidate material**) on its tensile properties and microstructure has been studied for a wide range of temperatures and He-concentrations. This work is close to comletition.

Research on Spallation Target and Moderator Materials

The emphasis of this research is on the most highly loaded components of the European Spallation Source (ESS), i.e. target and moderators. The integrity of these parts will be decisive for the duration of uninterrupted operation periods of the entire facility. The extraordinary loads on the mercury target are on the container proper and its secondary enclosure, in particular the respective proton beam windows. These loads have mainly two causes. First, the stress waves, which are due to the shock-like energy deposition into the target and its multiple shells. Stress waves within the container walls are generated by the direct heating of the beam window as well as by the pressure waves due to the pulsed heating of the mercury. The second concern is radiation damage and foreign atom production (mainly hydrogen and helium) induced by the high energetic protons and neutrons.

Radiation damage and foreign atom production are investigated with proton accelerators. Life time estimates of components are made by analyzing long term irradiated targets and proton beam windows of already operating medium power spallation sources (LANSCE, Los Alamos and ISIS, Rutherford Appleton Lab). The stress wave problem is studied with experiments on pulsed high power proton accelerators.

The **mechanical tests and micro-structural investigations** of samples cut from LANSCE components of existing spallation sources are nearly finished. The results show a remarkable strengthening and embrittlement with all three investigated materials classes (austenitic and martensitic steels as well as nickel-based alloys). The residual ductility observed with specimens subject to the highest available dose of 10 dpa (corresponding to about 2 months of operation of ESS) are, however, sufficient for being employed as structural materials of ESS targets.

An unexpected result was found in the investigation of the "spent" ISIS target: Pure tantalum remained a ductility of more than 10% after irradiation up to the maximum available dose of 13 dpa, making Ta an attractive candidate material for target structural components. Microstructural studies and simulation experiments (in collaboration with ORNL) are under way to uncover the reason for this behaviour.
A new tensile machine allowing tests in the temperature range from RT to 350°C was developed and installed in the FZJ Hot Cells. It will be used for testing he specimens from the STIP irradiation program at SINQ (PSI) which will arrive in Jülich in early 2001.

Cold moderators have gained increasing importance in the past. Quality and quantity of neutrons produced with a pulsed source can be particularly improved, if cold moderators can deliver and sustain short pulses over a broad energy range. The ideal slowing down medium for that purpose is methane because of its high proton density and many low lying rotational

vibration modes. Unfortunately, in the radiation field of a target, highly active radicals are formed in methane, in particular CH_3^- und H^+. In liquid methane (100-K-moderator) this gives rise to the formation of higher alkane homologues, which is eventually clogging the piping. In its solid state (20-K-moderator), in addition to radiolysis, crystal defects like interstitials are generated. The stored energy together with recombination of radicals can lead to spontaneous energy release (Wigner effect), which in turn may destroy the moderator vessels.

Within the present R&D phase several paths for developing radiation resistant or at least better manageable cold moderators are being followed. One way is the production of small methane pebbles (2 to 3 mm diameter), which as a bed are cooled by flowing liquid hydrogen. A second possibility is the inclusion of methane in porous substances (e.g. zeolites) or clathrates (e.g. from water ice), both again as small pebbles. Radiation damage and Wigner effect will thus be restricted to small particles. A timely and regular exchange of the pebble beds would prevent the destruction of the vessel and sustain the neutronic quality of the moderator. A third way would be the utilization of different hydrocarbons (with many freely rotating methyl groups), which do not exhibit the unfavorable radiolysis behavior of methane.

Irradiation behavior of moderator media are being performed at reactors (CARE in England and IBR-2 in Russia). The neutronic properties (intensities and pulse shapes) of the different variants will be studied in a to scale mock-up of the ESS target-moderator-reflector module. This test facility has been installed at the cooler synchrotron (COSY) of the Institut für Kernphysik of Forschungszentrum Jülich and first successful experiments have been performed. The experiments are performed under the auspices of the international collaboration JESSICA (Jülich Experimental Spallation target Set-up In COSY Area).

H. Ullmaier and H. Conrad

Collaboration

Internal (Forschungszentrum Jülich)
IKP, ZAT, ZEL, ZFK-HZ

External (international)
BNL (Upton, USA) , JINR (Dubna, Russland), KEK (Tsukuba, Japan), Kurchatov Inst. (Moskau, Russland), JAERI (Tokai, Japan), LANL (Los Alamos, USA), ORNL (Oak Ridge, USA), PSI (Villigen, CH), RAL (Chilton, UK), RISO (Roskilde, DK), Universita die Ancona (Ancona, IT)

Personnel 2000/2001 and areas of activities

Scientific Staff

Dr. J. Chen	Mechanical tests and TEM on irradiated spallation materials	23.60.0
Dr. H. Conrad (Institute for Scattering Methods)	European Spallation Source: Target and Moderators	23.60.0
Dr. P. Jung	Radiation damage and hydrogen effects in metals and ceramics, thermal desorption spectroscopy	23.80.5
Dr. W. Kesternich (until Oct. 00)	Radiation effects in metals and insulators, TEM	23.80.5
Dr. H. Tietze-Jaensch	Co-ordinator of international ESS-experiment "JESSICA" Instruments for pulsed neutron sources	23.60.0
Prof. H. Ullmaier (Head of Project "European spallation Source ESS" at FZJ)	Mechanical properties of irradiated metals,	23.60.0 23.80.5

Technical Staff

A. Fournier	Secretary, Project Assistant ESS	23.80.5 23.60.0
H. Klein	Instrumentation and data processing, TEM, irradiation experiments	23.80.5 23.60.0
W. Schmitz	SEM, irradiation experiments, specimen preparation	23.80.5

Guests

C. Byloos (Institute for Scattering Methods)	Shock waves in ESS target	23.60.0
Dr. F. Carsughi	(Univ. of Ancona, Italy) Investigations of spent spallation target components	23.60.0
A. Garcia-Borquez	(IPN Mexico) Radiation-induced segregation in metals and ceramics	23.80.5
C. Liu	(NPCI, Chengdu, China) Hydrogen embrittlement of ferritic/ martensitic steels	23.80.5
Dr. E. Shabalin	(JINR, Dubna) Radiation damage in solid methane and ice	23.60.0
G. Flores Diaz	(IPN Mexico) Radiation-induced segregation in metals and ceramics	23.80.5

Publications in refereed journals

Bauer G.S.; Carsughi F.; Dai Y.;Sommer W.F.; Ullmaier H.
Tensile Properties and Microstructure of Martensitic Steel DIN 1.4926 after 800 MeV Proton Irradiation
J. Nucl. Mater. 276 (2000) 289
23.60.0

Bräutigam W.; Filges D.; Ullmaier H.; Wagner R.
The Project "European Spallation Neutron Source (ESS)": Status of R & D Programme
Physica B 276 - 278 (2000) 38
23.60.0

Chen J.; Jung P.; Trinkaus H.
Microstructural evolution of helium-implanted (-SiC
Phys.Rev.B 61 (2000-I) 12923
23.80.5

Chen J.; Jung P.
Effect of helium on radiation damage in a SiC/C composite
Ceramics International 26 (2000) 513
23.80.5

Farrell K.; Jung P.; Stoller R.E.; Ullmaier H.
Hardening of ferritic alloys at 288°C by electron irradiation
J.Nucl.Mater. 279 (2000) 77
23.80.5

Golubov S.I.; Singh B.N.; Trinkaus H.
Defect accumulation in fcc and bcc metals and alloys under cascade damage conditions - Towards a generalisation of the production bias model
J.Nucl.Mater. 276 (2000) 78-89
23.80.5

Golubov S.I.; Singh B.N.; Trinkaus H.
Progress in modelling the microstructural evolution in metals under cascade damage conditions
J.Nucl.Mater. 283 (2001) 89
23.80.5

He Z.; Jung P.
Dimensional changes of Al2O3, MgO, MgAl2O4, AlN and Si3N4 by helium implantation
Nucl.Instr.Meth.Phys.Res. B 166-167 (2000) 165
23.80.5

Jung P.
Creep and electrical resistivity of metallic glass Ni78B14Si8 under proton irradiation
J.Appl.Phys. 86 (1999) 4876
23.80.5

Jung P.
Diffusion Processes in Radiation Damage of Metals
Metals Materials and Processes 11 (1999) 191
23.80.5

Kesternich W.
Difficulties in measuring electrical conductivities in highly insulating materials:
Radiation-induced electrical degradation is an artifact
J.Mater.Research 15 (2000)
23.80.5

Other publications

Carsughi F.; Fournier A.; Ullmaier H. (eds.)
Proceedings of 6th ESS General Meeting, Ancona, Italy, Sept. 20 - 23, 1999, ESS Report 99 - 99 - M 1 to M 5, ISSN 1433333 - 559 X
23.60.0

Treusch J.; Ullmaier H.; Wagner R.
Die Europäische Spallations-Neutronenquelle: ein Mikroskop zur Erforschung der Materie
Jahrbuch 2000/2001 des Wissenschaftszentrums Nordrhein-Westfalen
S. 12, Düsseldorf (2000)
23.60.0

Invited Talks

Jung P.; Liu C.
Diffusion of Hydrogen in Steel - Effect of Irradiation
5th International Workshop on Hydrogen Isotopes in Solids, Stockholm
17.5.2000
23.80.5

Jung P.; Ullmaier H.
Hydrogen and Helium in Target Materials at High Power Spallation Sources
5th International Workshop on Hydrogen Isotopes in Solids, Stockholm
18.5.2000
23.80.5

Jung P.
Hydrogen and Helium in Fusion Materials
The Institue of Modern Physics, Lanzhou, PR-China
6.7.2000
23.80.5

Jung P.
Materials for Fusion Power Reactors
Institute of Plasma Physics, Hefei, PR-China
12.7.2000
23.80.5

Jung P.
Materials for Fusion Power Reactors
The University of Science and Technology, Bejing, PR-China
30.6.2000
23.80.5

Trinkaus H.
Defect Interaction and Accumulation - Physical Concepts and Analytical Treatments
Barcelona,
7.9.00
23.80.5

Trinkaus H.
Dislocation - Defect Interaction - The Elastic Approach
Toledo,
4.4.00
23.80.5

Trinkaus H.
Does Pulsing in Spallation Neutron Sources Affect Radiation Damage
Schruns
11.10.00
23.80.5

Ullmaier H.
Forschungs- und Entwicklungsarbeiten zur Europäischen Spallations - Neutronenquelle ESS
Kolloquium des Forschungszentrums Jülich
25.02.00
23.60.0

Ullmaier H.
Spallationstargets - eine neue Herausforderung an nukleare Werkstoffe
Kolloqium des Forschungszentrums Karlsruhe
08.12.00, 23.60.0

Ullmaier H.
What is New in Spallation Materials? Reflections on the IWSMT-4 Meeting in Schruns
American Nuclear Society International Meeting, Washington, DC.
15.11.00
23.60.0

Other talks

Bauer G.S.; Chen J.; Dai Y.; Sommer W.F.; Viktoria M.
Microstructure in Deformed and Undeformed Austenitic Steel 304L Irradiated with 800 MeV Protons
4th International Workshop on Spallation Materials technology,
Schruns
8-13.10.2000
23.60.0

Broome T.; Carsughi F.; Chen J.; Floßdorf T.; Ullmaier H.
Mechanical Properties and Microstructure of Pure Tantalum after 800 MeV Proton Irrradiation
4th International Workshop on Spallation Materials technology
Schruns
8-13.10.2000
23.60.0

Chen J.; James M.R.; Maloy S.A.; Sommer W.F.; Ullmaier H.
The Mechanical Properties of an Alloy 718 Window after Irradiation in Spallation Environment
4th International Workshop on Spallation Materials technology,
Schruns
8-13.10.2000
23.60.0

Chen J.; Jung P.; Klein H.; Liu C.
Retention of Hydrogen and Helium in Martensitic Stainless Steels and their Effect on Mechanical Properties
4th International Workshop on Spallation Materials Technology, Schruns
10.10.2000.
23.80.5

Jung P.
Hydrogen Embrittlement
Data Base Evaluation Workshop, RAFM Steels, Brasimone
27.11.2000.
23.80.5

Jung P.
Microstructure of C-containing materials, Be, W, SiC and oxide ceramics with high helium concntrations
Monitoring Workshop, Underlying Technology of the European Fusion Programme, Garching
18.7.2000.
23.80.5

Ullmaier H.
Das ESS - Projekt
62. Sitzung des Wissenschaftlich-Technischen Ausschusses des Aufsichtsrats, Jülich
09.05.00
23.60.0

Ullmaier H.
Das Projekt Europäische Spallation - Neutronenquelle
2. Entwicklungskonferenz der beiden Kirchen, Jülich
18.05.00
23.60.0

Ullmaier H.
ESS-Project: Status and planned R & D with emphasis on materials activities
Internat. Workshop on Spallation Materials Technology (IWSMT-4)
Schruns
09.10.00
23.60.0

Ullmaier H.
Effects of Helium on Mechanical Properties of Structural Target Materials
Metals and Ceramics Seminar, Oak Ridge National Laboratory
20.03.00
23.60.0

Ullmaier H.
Materialforschung und -entwicklung für die Europäische Spallations - Neutronenquelle
Kolloquium des Instituts für Werkstoffe und Verfahren der Energietechnik, Jülich
11.05.00
23.60.0

Ullmaier H.
Radiation Damage in Spallation Materials
CEA - Saclay,
16.06.00
23.60.0

The number at the end of each contribution characterize the associated R&D program:

23.06.0	Special and guest program in solid state research
23.15.0	Cooperative phenomena in condensed matter
23.20.0	Electronic structure of solids, surfaces and layered systems
23.30.0	Polymer, membranes and complex fluids
23.42.0	Solid State Research for information technology
23.55.0	Research on novel and advanced materials
23.60.0	Material problems in target components
23.80.5	Materials under high doses of radiation
23.89.1	Applications of synchrotron and neutron radiation

Publications

Publications in refereed journals

IFF-00-11-001
Abbas B.; Schwahn D.; Willner L.
Concentrated diblock copolymer solutions in a pressure field
Physica B 276-278, 377-378, (2000)
23.30.0

IFF-00-11-002
Alefeld B.; Dohmen L.; Heidemann A.1
1ILL, Grenoble, France
GaAs as a backscattering crystal
Physica B 283 (2000) 299 - 301
23.89.1

IFF-00-11-003
Alefeld B.; Dohmen L.; Richter D.; Brückel Th.
Space technology from X-ray telescopes for focusing SANS and reflectometry
Physica B 276 - 278 (2000) 52 - 54
23.89.1

IFF-00-11-004
Alefeld B.; Dohmen L.; Richter D.; Brückel Th.
X-ray space technology for focusing small-angle neutron scattering and neutron reflectometry
Physica B 283 (2000) 330 - 332
23.89.1

IFF-00-11-005
Allen C.W.; Schroeder H.; Hiller J.M.
In situ study of dislocation behaviour in columnar Al thin films on Si-substrate during thermal cycling
Materials Research Society (MRS) Symposium Proceedings 594, 123 (2000)
23.42.0

IFF-00-11-006
Andoh H.; Harnach O.; Darula M.; Beuven St.; Kohlstedt H.
Superconductivity and its applications: Dynamics of order parameter and microwave emission for a YBa2Cu3O7-delta bicrystal junction
Physica C 339/4, 237 (2000)
23.42.0

IFF-00-11-007
Antal T.1,2; Schütz G.M.
1 Universite de Geneve, Switzerland
2 FZ Jülich, Germany
Asymmetric exclusion process with short-range interaction: Some remarks on traffic flow and a nonequilibrium reentrance transition
Phys. Rev. E. 62, 83 - 89 (2000)
23.15.0

IFF-00-11-008
Apostolopoulos G.1; Herfort J.1; Däweritz I.1; Ploog K.H.1; Luysberg M.
1 Paul Drude Institut, Berlin
Reentrant Mound Formation in GaAs(001) Homoepitaxy Observed by ex situ Atomic Force Microscopy
Phys. Rev. Lett. 84, 3358 (2000)
23.42.0

IFF-00-11-009
Baier F.1; Müller M.A.1; Grushko B.; Schäfer H.E.1
1 ITAP, Univ. Stuttgart 70569 Stuttgart, D
Atomic defects in quasicrystals: an approach with positron annihilation spectroscopy and time differential dilatometry.
Mat. Sci. Eng. A294-296, 650-653 (2000)
23.55.0

IFF-00-11-010
Ballone P.; Montanari B.; Jones R.O.
Catalytic reactions of living polymers - density functional study of reactivity of phenol and phenoxides with the cyclic tetramer of polycarbonate
J. Phys. Chem. A104, 2793-2798, 2000
23.20.0

IFF-00-11-011
Ballone P.; Montanari B.; Jones R.O.
Density functional study of carbonic acid clusters
J. Chem. Phys. 112, 6571-6575, 2000
23.20.0

IFF-00-11-012
Bartsch M.1; Geyer B.1; Häussler D.1; Feuerbacher M.; Urban K.; Messerschmidt U.1
1 Max-Planck-Institut für Mikrostrukturphysik, Weinberg 2, Halle/Saale, D-06120, Germany
Plastic properties of icosahedral Al-Pd-Mn single quasicrystals
Mat. Sci. Eng. A294-296, 761 (2000)
23.55.0

IFF-00-11-013
Bauer G.S.; Carsughi F.; Dai Y.;Sommer W.F.; Ullmaier H.
Tensile Properties and Microstructure of Martensitic Steel DIN 1.4926 after 800 MeV Proton Irradiation
J. Nucl. Mater. 276 (2000) 289
23.60.0

IFF-00-11-014
Bene J.1,; Bröcheler S.; Lustfeld H.
1Institute for Theoretical Physics, Eötvös University, Budapest, Ungarn
Simulating 2D Flows with Viscous Vortex Dynamics
J. Stat. Phys. 101, p. 567 (2000)
23.15.0

IFF-00-11-015
Berger R.; Blügel S.; Antons A.; Kromen Wi.; Schroeder K.
A Parallelized ab initio Molecular Dynamics Code for the Investigation of Atomistic Growth Processes
Proceedings of the NIC-Workshop "Molecular Dynamics on parallel Computers", Jülich, 08.-10. Februar 1999, p. 185-198 (World Scientific 2000)
23.42.0

IFF-00-11-016
Bihlmayer G.; Asada T.1; Blügel S.
1Shizuoka University, Hamamatsu, Japan
Electronic and magnetic structure of the (001)-surfaces of V, Cr, and V/Cr
Phys. Rev. B 62, R11937 (2000)
23.20.0

IFF-00-11-017
Bihlmayer G.; Kurz Ph.; Blügel S.
Overlayers, interlayers, and surface alloys of Mn on the Cu(111) surface
Phys. Rev. B 62, 4726 (2000)
23.20.0

IFF-00-11-018
Blüher R.1; Frank W.1,2; Grushko B.
1 ITAP, Univ. Stuttgart 70550 Stuttgart, D
2 MPI f. Metallforshung 70506 Stuttgart, D
Diffusion of 103Pd and 195Au in icosahedral Al 70.2Pd21.3Mn8.5 under proton irradiation.
Mat. Sci. Eng. A294-296, 689-692 (2000)
23.55.0

IFF-00-11-019
Bonn M.1,2; Hess Ch.1; Funk S.1; Miners J.1; Persson B.N.J.; Wolf M.1; Ertl G.1
1Fritz-Haber-Institut der MPG Berlin
2Leiden Institute of Chemistry, Leiden, Niederlande
Femtosecond surface vibrational spectroscopy of CO adsorbed on Ru(001) during desorption

Phys. Rev. Lett. 84, 4653 (2000)
23.20.0

IFF-00-11-020
Borbeley S.1.; Heiderich M.; Schwahn D.; Seidl E.2
1Research Institute for Solid State Physics and Optics, Hungary
2Atominstitut der Österreichischen Universitäten, Wien/Österreich
Resolution of the USANS diffractometer at the FRJ-2 reactor in Jülich
Physica B 276-278, 138-139 (2000)
23.30.0

IFF-00-11-021
Botti A.; Pyckhout-Hintzen W.; Richter D.; Straube E.1; Urban V.2; Kohlbrecher J.3
1Univ. Halle/Saale, FB Physik
2ESRF Grenoble, Frankreich
3PSI Villigen, Schweiz
Chain deformation in filled elastomers: a SANS approach
Physica B 276-278, 371-372 (2000)
23.30.0

IFF-00-11-022
Braun A.1; Bärtsch M.1; Schnyder B.1; Kötz R.1; Haas O.1; Haubold H.-G.; Goerigk G.
1PSI, Department of General Energy Research, Villigen, Switzerland
X-ray scattering and adsorption studies of thermally oxidized glassy carbon
Journal of Non-Crystalline Solids 260 (1999) 1 - 14
23.89.1

IFF-00-11-023
Brener E. A.; Müller-Krumbhaar H.; Temkin D.E.1
1I.P. Bardin Institute of Ferrous Metals, Moscow
Structure Formation in Diffusional Growth and Dewetting
Solid State Ionics 131, 23 (2000)
23.15.0

IFF-00-11-024
Brener E.; Marchenko V. I.1; Müller-Krumbhaar H.; Spatschek R.
1P.L. Kapitza Institute for Physical Problems, Moskau
Coarsening kinetics with elastic effects,
Phys. Rev. Lett. 84, 4914 (2000)
23.15.0

IFF-00-11-025
Brener E.; Marchenko V.1; Müller-Krumbhaar H.; Spatschek R.
1P.L. Kapitza Institute for Physical Problems, Moskau
Coarsening Kinetics with Elastic Effects
Phys. Rev. Lett. 84, 4914 (2000)
23.15.0

IFF-00-11-026
Brener E.; Müller-Krumbhaar,H.; Temkin D.; Abel T.
Structure formation in diffusional growth and dewetting
Solid State Ionics 131, 23 (2000)
2315.0

IFF-00-11-027
Bräutigam W.; Filges D.; Ullmaier H.; Wagner R.
The Project "European Spallation Neutron Source (ESS)": Status of R & D Programme
Physica B 276 - 278 (2000) 38
23.60.0

IFF-00-11-028
Buzza D.M.1; Fzea A.H.2; Allgaier J.; Young R.N.3; Hawkins R.J.1; Hamley I.W.4; McLeish T.C.B.1; Lodge T.P.5
1Dep. of Phys. and Astronomy & Polymer IRC, Univ. Leeds/UK
2Dep. of Chem., Univ. Dundee/UK
3Univ. Sheffield/UK
4School of Chemistry, Univ. Leeds/UK
5Univ. Minnesota/USA
Linear melt rheology and small angle X-ray scattering of AB diblock vs A2B2 four arm star block copolymers
Macromolecules 2000, 8399-8414 (2000)
23.30.0

IFF-00-11-029
Caprion D.; Kluge M.; Matsui J.1; Schober H.R.
1Kyushu University, Japan
Computer simulations of the dynamics in glasses and melts
Advances in Solid State Physics 40 (B. Kramer edt.), p. 469, Vieweg, Braunschweig, 2000
23.30.0

IFF-00-11-030
Caprion D.; Matsui J.1; Schober H.R.
1Kyushu University, Japan
Dynamic Heterogenity in Glasses and Liquids
Phys. Rev. 85, 4293 (2000)
23.30.0

IFF-00-11-031
Chen J.; Jung P.; Trinkaus H.
Microstructural evolution of helium-implanted (-SiC
Phys.Rev.B 61 (2000-I) 12923
23.80.5

IFF-00-11-032
Chen J.; Jung P.
Effect of helium on radiation damage in a SiC/C composite
Ceramics International 26 (2000) 513
23.80.5

IFF-00-11-033
Clarke S.; Bihlmayer G.; Blügel S.
Chemical effects in rare gas adsorption
Phys. Rev. B (accepted)
23.20.0

IFF-00-11-034
Corberi F.1; Gonnella G.2; Lamura A.
1 Univ. Salerno, Italy
2 Univ. Bari, Italy
Phase separation of binary mixtures in shear flow: A numerical study
Phys. Rev. E 62, 8064 - 8070 (2000)
23.30.0

IFF-00-11-035
Dallmeyer A.; Carbone C.; Eberhardt W.; Pampuch C.1; Rader O.1; Gudat W.1; Gambardella P.2; Kern K.2
1BESSY, Berlin
2Institut de Physique Experimentale, EPF-Lausanne, CH-1015 Lausanne
Electronic states and magnetism of monatomic Co and Cu wires
Phys. Rev. B 61, R5133 (2000)
23.20.0

IFF-00-11-036
Damson B.1; Weller M.1; Feuerbacher M.; Grushko B.; Urban K.
1 MPI f. Metallforschung 70174 Stuttgart
Mechanical spectroscopy of d-AlNiCo and i-AlPdMn.
Mat. Sci. Eng. A294-296, 806-809 (2000)
23.55.0

IFF-00-11-037
Damson B.1; Weller M.1; Feuerbacher M.; Grushko B.; Urban K.
1 MPI f. Metallforschung 70174 Stuttgart, D
Mechanical spectroscopy of quasicrystals.
J. of Alloys and Compounds 310, 184-189 (2000)
23.55.0

IFF-00-11-038

Dederichs P.H.; Mavropoulos Ph.; Papanikolaou N.
Complex Bandstructure and Tunneling through Insulators
Tagungsband Statusseminar Magnetoelektronik 2000, p. 263, VDI Technologiezentrum
23.20.0

IFF-00-11-039
Dhesi S.S.1; Dürr H.A.; Dudzik E.1; van der Laan G.1; Brookes N.B.2
1Daresbury Laboratory, Warrington, UK
2ESRF Grenoble, France
Magnetism and electron redistribution at Ni/Co interface
Phys. Rev. B 61, 6866 (2000)
23.20.0

IFF-00-11-040
Diehl H.W.1; Eckhardt B.1; Grossmann S.2; Müller-Krumbhaar H.; Zimmermann W.3
1Universität GHS Essen
2Universität Marburg
3Universität Saarbrücken
Strukturbildung und Selbstorganisation
Kapitel 3.4 in "Physik - Denkschrift der Deutschen Physikalischen Gesellschaft zum Jahr der Physik", Herausgeber: Deutsche Physikalische Gesellschaft e.V., Bad Honnef; November 2000
23.15.0

IFF-00-11-041
Divin Y.Y.; Poppe U.; Volkov O.Y.1; Pavlovskii V.V.1
1 Institute of Radioengineering & Electronics of RAS, Moscow 103907, Russian Federation
Frequency-selective incoherent detection of terahertz radiation by high-Tc Josephson junctions
Appl. Phys. Lett., Vol. 76, No. 20, 2826-2828 (2000)
23.42.0

IFF-00-11-042
Dudzik E.1; Dhesi S.S.1; Dürr H.A.; Collins S.P.1; Roper M.D.1; van der Laan G.1; Chesnel K.2
1Daresbury Laboratory, Warrington, UK
2CEA/Grenoble, France
Influence of perpendicular magnetic anisotropy on closure domains studied with x-ray resonant magnetic scattering
Phys. Rev. B 62, 5779 (2000)
23.20.0

IFF-00-11-043
Dudzinski M.1; Schütz G.M.
1 Univ. Köln
Relaxation spectrum of the asymmetric exclusion process with open boundaries
J. Phys. A 33, 8351-8364 (2000)
23.15.0

IFF-00-11-044
Döblinger M.1; Wittmann R.1; Gerthsen D.1; Grushko B.
1 Lab. Elektronenmikroskopie, Univ. Karlsruhe 76128 Karlsruhe, D
Structural relationship and mutual transformation of approximants of the decagonal Al-Co-Ni phase.
Mat. Sci. Eng. A294-296, 131-134 (2000)
23.55.0

IFF-00-11-045
Dürr H.A.; Dudzik E.1; Dhesi S.S.1; Goedkoop J.B.2; van der Laan G.1; Belakhovsky M.3; Mocuta C.3; Marty A.3; Samson Y.3
1Daresbury Laboratory, Warrington, UK
2University of Amsterdam, NL
3CEA/Grenoble, F
Magnetization profile of ultrathin FePd films
J. Synchrotron Rad. 7, 178 (2000)
23.20.0

IFF-00-11-046
Ebert Ph.; Chao K.J.1; Niu Q.1; Shih C.K.1; Plummer E.W.2; Urban K.
1 Department of Physics, University of Texas, Austin
2 Department of Physics, University of Tennessee, Knoxville
Scanning tunneling microscopy of defects in quasiperiodically ordered surfaces
Mat. Sci. Eng. A, 294-296, 826-829 (2000)
23.55.0

IFF-00-11-047
Ebert Ph.; Urban K.; Aballe L.1; Chen C.H.1; Horn K.1; Schwarz G.1; Neugebauer J.1; Scheffler M.1
1 Fritz-Haber-Institut Berlin
Symmetric versus non-symmetric structure of the phosphorous vacancy in InP(110)
Phys. Rev. Lett. 84, 5816-5819 (2000)
23.55.0

IFF-00-11-048
Ebert Ph.
Atomic structure of Point Defects in Compound Semiconductor Surfaces.
Current Opinion in Solid State and Materials Science, in press
23.55.0

IFF-00-11-049
Eisebitt S.; Eberhardt W.
Band structure information and resonant inelastic soft X-ray scattering in broad band solids
J. of Electron Spectroscopy and Related Phenomena 110-111, 335 (2000)
23.20.0

IFF-00-11-050
Eisebitt, S.; Wirth I.; Kann G.; Eberhardt W.
Statistical analysis of the electronic structure of single-wall carbon nanotubes
Phys. Rev. B 61, 5719 (2000) und Phys. Rev. B 62 , 4756 (2000)
23.20.0

IFF-00-11-051
Eisenriegler E.
Polymers interacting with mesoscopic particles
J. Phys.: Condens. Matter 12, A227-A232 (2000)

IFF-00-11-052
Eisenriegler E.
Small mesoscopic particles in dilute and semidilute solutions of nonadsorbing polymers
Journ. Chem. Phys.: 113, 5091-5097 (2000)

IFF-00-11-053
Endo H.; Allgaier J.; Gompper G.; Jakobs B.1; Monkenbusch M.; Richter D.; Sottmann T.1; Strey R.1
1Univ. Koeln, Germany
Membrane Decoration by Amphiphilic Block Copolymers in Bicontinuous Microemulsions",
Phys. Rev. Lett. 85 102-105 (2000)
23.30.0

IFF-00-11-054
Endo H.; Allgaier J.; Gompper G.; Jakobs B.1; Monkenbusch M.; Richter D.; Sottmann T.1; Strey R.1
1Univ. Köln, Inst. für Physik. Chemie
Membrane decoration by amphiphilic block copolymers in bicontinuous microemulsions
Phys. Rev. Lett. 85, 102-105 (2000)
23.30.0

IFF-00-11-055
Farrell K.; Jung P.; Stoller R.E.; Ullmaier H.
Hardening of ferritic alloys at 288°C by electron irradiation
J.Nucl.Mater. 279 (2000) 77
23.80.5

IFF-00-11-056

Feuerbacher M.; Klein H.1; Bartsch M.2; Messerschmidt U.2; Urban K.
1 European Synchrotron Radiation Facility, Pluo E202, BP 220, 38043 Grenoble Cedex, France
2 Max-Planck-Institut für Mikrostrukturphysik, Weinberg 2, D-06120 Halle, Saale, Germany
A comparative study of the plastic behaviour of icosahedral and x'-Al-Pd-Mn.
Mat. Sci. Eng. A 294-296, 736 (2000).

IFF-00-11-057
Franken K.; Maier H.; Prume K.; Waser R.
Finite-Element Analysis of Ceramic Multilayer Capacitors: Failure Probability Caused by Wave Soldering and Bending Loads
J. Am. Cer. Soc., 83 (6), 1433-40 (2000)
23.42.0

IFF-00-11-058
Futakawa M.1; Kikuchi K.1; Conrad H.; Stechemesser H.
1Japan Atomic Energy Research Institute, Tokai-mura, Japan
Pressure and stress waves in a spallation neutron source mercury target generated by high-power proton pulses
Nuclear Instruments and Methods in Physics Research A 439 (2000) 1 - 7
23.60.0

IFF-00-11-059
Gavilano J.L.1; Mushkolaj S.1; Ott H.R.1; Apih T.1; Dolinsek J.1; Dubois J.M.1; Urban K.
1 Ecole des Mines de Nancy, LSG2M, Nancy F
NMR Studies of an icosahedral Al72.4 Pd20.5 Mn 7.1 quasicrystal
Physica B 284-288, 1167-1168 (2000)
23.42.0

IFF-00-11-060
Gebauer J.1; Börner F.1; Krause-Rehberg R.1; Staab T.E.M.2; Bauer-Kugelmann W.1; Kögel G.1; Triftshäuser W.1; Specht P.3; Lutz R.C.3; Weber E.R.3; Luysberg M.
1 ISG, FZ Jülich
2 Laboratory of Physics, Helsinki University of Technology, Finnland
3 Department of Materials Science, University of California, Berkeley, Ca 94720, USA
Defect identification in GaAs grown at low temperatures by positron annihilation
J. Appl. Phys. 87, 8368 (2000)
23.42.0

IFF-00-11-061
Gebauer J.1; Krause-Rehberg R.1; Domke C.; Ebert Ph.; Urban K.; Staab T.E.M.2
1 FB Physik, Universität Halle
2 Lab. of Physics, Helsinki University of Technology
Direct identification of As vacancies in GaAs using positron annihilation calibrated by scanning tunneling microscopy
Phys. Rev. B, in press
23.55.0

IFF-00-11-062
Geyer B.1; Bartsch M.1; Feuerbacher M.; Urban K.; Messerschmidt U.1
1 Max-Planck-Institut für Mikrostrukturphysik, Weinberg 2, Halle/Saale, D-06120, Germany
Plastic deformation of icosahedral Al-Pd-Mn single quasicrystals.
I. Experimental Results
Phil. Mag. A 80, 1151-1163 (2000)
23.55.0

IFF-00-11-063
Golubov S.I.; Singh B.N.; Trinkaus H.
Defect accumulation in fcc and bcc metals and alloys under cascade damage conditions - Towards a generalisation of the production bias model
J.Nucl.Mater. 276 (2000) 78-89
23.80.5

IFF-00-11-064
Golubov S.I.; Singh B.N.; Trinkaus H.
Progress in modelling the microstructural evolution in metals under cascade damage conditions
J.Nucl.Mater. 283 (2001) 89
23.80.5

IFF-00-11-065
Gompper G.; Kroll D. M.1
1 Univ. Minnesota, Minneapolis, USA
Melting transition of a network model in two dimensions
Eur. Phys. J. E 1, 153-157 (2000)
23.30.0

IFF-00-11-066
Gompper G.; Kroll D. M.1
1 Univ. Minnesota, Minneapolis, USA
Statistical mechanics of membranes: freezing, undulations, and topology fluctuations
J. Phys.: Condens. Matter 12 A29-A37 (2000)
23.30.0

IFF-00-11-067
Grossmann M.1; Bolten D.1; Lohse O.1; Böttger U.1; Waser R.
1 Institut für Werkstoffe der Elektrotechnik, RWTH Aachen
Correlation between switching and fatigue in PbZr0.3Ti0.7O3 thin films
Applied Physics Letters, Vol. 77, No. 12, 1894-1896
23.42.0

IFF-00-11-068
Grossmann M.1; Lohse O.1; Bolten D.1; Boettger U.1; Waser R.
1 Institut für Werkstoffe der Elektrotechnik, RWTH Aachen
Lifetime estimation due to imprint failure in ferroelectric SrBi2 Ta2O9 thin films
Applied Physics Letters, Vol. 76, No.3, 363-365.(2000)
23.42.0

IFF-00-11-069
Grushko B.; Gwózdz J.; Yurechko M.
Investigation of the Al-Cu-Rh phase diagram in the vicinity of the decagonal phase
J. Alloys Comp., 305, 219-224 (2000)
23.55.0

IFF-00-11-070
Grushko B.
Composition and precipitation behavior of icosahedral Al-Pd-Mn quasicrystals.
Mat. Sci. Eng. A294-296, 45-48 (2000)
23.55.0

IFF-00-11-071
Grünberg P.
Layered magnetic structures in research and application
Acta mater. 48, 239 (2000)
23.42.0

IFF-00-11-072
Gutheim F.; Müller-Krumbhaar H.; Brener E.; Misbah C.1
1Lab. de Spectrometrie Phys., Univ. Joseph Fourier, Grenoble, Frankreich
Epitaxial Growth with Elastic Interaction: Layer and Cluster Growth
Stochastic Processes in Physics, Chemistry and Biology, J.A. Freud, T. Pöschel (Eds.), Lecture Notes in Physics, Vol. 557 (2000)
23.15.0

IFF-00-11-073
Gutheim F.; Müller-Krumbhaar H.; Brener E.; Misbah C.1
1Lab. de Spectrometrie Phys., Univ. Joseph Fourier, Grenoble, Frankreich

Epitaxial Growth with Elastic Interaction: Layer and Cluster Growth
Stochastioc Processes in Physics, Chemistry and Biology, p. 484,
J. A. Freund, T. Poeschel eds., Springer Verlag, Berlin 2000
23.15.0

IFF-00-11-074
Gwozdz J.1; Grushko B.; Surowiec M.1
1 University of Silesia, Inst. Phys. Chem. Metals. 40-007 Katowice, Poland
Mosaic structure of single quasicrystals.
Mat. Sci. Eng. A294-296, 49-52 (2000)
23.55.0

IFF-00-11-075
Harnack O.; Darula M.; Beuven St.; Kohlstedt H.
Noise and conversion properties of Y-Ba-Cu-O Josephson mixers at operating temperatures above 20 K
Appl. Phys. Lett. 76, 1764 (2000)
23.42.0

IFF-00-11-076
Hase T.P.A.1; Pape I.1; Read D.E.1; Tanner B.K.1; Dürr H.A.; Dudzik E.2; van der Laan G.2; Marrows C.H.3; Hickey B.J.3
1Department of Physics, University of Durham, UK
2Daresbury Laboratory, Warrington, UK
3Department of Physics and Astronomy, University of Leeds, UK
Soft x-ray magnetic scattering evidence for biquadratic coupling in Co/Cu multilayers
Phys. Rev. B 61, 15331 (2000)
23.20.0

IFF-00-11-077
Hase T.P.A.1; Pape I.1; Tanner B.K.1; Dürr H.A.; Dudzik E.2; van der Laan G.2; Marrows C.H.3; Hickey B.J.3
1Department of Physics, University of Durham, UK
2Daresbury Laboratory, Warrington, UK
3Department of Physics and Astronomy, University of Leeds
Soft x-ray resonant magnetic diffuse scattering from strongly coupled Cu/Co multilayers
Phys. Rev. B 61, R3792 (2000)
23.20.0

IFF-00-11-078
Hauck J.; Mika K.
Architecture of crystal structures from square planes
Acta Crystallogr. B56, 750-765 (2000)
23.55.0

IFF-00-11-079
Hauck J.; Mika K.
Magnetic Ordering
J. Magn. Magn. Mat. 212, 389-400 (2000)
23.55.0

IFF-00-11-080
Hauck J.; Mika K.
Structure Maps of Surface Structures
Surface Review and Letters 7, 37-53 (2000)
23.55.0

IFF-00-11-081
Hauck J.; Mika K.
Structure and Interactions of Clusters
Int. J. Modern Phys. B 14, 1075-1092 (2000)
23.55.0

IFF-00-11-082
Hauck J.; Mika K.
Structure families of ZrO2 and CaTiO3 related ionic conductors
Solid State Ionics 127,1-21 (2000)
23.55.0

IFF-00-11-083
Hauck J.; Mika K.
The Jig-saw Puzzle of Crystal Structures: Alloys, Superconducting Oscides, Semiconductors, Ionic Conductors, Surface Adsorbates and Magnetic Structures
Jül-3732, Januar 2000, to appear in Progr. Solid State Chemistry
23.55.0

IFF-00-11-084
He Z.; Jung P.
Dimensional changes of Al2O3, MgO, MgAl2O4, AlN and Si3N4 by helium implantation
Nucl.Instr.Meth.Phys.Res. B 166-167 (2000) 165
23.80.5

IFF-00-11-085
Heggen M.; Feuerbacher M.; Schall P.; Klein H.1; Fisher I.R.2; Canfield P.C.2 Urban K.
1 European Synchrotron Radiation Facility, Pluo E202, BP 220, 38043 Grenoble Cedex, France
2 Ames Laboratory and Department of Physics and Astonomy, Iowa State University, Ames, Iowa
50011, USA
Plastic deformation of icosahedral Zn-Mg-Dy single quasicrystals
Phil. Mag. Lett., Vol. 80, No. 3, 129-136 (2000)
23.55.0

IFF-00-11-086
Heggen M.; Feuerbacher M.; Schall P.; Klein H.1; Fisher I.R.2; Canfield P.C.2; Urban K.
1 European Synchrotron Radiation Facility, Pluo E202, BP 220, 38043 Grenoble Cedex, France
2 Ames Laboratory and Department of Physics and Astonomy, Iowa State University, Ames, Iowa
50011, USA
Plasticity of icosahedral Zn-Mg-Dy single quasicrystals
Mat. Sci. Eng. A 294-296, 781 (2000)
23.55.0

IFF-00-11-087
Heinze S.; Bode M.1; Kubetzka A.1; Pietzsch O.1; Nie X.; Blügel S; Wiesendanger R.1
1Zentrum für Mikrostrukturforschung, Universität Hamburg
Real-space imaging of two-dimensional antiferromagnetism on the atomic scale
Science 288, 1805 (2000)
23.20.0

IFF-00-11-088
Hoffmann S.; Willner L.; Richter D.; Arbe A.1; Colmenero J.1; Farago B.2
1Departamento de Fisica de Materiales, Universidad del Pais Vasco, San Sebastian/Spain
2Institut Laue Langevin, Grenoble/France
On the Origin of Dynamic Heterogeneities in Miscible Polymer Blends - A Quasielastic Neutron Scattering Study
Phys. Rev. Lett. 80, 772 (2000)
23.30.0

IFF-00-11-089
Hohlwein D.1,2; Zeiske Th.
1University, Institut für Kristallographie, Tübingen
2HMI, BENSC, 14109 Berlin
Paramagnetic short-range order in MnF2 beyond the critical region
Physica B 276 - 278 (2000) 584 - 585
23.89.1

IFF-00-11-090
Hupfeld D.; Schweika W.; Strempfer J.1; Mattenberger K.2; McIntyre G. J.3; Brückel Th.
1Ames Laboratory, Iowa State University, Ames, USA
2ETH, Laboratorium für Festkörperphysik, Zürich, Switzerland
3ILL, Grenoble, France
Element-specific magnetic order and competing interactions in Gd0.8Eu0.2S

Europhyics Letters 49 (1) (2000) 92 - 98
23.89.1

IFF-00-11-091
Hwang S.C.; Waser R.
Study of Electrical and Mechanical Contribution to Switching in Ferroelectric/Ferroelastic Polycrystals
Acta mater. 48, 3271-3282 (2000)
23.42.0

IFF-00-11-092
Ibberson R.M.1; David W.I.F.1; Parsons S.2; Prager M.; Shankland K.1
1RAL, Chilton, Didcot, UK
2Univ. of Edinburgh, UK
The crystal structures of m-xylene and p-xylene, C8D10, at 4.5K
J. Mol. Struct. 524, 121 (2000)
23.15.0

IFF-00-11-093
Ibberson R.M.1; Morrison C.2; Prager M.
1RAL, Chilton, Didcot, UK
2Univ. of Edinburgh, UK
Neutron powder and ab-initio structure of orthoxylene: the influence of crystal packing on the phenyl ring
Chem. Commun. 2000, 539 (2000)
23.15.0

IFF-00-11-094
Inamura Y.1; Arai M.1; Otomo T.1; Kitamura N.2; Buchenau U.
1Inst. of Material Structure Science, KEK, Tsukuba/Japan
2Government Industrial Research, Inst. of Osaka, Ikeda/Japan
Density dependence of the boson peak of vitreous silica
Physica B 284-288, 1157-1158 (2000)
23.15.0

IFF-00-11-095
Irmer G.1; Monecke J.1; Verma P.2; Goerigk G.; Herms M.3
1University of Mining and Technology, Institute of Theoretical Physics, Freiberg
2Institute of Technology, Department of Electronics and Information Science, Kyoto, Japan
3Fraunhofer-Institut für Zerstörungsfreie Prüfverfahren, Dresden
Size analysis of nanocrystals in semiconductor doped silicate glasses with anomalous small-angle x ray and Raman scattering
Journal of Applied Physics 88 (2000) 1873 - 1879
23.89.1

IFF-00-11-096
Jia C.L.; Siegert M.1; Urban K.
1 ISI, FZ Jülich
Structure and defects of the interface between BaTiO3 thin films and MgO substrates
23.42.0

IFF-00-11-097
Jiang X.1; Fryda M.1; Jia C.L.
1 Fraunhofer-Institut für Schicht- und Oberflächentechnik, Bienroder Weg 54, 38108 Braunschweig
High-quality CVD diamond films on silicon: recent progresses
Diamond Relat. Mater. 9, 1640 (2000)
23.42.0

IFF-00-11-098
Jiang X.1; Jia C.L.
1 Fraunhofer-Institut für Schicht- und Oberflächentechnik, Bienroder Weg 54, 38108 Braunschweig
Direct epitaxy of diamond on Si(100) and surface-roughening-induced crystal misorientation
Phys. Rev. Lett. 84, 3658 (2000)
23.42.0

IFF-00-11-099
Jung P.
Creep and electrical resistivity of metallic glass Ni78B14Si8 under proton irradiation
J.Appl.Phys. 86 (1999) 4876
23.80.5

IFF-00-11-100
Jung P.
Diffusion Processes in Radiation Damage of Metals
Metals Materials and Processes 11 (1999) 191
23.80.5

IFF-00-11-101
Kaendler I. D.1; Seeck O. H.; Schlomka J.-P.1; Tolan M.1; Press W.1; Stettner J.1; Kappius L.2; Dieker C.2; Mantl S.2
1University, Inst. f. Exp. und Angw. Physik, Kiel
2FZJ, ISI, Jülich
Structural characterisation of oxidized allotaxially grown CoSi2 layers by x-ray scattering
Journal of Applied Physics 87 (2000) 133 - 139
23.89.1

IFF-00-11-102
Kanaya T.1; Buchenau U.; Koizumi S.; Tsukushi I.1; Kaji K.1
1Inst. for Chem. Research, Kyoto University, Kyoto/Japan
Non-Gaussian behavior of crystalline and amorphous phases of polyethylene
Phys. Rev. B 61, 6451 (2000)
23.30.0

IFF-00-11-103
Kawasaki M.; Odagaki T.; Kehr K.W.
Absence of self-averaging in the complex admittance for transport through random media,
Phys. Rev. B 61, 5839-5842 (2000)
23.15.0

IFF-00-11-104
Kehr K.W.; Koza Z.1
1 Univ. Wroclaw, Poland
Hopping motion of lattice gases through nonsymmetric potentials under strong bias conditions
Phys. Rev. E 61, 2319-2326 (2000)
23.15.0

IFF-00-11-105
Kehr K.W.; Koza Z.1
1 Univ. Wroclaw, Poland
Hopping motion of lattice gases through nonsymmetric potentials under strong bias conditions
Phys. Rev. E 61, 72319-2326 (2000)
23.15.0

IFF-00-11-106
Kemner E.1; de Schepper I.M.1; Schmets A.J.M.1; Grimm H.; Overweg A.R.1,2; van Santen R.A.2
1Interfaculty Reactor Institute, Delft Univ. of Technology, The Netherlands
2Lab. of Inorganic Chem. and Catalysis, Eindhoven Univ. of Technology, The Netherlands
Molecular motion of ferrocene in a Faujaste-type zeolite: A quasielastic neutron scattering study
J. Phys. Chem. B 2000, 1560-1562 (2000)
23.15.0

IFF-00-11-107
Kemner E.1; de Schepper I.M.1; Schmets A.J.M.1; Grimm H.
1Interfaculty Reactor Institute, Delft Univ. of Technology, The Netherlands
Model independent determination of the elastic incoherent structure factor in neutron scattering experiments
Nuclear Instruments and Methods in Physics Research B 160, 544-549 (2000)
23.15.0

IFF-00-11-108

Kentzinger E.; Rücker U.; Caliebe W.; Goerigk G.; Werges F.; Nerger S.; Voigt J.; Schmidt W.; Alefeld B.; Fermon C.1; Brückel Th.
1DRECAM/SPEC, CEA Saclay, 91191 Gif-sur-Yvette, France
Structural and magnetic characterization of Fe/(-Mn thin films
Physica B 276 - 278 (2000) 586 - 587
23.89.1

IFF-00-11-109
Kentzinger E.; Schober H.R.
Migration energies in L12 intermetallic compounds
J. Phys. Condens. Matter 12, 8145 (2000)
23.15.0

IFF-00-11-110
Kentzinger E.; Schober H.R.
Migration energies in L12 intermetallic compounds
J. Phys.: Condens. Matter 12 (2000) 8145 - 8158
23.89.1

IFF-00-11-111
Kesternich W.
Difficulties in measuring electrical conductivities in highly insulating materials:
Radiation-induced electrical degradation is an artifact
J.Mater.Research 15 (2000)
23.80.5

IFF-00-11-112
Khoukaz C.1; Galler R.1; Mehrer H.1; Canfield P.C.2; Fisher I.R.2; Feuerbacher M.
1 Institut für Metallforschung1, Universität Münster, D-48149 Münster, Germany;
2 Ames Laboratory and Department of Physics and Astonomy, Iowa State University, Ames, Iowa
50011, USA
Diffusion of 57Co in Decagonal AlNiCo-Quasicrystals
Mat. Sci. Eng. A, 294-296, 697 (2000)
23.55.0

IFF-00-11-113
Kirstein O.; Kozielewski T.; Prager M.; Richter D.
The backscattering spectrometer for the FRM-II reactor in Munich
Physica B 291, 310-313 (2000)
23.89.1

IFF-00-11-114
Kirstein O.; Prager M.; Kozielewski T.; Richter D.
Phase space transformation used at the FRM II backscattering spectrometer: concepts and technical realization
Physica B 283, 361-364 (2000)
23.89.1

IFF-00-11-115
Klein H.1; Feuerbacher M.; Urban K.
1 European Synchrotron Radiation Facility, Pluo E202, BP 220, 38043 Grenoble Cedex, France
Dislocations in Al-Pd-Mn approximants: an HREM study.
Mat. Sci. Eng. A294-296, 769 (2000)
23.55.0

IFF-00-11-116
Klein H.; Feuerbacher M.; Schall P.; Urban K.
Bending experiments on the ('-(Al-Pd-Mn) quasicrystal approximant
Phil. Mag. Lett., Vol. 80, No. 1, 11-18 (2000)
23.55.0

IFF-00-11-117
Klingeler R.; Bechthold P.S.; Neeb M.; Eberhardt W.
Mass spectra of metal-doped carbon and fullerene clusters
J. of Chem. Physics 113, 1420 (2000)
23.20.0

IFF-00-11-118
Klingeler R.; Kann G.; Wirth I.; Eisebitt S.; Bechthold P.S.; Neeb M.; Eberhardt W.
La@C60, a metallic endohedral fullerene
Nature (submitted)
23.20.0

IFF-00-11-119
Kluge F.; Ebert Ph.; Grushko B.; Urban K.
Influence of grown-in voids on the structure of cleaved icosahedral Al-Pd-Mn quasicrystal surfaces
Mat. Sci. Eng. A 294-296, 874-877 (2000)
23.55.0

IFF-00-11-120
Kluge M.; Schober H.R.
Isotope effect of diffusion in a simple liquid
Phys. Rev. E. 62, 597 (2000)
23.30.0

IFF-00-11-121
Koizumi S.1; Annaka M.1; Borbeley S.2; Schwahn D.
1Advanced Science Research Center, Japan Atomic Energy Research Institute, Tokai-mura/Japan
2Research Institute for Solid State Physics and Optics, Hungary
Fractal structures of a Poly(N-Isopropylacrylamide) gel studied by small-angle neutron scattering over a Q-range from 10-5 to 0.1Å-1
Physica B 276-278, 367-368 (2000)
23.30.0

IFF-00-11-122
Korhonen T.1; Settels A.; Papanikolaou N.; Zeller R.; Dederichs P.H.
1Helsinki University of Technology, Helsinki, Finland
Lattice Relaxations and Hyperfine Fields of Heavy Impurities in Fe
Physical Review B62, 452 (2000)
23.20.0

IFF-00-11-123
Kurth D.G.1; Lehmann P.1; Volkmer D.2; Müller A.2; Schwahn D.
1MPI of Colloids and Interfaces, Potsdam
2University of Bielefeld, Dep. of Chemistrsy
Biologically inspired polyoxometalate-surfactant composite materials. Investigations on the structures of discrete, surfactant-encapsulated clusters, monolayers, and Langmuir-Blodgett films of (DODA)40(NH4)2[(H2O)n (Mo132O372(CH3CO2)30(H2O)72]
J. Chem. Soc., Dalton Trans., 3989-3998 (2000)
23.30.0

IFF-00-11-124
Kurz Ph.; Bihlmayer G.; Blügel S.; Hirai K.1; Asada T.2
1Department of Physics, Nara Medical University, Nara, Japan
21Shizuoka University, Hamamatsu, Japan
Comment on "Ultrathin Mn films on Cu(111) substrates: Frustrated antiferromagnetic order
Phys. Rev. B (accepted)
23.20.0

IFF-00-11-125
Kurz Ph.; Bihlmayer G.; Hirai K.1; Blügel S.
1Department of Physics, Nara Medical University, Nara, Japan
Three-dimensional spin-structure on a two-dimensional lattice: Mn/Cu(111)
Phys. Rev. Lett. (accepted)
23.20.0

IFF-00-11-126
Kümmerle E. A.1; Güthoff F.1; Schweika W.; Heger G.1
1University, Institute for Crystallography, Aachen
Single-Crystal Neutron Diffraction Investigations on the Phase Transitions in CeO1.800 and CeO1.765
Journal of Solid State Chemistry 153 (2000) 218 - 230
23.15.0

IFF-00-11-127
Lee S.A.1; Grimm H.; Pohle W.2; Scheiding W.2; van Dam L.3; Song Z.3; Levitt M.H.3; Korolev N.3.; Szabó A.1; Rupprecht A.3
1Dep. of Physics & Astronomy, Univ. Toledo, Ohio/USA
2Inst. für Molekularbiologie, Univ. Jena
3Division of Physical Chem., Univ. Stockholm/Schweden
NaDNA-bipyridyl-(ethylenediamine)platinum (II) complex: Structure in oriented wet-spun films and fibers
Phys. Rev. E 62, 7044, (2000)
23.15.0

IFF-00-11-128
Lei C.H.; Jia C.L.; Lisoni J.G.1; Siegert M.1; Schubert J.1; Buchal Ch.1; Urban K.
1 ISI, FZ Jülich
Structural studies of epitaxial BaTiO3 film deposited on MgO-buffered r-plane cut sapphire
J. Crystal Growth 219, 397 (2000)
23.42.0

IFF-00-11-129
Lei C.H.; Jia C.L.; Siegert M.1; Urban K.
1 ISI, FZ Jülich
Investigation of {111} stacking faults and nanotwins in epitaxial BaTiO3 thin films by high-resolution transmission electron microscopy
Phil. Mag. Lett., Vol. 80, No. 6, 371-380 (2000)
23.42.0

IFF-00-11-130
Lentzen M.; Urban K.
Reconstruction of the projected crystal potential in transmission electron microscopy by means of a maximum-likelihood refinement algorithm
Acta Cryst. A 56, 235-247 (2000)
23.42.0

IFF-00-11-131
Leube W.; Monkenbusch M.; Schneiders D.; Richter D.; Adamson D.1; Fetters L.1; Panagiotis D.2; Lovegrove R.2
1Exxon Mobil Research and Engineering Co., Strategic Corporate, Research Laboratories, Annandale, New Jersey, USA
2Infineum, Ltd. Milton Hill, Abingdon, England
Wax crystal modification for fuel oils by self-aggregating partially crystallizable hydrocarbon block copolymers
Energy&Fuels, Vol. 14 (2), 419-430 (2000)
23.30.0

IFF-00-11-132
Levanov N.A.1; Stepanyuk V.S.1; Hergert W.1; Bazhanov D.I.2; Dederichs P.H.; Katsnelson A.3; Massobrio C.4
1FB Physik, Martin-Luther-Universität, Halle
2MPI für Mikrostrukturphysik, Halle
3Solid State Physics Department, Moscow State University, Moscow
4Institut de Physique e de Chimie des Materiaux de Strasbourg, Strasbourg, Frankreich
Energetics of Co adatoms on the Cu(001) surface
Phys. Rev. B61, 2330 (2000)
23.20.0

IFF-00-11-133
Lichtenstein A.I.; Jones R.O.; de Gironcoli S.1; Baroni S.1
1Istituto Nazionale per la Fisica della Materia, Trieste, Italien
Anisotropic thermal expansion in silicates: A density functional study of ß-eurvptite and related materials
Physical Review B, 62, 17 (2000)
23.20.0

IFF-00-11-134
Liebsch A.; Liechtenstein A.1
1University of Nijmegen, Niederlande
Photoemission quasiparticle spectra of Sr2RuO4
Phys. Rev. Lett. 84, 1591 (2000)
23.20.0

IFF-00-11-135
Liedtke R.1; Grossmann M.1; Waser R.
1 Institut für Werkstoffe der Elektrotechnik, RWTH Aachen
Capacitance and admittance spectroscopy analysis of hydrogen-degraded Pt/(Ba,Sr)TiO/Pt thin-film capacitors,
Appl. Physics Letters, Vol. 77, No. 13, 2045-2047
23.42.0

IFF-00-11-136
Liedtke R.1; Hoffmann S.; Waser R.
1 Institut für Werkstoffe der Elektrotechnik, RWTH Aachen
Recrystallization of Oxygen Ion Implanted Ba0,7Sr0,3TiO3 Thin Films
Journal of the American Ceramic Society, 83, (2), 436-438 (2000)
23.42.0

IFF-00-11-137
Liedtke R.; Hoffmann S.; Waser R.
Recrystallization of Oxygen Ion Implanted Ba0.7Sr0.3TiO3 Thin Films
J. Am. Ceram. Soc. 83, 436-438 (2000)
23.42.0

IFF-00-11-138
Lin J.-H.; Baumgärtner A.
Molecular Dynamics simulations of hydrophobic and amphiphatic proteins interacting with a lipid bilayer membrane.
Comput. Theor. Poly. Sci. 10, 97 (2000)
23.30.0
46.10.0

IFF-00-11-139
Lin J.-H.; Baumgärtner A.
Stability of a melittin pore in a lipid bilayer a molecular dynamics study.
Biophys. J. 78, 1714 (2000)
23.30.0
46.10.0

IFF-00-11-140
Link S., Scholl A.; Jacquemin R.; Eberhardt W.
Electron dynamics at a Ag/C60 metal semiconductor interface
Solid State Comm. 113, 689 (2000)
23.20.0

IFF-00-11-141
Link S.; Dürr H.A.; Bihlmayer G.; Blügel S.; Eberhardt W.; Chulkov E.V.1; Silkin V.M.1; Echenique P.M.1
1Donostia International Physics Center (DIPC), San Sebastian, E
Electron dynamics of image potential states on the clean and oxygen covered Pt(111) surface
Phys. Rev. B (submitted)
23.20.0

IFF-00-11-142
Link S.; Dürr H.A.; Eberhardt W.
Lifetimes of image potential states on the Pt(111) surface probed by time-resolved two-photon photoemission spectroscopy
Appl. Phys. A 71, 525 (2000)
23.20.0

IFF-00-11-143
Link S.; Sievers J.; Dürr H.A.; Eberhardt W.
Lifetimes of image-potential states on the clean and hydrogen covered Ni(111) surface
J. Electron Spectrosc. & Rel. Phenom. (in press)
23.20.0

IFF-00-11-144
Luchnikov V. A.1; Medvedev N. N.1; Naberukhin Y. I.1; Schober H.R.

1Institute of Chemical Kinetics and Combustion, Novosibirsk, Russia
Voronoi-Delaunoy analysis of normal modes in a simple model glass
Phys. Rev. B 62, 3181 (2000)
23.30.0

IFF-00-11-145
Lüttgens G.; Pontius N.; Friedrich C.; Klingeler R.; Bechthold P.S.; Neeb M.; Eberhardt W.
Chemisorption of benzene on metal dimer anions: A study by photoelectron detachment spectroscopy
J. Chem. Phys. (submitted)
23.20.0

IFF-00-11-146
Maus M.; Ganteför G.; Eberhardt W.
The electronic structure and the band gap of nano-sized Si particles: competition between quantum confinement and surface reconstruction
Appl. Phys. A 70, 535 (2000)
23.20.0

IFF-00-11-147
Mavropoulos M.; Papanikolaou N.; Dederichs P.H.
Complex Bandstructure and Tunnelin throug Ferromagnet/Insulator/Ferromagnet Junctions
Phys. Rev. Lett. 85, 1088 (2000)
23.20.0

IFF-00-11-148
McGrady G.S.1; Turner J.F.C.2; Ibberson R.M.3; Prager M.
1Kings College, London, UK
2Univ. of Tennessee, USA
3RAL, Chilton, Didcot, UK
Structure of the trimethylaluminum dimer as determined by powder neutron diffraction at low temperature
J. Mol. Struct. 19, 4398 (2000)
23.15.0

IFF-00-11-149
Meier G.1; Pawelzik U.1; Schweika W.; Kockelmann W.2
1MPI-Polymerforschung, Mainz
2ISIS, Rutherford Laboratory, UK
The static structure factor S(Q) of partially deuterated ethyl- and hexylmethacrylate polymers
Physica B 276 - 278 (2000) 369 - 370
23.89.1

IFF-00-11-150
Messerschmidt U.1; Bartsch M.1; Geyer B.1; Feuerbacher M.; Urban K.
1 Max-Planck-Institut für Mikrostrukturphysik, Weinberg 2, Halle/Saale, D-06120, Germany
Plastic deformation of icosahedral Al-Pd-Mn single quasicrystals.
II. Interpretation of the experimental results
Philosophical Magazine A 80, 1165-1181 (2000)
23.55.0

IFF-00-11-151
Messerschmidt U.1; Bartsch M.1; Geyer G.1; Häussler D.1; Feuerbacher M.; Urban K.
1 Max-Planck-Institut für Mikrostrukturphysik, Weinberg 2, Halle/Saale, D-06120, Germany
Microprocesses of the plastic deformation of icosahedral Al-Pd-Mn single quasicrystals.
Mat. Sci. Eng. A.294-296, 761 (2000)
23.55.0

IFF-00-11-152
Mirone A.1; Sacchi M.1; Dudzik E.2; Dürr H.A.; van der Laan G.2; Vaures A.3; Petroff F.3
1LURE, Université Paris-Sud, Orsay, F
2Daresbury Laboratory, Warrington, UK
3Unite Mixte CNRS/Thompson-LRC, Orsay, F
Study of the magnetic order in a Co/Cr multilayer by magnetic Bragg diffraction at the Co 2p resonance
J. Magn.&Magn. Mat. 218, 137 (2000)
23.20.0

IFF-00-11-153
Monkenbusch M.; Schneiders D.; Richter D.; Willner L.; Leube W.; Fettes L.J.1; Huang J.S.1; Lin M.1
1Exxon Corporate Research, Annandale/USA
2Dept. of Mat. Sci., Princeton Univeristy/USA
Aggregation behavior of PE-PEP copolymers and the winterization of Diesel fuel
Physica B 276-278, 941 (2000), Conf. Proced. ICNS '99, Budapest/Hungary
23.30.0

IFF-00-11-154
Morenzin J.; Kietzmann, H.; Bechthold P.S.; Ganteför G.; Eberhardt W.
Localization and "Bandwidth" of the 3d-orbitals in "magnetic" Ni and Co clusters (invited paper)
Pure and Applied Chemistry (2000) (submitted)
23.20.0

IFF-00-11-155
Mortensen K.1; Schwahn D.; Frielinghaus H.; Almdal K.1
1Risø National Laboratory, Condensed Matter Physics and Chemistry Department, Roskilde, Denmark
Lifshitz critical line in the ternary mixture of homopolymer blend and diblock copolymer, studied by small-angle neutron scattering
J. Appl. Cryst. 33, 686-689 (2000)
23.30.0

IFF-00-11-156
Müller-Krumbhaar H.; Emmerich H.; Brener E.; Hartmann M.
Dewetting hydrodynamics in 1+1 dimensions
Accepted Phys. Rev. E. (2000)
23.15.0

IFF-00-11-157
Müller-Krumbhaar H.; Saito Y.1
1KEIO University, Deoartment of Physics, Yokohama, Japan
Crystal Growth and Solidification (Review)
in Computer Simulation in Colloid an Interface Science, ed. M. Borowko, Dekker, N.Y., 2000
23.15.0

IFF-00-11-158
Müller-Krumbhaar H.
Nachwuchsmangel in Physik - ein Problem der Schule?
Praxis der Naturwissenschaften - Physik, Bd. 49, 1 (2000)
23.15.0

IFF-00-11-159
Neeb M.; Klingeler R.; Bechthold P.S.; Kann G.; Wirth I.; Eisebitt S.; Eberhardt W.
Deposition of endohedral fullerenes from a laser evaporation cluster source
Appl. Phys. A (accepted)
23.20.0

IFF-00-11-160
Nielen H.; Goebel H.; Eppler I.; Schroeder H.; Schilling W.
Stress and plasticity in passivated interconnect lines
Proc. Of 5th Int. Workshop on "Stress-induced Phenomena in Metallization", Stuttgart (Germany), AIP Conf. Proc. 491, 277 (1999)
23.42.0

IFF-00-11-161
Nonas B.; Papanikolaou N.; Wildberger K.; Zeller R.; Dederichs P.H.
3d Impurities on the (001) surface of Fe
Clusters and Nanostructure Interfaces, ed. By P.Jena, S.N. Khanna and B.K. Rao (World Scientific, Singapore, 2000), p. 545-552

23.20.0

IFF-00-11-162
Nordlund K.; Partyka P.; Averback R.S.; Robinson L.K.; Ehrhart P.
Atomistic simulation of diffuse x-ray scattering from defects in solids
J. Appl. Phys. 88 (2000) 2278-2288
23.42.0

IFF-00-11-163
Pampuch C.1; Rader O.1; Kachel T.1; Gudat W.1; Carbone C.; Kläsges R.; Bihlmayer G.; Blügel S.; Eberhardt W.
1BESSY Berlin
One-dimensional spin-polarized quantum-wire states in Au on Ni(110)
Phys. Rev. Lett. 85, 2561 (2000)
23.20.0

IFF-00-11-164
Papanikolaou N.; Nonas B.; Heinze S.1; Zeller R.; Dederichs P.H.
1Universität Hamburg
Scanning tunneling spectra of impurities in the Fe(001) surface
Physical Review B62, 11118 (2000)
23.20.0

IFF-00-11-165
Persson B.N.J.; Ballone P.1
1Istituto Nazionale per la Fisica della Materia, University of Messina, Italien
Boundary lubrication: layering transition for curved solid surfaces with long-range elasticity
Solid State Communications 115, 599 (2000)
23.20.0

IFF-00-11-166
Persson B.N.J.; Ballone P.1
1Istituto Nazionale per la Fisica della Materia, University of Messina, Italien
Squeezing lubrication films: layering transition for curved solid surfaces with long-range elasticity
J. Chem. Phys. 112, 9524 (2000)
23.20.0

IFF-00-11-167
Persson B.N.J.; Popov V.L.1
1Institute of Strength Physics and Materials Science, Tomsk, Russland
On the origin of the transition from slip to stick
Solid State Communications 114, 261 (2000)
23.20.0

IFF-00-11-168
Persson B.N.J.; Tosatti E.1
1SISSA, Trieste, Italien
Qualitative theory of Rubber Friction
J. Chem. Phys. 112, 2021 (2000)
23.20.0

IFF-00-11-169
Persson B.N.J.; Volokitin A.I.1
1Samara State Technical University, Russland
Comments on "Brownian Motion of Microscopic Solids under the Action of Fluctuating Electromagnetic Fields
Phys. Rev. Lett. 84, 3504 (2000)
23.20.0

IFF-00-11-170
Persson B.N.J.; Volokitin A.I.1
1Samara State Technical University, Russland
Dynamical Interactions in Sliding Friction
Surface Science 457, 345 (2000)
23.20.0

IFF-00-11-171
Persson B.N.J.
Electronic friction on a superconductivity surface
Solid Sate Communications 115, 145 (2000)
23.20.0

IFF-00-11-172
Persson B.N.J.
Friction dynamics for curved solid surfaces with long-range elasticivity
J. Chem. Phys. 113, 5477 (2000)
23.20.0

IFF-00-11-173
Persson B.N.J.
Layering transition: Dynamical instabilities during squeeze-out
Chem. Phys. Lett. 324, 231 (2000)
23.20.0

IFF-00-11-174
Persson B.N.J.
Sliding Friction: Theory and Applications
Second Edition (extended version), Springer 2000
23.20.0

IFF-00-11-175
Persson B.N.J.
Theory of time-dependent plastic deformation
Phys. Rev. B61, 5949 (2000)
23.20.0

IFF-00-11-176
Pertsev N.A.; Koukhar V.G.; Waser R.; Hoffmann S.
Curie Weiss-type law for strain and stress effects on the dielectric response of ferroelectric thin films
Appl. Phys. Lett. 77, 2596-2598 (2000)
23.42.0

IFF-00-11-177
Petzelt J.; Ostapchuk T.; Kamba S.; Rychetsky I.; Savinov M.; Volkov A.; Gorshunov B.; Pronin A.; Hoffmann S.; Waser R.; Lindner J.
High-Frequency Dielectric Response of SrTiO3 Crystals, Ceramics and thin Films
Ferroelectrics 239, 117 (2000)
23.42.0

IFF-00-11-178
Petzelt J.; Ostapchuk T.; Kamba S.; Rychetsky I.; Savinov M.; Volkov A.; Gorshunov B.; Pronin A.; Hoffmann S.; Waser R.;. Lindner J.
High-Frequency Dielectric Response of SrTiO3 Crystals, Ceramics and thin Films
Ferroelectrics 239, 117 (2000)
23.42.0

IFF-00-11-179
Pigorsch C.; Schütz G.M.
Shocks in the asymmetric simple exclusion process in a discrete-time update
J. Phys. A 33, 7919-7935 (2000)
23.15.0

IFF-00-11-180
Pontius N.; Bechthold P.S.; Neeb M.; Eberhardt W.
Femtosecond multi-photon photoemission of small transition metal cluster anions
J. of Electron Spectrosc. and Rel. Phenomena 106, 107 (2000)
23.20.0

IFF-00-11-181
Pontius N.; Bechthold P.S.; Neeb M.; Eberhardt W.
Time-resolved photo-electron spectroscopy on mass-selected metal clusters using a regenerative femtosecond amplifier up to 100 Hz
Appl. Phys. B 71, 351 (2000)
23.20.0

IFF-00-11-182
Pontius N.; Bechthold P.S.; Neeb M.; Eberhardt W.
Time-resolved photoelectron spectra of optically excited states in Pd3-
J. of Electron Spectrosc. and Relat. Phenom (in press)
23.20.0

IFF-00-11-183
Pontius N.; Bechthold P.S.; Neeb M.; Eberhardt W.
Ultrafast hot-electron dynamics observed in Pt3- using time-resolved
photoelectron spectroscopy
Phys. Rev. Lett. 84, 1132 (2000))
23.20.0

IFF-00-11-184
Prager M.; Grimm H.; Parker S.F.1; McGrady S.2
1ISIS facility, RAL, Chilton Didcot, Oxon OX11 0QX, UK
2Kings College, London, UK
Rotational potentials of bridging and terminal methyl groups in trimethylaluminium-dimers
Physica B 276-278, 250-251 (2000)
23.30.0

IFF-00-11-185
Prager M.
The thermal time-of-flight spectrometer SV29 at FZ Jülich: focusing in space and time
Physica B283, 376 (2000)
23.89.1

IFF-00-11-186
Prume K.1; Waser R.; Franken K.; Maier H.
1 Institut für Werkstoffe der Elektrotechnik, RWTH Aachen
Finite-Element Analysis of Ceramic Multilayer Capacitors: Modeling and Electrical Impedance Spectroscopy for a Non-Destructive Failure Test
J. Am. Ceram. Soc., 83 (5), 1153-59 (2000)
23.42.0

IFF-00-11-187
Quadbeck P.; Ebert Ph.; Urban K.; Gebauer J.1; Krause-Rehberg K.1
1 FB Physik, Universität Halle
Effect of dopant atoms on the roughness of III-V semiconductor cleavage surfaces
Appl. Phys. Lett., Vol. 76, No. 3, 300-302 (2000)
23.55.0

IFF-00-11-188
Reif T.; Doerr M.1; Loewenhaupt M.1; Rotter M.1; Svoboda P.2; Welzel S.3
1Technische Universität, Institut für Angewandte Physik, Dresden
2Charles University, Department of Electron Systems, Prague,The Czech Republic
3HMI, Berlin
Magnetic structure of DyCu2 in the virgin and in the converted state
Physica B 276 - 278 (2000) 600 - 601
23.89.1

IFF-00-11-189
Richter D.; Monkenbusch M.; Allgaier J.; Arbe A.1; Colmenero J.1; Farago B.2; Cheol Bae Y.3; Faust R.3
1Departamento de Fisica de Materiales, Universidad del Pais Vasco, San Sebastian/Spain
2Insitut Laue Langevin, Grenoble, France
3Department of Chemistry, University of Massachusetts-Lowell, Lowell/Massachusetts, USA
From Rouse dynamics to local relaxation: A neutron spin echo study on polyisobutylene melts
Journal of Chem. Phys. 111, 6107 (1999)
23.30.0

IFF-00-11-190
Richter D.
Neutron scattering in polymer physics
Physica B 276-278, 22-29 (2000)
23.30.0

IFF-00-11-191
Rottländer P.; Kohlstedt H.; Grünberg P.; Girgis P.
Ultraviolet light oxidation for magnetic tunnel junctions
J. Appl. Phys. 87, 6067 (2000)
23.42.0

IFF-00-11-192
Rottländer P.; Kohlstedt H.; de Gronckel H.A.M.; Girgis E.; Schelten J.; Grünberg P.
Magnetic tunnel junctions prepared by ultraviolet light assisted oxidation
J. of Magnetism and Magnetic Materials 210, 251 (2000)
23.42.0

IFF-00-11-193
Rottländer P.; Kohlstedt H.; de Gronckel H.M.A.; Girgis E.; Schelten J.; Grünberg P.
Magnetic tunnel junctions prepared by ultravioet light assisted oxidation
J. Magn. Magn. Mat. 210, 251 (2000)
23.42.0

IFF-00-11-194
Rush J.J.1; Udovic T.J.1; Berk N.F.1; Richter D.; Magerl A.2
1Center for Neutron Research, National Institute for Standards and Technology, Gaithersburg, USA
2Lehrstuhl für Kristallographie und Strukturphysik, Universität Erlangen-Nürnberg
Excited-state vibrational tunnel splitting of hydrogen trapped by nitrogen in niobium
Europhys. Lett. 48 (2), 187-193 (1999)
23.30.0

IFF-00-11-195
Ryazanov A.I.1; Trinkaus H.; Volkov A.E.1
1Russian Research Center, "Kurchatov Institute", Moscow
Incubation Dose for Ion Beam Induced Anisotropic Growth of Amorphous Alloys: Insight into Amorphous State Modifications
Phys. Rev. Lett. 84, 919 (2000)

IFF-00-11-196
Rücker U.; Alefeld B.; Bergs W.; Kentzinger E.; Brückel Th.
The new polarized neutron reflectometer in Jülich
Physica B 276 - 278 (2000) 95 - 97
23.89.1

IFF-00-11-197
Rücker U.; Alefeld B.; Kentzinger E.; Brückel Th.
Monochromator design for the HADAS reflectometer in Jülich
Physica B 283 (2000) 422 - 425
23.89.1

IFF-00-11-198
Schall P.; Feuerbacher M.; Bartsch M.1; Messerschmidt U.1; Urban K.
1 Max-Planck-Institut für Mikrostrukturphysik, Weinberg 2, D-06120 Halle, Saale, Germany
Dislocation arrangement and density in deformed Al-Pd-Mn single quasicrystals
Mat. Sci. Eng. A 294-296, 697 (2000)
23.55.0

IFF-00-11-199
Schober H.R.; Caprion D.
Structure and Relaxation in liquid and amorphous selenium
Phys. Rev. B 62, 3709 (2000)
23.30.0

IFF-00-11-200
Schober T.; Bohn H.G.
Water vapor solubility and electrochemical characterization of the high temperature proton conductor BaZr0.9Y0.1O2.95

Solid State Ionics 127 (2000) 351-360
23.55.0

IFF-00-11-201
Schober T.; Szot K.; Barton M.; Kessler B.; Breuer U.1;
Penkalla H.J.1; Speier W.1
1 Institut für Chemie und Dynamik der Geosphäre, FZJ
Cation loss of BaCa0.393Nb0.606O2.91 in aqueous media: amorphization at room temperature,
J. Solid State Chemistry 149, 262-275 (2000)
23.55.0

IFF-00-11-202
Schober T.; Szot K.; Barton M.;.Kessler B.; Breuer U.;
.Penkalla H.J.; Speier W.
Cation Loss of BaCa0.393Nb0.606O2..91 in Aqueous Media: Amorphization at Room Temperature
Journal of Solid State Chemistry 149, 262 (2000)
23.42.0

IFF-00-11-203
Schroeder K.; Antons A.; Berger R.; Kromen Wi.; Blügel S.
Surface Diffusion and Models for the Kinetics of Epitaxial Growth
to be published in the Proceedings of the International Symposium on Structure and Dynamics of Heterogeneous Systems, Duisburg, 25.-26. Februar 1999, p. 71-94 (World Scientific 2000)
23.42.0

IFF-00-11-204
Schroers J.1; Holland-Moritz D.1; Herlach D.M.1; Urban K.
1 DLR Köln
Growth kinetics of quasicrystalline and polytetrahedral phases of Al-Pd-Mn, Al-Co, and Al-Fe from the undercooled melt
Phys. Rev. B, Vol. 61, No. 21, 14500-14506 (2000)
23.42.0

IFF-00-11-205
Schwahn D.; Mortensen K.1; Frielinghaus H.1; Almdal K.1; Kielhorn L.2
1Risø National Laboratory, Condensed Matter Physics and Chemistry Department, Roskilde, Denmark
2Bayer AG, Leverkusen
Thermal composition fluctuations near the isotropic Lifshitz critical point in a ternary mixture of a homopolymer blend and diblock copolymer
Journ. of Chem. Physics 112, 5454-5472 (2000)
23.30.0

IFF-00-11-206
Schwahn D.; Mortensen K.1; Frielinghaus H.; Almdal K.1
1Risø National Laboratory, Condensed Matter Physics and Chemistry Department, Roskilde, Denmark
3D-Ising and Lifshitz critical behavior in a mixture of a polymer blend and a corresponding diblock copolymer
Physica B 276-278, 353-354 (2000)
23.30.0

IFF-00-11-207
Schwahn D.
Ginzburg number and phase behavior of binary polymer blends in pressure fields
Macromol. Symp. 149, 43-52 (2000)
23.30.0

IFF-00-11-208
Schwarz U.S.1; Gompper G.
1 Weizmann Inst. Rehovot, Israel
Stability of Inverse Bicontinuous Cubic Phases in Lipid-Water Mixtures
Phys. Rev. Lett. 85 1472-1475 (2000).
23.30.0

IFF-00-11-209
Schwarz, U.S.1; Gompper G.
1MPI-KG, Golm and Weizmann Inst. Israel
Stability of bicontinuous cubic phases in ternary amphiphilic systems with spontaneous curvature
J. Chem. Phys. 112, 3792-3802 (2000)
23.30.0

IFF-00-11-210
Schäfer P.; Waser R.
MOCVD of perovskite thin films using an aerosol-assisted liquid delivery system
Adv. Mater. Opt. Electron. 10 (2000) 169-175
23.42.0

IFF-00-11-211
Schütz G.M.
Exact tracer diffusion coefficient in the asymmetric random average process.
J. Stat. Phys. 99, 1045-1049 (2000)
23.15.0

IFF-00-11-212
Schütz G.M.
Phasenübergänge in offenen Vielteilchensystemen fern vom Gleichgewicht
Phys. Blätt. 56, 69 - 73 (2000)
23.30.0

IFF-00-11-213
Seeck O. H.; Kaendler I. D.1; Sinha S. K.1; Tolan M.2; Shin K.3; Rafailovich M. H.3; Sokolov J.3; Kolb R.4
1ANL, APS, Argonne, USA
2University, Inst. f. Exp. und Angw. Physik, Kiel
3SUNY, Dept. of Mat. Sci. and Engin., Stony Brook, USA
4Exxon Research, Annadale, USA
Analysis of x-ray reflectivity data from low-contrast polymer bilayers using a Fourier method
Applied Physics Letters 76 (2000) 2713 - 2715
23.30.0, 23.89.1

IFF-00-11-214
Semmler U.; Ebert Ph.; Urban K.
Effect of charge carriers on the barrier height for vacancy formation on InP(110) surfaces
Appl. Phys. Lett., Vol. 77, No. 1, 61-63 (2000)
23.55.0

IFF-00-11-215
Semmler U.; Simon M.; Ebert Ph.; Urban K.
Stoichiometry changes by selective vacancy formation on (110) surfaces of III-V semiconductors: Influence of electronic effects
J. Chem. Phys., in press
23.55.0

IFF-00-11-216
Settels A.; Schroeder K.; Korhonen T.1; Papanikolaou N.; Aretz M.; Zeller R.; Dederichs P.H.
1Helsinki University of Technology, Helsinki, Finland
In-donor complexes in Si and Ge: structure and electric field gradients
Solid State Commun. 113, 239 (2000)
23.20.0

IFF-00-11-217
Settels A.; Schroeder K.; Korhonen T.1; Papanikolaou N.; Aretz M.; Zeller R.; Dederichs P.H.
1Laboratory of Physics, Helsinki University of Technology, Espoo, Finland
In-Donor Complexes in Si and Ge: Structure and Electric Field Gradients
Solid State Comm. 113, 239 (2000)
23.42.0

IFF-00-11-218
Setter N.1; Waser R.
1 EPFL, Lausanne, Switzerland
Electroceramic Materials
Acta mater. 48, 151-178 (2000)

23.42.0

IFF-00-11-219
Singh B.N.; Eldrup M.; Horsewell A.; Ehrhart P.; Dworschak F.
On recoil energy dependent void swelling in pure copper: part I. Experimental results
Phil. Mag. A 80 (2000) 2629-2650
23.42.0

IFF-00-11-220
Skripov A.V.1; Combet J.2; Grimm H.; Hempelmann R.3; Kozhanov V.N.1
1Institute of Metal Physics, Urals Branch of the Academy of Sciences, Ekatarinenburg/Russia
2Institut Laue Langevin, Grenoble/Frankreich
3Inst. für Physik. Chemie, Univ. des Saarlandes
Quasielastic neutron scattering study of H motion in the hydrogen-stabilized C15-type phases HfTi2Hx and ZrTi2Hx
J. Phys. Cond. Matt. 12, 3313-3324 (2000)
23.15.0

IFF-00-11-221
Slowak R.1; Hoffmann S.; Liedtke R.1; Waser R.
1 Institut für Werkstoffe der Elektrotechnik, RWTH Aachen
Functional graded high-K (Ba1-xSrx)TiO3 thin films for capacitor structures with low temperature coefficient
Integrated Ferroelectrics 24, 169-179 (1999)
23.42.0

IFF-00-11-222
Smith G.D.1; Paul W.2; Monkenbusch M.; Richter D.
1Dep. of Materials Science and Engineering / Dept. of Chemical Engineering and Fuels Engineering, Univ. Utah, USA
2Inst. für Physik, Univ. Mainz
A comparison of neutron scattering studies and computer simulations of polymer melts
Chem. Physics 261, 61-74 (2000)
23.30.0

IFF-00-11-223
Smith G.D.1; Paul W.2; Monkenbusch M.; Willner L.; Richter D.; Qiu X.H.; Ediger M.D.
1Dep. of Mat. Science and Engineering, University of Utah, Salt Lake City/USA
2Inst. für Physik, Universität Mainz
3Dep. of Chemistry, University of Wisconsin-Madison, Madison/USA
Molecular Dynamics of a 1,4-Polybutadiene Melt. Comparison of Experimental and Simulation
Macromolecules 32, 8857 (1999)
23.30.0

IFF-00-11-224
Sokolov A.P.1; Grimm H.; Kisliuk A.1; Dianoux A.J.2
1Dep. of Polymer Science, Univ. Akron/USA
2Institute Laue Langevin, Grenoble/Frankreich
Slow relaxation process in DNA at different levels of hydration
J. of Biological Physics 26, SN1-SN5, (2000)
23.15.0

IFF-00-11-225
Spettmann R.1; Entel P.1; Schroeder K.; Blügel S.
1Theoretische Tieftemperaturphysik, Gerhard-Mercator Universität Duisburg
Electronic Structure of Si(111):Sb((3 x (3) R30°: an ab initio Study
Proceedings of the International Symposium on Structure and Dynamics of Heterogeneous Systems, held at Duisburg, 25.-26.02.1999, p. 217-225 (World Scientific 2000)
23.42.0

IFF-00-11-226
Stellbrink J.; Allgaier J.; Monkenbusch M.; Richter D.; Lang A.1; Likos C.N.1; Watzlawek M.1; Löwen H.1; Ehlers G.2; Schleger P.2
1Univ. Düsseldorf, Theor Physik II
2Insitut Laue Langevin, Grenoble/Frankreich
Neither Gaussian chains nor hard spheres-star polymer seen as ultrasoft colloids
Progr. Colloid Polymer Sci. 115, 88-97 (2000)
23.30.0

IFF-00-11-227
Stepanyuk V.S.1; Hergert W.1; Bazhanov D.I.2; Kirschner J.2; Baranov D.I., Dederichs P.H.; Katsnelson A.3
1FB Physik, Martin-Luther-Universität, Halle
2MPI für Mikrostrukturphysik, Halle
3Solid State Physics Department, Moscow State University, Moscow
Atomic processes and the strain distribution in the early stages of thin films growth
Appl. Phys. A71, 1-4 (2000)
23.20.0

IFF-00-11-228
Stepanyuk V.S.1; Hergert W.1; Rennert P.1; Nonas B.; Zeller R.; Dederichs P.H.
1Martin-Luther-Universität Halle, Halle
Magnetic nanostructures on the fcc Fe/Cu(100) surfaces
Physical Review B61, 2356 (2000)
23.20.0

IFF-00-11-229
Strempfer J.1; Brückel Th.; Caliebe W.; Vernes A.2; Ebert H.2; Prandl W.3; Schneider J. R.1
1HASYLAB at DESY, Hamburg
2Universität, Institut für Physikalische Chemie, München
3Universität, Institut für Kristallographie, Tübingen
Form-factor measurements on chromium with high-energy synchrotron radiation
Eur. Phys. J. B 14 (2000) 63 - 72
23.89.1

IFF-00-11-230
Sturm A.; Gusarov A.1
1Faculte Polytechnique de Mons, Belgien
Dynamical correlations in the electron gas
Physical Review B, 62, 24 (2000)
23.20.0

IFF-00-11-231
Szot K.; Speier W.; Breuer U.; Meyer R.1; Szade J.; Waser R.
1 Institut für Werkstoffe der Elektrotechnik, RWTH Aachen
Formation of micro-crystals on the (100) surface of SrTiO3 at elevated temperatures
Surface Science 460, 112 (2000)
23.42.0

IFF-00-11-232
Szot K.; Speier W.; Pawelczyk M.; Kwapulinski J.; Huliger J.; Hesse H.; Breuer U.; Quadakkers W.;
Chemical inhomogeneity in the near-surface region of KTaO3
J.Phys. : Condens. Matter 12, 4687 (2000)

IFF-00-11-233
Thust A.; Lentzen M.; Urban K.
The Use of Stochastic Algorithms for Phase Retrieval in HRTEM
Scanning Microscopy Supplement, 11, 435-452 (2000)
23.42.0

IFF-00-11-234
Tillmann K.1; Jäger W.1; Rahmati B.; Trinkaus H.; Vescan L.; Urban K.
1 Centrum für Materialanalytik, Universität Kiel, D24143 Kiel
Finite element analysis of the strain induced vertical ordering of islands and determination of compositional modifications in LPCVD-grown GexSi1-x-Si bilayers on Si(001)
Phil. Mag. A, Vol. 80, 255-277 (2000)
23.42.0

IFF-00-11-235
Tillmann K.; Lentzen M.; Rosenfeld R.

Impact of column bending in high-resolution transmission electron microscopy on the strain evaluation of GaAs/InAs/GaAs heterostructures
Ultramicroscopy 83, 111-128 (2000)
23.42.0

IFF-00-11-236
Tolan M.1; Seeck O. H.; Wang J.2; Sinha S. K.2; Rafailovich M. H.3, Sokolov J.3
1University, Inst. f. Exp. und Angw. Physik, Kiel
2ANL, APS, Argonne, USA
3SUNY, Dept. of Mat. Sci. and Engin., Stony Brook, USA
X-ray scattering from polymer films
Physica B 283 (2000) 22 - 26
23.30.0, 23.89.1

IFF-00-11-237
Trautmann C.1; Klaumünzer S.2; Trinkaus H.
1Gesellschaft für Schwerionenforschung, Darmstadt
2 HMI Berlin
Effect of Stress on Track Formation in Amorphous Iron Boron Alloy: Ion Tracks as Elastic Inclusions
Phys. Rev. Lett. 85, 3648 (2000)
23.15.0

IFF-00-11-238
Trimper S.; Täuber U.C.; Schütz G.M.
Reaction-controlled diffusion
Phys. Rev. E 62, 6071-6078 (2000)
23.30.0

IFF-00-11-239
Trinkaus H.; Holländer B.1; Rongen St.1; Mantl S.1; Herzog H.-J.2; Kuchenbecker J.2; Hackbarth T.2
1ISI, Forschungszentrum Jülich, Jülich
2Daimler Chrysler AG, Research and Technology, Ulm
Strain relaxation mechanism for hydrogen-implanted Si1-x Gex/Si(100) heterostructures
App. Phys. Lett. 76, 3552 (2000)
23.42.0

IFF-00-11-240
Tyagi A.K.; Szot K.; Czyrska-Filemonowicz A.; Naumenko D.; Quadakkers W.J.
Significance of Crystallographic Grain Orientation for Oxide Scale Formation on FeCrAl ODS Alloys studied by AFM TEM and SIMS/SNMS
Materials at High Temperatures 17,159 (2000)
23.42.0

IFF-00-11-241
Ujma Z.; Szymczak L.; Handerek L.; Szot K.; Penkalla H.J.
Dielectric and pyroelectric properties of Nb-doped Pb(Zr0.92Ti0.08)O3 ceramics
Journal of the European Ceramic Society 20, 1003 (2000)
23.42.0

IFF-00-11-242
Waser R.; Hagenbeck R.
Grain Boundaries in Dielectric and Mixed-Conducting Ceramics
Overview No. 137, Acta mater. 48, 797-825 (2000)
23.42.0

IFF-00-11-243
Westermann S.1; Willner L.; Richter D.
1Goodyear Technical Center, Luxembourg
The evaluation of polyethylene chain dimensions as a function of concentration in nonadecane
Macromol. Chem. Phys. 201, 500-504 (2000)
23.30.0

IFF-00-11-244
Westermann S.; Pyckhout-Hintzen W.; Thiyagarajan P.1; Wozniak D.1; Richter D.; Straube E.2
1IPNS, Argonne, USA
2Universität Halle
A SANS study on thermal degradation kinetics in polyisoprene networks
Mat. Res. using cold neutrons at pulsed neutron sources, eds. P. Thiyagarajan, F. Trouw, B. Marzec, C.-K. Loong, World Scientific Publ., 210 - 213 (1999)
23.30.0

IFF-00-11-245
Willner L.; Poppe A.; Allgaier J.; Lindner P.1; Richter D.
1Institut Laue Langevin, Grenoble/France
Micellarization of Amphiphilic Diblockcopolymers in Water: Shape Transition and Meanfield to Scaling Cross Over
Europhysics Letters 51 (6), 628 (2000)
23.30.0

IFF-00-11-246
Wischnewski A.; Richter D.; Monkenbusch M.; Willner L.; Farago B.1; Ehlers G.1; Schleger P.1
Reptation in polyethylene-melts with different molecular weights
Physica B 276-278, 337 (2000)
23.30.0

IFF-00-11-247
Wischnewski A.; Richter D.
Comment on "What is the entanglement length in a polymer melt?" by M. Pütz, K. Kremer and G.S. Grest
Europhys. Lett. 52, 719-720 (2000)
23.30.0

IFF-00-11-248
Wortmann D.; Heinze S.; Bihlmayer G.; Blügel S.
Interpreting STM images of the MnCu/Cu(100) surface alloy
Phys. Rev. B 62, 2862 (2000)
23.20.0

IFF-00-11-249
Wortmann D.; Heinze S.; Kurz Ph.; Bihlmayer G.; Blügel S.
Resolving complex atomic-scale spin-structures by SP-STM
Phys. Rev. Lett (submitted)
23.20.0

IFF-00-11-250
Yan S.-S.; Schreiber R.; Grünberg P.; Schäfer R.
Magnetization reversal in (001) Fe thin films studied by combining domain images and MOKE hysteresis loops
J. Magn. Magn. Mat. 210, 305 (2000)
23.42.0

IFF-00-11-251
Yang W.1; Wang R.1; Feuerbacher M.; Schall P.; Urban K.
1 Department of Physics, Wuhan University, Wuhan 430072, China
Determination of the Burgers vector of dislocations in icosahedral quasicrystals by a high-resolution lattice-fringe technique
Phil. Mag. Lett., Vol. 80, No. 5, 281-288 (2000)
23.55.0

IFF-00-11-252
Yurechko M.; Grushko B.
A study of the Al-Pd-Co alloy system.
Mater. Sci. Eng. A294-296, 139.142 (2000)
23.55.0

IFF-00-11-253
Zeiske Th.; Hagdorn K.1; Hohlwein D.1; Ihringer J.1; Prandl W.1; Ritter H.1
1University, Institut für Kristallographie, Tübingen
Structure and magnetism of Ho0.2Ca0.8MnO3
Physica B 276 - 278 (2000) 624 - 625
23.89.1

IFF-00-11-254
Zorn R.; Monkenbusch M.; Richter D.; Matsuoka H.1; Yamamoto Y.1; Nakano M.1; Endo H.1; Yamaoka H.1; Seto H.2; Kawabata Y.2; Nagao M.3

1Dep. of Polymer Chemistry, Kyoto University/Japan
2FIAS, Hiroshima Univ./Japan
3Inst. of Solid State Physics, Univ. of Tokyo, Ibaraki/Japan
Neutron spin-echo study of the dynamic behavior of amphiphilic diblock copolymer micelles in aqueous solution
Langmuir 16, 9177-9185 (2000)
23.30.0

IFF-00-11-255
Zorn R.; Richter D.; Hartmann L.1; Kremer F.1; Frick B.2
1Univ. Leipzig, Inst. für Experimentalphysik
2Institut Laue Langevin, Grenoble/Frankreich
Inelastic neutron scattering experiments on the fast dynamics of a glass forming liquid in mesoscopic confinements
J. Phys. France IV, 10, Pr. 7-83 - Pr.7.86 (2000)
23.15.0

IFF-00-11-256
de Gronckel H.A.M.; Kohlstedt H.; Daniels C.
Prerequisites for high-quality magnetic tunnel junctions: XPS and NMR study of Co/Al bilayers
Appl. Phys. A 70 (4), 435 (2000)
23.42.0

List of references

Abbas B.	IFF-00-11-001		
Abel T.	IFF-00-11-026		
Alefeld B.	IFF-00-11-002	IFF-00-11-003	IFF-00-11-004
	IFF-00-11-108	IFF-00-11-196	IFF-00-11-197
Allgaier J.	IFF-00-11-028	IFF-00-11-053	IFF-00-11-054
	IFF-00-11-189	IFF-00-11-226	IFF-00-11-245
Antons A.	IFF-00-11-015	IFF-00-11-203	
Aretz M.	IFF-00-11-216	IFF-00-11-217	
Ballone P.	IFF-00-11-010	IFF-00-11-011	
Barton M.	IFF-00-11-201		
Baumgärtner A.	IFF-00-11-138	IFF-00-11-139	
Bechthold P.S.	IFF-00-11-117	IFF-00-11-118	IFF-00-11-145
	IFF-00-11-154	IFF-00-11-159	IFF-00-11-180
	IFF-00-11-181	IFF-00-11-182	IFF-00-11-183
Berger R.	IFF-00-11-015	IFF-00-11-203	
Bergs W.	IFF-00-11-196		
Bihlmayer G.	IFF-00-11-016	IFF-00-11-017	IFF-00-11-033
	IFF-00-11-124	IFF-00-11-125	IFF-00-11-140
	IFF-00-11-163	IFF-00-11-248	IFF-00-11-249
Blügel S.	IFF-00-11-015	IFF-00-11-016	IFF-00-11-017
	IFF-00-11-033	IFF-00-11-087	IFF-00-11-124
	IFF-00-11-125	IFF-00-11-140	IFF-00-11-163
	IFF-00-11-203	IFF-00-11-225	IFF-00-11-248
	IFF-00-11-249		
Bohn H.G.	IFF-00-11-200		
Botti A.	IFF-00-11-021		
Brener E.	IFF-00-11-023	IFF-00-11-024	IFF-00-11-025
	IFF-00-11-026	IFF-00-11-072	IFF-00-11-073
	IFF-00-11-156		
Bräutigam W.	IFF-00-11-027		
Bröcheler S.	IFF-00-11-014		
Brückel Th.	IFF-00-11-003	IFF-00-11-004	IFF-00-11-090
	IFF-00-11-108	IFF-00-11-196	IFF-00-11-197
	IFF-00-11-229		
Buchenau U.	IFF-00-11-094	IFF-00-11-102	
Caliebe W.	IFF-00-11-108	IFF-00-11-229	
Caprion D.	IFF-00-11-029	IFF-00-11-030	IFF-00-11-199
Carbone C.	IFF-00-11-035	IFF-00-11-163	
Carsughi F.	IFF-00-11-013		
Chen J.	IFF-00-11-031	IFF-00-11-032	
Clarke S.	IFF-00-11-033		
Conrad H.	IFF-00-11-058		
Dallmeyer A.	IFF-00-11-035		
Dederichs P.H.	IFF-00-11-038	IFF-00-11-122	IFF-00-11-132
	IFF-00-11-147	IFF-00-11-161	IFF-00-11-164
	IFF-00-11-216	IFF-00-11-217	IFF-00-11-227

Heinze S.	IFF-00-11-087	IFF-00-11-248	IFF-00-11-249
Hoffmann S.	IFF-00-11-088	IFF-00-11-136	IFF-00-11-137
	IFF-00-11-176	IFF-00-11-177	IFF-00-11-178
	IFF-00-11-221		
Hupfeld D.	IFF-00-11-090		
Hwang S.C.	IFF-00-11-091		
Jacquemin R.	IFF-00-11-142		
Jia C.L.	IFF-00-11-096	IFF-00-11-097	IFF-00-11-098
	IFF-00-11-128	IFF-00-11-129	
Jones R.O.	IFF-00-11-010	IFF-00-11-011	IFF-00-11-133
Jung P.	IFF-00-11-031	IFF-00-11-032	IFF-00-11-055
	IFF-00-11-084	IFF-00-11-099	IFF-00-11-100
Kann G.	IFF-00-11-050	IFF-00-11-118	IFF-00-11-159
Kehr K.W.	IFF-00-11-103	IFF-00-11-104	IFF-00-11-105
Kentzinger E.	IFF-00-11-108	IFF-00-11-109	IFF-00-11-110
	IFF-00-11-196	IFF-00-11-197	
Kessler B.	IFF-00-11-201		
Kesternich W.	IFF-00-11-111		
Kietzmann, H.	IFF-00-11-154		
Kirstein O.	IFF-00-11-113	IFF-00-11-114	
Klein H.	IFF-00-11-116		
Klein H.1	IFF-00-11-056		
Klingeler R.	IFF-00-11-117	IFF-00-11-118	IFF-00-11-145
	IFF-00-11-159		
Kluge F.	IFF-00-11-119		
Kluge M.	IFF-00-11-029	IFF-00-11-120	
Kläsges R.	IFF-00-11-163		
Kohlstedt H.	IFF-00-11-006	IFF-00-11-075	IFF-00-11-191
	IFF-00-11-192	IFF-00-11-193	IFF-00-11-256
Koizumi S.	IFF-00-11-102		
Kozielewski T.	IFF-00-11-113	IFF-00-11-114	
Kromen Wi.	IFF-00-11-015	IFF-00-11-203	
Kurz Ph.	IFF-00-11-017	IFF-00-11-124	IFF-00-11-125
	IFF-00-11-249		
Lamura A.	IFF-00-11-034		
Lei C.H.	IFF-00-11-128	IFF-00-11-129	
Lentzen M.	IFF-00-11-130	IFF-00-11-233	IFF-00-11-235
Leube W.	IFF-00-11-131	IFF-00-11-153	
Lichtenstein A.	.	IFF-00-11-133	
Liebsch A.	IFF-00-11-134		
Lin J.-H.	IFF-00-11-138	IFF-00-11-139	
Link S.	IFF-00-11-140	IFF-00-11-141	IFF-00-11-142
	IFF-00-11-143		

Lustfeld H.	IFF-00-11-014		
Luysberg M.	IFF-00-11-008	IFF-00-11-060	
Lüttgens G.	IFF-00-11-145		
Maus M.	IFF-00-11-146		
Mavropoulos M.	IFF-00-11-147		
Mavropoulos Ph.	IFF-00-11-038		
Mika K.	IFF-00-11-078	IFF-00-11-079	IFF-00-11-080
	IFF-00-11-081	IFF-00-11-082	IFF-00-11-083
Monkenbusch M.	IFF-00-11-053	IFF-00-11-054	IFF-00-11-131
	IFF-00-11-153	IFF-00-11-189	IFF-00-11-222
	IFF-00-11-223	IFF-00-11-226	IFF-00-11-246
	IFF-00-11-254		
Montanari B.	IFF-00-11-010	IFF-00-11-011	
Morenzin J.	IFF-00-11-154		
Müller-Krumbhaar H.	IFF-00-11-023	IFF-00-11-024	IFF-00-11-025
	IFF-00-11-026	IFF-00-11-040	IFF-00-11-072
	IFF-00-11-073	IFF-00-11-156	IFF-00-11-157
	IFF-00-11-158		
Neeb M.	IFF-00-11-117	IFF-00-11-118	IFF-00-11-145
	IFF-00-11-159	IFF-00-11-180	IFF-00-11-181
	IFF-00-11-182	IFF-00-11-183	
Nerger S.	IFF-00-11-108		
Nie X.	IFF-00-11-087		
Nonas B.	IFF-00-11-161	IFF-00-11-164	IFF-00-11-228
Papanikolaou N.	IFF-00-11-038	IFF-00-11-122	IFF-00-11-147
	IFF-00-11-161	IFF-00-11-164	IFF-00-11-216
	IFF-00-11-217		
Persson B.N.J.	IFF-00-11-019	IFF-00-11-165	IFF-00-11-166
	IFF-00-11-167	IFF-00-11-168	IFF-00-11-169
	IFF-00-11-170	IFF-00-11-171	IFF-00-11-172
	IFF-00-11-173	IFF-00-11-174	IFF-00-11-175
Pontius N.	IFF-00-11-145	IFF-00-11-180	IFF-00-11-181
	IFF-00-11-182	IFF-00-11-183	
Poppe A.	IFF-00-11-245		
Poppe U.	IFF-00-11-041		
Prager M.	IFF-00-11-092	IFF-00-11-093	IFF-00-11-113
	IFF-00-11-114	IFF-00-11-148	IFF-00-11-184
	IFF-00-11-185		
Pyckhout-Hintzen W.	IFF-00-11-021	IFF-00-11-244	
Quadbeck P.	IFF-00-11-187		
Rahmati B.	IFF-00-11-234		
Reif T.	IFF-00-11-188		
Richter D.	IFF-00-11-003	IFF-00-11-004	IFF-00-11-021
	IFF-00-11-053	IFF-00-11-054	IFF-00-11-088
	IFF-00-11-113	IFF-00-11-114	IFF-00-11-131
	IFF-00-11-153	IFF-00-11-189	IFF-00-11-190
	IFF-00-11-194	IFF-00-11-222	IFF-00-11-223
	IFF-00-11-226	IFF-00-11-243	IFF-00-11-244
	IFF-00-11-245	IFF-00-11-246	IFF-00-11-247
	IFF-00-11-254	IFF-00-11-255	

Rosenfeld R.	IFF-00-11-235		
Rottländer P.	IFF-00-11-192		
Rücker U.	IFF-00-11-108	IFF-00-11-196	IFF-00-11-197
Schall P.	IFF-00-11-085	IFF-00-11-086	IFF-00-11-116
	IFF-00-11-198	IFF-00-11-251	
Schelten J.	IFF-00-11-192		
Schmidt W.	IFF-00-11-108		
Schneiders D.	IFF-00-11-131		
Schober H.R.	IFF-00-11-029	IFF-00-11-030	IFF-00-11-109
	IFF-00-11-110	IFF-00-11-120	IFF-00-11-144
	IFF-00-11-199		
Schober T.	IFF-00-11-200	IFF-00-11-201	IFF-00-11-202
Scholl A.	IFF-00-11-142		
Schreiber R.	IFF-00-11-250		
Schroeder H.	IFF-00-11-005	IFF-00-11-160	
Schroeder K.	IFF-00-11-015	IFF-00-11-203	IFF-00-11-216
	IFF-00-11-217	IFF-00-11-225	
Schwahn D.	IFF-00-11-001	IFF-00-11-020	IFF-00-11-121
	IFF-00-11-123	IFF-00-11-155	IFF-00-11-205
	IFF-00-11-206	IFF-00-11-207	
Schweika W.	IFF-00-11-090	IFF-00-11-126	IFF-00-11-149
Schäfer P.	IFF-00-11-210		
Schäfer R.	IFF-00-11-250		
Schütz G.M.	IFF-00-11-007	IFF-00-11-043	IFF-00-11-179
	IFF-00-11-211	IFF-00-11-212	IFF-00-11-238
Seeck O. H.	IFF-00-11-101	IFF-00-11-213	IFF-00-11-236
Semmler U.	IFF-00-11-214	IFF-00-11-215	
Settels A.	IFF-00-11-122	IFF-00-11-216	IFF-00-11-217
Sievers J.	IFF-00-11-143		
Simon M.	IFF-00-11-215		
Spatschek R.	IFF-00-11-023	IFF-00-11-024	
Stechemesser H.	IFF-00-11-058		
Stellbrink J.	IFF-00-11-226		
Sturm A.	IFF-00-11-230		
Szot K.	IFF-00-11-201	IFF-00-11-202	IFF-00-11-231
	IFF-00-11-232	IFF-00-11-240	IFF-00-11-241
Temkin D.	IFF-00-11-026		
Thust A.	IFF-00-11-233		
Tillmann K.	IFF-00-11-235		
Trinkaus H.	IFF-00-11-031	IFF-00-11-063	IFF-00-11-064
	IFF-00-11-195	IFF-00-11-237	IFF-00-11-239
Ullmaier H.	IFF-00-11-013	IFF-00-11-027	IFF-00-11-055
Urban K.	IFF-00-11-012	IFF-00-11-036	IFF-00-11-037
	IFF-00-11-046	IFF-00-11-047	IFF-00-11-056

	IFF-00-11-059	IFF-00-11-061	IFF-00-11-062
	IFF-00-11-085	IFF-00-11-086	IFF-00-11-096
	IFF-00-11-115	IFF-00-11-116	IFF-00-11-119
	IFF-00-11-128	IFF-00-11-129	IFF-00-11-130
	IFF-00-11-150	IFF-00-11-151	IFF-00-11-187
	IFF-00-11-198	IFF-00-11-204	IFF-00-11-214
	IFF-00-11-215	IFF-00-11-233	IFF-00-11-234
	IFF-00-11-251		
Voigt J.	IFF-00-11-108		
Wagner R.	IFF-00-11-027		
Waser R.	IFF-00-11-057	IFF-00-11-067	IFF-00-11-068
	IFF-00-11-091	IFF-00-11-135	IFF-00-11-136
	IFF-00-11-137	IFF-00-11-176	IFF-00-11-177
	IFF-00-11-178	IFF-00-11-186	IFF-00-11-210
	IFF-00-11-218	IFF-00-11-221	IFF-00-11-231
	IFF-00-11-242		
Werges F.	IFF-00-11-108		
Westermann S.	IFF-00-11-244		
Wildberger K.	IFF-00-11-161		
Willner L.	IFF-00-11-001	IFF-00-11-088	IFF-00-11-153
	IFF-00-11-223	IFF-00-11-243	IFF-00-11-245
	IFF-00-11-246		
Wirth I.	IFF-00-11-050	IFF-00-11-118	IFF-00-11-159
Wischnewski A.	IFF-00-11-246	IFF-00-11-247	
Wortmann D.	IFF-00-11-248	IFF-00-11-249	
Yan S.-S.	IFF-00-11-250		
Yurechko M.	IFF-00-11-069	IFF-00-11-252	
Zeiske Th.	IFF-00-11-089	IFF-00-11-253	
Zeller R.	IFF-00-11-122	IFF-00-11-161	IFF-00-11-164
	IFF-00-11-216	IFF-00-11-217	IFF-00-11-228
Zorn R.	IFF-00-11-254	IFF-00-11-255	
de Gronckel H.A.M.	IFF-00-11-192		

Other publications

IFF-00-12-001
Allgaier J.; Poppe A.; Willner L.; Stellbrink J.; Richter D.
PEP-PEO block copolymers as model system for the investigation of micellization in aqueous solution
ACS Symposium Series 765, Ed. J. Edward Glass (2000)
23.30.0

IFF-00-12-002
Asada T.1; Blügel S.; Bihlmayer G.; Handschuh S.; Abt R.
1Shizuoka University, Hamamatsu, Japan
First-principles investigation of the stability of 3d monolayer/Fe(001) against bilayer formation
(44th Magnetism and Magnetic Materials Conference)
J. Appl. Phys. 87, 5935 (2000)
23.20.0

IFF-00-12-003
Baumgaertner A.; Sambeth R.
Models of Cell Locomotion
In Stochastic Dynamics and Pattern Formation in Biological and Complex Systems, ed. by S.Kim, K.Lee, W.Sung,
AIP Conference Proceedings 501, Melville, New York, 2000.
23.30.0
46.10.0

IFF-00-12-004
Belin E.1; Thiel P.A.2; Tsai A.-P.3; Urban K.
1 Laboratoire de Chime Physique-Mat. et Rayonnement, Paris
2 Iowa State University, Ames
3 National Research Institute for Metals, Tsukuba
Quasicrystals
Materials Research Society Symposium Proceedings, to be published (2000)
23.55.0

IFF-00-12-005
Bihlmayer G.; Abt R.; Blügel S.; Asada T.1
1Shizuoka University, Hamamatsu, Japan
Influence of magnetism for the alloy formation of ultrathin films
(International Symposium on Structure and Dynamics of Heterogeneous Systems)
Editors: P. Entel and S.E. Wolf, page 179 (World Scientific, 2000)
23.20.0

IFF-00-12-006
Brückel Th.; Eberhardt W.
Dynamik in kondensierter Materie
Vorlesungsmanuskripte des 31. IFF-Ferienkurses vom 13. - 24.03.2000 (2000), Schriften des Forschungszentrums Jülich, Reihe Materie und Material/Matter and Materials, Band 3, ISBN 3-89336-256-8, 1 - 32
23.89.1

IFF-00-12-007
Brückel Th.; Eberhardt W.
Vorwort zum 31. IFF-Ferienkurs 2000 "fs und neV: Dynamik in kondensierter Materie"
Schriften des Forschungszentrums Jülich, Reihe Materie und Material/Matter and Materials, Band 3, ISBN 3-89336-256-8
23.89.1

IFF-00-12-008
Brückel Th.
Elastic Scattering from Many-Body Systems
Schriften des Forschungszentrums Jülich, Reihe Materie und Material / Matter and Materials, Volume 5 (2000) 3-1 - 3-18
23.89.1

IFF-00-12-009
Brückel Th.
Magnetism
Schriften des Forschungszentrums Jülich, Reihe Materie und Material / Matter and Materials, Volume 5 (2000) 16-1 - 16-19
23.89.1

IFF-00-12-010
Buchenau U.
Relaxationsprozesse in Gläsern
Vorlesungsmanuskript des 31. IFF-Ferienkurs "Femtosekunden und Nano-eV", Vol. 3, C7.1 - 18 (2000)
23.15.0

IFF-00-12-011
Carsughi F.; Fournier A.; Ullmaier H.
Proceedings of 6th ESS General Meeting, Ancona, Italy, Sept. 20 - 23, 1999, ESS Report 99 - 99 - M 1 to M 5, ISSN 1433333 - 559 X
23.60.0

IFF-00-12-012
Conrad H.
Die Europäische Spallations-Neutronenquelle ESS - Spallationsmethoden
Vorlesungsmanuskripte des 31. IFF-Ferienkurses vom 13. - 24.03.2000 (2000), Schriften des Forschungszentrums Jülich, Reihe Materie und Material/Matter and Materials, Band 3, ISBN 3-89336-256-8, B4.1 - 20
23.89.1

IFF-00-12-013
Conrad H.
Neutron Sources
Schriften des Forschungszentrums Jülich, Reihe Materie und Material / Matter and Materials, Volume 5 (2000) 1-1 - 1-15
23.89.1

IFF-00-12-014
Dhesi S.S.1; Dudzik E.1; Dürr H.A.; Brookes N.B.2; van der Laan G.1
1Daresbury Laboratory, Warrington, UK
2ESRF Grenoble, F
Correlation between L3 absorption satellite and spin moment in ultrathin Ni films
Surf. Sci. 454-456, 930 (2000)
23.20.0

IFF-00-12-015
Dhesi S.S.1; Dudzik E.1; Dürr H.A.; van der Laan G.1; Brookes N.B.2
1 Daresbury Laboratory, Warrington, UK
2ESRF Grenoble, F
Electron correlation and charge transfer at the Ni/Co interface
J. Appl. Phys. 87, 5466 (2000)
23.20.0

IFF-00-12-016
Dudzik E.1; Dhesi S.S.1; Collins S.P.1; Dürr H.A.; van der Laan G.1; Chesnel K.2; Belakhovsky M.2; Marty A.2; Samson Y.2; Goedkoop J.B.3
1 Daresbury Laboratory, Warrington, UK
2CEA/Grenoble, F
3University of Amsterdam, NL
X-ray resonant magnetic scattering from FePd thin films
J. Appl. Phys. 87, 5469 (2000)
23.20.0

IFF-00-12-017
Eberhardt W.; Klingeler R.; Bechthold P.S.; Neeb M.
Metal doped fullerenes: Endohedral and networked dopants
Proceedings of the International Winterschool on Electronic Properties and Novel Materials, Kirchberg, Austria (submitted)
23.20.0

IFF-00-12-018
Eisebitt S.; Eberhardt W.
Soft X-ray spectroscopy as a probe of the electronic structure of nanostructured solids
In: Frontiers of Nano-Optoelectronic Systems, Ed. L. Pavesi, E. Buzaneva, Nato Science Series II, 6, p. 347 (Kluwer Aacademic, London, in print)
23.20.0

IFF-00-12-019
Eisebitt S.; Karl A.; Zimina A.; Scherer R.; Freiwald M.; Eberhardt W.; Hauke F.1; Hirsch A.1; Achiba Y.2
Electronic structure of doped fullerenes and single wall carbon nanotubes
In: Electronic Properties of Novel Materials: MolecularNanostructures, Ed. H. Kuzmany, J. Fink, M. Mehring. S. Roth (AIP Conference Proceedings, Melville, in print)
23.20.0

IFF-00-12-020
Fetters L.J.1; Wheeler L.M.1; Xenidou M.; Richter D.
1Exxon Research and Engineering Co., Annandale/USA
Modification Potential for ShellvisTM Star Polymers
Exxon Research and Engineering Company; Proprietary Information, CR.17BU.99 (1999)
23.30.0

IFF-00-12-021
Gaehler F.1; Kramer P.2; Trebin H.-R.1; Urban K.
1 Universität Stuttgart
2 Universität Tübingen
Mat. Sci. Eng. A, 294-296, 1 (2000)
23.55.0

IFF-00-12-022
Grünberg P.; Rottländer P.; Girgis E.; Bürgler D.E.; Eberhardt W.; Kohlstedt H.; Gareev R.; Herrnsdorf J.1.; Schneider M.1
1HL-Planar, Dortmund
Preparation of materials for TMR type sensors
Tagungsband des Statusseminars über Magnetoelektronik, ed. by St. Mengel, VDI Düsseldorf, Juni 2000
23.42.0

IFF-00-12-023
Kurz Ph.; Bihlmayer G.; Blügel S.
Non-collinear magnetism of Cr and Mn monolayers on Cu(111)
(44th Magnetism and Magnetic Materials Conference)
J. Appl. Phys. 87, 6101 (2000)
23.20.0

IFF-00-12-024
Marty A.A.1; Samson Y.1; Gilles B.1; Belakhovsky M.1; Dudzik E.2; Dürr H.A.; Dhesi S.S.2; van der Laan G.2; Goedkoop J.B.3
1CEA Grenoble, F
2Daresbury Laboratory, Warrington, UK
3University of Amsterdam, NL
Weak-stripe magnetic domain evolution with an in-plane field in epitaxial FePd thin films: Model versus experimental results
J. Appl. Phys. 87, 5472 (2000)
23.20.0

IFF-00-12-025
Monkenbusch M.
Introduction to soft matter systems
Neutron Scattering in Novel Materials, Proceedings of the 8th Summer School on Neutron Scattering, 102-116 (2000)
23.30.

IFF-00-12-026
Monkenbusch M.
Neutron spin-echo spectrometer, NSE
Lecture Notes of the Laboratory Course on "Neutron Scattering", Vol. 5, 11-1 - 11-18 (2000)
23.30.0

IFF-00-12-027
Monkenbusch M.
Neutronenspektroskopie
Vorlesungsmanuskript des 31. IFF-Ferienkurs "Femtosekunden und Nano-eV", Vol.3, B5.1 - 40 (2000)
23.30.0

IFF-00-12-028
Monkenbusch M.
Time-of-flight spectrometers
Lecture Notes of the Laboratory Course on "Neutron Scattering", Vol. 5, 10-1 - 10-23 (2000)
23.30.0

IFF-00-12-029
Prager M.
Translation an Rotation
Lecture Notes of the Laboratory Course on "Neutron Scattering", Vol. 5, 17-1 - 17-20 (2000)
23.30.0

IFF-00-12-030
Pyckhout-Hintzen W.; Botti A.; Heinrich M.; Richter D.; Straube E.1; Westermann S.2; Urban V.3
1Univ. Halle/Saale, FB Physik
2Goodyear Technical Center, Luxembourg
3ESRF Grenoble, France
SANS of polymer networks under deformation
Novel Materials, World Science Press (Singapore), 117-130 (2000)
23.30.0

IFF-00-12-031
Pyckhout-Hintzen W.; Westermann S.1; Botti A.; Richter D.; Straube E.2
1Goodyear Technical Center, Luxembourg
2Univ. Halle/Saale, FB Physik
Chain deformation in unfilled and filled polymer networks: a SAS approach
Notiziario Neutroni e Luce di Sincrotone 5, 34-40 (2000)
23.30.0

IFF-00-12-032
Richter D.; Monkenbusch M.; Farago B.1; Schleger P.1; Montes H.2
1Institut Laue Langevin, Grenoble/France
2ESPCI, Paris/France
Large scale motions in dense polymer systems
AIP Conference Proceedings 469, 587 - 598 (1999)
23.30.0

IFF-00-12-033
Richter D.
Dynamik von Polymeren
Vorlesungsmanuskript des 31. IFF-Ferienkurs "Femtosekunden und Nano-eV", Vol. 3, C6.1 - 36 (2000)
23.30.0

IFF-00-12-034
Richter D.
Polymer dynamics
Lecture Notes of the Laboratory Course on "Neutron Scattering", Vol. 5, 15-1 - 15-29 (2000)
23.30.0

IFF-00-12-035
Richter D.
Polymer dynamics by neutron spin echo spectroscopy
in "Scattering in Polymeric and Colloidal Systems" Ed. by W. Brown and K. Mortensen, Gordon and Breach Science Publishers, London, Chap. 12, 535-575 (2000)
23.30.0

IFF-00-12-036
Richter D.
Properties of the neutron, elementary scattering processes
Lecture Notes of the Laboratory Course on "Neutron Scattering", Vol. 5, 2-1 - 2-21 (2000)
23.30.0

IFF-00-12-037
Rosov N.1; Rathgeber S.1; Monkenbusch M.
1NIST, Gaithersburg/USA
Neutron spin echo spectroscopy at the NIST Center

ACS Symposium Series 739 "Scattering from Polymers", Characterization by X-rays, Neutrons and Light, Ed. P. Cebe, B.S. Hsiao, D.J. Lohse
23.89.1 / 23.30.0

IFF-00-12-038
Schwahn D.; Mortensen K.1
1Risø National Laboratory, Condensed Matter Physics and Chemistry Department, Roskilde/Denmark
Thermal composition fluctuations in polymer blends studied with small angle neutron scattering
Chapter 8 in "Scattering in polymeric and colloidal systems", eds. W. Brown and K. Mortensen, Gordon and Breach Science Publishers (2000)
23.30.0

IFF-00-12-039
Schwahn D.
Small-angle scattering and reflectometry
Lecture Notes of the Laboratory Course on "Neutron Scattering", Vol. 5, 8-1 - 8-16 (2000)
23.30.0

IFF-00-12-040
Schwahn D.
Soft Matter Structure
Lecture Notes of the Laboratory Course on "Neutron Scattering", Vol. 5, 14-1 - 14-18 (2000)
23.30.0

IFF-00-12-041
Schweika W.
Polarization analysis
Schriften des Forschungszentrums Jülich, Reihe Materie und Material / Matter and Materials, Volume 5 (2000) 4-1 - 4-19
23.89.1

IFF-00-12-042
Schweika W.
Quellen und Eigenschaften der Neutronen- und Synchrotronstrahlung
Vorlesungsmanuskripte des 31. IFF-Ferienkurses vom 13. - 24.03.2000 (2000), Schriften des Forschungszentrums Jülich, Reihe Materie und Material/Matter and Materials, Band 3, ISBN 3-89336-256-8, B1.1 - 20
23.89.1

IFF-00-12-043
Schütz G.M.
Dynamical theory of steady state selection in open driven diffusive systems, in: Traffic and Granular Flow '99, pp. 227 - 232, D. Helbing, H. J. Herrmann, M. Schreckenberg and D. E. Wolf (eds.), (Springer Verlag, Berlin, 2000)
23.30.0

IFF-00-12-044
Schütz G.M.
Exactly Solvable Models for Many-Body Systems Far From Equilibrium, in: Phase Transitions and Critical Phenomena 19, pp. 1 - 251, C. Domb and J. Lebowitz (eds.), (Academic Press, London, 2000)
23.15.0

IFF-00-12-045
Seeck O. H.; Sinha S. K.1; Kaendler I. D.1; Shu D.1; Shin K.2; Rafailovich M.2; Sokolov J.2; Tolan M.3
1ANL, APS, Argonne, USA
2SUNY, Dept. of Mat. Sci. and Engin., Stony Brook, USA
3University, Inst. f. Exp. and Angw. Physik, Kiel
Interfacial properties of soft matter thin films studied by x-ray scattering
in: Interfacial Properties on the Submicron Scale, ACS/Oxford Press (2000) ed. by J. Frommer, R. Overney
23.89.1

IFF-00-12-046
Seeck O. H.; Sinha S. K.1; Kaendler I. D.1; Wang J.1
1ANL, APS, Argonne, USA
Investigation of confined liquids with x-ray and neutron scattering
in: Exploration of subsurface phenomena by particle scattering, IAS Press (2000) ed. by N. Q. Lam, C. A. Melendres, S. K. Sinha
23.89.1

IFF-00-12-047
Seeck O. H.
Continuum description: Grazing Incidence Neutron Scattering
in: Neutron Scattering, Forschungszentrum Jülich GmbH (2000) 6-1 - 6-18, ed. by Th. Brückel, G. Heger, D. Richter
23.89.1

IFF-00-12-048
Tolan M.1; Seeck O. H.; Wang J.2; Sinha S. K.2; Rafailovich M. H.3; Sokolov J.3
1University, Inst. f. Exp. and Angw. Physik, Kiel
2ANL, APS, Argonne, USA
3SUNY, Dept. of Mat. Sci. and Engin., Stony Brook, USA
Surface structure of soft-matter thin films probes by diffuse x-ray scattering
in: Exploration of subsurface phenomena by particle scattering, IAS Press (2000) ed. by N. Q. Lam, C. A. Melendres, S. K. Sinha
23.89.1

IFF-00-12-049
Treusch J.; Ullmaier H.; Wagner R.
Die Europäische Spallations-Neutronenquelle: ein Mikroskop zur Erforschung der Materie
Jahrbuch 2000/2001 des Wissenschaftszentrums Nordrhein-Westfalen
S. 12, Düsseldorf (2000)
23.60.0

IFF-00-12-050
Urban K.; Paul G.1
1 Frankfurter Allgemeine Zeitung (FAZ), Frankfurt/Main
Physik im Wandel
Rotbuch Verlag (2000).
23.55.0

IFF-00-12-051
Van der Laan G.1; Dudzik E.1; Collins S.P.1; Dhesi S.S.1; Dürr H.A.; Belakhovsky M.2; Chesnel K.2; Marty A.2; Samson Y.2; Gilles B.2
1Daresbury Laboratory, UK
2CEA/Grenoble, F
Soft X-ray magnetic scattering from striped magnetic domain structures
Physica B 283, 171 (2000)
23.20.0

IFF-00-12-052
Vasiliu-Doloc L.1; Rosenkranz S.2; Osborn R.2; Sinha S. K.3; Lynn J. W.1; Mesot J.2; Seeck O. H.; Preosti G.4; Fredo A.J.4; Mitchell J. F.2
1NIST Center for Neutron Research, Gaithersburg, USA
2ANL/MSD, Argonne, USA
3ANL, APS, Argonne, USA
4Northern Illinois University, Dept. of Phys., DeKalb, USA
Charge melting and polaron collapse in La1.2Sr1.8Mn2O7
Advanced Photon Source Research No. 3, April 2000
23.89.1

IFF-00-12-053
Zorn R.
Correlations functions measured by scattering experiments
Lecture Notes of the Laboratory Course on "Neutron Scattering", Vol. 5, 5.1 - 5-24 (2000)
23.15.0

IFF-00-12-054
Zorn R.
Ionentransport in Elektrolyten

Vorlesungsmanuskript des 31. IFF-Ferienkurs
"Femtosekunden und Nano-eV", Vol. 3, D1.1 - 20 (2000)
23.15.0

List of references

Abt R.	IFF-00-12-002	IFF-00-12-005	
Allgaier J.	IFF-00-12-001		
Baumgaertner A.	IFF-00-12-003		
Bechthold P.S.	IFF-00-12-017		
Bihlmayer G.	IFF-00-12-002	IFF-00-12-005	IFF-00-12-023
Blügel S.	IFF-00-12-002	IFF-00-12-005	IFF-00-12-023
Botti A.	IFF-00-12-030	IFF-00-12-031	
Brückel Th.	IFF-00-12-006 IFF-00-12-009	IFF-00-12-007	IFF-00-12-008
Buchenau U.	IFF-00-12-010		
Bürgler D.E.	IFF-00-12-022		
Carsughi F.	IFF-00-12-011		
Conrad H.	IFF-00-12-012	IFF-00-12-013	
Dürr H.A.	IFF-00-12-014 IFF-00-12-024	IFF-00-12-015 IFF-00-12-051	IFF-00-12-016
Eberhardt W.	IFF-00-12-006 IFF-00-12-018	IFF-00-12-007 IFF-00-12-019	IFF-00-12-017 IFF-00-12-022
Eisebitt S.	IFF-00-12-018	IFF-00-12-019	
Fournier A.	IFF-00-12-011		
Freiwald M.	IFF-00-12-019		
Gareev R.	IFF-00-12-022		
Girgis E.	IFF-00-12-022		
Grünberg P.	IFF-00-12-022		
Handschuh S	IFF-00-12-002		
Heinrich M.	IFF-00-12-030		
Karl A.	IFF-00-12-019		
Klingeler R.	IFF-00-12-017		
Kohlstedt H.	IFF-00-12-022		
Kurz Ph.	IFF-00-12-023		
Monkenbusch M.	IFF-00-12-025 IFF-00-12-028	IFF-00-12-026 IFF-00-12-032	IFF-00-12-027 IFF-00-12-037
Neeb M.	IFF-00-12-017		
Poppe A.	IFF-00-12-001		
Prager M.	IFF-00-12-029		
Pyckhout-Hintzen W.	IFF-00-12-030	IFF-00-12-031	
Richter D.	IFF-00-12-001 IFF-00-12-031 IFF-00-12-034	IFF-00-12-020 IFF-00-12-032 IFF-00-12-035	IFF-00-12-030 IFF-00-12-033 IFF-00-12-036
Rottländer P.	IFF-00-12-022		
Sambeth R.	IFF-00-12-003		
Scherer R.	IFF-00-12-019		

Schwahn D.	IFF-00-12-038	IFF-00-12-039	IFF-00-12-040
Schweika W.	IFF-00-12-041	IFF-00-12-042	
Schütz G.M.	IFF-00-12-043	IFF-00-12-044	
Seeck O. H.	IFF-00-12-045 IFF-00-12-048	IFF-00-12-046 IFF-00-12-052	IFF-00-12-047
Stellbrink J.	IFF-00-12-001		
Treusch J.	IFF-00-12-049		
Ullmaier H.	IFF-00-12-011	IFF-00-12-049	
Urban K.	IFF-00-12-004	IFF-00-12-021	IFF-00-12-050
Wagner R.	IFF-00-12-049		
Willner L.	IFF-00-12-001		
Zimina A.	IFF-00-12-019		
Zorn R.	IFF-00-12-053	IFF-00-12-054	

Talks / Posters

Invited Talks

IFF-00-21-001
Baumgärtner A.
MD Simulations of Ionchannels
Second workshop on Protein-Lipid Interactions.
Brüssel, Belgien
17.11.-19.11. 2000
23.30.0

IFF-00-21-002
Baumgärtner A.
MD simulations of membrane proteins
Univ. Wageningen
20.12.2000,
23.30.0

IFF-00-21-003
Baumgärtner A.
Motility of biological cells.
Debye Winterschool.
Utrecht, Niederlande
22.3.-23.3. 2000
23.30.0

IFF-00-21-004
Baumgärtner A.
The protein-lipid interface
First meeting on protein-lipid interaction.
Brüssel, Belgien
23.4.-24.4. 2000
23.30.0

IFF-00-21-005
Baumgärtner A.
The protein-lipid interface
Univ. Utrecht, Niederlande
14.12.2000
23.30.0

IFF-00-21-006
Bechthold P.S.
Electronic structure of small metal clusters (invited lecture)
10th Int. IUPAC Conf. on High Temperature Materials Chemistry, Jülich
13.04.2000
23.20.0

IFF-00-21-007
Bihlmayer G.; Kurz Ph.; Förster F.; Blügel S.
The FLAPW method applied to complex magnetic systems
Psi-k-2000: Network conference on electronic structure theory, Schwäbisch-Gmünd
22. - 26.08.2000
23.20.0

IFF-00-21-008
Blügel S.; Nie X.; Bihlmayer G.
Magnetic anisotropy in low dimensional systems
Psi-k-2000: Network conference on electronic structure theory, Schwäbisch-Gmünd
22. - 26.08.2000
23.20.0

IFF-00-21-009
Blügel S.
Der Schatz im Quantensee
Stein der Weisen, Veranstaltung im Rahmen des Jahres der Physik, Bundeshaus Bonn
21.09.2000
23.20.0

IFF-00-21-010
Blügel S.
Elektronen, Atome und Magnetismus im Nanokosmos
Fachbereich Physik der Universität Regensburg
05.05.2000
23.20.0

IFF-00-21-011
Blügel S.
Kristallwachstum von Halbleitern mit Surfactants aus mikroskopischer Sichtweise
Seminar and der LMU München, Institut für Kristallografie und Mineralogie
12.05.2000
23.20.0

IFF-00-21-012
Blügel S.
Magnetism in the nano-world
Talk at the electron group (National Institut for Standards (NIST)
24.07.2000
23.20.0

IFF-00-21-013
Blügel S.
Nanomagnetism meets magnetoelectronics
Symposium am Institut für Angewandte Physik, Universität
22.06.2000
23.20.0

IFF-00-21-014
Blügel S.
Nanomagnetismus im Zeitalter der Magnetoelektronik
Kolloquiumsvortrag am Fachbereich Physik, Christian-Albrecht-Universität zu Kiel
14.11.2000
23.20.0

IFF-00-21-015
Blügel S.
Von der Quantentheorie der Elektronen zu neuen Nanomaterialien
Fachbereich Physik, TU Clausthal, Osnabrück
24.01.2000
23.20.0

IFF-00-21-016
Blügel S.
Von der Quantentheorie der Elektronen zu neuen Nanomaterialien
Kolloquium am Fachbereich Physik, Universität Kaiserslautern
12.12.2000
23.20.0

IFF-00-21-017
Blügel S.
Von der Quantentheorie der Elektronen zu neuen Nanomaterialien
Zentrales Kolloquium des Hahn-Meitner-Instituts Berlin
01.03.2000
23.20.0

IFF-00-21-018
Brückel Th.
Magnetism in a new light: Applications of resonant and non-resonant magnetic x-ray diffraction
USA, Iowa State University/Ames Laboratory, Seminar of the Solid State Physics Group, 05.10.2000
23.89.1

IFF-00-21-019
Brückel Th.
The High Energy Side Station at the MuCAT Beamline
USA, Advanced Light Source APS, Seminar, 12.10.2000
23.89.1

IFF-00-21-020
Buchenau U.

A new view of the glass transition
Workshop CPG 2000, Univ. Dresden, 02. - 13.10.00
23.15.0

IFF-00-21-021
Buchenau U.
Dynamics of glass formers
EPS CMD-18 Conference, Montreux/Switzerland, 14.03.00
23.30.0

IFF-00-21-022
Buchenau U.
Fast and slow relaxations at the glass transition
Workshop "Neutron scattering and computer simulation", Univ. San Sebastian/Spain, 15. - 17.06.00
23.30.0

IFF-00-21-023
Buchenau U.
I. Glasses; II. Glass transition; III. Inelastic scattering from glasses
Euroschool Dyn. Mat. 2000, Univ. Rostock, 04. - 05.09.00
23.15.0

IFF-00-21-024
Böttger U.1; Waser R.
1 Institut für Werkstoffe der Elektrotechnik, RWTH Aachen
Dielectric losses in ferroelectric thin films by reversible domain wall motion
12th IEEE Int. Symp. on the Applications of Ferroelectrics, Honolulu, Hawaii, 31.07.-02.08.2000
23.42.0

IFF-00-21-025
Bürgler D.E.
Magnetische Zwischenschichtkopplung in Fe/Cr/Fe Schichtungen: Morphologie und Fermiologie
SFB-Kolloquium TU Dresden
27.04.2000

IFF-00-21-026
Bürgler D.E.
Magnetische Zwischenschichtkopplung und Magnetowiderstand in Fe/Cr-Schichtungen: Morphologie und Fermiologie
SFB-Kolloquium, Universität Göttingen
13.11.2000
23.42.0

IFF-00-21-027
Bürgler D.E.
Magnetische Zwischenschichtkopplung und Magnetowiderstand in magnetischen Schichtungen: Morphologie und Fermiologie
Kolloquium Universität Halle-Wittenberg
16.12.2000
23.42.0

IFF-00-21-028
Bürgler D.E.
Magnetoelektronik
Universität Regensburg
22.05.2000
23.42.0

IFF-00-21-029
Bürgler D.E.
Magnetoelektronik: Vom Kompass zum Datenspeicher von morgen
Kolloquium, Universität Basel
09.06.2000
23.42.0

IFF-00-21-030
Caprion D.
Dynamics of amorphous and liquid selenium
ESRF, Grenoble, 06.06.2000
23300

IFF-00-21-031
Caprion D.
Relaxation dons les verres de selenium
Lab. de Matiere Condensee, Universite Paris 6, 20.03.2000
23.30.0

IFF-00-21-032
Conrad H.
Introduction to the ESS Mercury Target System Design
Tokai, Japan, 2nd International Workshop on Mercury Target and Cold Moderator Engineering, 13.11.2000
23.60.0

IFF-00-21-033
Conrad H.
Probleme in Target- und Moderatormaterialien
Simonskall, ESS-Tag, 17.04.2000
23.60.0

IFF-00-21-034
Conrad H.
Status Report on the Jülich ESS-related activities
Tsukuba, Japan, ICANS-XV, 09.11.2000
23.60.0

IFF-00-21-035
Dederichs P.H.; Papanikolaou N.; Zeller R.
Conceptional Improvements of the KKR Method
Psi-k conference: Ab-initio (from electronic structure) calculation of complex processes in materials
Schwäbisch Gmünd, 22-26.08.2000
23.20.0

IFF-00-21-036
Dederichs P.H.
A Contribution to Understanding Tunneling Magnetoresistance
International Workshop on First-principles Simulation of Advanced Magnetic Materials
Suwa, Japan, 06.-07.03.2000
23.20.0

IFF-00-21-037
Dederichs P.H.
Ab-initio Rechnungen zum Tunnelmagnetowiderstand in Ferromagnet / Isolator Schichten
Kolloquium des MPI Metalphysik, Stuttgart, 11.07.2000
23.20.0

IFF-00-21-038
Dederichs P.H.
Ab-initio Rechnungen zum Tunnelmagnetowiderstand in Ferromagnet / Isolator Schichten
Seminar, 1. Physikalisches Institut, RWTH Aachen,
23.11.2000
23.20.0

IFF-00-21-039
Dederichs P.H.
Ein Beitrag zum Verständnis des Tunnelmagnetowiderstandes in Ferromagnet / Isolator / Ferromagnet Schichten
Forschergruppenseminar, Universität Regensburg, 25.02.2000
23.20.0

IFF-00-21-040
Divin Y.Y.; Poppe U.; Jia C.L.; Seo J.W.1; Glyantsev V.2
1 Institute de Physique Universite de Neuchatel,CH-2000, Switzerland
2 Conductus Inc., Sunnyvale, CA 94086, USA
Epitaxial (101) YBa2Cu3O7-x thin films on (103)NdGaO3 bicrystal substrates
Applied Superconductivity 1999. Ed.: X. Obradors, F. Sandiumenge and J. Fontcuberta, Inst. of Physics Conf. Ser. No.167, IOP Publishing Ltd., Bristol, p.p. 29-32 (2000)
23.42.0

IFF-00-21-041
Divin Y.Y.; Poppe U.; Shirotov V.V.; Volkov O.Y.1; Pavlovskii V.V.1; Urban K.
1 Institute of Radioengineering & Electronics of RAS, Moscow 103907, Russian Federation
Applications of Hilbert-Transform-Spectroscopy and terahertz spectral analysis by ac Josephson effect in high-Tc bicrystal junctions
Proceedings of the 7. Statusseminar "Supraleitung und Tieftemperaturtechnik" 14./15. Dezember 2000, Garmisch Partenkirchen, Germany
23.42.0

IFF-00-21-042
Divin Y.Y.; Poppe U.; Urban K.; Volkov O.Y.1; Pavlovskii V.V.1
1 Institute of Radioengineering & Electronics of RAS, Moscow 103907, Russian Federation
Terahertz Spectral Analysis by Frequency-Selective Incoherent Detection in High-Tc Josephson Junctions
8th International Conf. on Terahertz Electronics, 28-29 September 2000, Darmstadt, Germany
23.42.0

IFF-00-21-043
Divin Y.Y.; Volkov O.1; Pavlovskii V.1; Poppe U.; Urban K.
1 Institute of Radioengineering & Electronics of RAS, Moscow 103907, Russian Federation
Terahertz Spectral Analysis by ac Josephson Effect in High-Tc Bicrystal Junctions
Applied Superconductivity Conference, ASC 2000, Virginia, USA, September 17 - 22, 2000
23.42.0

IFF-00-21-044
Dürr H.A.
Angular resolved photoelectron spectroscopy
International Symposium on Spectroscopy of Materials
Schloss Ringberg
07.03.2000
23.20.0

IFF-00-21-045
Dürr H.A.
Anisotropic magnetic ground-state moments probed by soft X-ray spectroscopy
WE-Heraeus Seminar "Ground-state and Finite-temperature Bandferromagnetism", Berlin
04.10.2000
23.20.0

IFF-00-21-046
Dürr H.A.
Electron correlation and magnetism in low-dimensional solids
Seminar , Physikalisches Institut, Universität zu Köln
10.07.2000
23.20.0

IFF-00-21-047
Dürr H.A.
Femtosecond Laser Spectroscopy
Euro Summer School 2000, Rostock
29.08.2000
23.20.0

IFF-00-21-048
Dürr H.A.
Femtosecond spectromicroscopy of magnetic nanostructures
XFEL - Workshop on Hard Condensed Matter
20.07.2000
23.20.0

IFF-00-21-049
Dürr H.A.
Image potential state lifetime on transition metal fcc (111) surfaces
Image Potential State Workshop, San Sebastian, Spain
25.06.2000
23.20.0

IFF-00-21-050
Dürr H.A.
Magnetic domain correlations in transition metal films and multilayers
INFP Kolloquium, Forschungszentrum Karlsruhe
12.01.2000
23.20.0

IFF-00-21-051
Dürr H.A.
Magnetocrystalline anisotropy at interfaces probed by soft x-ray spectroscopy
Seminar im Physikalischen Institut, Universität Göttingen
19.06.2000
23.20.0

IFF-00-21-052
Dürr H.A.
Magnetocrystalline anisotropy of low dimensional systems probed by soft x-ray spectroscopy
Seminar
Hahn-Meitner-Institut Berlin
05.04.2000
23.20.0

IFF-00-21-053
Dürr H.
Stars and stripes in magnetism
Ward Plummer Symposium: Frontiers in Surface Science, Knoxville, TN, USA
14.10.2000
23.20.0

IFF-00-21-054
Eberhardt W.
Cluster als neue Materialien; elektronische Struktur und atomare Geometrie
11. Edgar-Lüscher-Seminar, Serneus, Schweiz
Februar 2000
23.20.0

IFF-00-21-055
Eberhardt W.
Clusters as new materials
Oak Ridge National Laboratory, USA
16.03.2000
23.20.0

IFF-00-21-056
Eberhardt W.
Clusters as new materials
Physik-Kolloquium, Universität Greifswald
11.05.2000
23.20.0

IFF-00-21-057
Eberhardt W.
Clusters as new materials
Universität Basel
23.06.2000
23.20.0

IFF-00-21-058
Eberhardt W.
Combination of lasers and synchrotron radiation sources
ESF/PESC Workshop on "Future Advanced Light Sources", Zürich, Schweiz
24.10.2000
23.20.0

IFF-00-21-059
Eberhardt W.
Forschung mit Synchrotronstrahlung
Kolloquium, TU Berlin
06.06.2000

23.20.0

IFF-00-21-060
Eberhardt W.
Fs-spectroscopy of clusters
Workshop on Atomic, Molecular and Cluster Physics with Free Electron Lasers, Hasylab, Hamburg
04.09.2000
23.20.0

IFF-00-21-061
Eberhardt W.
Future direction for research with lasers and synchrtron radiation
LS WAVE 2000, Berlin
26.08.2000
23.20.0

IFF-00-21-062
Eberhardt W.
Metal doped fullerenes: Endohedral and networked dopants
International Winterschool on Electronic Properties and Novel Materials, Kirchberg, Austria
23.20.0

IFF-00-21-063
Eberhardt W.
Opportunities for science using the time structure and coherence of a VUV-FEL
Erstes Blankeneser Gespräch über Forschung mit Synchrotronstrahlung, Workshop zum BESSY FEL, Blankensee
01.07.2000
23.20.0

IFF-00-21-064
Eberhardt W.
Overview of soft X-ray techniques
Workshop on "Soft X-ray Science in the Next Millennium: The Future of Photon-/In/Photon-Out Experiments, Pikeville, Tennesse, USA
18.03.2000
23.20.0

IFF-00-21-065
Eberhardt W.
Soft X-ray emission spectroscopy
Workshop Research with Synchrotron Radiation, Berlin
07.07.2000
23.20.0

IFF-00-21-066
Eberhardt W.
Ward Plummer Symposium: Frontiers in Surface Science, Knoxville, TN, USA
14.10.2000
23.20.0

IFF-00-21-067
Ebert Ph.; Chao K.-J.; Niu Q.; Shih C.K.1
1 University of Tennessee, Knoxville
Dislocations, phason defects, and domain wall in a one-dimensional superstructure of a metallic thin film.
DFG Schwerpunktkolloquium 'Quasicrystals, Structure and Physical Properties', Jülich, Germany, 5.-7. April 2000.
23.42.0

IFF-00-21-068
Ebert Ph.; Kluge F.; Semmler U.; Zhang Tianjiao; Simon M.; Zhang Zhenyu; Urban K.
Clusterung von geladenen Zn-Dotieratomen in GaAs
Frühjahrtagung der Deutschen Physikalischen Gesellschaft, Regensburg, Germany, 27.-31.3.2000.
23.42.0

IFF-00-21-069
Ebert Ph.; Shih C.K.1
1 University of Tennessee, Knoxville
Critical thicknesses and quasiperiodic superstructures of ultrathin Ag overlayers on (110) surfaces of III-V semiconductors.
Materials Research Society Fall Meeting, Boston, Massachusetts, November 27-December 1, 2000.
23.42.0

IFF-00-21-070
Ebert Ph.
Cleavage Surfaces of Quasicrystals.
219th National Meeting of the American Chemical Society, San Francisco, California, March 26-30, 2000.
23.55.0

IFF-00-21-071
Ebert Ph.
Defekte auf III-V-Halbleiteroberflächen.
Symposium Rekonstruktion und Wachstum von III-V-Halbleiteroberflächen der Fachverbände Halbleiter- und Oberflächenphysik. DPG Frühjahrstagung des Arbeitskreises Festkörperphysik, Hamburg, Germany, 26.-30.3.2001.
23.42.0

IFF-00-21-072
Ebert Ph.
Factors affecting the structure and composition of cleavage surfaces of quasicrystals.
Materials Research Society Fall Meeting, Boston, Massachusetts, November 27-December 1, 2000.
23.55.0

IFF-00-21-073
Ebert Ph.
Spaltoberflächen von Quasikristallen.
Symposium 'Quasicrystalline Surfaces' des Schwerpunkts Quasikristalle der Deutschen Forschungsgemeinschaft, Bommerholz bei Dortmund, Germany, 9.-11. November 2000.
23.55.0

IFF-00-21-074
Ehrhart P.; Fitsilis F.; Regnery S.; Waser R.; Schienle F.1; Schumacher M.1; Dauelsberg M.1; Strzyzewski P.1; Jürgensen H.1
1 Aixtron AG, Aachen, Germany
Growth of (Ba,Sr) TiO3 thin films in a multiwafer MOCVD reactor
MRS Fall Meeting, Boston, 27.11.-01.12.00
23.42.0

IFF-00-21-075
Ehrhart P.; Waser R.; Schneller T.; Hoffmann-Eifert S.
Chemical deposition methods for ferroelectric thin films
Asian Meeting on Ferroelectrics, Hongkong, 13.12.00
23.42.0

IFF-00-21-076
Ehrhart P.
Chemical deposition methods II: MOCVD
12th Int. Symp. Integrated Ferroelectrics, Aachen, 12.03.-15.03.00
23.42.0

IFF-00-21-077
Faley M.; Jia C.L.; Wu J.S.; Poppe U.; Urban K.
Dependence of the microstructure of ReBa2Cu3O7-x films on the conditions of high-oxygen pressure dc-sputtering (INVITED PAPER)
M2S-HTSC-VI: 6th International Conference, Materials and Mechanisms of Superconductivity and High Temperature Superconductors, Houston, Texas, February 20-25 (2000)
23.42.0

IFF-00-21-078
Faley M.I.; Poppe U.; Urban K.; Paulson D.N.1; Starr T.1; Fagaly R.L.1
1 Tristan Technologies Inc. San Diego, CA 92121, USA

HTS dc-SQUID with gradiometric multilayer flux transformer
Applied Superconductivity 1999. Ed.: X. Obradors, F. Sandiumenge and J. Fontcuberta, Inst. of Physics Conf. Ser. No.167, IOP Publishing Ltd., Bristol, p.p.509-512 (2000)
23.42.0

IFF-00-21-079
Faley M.I.; Poppe U.; Urban K.; Paulson D.N.1; Starr T.1; Fagaly R.L.1
1 Tristan Technologies Inc. San Diego, CA 92121, USA
HTS dc-SQUID with gradiometric multilayer flux transformer
Proceedings of the 4rd European Conference on Applied Superconductivity (EUCAS 99), Barcelona, Spanien; Published in: Inst. Phys. Conf. Ser., No. 167, 509-512 (2000)
23.42.0

IFF-00-21-080
Faley M.I.; Poppe U.; Urban K.; Paulson D.N.1; Starr T.N.1; Fagaly R.L.1
1 Tristan Technologies Inc. San Diego, CA 92121, USA
HTS dc-SQUID flip-chip magnetometers and gradiometers
12th International Conference on Biomagnetism, Biomag 2000, Helsinki, 13.-17. August (2000)
23.42.0

IFF-00-21-081
Faley M.I.; Poppe U.; Urban K.; Paulson D.N.1; Starr T.N.1; Fagaly R.L.1
1 Tristan Technologies Inc. San Diego, CA 92121, USA
Low noise HTS dc-SQUID flip-chip magnetometers and gradiometers
Submitted to Applied Superconductivity Conference, ASC 2000, Virginia Beach (2000)
23.42.0

IFF-00-21-082
Fitsilis F.; Regnery S.; Ehrhart P.; Waser R.; Schienle F.1; Schumacher M.1; Lindner J.1; Miedl S.1; Jürgensen H.1
1 Aixtron AG, Aachen, Germany
BST thin films growth in a multiwafer MOCVD reactor
Int. Conf. on Electroceramics VII, Portoroz, Slovenia, 03.-06.09.2000
23.42.0

IFF-00-21-083
Förster F.
Untersuchung vonnichtkollinearem Magnetismus in ultradünnen Filmen
Seminarvortrag am 1. Physikalischen Institut der RWTH Aachen
07.11.2000
23.20.0

IFF-00-21-084
Goerigk G.
Anomalous Small Angle X-ray Scattering
Budapest, Technische Universität, Institutsseminar des Instituts für Physikalische Chemie, 09.11.2000
23.89.1

IFF-00-21-085
Goerigk G.
Materialuntersuchungen mit anomaler Röntgen-Kleinwinkelstreuung
Berlin, Kolloquium des Komitees Forschung mit Synchrotronstrahlung, 07. - 08.07.2000
23.89.1

IFF-00-21-086
Goerigk G.
Materialuntersuchungen mit anomaler Röntgen-Kleinwinkelstreuung
Rostock, Universität, Fachbereich Physik, Institutsseminar, 11.05.2000
23.89.1

IFF-00-21-087
Gompper G.
Applications of Random Surfaces to Fluid Mixtures
Reihe von zwei eingeladenen Vorträgen beim "10th Workshop on Statistical Mechanics and Non-perturbative Field Theory (SMFT 2000)"
Bari (Italy), 25. - 27. September 2000
23.30.0

IFF-00-21-088
Gompper G.
Recent Results on the Physics of Membranes
Eingeladener Vortrag beim "French-German Symposium on Present and Future Topics in Wetting"
Bad Honnef, 18. - 20. September 2000
23.30.0

IFF-00-21-089
Gompper G.
Soft Matter: Amphiphile, Membranen, Mikroemulsionen
Fachbereich Physik, Universität Essen
2. 2. 2000
23.30.0

IFF-00-21-090
Gompper G.
Statistical Physics of Membranes: Undulations, Defects, Topology Fluctuations
Institut für Biologische Informationsverarbeitung, FZJ
10. 3. 2000
23.30.0

IFF-00-21-091
Gompper G.
Weiche Materie: Amphiphile, Membranen, Schwamm-Phasen
Fakultät für Naturwissenschaften, Universität Magdeburg
7. 11. 2000
23.30.0

IFF-00-21-092
Grossmann M.1; Bolten D.1; Böttger U.1; Lohse O.1; Waser R.; Tiedke S.1; Schmitz T.1; Kall U.1; Hartner W.; Kastner M.; Schindler G.
1 Institut für Werkstoffe der Elektrotechnik, RWTH Aachen
The influence of the experimental procedures on the reliability issues of ferroelectric thin films in view of memory applications
12th Int. Symp. Integrated Ferroelectrics, Aachen, 12.03.-15.03.00
23.42.0

IFF-00-21-093
Grünberg P.
Exchange anisotropy, interlayer exchange coupling and GMR in research and application
3rd European Conference on Magnetic Sensors and Actuators (EMSA), Dresden
Juli 2000
23.42.0

IFF-00-21-094
Grünberg P.
Kompass zum Datenspeicher: Magnetoelektronik
Veranstaltung "Stein der Weisen", Bonn
September 2000
23.42.0

IFF-00-21-095
Grünberg P.
Layered magnetic structures - history, highlights, applications
International, Conference on Magnetism 2000, Recife, Brazil
August 2000
23.42.0

IFF-00-21-096
Grünberg P.
Layered magnetic structures: Facts, figures, future
Euro Summer School 2000, Rostock
03.09.2000

23.42.0

IFF-00-21-097
Grünberg P.
Layered magnetic structures: History, highlights, applications
International Symposium on Nanoscale Magnetism and Transport, Sendai, Japan
März 2000
23.42.0

IFF-00-21-098
Grünberg P.
Layered magnetic structures: History, highlights, applications
Symposium on Magnetic Materials for Magnetoelectronic Devices, Ames Iowa, USA
Mai 2000
23.42.0

IFF-00-21-099
Grünberg P.
Magnetische Schichtstrukturen in Forschung und Anwendung
Physikalisches Kolloquium der RWTH Aachen
Januar 2000
23.42.0

IFF-00-21-100
Grünberg P.
Magnetische Schichtstrukturen in Forschung und Anwendung
Physikalisches Kolloquium der Universität Regensburg
Juli 2000
23.42.0

IFF-00-21-101
Grünberg P.
Magnetoelektronik: Vom Kompass zum Datenspeicher
Helmholtz Syposium 2000, Zukunft braucht Wissenschaftsthemen aus der Physik,
November 2000
23.42.0

IFF-00-21-102
Grünberg P.
Preparation of materials for TMR type sensors
Statusseminar Magnetoelektronik, Dresden
Juni 2000
23.42.0

IFF-00-21-103
Harris J.
Calculation of Elastic Constants of Materials using Density Functional Theory
Washington, DC, American Chemical Society Meeting, 16.8.2000
23.20.0

IFF-00-21-104
Haubold H.-G.
Röntgenkleinwinkel-Streuung an Realkatalysatoren
Bochum, Ruhr-Universität, Graduiertenkolleg, 18.01.2000
23.89.1

IFF-00-21-105
Heinze S.
Interpretation of STM experiments on transition-metal structures by ab initio calculations
Research Institute for Materials, University Nijmegen, NL
19.01.2000
23.20.0

IFF-00-21-106
Hoffmann-Eifert S.
Processing-microstructure-property relationship of CSD and MOCVD derived oxide thin films
12th IEEE Int. Symp. on the Applications of Ferroelectrics, Honolulu, Hawaii, 31.07.-02.08.2000
23.42.0

IFF-00-21-107
Ioffe A.
Neutron Speed Echo Spectroscopy
Berlin, International Workshop on Neutron Spin Echo Spectroscopy, 16. - 17.10.2000
23.89.1

IFF-00-21-108
Jahnen B.; Luysberg M.; Urban K.; Ungermanns Ch.1; Schmidt R.1
Bestimmung von Konzentrationsprofilen in GaSb/AlSb Heterostrukturen
1 ISG, FZ Jülich
Proceedings of the General Conference of the Condensed Matter Division European Physical Society, Regensburg, Europhysics Conference Abstracts (2000)
23.42.0

IFF-00-21-109
Jones R.O.
Density functional calculations and force field parameters
Workshop on: Multiscale Modeling of Macromolecularsystems, Mainz 6.9.2000
23.20.0

IFF-00-21-110
Jones R.O.
Density functional calculations for polymers and clusters - present experience and future prospects
10. Workshop on Computational Materials Science, Villasimius (CA), Italien 8.-11.9.2000
23.20.0

IFF-00-21-111
Jones R.O.
Density functional study of molecules and polymers - structure, energetics, reactions
Department of Chemistry, University of Jyväskylä, Finland, 29.3.2000
23.20.0

IFF-00-21-112
Jones R.O.
Strukturen, Energien und Reaktionen in organischen Molekülen und Polymeren - eine Dichtfunktionalstudie des Polycarbonats
Institut für Theoretische Physik, Universität Paderborn
8.5.2000
23.20.0

IFF-00-21-113
Jones R.O.
Thermal expansion in silicates - or the remarkable stability of cook-tops towards thermal shock
Department of Physics, University of Jyväskylä, Finland
30.3.2000
23.20.0

IFF-00-21-114
Jones R.O.
Thermische Ausdehnung in Kochfeldern - ein Beispiel der vielen Anwendungen von Silikaten
Workshop BMBF Kompetenzentrum, MPI für Polymerforschung, Mainz 7.11.2000
23.20.0

IFF-00-21-115
Jung P.; Liu C.
Diffusion of Hydrogen in Steel - Effect of Irradiation
5th International Workshop on Hydrogen Isotopes in Solids, Stockholm
17.5.2000
23.80.5

IFF-00-21-116
Jung P.; Ullmaier H.

Hydrogen and Helium in Target Materials at High Power Spallation Sources
5th International Workshop on Hydrogen Isotopes in Solids, Stockholm
18.5.2000
23.80.5

IFF-00-21-117
Jung P.
Hydrogen and Helium in Fusion Materials
The Institue of Modern Physics, Lanzhou, PR-China
6.7.2000
23.80.5

IFF-00-21-118
Jung P.
Materials for Fusion Power Reactors
Institute of Plasma Physics, Hefei, PR-China
12.7.2000
23.80.5

IFF-00-21-119
Jung P.
Materials for Fusion Power Reactors
The University of Science and Technology, Bejing, PR-China
30.6.2000
23.80.5

IFF-00-21-120
Kann G.
Rastertunnelmikroskopische Untersuchungen an Buckypaper und endohedralen Lanthanid-C60-Fullerenen
Seminar, Institut für Materialphysik, Universität Wien
11.12.2000
23.20.0

IFF-00-21-121
Khoukaz C.1; Galler R.1; Feuerbacher M.; Mehrer H.1
1 Institut für Metallforschung, Universität Münster, D-48149 Münster
Self-Diffusion of Ni and Co in decagonal Al-Ni-Co quasicrystals.
Proc. DIMAT 2000
23.55.0

IFF-00-21-122
Kim J.; Maciel A.; O'Sullivan E.D.; Ryan J.F.; Schwarz A.; Kaluza A.; Hardtdegen H.H.; Schapers T.; Lüth H.; Meertens D.; Dieker C.
Fermi-edge singularities in the photoluminescence spectrum of modulation-doped GaAs v-groove quantum wires
9th International Conference on Modulated Semiconductor Structures. MSS9
May 2000
Physica E, Vol.7, No.3-4, 517 (2000)
23.42.0

IFF-00-21-123
Kluge F.; Grushko B.; Ebert Ph.; Urban K.
Investigations of the structure and composition of decagonal Al-Ni-Co cleavage surfaces.
DFG Schwerpunktkolloquium 'Quasicrystals, Structure and Physical Properties', Jülich, Germany, 5.-7. April 2000.
23.42.0

IFF-00-21-124
Kluge M.
Molecular Dynamics Simulations an Melts and Glasses of Cu33 Zr67
Ioffe-Institute, St. Petersburg, 15.06.2000
23.30.0

IFF-00-21-125
Kohlstedt H.H.
Al2O3 Tunnelbarrieren in supraleitenden und magnetischen Tunnelkontakten
Ruhr-Universität Bochum, 19.05.00
23.42.0

IFF-00-21-126
Kohlstedt H.H.
Bauelemente zur nicht-flüchtigen Informationsspeicherung: Grundlagen und Entwicklungstendenzen
Graduierten Kolleg Workshop, Institut für Angewandte Physik der Universität Karlsruhe, 21.02.-22.02.2000
23.42.0

IFF-00-21-127
Kohlstedt H.H.
Dry-etching of oxides materials and refractory metal electrodes
Penn State University, USA, 21.11.2000
23.42.0

IFF-00-21-128
Kohlstedt H.H.
Magnetic tunnel junctions for non-volatile memory application
Wilhelm-Else Hereaus Stiftung, Metal-Nonmetal Structures for Magnetoelectronics, Bad Honnef, 05.01.-07.01.2000
23.42.0

IFF-00-21-129
Kohlstedt H.H.
Physics and technology of superconducting and magnetic tunnel junctions with aluminium oxide barriers
Universität Saarbrücken, 15.12.2000
23.42.0

IFF-00-21-130
Kohlstedt H.H.
Ätztechniken bei der Herstellung elektronischer Bauelemente
Arbeitskreis "Dünnschichten in der Mikroelektronik, Caesar, Bonn, 17.11.2000
23.42.0

IFF-00-21-131
Kurz Ph.; Bihlmayer G.; Blügel S.; Hirai K.1
1Department of Physics, Nara Medical University, Nara, Japan
Magnetism of two-dimensional itinerant antiferromagnets on a triangular lattice
ESCM-2000: Electronic Structure and Magnetism in Complex Materials, Washington, D.C., USA
26. - 28.07.2000
23.20.0

IFF-00-21-132
Kurz Ph.; Bihlmayer G.; Blügel S.; Hirai K.1
1Department of Physics, Nara Medical University, Nara, Japan
Magnetism of two-dimensional itinerant antiferromagnets on a triangular lattice
SDHS'00: International Symposium on Structure and Dynamics of Heterogeneous Systems, Duisburg
28.- 29.08.2000
23.20.0

IFF-00-21-133
Köbler U.
Die dominierende Rolle der Austauschwechselwirkungen 4. Ordnung in reinen Spinmaterialien
Aachen, RWTH, Seminar über Kristall- und Strukturchemie, 03.11.2000
23.15.0

IFF-00-21-134
Lentzen M.
Prospects of Cs-correction for structure imaging in HRTEM
4th Meeting of the Societe Francaise des Microscopies, 6-8 September 2000, Toulouse/F
23.42.0

IFF-00-21-135
Liebsch A.
Photoemission quasi-particle spectra of Sr2RuO4
European Physical Society Meeting

Montreux 17.3.2000
23.20.0

IFF-00-21-136
Liebsch A.
Quantum well behavior induced by dynamical screening in alkali metal films
Workshop Epioptics Erice 21.7.2000
23.20.0

IFF-00-21-137
Liebsch A.
Surface optics of Ag: influence of localized d electrons
Workshop Epioptics Erice 22.7.2000
23.20.0

IFF-00-21-138
Liedtke R.1; Waser R.
1 Institut für Werkstoffe der Elektrotechnik, RWTH Aachen
Capacitance and admittance spectroscopy analysis of hydrogen-degraded Ba0.7Sr0.3TiO3 thin films
12th IEEE Int. Symp. on the Applications of Ferroelectrics, Honolulu, Hawaii, 31.07.-02.08.2000
23.42.0

IFF-00-21-139
Lohse O.1; Grossmann M.1; Bolten D.1; Böttger U.1; Waser R.
1 Institut für Werkstoffe der Elektrotechnik, RWTH Aachen
Relaxation mechanisms in ferroelectric thin film capacitors for FERAM application
12th Int. Symp. Integrated Ferroelectrics, Aachen, 12.03.-15.03.00
23.42.0

IFF-00-21-140
Luysberg M.; Specht P.1; Weber E.R.1
1 Department of Materials Science, University of California, Berkeley, Ca 94720, USA
Influence of Be doping on the structural properties of low-temperature grown GaAs
SIMC XI 2000, Canberra, Australien (accepted for publication) (2000)
23.42.0

IFF-00-21-141
Maciel A.C.; Kim J.; Davies H.D.M.; O'Sullivan E.D.; Ryan J.F.; Schwarz A.; Kaluza A.; Hardtdegen H.H.; Schapers T.; Meertens D.; Dieker C.; Lüth H.
Fermi-edge singularities in the photoluminescence and magneto-optical spectra of modulation-doped v-groove quantum wires
Proceedings of 13th International Conference on the Electronic Properties of Two-Dimensional Systems
Physica E, Vol.6, No.1-4, 530 (2000)
23.42.0

IFF-00-21-142
Meyer R.1; Waser R.; Helmbold J.; Borchardt G.
Thermodynamics versus kinetics of perovskites: defect chemistry in the transition state
12th IEEE Int. Symp. on the Applications of Ferroelectrics, Honolulu, Hawaii, 31.07.-02.08.2000
23.42.0

IFF-00-21-143
Meyer R.1; Waser R.
1 Institut für Werkstoffe der Elektrotechnik, RWTH Aachen
Advances in point defect chemistry: space-charge controlled surface reactions
Int. Conf. on Electroceramics VII, Portoroz, Slovenia, 03.-06.09.2000
23.42.0

IFF-00-21-144
Monkenbusch M.
Dynamics of homo- and blockcopolymer melts - Recent advances from neutron spin echo
CEA-CMRS Conference, Nagoya/Taiwan, 22.09.00
23.30.0

IFF-00-21-145
Monkenbusch M.
Next generation NSE instruments, What are the challenges?
Int. Workshop on NSE, HMI Berlin, 16.10.00
23.89.1

IFF-00-21-146
Mueller R.
The Yb fiber LASER for metastable 3He optical pumping at Jülich
Sanct Petersburg, Russia, PNCMI-2000 International Workshop, 22.06.2000
23.89.1

IFF-00-21-147
Müller-Krumbhaar H.
Ist Physik morgen noch interessant?
Studienkreis Schule + Wirtschaft in NRW, Leverkusen, 21.11.2000
23.15.0

IFF-00-21-148
Müller-Krumbhaar H.
Nachwuchsmangel in Physik - ein Bildungsproblem?
DPG-Frühjahrstagung, FV Didaktik, Hauptvortrag, 20.03.2000
23.15.0

IFF-00-21-149
Müller-Krumbhaar H.
Wie wächst ein Keim?
Physikalisches Kolloquium, Uni. Erlangen, 10.7.2000
23.15.0

IFF-00-21-150
Nasini A.1; Dernovsek O.1; Fritz M.1; Waser R.; Wersing W.1
1 Siemens AG München
Innovative microwave filter design with a new high dielectric LTCC-material
MIOP Conference, 2001, Stuttgart
23.42.0

IFF-00-21-151
Neeb M.
Metalldotierte Fullerencluster aus der Laserverdampfung
Symposium Cluster und Fullerene, Hauptvortrag, DPG-Tagung, Bonn
April 2000
23.20.0

IFF-00-21-152
Ohl M.
Studies of dynamic and static properties of the orientational glasses
CEA, Grenoble/France, 09.12.99
23.15.0

IFF-00-21-153
Ohly C.; Hoffmann S.; Szot K., Waser R.
Electrical conductivity and segregation effects of doped SrTiO3 thin films at high temperatures
Int. Conf. on Electroceramics VII, Portoroz, Slovenia, 03.-06.09.2000
23.42.0

IFF-00-21-154
Ohly Ch.
Chemical Solution Deposition und elektrische Leitfähigkeit von SrTiO3-Dünnschichten
Universität Karlsruhe, 24.10.2000
23.42.0

IFF-00-21-155

Papanikolaou N.; Freyss M.; Bellini V.; Mavropoulos Ph.; Zeller R.; Dederichs P.H.
Ab-initio calculations for the electronic structure and transport properties of TMR junctions
Symposium on Spin-Electronics
Halle, 03.-06.07.2000
23.20.0

IFF-00-21-156
Papanikolaou N.; Mavropoulos Ph.; Dederichs P.H.
Complex band structure and tunneling through Metal/Insulator/Metal junctions
GMR-TMR miniworkshop, Prague, 12-13.04.2000,
23.20.0

IFF-00-21-157
Papanikolaou N.; Mavropoulos Ph.; Freyss M.; Zeller R.; Dederichs P.H.
Spin dependent transport in metal-insulator junctions
Psi-k conference: Ab-initio (from electronic structure) calculation of complex processes in materials
Schwäbisch Gmünd, 22-26.08.2000
23.20.0

IFF-00-21-158
Persson B.N.J.
10 Lectures on Friction presented at Dipartimento di Fisica G. Galilei,
Padova, Italien April und Mai 2000
23.20.0

IFF-00-21-159
Persson B.N.J.
12 Lectures presented "Troisieme cycle de la Physique"
Lausanne 13.4.2000; 27.5.2000; 4.11.2000
23.20.0

IFF-00-21-160
Persson B.N.J.
Dynamics of Small Confined Systems
MRS Fall meeting, Boston, USA 27.11.-1.12.2000
23.20.0

IFF-00-21-161
Persson B.N.J.
Four invited lectures presented at spring school on friction
Oulanka Biological Station, Finland 26.-30.3.2000
23.20.0

IFF-00-21-162
Persson B.N.J.
Participated as expert (presented a talk on friction) in an EU-meeting related to the founding of nano-scale materials physics by the European union
Brüssel 10.3.2000
23.20.0

IFF-00-21-163
Persson B.N.J.
Reibungsprobleme in dynamischen Systeme
Hannover 7.-8.12.2000
23.20.0

IFF-00-21-164
Persson B.N.J.
Summer School "Imaging and manipulation of matter at the nanometer scale
Mi-ra ores de la Sierra, Spanien 11.-16.9.2000
23.20.0

IFF-00-21-165
Persson B.N.J.
Third Swedish meeting on vacuum and materials science
CTH Gothenburg, Schweden 14.-16.8.2000
23.20.0

IFF-00-21-166
Persson B.N.J.
Workshop on Tribology
The Wiezmann Institute, Tel Aviv, Israel 3.4.2000
23.20.0

IFF-00-21-167
Persson B.N.J.
Workshop on nonequilibrium phenomena in confied systems and on solid friction
CECAM, Lyon 28.-31.8.2000
23.20.0

IFF-00-21-168
Pertsev N.A.; Koukhar V.G.; Waser R.; Hoffmann S.
Effects of domain formation on the dielectric properties of ferroelectric thin films
12th Int. Symp. Integrated Ferroelectrics, Aachen, 12.03.-15.03.00
23.42.0

IFF-00-21-169
Petukhov B.V.1; Messerschmidt U.1; Bartsch M.1; Dietzsch Ch.1; Geyer G.1; Häussler D.1; Ledig L.1; Feuerbacher M.; Schall P.; Urban K.
1 Max-Planck-Institut für Mikrostrukturphysik, Weinberg 2, Halle/Saale, D-06120, Germany
Dislocation mobility versus dislocation substructure controlled deformation of icosahedral Al-Pd-Mn single quasicrystals.
Proc. ICSMA 2000
23.55.0

IFF-00-21-170
Petzelt J.; Gregora I.; Ostapchuk T.; Kamba S.; Pokorny J.; Bovtun V.; Porokhonskyy V.; Savinov M.; Kadlec F.; Vanek P.; Rychetsky I.; Yuzyuk Y.; Almeida A.; Chavez R.; Hoffmann S.; Waser R.; Rafaja D.; Dobiasova L.; Perina V.
Polar clusters in pure bulk SrTiO3 ceramics
Int. Conf. on Electroceramics VII, Portoroz, Slovenia, 03.-06.09.2000
23.42.0

IFF-00-21-171
Petzelt J.; Ostapchuk T.; Kamba S.; Gregora I.; Rychetsky I.; Pokorny J.; Bovtun V.; Porokhonsky V.; Savinov M.; Hoffmann S.; Waser R.; Lindner J.
Far infrared, microwave and Raman spectroscopy of the ferroelectric soft mode in SrTiO3 thin films and ceramics
12th Int. Symp. Integrated Ferroelectrics, Aachen, 12.03.-15.03.00
23.42.0

IFF-00-21-172
Poppe U.; Divin Y.Y.; Faley M.I.; Wu J.S.; Jia C.L.; Shadrin P.; Urban K.
Properties of YBa2Cu3O7 Thin Films Deposited on Substrates and Bicrystals with Vicinal Offcut and Realization of High IcRn Junctions
Applied Superconductivity Conference, ASC 2000, Virginia Beach (2000)
23.42.0

IFF-00-21-173
Pyckhout W.
Local chain deformation in polymer networks by SANS
EPS CMD-18 Conference, Montreux/Switzerland, 13. - 17.03.2000
23.30.0

IFF-00-21-174
Pyckhout-Hintzen W.
SANS of polymer networks under deformation
Summerschool on Neutron Scattering, Zuoz/Switzerland, 08. - 12.08.00
23.30.0

IFF-00-21-175

Reichmann K.; Hoffmann S.; Schneller T.; Hasenkox U.; Waser R.
Morphology and electrical properties of SrTiO3-films on conductive oxide films
Int. Conf. on Electroceramics VII, Portoroz, Slovenia, 03.-06.09.2000
23.42.0

IFF-00-21-176
Richter D.
Amphiphilic polymers as amphiphilicity boosters in microemulsion systems
219th ACS Conference, San Francisco/USA, 26. - 30.03.00
23.30.0

IFF-00-21-177
Richter D.
Die europäische Spallationsneutronenquelle - ein Leuchtturm für die Forschung
Jahresempfang des Forschungszentrum Jülich, Bonn, 20.09.00
23.30.0

IFF-00-21-178
Richter D.
Dynamics of homo- and blockcopolymer melts - recent advances from neutron spin echo
APS March Meeting, Minneapolis/USA, 20. - 24.03.00
23.30.0

IFF-00-21-179
Richter D.
Neutron scattering and the glass transition in polymers - Present status and future opportunities
VI Int. Workshop on "Non Crystalline Solids", Bilbao/Spain, 13.- 15.09.00
23.30.0

IFF-00-21-180
Richter D.
Neutron scattering and the glass transition in polymers - Present status and future opportunities
Workshop "Future perspectives for understanding the unsolved problem of the glass-transition by neutron scattering and computer simulation", San Sebastian/Spain, 15. - 17.06.00
23.30.0

IFF-00-21-181
Richter D.
Neutron scattering in polymer physics - recent highlights
Summer School "Recent developments in neutron scattering", Les Houches/France, 02. - 12.05.00
23.30.0

IFF-00-21-182
Richter D.
Neutron spin echo
Workshop on "Neutron Scattering in Soft Matter", Lungtan/Taiwan, 29. - 31.03.00
23.30.0

IFF-00-21-183
Richter D.
Polymer dynamics from local to the global scale
Workshop on "Neutron Scattering in Soft Matter", Lungtan/Taiwan, 29. - 31.03.00
23.30.0

IFF-00-21-184
Richter D.
The role of amphiphilic polymers in emulsification boosting in oil water microemulsion - a SANS and NSE Study
Kolloquium, MPI für Kolloid- und Grenzflächenforschung, Potsdam, 12.12.00
23.30.0

IFF-00-21-185
Richter D.
The role of amphiphilic polymers in emulsification boosting in oil-water microemulsions
Conference on "Scattering Studies of Mesoscopic Scale Structure and Dynamics in Soft Matter", Messina/Italy, 22. - 25.11.00
23.30.0

IFF-00-21-186
Rickes J.; Waser R.; Kall U.1; Bartic A.2; Wouters D.2
1 Institut für Werkstoffe der Elektrotechnik, RWTH Aachen
2 IMEC Leuven, Belgium
Comparison between standard and chain-type FERAM architectures employing a sophisticated ferroelectric capacitor model
12th Int. Symp. Integrated Ferroelectrics, Aachen, 12.03.-15.03.00
23.42.0

IFF-00-21-187
Rotenberg E.; Barman S.R.; Paggel J.J.; Theis W.; Horn K.; Ebert Ph.; Urban K.; Gille P.
Photoemission study of valence band dispersion in quasicrystals. Aperiodic 2000, Nijmegen, The Netherlands, July 4-8, 2000.
23.55.0

IFF-00-21-188
Schneider St.; Kohlstedt H.H.; Waser R.
Etching characteristics of noble metal electrode
MRS Fall Meeting, Boston, 27.11.-01.12.00
23.42.0

IFF-00-21-189
Schneller T.1; Ehrhart P.
1 Institut für Werkstoffe der Elektrotechnik, RWTH Aachen
Chemical deposition methods CSD and MOCVD
12th Int. Symp. Integrated Ferroelectrics, Aachen, 12.03.-15.03.00
23.42.0

IFF-00-21-190
Schober H.R.; Caprion D.; Kluge M.
Simulationen zur Dynamik in Gläsern und Schmelzen
Regensburg 27.03.2000, DPG Frühjahrstagung
23.30.0

IFF-00-21-191
Schober H.R.
Collectivity of motion in glasses and supercooled liquids
MPI Dresden, 11.10.2000
Int. Workshop on Collective Phenomena in the Low Temperature Physics of Glasses
23.30.0

IFF-00-21-192
Schober T.
Tubular high-temperature proton conductors: transport numbers and hydrogen injection
7th Euroconference on Ionics, Calcatoggio, Corsica, 02.10.2000
23.55.0

IFF-00-21-193
Schober T.
Water vapor solubility and impedance of the high temperature proton conductor SrZr0.9Y0.1O3-x
10th Int. Conf. on Solid State Protonic Conductors, Montpellier, France, 25.09.2000
23.55.0

IFF-00-21-194
Schroeder K.; Antons A.; Berger R.; Blügel S.
Ab initio Rechnungen für Adatome auf Halbleiteroberflächen
Tagung der Theorie-Institute der RWTH Aachen, Altenberg, 18.02.2000

23.42.0

IFF-00-21-195
Schroeder K.; Antons A.; Berger R.; Blügel S.
Theory of surfactant-mediated growth
PSI-K 2000 Conference, Schwäbisch Gmünd, 22-26.08.2000
23.42.0

IFF-00-21-196
Schroeder K.; Antons A.; Berger R.; Blügel S.
Understanding surfactant-mediated growth, contributions from ab initio calculations
International Symposium on Structure and Dynamics of Heterogeneous Sytems, Duisburg, 28-29.08.2000
23.42.0

IFF-00-21-197
Schroeder K.
Mikroskopie des Kristallwachstums mit Surfactants: ab initio Rechnungen zur Kinetik von Adatomen auf Halbleiteroberflächen
Kolloquium des SFB 418, Fachbereich Physik der Martin-Luther-Universität Halle-Wittenberg, 03.05.2000
23.42.0

IFF-00-21-198
Schulte T.; Waser R.; Römer E.W.J.; Bouwmeester H.J.M.; Nigge U.; Wiemhöfer H.-D.
Development of oxygen-permeable ceramic-membranes for NOx-sensors
Int. Conf. on Electroceramics VII, Portoroz, Slovenia, 03.-06.09.2000
23.42.0

IFF-00-21-199
Schwahn D.
Investigations of polymer blends with small angle neutron scattering
The Dutch Polymer Institute (DPI), Eindhoven University of Technology/The Netherlands, 08.06.00
23.30.0

IFF-00-21-200
Schwarz A.; Kaluza A.; Schapers T.; Hardtdegen H.H.; Lüth H.; Meertens D.; Dieker C.; Maciel A.C.; Kim J.; O'Sullivan E.D.; Ryan J.F.
Electron transport in modulation-doped GaAs v-groove quantum wires
Ninth International Conference on Modulated Semiconductor Structures. MSS9
May 2000
Physica E, Vol.7, No.3-4, 760 (2000)
23.42.0

IFF-00-21-201
Schütz G.
Aging in Reaction-diffusion systems
Fachbereich Physik, Universität Halle
27. 4. 2000
23.15.0

IFF-00-21-202
Schütz G.
Nonequilibrium relaxation law for entangled polymers
83th Statistical Mechanics Conference, Ruttgers University, USA
7. 5. 2000
23.30.0

IFF-00-21-203
Schütz G.
Nonequilibrium relaxation law for entangled polymers
Department of Chemistry and Chemical Biology, Cornell University, USA
21. 5. 2000
23.30.0

IFF-00-21-204
Schütz G.
Phasenübergänge in offenen Vielteilchensystemen fern vom Gleichgewicht
64. Physikertagung, Dresden
22. 3. 2000
23.15.0

IFF-00-21-205
Seeck O. H.
Coherent X-ray Scattering on Layer Systems with Magnetic Roughness
Hamburg, DESY/HASYLAB, XFEL-Workshop, 20. - 21.07.2000
23.89.1

IFF-00-21-206
Seeck O. H.
Investigation of polymer bilayer interfaces with x-ray scattering
Amsterdam, The Netherlands, AMOLF, Seminar, 24.07.2000
23.89.1

IFF-00-21-207
Seeck O. H.
Untersuchung der Grenzflächeneigenschaften dünner "Soft-Matter"-Filme mittels Röntgenstreuung
Berlin, Hahn-Meitner-Institut, Seminar, 17.02.2000
23.30.0, 23.9.1

IFF-00-21-208
Semmler U.; Ebert Ph.; Urban K.
Einfluß der Ladungsträger auf die Bildungsbarriere von Leerstellen in InP(110) Oberflächen
Frühjahrtagung der Deutschen Physikalischen Gesellschaft, Regensburg, Germany, 27.-31.3.2000.
23.42.0

IFF-00-21-209
Shadrin P.M.; Divin Y.Y.
Spread of critical currents in thin-film YBa2Cu3O7-x bicrystal junctions
Applied Superconductivity Conference, ASC 2000, Virginia, USA, September 17 - 22, 2000.
23.42.0

IFF-00-21-210
Shirotov V.; Divin Y.Y.; Urban K.
Dynamic Range of Frequency-Selective Response of High-Tc Josephson Detector to Millimeter-Wave Radiation
Applied Superconductivity Conference, ASC 2000, Virginia, USA, September 17 - 22, 2000.
23.42.0

IFF-00-21-211
Shur V.Ya.; Blankova E.B.; Subbotin A.L.; Borisova E.A.; Barannikov A.V.; Bolten D.1; Gerhardt R.1; Waser R.
1 Institut für Werkstoffe der Elektrotechnik, RWTH Aachen
Kinetics of pyrochlore-perovskite transformation during rapid thermal annealing of sol-gel PZT films
Int. Conf. on Electroceramics VII, Portoroz, Slovenia, 03.-06.09.2000
23.42.0

IFF-00-21-212
Specht P.1; Cich M.J.1; Zhao R.1; Jäger N.D.1; Weber E.R.1; Gebauer J.2; Börner F.2; Krause-Rehberg R.2; Luysberg M.
1 Department of Materials Science, University of California, Berkeley, Ca 94720, USA
2 Fachbereich Physik, Universität Halle/Saale
Defect engineering in MBE grown GaAs-based materials
SIMC XI 2000, Canberra, Australien (accepted for publication) (2000)
23.42.0

IFF-00-21-213
Stellbrink J.
Partial structure factors in star polymer/colloid mixtures

COST WG1-Meeting, Fribourg/Switzerland, 15.-16.12.2000
23.30.0

IFF-00-21-214
Szot K.; Hoffmann S.; Speier W.; Breuer U.; Siegert M.; Waser R.
Segregation phenomena in thin films of BaTiO3
12th Int. Symp. Integrated Ferroelectrics, Aachen, 12.03.-15.03.00
23.42.0

IFF-00-21-215
Szot K.
Oberflächenschicht in Perowskit-Materialien
Institut für Angewandte Photophysik, Universität Dresden, 18.01.00
23.42.0

IFF-00-21-216
Szot K.
Restructuring of the surface region in ABO3 materials
University of Mining and Metallurgy, Krakow, 10.04.00
23.42.0

IFF-00-21-217
Szot K.
Solid state reaction in surface layer of perovskite
Silesian University of Katowice, 15.12.00
23.42.0

IFF-00-21-218
Thust A.; Jia C.L.
Advances in atomic structure determination using the focal-series reconstruction method
12th European Congress on Electron Microscopy, Brno, Czech Republic, July 9 - 14, 2000.
Proceedings 12th EUREM, Vol III, p. 107.
23.42.0

IFF-00-21-219
Thust A.
Advanced Techniques for HRTEM of Defects
Euro Summer School on Electron Crystallography, Aachen, Germany, July 31 - August 4, 2000.
23.42.0

IFF-00-21-220
Thust A.
Obtaining 0.1 nm Interpretable resolution in electron microscopy by combining a series of images
Fall Meeting of the Dutch and Belgian Societies for Electron Microscopy,
Papendal, The Netherlands, December 7-8, 2000.
23.42.0

IFF-00-21-221
Thust A.
Techniques for direct atomic structure determination in HRTEM
International symposium on the occasion of the inauguration of the Tecnai F30 electron microscope at the Angstrom Laboratory, Uppsala, Sweden, April 14, 2000.
23.42.0

IFF-00-21-222
Thust A.
The technique of focal-series reconstruction
7th Annual Summer School on Computer-Interactive HRTEM at the Lawrence Berkeley Labs,
Berkeley, California, June 24 - 30, 2000.
23.42.0

IFF-00-21-223
Trinkaus H.
Defect Interaction and Accumulation - Physical Concepts and Analytical Treatments
Barcelona,
7.9.00
23.80.5

IFF-00-21-224
Trinkaus H.
Dislocation - Defect Interaction - The Elastic Approach
Toledo,
4.4.00
23.80.5

IFF-00-21-225
Trinkaus H.
Does Pulsing in Spallation Neutron Sources Affect Radiation Damage
Schruns
11.10.00
23.80.5

IFF-00-21-226
Ullmaier H.
Forschungs- und Entwicklungsarbeiten zur Europäischen Spallations - Neutronenquelle ESS
Kolloquium des Forschungszentrums Jülich
25.02.00
23.60.0

IFF-00-21-227
Ullmaier H.
Spallationstargets - eine neue Herausforderung an nukleare Werkstoffe
Kolloqium des Forschungszentrums Karlsruhe
08.12.00
23.60.0

IFF-00-21-228
Ullmaier H.
What is New in Spallation Materials? Reflections on the IWSMT-4 Meeting in Schruns
American Nuclear Society International Meeting, Washington, DC.
15.11.00
23.60.0

IFF-00-21-229
Urban K.
High- and low-speed plastic deformation of quasicrystals and their intermetallic approximants (INVITED PAPER)
Int. Workshop on High-Speed Plastic Deformation, Hiroshima 2000, Radiation Effets and Defects in Metals, in press
23.55.0

IFF-00-21-230
Urban K.
Spherical aberration corrected transmission electron microscopy
Congress of the Int. Mat. Res. Soc. Beijing 1999
23.42.0

IFF-00-21-231
Vetterl O.1; Carius R.1; Houben L.; Scholten C.; Luysberg M.; Lambertz A.1; Finger F.1; Wagner H.1
1 IPV, FZ Jülich
Effects of structural properties of (c-Si:H absorber layers on solar cell performance
MRS Spring Meeting, San Francisco (accepted for publication) (2000)
23.42.0

IFF-00-21-232
Volkov O.Y.1; Pavlovskii V.V.1; Divin Y.Y; Poppe U.
1 Institut für Festkörperforschung, Forschungszentrum Jülich GmbH, 52425 Jülich, Germany
2 Institute of Radioengineering & Electronics of RAS, Moscow 103907, Russian Federation
Far-infrared Hilbert-transform spectrometer based on Stirling cooler

Applied Superconductivity 1999. Ed.: X. Obradors, F. Sandiumenge and J. Fontcuberta, Inst. of Physics Conf. Ser. No.167, IOP Publishing Ltd., Bristol, p.p. 623-626 (2000)
23.42.0

IFF-00-21-233
Waser R.; Lohse O.1; Grossmann M.1; Bolten D.1; Böttger U.1
1 Institut für Werkstoffe der Elektrotechnik, RWTH Aachen
Transient behavior of the polarization in ferroelectric thin film capacitors
MRS Fall Meeting, Boston, 27.11.-01.12.00
23.42.0

IFF-00-21-234
Waser R.; Schneller T.1; Hoffmann S.
1 Institut für Werkstoffe der Elektrotechnik, RWTH Aachen
Advances in CSD technology for electroceramic thin films
Int. Conf. on Electroceramics VII, Portoroz, Slovenia, 03.-06.09.2000
23.42.0

IFF-00-21-235
Waser R.
Chemical solution deposition of complex electronic oxide thin films
Material Science Division, Argonne National Labs., Chicago, 01.12.00
23.42.0

IFF-00-21-236
Waser R.
Dielectric losses in ferroelectric thin films by reversible domain wall motion
12th IEEE Int. Symp. on the Applications of Ferroelectrics, Honolulu, Hawaii, 31.07.-02.08.2000
23.42.0

IFF-00-21-237
Waser R.
Oxidkeramische Materialien in der Mikroelelektronik und Nanotechnologie
10. Vortragstagung der Gesellschaft Deutscher Chemiker-Fachgruppe Festkörperchemie und Materialforschung: Anorganische Funktionsmaterialien, Münster, 26.09.-29.09.2000
23.42.0

IFF-00-21-238
Weber U.; Greuel G.; Böttger U.; Weber S.; Hennings D.; Waser R.
Dielectric properties of Ba(Zr,Ti)O3-based ferroelectrics for capacitor applications
Int. Conf. on Electroceramics VII, Portoroz, Slovenia, 03.-06.09.2000
23.42.0

IFF-00-21-239
Wischnewski A.; Richter D.; Monkenbusch M.; Willner L.; Farago B.1; Ehlers G.1; Schleger P.1
1Institute Laue Langevin, Grenoble/France
Reptation in polymer melts - What's new?
EPS CMD-18 Conference, Montreux/Switzerland, 13. - 17.03.2000
23.30.0

IFF-00-21-240
Wischnewski A.; Willner L.; Monkenbusch M.; Richter D.; Farago B.1; Ehlers G.1; Schleger P.1
1Institut Laue Langevin, Grenoble/France
NSE: A method to observe constraints of motion in polymer melts
Int. Workshop on NSE, HMI, Berlin, 16.10.00
23.30.0

IFF-00-21-241
Wortmann D.; Heinze S.; Bihlmayer G.; Blügel S.
STM-Theorie von Übergangsmetalloberflächen und -grenzflächen
Seminarvortrag im Rahmen Forschergruppe 353, Christian-Albrecht-Universität zu Kiel
13.11.2000
23.20.0

IFF-00-21-242
Zeller R.
Calculations for the electronic structure and lattice relaxations of defets
Berlin, 11.05.2000
23.20.0

IFF-00-21-243
Zorn R.; Richter D.; Hartmann L.1; Kremer F.1; Frick B.2
1Fakultät für Physik und Geowissenschaften, Universität Leipzig
2Institut Laue Langevin, Grenoble/Frankreich
Inelastic Neutron Scattering Experiments on the Fast Dynamics of a Glass-Forming Liquid in Mesoscopic Confinements
Workshop "Dynamics in Confinement", Grenoble/France, 29.01.00
23.15.0

IFF-00-21-244
Zorn R.
Inelastische Neutronenstreuung als Werkzeug zur Beobachtung der mikroskopischen Dynamik in Polymersystemen
Kolloquium Physikalische Chemie, Univ. Hannover, 17.01.00
23.15.0

IFF-00-21-245
Zorn R.
Multiple scattering correction for polarized-neutron diffraction
Universität San Sebastian/Spanien, 28.07.00
23.15.0

List of references

Antons A.	IFF-00-21-194	IFF-00-21-195	IFF-00-21-196
Baumgärtner A.	IFF-00-21-001	IFF-00-21-002	IFF-00-21-003
	IFF-00-21-004	IFF-00-21-005	
Bechthold P.S.	IFF-00-21-006		
Bellini V.	IFF-00-21-155		
Berger R.	IFF-00-21-194	IFF-00-21-195	IFF-00-21-196
Bihlmayer G.	IFF-00-21-007	IFF-00-21-008	IFF-00-21-131
	IFF-00-21-132	IFF-00-21-241	
Blügel S.	IFF-00-21-007	IFF-00-21-008	IFF-00-21-009
	IFF-00-21-010	IFF-00-21-011	IFF-00-21-012
	IFF-00-21-013	IFF-00-21-014	IFF-00-21-015
	IFF-00-21-016	IFF-00-21-017	IFF-00-21-131
	IFF-00-21-132	IFF-00-21-194	IFF-00-21-195
	IFF-00-21-196	IFF-00-21-241	
Brückel Th.	IFF-00-21-018	IFF-00-21-019	
Buchenau U.	IFF-00-21-020	IFF-00-21-021	IFF-00-21-022
	IFF-00-21-023		
Bürgler D.E.	IFF-00-21-025	IFF-00-21-026	IFF-00-21-027
	IFF-00-21-028	IFF-00-21-029	
Caprion D.	IFF-00-21-030	IFF-00-21-031	IFF-00-21-190
Conrad H.	IFF-00-21-032	IFF-00-21-033	IFF-00-21-034
Dederichs P.H.	IFF-00-21-035	IFF-00-21-036	IFF-00-21-037
	IFF-00-21-038	IFF-00-21-039	IFF-00-21-155
	IFF-00-21-156	IFF-00-21-157	
Divin Y.Y.	IFF-00-21-040	IFF-00-21-041	IFF-00-21-042
	IFF-00-21-043	IFF-00-21-172	IFF-00-21-209
	IFF-00-21-210	IFF-00-21-232	
Dürr H.A.	IFF-00-21-044	IFF-00-21-045	IFF-00-21-046
	IFF-00-21-047	IFF-00-21-048	IFF-00-21-049
	IFF-00-21-050	IFF-00-21-051	IFF-00-21-052
	IFF-00-21-053		
Eberhardt W.	IFF-00-21-054	IFF-00-21-055	IFF-00-21-056
	IFF-00-21-057	IFF-00-21-058	IFF-00-21-059
	IFF-00-21-060	IFF-00-21-061	IFF-00-21-062
	IFF-00-21-063	IFF-00-21-064	IFF-00-21-065
	IFF-00-21-066		
Ebert Ph.	IFF-00-21-067	IFF-00-21-068	IFF-00-21-069
	IFF-00-21-070	IFF-00-21-071	IFF-00-21-072
	IFF-00-21-073	IFF-00-21-123	IFF-00-21-187
	IFF-00-21-208		
Ehrhart P.	IFF-00-21-074	IFF-00-21-075	IFF-00-21-076
	IFF-00-21-082	IFF-00-21-189	
Faley M.	IFF-00-21-077	IFF-00-21-078	IFF-00-21-079
	IFF-00-21-080	IFF-00-21-081	IFF-00-21-172
Feuerbacher M.	IFF-00-21-121	IFF-00-21-169	
Fitsilis F.	IFF-00-21-074	IFF-00-21-082	
Freyss M.	IFF-00-21-155	IFF-00-21-157	
Förster F.	IFF-00-21-007	IFF-00-21-083	
Goerigk G.	IFF-00-21-084	IFF-00-21-085	IFF-00-21-086
Gompper G.	IFF-00-21-087	IFF-00-21-088	IFF-00-21-089
	IFF-00-21-090	IFF-00-21-091	

Grushko B.	IFF-00-21-123		
Grünberg P.	IFF-00-21-093	IFF-00-21-094	IFF-00-21-095
	IFF-00-21-096	IFF-00-21-097	IFF-00-21-098
	IFF-00-21-099	IFF-00-21-100	IFF-00-21-101
	IFF-00-21-102		
Harris J.	IFF-00-21-103		
Haubold H.-G.	IFF-00-21-104		
Heinze S.	IFF-00-21-105	IFF-00-21-241	
Hoffmann S.	IFF-00-21-153	IFF-00-21-168	IFF-00-21-170
	IFF-00-21-171	IFF-00-21-175	IFF-00-21-214
	IFF-00-21-234		
Hoffmann-Eifert S.	IFF-00-21-075	IFF-00-21-106	
Houben L.	IFF-00-21-231		
	offe A.	IFF-00-21-107	
Jahnen B.	IFF-00-21-108		
Jia C.L.	IFF-00-21-040	IFF-00-21-077	IFF-00-21-172
	IFF-00-21-218		
Jones R.O.	IFF-00-21-109	IFF-00-21-110	IFF-00-21-111
	IFF-00-21-112	IFF-00-21-113	IFF-00-21-114
Jung P.	IFF-00-21-115	IFF-00-21-116	IFF-00-21-117
	IFF-00-21-118	IFF-00-21-119	
Kann G.	IFF-00-21-120		
Kluge F.	IFF-00-21-068	IFF-00-21-123	
Kluge M.	IFF-00-21-124	IFF-00-21-190	
Kohlstedt H.H.	IFF-00-21-125	IFF-00-21-126	IFF-00-21-127
	IFF-00-21-128	IFF-00-21-129	IFF-00-21-130
	IFF-00-21-188		
Kurz Ph.	IFF-00-21-007	IFF-00-21-131	IFF-00-21-132
Köbler U.	IFF-00-21-133		
Lentzen M.	IFF-00-21-134		
Liebsch A.	IFF-00-21-135	IFF-00-21-136	IFF-00-21-137
Liu C.	IFF-00-21-115		
Luysberg M.	IFF-00-21-108	IFF-00-21-140	IFF-00-21-212
	IFF-00-21-231		
Mavropoulos Ph.	IFF-00-21-155	IFF-00-21-156	IFF-00-21-157
Meertens D.	IFF-00-21-122	IFF-00-21-141	IFF-00-21-200
Monkenbusch M.	IFF-00-21-144	IFF-00-21-145	IFF-00-21-239
	IFF-00-21-240		
Mueller R.	IFF-00-21-146		
Müller-Krumbhaar H.	IFF-00-21-147	IFF-00-21-148	IFF-00-21-149
Neeb M.	IFF-00-21-151		
Nie X.	IFF-00-21-008		
Ohl M.	IFF-00-21-152		
Ohly C.	IFF-00-21-153		

Ohly Ch.	IFF-00-21-154		
Papanikolaou N.	IFF-00-21-035	IFF-00-21-155	IFF-00-21-156
	IFF-00-21-157		
Persson B.N.J.	IFF-00-21-158	IFF-00-21-159	IFF-00-21-160
	IFF-00-21-161	IFF-00-21-162	IFF-00-21-163
	IFF-00-21-164	IFF-00-21-165	IFF-00-21-166
	IFF-00-21-167		
Poppe U	IFF-00-21-040	IFF-00-21-041	IFF-00-21-042
	IFF-00-21-043	IFF-00-21-077	IFF-00-21-078
	IFF-00-21-079	IFF-00-21-080	IFF-00-21-081
	IFF-00-21-172	IFF-00-21-232	
Pyckhout-Hintzen W.	IFF-00-21-173	IFF-00-21-174	
Regnery S.	IFF-00-21-074	IFF-00-21-082	
Richter D.	IFF-00-21-176	IFF-00-21-177	IFF-00-21-178
	IFF-00-21-179	IFF-00-21-180	IFF-00-21-181
	IFF-00-21-182	IFF-00-21-183	IFF-00-21-184
	IFF-00-21-185	IFF-00-21-239	IFF-00-21-240
	IFF-00-21-243		
Rickes J.	IFF-00-21-186		
Schall P.	IFF-00-21-169		
Schneider St.	IFF-00-21-188		
Schober H.R.	IFF-00-21-190	IFF-00-21-191	
Schober T.	IFF-00-21-192	IFF-00-21-193	
Scholten C.	IFF-00-21-231		
Schroeder K.	IFF-00-21-194	IFF-00-21-195	IFF-00-21-196
	IFF-00-21-197		
Schwahn D.	IFF-00-21-199		
Schütz G.	IFF-00-21-201	IFF-00-21-202	IFF-00-21-203
	IFF-00-21-204		
Seeck O. H.	IFF-00-21-205	IFF-00-21-206	IFF-00-21-207
Semmler U.	IFF-00-21-068	IFF-00-21-208	
Shadrin P.	IFF-00-21-172		
Shadrin P.M.	IFF-00-21-209		
Shirotov V.	IFF-00-21-210		
Shirotov V.V.	IFF-00-21-041		
Stellbrink J.	IFF-00-21-213		
Szot K.	IFF-00-21-153	IFF-00-21-214	IFF-00-21-215
	IFF-00-21-216	IFF-00-21-217	
Thust A.	IFF-00-21-218	IFF-00-21-219	IFF-00-21-220
	IFF-00-21-221	IFF-00-21-222	
Trinkaus H.	IFF-00-21-223	IFF-00-21-224	IFF-00-21-225
Ullmaier H.	IFF-00-21-116	IFF-00-21-226	IFF-00-21-227
	IFF-00-21-228		
Urban K.	IFF-00-21-041	IFF-00-21-042	IFF-00-21-043
	IFF-00-21-068	IFF-00-21-077	IFF-00-21-078
	IFF-00-21-079	IFF-00-21-080	IFF-00-21-081
	IFF-00-21-108	IFF-00-21-123	IFF-00-21-169
	IFF-00-21-172	IFF-00-21-187	IFF-00-21-208
	IFF-00-21-210	IFF-00-21-229	IFF-00-21-230

Waser R.	IFF-00-21-024	IFF-00-21-074	IFF-00-21-075
	IFF-00-21-082	IFF-00-21-092	IFF-00-21-138
	IFF-00-21-139	IFF-00-21-142	IFF-00-21-143
	IFF-00-21-150	IFF-00-21-153	IFF-00-21-168
	IFF-00-21-170	IFF-00-21-171	IFF-00-21-175
	IFF-00-21-186	IFF-00-21-188	IFF-00-21-198
	IFF-00-21-211	IFF-00-21-214	IFF-00-21-233
	IFF-00-21-234	IFF-00-21-235	IFF-00-21-236
	IFF-00-21-237	IFF-00-21-238	
Willner L.	IFF-00-21-239	IFF-00-21-240	
Wischnewski A.	IFF-00-21-239	IFF-00-21-240	
Wortmann D.	IFF-00-21-241		
Wu J.S.	IFF-00-21-077	IFF-00-21-172	
Zeller R.	IFF-00-21-035	IFF-00-21-155	IFF-00-21-157
	IFF-00-21-242		
Zorn R.	IFF-00-21-243	IFF-00-21-244	IFF-00-21-245

Other talks

IFF-00-22-001
Allgaier J.; Poppe A.; Willner L.; Stellbrink J.; Richter D.
PEP-PEO block copolymers as model system for the investigation of micellization in aqueous solution
ACS Symposium Series 765, Ed. J. Edward Glass (2000)
23.30.0

IFF-00-22-002
Antons A.; Berger R.; Blügel S.; Kromen Wi.; Schroeder K.
Ab initio Untersuchungen der Struktur von Inseln und Stufenkanten As-bedeckter Si(111)-Oberflächen
DPG-Frühjahrstagung Regensburg, 27.03.2000
23.42.0

IFF-00-22-003
Bauer G.S.; Chen J.; Dai Y.; Sommer W.F.; Viktoria M.
Microstructure in Deformed and Undeformed Austenitic Steel 304L Irradiated with 800 MeV Protons
4th International Workshop on Spallation Materials technology, Schruns
8-13.10.2000
23.60.0

IFF-00-22-004
Bene J.1; Bröcheler S.; Lustfeld H.
1Institute for Theoretical Physics, Eötvös University, Budapest, Ungarn
Simulating 2D-flows with viscous order dynamics
General Assembly der European Geophysical Society, Nizza
29.4.2000
23.15.0

IFF-00-22-005
Blügel S.; Kurz Ph.; Bihlmayer G.
Nichtkollinearer Magnetismus von Monolagen auf Ag(111) und Cu(111)
DPG-Frühjahrstagung Regensburg
März 2000
23.20.0

IFF-00-22-006
Blügel S.
Magnetism of two-dimensional itinerant antiferromagnets on a triangular lattice
1st Washington Conference on Electronic Structure of Complex Materials
27.07.2000
23.20.0

IFF-00-22-007
Breidbach M.; Bürgler D.E.; Olligs D.; Grünberg P.
Strukturuntersuchungen dünner Goldpuffer auf GaAs (001)
DPG-Frühjahrstagung Regensburg
März 2000
23.42.0

IFF-00-22-008
Breidbach M.
Strukturuntersuchungen dünner Goldpuffer auf GaAs
DPG-Frühjahrstagung Regensburg
März 2000
23.42.0

IFF-00-22-009
Broome T.; Carsughi F.; Chen J.; Floßdorf T.; Ullmaier H.
Mechanical Properties and Microstructure of Pure Tantalum after 800 MeV Proton Irrradiation
4th International Workshop on Spallation Materials technology Schruns
8-13.10.2000
23.60.0

IFF-00-22-010
Brückel Th.; Ioffe A.; Küssel E.; Massalovitch S.; Schlapp M.; Schmitz B.
Development of the high resolution image plate detector at the FZ Jülich
Grenoble, France, ILL, 2nd TECHNI Meeting, 12. - 13.10.2000
23.89.1

IFF-00-22-011
Brückel Th.; Rücker U.
Weiterentwicklung von Beugungsmethoden zur Untersuchung magnetischer Materialien mit Hilfe von Synchrotronstrahlung
Konferenzraum des IFF, Vollversammlung BMBF Verbund 04, 14. - 15.02.2000
23.89.1

IFF-00-22-012
Brückel Th.
Image Plate Detector for Thermal Neutrons
Abingdon, UK, The Cosener's House; TECHNI-Meeting, 30. - 31.03.2000
23.89.1

IFF-00-22-013
Brückel Th.
Polarised Neutron Scattering at the Jülich Research Center
Grenoble, France, ILL, ENPI-Meeting, 24. - 25.02.2000
23.89.1

IFF-00-22-014
Buchenau U.
Relaxationsprozesse in Gläsern
Vorlesungsmanuskript des 31. IFF-Ferienkurs "Femtosekunden und Nano-eV", Vol. 3, C7.1 - 18 (2000)
23.15.0

IFF-00-22-015
Buchmeier M.
Inverser GMR-Effekt in Fe/Cr/Au/Co-Schichtsystemen
DPG-Frühjahrstagung Regensburg
März 2000
23.42.0

IFF-00-22-016
Bürgler D.E.; Meisinger F.1; Schmidt C.M.1; Schaller D.M.1, Güntherodt H.-J.1; Grünberg P.
1Universität Basel
In-plane momentum conservation and Fermi surface effects in magnetic interlayer coupling
EPS-CMD18, Montreux (CH)
16.03.2000
23.42.0

IFF-00-22-017
Caprion D.; Schober H.R.
Does selenium have heterogeneous or homogeneous diffusion behaviour
DIMAT 2000, Paris 19.07.2000
23.30.0

IFF-00-22-018
Chen J.; James M.R.; Maloy S.A.; Sommer W.F.; Ullmaier H.
The Mechanical Properties of an Alloy 718 Window after Irradiation in Spallation Environment
4th International Workshop on Spallation Materials technology, Schruns
8-13.10.2000
23.60.0

IFF-00-22-019
Chen J.; Jung P.; Klein H.; Liu C.
Retention of Hydrogen and Helium in Martensitic Stainless Steels and their Effect on Mechanical Properties
4th International Workshop on Spallation Materials Technology, Schruns
10.10.2000.
23.80.5

IFF-00-22-020
Clarke S.; Nie X.; Weinert M.1; Bihlmayer G.; Blügel S.

1Physics Department, Brookhaven National Laboratory, Upton, New York, USA
Ab initio investigations of the effect of an applied electric field on the Fe(001) surface
DPG-Frühjahrstagung Regensburg
März 2000
23.20.0

IFF-00-22-021
Clarke S.
An ab initio investigation of the effect of an applied field on the Fe(001) surface
DPG-Frühjahrstagung Regensburg
März 2000
23.20.0

IFF-00-22-022
Conrad H.
JESSICA, the ESS-like Target/Moderator/Reflector Mock-up and Cold Moderator Test Facility
Tsukuba, Japan, ICANS-XV, 08.11.2000
23.60.0

IFF-00-22-023
Conrad H.
Overview of the ESS Target and Moderator R&D
Tsukuba, Japan, ICANS-XV, 07.11.2000
23.60.0

IFF-00-22-024
Dallmeyer A.; Gambardella P.1; Maiti K.; Malagoli M.; Carbone C.; Eberhardt W.; Kern K.1
1Institut de Physique Experimentale, EPF-Lausanne, Switzerland
Magnetismus von eindimensionalen Co-Drähten
DPG-Frühjahrstagung Regensburg
März 2000
23.20.0

IFF-00-22-025
Dallmeyer A.; Malagoli M.; Maiti K.; Wingbermühle J.; Carbone C.; Eberhardt W.; Nagy D.L.1; Deak L.1; Bottyan L.1; Rüffer R.2; Leupold O.2
1KFKI Research Institute for Particle and Nuclear Physics, Budapest, Hungary
2European Synchrotron Radiation Facility , Grenoble, France
Nicht-kollinearer Magnetismus in fcc-Fe/Co(100)-Filmen
DPG-Frühjahrstagung Regensburg
März 2000
23.20.0

IFF-00-22-026
Dürr H.A.; Münzenberg M.1; Felsch W.1; Dhesi S.S.1
1Universität Göttingen
Interface magnetic anisotropy in Fe/CeH2 multilayers
International Workshop on X-ray Spectroscopies of Magnetic Solids
09.12.2000
23.20.0

IFF-00-22-027
Dürr H.A.
Magnetic stripe domains probed by soft x-ray resonant magnetic scattering
ESRF Monday Seminar, ESRF Grenoble, France
21.02.2000
23.20.0

IFF-00-22-028
Dürr H.A.
Magnetization dynamics of magneto-electronics devices probed by femtosecond photoelectron microscopy
Kolloquium zum Schwerpunktprogramm "Dynamik von Elektronentransferprozessen an Grenzflächen", Walberberg
14.02.2000
23.20.0

IFF-00-22-029
Eberhardt W.
Spektroskopie an Clustern im Molekularstrahl
Erstes Blankeneser Gespräch über Forschung mit Synchrotronstrahlung bei BESSY
01.07.2000
23.20.0

IFF-00-22-030
Ebert Ph.
Quasikristalle und ihre Oberflächen.
Kolloquium des Instituts für Festkörperforschung, Forschungszentrum Jülich, Germany, February 4, 2000.
23.55.0

IFF-00-22-031
Ebert Ph.
Surfaces of Quasicrystals.
Seminar at the Institut d'Electronique et de Microélectronique du Nord, Villeneuve d'Ascq, France, May 25, 2000. (Prof. Dr. D. Stiévenard)
23.55.0

IFF-00-22-032
Eisebitt S.
Soft X-ray Speckle from antiferromagnetic domains
International Workshop on Soft X-ray Science in the Next Millennium:
The Future of Photon-in/Photon-out Experiments
Pikeville, USA
16.03.2000
23.20.0

IFF-00-22-033
Fetters L.J.1; Wheeler L.M.1; Xenidou M.; Richter D.
1Exxon Research and Engineering Co., Annandale/USA
Modification Potential for ShellvisTM Star Polymers
Exxon Research and Engineering Company; Proprietary Information, CR.17BU.99 (1999)
23.30.0

IFF-00-22-034
Grushko B.
Composition and precipitation behavior of icosahedral quasicrystals in Al-Pd-Mn.
Frühjahrstagung des Arbeitskreises Festkörperphysik bei der DPG. Regensburg, Germany. März 2000.
23.55.0

IFF-00-22-035
Grushko B.
Decagonal and related phases in Al-Cu-Rh
Lab. f. Kristallogr., ETH Zürich, Schweiz
23.55.0

IFF-00-22-036
Grushko B.
Metallurgy of the aluminum-transition metals alloy systems forming quasicrystals
CRMC2/CNRS, Marseille, France June 2000
23.55.0

IFF-00-22-037
Harris J.
Computational Methods in Materials Science
Institut Superieure des Materiaux du Mans, Le Mans, Frankreich 26.3.2000
23.20.0

IFF-00-22-038
Haubold H.-G.; Vad Th.; Jungbluth H.; Hiller P.
Nano Structure of Nafion: A SAXS Study
Noosa, Australia, ISPE 7, 06. - 11.08.2000
23.89.1

IFF-00-22-039
Heinze S.; Abt. R.; Blügel S.; Gilarowski G.1.; Niehus H.1

1Institut für Physik, Humboldt-Universität zu Berlin
Vergrabene Übergangsmetallstrukturen auflösbar durch STM
DPG-Frühjahrstagung Regensburg
März 2000
23.20.0

IFF-00-22-040
Heinze S.; Bode M.1; Kubetzka A.1; Pietzsch O.1; Wortmann D.; Kurz Ph.; Nie X.; Blügel S.; Wiesendanger R.1
1Institut für Angewandte Physik, Universität Hamburg
Real space imaging of two-dimensional antiferromagnetism on the atomic scale
ICSFS-10: International Conference on Solid Films and Surfaces, Princeton University, N.J., USA
09. - 13.07.2000
23.20.0

IFF-00-22-041
Heinze S.; Wortmann D.; Bihlmayer G.; Blügel S.
Ab-initio calculations of tunneling through MgO barriers on Fe(001)
228. WE-Heraeus-Seminar "Metal-Nonmetal Structures for Magnetoelectronics"
Bad Honnef
5. - 7. Januar 2000
23.20.0

IFF-00-22-042
Heinze S.; Wortmann D.; Blügel S.; Bode M.1; Wiesendanger R.1
1Zentrum für Mikrostrukturforschung, Universität Hamburg
Ab initio Rechnungen zum spinpolarisierten STM
DPG-Frühjahrstagung Regensburg
März 2000
23.20.0

IFF-00-22-043
Hupfeld D.
The mu-CAT Undulator High Energy Side Station
APS, Argonne, USA, Technical Workgroup Meeting,
16.11.2000
23.89.1

IFF-00-22-044
Jung P.
Hydrogen Embrittlement
Data Base Evaluation Workshop, RAFM Steels, Brasimone
27.11.2000.
23.80.5

IFF-00-22-045
Jung P.
Microstructure of C-containing materials, Be, W, SiC and oxide ceramics with high helium concntrations
Monitoring Workshop, Underlying Technology of the European Fusion Programme, Garching
18.7.2000.
23.80.5

IFF-00-22-046
Klingeler R.
Mass spectra of metal-doped fullerene clusters and electronic structure of Ce@44
DPG-Frühjahrstagung Bonn
April 2000
23.20.0

IFF-00-22-047
Kluge M.; Schober H.R.
Molekulardynamik-Simulationen an Schmelzen und Gläsern aus Cu33 Zr67
28.03.2000, DPG Frühjahrstagung, Regensburg
23.30.0

IFF-00-22-048
Kromen Wi.; Blügel S.; Schroeder K.
Implementierung einer Projektor-augmentierten Pseudopotentialmethode
DPG-Frühjahrstagung Regensburg, 29.03.2000
23.42.0

IFF-00-22-049
Kuanr B.; Wingbermühle J.; Bürgler D.E.; Grünberg P.
Influence of anisotropy on FMR frequency of polycrystalline pinned and unpinned thin Permalloy and epitaxial Fe films
16th ICMFS, 16th International Colloquium of Magnetic Films and Surfaces
Natal, Brazil
15.08.2000
23.42.0

IFF-00-22-050
Kuanr B.
Magnetic interlayer exchange coupling investigated by means of Brillouin-Light Scattering
Workshop 2000 des DEGA - Fachausschuss Physikalisches Akustik der DPG
Bad Honnef
05.10.2000
23.42.0

IFF-00-22-051
Liebsch A.
Quantum well behavior induced by dynamical screening in alkali metal films
Physics Department, University of San Sebastian 4.7.2000
23.20.0

IFF-00-22-052
Liebsch A.
Role of d electrons in electronic surface excitations
Physics Department, University of San Sebastian 5.7.2000
23.20.0

IFF-00-22-053
Link S.; Dürr H.A.; Eberhardt W.
Lifetimes of image-potential states on the clean and oxygen covered Pt(111) surface
DPG-Frühjahrstagung, Regensburg
März 2000
23.20.0

IFF-00-22-054
Lustfeld H.; Kaufmann Z.1
1Department of Physics of Complex Systems, Eötvös University, Budapest, Ungarn
Comparison between flow and Poincare maps of simple repelelrs
MPI für Physik komplexer Systeme, Dresden 6.11.2000
23.15.0

IFF-00-22-055
Lustfeld H.; Poppe D.1; Bröcheler S.
1FZJ -ICG3
Charakterisierung periodischen Verhaltens der Reaktionsgleichungen von Spurengasen in der Troposphäre
Frühjahrstagung 2000 der AEFF der DPG, Bremen 24.3.2000
23.15.0

IFF-00-22-056
Lüttgens G.; Pontius N.; Friedrich Ch.; Klingeler R.; Bechthold P.S.; Neeb M.; Eberhardt W.
Chemisorption von Benzol an kleinen Metallclusteranionen: Eine photoelektronen-spektroskopische Studie
DPG-Frühjahrstagung Bonn
April 2000
23.20.0

IFF-00-22-057
Malagoli M.; Maiti K.; Magnano E.1; Dallmeyer A.; Carbone C.
1Laboratorio Nazionale TASC, Padriciano, Trieste, Italy
Lifetime and correlation effects in photoemission from the Gd valence band

DPG-Frühjahrstagung Regensburg
März 2000
23.20.0

IFF-00-22-058
Mika K.
A linear programming approach to the high temperature degeneracy of simple Ising systems
Ising Centenuial Conference, Universität Köln, 15.06.2000
23.15.0

IFF-00-22-059
Monkenbusch M.
Introduction to soft matter systems
Neutron Scattering in Novel Materials, Proceedings of the 8th Summer School on Neutron Scattering, 102-116 (2000)
23.30.

IFF-00-22-060
Monkenbusch M.
Neutron spin-echo spectrometer, NSE
Lecture Notes of the Laboratory Course on "Neutron Scattering", Vol. 5, 11-1 - 11-18 (2000)
23.30.0

IFF-00-22-061
Monkenbusch M.
Neutronenspektroskopie
Vorlesungsmanuskript des 31. IFF-Ferienkurs "Femtosekunden und Nano-eV", Vol.3, B5.1 - 40 (2000)
23.30.0

IFF-00-22-062
Monkenbusch M.
Time-of-flight spectrometers
Lecture Notes of the Laboratory Course on "Neutron Scattering", Vol. 5, 10-1 - 10-23 (2000)
23.30.0

IFF-00-22-063
Müller-Krumbhaar H.
2000: Jahr der Physik
mehrere Pressekonferenzen im Rahmen der Aktion von DPG und BMBF
23.15.0

IFF-00-22-064
Neeb M.
Time-resolved photodetachment spectroscopy on transition metal cluster anions
International Conference on Small Particles and Inorganic Clusters ISSPIC, Atlante, USA
12.10.2000-09-26
23.20.0

IFF-00-22-065
Neeb M.
Time-resolved photodetachment spectroscopy on transition metal cluster anions
International Workshop on Photoionization IWP 2000, Carry le Rouet, France
08.10.2000
23.20.0

IFF-00-22-066
Nie X.; Blügel S.
Investigation of chemical trends of the magnetocrystalline anisotropy for monolayers
DPG-Frühjahrstagung Regensburg
März 2000
23.20.0

IFF-00-22-067
Olligs D.; Bürgler D.E.; Grünberg P.
GMR in epitaktischen Fe/Cr/Fe-Schichten
DPG-Frühjahrstagung Regensburg
März 2000
23.42.0

IFF-00-22-068
Olligs D.; Bürgler D.E.; Grünberg P.
GMR in epitaktischen Fe/Cr/Fe-Schichten: Einfluss der Grenzflächenrauhigkeit
DPG-Frühjahrstagung Regensburg
März 2000
23.42.0

IFF-00-22-069
Pontius N.; Bechthold P.S.; Neeb M.; Eberhardt W.
Dynamik heißer Elektronen in kleinen Übergangsmetall-Clustern
DPG-Frühjahrstagung Bonn
April 2000
23.20.0

IFF-00-22-070
Prager M.
Translation an Rotation
Lecture Notes of the Laboratory Course on "Neutron Scattering", Vol. 5, 17-1 - 17-20 (2000)
23.30.0

IFF-00-22-071
Pyckhout-Hintzen W.; Botti A.; Heinrich M.; Richter D.; Straube E.1; Westermann S.2; Urban V.3
1Univ. Halle/Saale, FB Physik
2Goodyear Technical Center, Luxembourg
3ESRF Grenoble, France
SANS of polymer networks under deformation
Novel Materials, World Science Press (Singapore), 117-130 (2000)
23.30.0

IFF-00-22-072
Pyckhout-Hintzen W.; Westermann S.1; Botti A.; Richter D.; Straube E.2
1Goodyear Technical Center, Luxembourg
2Univ. Halle/Saale, FB Physik
Chain deformation in unfilled and filled polymer networks: a SAS approach
Notiziario Neutroni e Luce di Sincrotone 5, 34-40 (2000)
23.30.0

IFF-00-22-073
Richter D.; Monkenbusch M.; Farago B.1; Schleger P.1; Montes H.2
1Institut Laue Langevin, Grenoble/France
2ESPCI, Paris/France
Large scale motions in dense polymer systems
AIP Conference Proceedings 469, 587 - 598 (1999)
23.30.0

IFF-00-22-074
Richter D.
Dynamik von Polymeren
Vorlesungsmanuskript des 31. IFF-Ferienkurs "Femtosekunden und Nano-eV", Vol. 3, C6.1 - 36 (2000)
23.30.0

IFF-00-22-075
Richter D.
Polymer dynamics
Lecture Notes of the Laboratory Course on "Neutron Scattering", Vol. 5, 15-1 - 15-29 (2000)
23.30.0

IFF-00-22-076
Richter D.
Polymer dynamics by neutron spin echo spectroscopy
in "Scattering in Polymeric and Colloidal Systems" Ed. by W. Brown and K. Mortensen, Gordon and Breach Science Publishers, London, Chap. 12, 535-575 (2000)
23.30.0

IFF-00-22-077
Richter D.
Properties of the neutron, elementary scattering processes
Lecture Notes of the Laboratory Course on "Neutron Scattering", Vol. 5, 2-1 - 2-21 (2000)
23.30.0

IFF-00-22-078
Rosov N.1; Rathgeber S.1; Monkenbusch M.
1NIST, Gaithersburg/USA
Neutron spin echo spectroscopy at the NIST Center
ACS Symposium Series 739 "Scattering from Polymers", Characterization by X-rays, Neutrons and Light, Ed. P. Cebe, B.S. Hsiao, D.J. Lohse
23.89.1 / 23.30.0

IFF-00-22-079
Rücker U.; Bergs W.; Alefeld B.; Kentzinger E.; Brückel Th.
The new polarized neutron Reflectometer in Juelich
Sanct Petersburg, Russia, PNCMI-2000 International Workshop, 21.06.2000
23.89.1

IFF-00-22-080
Schondelmaier D.
Orientation and self-assembly of hydrophobic fluoro-alcyl-silanes
DPG-Frühjahrstagung Regensburg
März 2000
23.20.0

IFF-00-22-081
Schroeder K.; Antons A.; Berger R.; Blügel S.
Adatome auf Si(111): Sb, Gleichgewichtslagen und Diffusion
DPG-Frühjahrstagung Regensburg, 27.03.2000
23.42.0

IFF-00-22-082
Schwahn D.; Mortensen K.1
1Risø National Laboratory, Condensed Matter Physics and Chemistry Department, Roskilde/Denmark
Thermal composition fluctuations in polymer blends studied with small angle neutron scattering
Chapter 8 in "Scattering in polymeric and colloidal systems", eds. W. Brown and K. Mortensen, Gordon and Breach Science Publishers (2000)
23.30.0

IFF-00-22-083
Schwahn D.
Small-angle scattering and reflectometry
Lecture Notes of the Laboratory Course on "Neutron Scattering", Vol. 5, 8-1 - 8-16 (2000)
23.30.0

IFF-00-22-084
Schwahn D.
Soft Matter Structure
Lecture Notes of the Laboratory Course on "Neutron Scattering", Vol. 5, 14-1 - 14-18 (2000)
23.30.0

IFF-00-22-085
Schütz G.
Nonequilibrium relaxation law for entangled polymers
Meco 25, Pont-a-Mousson, Frankreich
11. 3. 2000
23.30.0

IFF-00-22-086
Schütz G.
Stability and Branching of Shocks
DPG-Frühjahrstagung, Regensburg
30. 3. 2000
23.15.0

IFF-00-22-087
Spatschek R.; Brener E.; Marchenko V.1; Müller-Krumbhaar H.
1 P.L. Kapitza Insitute for Physical Problems, Moskau
Vergröberungsübergang unter Berücksichtigung elastischer Effekte
Frühjahrstagung der DPG, Regensburg, März 2000
23.15.0

IFF-00-22-088
Spatschek R.; Müller-Krumbhaar H.; Brener E.
Ostwald-Reifung unter elastischer Wechselwirkung
DFG-KickOff-Meeting zum SPP: "Phasenumwandlungen in mehrkomponentigen Schmelzen", Bonn, Okt. 2000
23.15.0

IFF-00-22-089
Ullmaier H.
Das ESS - Projekt
62. Sitzung des Wissenschaftlich-Technischen Ausschusses des Aufsichtsrats, Jülich
09.05.00
23.60.0

IFF-00-22-090
Ullmaier H.
Das Projekt Europäische Spallation - Neutronenquelle
2. Entwicklungskonferenz der beiden Kirchen, Jülich
18.05.00
23.60.0

IFF-00-22-091
Ullmaier H.
ESS-Project: Status and planned R & D with emphasis on materials activities
Internat. Workshop on Spallation Materials Technology (IWSMT-4)
Schruns
09.10.00
23.60.0

IFF-00-22-092
Ullmaier H.
Effects of Helium on Mechanical Properties of Structural Target Materials
Metals and Ceramics Seminar, Oak Ridge National Laboratory
20.03.00
23.60.0

IFF-00-22-093
Ullmaier H.
Materialforschung und -entwicklung für die Europäische Spallations - Neutronenquelle
Kolloquium des Instituts für Werkstoffe und Verfahren der Energietechnik, Jülich
11.05.00
23.60.0

IFF-00-22-094
Ullmaier H.
Radiation Damage in Spallation Materials
CEA - Saclay,
16.06.00
23.60.0

IFF-00-22-095
Wingbermühle J.; Grünberg P.; Bürgler D.E.
Exchange Bias Eigenschaften von NiO/Permalloy Schichten, hergestellt mit Hilfe von Ionenstrahlsputtern
DPG-Frühjahrstagung Regensburg
März 2000
23.42.0

IFF-00-22-096
Wortmann D.; Heinze S.; Bihlmayer G.; Blügel S.
Ab initio calculations of tunneling through MgO barriers on Fe(001)
Workshop on TMR and GMR, Dresden

Dezember 2000
23.20.0

IFF-00-22-097
Wortmann D.; Heinze S.; Bihlmayer G.; Blügel S.
Ab-initio Berechnungen von STM-Aufnahmen einer Oberflächenlegierung: c(2x2)MnCu/Cu(100)
DPG-Frühjahrstagung Regensburg
März 2000
23.20.0

IFF-00-22-098
Wortmann D.; Heinze S.; Bihlmayer G.; Blügel S.
Ab-initio Berechnungen zum Tunneln durch eine MgO-Barriere auf Fe(001)
DPG-Frühjahrstagung Regensburg
März 2000
23.20.0

IFF-00-22-099
Wortmann D.; Heinze S.; Kurz Ph.; Bihlmayer G.; Blügel S.
Resolving complex atomic-scale spin-structures by SP-STM
Workshop on TMR and GMR, Dresden
Dezember 2000
23.20.0

IFF-00-22-100
Zorn R.
Correlations functions measured by scattering experiments
Lecture Notes of the Laboratory Course on "Neutron Scattering", Vol. 5, 5.1 - 5-24 (2000)
23.15.0

IFF-00-22-101
Zorn R.
Ionentransport in Elektrolyten
Vorlesungsmanuskript des 31. IFF-Ferienkurs "Femtosekunden und Nano-eV", Vol. 3, D1.1 - 20 (2000)
23.15.0

List of references

Abt. R.	IFF-00-22-039		
Alefeld B.	IFF-00-22-079		
Allgaier J.	IFF-00-22-001		
Antons A.	IFF-00-22-002	IFF-00-22-081	
Bechthold P.S.	IFF-00-22-056	IFF-00-22-069	
Berger R.	IFF-00-22-002	IFF-00-22-081	
Bergs W.	IFF-00-22-079		
Bihlmayer G.	IFF-00-22-005	IFF-00-22-020	IFF-00-22-041
	IFF-00-22-096	IFF-00-22-097	IFF-00-22-098
	IFF-00-22-099		
Blügel S.	IFF-00-22-002	IFF-00-22-005	IFF-00-22-006
	IFF-00-22-020	IFF-00-22-039	IFF-00-22-040
	IFF-00-22-041	IFF-00-22-042	IFF-00-22-048
	IFF-00-22-066	IFF-00-22-081	IFF-00-22-096
	IFF-00-22-097	IFF-00-22-098	IFF-00-22-099
Botti A.	IFF-00-22-071	IFF-00-22-072	
Breidbach M.	IFF-00-22-007	IFF-00-22-008	
Brener E.	IFF-00-22-087	IFF-00-22-088	
Bröcheler S.	IFF-00-22-004	IFF-00-22-055	
Brückel Th.	IFF-00-22-010	IFF-00-22-011	IFF-00-22-012
	IFF-00-22-013	IFF-00-22-079	
Buchenau U.	IFF-00-22-014		
Buchmeier M.	IFF-00-22-015		
Bürgler D.E.	IFF-00-22-007	IFF-00-22-016	IFF-00-22-049
	IFF-00-22-067	IFF-00-22-068	IFF-00-22-095
Caprion D.	IFF-00-22-017		
Carbone C.	IFF-00-22-024	IFF-00-22-025	IFF-00-22-057
Carsughi F.	IFF-00-22-009		
Chen J.	IFF-00-22-003	IFF-00-22-009	IFF-00-22-018
	IFF-00-22-019		
Clarke S.	IFF-00-22-020	IFF-00-22-021	
Conrad H.	IFF-00-22-022	IFF-00-22-023	
Dallmeyer A.	IFF-00-22-024	IFF-00-22-025	IFF-00-22-057
Dürr H.A.	IFF-00-22-026	IFF-00-22-027	IFF-00-22-028
	IFF-00-22-053		
Eberhardt W.	IFF-00-22-024	IFF-00-22-025	IFF-00-22-029
	IFF-00-22-053	IFF-00-22-056	IFF-00-22-069
Ebert Ph.	IFF-00-22-030	IFF-00-22-031	
Eisebitt S.	IFF-00-22-032		
Floßdorf T.	IFF-00-22-009		
Friedrich Ch.	IFF-00-22-056		
Grushko B.	IFF-00-22-034	IFF-00-22-035	IFF-00-22-036
Grünberg P.	IFF-00-22-007	IFF-00-22-016	IFF-00-22-049
	IFF-00-22-067	IFF-00-22-068	IFF-00-22-095

Harris J.	IFF-00-22-037		
Haubold H.-G.	IFF-00-22-038		
Heinrich M.	IFF-00-22-071		
Heinze S.	IFF-00-22-039 IFF-00-22-042 IFF-00-22-098	IFF-00-22-040 IFF-00-22-096 IFF-00-22-099	IFF-00-22-041 IFF-00-22-097
Hiller P.	IFF-00-22-038		
Hupfeld D.	IFF-00-22-043		
	offe A.	IFF-00-22-010	
Jung P.	IFF-00-22-019 IFF-00-22-045	IFF-00-22-044	
Jungbluth H.	IFF-00-22-038		
Kentzinger E.	IFF-00-22-079		
Klein H.	IFF-00-22-019		
Klingeler R.	IFF-00-22-046	IFF-00-22-056	
Kluge M.	IFF-00-22-047		
Kromen Wi.	IFF-00-22-002	IFF-00-22-048	
Kuanr B.	IFF-00-22-049	IFF-00-22-050	
Kurz Ph.	IFF-00-22-005	IFF-00-22-040	IFF-00-22-099
Küssel E.	IFF-00-22-010		
Liebsch A.	IFF-00-22-051	IFF-00-22-052	
Link S.	IFF-00-22-053		
Liu C.	IFF-00-22-019		
Lustfeld H.	IFF-00-22-004	IFF-00-22-054	IFF-00-22-055
Lüttgens G.	IFF-00-22-056		
Maiti K.	IFF-00-22-024	IFF-00-22-025	IFF-00-22-057
Malagoli M.	IFF-00-22-024	IFF-00-22-025	IFF-00-22-057
Massalovitch S.	IFF-00-22-010		
Mika K.	IFF-00-22-058		
Monkenbusch M.	IFF-00-22-059 IFF-00-22-062	IFF-00-22-060 IFF-00-22-073	IFF-00-22-061 IFF-00-22-078
Müller-Krumbhaar H.	IFF-00-22-063	IFF-00-22-087	IFF-00-22-088
Neeb M.	IFF-00-22-056 IFF-00-22-069	IFF-00-22-064	IFF-00-22-065
Nie X.	IFF-00-22-020	IFF-00-22-066	
Ollígs D.	IFF-00-22-007	IFF-00-22-067	IFF-00-22-068
Pontius N.	IFF-00-22-056	IFF-00-22-069	
Poppe A.	IFF-00-22-001		
Prager M.	IFF-00-22-070		
Pyckhout-Hintzen W.	IFF-00-22-071	IFF-00-22-072	
Richter D.	IFF-00-22-001	IFF-00-22-033	IFF-00-22-071

	IFF-00-22-072	IFF-00-22-073	IFF-00-22-074
	IFF-00-22-075	IFF-00-22-076	IFF-00-22-077
Rücker U.	IFF-00-22-011	IFF-00-22-079	
Schlapp M.	IFF-00-22-010		
Schmitz B.	IFF-00-22-010		
Schober H.R.	IFF-00-22-017	IFF-00-22-047	
Schondelmaier D.	IFF-00-22-080		
Schroeder K.	IFF-00-22-002	IFF-00-22-048	IFF-00-22-081
Schwahn D.	IFF-00-22-082	IFF-00-22-083	IFF-00-22-084
Schütz G.	IFF-00-22-085	IFF-00-22-086	
Spatschek R.	IFF-00-22-087	IFF-00-22-088	
Stellbrink J.	IFF-00-22-001		
Ullmaier H.	IFF-00-22-009	IFF-00-22-018	IFF-00-22-089
	IFF-00-22-090	IFF-00-22-091	IFF-00-22-092
	IFF-00-22-093	IFF-00-22-094	
Vad Th.	IFF-00-22-038		
Willner L.	IFF-00-22-001		
Wingbermühle J.	IFF-00-22-025	IFF-00-22-049	IFF-00-22-095
Wortmann D.	IFF-00-22-040	IFF-00-22-041	IFF-00-22-042
	IFF-00-22-096	IFF-00-22-097	IFF-00-22-098
	IFF-00-22-099		
Zorn R.	IFF-00-22-100	IFF-00-22-101	

Posters

IFF-00-23-001
Alefeld B.; Dohmen L.; Brückel Th.
GaAs as a backscattering crystal
Aachen, RWTH, 8. DGK Jahrestagung, 13. - 16.03.2000
23.89.1

IFF-00-23-002
Antons A.; Berger R.; Blügel S.; Schroeder K.
Structure of Steps and small Islands on Si(11): As
CHIPPS'2000, Wandlitz bei Berlin, 15.-18.05.2000
23.42.0

IFF-00-23-003
Antons A.; Berger R.; Blügel S.; Schroeder K.
Structure of Steps and small Islands on Si(11): As
PSI-K 2000 Conference, Schwäbisch Gmünd, Germany, 22.-26.08.2000
23.42.0

IFF-00-23-004
Bachhofer H.1; Reisinger H.1; Dehm D.; von Philipsborn H.1; Waser R.
1 Siemens AG, München, Germany
Relaxation effects and steady-state conduction in non-stoichiometric SBT films
12th Int. Symp. Integrated Ferroelectrics, Aachen, 12.03.-15.03.00
23.42.0

IFF-00-23-005
Baldus O.; Krasser W.; Hoffmann S.; Waser R.; Kreutz E.
Laserannealing studies of strontium-titanate thin films using short laser pulses
12th Int. Symp. Integrated Ferroelectrics, Aachen, 12.03.-15.03.00
23.42.0

IFF-00-23-006
Bellini V.; Papanikolaou N.; Zeller R.; Dederichs P.H.
Magnetic 4d monoatomic rows on Ag substrates
Psi-k Conference: Ab initio (from electronic structure) calculation of complex processes in materials
Schwäbisch Gmünd, 22.-26-08.2000
23.20.0

IFF-00-23-007
Bihlmayer G.; Nie X.; Blügel S.
Magnetismus von dekorierten Stufenkanten
DPG-Frühjahrstagung Regensburg
März 2000
23.20.0

IFF-00-23-008
Bolten D.1; Böttger U.1; Grossmann M.1; Lohse O.1; Waser R.
1 Institut für Werkstoffe der Elektrotechnik, RWTH Aachen, Germany
Irreversible processes in donor and acceptor doped Pb(zr,Ti)O3 thin films
12th Int. Symp. Integrated Ferroelectrics, Aachen, 12.03.-15.03.00
23.42.0

IFF-00-23-009
Bolten D.1; Böttger U.1; Grossmann M.1; Lohse O.1; Waser R.
1 Institut für Werkstoffe der Elektrotechnik, RWTH Aachen, Germany
Reversible and irreversible polarization processes in ferroelectric thin films
12th IEEE Int. Symp. on the Applications of Ferroelectrics, Honolulu, Hawaii, 31.07.-02.08.2000
23.42.0

IFF-00-23-010
Buchmeier M.; Schreiber R.; Bürgler D.E.; Grünberg P.
Inverse GMR effect in Fe/Cr/Au/Co systems
VDI Statusseminar "Magnetoelektronik", Dresden
14. - 16.06.2000
23.42.0

IFF-00-23-011
Böttger U.1; Bolten D.1; Lohse O.1; Grossmann M.1; Waser R.
1 Institut für Werkstoffe der Elektrotechnik, RWTH Aachen, Germany
Dielectric losses in ferroelectric thin films by reversible domain wall motion
12th Int. Symp. Integrated Ferroelectrics, Aachen, 12.03.-15.03.00
23.42.0

IFF-00-23-012
Bürgler D.E.; Meisinger F.1; Schmidt C.M.1; Schaller D.M.1; Güntherodt H.-J.1; Grünberg P.
1Universität Basel
In-plane momentum conservation and Fermi surface effects in magnetic interlayer coupling
EPS-CMD18, Montreux (CH)
16.03.2000
23.42.0

IFF-00-23-013
Bürgler D.E.; Meisinger; F.1; Schmidt C.M.1; Schaller D.M.1; Güntherodt J.-J.1; Grünberg P.
1Universität Basel
In-plane momentum conservation and Fermi surface effects in magnetic interlayer coupling
Gordon Research Conference on Magnetic Nanostructures, Ventura, CA (USA)
14.02.2000
23.42.0

IFF-00-23-014
Cabria I.; Nonas B.; Zeller R.; Dederichs P.H.
Strong enhancement of orbital moments and anisotropy energies of adatoms on the Ag(001)surface
Psi-k Conference: Ab initio (from electronic structure) calculation of complex processes in materials
Schwäbisch Gmünd, 22.-26-08.2000
23.20.0

IFF-00-23-015
Clarke S.; Nie X.; Blügel S.; Bihlmayer G.; Weiner M.1
1Department of Physics, Brookhaven National Laboratory, Upton, NY, USA
An investigation of the effect of applied static electric fields on magnetic surfaces
Psi-k2000 Konferenz, Schwäbisch-Gmünd
August 2000
23.20.0

IFF-00-23-016
Dederichs P.H.; Mavropoulos Ph.; Papanikolaou N.
Complex band structure and tunneling through Metal/Insulator/Metal junctions
3rd Gordon Research Conference on Magnetic Nanostructures, February 2000, Ventura, California
23.20.0

IFF-00-23-017
Döbereiner H.-G.; Gompper G.; Haluska C.; Petrov P. G.
Measurement of Spontaneous Curvature
Poster beim "3rd European Biophysics Congress", München, 9. - 13. September 2000
23.30.0

IFF-00-23-018
Dürr H.A.
Magnetic domain correlations in transition metal films and multilayers

228. WE-Heraeus-Seminar "Metal-Nonmetal Structures for Magnetoelectronics"
Physikzentrum Bad Honnef
07.01.2000
23.20.0

IFF-00-23-019
Eberhardt W.
Magnetoelectronics: Basic research, characterization and optimization of multilayer-
Systems for GMR-sensors and nonvolatile memeory diveces (MRAM)
BMBF-Statusseminar "Magnetoelektronik"
IFW Dresden
16.06.2000
23.20.0

IFF-00-23-020
Edelmann K.1; Janich M.1; Hoinkis E.2; Pyckhout-Hintzen W.; Höring S.3
1Technische Hochschule Merseburg
2HMI, Berlin
3Universität Halle
Aggregationsverhalten von Ethylenoxid/Methylmethacrylat Diblock-Copolymeren in organischen Lösungsmitteln
GDCH, Merseburg, 20. - 21.03.2000
23.30.0

IFF-00-23-021
Ehrhart P.; Fitsilis F.; Regnery S.; Waser R.; Schienle F.1; Schumacher M.1; Lindner J.1; Dauelsberg M.1; Strzyzewski P.1; Jürgensen H.1
1 Aixtron AG, Aachen, Germany
Deposition of BST thin films in a multi-wafer MOCVD reactor
12th Int. Symp. Integrated Ferroelectrics, Aachen, 12.03.-15.03.00
23.42.0

IFF-00-23-022
Eisebitt S.; Karl A.; Zimina A.; Scherer R.; Freiwald M.; Cramm S.; Schondelmaier D.; Bringer A.; Eberhardt W.
The electronic structure of doped fullerenes investigated by soft X-ray emission
14th International Winterschool on Electronic Properties of Novel Materials - Molecular Nanostructures, Kirchberg, Tirol
08.03.2000
23.20.0

IFF-00-23-023
Eisebitt S.; Karl A.; Zimina A.; Scherer R.; Freiwald M.; Cramm S.; Schondelmaier D.; Bringer A.; Eberhardt W.
The electronic structure of doped fullerenes investigated by soft X-ray emission
14th International Winterschool on Electronic Properties of Novel Materials: Molecular Nanostructures, Kirchberg, Österreich
März 2000
23.20.0

IFF-00-23-024
Falter S.T.; Du K.M.; Loosen P.; Poprawe R.; Baldus O.; Waser R.
UV beam sources for double pulse generation
Conference on Lasers and Electrooptics 2000, Nizza, France, 04.-08.09.2000
23.42.0

IFF-00-23-025
Freyss M.; Papanikolaou N.; Mavropoulos Ph.; Zeller R.; Dederichs P.H.
Ab-initio calculations for the electronic structure and transport properties of TMR junctions
Psi-k Conference: Ab initio (from electronic structure) calculation of complex processes in materials
Schwäbisch Gmünd, 22.-26.08.2000
23.20.0

IFF-00-23-026
Friedrich Ch.; Lüttgens G.; Pontius N.; Neeb M.; Bechthold P.S.; Eberhardt W.
Erhöhung der Massenauflösung zur Photoelektronenspektroskopie von Cluster-Adsorbat-Systemen im Molekularstrahl
DPG-Frühjahrstagung Bonn
April 2000
23.20.0

IFF-00-23-027
Gebhardt R.; Lauer I.; Nawroth T.; Decker H.; Goerigk G.; von Krosigk G.
Structural Changes of Oxygen Transport Protein Hemocyamin Detected by pH-Dependent USAXS
Hamburg, HASYLAB, Usermeeting, 28.01.2000
23.89.1

IFF-00-23-028
Glück S.; Fischer P.; Schütz G.; Goerigk G.
Monitoring of the Circular Polarization State of Synchrotron Radiation at B1 (JUSIFA) Beamline
Hamburg, HASYLAB, Usermeeting, 28.01.2000
23.89.1

IFF-00-23-029
Goerigk G.; Williamson D. L.
Nanostructured Ge-Distribution in a-SiGe Alloys from Anomalous Small Angle X-ray Scatterinbg Studies
Hamburg, HASYLAB, Usermeeting, 28.01.2000
23.89.1

IFF-00-23-030
Grossmann M.1; Bolten D.1; Böttger U.1; Lohse O.1; Waser R.; Hartner W.; Kastner M.; Schindler G.
1 Institut für Werkstoffe der Elektrotechnik, RWTH Aachen, Germany
Imprint properties of SBT thin films
12th Int. Symp. Integrated Ferroelectrics, Aachen, 12.03.-15.03.00
23.42.0

IFF-00-23-031
Grossmann M.1; Lohse O.1; Bolten D.1; Böttger U.1; Waser R.
1 Institut für Werkstoffe der Elektrotechnik, RWTH Aachen, Germany
Imprint in ferroelectric thin films: trapped charges model
12th IEEE Int. Symp. on the Applications of Ferroelectrics, Honolulu, Hawaii, 31.07.-02.08.2000
23.42.0

IFF-00-23-032
Gutheim F.; Brener E.; Müller-Krumbhaar H.
Cluster und Stufenwachstum unter elastischer Verspannung
Frühjahrstagung der DPG, Regensburg, März 2000
23.15.0

IFF-00-23-033
Gwan J.-F.; Baumgärtner A.; Seifert R.; Kaupp U.B.
Computer simulation study of the binding effect of various ions in cyclic
nuleotide-gated channels.
3rd European Biophysics Congress
9.-13.Sept. 2000, Muenchen
23.30.0
42.50.0

IFF-00-23-034
Haegel F.-H.; Janssen M.; Dams P.; Dornseiffer J.; Otterstedt R.; Triefenbach D.; Pithan C.
Synthesis of oxidic nanoparticles from microemulsions
10th Int. Conf. On Colloid and Interface Science, Bristol, Great Britain, 23.07.-28.07.2000
23.42.0

IFF-00-23-035

Hartner W.1; Bosk P.1; Schindler G.2; Dehm C.1; Mazuré C.2; Schroeder H.; Waser R.
1 Siemens AG, München, Germany,
2 Infineon Technologies, München, Germany
Degradation mechanisms of SrBi2Ta2O9 ferroelectric thin film capacitors during forming gas annealing
12th Int. Symp. Integrated Ferroelectrics, Aachen, 12.03.-15.03.00
23.42.0

IFF-00-23-036
Heinrich M.; Pyckhout-Hintzen W.; Perny S.; Allgaier J.; Richter D.; Straube E.1
1Fachbereich Physik, Universität Halle
A SANS study of strained H-polymer melts in the quenched state
EPS, CMD-18, Montreux/Schweiz, 13. - 17.03.2000
23.30.0

IFF-00-23-037
Heinze S.; Bode M.1; Kubetzka A.1; Wortmann D.; Kurz Ph.; Pietzsch O.1; Nie X.; Blügel S.; Wiesendanger R.1
1Institut für Angewandte Physik, Universität Hamburg
Real space imaging of surface antiferromagnetism on the atomic scale
2nd Internationl Conference on Scanning Probe Spectroscopy , Hamburg
19.07.2000
23.20.0

IFF-00-23-038
Heinze S.; Wortmann D.; Bihlmayer G.; Blügel S.
Ab-initio calculations of tunneling through MgO barriers on Fe(001)
228. WE-Heraeus Seminar "Metal-Nonmetal Structures for Magnetoelectronics"
Physikzentrum Bad Honnef
05.01.2000
23.20.0

IFF-00-23-039
Hofer C.1; Weber U.1; Waser R.
1 Institut für Werkstoffe der Elektrotechnik, RWTH Aachen, Germany
Electrical characterization of grain boundary decorated strontiumtitanate ceramics
Int. Conf. on Electroceramics VII, Portoroz, Slovenia, 03.-06.09.2000
23.42.0

IFF-00-23-040
Hoffmann M.1; Küppers H.1; Schneller T.1; Böttger U.1; Schnakenberg U.1; Mokwa W.1; Waser R.
1 Institut für Werkstoffe der Elektrotechnik, RWTH Aachen, Germany
A new concept and first development results of a PZT thin film actuator
12th IEEE Int. Symp. on the Applications of Ferroelectrics, Honolulu, Hawaii, 31.07.-02.08.2000
23.42.0

IFF-00-23-041
Hupfeld D.; Brückel Th.; Schweika W.; Strempfer J.1; Mattenberger K.2
1APS at ANL, Argonne, USA
2ETH, Zürich, Switzerland
Resonante Austauschstreuung an GdxEu1-xS-Mischkristallen
Aachen, RWTH, 8. DGK Jahrestagung, 13. - 16.03.2000
23.89.1

IFF-00-23-042
Hupfeld D.; Strempfer J.1; Voigt J.; Goldman A.2; Brückel Th.
1Northern Illinois University, de Kalb, USA
2Ames Laboratory, Iowa State University, Ames, USA
X-ray resonance exchange scattering from a Tb single crystal
Chicago, USA, 10th Advanced Photon Source (APS) User Meeting, 02. - 04.05.2000
23.89.1

IFF-00-23-043
Jakobs B.1; Sottmann T.1; Strey R.1; Endo H.; Allgaier J.; Richter D.; Gompper G.
Amphiphilic blockcopolymers: Efficiency boosters for microemulsions
14. Vortragstagung der Fachgruppe Waschmittelchemie der GDCH, Würzburg, April 2000
23.30.0

IFF-00-23-044
Kann G.; Wirth I.; Eisebitt S.; Klingeler R.; Neeb M.; Eberhardt W.
Scanning tunnelling spectroscopy of La@C60: A metallic endohedral fullerene
8th International Conference on Electronic Spectroscopy and Structures
Berkeley, USA
08. - 12.08.2000-07-06
23.20.0

IFF-00-23-045
Kentzinger E.; Rücker U.; Nerger S.; Caliebe W.; Goerigk G.; Werges F.; Brückel Th.
Charakterisierung von dünnen epitaktischen (-Mn-Schichten mit Elektronenbeugung sowie Reflektometrie und diffuser Streuung von Synchrotronstrahlung
Aachen, RWTH, 8. DGK Jahrestagung, 13. - 16.03.2000
23.89.1

IFF-00-23-046
Kirstein O.; Kozielewski T.; Prager M.; Richter D.
Das Rückstreuspektrometer am FRM-II Reaktor
Wissenschaftliche Perspektiven 2001, Univ. München, 13.10.00
23.89.1

IFF-00-23-047
Klingeler R.
La@C60: A metallic endohedral fullerene
10th International Symposium on Small Particles and Inorganic Clusters, Atlanta, USA
13.10.2000
23.20.0

IFF-00-23-048
Klingeler R.
Mass spectra of metal-doped fullerene clusters MxCn>120 (M = Ce, Gd; x = 1,2
DPG-Frühjahrstagung Bonn
06.04.2000
23.20.0

IFF-00-23-049
Klingeler R.
Metal doped fullerenes: Endohedral and networked dopants
14th International Winterschool on Electronic Properties of Novel Materials: Molecular Nanostructures, Kirchberg, Österreich
März 2000
23.20.0

IFF-00-23-050
Kluge M.; Schober H.
Diffusion in Amorphous Solids and Liquids
DIMAT 2000, Paris, 18.07.2000
23.30.0

IFF-00-23-051
Knerr M.1; Krosigk G.2; Pyckhout-Hintzen W.; Göritz D.1
1Institut für Experimentelle und Angewandte Physik, Universität Regensburg
2DESY, Hamburg
Analyse der Dispergierung von Füllstoffen in Elastomeren mittels Ultrakleinwinkelstreuung
DPG Frühjahrstagung, Potsdam, 13. - 16.03.2000

23.30.0

IFF-00-23-052
Kuanr B.K.; Wingbermühle J.; Grünberg P.
Influence of anisotropy on FMR frequency of thin Permalloy and epitaxial Fe
Symposium on Spin-Electronics, Halle
05.07.2000
23.42.0

IFF-00-23-053
Köbler U.
Fourth-order exchange interactions - the driving forces in magnetism
Berlin, HMI, Nutzertreffen, 05.05.2000
23.15.0

IFF-00-23-054
Küppers H.1; Hoffmann M.1; Leuerer T.1; Schneller T.1; Böttger U.1; Schnakenberg U.1; Waser R.; Mokwa W.
1 Institut für Werkstoffe der Elektrotechnik, RWTH Aachen, Germany
Piezoelectric bending actuator for microelectro-mechanical applications
12th Int. Symp. Integrated Ferroelectrics, Aachen, 12.03.-15.03.00
23.42.0

IFF-00-23-055
Lemster K.1; Estermann M.A.1; Haibach T.1; Steurer W.1; Grushko B.
1 ETH Zuerich, 8092 Zurich, Switzerland
Dekagonale Approximanten hoher Ordnung im System Al-Co-X (X=Ni, Ta).
8. Jahrestagung der Deutschen Gesellschaft für Kristallographie. Aachen, Germany. März 2000.
23.55.0

IFF-00-23-056
Liedtke R.1; Hoffmann S.; Waser R.
1 Institut für Werkstoffe der Elektrotechnik, RWTH Aachen, Germany
Hydrogen induced degradation of (Ba,Sr)TiO3 thin films
12th Int. Symp. Integrated Ferroelectrics, Aachen, 12.03.-15.03.00
23.42.0

IFF-00-23-057
Liedtke R.1; Hoffmann S.; Waser R.
1 Institut für Werkstoffe der Elektrotechnik, RWTH Aachen, Germany
Recrystallization of oxygen ion implanted Ba0.7Sr0.3TiO3 thin films
12th IEEE Int. Symp. on the Applications of Ferroelectrics, Honolulu, Hawaii, 31.07.-02.08.2000
23.42.0

IFF-00-23-058
Link S.; Sievers J.; Dürr H.A.; Eberhardt W.
Lifetimes of image-potential states on the transition metal surfaces of Pt(111) and Ni(111)
8th International Conference on Electronic Spectroscopy and Structures
Berkeley, USA
08. - 12.08.2000
23.20.0

IFF-00-23-059
Lustfeld H.
Fast Slow behavior in the pollutant reaction equations of the troposphere
MPI für Physik komplexer Systeme, Dresden 18.5.-19.05.2000
23.15.0

IFF-00-23-060
Ma W.; Schäfer P.; Ehrhart P.; Waser R.
Metalorganic chemical vapor deposition of BaTiO3 and SrTiO3 thin films using a single solution source with a non-contact vaporizer
12th Int. Symp. Integrated Ferroelectrics, Aachen, 12.03.-15.03.00
23.42.0

IFF-00-23-061
Mavropoulos Ph.; Papanikolaou N.; Dederichs P.H.
Complex band structure and tunneling through Metal/Insulator/Metal junctions
International Symposium on Nanoscale Magnetism and Transport
Sendai, Japan, 08.-10.03.2000
23.20.0

IFF-00-23-062
Meyer R.1; Liedtke R.1; Waser R.
1 Institut für Werkstoffe der Elektrotechnik, RWTH Aachen, Germany
Modeling of the time dependent current in BST thin films in the short time range
12th IEEE Int. Symp. on the Applications of Ferroelectrics, Honolulu, Hawaii, 31.07.-02.08.2000
23.42.0

IFF-00-23-063
Mihailescu M.
Dynamics of microemulsions with polymeric cosurfactant
EPS, CMD-18, Montreux/Schweiz, 13. - 17.03.2000
23.30.0

IFF-00-23-064
Mitze C.1; Hasenkox U.1; Waser R.
1 Institut für Werkstoffe der Elektrotechnik, RWTH Aachen, Germany
On the magnetic structure of grain boundaries in doped manganates
12th Int. Symp. Integrated Ferroelectrics, Aachen, 12.03.-15.03.00
23.42.0

IFF-00-23-065
Morenzin J.; Kietzmann H.; Ganteför G.; Bechthold P.S.; Eberhardt W.
Magnetic properties of transition-metal clusters
10th Int. IUPAC Conf. on High Temperature Materials Chemistry, Jülich
11.04.2000
23.20.0

IFF-00-23-066
Morenzin J.; Kietzmann H.; Ganteför G.; Bechthold P.S.; Eberhardt W.
Spectroscopic evidence for the magnetic behavior of rhodium and ruthenium clusters
International Symposium on Small Particles and Inorganic Clusters (ISSPIC 10),. Atlanta, USA
11.10.2000
23.20.0

IFF-00-23-067
Mört M.1; Schindler G.2; Hartner W.1; Kasko I.1; Kastner M.1; Dehm C.1; Waser R.
1 Siemens AG München, Germany
2 Infineon Technologies, München, Germany
Low-temperature-process and thin-SBT-films for ferroelectric memory devices
12th Int. Symp. Integrated Ferroelectrics, Aachen, 12.03.-15.03.00
23.42.0

IFF-00-23-068
Nawroth T.; Gebhardt R.; Decker H.; Goerigk G.
XANES and EXAFS of Metalloproteins by Subtraction of True Reference Spectra Obtained with a Flow-Through Cell
Hamburg, HASYLAB, Usermeeting, 28.01.2000

23.89.1

IFF-00-23-069
Nerger S.; Kentzinger E.; Rücker U.; Voigt J.; Ott F.1; Seeck O.H.; Brückel Th.
1LLB, CEA/CNRS, France
Proximity effects in Fe1-xCox/Mn/Fe1-xCox trilayers
Sanct Petersburg, Russia, PNCMI-2000 International Workshop, 21.06.2000
23.89.1

IFF-00-23-070
Ohly C.; Hoffmann S.; Szot K.; Waser R.
Doped alkaline earth titanates: from the defect chemistry of bulk ceramics to the conduction behavior of thin films
12th IEEE Int. Symp. on the Applications of Ferroelectrics, Honolulu, Hawaii, 31.07.-02.08.2000
23.42.0

IFF-00-23-071
Ohly C.; Hoffmann S.; Szot K.; Waser R.
High temperature conductivity behaviour of doped SrTiO3 thin films
12th Int. Symp. Integrated Ferroelectrics, Aachen, 12.03.-15.03.00
23.42.0

IFF-00-23-072
Papanikolaou N.; Mavropoulos Ph.; Dederichs P.H.
Complex band structure and tunneling through Metal/Insulator/Metal junctions
Symposium on Spin-Electronics, Halle, 3-6.07.2000
23.20.0

IFF-00-23-073
Papanikolaou N.; Nonas B.; Zeller R.; Dederichs P.H.
Scanning Tunneling Spectra of Impurities in the Fe (001)surface
3rd Gordon Research Conference on Magnetic Nanostructures, February 2000, Ventura, California
23.20.0

IFF-00-23-074
Pontius N.; Bechthold P.S.; Neeb M.; Eberhardt W.
Time-resolved photoelectron spectroscopy of small metal cluster anions
8th International Conference on Electronic Spectroscopy and Structures
Berkeley, USA
08. - 12.08.2000
23.20.0

IFF-00-23-075
Prager M.
The thermal TOF spectrometer SV29 at the FRJ2-DIDO reactor, Jülich
FRM-2, Univ. München, 13.10.00
23.89.1

IFF-00-23-076
Prume K.1; Hoffmann S.; Waser R.
1 Institut für Werkstoffe der Elektrotechnik, RWTH Aachen, Germany
Finite-element simulations of interdigital electrode structures on high permittivity thin films
12th Int. Symp. Integrated Ferroelectrics, Aachen, 12.03.-15.03.00
23.42.0

IFF-00-23-077
Prume K.1; Waser R.
1 Institut für Werkstoffe der Elektrotechnik, RWTH Aachen, Gemany
Finite element simulation of multiplayer structures and devices
12th IEEE Int. Symp. on the Applications of Ferroelectrics, Honolulu, Hawaii, 31.07.-02.08.2000
23.42.0

IFF-00-23-078
Pyckhout-Hintzen W.; Westermann S.; Botti A.; Richter D.; Straube E.1
1Fachbereich Physik, Universität Halle
Local chain deformation in polymer networks by SANS
EPS, CMD-18, Montreux/Schweiz, 13. - 17.03.2000
23.30.0

IFF-00-23-079
Rickes J.T.; Waser R.
The effect of imprint on read and write operations in ferroelectric random access memories for lifetime prediction
12th IEEE Int. Symp. on the Applications of Ferroelectrics, Honolulu, Hawaii, 31.07.-02.08.2000
23.42.0

IFF-00-23-080
Roelofs A.1; Grossmann M.1; Hoffmann M.1; Schneller T.1; Böttger U.1; Waser R.; Schlaphof F.2; Eng L.M.2
1 Institut für Werkstoffe der Elektrotechnik, RWTH Aachen, Germany
2 TU Dresden, Germany
Nanoscale characterization of chemical solution deposition derived Ba{0.5}Pb{0.5}TiO3 thin films with scanning force microscopy
12th Int. Symp. Integrated Ferroelectrics, Aachen, 12.03.-15.03.00
23.42.0

IFF-00-23-081
Roelofs A.1; Schlaphof F.2; Schneller T.1; Grossmann M.1; Böttger U.1; Waser R.; Eng L.M.2
1 Institut für Werkstoffe der Elektrotechnik, RWTH Aachen, Germany
2 TU Dresden, Germany
Nanoscale characterization of chemical solution deposited PbTiO3 thin films with scanning force microscopy
12th IEEE Int. Symp. on the Applications of Ferroelectrics, Honolulu, Hawaii, 31.07.-02.08.2000
23.42.0

IFF-00-23-082
Rottländer P.; Kohlstedt H.; Girgis E.; Schelten J.; Grünberg P.
Transportmessungen an UV-oxidierten Tunnelmagnetowiderstandselementen
DPG-Frühjahrstagung Regensburg
März 2000
23.20.0
23.42.0

IFF-00-23-083
Rücker U.; Bergs W.; Alefeld B.; Kentzinger E.; Brückel Th.
The new polarized neutron Reflectometer in Juelich
Sanct Petersburg, Russia, PNCMI-2000 International Workshop, 21.06.2000
23.89.1

IFF-00-23-084
Sambeth R.; Baumgärtner A.
A 2-d model for cell locomotion based on actin polymerization.
Biophysics and biochemistry of motor proteins
27.9.-1.10.2000, Banff, Canada
23.30.0
46.10.0

IFF-00-23-085
Sambeth R.; Baumgärtner A.
A complete one dimensional model for force generation based on the
treadmilling of filaments.
Numerical simulations on polymer and cell dynamics.
13.6.-16.6.2000, Honnef
23.30.0
46.10.0

IFF-00-23-086

Sambeth R.; Baumgärtner A.
Signal induced motility in a complete two dimensional model for amoeboid
motion based on the polymerization of actin.
3rd European Biophysics Congress
9.-13.Sept. 2000, Muenchen
23.30.0
46.10.0

IFF-00-23-087
Schroeder H.
On leakage current models applied to thin films
12th Int. Symp. Integrated Ferroelectrics, Aachen, 12.03.-15.03.00
23.42.0

IFF-00-23-088
Schroeder K.; Antons A.; Berger R.; Kromen W.; Blügel S.
Kinetics of group-IV adatoms on As-covered Si(111): diffusion and exchange processes
CHIPPS'2000, Wandlitz bei Berlin, 15.-18.05.2000
23.42.0

IFF-00-23-089
Schweika W.; Ice G. E.1; Robertson J. L.1; Sparks C. J.1; Bai J.1
1ORNL, Oak Ridge, USA
Gitterverschiebungen und Fermiflächeneffekte in Cu3Au
Aachen, RWTH, 8. DGK Jahrestagung, 13. - 16.03.2000
23.89.1

IFF-00-23-090
Schweika W.
The Instrument DNS: Polarization Analysis for Diffuse Neutron Scattering
Sanct Petersburg, Russia, PNCMI-2000 International Workshop, 21.06.2000
23.89.1

IFF-00-23-091
Schäfer P.; Ma W.; Waser R.
Preparation of (Pb,Ba)TiO3 thin films by MOCVD using an aerosol-assisted liquid delivery system
12th Int. Symp. Integrated Ferroelectrics, Aachen, 12.03.-15.03.00
23.42.0

IFF-00-23-092
Schäfer P.; Ritter S.; Ganster R.; Hoffmann S.; Waser R.
Preparation of (Pb,Ba)TiO3 thin films by MOCVD using an aerosol-assisted liquid delivery system
12th Int. Symp. Integrated Ferroelectrics, Aachen, 12.03.-15.03.00
23.42.0

IFF-00-23-093
Schäfer P.; Ritter S.; Hoffmann S.; Waser R.
(Pb1-xBax)TiO3 thin films prepared by MOCVD: film formation and electrical properties
Int. Conf. on Electroceramics VII, Portoroz, Slovenia, 03.-06.09.2000
23.42.0

IFF-00-23-094
Schütz G.
Emergence of macroscopic non-equilibrium behaviour from microscopic dynamics in quantum spin chains
DPG-Frühjahrstagung, Regensburg
27. 3. 2000
23.15.0

IFF-00-23-095
Shur V.Y.; Nikolaeve E.V.; Shishkin E.I.; Baturin I.S.; Bolten D.; Waser R.
Fatigue in PZT thin films
MRS Fall Meeting, Boston, 27.11.-01.12.00
23.42.0

IFF-00-23-096
Slowak R.1; Schneller T.1; Waser R.
1 Institut für Werkstoffe der Elektrotechnik, RWTH Aachen, Germany
High-permittivity temperature independent devices up to 2000C by modified graded thin films
12th Int. Symp. Integrated Ferroelectrics, Aachen, 12.03.-15.03.00
23.42.0

IFF-00-23-097
Wang Y.G.; Kentzinger E.; Rücker U.; Caliebe W.; Goerigk G.; Babik W.; Brückel Th.
Strukturelle Charakterisierung von Fe/Cr/Fe Schichtsystemen
Aachen, RWTH, 8. DGK Jahrestagung, 13. - 16.03.2000
23.89.1

IFF-00-23-098
Wang Y.G.; Kentzinger E.; Rücker U.; Seeck O.H.; Brückel Th.; Schreiber R.; Bürgler D.E.; Grünberg P.
Characterization of the buried interfaces in Fe/Cr/Fe trilayers using synchrotron radiation
VDI Statusseminar "Magnetoelektronik", Dresden
14. - 16.06.2000
23.42.0

IFF-00-23-099
Wang Y.G.; Kentzinger E.; Rücker U.; Seeck O.H.; Brückel Th.; Schreiber R.; Bürgler D.aE.; Grünberg P.
Characterization of the Buried Interfaces in Fe/Cr/Fe Trilayers using Synchrotron Radiation
Dresden, VDI-Tagung, 13. - 16.06.2000
23.89.1

IFF-00-23-100
Waser R.; Hölbling Th.1
1 Institut für Werkstoffe der Elektrotechnik , RWTH Aachen, Germany
1D modelling of charge transport in SrTiO3 ceramics
Int. Conf. on Electroceramics VII, Portoroz, Slovenia, 03.-06.09.2000
23.42.0

IFF-00-23-101
Willner L.; Allgaier J.
Synthese von amphiphilen Di-, Tri- und Sternblockcopolymeren via HO-funktionalisierter Polydiene
Vortragstagung: "Maßgeschneiderte Polymere", Merseburg, 20. - 21.03.00
23.30.0

IFF-00-23-102
Wortmann D.; Heinze S.; Bihlmayer G.; Blügel S.
Ab-initio calculations of tunneling through MgO barriers on Fe(001)
SSE-2000: Symposium on Spin-Electronics, Halle, Germany
03.-06.07.2000
23.20.0

IFF-00-23-103
Yurechko M.; Grushko B.
Orthorhombic "Al3TM" phases in Al-Pd and Al-Rh
Frühjahrstagung des Arbeitskreises Festkörperphysik bei der DPG. Regensburg, Germany. März 2000
23.55.0

IFF-00-23-104
Yurechko M.; Gwózdz J.1; Grushko B.
1 University of Silesia, Inst. Phys. Chem. Metals. 40-007 Katowice, Poland
Phase equilibrium in Al-Cu-Rh in the vicinity of the decagonal phase.
SPQK-Kolloquium 2000 Jülich, Germany, April 2000.
23.55.0

IFF-00-23-105
Zeller R.
Energy Interpolation for the Tight-Binding Korringa-Kohn-Rostoker Structure Constants
Schwäbisch-Gmünd, 23.08.2000
23.20.0

List of references

Alefeld B.	IFF-00-23-001	IFF-00-23-083	
Allgaier J.	IFF-00-23-036	IFF-00-23-043	IFF-00-23-101
Antons A.	IFF-00-23-002	IFF-00-23-003	IFF-00-23-088
Babik W.	IFF-00-23-097		
Baldus O.	IFF-00-23-005	IFF-00-23-024	
Baumgärtner A.	IFF-00-23-033 IFF-00-23-086	IFF-00-23-084	IFF-00-23-085
Bechthold P.S.	IFF-00-23-026 IFF-00-23-074	IFF-00-23-065	IFF-00-23-066
Bellini V.	IFF-00-23-006		
Berger R.	IFF-00-23-002	IFF-00-23-003	IFF-00-23-088
Bergs W.	IFF-00-23-083		
Bihlmayer G.	IFF-00-23-007 IFF-00-23-102	IFF-00-23-015	IFF-00-23-038
Blügel S.	IFF-00-23-002 IFF-00-23-015 IFF-00-23-088	IFF-00-23-003 IFF-00-23-037 IFF-00-23-102	IFF-00-23-007 IFF-00-23-038
Botti A.	IFF-00-23-078		
Brener E.	IFF-00-23-032		
Bringer A.	IFF-00-23-022	IFF-00-23-023	
Brückel Th.	IFF-00-23-001 IFF-00-23-045 IFF-00-23-097	IFF-00-23-041 IFF-00-23-069 IFF-00-23-098	IFF-00-23-042 IFF-00-23-083 IFF-00-23-099
Buchmeier M.	IFF-00-23-010		
Bürgler D.E.	IFF-00-23-010 IFF-00-23-098	IFF-00-23-012 IFF-00-23-099	IFF-00-23-013
Cabria	.	IFF-00-23-014	
Caliebe W.	IFF-00-23-045	IFF-00-23-097	
Clarke S.	IFF-00-23-015		
Cramm S.	IFF-00-23-022	IFF-00-23-023	
Dederichs P.H.	IFF-00-23-006 IFF-00-23-025 IFF-00-23-073	IFF-00-23-014 IFF-00-23-061	IFF-00-23-016 IFF-00-23-072
Dohmen L.	IFF-00-23-001		
Dürr H.A.	IFF-00-23-018	IFF-00-23-058	
Eberhardt W.	IFF-00-23-019 IFF-00-23-026 IFF-00-23-065	IFF-00-23-022 IFF-00-23-044 IFF-00-23-066	IFF-00-23-023 IFF-00-23-058 IFF-00-23-074
Ehrhart P.	IFF-00-23-021	IFF-00-23-060	
Eisebitt S.	IFF-00-23-022	IFF-00-23-023	IFF-00-23-044
Endo H.	IFF-00-23-043		
Fitsilis F.	IFF-00-23-021		
Freiwald M.	IFF-00-23-022	IFF-00-23-023	
Freyss M.	IFF-00-23-025		

Mihailescu M.	IFF-00-23-063		
Morenzin J.	IFF-00-23-065	IFF-00-23-066	
Müller-Krumbhaar H.	IFF-00-23-032		
Neeb M.	IFF-00-23-026	IFF-00-23-044	IFF-00-23-074
Nerger S.	IFF-00-23-045	IFF-00-23-069	
Nie X.	IFF-00-23-007	IFF-00-23-015	IFF-00-23-037
Nonas B.	IFF-00-23-014	IFF-00-23-073	
Ohly C.	IFF-00-23-070	IFF-00-23-071	
Otterstedt R.	IFF-00-23-034		
Papanikolaou N.	IFF-00-23-006 IFF-00-23-061	IFF-00-23-016 IFF-00-23-072	IFF-00-23-025 IFF-00-23-073
Perny S.	IFF-00-23-036		
Pithan C.	IFF-00-23-034		
Pontius N.	IFF-00-23-026	IFF-00-23-074	
Prager M.	IFF-00-23-046	IFF-00-23-075	
Pyckhout-Hintzen W.	IFF-00-23-020 IFF-00-23-078	IFF-00-23-036	IFF-00-23-051
Regnery S.	IFF-00-23-021		
Richter D.	IFF-00-23-036 IFF-00-23-078	IFF-00-23-043	IFF-00-23-046
Rickes J.T.	IFF-00-23-079		
Ritter S.	IFF-00-23-092	IFF-00-23-093	
Rottländer P.	IFF-00-23-082		
Rücker U.	IFF-00-23-045 IFF-00-23-097	IFF-00-23-069 IFF-00-23-098	IFF-00-23-083 IFF-00-23-099
Sambeth R.	IFF-00-23-084	IFF-00-23-085	IFF-00-23-086
Schelten J.	IFF-00-23-082		
Scherer R.	IFF-00-23-022	IFF-00-23-023	
Schober H.	IFF-00-23-050		
Schondelmaier D.	IFF-00-23-022	IFF-00-23-023	
Schreiber R.	IFF-00-23-010	IFF-00-23-098	IFF-00-23-099
Schroeder H.	IFF-00-23-035	IFF-00-23-087	
Schroeder K.	IFF-00-23-002	IFF-00-23-003	IFF-00-23-088
Schweika W.	IFF-00-23-041	IFF-00-23-089	IFF-00-23-090
Schäfer P.	IFF-00-23-060 IFF-00-23-093	IFF-00-23-091	IFF-00-23-092
Schütz G.	IFF-00-23-094		
Seeck O.H.	IFF-00-23-069	IFF-00-23-098	IFF-00-23-099
Seifert R.	IFF-00-23-033		
Sievers J.	IFF-00-23-058		
Szot K.	IFF-00-23-070	IFF-00-23-071	

Triefenbach D.	IFF-00-23-034		
Voigt J.	IFF-00-23-042	IFF-00-23-069	
Wang Y.G.	IFF-00-23-097	IFF-00-23-098	IFF-00-23-099
Waser R.	IFF-00-23-004	IFF-00-23-005	IFF-00-23-008
	IFF-00-23-009	IFF-00-23-011	IFF-00-23-021
	IFF-00-23-024	IFF-00-23-030	IFF-00-23-031
	IFF-00-23-035	IFF-00-23-039	IFF-00-23-040
	IFF-00-23-054	IFF-00-23-056	IFF-00-23-057
	IFF-00-23-060	IFF-00-23-062	IFF-00-23-064
	IFF-00-23-067	IFF-00-23-070	IFF-00-23-071
	IFF-00-23-076	IFF-00-23-077	IFF-00-23-079
	IFF-00-23-080	IFF-00-23-081	IFF-00-23-091
	IFF-00-23-092	IFF-00-23-093	IFF-00-23-095
	IFF-00-23-096	IFF-00-23-100	
Werges F.	IFF-00-23-045		
Westermann S.	IFF-00-23-078		
Willner L.	IFF-00-23-101		
Wingbermühle J.	IFF-00-23-052		
Wirth	.	IFF-00-23-044	
Wortmann D.	IFF-00-23-037	IFF-00-23-038	IFF-00-23-102
Yurechko M.	IFF-00-23-103	IFF-00-23-104	
Zeller R.	IFF-00-23-006	IFF-00-23-014	IFF-00-23-025
	IFF-00-23-073	IFF-00-23-105	
Zimina A.	IFF-00-23-022	IFF-00-23-023	

Patents

Patents granted

IFF-00-31-001
Allgaier J.; Willner L.; Richter D.
Verfahren zur Herstellung von Hydrophob-Hydrophilen AB-Blockcoplymeren
EP 0904307 (28.06.2000) (DE,FR,GB,IT); PT 1.1375
23.30.0

IFF-00-31-002
Divin Y.Y.: Seo J.W.; Poppe U.
Schichtenfolge mit wenigstens einer epitaktischen nicht c-Achsen orientierten Schicht aus einer mit Hochtemperatursupraleitern kristallographisch vergleichbaren Struktur
EP: 0868753 (12.04.2000) (DE, FR, GB)
PT 1.333
23.42.0

IFF-00-31-003
Klein A.; Scholen A.
"Dual-mode"-Mikrowellen-Bandpaßfilter aus Hochgüterresonatoren
EP: 0896744 (31.05.2000) (De, ES, IT, FR, GB, SE)
PT 1.1369
23.42.0

IFF-00-31-004
Soltner J.; Zhang Y.1; Zander W.1; Banzet M.1; Schubert J.1
1ISI
Anordnung zur Ankopplung eines rf-SQUID-Magnetometers an einem supraleitenden Tankschwingkreis auf einem Substrat
DE: 196 11 900 (1007.2000)
PT 1.1356
29.85.0

List of references

Allgaier J.	IFF-00-31-001
Divin Y.Y.	IFF-00-31-002
Klein A.	IFF-00-31-003
Poppe U.	IFF-00-31-002
Richter D.	IFF-00-31-001
Scholen A.	IFF-00-31-003
Seo J.W.	IFF-00-31-002
Soltner J.	IFF-00-31-004
Willner L.	IFF-00-31-001

Patents applied for

IFF-00-32-001
Dohmen L.; Alefeld B.
Geschwindigkeitsselektor zur Monochromatisierung eines Neutronenstrahls
Deutsche Patentanmeldung PCT/DE 00/00238 (23.01.2000) (EP,US,JP)
PT 1.1656
23.89.1

IFF-00-32-002
Hoffmann S.; Waser R.; Slowak R.1; Liedtke R.1
1RWTH Aachen
Dünnschichtkondensator
PCT: PCT/EP 00/09319 (26.08.2000) (EP,US,JP,KR)
PT 1.1726
17.22.0

IFF-00-32-003
Kohlstedt H.; Rodriguez J.
Verfahren zur Erzeugung eines Tunnelkontaktes sowie eine Vorrichtung umfassende Mittel zur Erzeugung eines Tunnelkontaktes
DE: 100 59 357.7 (29.11.2000)
PT 1.1859
23.42.0

IFF-00-32-004
Kohlstedt H.; Rottländer P.
Verfahren zur Herstellung eines magnetischen Tunnelkontaktes sowie magnetischer Tunnelkontakt
PCT: PCT/EP 00/07012 (21.07.2000) (EP, US,JP;KR)
PT 1.1721
23.42.0

IFF-00-32-005
Kohlstedt H.; Stein S.
Dreitorbauelement
DE: 100 31 401.5-33 (03.07.2000)
PT 1.1810
23.42.0

IFF-00-32-006
Kohlstedt H.
Anordnung zum Messen eines Magnetfeldes und Verfahren zum Herstellen einer Anordnung zum Messen eines Magnetfeldes
DE: 100 09 944.0 (02.03.2000)
PT 1.1782
23.42.0

IFF-00-32-007
Kohlstedt H.
Speicherkondensator
PCT: PCT/DE 00/02184 (04.07.2000) (EP,US,JP)
PT 1.1713
23.42.0

IFF-00-32-008
Nie X.
Magnetisches Schichtsystem sowie ein solches Schichtsystem aufweisendes Bauelement
DE: 10046782.2 (21.09.2000)
PT 1.1832
23.20.0

IFF-00-32-009
Morenzin J.; Eberhardt W.
Markierungseinrichtung sowie Verfahren zum Auslesen einer solchen Markierungseinrichtung
DE: 100 08 097.9 (22.02.2000); PT 1.1777
23.20.0

IFF-00-32-010
Morenzin J.; Eberhardt W.
Positionsmeßeinrichtung
DE: 100 52 086.3 (20.10.2000); PT 1.1853
23.20.0

IFF-00-32-011
Poppe U.; Faley M.; Zimmermann E.1; Halling H.1
1ZEL
Magnetflußsensor mit schleifenförmigen Magnetfeldleiter sowie dessen Herstellung
PCT: PCT/DE 00/00962 (30.03.2000) (EP, US, JP)
PT 1.1674
23.42.0, 52.90.0

IFF-00-32-012
Schober T.; Meuffels P.; Friedrich J.
Verfahren zur Wasserstoffdosierung
DE: 100 53 986.6 (31.10.2000)
PT 1.1850
23.42.0

IFF-00-32-013
Schondelmaier D.; Eberhardt W.
Verfahren zur Behandlung von Oberflächen sowie mit diesem Verfahren hergestellte Gegenstände und Verwendung von Verbindungen als photochemisch spaltbare Reagenzien
DE: 100 30 797.3 (29.06.2000), PT 1.1798
23.20.0

IFF-00-32-014
Sonnenberg K.; Küssel E.
Verfahren und Vorrichtung zur Herstellung von Einkristallen sowie Kristallkeim
Deutsche Patentanmeldung 199 12 486.8-43 EP: 00105206.7 (13.03.2000)
PT 1.1681
23.89.1

IFF-00-32-015
Sonnenberg K.; Küssel E.
Vorrichtung zur Herstellung von Einkristallen
Deutsche Patentanmeldung 199 12 484.1-43 PCT/DE 00/02349 (16.03.2000) (EP,US,JP)
PT 1.1680
23.89.1

IFF-00-32-016
Szot K.; Speier W.
Teleskopartiger Mikromanipulator mit Piezomaterialien
PCT: PCT/DE 00/01070 (05.04.2000) (EP,US,JP,KR,CN)
PT 1.1679
23.42.0

IFF-00-32-017
Waser R.; Baldus O.; Krasser W.
Lasersystem mit steuerbarer Pulsdauer
PCT: PCT/DE 00/04314 (04.12.2000) (EP,US,JP,KR)
PT 1.1754
23.42.0

IFF-00-32-018
Waser R.; Baldus O.; Krasser W.
Verfahren zur Herstellung einer kristallisierten keramischen Schicht durch Laser-Annealing
PCT: PCT/DE 00/04313 (04.12.2000) (EP,US,JP,KR)
PT 1.1755
23.42.0

IFF-00-32-019
Zimmermann E.1; Glass W.1; Halling H1.; Soltner H.; Faley M.
1ZEL
SQUID-Mikroskop
DE: 100 53 034.6 (26.10.2000)
PT 1.1838
FE 23.420

List of references

Alefeld B.	IFF-00-32-001		
Baldus O.	IFF-00-32-018	IFF-00-32-019	
Dohmen L.	IFF-00-32-001		
Eberhardt W.	IFF-00-32-009 IFF-00-32-014	IFF-00-32-010	IFF-00-32-011
Faley M.	IFF-00-32-012	IFF-00-32-020	
Friedrich J.	IFF-00-32-013		
Hoffmann S.	IFF-00-32-002		
Kohlstedt H.	IFF-00-32-003 IFF-00-32-006	IFF-00-32-004 IFF-00-32-007	IFF-00-32-005
Krasser W.	IFF-00-32-018	IFF-00-32-019	
Küssel E.	IFF-00-32-015	IFF-00-32-016	
Meuffels P.	IFF-00-32-013		
Morenzin J.	IFF-00-32-009	IFF-00-32-010	IFF-00-32-011
Nie X.	IFF-00-32-008		
Poppe U.	IFF-00-32-012		
Rodriguez J.	IFF-00-32-003		
Rottländer P.	IFF-00-32-004		
Schober T.	IFF-00-32-013		
Schondelmaier D.	IFF-00-32-014		
Soltner H.	IFF-00-32-020		
Sonnenberg K.	IFF-00-32-015	IFF-00-32-016	
Speier W.	IFF-00-32-017		
Stein S.	IFF-00-32-005		
Szot K.	IFF-00-32-017		
Waser R.	IFF-00-32-002	IFF-00-32-018	IFF-00-32-019

Lecture

Lecture courses

IFF-00-41-001
Baumgärtner A.
Einführung in die theoretische Biophysik I.
Universität Duisburg, V2
SS 2000

IFF-00-41-002
Baumgärtner A.
Einführung in die theoretische Biophysik II.
Universität Duisburg, V2
WS 2000/2001

IFF-00-41-003
Baumgärtner A.
Theoretische Physik fürs Lehramt II.
Universität Duisburg, V2, Ue2
WS 1999/2000

IFF-00-41-004
Bechthold P.S.
Cluster und Clustermaterie
Universität zu Köln
SS2000
23.20.0

IFF-00-41-005
Bechthold P.S.
Ultrakurze Laserimpulse: Erzeugung, Handhabung, Nachweis
31. IFF-Ferienschule 2000 Femtosekunden und Nano-eV:
Dynamik in kondensierter Materie
13. - 23.03.2001
23.20.0

IFF-00-41-006
Blügel S.; Dederichs P.H.; Müller-Krumbhaar H.; Schroeder K.
Computeranwendungen in der Festkörperphysik,
Physikalisches Seminar (6h), WS 2000/2001, RWTH Aachen
23.20.0

IFF-00-41-007
Blügel S.; Dederichs P.H.; Müller-Krumbhaar H.; Schroeder K.
Computeranwendungen in der Festkörperphysik,
Physikalisches Seminar (6h), WS 2000/2001, RWTH Aachen
23.42.0

IFF-00-41-008
Blügel S.
Dynamik in kondensierter Materie
31. IFF-Ferienschule 2000 Femtosekunden und Nano-eV:
Dynamik in kondensierter Materie
13. - 23.03.2001
23.20.0

IFF-00-41-009
Bringer, A.
SS 2000: Numerische Methoden in der Physik
23.20.0

IFF-00-41-010
Brückel Th.; Schweika W.
Ferienschule (Praktikum) über Neutronenstreuung
TV 10 / TÜ 30, WS 00/01

IFF-00-41-011
Brückel Th.
Festkörpermagnetismus und hochkorrelierte
Elektronensysteme
RWTH Aachen, V2, SS 00
1.2 FKF

IFF-00-41-012
Buchenau U.; Schmid D.1
1Univ. Düsseldorf, Inst. für Festkörperspektroskopie
Experimentalphysik VI (Festkörperphysik)
SS 00, Univ. Düsseldorf
23.15.0

IFF-00-41-013
Bürgler D.E.; Grünberg P.
Magnetoelektronik in Forschung und Anwendung
31. IFF-Ferienschule 2000 Femtosekunden und Nano-eV:
Dynamik in kondensierter Materie
13. - 23.03.2001
23.42.0

IFF-00-41-014
Bürgler D.E.
Beitrag zur Ringvorlesung "Kondensierte Materie III"
Universität Basel
SS2000
23.42.0

IFF-00-41-015
Bürgler D.E.
Magnetoelektronik in Forschung und Anwendung
31. IFF-Ferienschule 2000 Femtosekunden und Nano-eV:
Dynamik in kondensierter Materie
13. - 23.03.2001
23.42.0

IFF-00-41-016
Capellmann H.1; Schroeder K.
1Institut für Theoretische Physik, RWTH Aachen
Theoretische Festskörperphysik I, Vorlesung (4h) und Übung
(2h), SS 2000, RWTH Aachen
23.42.0

IFF-00-41-017
Dederichs P.H.
Grundlagen der Elektronentheorie
31. IFF Ferienkurs "Femtosekunden und Nano-eV:Dynamik in
kondensierter Materie", Jülich 13.-24.03.2000
23.20.0

IFF-00-41-018
Dürr H.A.
Fsec-Magnetism
31. IFF-Ferienschule 2000 Femtosekunden und Nano-eV:
Dynamik in kondensierter Materie
13. - 23.03.2001
23.20.0

IFF-00-41-019
Eberhardt W.
Oberseminar "Magnetoelektronik"
Universität zu Köln
WS2000/01
23.20.0

IFF-00-41-020
Ebert Ph.
Oberflächen von Quasikristallen
Physikalisches Kolloquium, RWTH Aachen, Germany, April
10, 2000.
23.55.0

IFF-00-41-021
Eilenberger G.
WS 2000/2001: 5-stündige Vorlesung. Universität zu Köln:
Analysis 1 für Physiker
23.20.0

IFF-00-41-022
Eisebitt S.
Resonante inelastische Röntgenstreuung: Messungen mit
atomarer Stoppuhr
31. IFF-Ferienschule 2000 Femtosekunden und Nano-eV:
Dynamik in kondensierter Materie
13. - 23.03.2001

23.20.0

IFF-00-41-023
Eisenriegler E.
Statistische Physik von Polymeren
Universität Düsseldorf, 2-std.
SS 2000

IFF-00-41-024
Grimm H.
Crystal spectrometer: triple-axis and back-scattering spectrometer
WS 00/01, Laboratory Course Neutron Scattering, FZ Jülich, 26.09. - 06.10.00
23.15.0

IFF-00-41-025
Grimm H.
Rotation and Translation
SS 00, Laboratory Course Neutron Scattering, FZ Jülich, 26.09. - 06.10.00
23.15.0

IFF-00-41-026
Monkenbusch M.
Introduction to soft matter systems
SS 00, Summerschool on Neutron Scattering, Zuoz/Switzerland, 08. - 12.08.00
23.30.0

IFF-00-41-027
Monkenbusch M.
Neutronenspektroskopie
WS 99/00, IFF Ferienschule: Femtosekunden und Nano-eV, FZ Jülich, 13.03. - 24.03.00
23.30.0

IFF-00-41-028
Monkenbusch M.
Time-of-flight spectrometers
WS 00/01, Laboratory Course Neutron Scattering, FZ Jülich, 26.09. - 06.10.00
23.89.1

IFF-00-41-029
Müller-Krumbhaar H.
Computeranwendungen in der Festkörperphysik
RWTH-Aachen, WS 00/01
23.15.0

IFF-00-41-030
Müller-Krumbhaar H.
Praktisches Rechnen für Naturwissemschaftler
RWTH-Aachen, WS 99/00.
23.15.0

IFF-00-41-031
Neeb M.
Molekulardynamik chemischer Reaktionen auf der Femtosekundenskala: "Die schnellste Kamera der Welt"
31. IFF-Ferienschule 2000 Femtosekunden und Nano-eV: Dynamik in kondensierter Materie
13. - 23.03.2001
23.20.0

IFF-00-41-032
Prager M.
Rotation and Translation
WS 00/01, Laboratory Course Neutron Scattering, FZ Jülich, 26.09. - 06.10.00
23.15.0

IFF-00-41-033
Richter D.
Dynamik von Polymeren
WS 99/00, IFF Ferienschule: Femtosekunden und Nano-eV, FZ Jülich, 13.03. - 24.03.00
23.30.0

IFF-00-41-034
Richter D.
Polymer dynamics
WS 00, Laboratory Course Neutron Scattering, FZ Jülich, 26.09. - 06.10.00
23.30.0

IFF-00-41-035
Richter D.
Properties of the neutron, elementary scattering process
WS 00, Laboratory Course Neutron Scattering, FZ Jülich, 26.09. - 06.10.00
23.30.0

IFF-00-41-036
Schroeder H.
Ausgewählte Kapitel der Metallkunde
Fakultät für Bergbau, Hüttenwesen und Geowissenschaften der RWTH Aachen, WS 99/2000 und WS 2000/01
23.42.0

IFF-00-41-037
Schroeder K.
Elementare Anregungen: Phononen und Magnonen
31. IFF-Ferienkurs "fs und neV: Dynamik in kondensierter Materie", Jülich, 13.-24.03.2000
23.42.0

IFF-00-41-038
Schwahn D.
Small angle scattering and reflectometry
WS 00/01, Laboratory Course Neutron Scattering, FZ Jülich, 26.09. - 06.10.00
23.30.0

IFF-00-41-039
Schwahn D.
Soft matter structure
WS 00/01, Laboratory Course Neutron Scattering, FZ Jülich, 26.09. - 06.10.00
23.30.0

IFF-00-41-040
Schütz G.
Gläser: Physikalische Konzepte und numerische Methoden
Universität Bonn, 2-std.
WS 2000/2001

IFF-00-41-041
Sturm K.
SS 2000: 2-stündige Vorlesung an der Universität Düsseldorf: Elektronische Anregungen im Festkörper
23.20.0

IFF-00-41-042
Sturm K.
WS 1999/2000: Vorlesung im 31. IFF-Ferienkurs: Dynamik in kondensierter Materie
März 2000
23.20.0

IFF-00-41-043
Waser R.; Ehrhart P.; Hoffmann S.; Kohlstedt H.H.; Schroeder H.
Neue Materialien und Bauelemente für die Informationstechnik I (WS 99/2000)
Vertiefungsfach II
RWTH Aachen, WS 1999/2000
23.42.0

IFF-00-41-044
Waser R.
Vorlesung Werkstoffe der Elektrotechnik
Sensoren und Sensormeßtechnik I+II
RWTH Aachen

23.42.0

IFF-00-41-045
Zorn R.
Correlation functions measured by scattering experiments
WS 00/01, Laboratory Course Neutron Scattering, FZ Jülich, 26.09. - 06.10.00
23.15.0

IFF-00-41-046
Zorn R.
Inelastic neutron scattering: dynamics of polymers
5th European School on Neutron Scattering Methods Applied to Soft Condensed Matter, Bombannes/France, 28.05. - 03.06.00
23.15.0

IFF-00-41-047
Zorn R.
Ionentransport in Elektrolyten
WS 99/00, IFF Ferienschule: Femtosekunden und Nano-eV, FZ Jülich, 13.03. - 24.03.00
23.15.0

IFF-00-41-048
Zorn R.
Neutron Spin Echo Spectrometer
WS 00/01, Laboratory Course Neutron Scattering, FZ Jülich, 26.09. - 06.10.00
23.15.0

Scientific degrees, further education

Program	Diplomas granted	Doctor. comp.	Habil. comp.	Prof. Pos. off.
1.2 FKF	11	11		3
2.1 PGI	2	1	1	
Sum	13	12	1	3

List of references

Baumgärtner A.	IFF-00-41-001	IFF-00-41-002	IFF-00-41-003
Bechthold P.S.	IFF-00-41-004	IFF-00-41-005	
Blügel S.	IFF-00-41-006	IFF-00-41-007	IFF-00-41-008
Bringer, A.	IFF-00-41-009		
Brückel Th.	IFF-00-41-010	IFF-00-41-011	
Buchenau U.	IFF-00-41-012		
Bürgler D.E.	IFF-00-41-013	IFF-00-41-014	IFF-00-41-015
Dederichs P.H.	IFF-00-41-006	IFF-00-41-007	IFF-00-41-017
Dürr H.A.	IFF-00-41-018		
Eberhardt W.	IFF-00-41-019		
Ebert Ph.	IFF-00-41-020		
Ehrhart P.	IFF-00-41-043		
Eilenberger G.	IFF-00-41-021		
Eisebitt S.	IFF-00-41-022		
Eisenriegler E.	IFF-00-41-023		
Grimm H.	IFF-00-41-024	IFF-00-41-025	
Grünberg P.	IFF-00-41-013		
Hoffmann S.	IFF-00-41-043		
Monkenbusch M.	IFF-00-41-026	IFF-00-41-027	IFF-00-41-028
Müller-Krumbhaar H.	IFF-00-41-006 IFF-00-41-030	IFF-00-41-007	IFF-00-41-029
Neeb M.	IFF-00-41-031		
Prager M.	IFF-00-41-032		
Richter D.	IFF-00-41-033	IFF-00-41-034	IFF-00-41-035
Schroeder H.	IFF-00-41-036	IFF-00-41-043	
Schroeder K.	IFF-00-41-006 IFF-00-41-037	IFF-00-41-007	IFF-00-41-016
Schwahn D.	IFF-00-41-038	IFF-00-41-039	
Schweika W.	IFF-00-41-010		
Schütz G.	IFF-00-41-040		
Sturm K.	IFF-00-41-041	IFF-00-41-042	
Waser R.	IFF-00-41-043	IFF-00-41-044	
Zorn R.	IFF-00-41-045 IFF-00-41-048	IFF-00-41-046	IFF-00-41-047

Internal reports

IFF-00-51-001
Blügel S.
Nanomagnetismuslabor: Supercomputer
ZAM-aktuell Nr. 86, Juni 2000
23.20.0

IFF-00-51-002
Nerger S.
Struktur und magnetische Kopplung in FexCo1-x/Mn/FexCo1-x-Schichtsystemen
Diplomarbeit in Physik, vorgelegt der RWTH, angefertigt am IFF
23.89.1

IFF-00-51-003
Voigt J.
Elementspezifische Magnetisierungsdichteverteilung in Seltenen-Erd-Übergittern
Diplomarbeit in Physik, vorgelegt der RWTH, angefertigt am IFF
23.89.1

List of references

Blügel S.	IFF-00-51-001
Nerger S.	IFF-00-51-002
Voigt J.	IFF-00-51-003

Internal seminars

IFF-00-61-001
Allgaier J.
Polymersynthese
Jülich Soft Matter Days, Heimbach, 18. - 20.10.00
23.30.0

IFF-00-61-002
Baumgärtner A.
Simulationen von Membranproteinen
Soft Matter Tagung
Heimbach, 18.-20.10.2000
23.30.0

IFF-00-61-003
Baumgärtner A.
Simulationen von Membranproteinen
VSR-Kommission
Juelich, 7.11.2000
23.30.0

IFF-00-61-004
Blügel S.
Magnetismus im Nanokosmos
Vortragsveranstaltung der VSR-Kommission des FZJ
19.06.2000
23.20.0

IFF-00-61-005
Brückel Th.; Eberhardt W.
Dynamik in kondensierter Materie
Auditorium der Zentralbibliothek, IFF-Ferienschule,
13.03.2000
23.89.1

IFF-00-61-006
Brückel Th.
Elastic Scattering from Many-Body Systems
IFF-Hörsaal, Neutron Laboratory Course, 26.09.2000
23.89.1

IFF-00-61-007
Brückel Th.
Magnetism
IFF-Hörsaal, Neutron Laboratory Course, 29.09.2000
23.89.1

IFF-00-61-008
Conrad H.
Die Europäische Spallations-Neutronenquelle ESS - Spallationsmethoden
Auditorium der Zentralbibliothek, IFF-Ferienschule,
13.03.2000
23.89.1

IFF-00-61-009
Conrad H.
Neutron Sources
IFF-Hörsaal, Neutron Laboratory Course, 26.09.2000
23.89.1

IFF-00-61-010
Endo H.
Polymer efficiency boosters in microemulsions: A SANS study to investigate the role of the polymer
Jülich Soft Matter Days, Heimbach, 18. - 20.10.00
23.30.0

IFF-00-61-011
Gompper G.
Fluctuation Spectra of Non-Spherical Vesicles
Soft Matter Tagung
Heimbach, 18.-20.10.2000
23.30.0

IFF-00-61-012
Kahle S.
Glass transition and glassy state
Jülich Soft Matter Days, Heimbach, 18. - 20.10.00
23.30.0

IFF-00-61-013
Kentzinger E.
Characterization of the buried interfaces in metallic multilayers using synchrotron radiation
IFF-Hörsaal, Informationstagung aus Anlaß der 15. Sitzung des Wissenschaftlichen Beirats, 13.04.2000
23.89.1

IFF-00-61-014
Kirstein O.; Kozielewski T.; Prager M.; Richter D.
Rückstreuspektrometer für den FRM-II Reaktor
KFN-Tagung, FZ Jülich, 18. - 19.09.00
23.89.1

IFF-00-61-015
Lamura A.
Equilibrium and Dynamical Properties of Microemulsions
Soft Matter Tagung
Heimbach, 18.-20.10.2000
23.30.0

IFF-00-61-016
Lamura A.
Phase separation of binary mixtures in shear flow
Seminarvortrag, IFF, FZ Jülich, 25.5.2000
23.30.0

IFF-00-61-017
Mihailescu M.
Experiments describing the dynamics of microemulsions
Jülich Soft Matter Days, Heimbach, 18. - 20.10.00
23.30.0

IFF-00-61-018
Monkenbusch M.
Neutronenstreuung und Dynamik in "Soft Matter" Systemen
Jülich Soft Matter Days, Heimbach, 18. - 20.10.00
23.30.0

IFF-00-61-019
Poppe U.; Divin Y.Y.
Hilbert-Transform-Spetroskopie
INFO-PHYS-TECH, Nr.29/ Juni 2000, VDI-Technologiezentrum , Düsseldorf, Germany
23.42.0

IFF-00-61-020
Pyckhout-Hintzen W.
Untersuchungen mit Neutronen and Netzwerken und verzweigten Polymerschmelzen
Jülich Soft Matter Days, Heimbach, 18. - 20.10.00
23.30.0

IFF-00-61-021
Schwahn D.
Phase behavior in ternary polymer mixtures
Jülich Soft Matter Days, Heimbach, 18. - 20.10.00
23.30.0

IFF-00-61-022
Schweika W.
Polarization analysis
IFF-Hörsaal, Neutron Laboratory Course, 27.09.2000
23.89.1

IFF-00-61-023
Schweika W.
Quellen und Eigenschaften der Neutronen- und Synchrotronstrahlung
Auditorium der Zentralbibliothek, IFF-Ferienschule,
13.03.2000
23.89.1

IFF-00-61-024
Schütz G.
Non-equilibrium relaxation law for entangled polymers
Joint Soft Matter Seminar, IFF, FZ Jülich, 24.2.2000
23.30.0

IFF-00-61-025
Seeck O.H.
Continuum description: Grazing Incidence Neutron Scattering
IFF-Hörsaal, Neutron Laboratory Course, 27.09.2000
23.89.1

IFF-00-61-026
Stellbrink J.
Kolloidale Aspekte von Sternsystemen
Jülich Soft Matter Days, Heimbach, 18. - 20.10.00
23.30.0

IFF-00-61-027
Willner L.
Mizellarisierung von Polymeren
Jülich Soft Matter Days, Heimbach, 18. - 20.10.00
23.30.0

IFF-00-61-028
Wischnewski A.; Richter D.; Monkenbusch M.; Willner L.;
Farago B.1; Ehlers G.1; Schleger P.1
1Institute Laue Langevin, Grenoble/France
Dynamik in Polymerschmelzen - Grenzen des
Reptationsmodells
Beiratssitzung, IFF, FZ-Jülich, 13.04.2000
23.30.0

IFF-00-61-029
Zorn R.
Glass dynamics in confinement
Jülich Soft Matter Days, Heimbach, 18. - 20.10.00
23.15.0

List of references

Allgaier J.	IFF-00-61-001		
Baumgärtner A.	IFF-00-61-002	IFF-00-61-003	
Blügel S.	IFF-00-61-004		
Brückel Th.	IFF-00-61-005	IFF-00-61-006	IFF-00-61-007
Conrad H.	IFF-00-61-008	IFF-00-61-009	
Divin Y.Y.	IFF-00-61-019		
Eberhardt W.	IFF-00-61-005		
Endo H.	IFF-00-61-010		
Gompper G.	IFF-00-61-011		
Kahle S.	IFF-00-61-012		
Kentzinger E.	IFF-00-61-013		
Kirstein O.	IFF-00-61-014		
Kozielewski T.	IFF-00-61-014		
Lamura A.	IFF-00-61-015	IFF-00-61-016	
Mihailescu M.	IFF-00-61-017		
Monkenbusch M.	IFF-00-61-018	IFF-00-61-028	
Poppe U.	IFF-00-61-019		
Prager M.	IFF-00-61-014		
Pyckhout-Hintzen W.	IFF-00-61-020		
Richter D.	IFF-00-61-014	IFF-00-61-028	
Schwahn D.	IFF-00-61-021		
Schweika W.	IFF-00-61-022	IFF-00-61-023	
Schütz G.	IFF-00-61-024		
Seeck O.H.	IFF-00-61-025		
Stellbrink J.	IFF-00-61-026		
Willner L.	IFF-00-61-027	IFF-00-61-028	
Wischnewski A.	IFF-00-61-028		
Zorn R.	IFF-00-61-029		

Institute for Solid State Researcj (IFF)

Research Center Jülich GmbH

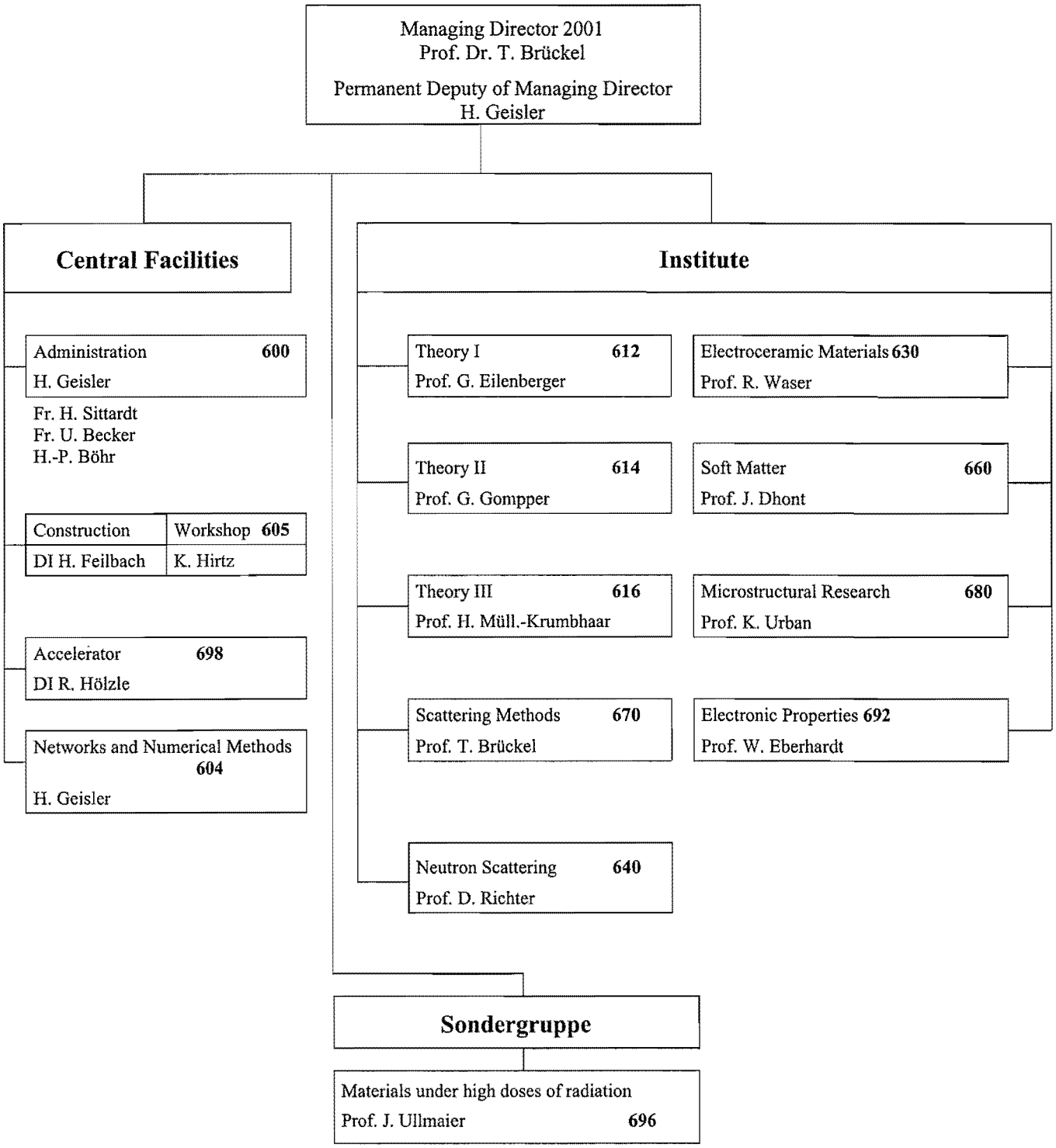

Stand 01.01.2001

Scientific Advisory Board 2001

The 2001 meeting of the Scientific Advisory Board will take place on the 26./27. April. Currently, the board consists of the following members:

Dr. C. **Carlile**, Institute Laue-Langevin, Grenoble, France

Prof. R. **Dronskowski**, RWTH Aachen

Prof. H. **Eschrig**, IFW Dresden, **Vice chairman**

Prof. W.M. **Finnis**, Queen's University of Belfast, UK

Prof. U. **Gösele**, MPI Halle/Saale

Prof. S. **Hess**, TU Berlin

Dr. J. **Joosten**, DSM Research, Geleen, NL

Prof. H. **Lüth**, Forschungszentrum Jülich, ISI

Prof. H. **Micklitz**, Universität zu Köln

Prof. W. **Press**, Universität Kiel

Dr. J. **Rieger**, BASF, Ludwigshafen

Prof. J. **Schnakenberg**, RWTH Aachen, **Chairman**

Prof. L. **Singheiser**, Forschungszentrum Jülich, IWV2

Prof. U.W. **Suter**, ETH Zürich, Switzerland

Prof. H. **Thomann**, Siemens AG München

Prof. E. **Umbach**, Universität Würzburg

Prof. P. **Wyder**, Centre National de la Recherche Scientifique (MPI), Grenoble, France

Personnel 2000/2001

Staff members (centrally financial)	
- **Scientific Staff**	**96**
including those funded externally	15
- **Technical Staff**	**49**
including those funded externally	2
Post-doc (HGF)	**16**
Staff members of service-groups	**42**
Administrations incl. Secretaries	**19**
Graduate students	**71**
including those funded externally	13
Diploma students	**25**
Trainees	**28**
Guests Scientists staying for two weeks or longer	**64**
Invited lectures	**127**

IFF-Scientists Teaching at Universities

Lecturer:	University:
Dr. A. Baumgärtner	Duisburg
Dr. P.S. Bechthold	Köln
Dr. S. Blügel	Aachen
Dr. A. Bringer	Düsseldorf
Prof. Th. Brückel	Aachen
Prof. U. Buchenau	Düsseldorf
Prof. P. Dederichs	Aachen
Prof. J.K.G. Dhont	Düsseldorf
Prof. W. Eberhardt	Köln
Dr. P. Ehrhart	Aachen
Prof. G. Eilenberger	Köln
Prof. E. Eisenriegler	Düsseldorf
Prof. P. Grünberg	Köln
Dr. H. Lustfeld	Duisburg
Prof. H. Müller-Krumbhaar	Aachen
Prof. D. Richter	Münster
Prof. T. Schober	Aachen
Dr. H. Schroeder	Aachen
Prof. K. Schroeder	Aachen
Dr. G. Schütz	Bonn
Dr. W. Schweika	Aachen
Prof. K. Sturm	Düsseldorf
Prof. H. Ullmaier	Aachen
Prof. K. Urban	Aachen
Prof. R. Waser	Aachen
Dr. R. Zorn	Münster

IFF Scientists on leave 2000

Prof. T. Brückel	APS Argonne, USA
Dr. St. Eisebitt	University Stanford, USA
Dr. G. Goerigk	HASYLAB at DESY, Hamburg, Germany
Dr. D. Hupfeld	APS Argonne, USA
Dr. R. Lässer	Forschungszentrum Karlsruhe, Germany
Dr. M. Ohl	ILL Grenoble, France
Dr. U. Rücker	Laboratoire Leon Brillouin, Saclay, France
Dr. W. Schmidt	ILL Grenoble, France
Dr. O. Seeck	HASYLAB at DESY, Hamburg, Germany
Dr. J. Stellbrink	University of Edinburgh, UK

List of IFF-Scientists

(G: Guests; GS: Graduate students)

Abdel-Goad, M	(Neutron Scattering, GS)
Akola, J.	(Theory I, G)
Alefeld, B.	(Scattering Methods)
Allgaier, J.	(Neutron Scattering)
Antons, A.	(Theory III, GS)
Arons, R.	(Electroceramic Materials)
Babik, W.	(Scattering Methods, GS)
Baldus, O.	(Electroceramic Materials, GS)
Baumgarten, L.	(Electronic Properties)
Baumgärtner, A.	(Theory II)
Bechthold, P.	(Electronic Properties)
Bellini, V.	(Theory III, GS)
Biermann, S.	(Theory I, GS)
Bihlmayer, G.	(Electronic Properties, G)
Blügel, S.	(Electronic Properties)
Botti, A.	(Neutron Scattering, GS)
Breidbach, M.	(Electronic Properties, GS)
Brener, E.	(Theory III)
Bringer, A.	(Theory I)
Brückel, T.	(Scattering Methods)
Buchenau, U.	(Neutron Scattering)
Buchmeier, M.	(Electronic Properties, GS)
Bürgler, D. E.	(Electronic Properties)
Bukhvalov, D.	(Theory I, GS)
Burkhardt, T.	(Theory I, G)
Byelov, D.	(Neutron Scattering, GS)
Byloss, C.	(Neutron Scattering, G)
Cao, Y.	(Theory III, GS)
Caprion, D.	(Theory III, G)
Carbone, C.	(Electronic Properties)
Chen, J. H.	(Microstructure Research)
Chen, J.	(Special Group)
Chen, X.	(Theory II, G)
Clarke, S.	(Electronic Properties, G)
Conrad, H.	(Scattering Methods)
Cramm, S.	(Electronic Properties)

Dallmeyer, A.	(Electronic Properties, GS)
Dederichs, P.-H.	(Theory III)
Dhont, J.-K.	(Soft Matter)
Divin, Y.	(Microstructure Research)
Dogic, Z.	(Soft Matter, G)
Dürr, H.	(Electronic Properties)
Eberhardt, W.	(Electronic Properties)
Ebert, P.	(Microstructure Research)
Ehrhart, P.	(Electroceramic Materials)
Eilenberger, G.	(Theory I)
Eisebitt, S.	(Electronic Properties)
Eisenriegler, E.	(Theory II)
Endo, H.	(Neutron Scattering, GS)
Faley, M.	(Microstructure Research)
Fetters, L. J.	(Neutron Scattering, G)
Feuerbacher, M.	(Microstructure Research)
Fitsilis, F.	(Electroceramic Materials, GS)
Freiwald, M.	(Electronic Properties, GS)
Freyss, M.	(Theory III, G)
Galanakis, I.	(Theory III, G)
Ganster, R.	(Electroceramic Materials, GS)
Goerigk, G.	(Scattering Methods)
Gompper, G.	(Theory II)
Grimm, H.	(Neutron Scattering)
Grünberg, P.	(Electronic Properties)
Grushko, B.	(Microstructure Research)
Gutheim, F.	(Theory III, GS)
Harris, J.	(Theory I)
Hartmann, M.	(Theory III, GS)
Haubold, H.-G.	(Scattering Methods)
Hauck, J.	(Soft Matter)
Heggen, M.	(Microstructure Research, GS)
Heinrich, M.	(Neutron Scattering, G)
Hermes, H.	(Neutron Scattering)
Hoffmann-Eifert, S.	(Electroceramic Materials)
Höhler, H.	(Theory III, GS)
Houben, L.	(Microstructure Research)
Hupfeld, D.	(Scattering Methods)
Istomin, K.	(Scattering Methods, GS)
Jacquemin, R.	(Electronic Properties)
Jahnen, B.	(Microstructure Research, GS)

Jia, C.	(Microstructure Research)
Jin, H.-Z.	(Microstructure Research, GS)
Jones, R.	(Theory I)
Jung, P.	(Special Group)
Kahle, S.	(Neutron Scattering)
Kann, G.	(Electronic Properties, GS)
Karl, A.	(Electronic Properties, GS)
Kaya, U. L.	(Neutron Scattering, GS)
Kentzinger, E.	(Scattering Methods)
Kesternich, W.	(Special Group)
Kienle, D.	(Theory III, GS)
Kirstein, O.	(Neutron Scattering)
Klingeler, R.	(Electronic Properties, GS)
Kluge, F.	(Microstructure Research, GS)
Kluge, M.	(Theory III, GS)
Köbler, U.	(Scattering Methods)
Kohlstedt, H.	(Electroceramic Materials)
Krasser, W.	(Electroceramic Materials)
Kreitschmann, M.	(Neutron Scattering)
Kromen, W.	(Theory III, GS)
Kurz, P.	(Electronic Properties, GS)
Küssel, E.	(Scattering Methods)
Lamura, A.	(Theory II, G)
Lang, P.	(Soft Matter)
Lei, C.	(Microstructure Research, GS)
Lentzen, M.	(Microstructure Research)
Lettinga, P.	(Soft Matter)
Leube, W.	(Neutron Scattering)
Liebsch, A.	(Theory I)
Link, S.	(Electronic Properties, GS)
Liu, C.	(Special Group, G)
Lörgen, M.	(Electronic Properties, GS)
Lustfeld, H.	(Theory I)
Lüttgens, G.	(Electronic Properties, GS)
Luysberg, M.	(Microstructure Research)
Maassen, R.	(Theory I, GS)
Maiti, K.	(Electronic Properties, G)
Malagoli, M.	(Electronic Properties, GS)
Meier, G.	(Soft Matter)
Meuffels, Paul	(Electroceramic Materials)
Mi, S.	(Microstructure Research, GS)

Schmitz, R.	(Electroceramic Materials, GS)
Schmitz, S.	(Electroceramic Materials, GS)
Schneider, S.	(Electroceramic Materials, GS)
Schober, H.	(Theory III)
Schober, T.	(Electroceramic Materials)
Scholl, A.	(Electronic Properties)
Schondelmaier, D.	(Electronic Properties, GS)
Schröder, H.	(Electroceramic Materials)
Schröder, K.	(Theory III)
Schütz, G.	(Theory II)
Schwahn, D.	(Neutron Scattering)
Schweika, W.	(Scattering Methods)
Seeck, O.	(Scattering Methods)
Semmler, U.	(Microstructure Research, GS)
Settels, A.	(Theory III)
Shadrin, P.	(Microstructure Research, G)
Shirotov, V.	(Microstructure Research, GS)
Smith, N.	(Electronic Properties, G)
Soltner, H.	(Microstructure Research)
Spatschek, R.	(Theory III, GS)
Stein, S.	(Electroceramic Materials, GS)
Stellbrink, J.	(Neutron Scattering)
Sturm, K.	(Theory I)
Szot, K.	(Electroceramic Materials)
Thust, A.	(Microstructure Research)
Tietze-Jaensch, B.-H.	(Special Group)
Tillmann, K.	(Microstructure Research)
Toperverg, B.	(Scattering Methods, G)
Trinkaus, H.	(Theory III)
Ullmaier, J.	(Special Group)
Urban, K.	(Microstructure Research)
Vad, T.	(Scattering Methods)
Vijayalakshmi, M.	(Microstructure Research, G)
Voigt, J.	(Scattering Methods, GS)
Volokitin, A.	(Theory I, G)
Wang, J.	(Microstructure Research, GS)
Wang, Y.-g.	(Scattering Methods, G)
Waser, R.	(Electroceramic Materials)
Willner, L.	(Neutron Scattering)
Wingbermühle, J.	(Electronic Properties, GS)
Wirth, I.	(Electronic Properties, GS)

Wischnewski, A.	(Neutron Scattering)
Wortmann, D.	(Electronic Properties, GS)
Wu, J.	(Microstructure Research, G)
Wunnicke, O.	(Theory III, GS)
Yan, S.-S.	(Electronic Properties, G)
Yurechko, M.	(Microstructure Research, GS)
Zeller, R.	(Theory III)
Zilkens, C.	(Electronic Properties, GS)
Zorn, Reiner	(Neutron Scattering)

Guest Scientists

J.A. Abasolo-Hermandes	Instituto Politecnico Nacional, Mexico
Dr. J. Akola	University of Jyväskylä, Finland
Dr. M. Arbe	Universidad Pais Vasco, St. Sebastian, Spain
M.Sc.. N. Atodiresei	University "Al. I CUZA", Iasi, Romania
DP T. Auth	Johann Wolfgang Goethe-University, Frankfurt/M., Germany
Prof. P. Ballone	University Messina, Italy
Dr. G. Bihlmayer	University Vienna, Austria
Prof. T. Burkhardt	Temple University, Philadelphia, USA
DP C. Byloss	University Ferrara, Italy
Dr. I. Cabria Alvaro	University Santander, Spain
Dr. D. Caprion	University Montpellier II, France
Prof. X. Chen	Hua-Zhong Normal University, Wuhan, China
Prof. S. Clarke	University of Wales, Great Britain
Dr. Z. Dogic	Brandeis University, Waltham, USA
V. Ermakov	Joint Institute for Nuclear Research, Bubna, Russia
Dr. L. J. Fetters	Exxon, Annandale, New Jersey, USA
DI G. Flores-Diaz	Instituto Polytecnico National, Mexico
M. Fouladvand	Sharif University, Teheran, Iran
Dr. M. Freyss	University Louis Pasteur, Strasbourg, France
Prof. V. Fridkin	Russian Academy of Sciences, Moscow, Russia
Dr. A. Garcia-Borques	Instituto Politecnico Nacional, Mexico
Dr. R. Gareev	Russian Academy of Sciences, Moscow, Russia
Dr. I. Galanakis	University Louis Pasteur, Strasbourg, France
Dr. W. Gozdz	Polish Academy of Sciences and College of Science, Warsaw, Poland
Prof. J. Gui	Wuhan University, China
Prof. V.L. Gruevich	IOFFE-Institut, St. Petersburg, Russia
Dr. M. Heinrich	University Louis Pasteur, Strasbourg, France
Dr. H. Hölscher	University Hamburg, Germany
Dr. T. Ihle	University of Minnesota, Minneapolis, USA
Dr. A. Ioffe	St. Petersburg Technical University, Russia
Dr. S. Koizumi	Japan Atomic Energy Resarch Institute, Ibaraki-ken, Japan
E. Koulaguine	Joint Institute for Nuclear Research, Dubna, Russia
Prof. B. Kuanr	University of Delhi, India
Dr. A. Lamura	University of Bari, Italy
Dr. T. Lenstra	University Ütrecht, Netherlands
M.Sc. C. Liu	The 4th Institute, Nurclear Power Institute of China, Chengdu, China
Dr. C. Lopez-Bastida	University Cuernavaca, Mexico
Dr. G. Madsen	University of Aarhus, Denmark
Dr. K. Maiti	Indian Institute of Science, Bangalore, India

Dr. S. Masalovich	Kurchatov Institut, Moscow, Russia
Dr. P. Mavropoulos	University Athen, Greece
Dr. J. A. Maxtorena Cordova	University Cuernavaca, Mexico
Dr. X. Nie	Massachusetts Ist. Of Technology, Cambridge, USA
Prof. M. Olmstead	University of Washington, Seattle, USA
Dr. N. Papanikolaou	University Athens, Greece
Dr. S. Perny	Thomson CSF-LCR, ENS Cachan, France
Dr. N. Pertsev	Russian Academy of Sciences, St. Petersburg, Russia
Prof. V. Plaghty	St. Petersburg Nuclear Physics Institute, Gatchna, Russia
Prof. V.L. Popcov	Russian Academy of Sciences, Tomsk, Russia
L. Sacharow	University Hamburg, Germany
Dr. E. Shabalin	Joint Institute for Nuclear Research, Dubna, Russia
Dr. P. Shadrin	Intitute of Radioengineering and Electronics, Moscow, Russia
Prof. V. Shur	Ural State University, Ekaterinburg, Russia
Prof. N. Smith	Law. Berkeley National Laboratory, Berkeley, USA
Prof. E. Straube	University Merseburg, Germany
Dr. B. Topeverg	Petersburg Nuclear Physics Institute, Russia
Dr. M. Vijayalakshmi	Indira Ghandi Centre, Kalpakkam, India
Prof. A. Volokitin	Polytechnic Institut Kuibyshev, Russia
Prof. R. Wang	Department of Physics, Wuhan University, China
Dr. Y.-G. Wang	Southeast University, Nanjing, China
Dr. G. Wignall	Oak Ridge International Laboratory, USA
Dr. J. Wu	Beijing Laboratory of Electron Microscopy, China
Dr. S.-S. Yan	Shandong University, Jinan, China
A. Zimina	State University Saint Petersburg, Russia

Spring Schools of the IFF

Beginning in 1970, our institute has organized an annual two-week Spring School on modern topics in solid state physics.

The topics of the Spring Schools over the past 12 years were:

1990	Solid State research for Information Technology
1991	Physics of Polymers
1992	Synchrotron Radiation for investigating Condensed Matter
1993	Magnetism of Solids and Boundaries
1994	Complex Systems between Atoms and Solids
1995	Electroceramics – Basics and Applications
1996	Scattering Methods for investigating Condensed Matter
1997	Dynamics and Pattern Formation in Condensed Matter
1998	Physics of Nanostructures
1999	Magnetic Layer Structures
2000	fsec and neV: Dynamics of Condensed Matter
2001	New materials for the information technology

Spring School 2001 on "New Materials for information technology"

This event was the 32. spring school offered by the IFF. It took place from 05.-16. March 2001 and included the latest developments in the fields of spectroscopic investigations of the dynamics in condensed matter.

The following lectures were presented (in chronological order):

R. Waser	Introduction
S. Hoffmann-Eifert	Dielectrics and Optics
D. Richter	Ferroelectrics
M. Dolle	Circuit and System Design
K. Sturm	Electronic Properties and Quantum Effects
H. Schroeder	High-permittivity Materials for DRAMs
P. Ehrhart	Deposition methods
Ph. Ebert/ K. Szot	Scanning Probe Techniques
U. Böttger	Ferroelectric RAMs
H. Kohlstedt	Ferroelectric FETs
U.B. Kaupp	Molecular Biology
P. Fromherz	Biological Interface
R. Waser	Molecular Electronics
O. Seeck	Analysis by Diffraction and Fluorescence Methods
J. Moers	Lithography
D. Bürgler/ P. Grünberg	Magnetics and Magnetoelectronics
H. Dürr	Magnetoresistive RAMs
Ch. Buchal	Lightwave Systems
A. Dietzel	Hard Discs
P. Vettiger	MEMS-based Data Storage
B. Spangenberger	Non-lithography Patterning
K. Röll	Magneto-optic Discs
S. Mantl	Alternative Gate Oxides for FETs
M. Siegel	Concepts for Superconducting Logic
A. Ustinov	Quantum Computing using Superconductors
H. Bechtel	Plasma and Field-emission Displays
R. Zorn	Liquid Crystal Displays
M. Wuttig	Rewritable DVDs based on Phase Change Materials
Ch. Buchal	Holographic 3D Memories
W. Mokwa	Transmission on Chip and Board Level
N. Klein	Microwave Communications Systems

Atomic view of a monatomic film of magnetic manganese atoms deposited on a (110) oriented tungsten surface, Mn/W (110). The magnetic moments indicated by arrows are arranged in an antiferromagnetic order, a checkerboard arrangement of red and green atoms. All Mn atoms are chemically and structurally indistinguishable and differ only in the relative orientation of the magnetic moments. The total magnetization is zero. This atomic scale magnetic structure can be detected using a spin-polarized scanning tunneling microscope (SP-STM) operated in the constant current mode. Using a magnetic probe tip (gold colored cone), the calculated STM-image (movement of the tip normal to the surface as the tip scans across the surface, grey scale cloud superimposed on the atoms) does not follow the chemical – but the magnetic unit cell. Although spin-polarization is in general a small effect, here it is exponentially enhanced due to the slow decay of the tunneling current into the vacuum in case of a long-wavelength modulation due to the magnetic super-structure. This opens a route to the understanding of the magnetic properties of nanoscale magnets with complex magnetic strutures, which is a key issue in the magnetic recording industry and in magnetoelectronics (S. Heinze et al., Science 288, 1805 (2000).)

Forschungszentrum Jülich